Interactions between coarse sediment transfer, channel change, river engineering and flood risk in an upland gravel-bed river

Emma Kate Waterhouse

Interactions Between Coarse Sediment Transfer, Channel Change, River Engineering and Flood Risk in an Upland Gravel-Bed River

Emma Kate Waterhouse

Department of Geography
Durham University

2008

Durham University

DECLARATION OF COPYRIGHT

I confirm that no part of the material presented in this thesis has previously been submitted by me or any other persons for a degree in this or any other University. In all cases, where it is relevant, material from the work of others has been acknowledged.

Signed: 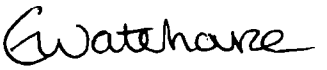

Date: 4/12/08

Research and running; similar in so many ways.

"Running requires endurance, character, pride, physical strength and mental toughness. Running is a test, not a game. A test of faith, belief, will and trust in ones self. So hardcore that it needs a category all to itself to define the pain. Running is more than a sport; it's a lifestyle. If you have to ask us why we run, you'll never understand, so just accept"

Jessica Propst

THESIS SUMMARY

Coarse sediment transfer in upland gravel-bed river systems is often neglected in the design and operation of river management schemes. Yet, it is increasingly attributed to problems within upland environments including bank erosion and enhanced flood risk. Developing a sufficient understanding of coarse sediment transfer and channel change requires strategic field monitoring. Predicting future channel change and flood risk under varying management options requires numerical modelling. This thesis employs a combined field monitoring and numerical modelling approach to explore the relationship between coarse sediment transfer, lateral channel change, river engineering and flood risk.

Intensive field monitoring is used to understand sediment transfer and channel change. Methods include repeat cross-sectional resurvey, bank erosion pins and bank-top surveys, and sediment impact sensors. These data are used to illustrate the spatial and temporal variability of in-channel sedimentation and rates and mechanisms of bank erosion. When analysed further, these data explain patterns of sedimentation and demonstrate implications of coarse sediment accumulation for flood risk. The data are then used in the development and application of a quasi two-dimensional model of channel change. The model couples a one-dimensional sediment routing model with a lateral adjustment component to simulate patterns of downstream fining alongside vertical and lateral channel changes. By using a split channel approach, asymmetrical width adjustments are simulated based on critical shear stress thresholds. Lateral differences in bed elevation and curvature are used to distribute shear stress across the channel. Simulations are run to explore scenarios including changing the flow regime, removing bank protection and implementing a river engineering scheme on a reach with high sedimentation and bank erosion problems. The results highlight the potential impact that poor river management can have on upland rivers, demonstrating enhanced bank erosion upstream and greater sedimentation downstream of the engineered reach. The accumulation of sediment results in increased flood risk.

ACKNOWLEDGEMENTS

There are a number of people I would like to thank for their help, advice and support throughout my PhD.

At Durham University, I would firstly like to thank my supervisors, Professor Stuart Lane, Professor Rob Ferguson and Dr Louise Bracken for their academic guidance in all aspects of my work. In addition, thanks to the other academic staff in the Department who offered advice throughout my research. Second are my fellow students and friends who helped out on field-work (particularly those who stood in the Wharfe in the cold winter months), provided technical support with software and who I shared the ups and downs of Ph.D. life with. Particular thanks go to Dave, Mouldo, Mark, James, Katie O, Katie T, Emma, Tasha, Lisa, Stefano, Friz, Chris, Beth and Ian. Third, the lab staff in the Department who put up with my demands for erosion pins, stakes, GPSs etc. and never tired of me returning leaking waders.

My second group of thanks go to those who helped provide data or the means to collect data. These include: Simon Reid, a Ph.D. student from Leeds University, who preceded me in the time-consuming task of repeat cross-sectional surveying and supplied other valuable data for this project; the National Trust and the Upper Wharfe tenants and landlords for granting me access to the river to carry out my data collection; Ian Benson, who designed and installed my new impact sensors into the Wharfe; and the EPSRC for providing funding for this research as part of the Flood Risk Management Research Consortium.

Finally, a great big "thank-you" to my close friends and family, particularly Mum, Dad and James for all your encouragement, advice and support on a non-academic level, and for putting up with my enthusiasm about gravel, bank erosion and big floods!

Table of Contents, Figures, Table List & Notation

Table of Contents

LIST OF FIGURES

LIST OF TABLES

NOTATION

A	cross-sectional area
C	Chezy coefficient
c	Curvature
c_r	radius of curvature (1/c)
D_x	grain size diameter at which x% of grains are larger
d	flow depth
D_c	channel depth (from bed elevation to highest banktop)
E_{diff}	difference in elevation between left and right channel sides
w_e	rate of width increase through erosion
w_d	rate of width decrease through deposition
e_g	uncertainty in elevation due to grain roughness
e_z	uncertainty in elevation due to GPS location
f	Darcy-Weisbach friction factor
F_i	proportion of size fraction I in a mixture
F_s	proportion of sand in a mixture of sediment
g	gravity due to acceleration
h	bed elevation
L	is active layer thickness
n	Mannings roughness value
P_i	wetted perimeter
q	bedload flux / sediment transport rate
Q	discharge
R	hydraulic radius
r	routing potential in cellular models
r_n	relative transport intensity using pings
S	slope
t	time
t_n	transport intensity of pings
u*	shear velocity
V	volume change between two surveys
V_c	volume of sediment lost / gained during width adjustment
V_w	width-averaged V_c
v	cross-sectionally averaged velocity
w	channel width
w_i	inital half channel width
w_n	new half channel width after adjustment
w_l	width of logger plate
x	distance downstream from top of reach
z	horizontal distance across the channel
ε	porosity of sediment
ρ	density of water
τ	shear stress
τ_{cD}	critical shear stress for deposition
τ_{cE}	critical shear stress for erosion
τ_{di}	lateral shear stress distribution
ϕ	grain size diameter in phi

CHAPTER ONE:
CONTEXT, AIMS AND OBJECTIVES

1.1 AIMS AND RESEARCH QUESTIONS

This Ph.D. research has two overall aims:

- *to explore sediment dynamics and channel change in an upland gravel-bed river and to assess the impacts of such changes on flood risk; and*
- *to develop a model that simulates annual to decadal scale channel change for exploring the impacts of river management.*

These aims are achieved by answering the following key research questions which are answered throughout the thesis and are revisited in the conclusions.

1) How does in-channel sedimentation in an upland gravel-bed river vary through space and time?
2) At what rate do unprotected river banks, in upland gravel-bed rivers, erode and what processes drive this bank erosion?
3) What are the mechanisms that drive these spatial and temporal patterns of channel change?
4) What implications do in-channel sedimentation and bank erosion have for flood risk?
5) Can a simple quasi two-dimensional modelling approach be used to simulate vertical and lateral channel change in a natural, sinuous upland gravel-bed river?
6) Within the model, how important are the inclusion of a variable discharge and curvature driven shear stress distribution for predictions of channel change through space and time?
7) What are the implications of changes in hydrology and river management for channel change and flood risk?

1.2 SCIENTIFIC CONTEXT OF RESEARCH

It is becoming increasingly accepted that many problems in upland river systems, including bank erosion and increased flooding, stem from in-channel sedimentation (e.g. James, 1999; Stover and Montgomery, 2001; Korup *et al.*, 2004; Pinter and Heine, 2005; Lane *et al.*, 2008). Traditionally, river systems have responded to sediment delivery through lateral migration, with bank erosion countering the loss of flow capacity resulting from aggradation. As the timescale of adjustment through channel migration is commonly longer than the individual event timescale, sediment delivery events are expected to lead to a short-term increase in flood risk whilst channel capacity re-establishes itself. However, there are at least two scenarios where this might not be the case: (1) where the return period of coarse sediment delivery events is sufficiently short that the channel capacity does not re-establish itself before a subsequent coarse sediment delivery event; and (2) where management activities have been adopted to prevent bank erosion and to protect flood infrastructure, and hence channel capacity cannot be re-established. Modelling suggests that, under future climate change scenarios, and particularly in upland catchments sensitised to rainfall events as a result of deforestation (Macklin and Lewin, 2003), coarse sediment delivery rates may increase dramatically (Lane *et al.*, 2007). This is primarily through reductions in event return period. In addition, river bank erosion, even in rural areas, has traditionally been seen as a problem that has to be prevented rather than an aspect of natural channel response to sediment delivery (Reid *et al.*, 2007a). Thus, there remains a tradition of active intervention to reduce bank erosion rates, whether through traditional 'hard' engineering or more recent 'soft' engineering. Taken together, the changing return period of sediment delivery events, coupled to constraints on the capacity of a river to migrate in response to delivered sediment, could lead to dramatic increases in flood risk in systems associated with coarse sediment delivery.

Thus far, the primary focus of the effects of possible climate changes, and their interaction with land management impacts, upon flood risk has been in terms of impacts on runoff (e.g. Robinson, 1990; Tollan, 2002; O'Connell *et al.*, 2004; Sullivan *et al.*, 2004). There has been much less attention given to the effects of river bed level changes upon flood risk, and their sensitivity to climate and land use change impacts upon sediment delivery (Stover and

Montgomery, 2001; Lane *et al.*, 2007). If understanding the sediment transfer system is crucial to effective understanding of flood risk, then it needs to be based upon evidence that captures morphological response over longer timescales than single sediment delivery events. Evidence is needed that encompasses a number of sediment delivery events and quantifies the detailed morphological response to those events. Longer term quantification of sediment and river channel histories is possible through the analysis of historical maps and aerial photography (e.g. Hooke, 1977; Winterbottom, 2000; Parsons and Gilvear, 2002), but this is rarely of high enough frequency to capture system response to individual events or clusters of events. Spatially-detailed, repeated river bed surveys are rarely undertaken over more than one or two years as they are time consuming and rarely attract funding for more than three years. Also, to date, these surveys have emphasised planform change rather than the coupled vertical adjustment and lateral migration which is central to understanding changes in channel capacity. This also reflects the established view that river engineering and fluvial geomorphology are separate disciplines. Despite the gradual convergence of the disciplines that began in the late 1980s (e.g. Chang, 1988) there remains a lack of consideration for fluvial geomorphology in the design and implementation of engineering structures. Thus, there are no research models that allow for the inclusion of bank protection measures that prevent the natural adjustment process.

Whilst field studies can be used to monitor on-going changes in a river channel, predicting the morphological response of a river system to management options, specifically river engineering, requires a numerical modelling approach. The implications of river response can be environmental and economic, including increased flood-risk, loss of land, damage to riverbank infrastructure and negative impacts on aquatic and riparian ecosystems. Previous modelling approaches have explored the lateral adjustment of river systems (e.g. Mosselman, 1995; Darby and Thorne, 1996; Lancaster and Bras, 2002). However, they have several inherent weaknesses. Many width adjustment models are developed for straight rectangular channels, failing to simulate channel change processes occurring at meander bends in natural channels (e.g. Chang, 1988; Yang *et al.*, 1988). In contrast, meander evolution and migration models typically simulate outer bank erosion but neglect inner bank deposition processes, instead assuming deposition rates that match erosion rates

thus maintaining channel width (e.g. Ikeda *et al.*, 1981). This is problematic as it fails to capture the asymmetrical adjustment process which may be attributed to changes in channel capacity. The channel's capacity to hold flow is crucial for flood risk. These models are often limited to steady state conditions (e.g. Osman, 1985) and they provide limited information on the rate of change. In addition, most morphological channel change models express a weakness due to a lack of data for model testing and a dependence upon data sourced in a flume (e.g. Simon and Darby, 1997). Hence, there are no suitable models available to explore sediment transport and vertical and lateral channel change in upland gravel-bed rivers with coarse sediment.

Research is required that combines a field-based and modelling approach: (1) to highlight the important role that in-channel sedimentation plays in flood risk; (2) to explore the spatial and temporal nature of this sedimentation; (3) to examine factors underlying the nature of the sediment supply and transfer system; and (4) to investigate the impacts that river engineering strategies have on the sediment transfer system and channel change.

1.3 THESIS STRUCTURE

The two thesis aims and key research questions are fulfilled using the following methodological objectives which structure the thesis as shown in Figure 1.1:

1) to use literature review:
    a. to develop an understanding of the channel change process and the factors driving it;
    b. to provide knowledge about the chosen study site;
    c. to develop a suitable methodology for monitoring channel change using a field-based approach; and
    d. to explore previous modelling approaches to assess their applicability to the research aim and to aid with model development;
2) to select a study site that allows the research aims and objectives to be achieved;
3) to use field-based techniques to monitor channel change and the variables driving these changes;

4) to use field-based findings from (3) to analyse the sediment transfer and channel change process and assess its impact on flood risk;
5) to develop a model of vertical and lateral channel change using data from (3); and
6) to run scenarios to produce model outputs for analysis.

The thesis is split into ten chapters which are linked together as shown in the thesis map (Figure 1.1). This map shows where the six methodological objectives are achieved and how the chapters link together.

Figure 1.1: Thesis Map

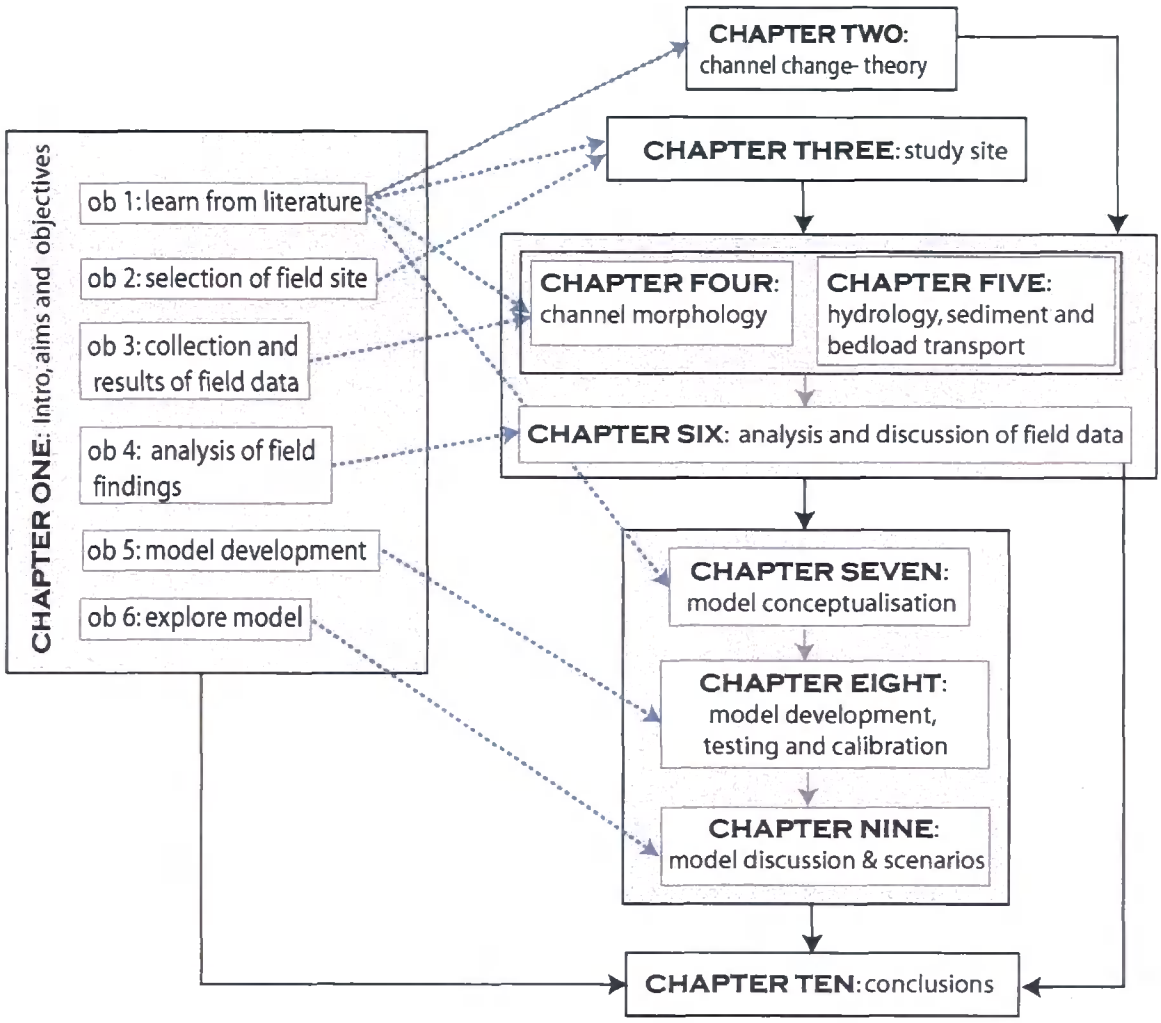

Objective 1: to use literature review to develop an understanding about channel change processes, the field site, field methodologies and modelling techniques.

This objective is addressed in Chapters 2, 3, 4, 5 and 7. There are two main sections of literature review. The first is in Chapter 2 which explores channel change in upland river systems. This begins by considering the catchment wide factors that control channel morphology. Three main within-channel factors are identified and explored in more detail. These include the discharge, the sediment supply and the nature of the channel boundary. This is followed by an overview of the broader factors that directly or indirectly alter these three factors. River channel engineering is focussed on as this forms a key part of conventional management interventions. The mechanisms of channel change are then discussed with attention concentrating on bank erosion, widely recognised to be complex and multifaceted. Other processes, including deposition and meander migration, are summarised as these are discussed later in the thesis.

The second main section of literature review is within Chapter 7. This provides an overview of previous modelling approaches to simulate channel change. These are split into empirical models, width adjustment models for straight channels, meander evolution and migration models and methods of modelling width adjustment in meandering channels. The main limitations of these modelling approaches are discussed, thereby justifying the development of a new model. Details of the three sub-models used in width adjustment models for straight channels are included as a similar sub-model approach is fully developed in Chapter 8. Within this chapter, key modelling questions are raised. These form the structure of the model development in Chapter 8.

Objective 1 is also addressed in Chapters 3, 4 and 5. In Chapter 3, the study site, literature and reports from previous studies in the catchment are consulted to provide details on the catchment's characteristics, history and river management strategies. In Chapters 4 and 5 literature is used to develop methodologies for each of the field monitoring techniques adopted. Literature is also used to compare the results from this research with findings from previous research.

Objective 2: the selection of a suitable study site.

Objective 2 is achieved in Chapter 3 where the reasons behind the Upper Wharfe being chosen as a study site are outlined. In addition, this chapter provides an overview of the catchment and channel characteristics. This helps with understanding the locations of the field-based monitoring and in the analysis of the results. Furthermore, the catchment and channel description shows that the Wharfe has similarities with other UK gravel-bed rivers, allowing many of the findings to be transferred to similar catchments. Outlining the channel and catchment characteristics and providing details of the history of the catchment and the river management that has taken place along the study reach are also important for understanding the processes operating in the study reach.

Objective 3: monitoring channel change and river system response using a field-based approach.

Field data are required for three reasons: (1) to explore links between coarse sediment transfer, vertical and lateral channel change and flood risk (Chapter 6); (2) to allow the reconstruction of a sediment budget for estimating bedload transport rates (Chapter 6); (3) to provide the required input and boundary conditions for the development and application of the model in Chapter 8 and Chapter 9. A monitoring strategy was required to provide these data. Chapter 4 and Chapter 5 both begin by outlining the data required to monitor and to characterise channel morphology (Chapter 4) and to provide data on the hydrology and the supply and transfer of sediment in the study reach (Chapter 5). For each method, options for monitoring are explored using evidence from the literature, before the adopted monitoring strategies are described in full. Results for each method are then presented.

Chapter 4 aims to monitor and characterise the channel morphology and this is achieved using five methods including: (1) field surveys; (2) repeat cross-sectional surveys; (3) a bank erosion study using erosion pins and bank-top resurveys; (4) characterising curvature from a digitized LiDAR image; and (5) measuring the flow around a meander bend.

Chapter 5 provides data on the main factors that determine the channel morphology as outlined in the literature review. These include: (1) describing the channel's hydrological regime; (2) characterising the bed material using a hybrid approach of pebble counts and bulk samples; and (3) monitoring sediment transport within the study reach.

Objective 4: to use field-based findings to analyse sediment transfer and channel change, and its impacts on flood risk.

This objective uses the results from Chapter 4 and Chapter 5 to explore several key research themes in Chapter 6. Many of the results from individual methods are combined in this analysis. The first key area of synthesis is explaining spatial and temporal patterns of sedimentation by exploring the links between the sedimentation results and: (a) hydrology; (b) sediment supply; (c) survey frequency; and (d) channel geometry characteristics. Second, locations of channel change are explored in relation to channel width, curvature and bank protection. Third, results from Chapters 4 and 5 are combined to provide additional data for the modelling. This includes estimating the bedload transport rate. Fourth, the ability to infer changes in bed level from the impact sensor data are discussed. Finally, the impacts of aggradation on flood risk are explored.

Objective 5: to develop a model capable of simulating vertical and lateral channel change in the study reach.

Knowledge on the channel change process obtained from literature in Chapter 2, and from data analysed in Chapters 4, 5 and 6 are used alongside the modelling literature review in Chapter 7 to produce a conceptual model of channel change. Ten key modelling questions are posed within Chapter 7. These are addressed during Chapter 8, through the development and testing of the research model. Modifications and decisions made are discussed alongside supporting model outputs. Following development, several of the model parameters are tested for sensitivity. The model is then calibrated to optimise the parameters on field observations (Chapters 4, 5 and 6). Chapter 9 begins by providing a

discussion of the model capabilities and limitations before a range of scenarios are tested later in the chapter.

Objective 6: to run scenarios to produce model outputs for analysis.

Chapter 9 uses the fully developed and calibrated model to run a range of scenarios. These scenarios include: (1) running the model for 2, 4 and 6 years; (2) removing bank protection from the Wharfe study reach; (3) simulating different hydrological regimes; and (4) exploring engineering options around a problematic reach of the Upper Wharfe. The key model outputs that are explored include bed level changes and bank erosion rates. The implications of channel changes following each scenario are considered.

Overall aims and research questions.

The two main thesis aims and each of the key research questions set out in Section 1.1 are revisited in the final conclusions chapter (Chapter 10). This chapter is split into questions about the field-based approach and questions about the modelling. Answers to these questions are provided alongside some concluding comments about the methodologies adopted. Some final concluding remarks bring the thesis to a close.

CHAPTER TWO: CHANNEL CHANGE IN UPLAND GRAVEL-BED RIVERS

2.1 INTRODUCTION

Reviewing literature is important for three reasons. First, it provides an introduction and background into many of the ideas, theories and methodologies that are dealt with in the thesis. Second, doing so highlights fields of strength where extensive research has been carried out, alongside establishing gaps in knowledge that require further research. Finally, literature review provides essential details on approaches and methodologies which allow research, specifically field data collection and modelling, to be carried out effectively.

This chapter concentrates on reviewing channel change in upland environments. It is essential to develop an understanding into the factors that drive channel change at both the channel and catchment scale. This background will be required when the findings made in Chapters 4, 5 and 6 are explored. The discussion concentrates on the driving factors of discharge and sediment supply and the boundary conditions imposed by the channel (Section 2.3). The morphological effects of human disturbances, specifically channel engineering are introduced (Section 2.4) and channel change mechanisms are discussed with a focus on bank erosion (Section 2.5). Understanding bank erosion is required when the bank erosion results are analysed and for modelling the lateral adjustment process. Further adjustment processes including deposition and meander migration are summarised (Section 2.5) again providing valuable background information for the modelling phase of the thesis. The final part of this chapter is a short summary into the implications that channel change has on flood risk, habitats and bank erosion (Section 2.6).

2.2 Overview of Processes

To understand processes of channel change, the channel must be placed within a catchment scale context as these broader controls ultimately drive changes. Figure 2.1 provides a schematic representation of an upland environment and shows the wide range of factors that are capable of directly or indirectly influencing the *geometry* of a channel cross-section (e.g. width, depth, shape) and the *planform* of the channel in the downstream direction (e.g. slope, sinuosity, meanders). Together these are referred to as the channel *morphology*. Figure 2.2 groups these processes and provides a summary of the main linkages between them.

Figure 2.1: Factors influencing channel morphology.

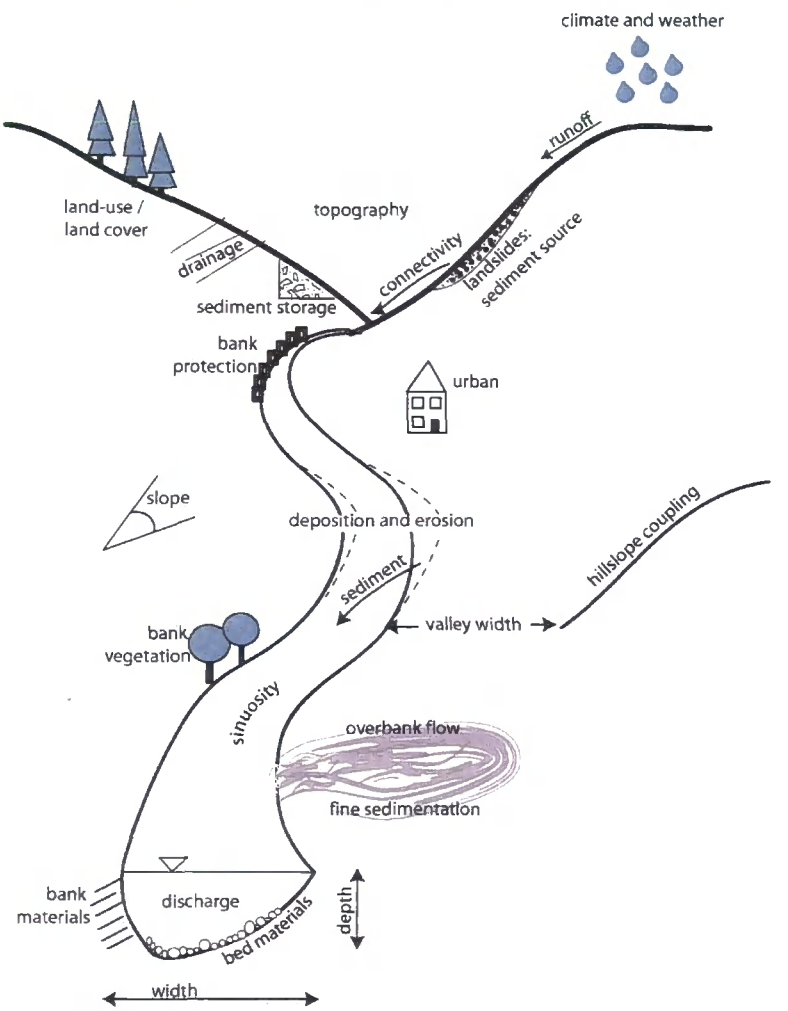

Figure 2.2: Linkages between factors influencing channel morphology.

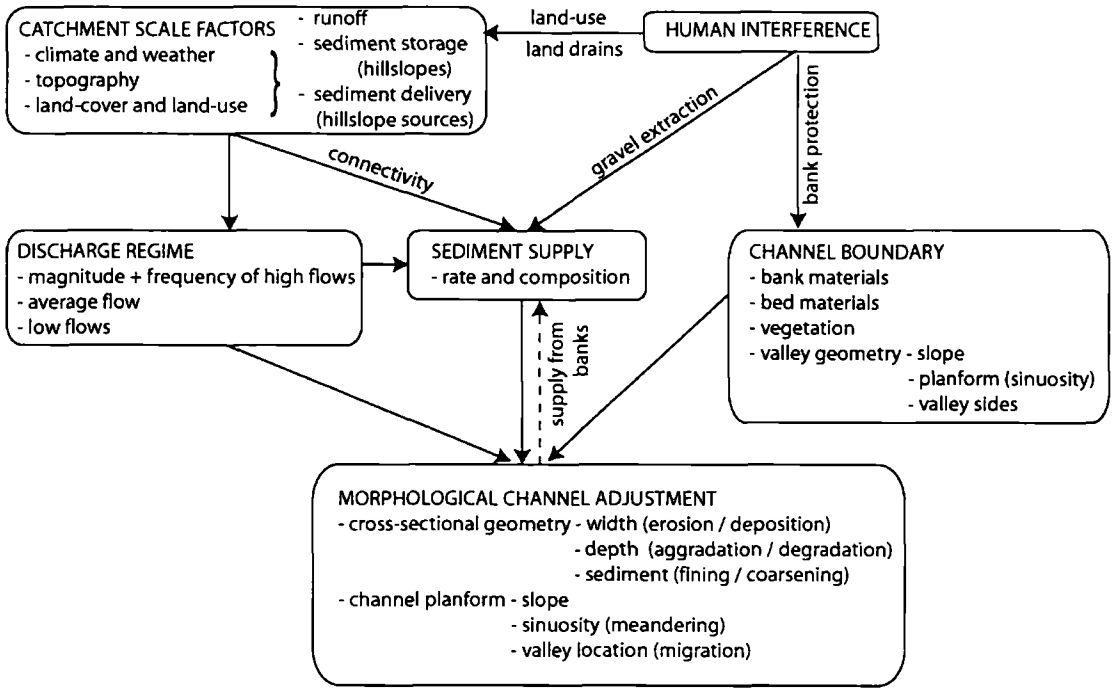

Changes in any of the variables shown in Figure 2.1 and Figure 2.2 can trigger instabilities within the channel leading to channel change. The relative importance of each of these factors varies between catchments and channels. Yet it is widely agreed that the channel's discharge (e.g. Harvey, 1969; Knighton, 1987), sediment supply (e.g. Harvey, 1991; Kondolf *et al.*, 2002; Rinaldi, 2003) and the nature of the channel boundary (Thorne, 1981, 1982; Ikeda *et al.*, 1988; Beschta, 1998) are the most important controls (e.g. Wolman, 1959; Knighton, 1998; Pickup, 1976; Hey and Thorne, 1986; Beschta, 1988; Werritty, 1997). As shown in Figure 2.2, these are ultimately driven by catchment scale factors and human disturbances. Whilst controls such as climate (e.g. Arnell and Reynard, 1996) and land-use (e.g. Kondolf *et al.*, 2002) can significantly alter the discharge and sediment regime of a river, additional concerns arise from the impacts of river engineering and management schemes on the channel (e.g. Brookes, 1997; Gilvear, 1999). These schemes can directly alter the channel boundary; for example bed lowering from gravel extraction or by preventing bank erosion through bank protection. Furthermore, they often feedback to

trigger morphological adjustments upstream, downstream and within the engineered or managed reach.

Any triggered instability in the channel can lead to the channel adjusting in a variety of ways to accommodate the new conditions (Hey, 1997). The effect of an instability on channel morphology is a reflection of the balance between the magnitude of the perturbation and the ability of the channel to resist or to accommodate the impact of the disturbance (Werritty, 1997). Therefore, some changes in the controlling variables will trigger large channel changes whilst others may be resisted. Werritty and Leys (2001) explain that landscapes respond to changes in two ways. First, *robust* changes are absorbed by the landscape with only modest adjustments occurring. These include meandering channels which steadily migrate. Second, *responsive* adjustments involve the channel undergoing a fundamental or persistent change in their morphology. For example, a catastrophic flood which changes the meandering planform to braided. Changes are accommodated through the complex and interlinked processes of erosion (both bed and bank) and deposition through which the channel adjusts in a variety of ways. These adjustments can then feedback promoting further adjustments. For example, bar deposition may result in bank erosion as the flow is shifted to the outer bank. Conversely, bank erosion may result in bar deposition as the bank erosion shifts the flow further from the inner bank. This continual adjustment challenges the traditional idea that a channel adjusts to reach equilibrium (e.g. Pickup, 1976; Lane, 1995; Millar, 2005). This equilibrium geometry is thought to be the optimum for the transport of bedload which varies with discharge (Pickup, 1976). It is perhaps more appropriate to consider an upland river system as one which is constantly evolving and adjusting to the prevailing flow and sediment conditions. The discussion that follows initially examines the three main controls on channel morphology: discharge, sediment supply and the channel boundary (Section 2.3), and summarises the catchment controls that are ultimately responsible for them (Section 2.4). It then explores the mechanisms by which the channel can adjust to accommodate these changes (Section 2.5) and the impacts of such changes specifically on flood risk and habitats (Section 2.6).

2.3 INTERNAL CONTROLS ON CHANNEL MORPHOLOGY

As identified, the three main controls on channel morphology are the driving forces of discharge and sediment supply and the resisting forces of the channel boundary. The first of these is the channel discharge, or the flow regime. A statistical relationship between flow and the channel geometry has long been acknowledged and is supported by numerous studies (e.g. Harvey, 1991; Pizzuto, 1994; Allred and Schmidt, 1999). This relationship formed the basis of Leopold and Maddock's (1953) "hydraulic geometry theory" which was used to determine the channel-forming or dominant discharge (i.e. the flow that created the average channel geometry). There is a large body of evidence from flume and field data to suggest that this dominant discharge is the bank full flow (Ackers and Charlton, 1970). For example, Harvey (1991) found a clear correlation between channel width and discharge in the Howgill Fells, Cumbria; Sloan *et al.* (2001) found an 80% increase in channel width following a large flood on the Eel River, California; and Allred and Schmidt (1999) attributed narrowing on the Green River, Utah, to a reduction in discharge from an upstream dam. Nevertheless, whilst a channel-forming discharge is empirically evident, many argue that the magnitude and frequency of flows also need considering: an idea first proposed by Wolman and Miller (1960). Their concept suggests that frequent low-magnitude events can be as effective at shaping channel geometry as infrequent high-magnitude events. Pickup and Warner (1976) support this and conclude that the most effective discharge was more frequent than bank full, occurring 3-5 times a year. Furthermore, some have found that the importance of the flow regime can also depend on other channel factors. Both Baker (1977) and Wolman and Gerson (1978) argue that rare high magnitude flows are the most effective channel forming discharges in arid environments, Pickup and Reiger (1979) proposed that channel form is a result of antecedent conditions whilst Osterkamp (1980) suggest that a river with a flashier regime and relatively high peak flows tends to develop wider channels. This explains why arid systems tend to increase their widths at a faster rate than channels in humid climates.

The second key control on channel morphology is coarse sediment supply. Some argue that changes in sediment supply are the most probable cause of channel planform change in upland rivers (e.g. Carson, 1984; Harvey, 1987; Martin and Church, 1995; Warburton *et*

al., 2002). It is important to understand the main sources of sediment in a channel. In upland river systems, coarse sediment originates from the hillslopes and from within the channel itself as it reworks the bed and bank material. In upland areas in temperate regions, the hillslope sources of coarse sediment are predominantly activated by rainfall-triggered shallow translational landslides (e.g. Dietrich *et al.*, 1995; Montgomery and Dietrich, 1995; Dhakal and Sidle, 2004). These slides typically occur following periods of wet antecedent conditions, typically after periods of prolonged rainfall. This reduces soil moisture deficits (Page *et al.*, 1994), pore water pressure increase and reduce the shear strength of the soil. At the same time, the downslope weight of soil mass increases. Once the downslope forces exceed the slope's critical threshold (often termed the factor of safety), a landslip will initiate. In addition, some landslides can be triggered by a short period of higher intensity rainfall (such as storm events and summer thunderstorms) which result in a rapid rise in downslope pressure as the soil rapidly saturates (Montgomery *et al.*, 1997; 2002). Within channel sources of sediment have also been found to be important and can contribute greater than 50% of the total sediment output from a channel (e.g. Grimshaw and Lewin, 1980; Church and Slaymaker, 1989; Johnson and Warburton, 2002). The supply of sediment from the channel comes from sediment transport of the bed material and from bank erosion. Therefore, the supply of sediment within the channel is explicitly linked to channel discharge. For example Gintz *et al.* (1996) report longer sediment transport times under higher magnitude floods whilst Hassan *et al.* (1992) and Haschenburger and Church (1998) report greater sediment transport associated with longer event durations. The mechanisms responsible for sediment transport and bank erosion are discussed more fully in Section 2.5.

Several studies have explored the relative contribution of sediment supply from the hillslopes and from the channel itself. Keinholz *et al.* (1991) estimated that 17% of bedload sediment was sourced from the hillslopes and 83% from the channel bed and banks in a study of 21 Swiss catchments. Schmidt (1994) recorded values of 24% from the hills and 76% from the channel in Bavaria, whilst Johnson and Warburton (2002) recorded similar values of 25% and 75% respectively from the Lake District. These findings all outline the significance of channel re-working in the availability of sediment in channels. Hillslope

sources do however remain important as the in-channel re-working of the sediment is finite and sediment must continue to be supplied to the channel. This raises the role played by sediment connectivity to explain how sources of sediment, both hillslope and within channel are linked or connected together (Hooke, 2003). Understanding the connectivity of coarse sediment transfer is important to determine the level of coupling between the hillslope and the channel network (Brunsden and Thornes, 1979). This coupling involves the transfer of sediment between the source areas, the hillslopes, and the channel (e.g. Harvey, 2001). Transfer is dependent on the proximity of a source to the network and the fluvial power available to transfer the sediment. For example if a landslide runs out into a river channel, coupling is high and the source is well connected to the fluvial system. On the other hand, a landslide may be isolated on a hillslope; thus connectivity is low. In upland systems, where the channel sides are steep, coupling tends to be high with sediment readily supplied to steep, often bedrock, channels (Stelczer, 1981). In lowland systems, where the valley is wide, the coupling between hillslopes and the channel can be some distance and the system is often deemed partially or completely unconnected (Hooke, 2003).

Second, the connectivity of sediment within a channel is important for: (1) the interaction between different reaches of the channel; (2) the influence of sediment sources and transfer upon channel morphology and landscape evolution (e.g. Leopold, 1992; Friend, 1993); and (3) the potential for a specific particle to move through the system. Early work by Schumm (1977) demonstrates the relationship between channel geometry, stability and sediment supply. Figure 2.3 shows this classic study and suggests that as sediment supply increases, the channel becomes more unstable, wider and shallower until it becomes anastomosing and then fully braided. Following on from Schumm (1977) numerous studies have demonstrated the impact that the quantity of sediment supplied to a channel has on its geometry. Kondolf *et al.* (2002) concluded that changes in bedload yield (due to land-use change) in rivers in France and Idaho resulted in significant channel changes, Parker (1979) suggested that for a given discharge, a 30% increase in gravel load would require a 40% increase in channel width, and Beschta (1998) attributed channel widening in the Kowai River in New Zealand to an increased sediment supply from storm triggered landslides.

Conversely, Rinaldi (2003) documented various alluvial adjustments on several Tuscan Rivers (Italy) and attributed them to reductions in sediment supply due to the cessation of mining, and Liebault and Piegay (2001) report degradation and channel narrowing in response to a decrease in bedload supply, linked to an increase in forest cover on the Upper-Roubion River, France. They also report a decrease in peak flow due to the increase in forest cover.

In addition, the coupling that exists between different elements of the river system is important. This includes the movement of sediment from sedimentation zones, particularly from one gravel bar to the next and the influence of tributary inputs on mainstream sediment dynamics. Much work has explored the interaction between tributary and mainstream sediment connectivity (e.g. Rice, 1998; Ferguson *et al.*, 2006; Rice *et al.*, 2008). The latter two studies suggest that the ratio of flow and sediment influx is largely attributable to channel response both in terms of downstream fining and levels of aggradation. These interactions are particularly important in river systems where tributaries are considered important.

Figure 2.3: Channel type based on sediment load and system stability. Schumm (1977): initially adapted by Thorne (1997).

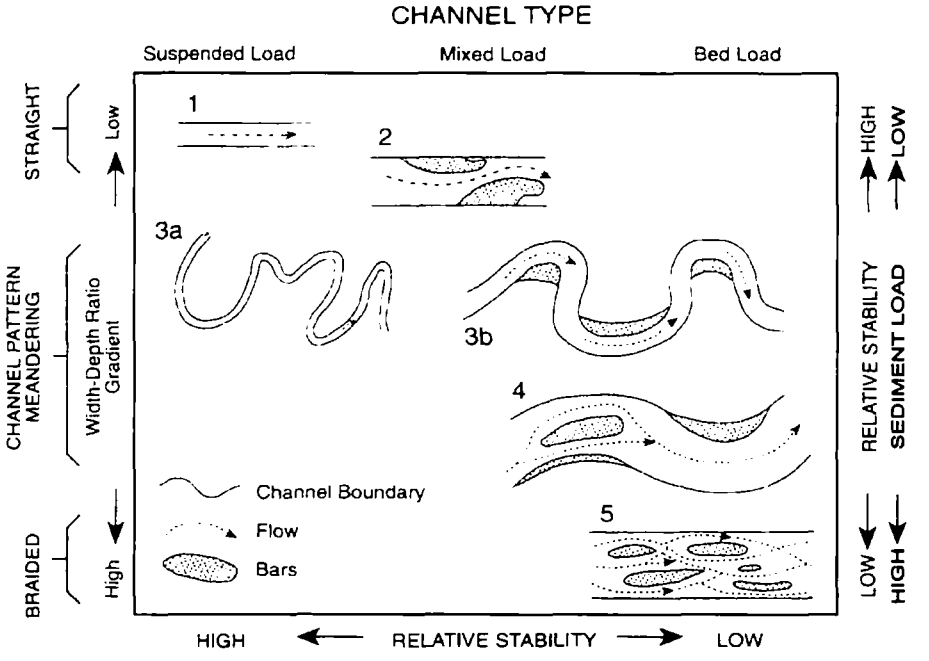

The third main factor influencing the nature and amount of channel change is the channel boundary. Whilst discharge and sediment supply are the variables driving the changes, the stability of the bed and bank determine the channel's ability to adjust (Thorne, 1981; Andrews, 1982). Consequently there is a link between channel geometry (particularly channel width) and bank strength (Dury, 1984; Abernethy and Rutherfurd, 1998). Bank stability is determined by several factors including the climate which controls weathering processes (Thorne, 1982), vegetation (Thorne, 1990), bank height, slope angle and sediment composition (Osterkamp and Hedmand, 1982; Ikeda *et al.*, 1988) and human and animal disturbance (Madje *et al.*, 1994). Vegetation is particularly important since root systems enhance cohesion (Beschta, 1998; Abernethy and Rutherfurd, 2000) by adding tensile strength. This concept is supported by Hey and Thorne (1986) who suggested that grass lined channels can be up to 1.8 times wider than tree-lined channels. Heritage and Newson (1998) also report that bank stability is enhanced by good tree cover. This resulted in an irregular bank profile in tree lined sections of the River Wharfe with erosion occurring between trees. On the other hand, vegetation may also have a negative effect on bank stability. Osman and Thorne (1988) argue that the increased loading effect of greater biomass, the effect of wind throw from trees on the bank and the development of lines of weakness from dead roots can all reduce bank stability leading to erosion and wider channels.

2.4 DRIVERS OF CHANNEL CHANGE: NATURAL AND HUMAN

These three internal controls are all ultimately responsible for driving channel changes, but are themselves products of the drivers shown in Figure 2.2. The dominant catchment controls are those which can significantly alter the discharge, the sediment supply and / or the channel boundary. They can be split into natural catchment controls and human disturbances.

Natural controls typically operate over longer timescales (e.g. Macklin *et al.*, 1998; Coulthard and Macklin, 2001) than human disturbances. Climate is the predominant control in upland UK rivers systems as it directly determines flow regime and indirectly controls

glaciations, vegetation land cover and human land use. Several studies have demonstrated the impact that changes in climate and land cover over the Holocene period (since around 10,000 years ago) have had on river systems (e.g. Knox, 2000; Coulthard *et al.,* 2000; Macklin and Lewin, 2003). Studies have explored the links between rainfall (including the effect of climate change) and coarse sediment delivery and the effects of this link on geomorphology (e.g. Dunne, 1991; Rumsby and Macklin, 1994), coarse sediment yields (Coulthard, 1999; Coulthard *et al.,* 2000; Coulthard and Macklin, 2001) and on shallow landsliding (Buma and Dehn, 1998; Brooks *et al.,* 2004; Dhakal and Sidle, 2004). For example Coulthard *et al.* (1998, 2000) used cellular modelling approaches to explore the effects of different climate scenarios on sediment discharges in upland river systems. They note that over a 100 year simulation, a 33% increase in the magnitude of rainfall events increased sediment supply by 100%. Coulthard and Macklin (2001) perform similar model runs over much longer timescales of 9000 years. Results emphasise that Holocene river evolution in temperate catchments is driven primarily by climate change but is also influenced by land cover and sediment storage. In addition, numerous studies have addressed concerns over the future effect of climate change associated with global warming, on the hydraulic regime and on flooding (e.g. Jones and Bradley, 1992; Arnell and Reynard, 1996; Werritty and Foster, 1998; Knox, 1999; Booij, 2005; Cameron, 2006; Fowler and Kilsby, 2007). Arnell and Reynard (1996) showed that under most climate change scenarios, the range of flows in UK rivers would increase with higher winter flows and lower summer flows. But the reduction in snowfall in the UK due to higher temps is likely to reduce the magnitude of the snowmelt flood event. Cameron (2006) demonstrated that under all UKCIP02 climate change scenarios derived from the HadCm3 GCM, flood magnitudes will increase. Fowler and Kilsby (2007) predict significant changes in monthly flow distributions with 40-80% reductions in summer flows and up to 20% increases in winter flows. The highest magnitude flows are projected to increase in magnitude by up to 25% with these effects felt greatest in high elevation catchments. Whilst all these findings are similar, Cameron (2006) highlights the complexities associated with modelling the impact of climate change on flood frequency and magnitude which result in large uncertainties in predictions. Meanwhile, Macklin and Lewin (2003) stress that climate

change impacts on flooding may be enhanced dramatically by the combined influence of land use change such as deforestation.

As such, the effects of human disturbances are generally considered to be greater than those from natural forcings. This was illustrated by Surian and Rinaldi (2003) who suggested that in Italy most rivers have experienced significant channel adjustments due to human disturbances. Land use change (e.g. Kondolf *et al.*, 2002; Sullivan *et al.*, 2004) has been identified as a particularly important driver of channel changes across the world (Surian and Rinaldi, 2003). Deforestation (e.g. Leeks, 1992; Gustard and Wesselink, 1993; Whitehead and Calder, 1993; Johnson and Thompson, 2002; Stott and Mount, 2004), mining (Lewin and Macklin, 1987; Rinaldi, 2003) and urbanisation are particularly problematic (Wolman and Schick, 1967). Urbanisation is thought to increase peak flows by a factor of two or more (Robinson, 1980) and significantly reduce sediment supply. Deforestation alters both the discharge and sediment regime. In Leek's (1992) study of deforestation in the UK, suspended and bedload transport were found to increase during deforestation but the impact of such changes were highly dependent on the connectivity of the sediment to the fluvial system; in this case to drainage ditches. Furthermore, the impact of the forestry process is strongly dependent on the forestry phase. During the ground preparation and planting phase, ditches are dug and sediment supply is often high. As the forest becomes more established, runoff and sediment yields reduce (Gustard and Wesselink, 1993; Whitehead and Calder, 1993; Johnson and Thompson, 2002). Human disturbances within the channel are also important. These include dam construction (e.g. Gregory and Park, 1974; Allred and Schmidt, 1999; Batalla *et al.*, 2004;), gravel mining (e.g. Knighton, 1989; Kondolf, 1994; Surian, 1999; Gob *et al.*, 2005; Sear and Archer, 1998; Wishart *et al.*, 2008) and channel engineering (e.g. Gilvear and Bradley, 1997), all of which exhibit strong controls on river dynamics as they alter the discharge or the sediment regime and in many cases both. Gravel extraction in the UK was widespread during the 1930s and the 1960s for commercial purposes. Only a few gravel extraction operations function today to reduce flood risk and for navigation. Wishart *et al.* (2008) note that a common morphological response to gravel extraction is the upstream progression of incision.

River engineering schemes, which directly alter the channel boundary, arguably have the greatest impact on the channel. River engineering is traditionally used to reduce flood risk and to prevent unwanted bank erosion. Typical channel management options that directly alter the channel's morphology and boundary include: (1) straightening a channel to increase the channel slope, reduce energy loss through meanders and enhance sediment throughput (Brookes, 1988; 1997); (2) widening a channel to increase its capacity to hold flow; (3) constructing bank protection to prevent problematic bank erosion. This is typically carried out when property and infrastructure are through to be at risk from bank erosion; and (4) channelisation through the construction of embankments which often consist of narrowing the channel and making the channel concrete. The aim here is to reduce flow resistance thereby increasing transport capacity. These schemes were traditionally undertaken with little consideration for the sediment transfer process or the fluvial geomorphology. James (1999) suggests that the traditional differences between river engineering fields and fluvial geomorphology reveal that both are valuable disciplines that have much to learn from each other. Thus, progress has been made in bringing the two disciplines together in river management operations (Thorne and Osman, 1988; Hey, 1990; Thorne *et al.,* 1997b). This is reflected in the scientific literature by numerous studies that have explored the morphological impacts that engineering has on the river system.

Numerous studies have explored the impacts of river management on the Rivers Tay and Tummel in Perthshire, Scotland (e.g. Gilvear *et al.,* 1994; Winterbottom, 1992; Gilvear and Winterbottom, 1992, 1998; Bryant and Gilvear, 1999; Winterbottom and Gilvear, 2000; Winterbottom, 2000; Parsons and Gilvear, 2002). The natural planform of the channel was documented to be gravel-bed and wandering with channel migration and avulsions (where the channel reverts back to a previously abandoned channel) being characteristic (e.g. Gilvear and Winterbottom, 1992, 1998; Bryant and Gilvear, 1999; Winterbottom and Gilvear, 2000; Winterbottom, 2000). During the 18th and 19th centuries, flood embankments and bank protection resulted in the channel being constrained. It became around 50% narrower and switched from multi thread to single channel (Gilvear and Winterbottom, 1992). This management was predominantly for agricultural purposes. During the 19th century, large flood events breached the embankments (Gilvear *et al.*, 1994) and today the

river has returned to a more natural state (Parsons and Gilvear, 2002) with lateral channel instability dominant (Winterbottom, 1992).

The narrowing and incision noted on the Tay and Tummel, echoes findings from other Scottish rivers and also from across Europe following channel regulation. For example, narrowing after regulation was recorded on the River Dee (McEwen, 1989) and the River Spey. Werritty and Ferguson (1980) agree that the opposite, an increase in width and braiding, occurs when a river is unconfined by bank protection or flood embankments. In Europe, Wyzga (1993) recorded between 1.5 and 3 m of narrowing by direct regulation works in Polish rivers. 4.5 m of incision was attributed to channelisation on the Rhone between 1847 and 1952 (Petit *et al.*, 1996) and Marston *et al.* (1995) attributed channel entrenchment or incision on the Ain River, France, to channelisation, flow regulation and flood embankment construction. Surian (1999) and Surian and Rinaldi (2003) noted similar findings in Italian rivers. Surian (1999) found an abrupt reduction in channel width and braiding indices after flow regulation and embankment construction on the River Piave and Surian and Rinaldi (2003) compared 25 Italian rivers and recorded incision in the order of 3-4 m. In some cases this was more than 10 m and occurred alongside channel narrowing of the active channel, in some cases by up to 50%. These changes were largely attributed to river management interventions but were also from sediment extraction and changes in land use. Finally, degradation was attributed to constraining channel width through engineering in Western European Rivers (Habersack and Smart, 1999).

These findings demonstrate a range of responses to both natural and human induced channel change, many of which are problematic. This makes it difficult to predict the response of a given catchment to future changes in climate and land use and from river management schemes. To develop a better understanding of channel change, the mechanisms underlying change require consideration.

2.5 CHANNEL ADJUSTMENT MECHANISMS

Alluvial rivers possess numerous degrees of freedom in which they can adjust through the processes of erosion and deposition. Examples include: width, depth, velocity, sinuosity and grain size (Hey, 1997). As Hooke (1997) states, the nature of channel response depends on the inherent instability and the freedom of a particular channel reach to adjust (e.g. channels cannot widen if the banks are concrete). Furthermore, channel change is both spatially and temporally variable. The location of the adjustment can extend significantly upstream or downstream from where the perturbation occurred (Andrews, 1986) and the adjustment itself can lead to further changes. Furthermore, since both current and previous channel conditions can play a role in determining the nature of the change (Brewer and Lewin, 1998), similar changes in inputs can result in a variety of channel adjustments (Gaeuman *et al.*, 2005). Table 2.1 shows the potential response of an alluvial channel to changes in both discharge and sediment supply.

Table 2.1: Morphological responses to changes in discharge and sediment supply. Adapted from Werritty (1997) after Schumm (1997).

Change		Morphological response
Sediment discharge	**Water discharge**	
Increase	Stable	Aggradation, channel instability, wider and shallower channel
Decrease	Stable	Incision, channel instability, narrower and deeper channel
Stable	Increase	Incision, channel instability, wider and deeper channel
Stable	Decrease	Aggradation, channel instability, narrower and shallower channel
Increase	Decrease	Aggradation
Increase	Increase	Processes increase in intensity
Decrease	Decrease	Processes decrease in intensity
Decrease	Increase	Incision, channel instability, deeper, wider ? channel

Sediment transport underpins these adjustments. Upland environments are characterised by coarse sediment which is eroded from the hillslopes and then enters the fluvial network. Once in the channel, sediment will be entrained and transported when a condition is reached where the flow conditions (fluid forces of lift and drag) acting on a sediment grain exceed those that resist its motion (e.g. submerged weight). Thus, a wide range of factors

control the incipient motion of sediment. These include grain properties such as the composition and arrangement of the bed (e.g. Reid *et al.*, 1997), grain hiding and protrusion effects and the grain pivoting angle (Li and Komar, 1986). In addition, flow properties such as shear stress and turbulence are also important.

From the headwaters, the sediment gradually works its way through the system in a complex and dynamic way, typically decreasing in size towards the middle and lower reaches. This downstream fining occurs due to abrasion (the breaking down of particles through collision) and selective transport (where smaller particles travel further than larger particles). Previous research suggests that rates of abrasion are not comparable to rates of downstream fining and that fining is largely controlled by selective transport (e.g. Ferguson and Ashworth, 1991; Werritty, 1992; Hoey and Ferguson, 1994; Ferguson *et al.*, 1998; Hoey and Bluck, 1999). This leaves a fundamental question; where does the coarse sediment go? One hypothesis suggests that the sediment becomes incorporated into the floodplain through the processes of lateral bank erosion, bar deposition and channel migration (Pizzuto, 1994; Darby and Thorne, 1996; Knighton, 1998). This process releases fine sediment back into the river system whilst the coarse sediment moves into long-term storage. These three processes are examined in more detail as follows.

Bank erosion is a more complex process than bed erosion and operates over a range of spatial and temporal scales (Couper, 2004). It forms a central component of channel evolution and adjustment determining processes such as meander formation and lateral channel migration (Lawler *et al.*, 1997). Bank erosion processes and rates are an extensively researched area with authors such as Thorne (1982, 1998) providing excellent reviews of the governing processes and mechanisms. However, many uncertainties, such as "process dominance", remain (Lawler *et al.*, 1997; Lawler, 2005), providing plenty of opportunities for further research.

The main bank erosion processes and mechanisms are typically grouped for analysis and discussion (e.g. Hooke, 1995) into: (1) bank weakening and weathering; (2) fluvial erosion / entrainment; and (3) mass failure. Several studies have also identified other bank erosion

mechanisms. For example, Hooke (1995) mentions the power of waves (Nanson *et al.*, 1994; Dorava, 2001) and bank trampling by either cattle or people (e.g. Trimble, 1994; Madje *et al.*, 1994). These different processes typically operate together (e.g. Hooke, 1979) but at different levels of magnitude and frequency (Couper and Maddock, 2001) and over varying seasonal and sub-seasonal timescales. Hence, establishing the dominant mechanism acting on a particular bank at a particular time can be very difficult.

The first group of processes are often underestimated and viewed as preparatory processes. However Couper and Maddock (2001) found that *weakening and weathering processes*, are also important erosion processes. Thorne (1982) suggests that soil moisture conditions which are dependent on both climatic conditions and the bank's geotechnical properties (e.g. particle size, gradation, cohesion, stratification and strength due to vegetation) are the dominant controls on weakening and weathering processes. These processes can be split into those which reduce bank strength and those which loosen and detach particles and aggregates. In so doing they enhance the likelihood of mass failure and supply fine sediment to the bank face for removal by fluvial erosion.

The reduction in strength of the bank can result from: (1) a loss of matrix suction (e.g. Rinaldi and Casagli, 1999; Simon *et al.*, 2000) which is linked to pore-water pressure; the pressure of water filling the voids between solid particles (Casagli *et al.*, 1999); (2) saturation which reduces cohesion (Rinaldi and Casagli, 1999) and can increase soil bulk weight (Simon *et al.*, 2000); (3) cycles of wetting and drying which cause the bank to swell, shrink and desiccation cracks to form (Osman and Thorne, 1988); and (4) freeze-thaw cycles (Lawler, 1993a). The loosening and detachment of particles or aggregates occur through seepage and piping effects (Hagerty, 1991) where the movement of water within the banks entrains and removes the finer grains supplying them to the bank face for removal during the next high flow event (Thorne, 1998).

The processes of *fluvial erosion and entrainment* describe the direct removal of individual grains and aggregates from the bank. Hence the nature of the hydraulic regime and the geotechnical properties of the bank determine erosion capacity (Simon *et al.*, 2000), whilst

sediment availability on the bank face, determines fluvial erosion rates. This process is more common on non-cohesive banks (Thorne, 1982) since the existence of electrochemical bonds between particles in cohesive banks increases resistance to erosion (Simon and Collinson, 2001). Fluvial entrainment predominantly occurs on the rising limb of a flood with the removal of the loose sediment and the initiation of new sources of sediment.

Mass failures are typically associated with cohesive and composite banks (Hooke, 1995) with the nature of the failure again determined by bank properties and hydraulic forces (Thorne, 1982, 1998). Failures occur when the gravitational force acting on a bank exceeds the shear strength of the bank material. This can be initiated when either erosion of the bank toe by fluvial entrainment oversteepens the angle of the slope beyond a critical threshold (Simon *et al.*, 2000), when a weaker sediment layer underlying a stronger layer is selectively eroded or when the bank's shear strength is weakened. Figure 2.4 shows the four main bank failure mechanisms which include *planar failure* (Lohnes and Handy, 1968; Osman and Thorne, 1988), *rotational failure* which is typical of highly cohesive banks Thorne, 1982), *cantilever failure* which is characteristic of failures on composite banks (Thorne and Tovey, 1981) and *piping/sapping failure* (Hagerty, 1991). Unlike fluvial erosion, failures are more common on the falling limb of a flood due to the supporting influence high stage has on the bank. Once the flood recedes, the support is removed from a weakened bank and a collapse is more likely.

Figure 2.4: Bank failure mechanisms: (A) planar failure, (B) rotational failure, (C) cantilever failure and (D) piping/ sapping failure. Darby (1998b).

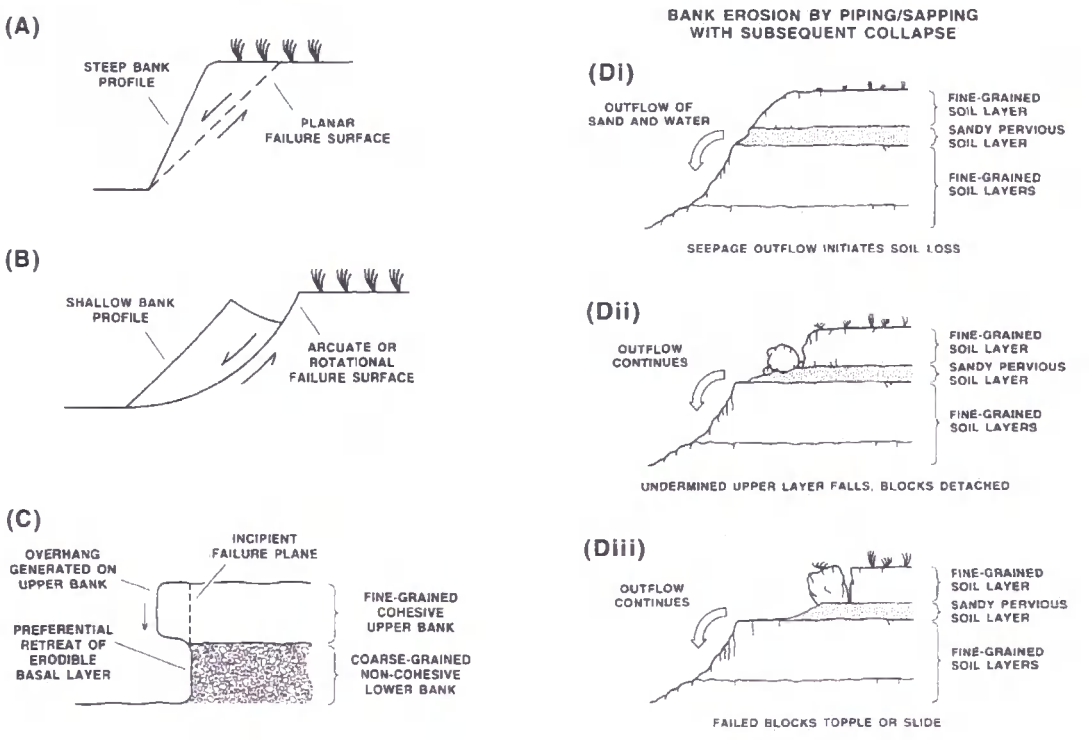

Despite being studied to a lesser extent than bank erosion, processes of deposition can be equally as diverse (Darby, 1998b). Following entrainment, the prevailing flow characteristics determine the transport fate of the particle in motion. When the flow or bed-level turbulence drops below the settling velocity of the particle, deposition will begin (Hooke, 1995). This deposition is selective with the coarsest grains being deposited before the finer grains. Hence sediment deposits are typically sorted vertically, laterally and longitudinally (e.g. Blom and Parker, 2004).

Sediment deposition occurs in several forms (e.g. Thorne, 1998) and where substantial, sedimentation zones develop (Xu, 1997). First, sediment can be deposited within the channel either directly onto the sloping banks, as alternate bars which are attached to the channel banks and typically found in straight channels (Hooke, 1995), or as point bars on the apex of meander bends which develop slowly through vertical accretion (e.g. Hooke,

1975; Dietrich and Smith, 1983). Lateral deposition can also occur directly from mass failures. These deposits are often termed berms or benches (Thorne, 1998). Secondly, deposition can occur within the centre of the channel as mid-channel, longitudinal or transverse bars. Church and Jones (1982) explain that these grow by the upstream accumulation of coarse sediments and the downstream accumulation of the finer material. Transverse bars are relatively uncommon except at channel confluences (Church and Jones, 1982). Thirdly, deposition can occur on the floodplain during overbank flows. These deposits are typically fine grains due to the lower transport capacity on the floodplain. Finally, deposition can occur as aggradation which is uniform deposition throughout a reach. Gaeuman *et al.* (2005) explains that aggradation typically occurs when the sediment supply increases or the discharge decreases for a sustained period of time.

As has been shown, both erosion and deposition are complex processes and can be initiated or enhanced following a disturbance in the variables previously discussed. Furthermore, these two processes are closely coupled together with the occurrence of one usually echoed by the onset of the other, which in turn determines spatial patterns of future erosion and deposition. This relationship can be described using the term "connectivity" (Hooke, 2003). For example, Gaeuman *et al.* (2005) concluded that aggradation in the gravel bed reaches of the lower Duchesne River in Colorado only occurred following local bank-erosion. M^{c}Donald *et al.* (2004) also explain that bar deposition causes flow divergence and the formation of a secondary circulation which subsequently alters the flow distribution enhancing bank erosion. This explains why point bars are found on the inside of meander bends whilst erosion occurs on the outside of the bed and why the deposition of a bar often results in channel widening through erosion. Similarly, the survival of a bench or berm following bank collapse, depends on ability of the channel to erode the deposited material (Thorne, 1982). This concept, which is termed basal end point control (Carson and Kirkby, 1972; Thorne, 1982; Darby and Thorne, 1992) shows how the deposit from a collapse can increase bank stability (as the slope angle is reduced) and reduce the likelihood of further bank collapse.

Channel migration occurs through the combined processes of deposition and erosion and typically occurs at meander bends. It may occur in straighter reaches if a secondary circulation develops. Deposition occurs on one side of the channel whilst the opposite site erodes. Secondary circulations form in the lateral, across channel direction and initiate from the effects of the channel geometry and planform on the flow. Concurrently, the circulation alters the channel morphology further enhancing the secondary circulation. In straight channels, secondary circulations are typically weak and may develop in the presence of lateral channel bars. This may indeed be the initial stages of meander development. Secondary circulation is more commonly considered at confluences (e.g. Bradbrook *et al.*, 1998; Lane *et al.*, 2000) and at bends (Dietrich and Smith, 1983; Ferguson *et al.*, 2003) where curvature is high. Curvature induces not only a secondary circulation but also large cross-sectional variations in the boundary shear stress and velocity fields (Dietrich, 1987). Around a bend there is a downstream increase in shear stress along the outside of the bank and a decrease along the inside bank (e.g. Hooke, 1975; Dietrich *et al.*, 1979; Nouh and Townsend, 1979; Bridge and Jarvis, 1982). Faster near-surface flow is forced to the outer bank because of centrifugal acceleration. These leads to super-elevation of flow by the bank face. A slower moving near-bed flow scours the bend leading to a deeper pool at the outer bank whilst a point bar develops through deposition near the inside (Hooke, 1975; Dietrich and Smith, 1983). Figure 2.5 shows this process. The lateral deviation of flow from the primary flow direction is exacerbated in coarse grained channels due to inertia effects. This means that the sediment transport direction responds more slowly to changes in primary flow direction, resulting in the typical channel geometry around a bend.

This channel geometry consists of three zones (Markham and Thorne, 1992): (1) the inner bank where shoaling over the point bar induces a net outward flow, forcing the core of maximum velocity more rapidly towards the outer bank. An increase in stage will reduce the shoaling effect and allow and inward component of near-bed flow over the bar top (Dietrich and Smith, 1983; Dietrich, 1987). (2) the mid-channel zone where the majority of flow passes and the classic helicoidal motion is well established; and (3) the outer region where a cell of opposite circulation develops and bank erosion prevails. The strength of the secondary circulation will be dependent on stage, the tightness of the bend and the

steepness of the outer bank. Thus the flow pattern that develops around a bend is spatially and temporally variable. In addition, at high discharges the secondary circulation can break down. The primary downstream currents dominate as flow follows a straighter path (Bathurst *et al.*, 1979).

With erosion occurring on the outside of a meander bend, the deposited bar on the inside of the bend becomes gradually wider as it follows the eroding bank in shifting laterally. Thus, as the bar grows, the far inner parts of the bar are subjected to less frequent inundation. Vegetation can now establish and gradually the inner part of the channel bar becomes incorporated into the floodplain as vegetation fully establishes. Thus the coarse sediment deposited on the bar becomes incorporated into the floodplain. Figure 2.5c shows this migration process. Meander migration involves several types of movement as noted by Hooke (1984) from a study of over 100 bends on the River Dane in Cheshire. *Translation* was the most common migration type accounting for 25% of bends. Translation describes a bend that shifts in position without changing its basic shape. This is typically movement in the downstream direction and is characteristic of low curvature bends. When curvature is higher, *extension* is more typical accounting for 15% of bends on the River Dane. When a bend migrates through extension it predominantly moves in the lateral direction. Other less common migration movements include *rotation* where a bend changes its orientation through its axis and *lobing and compound growth.* This later movement term describes bends which grow an additional lobe so that the curve has an additional "bumb". The rate of channel migration in unconfined channels is largely controlled by bend geometry and channel curvature (Hickin and Nanson, 1975; 1984).

Figure 2.5: Secondary circulation across a meander bend and channel migration. (A) is after Dietrich (1987).

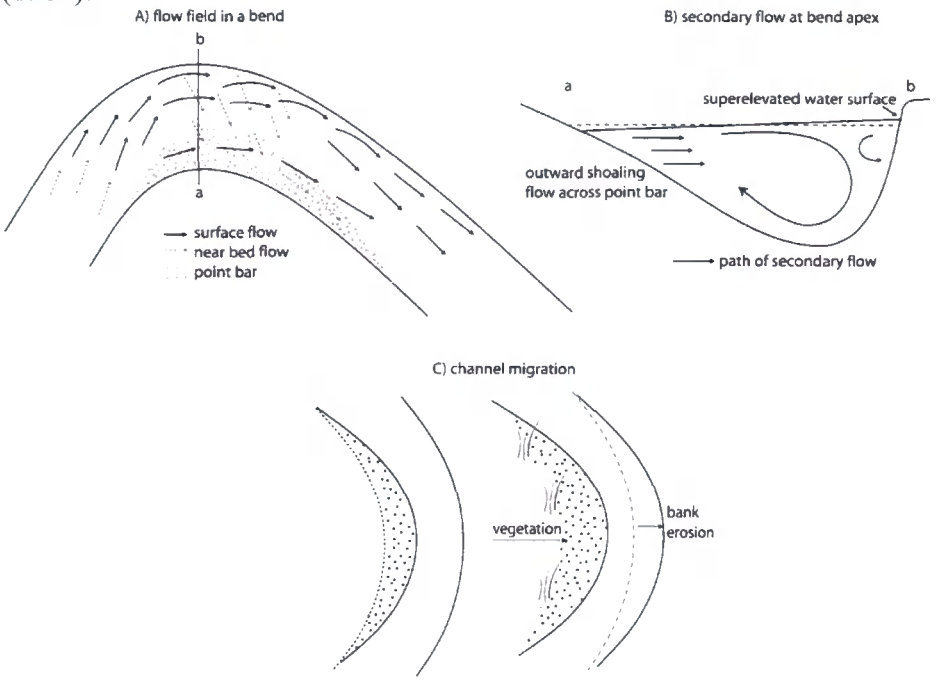

2.6 Implications of Adjustments

Natural or human induced channel adjustments can have implications for flood risk and for the availability of habitats. Furthermore they can feedback to create further adjustments which may be unwanted; particularly bank erosion. Much work thus far has concentrated on the impacts of increased flow from climate change on discharge and much less emphasis has been placed on the effects of river bed level changes upon flood risk, and their sensitivity to climate and land use changes impacts upon sediment delivery (Stover and Montgomery, 2001; Lane *et al.*, 2007). Flood risk will increase if the channel's ability to convey flow is reduced. This may occur through a decrease in channel capacity through a reduction in cross-sectional area, or a decrease in flow conveyance through an increase in bed roughness. The sediment regime is central to this with enhanced sediment delivery, which reduces channel capacity, associated with an increase in flood risk (e.g. James, 1999; Stover and Montgomery, 2001; Korup *et al.*, 2004; Pinter and Heine, 2005; Lane *et al.*, 2007). For example, increased flood risk in the River Wharfe was attributed to enhanced gravel accumulation (M^{c}Donald *et al.*, 2004), aggradation raised concerns of flood risk on the Pine Creek, Idhao such that a management plan now aims to reduce sedimentation

downstream (Kondolf *et al.*, 2002) and Stover and Montgomery (2001) report increases in flooding due to sedimentation in the Skokomish River, Washington.

When engineering is constructed without consideration of the sediment transport system, further problems arise. For example, engineering work on the River Tame in Birmingham resulted in further problems due to sedimentation. This river was artificially widened in an attempt to convey peak flood discharges within the banks. However, the widening reduced the sediment discharge capacity through reductions in stream power and velocity and this promoted aggradation in the channel. The flood capacity of the channel was reduced and the original flood problem returned. Other engineering works can enhance flood risk such as bank protection schemes. These prevent channel migration through lateral bank erosion but do not inhibit bar deposition. The result is that the bar increasingly grows reducing the channel capacity. Furthermore as Brookes (1988, 1997) explains, channel straightening reduces channel length which steepens the channel and increases the channel's velocity whilst also reducing energy loss in meanders. This increases flow conveyance and enhances sediment transport leading to scour. Scour increases the channel capacity. The combined effect is a reduction in flood risk for the engineered reach. However, the problem may simply be shifted upstream or downstream of the un-engineered reach. In the upstream reach, the elevated sediment capacity may be higher than the sediment supply leading to erosion and a destabilisation of the banks. In the downstream reach the reduction in channel gradient can cause sediment deposition reducing the channel capacity or leading to channel widening. Hence the flood risk may be enhanced in the downstream reach.

The impacts of channel adjustment on habitat availability and biodiversity are also of great concern. Natural channels are noted for their spatial heterogeneity and dramatic, rapid fluctuations in habitats (Power, 2001). Spatial and temporal variations in discharge, sediment supply and channel morphology can help to enhance the habitat diversity and thus increase species richness. For example, sustained bank erosion and lateral channel shift can maintain high biodiversity on floodplains and continually create new opportunities for pioneering species within the channel (Salo *et al.*, 1986). However, some channel adjustments, particularly those which upset the channel dynamics, can have negative effects on the channel ecosystem. In recent decades there has been an increasing interest in aquatic

and riparian habitats due to a generally perceived decline in biodiversity following morphological changes (Newbold *et al.*, 1983; Reiser, 1998; Newson and Newson, 2000) and human induced channel adjustments (Richards, 2001). Many studies have examined the link between sediment delivery and habitat availability (e.g. Kondolf and Wolman, 1993; Slaymaker, 2000; Pitlick and Wilcock, 2001) whilst others have concentrated on linking hydrology to ecology (e.g. Gurnell *et al.*, 2000; Bendix and Hupp, 2000). Thus, it is noted that channel changes that remove habitats and those which create inhospitable conditions can alter the diversity of the channel. This is particularly severe when adjustments are induced by human activities (Richards, 2001) such as flow regulation and channelisation (e.g. Bravard *et al.*, 1986; Large *et al.*, 1994). Examples include, removing fish spawning gravels through gravel extraction or channel incision, enhanced flow velocities in an engineered reach and enhanced sediment transport which severely alters life by crushing, burying and exporting organisms (Power, 2001). The impacts of channel adjustment can be important. As such, it is essential that the morphological adjustment process is more fully understood to protect habitats and to improve management of flood risk and bank erosion. Field-observations can provide valuable information on past changes. However they can only be used to suggest future impacts.

2.7 CHAPTER SUMMARY

Objective 1a, aimed to use literature review to develop an understanding of the channel change in upland catchments. Several key findings include: (1) channel change is a complex process with both natural and human catchment scale factors altering the three main driving and resisting forces in the channel; (2) these main factors were identified as the discharge, the sediment supply and the nature of the channel boundary. (3) With all three linked together (e.g. increased discharge increasing sediment delivery downstream) and a range of catchment scale factors acting simultaneously (e.g. climate and land-use change) the morphological response of a channel is difficult to predict; and (4) channel changes may have an adverse effect on flood risk, bank erosion and habitats. Thus it is essential that a combination of field-based monitoring and modelling are used to study upland channels to identify past and predict future channel change.

CHAPTER THREE:
INTRODUCTION TO THE STUDY SITE

3.1 INTRODUCTION

The second objective in this thesis was to select a suitable field site for monitoring and modelling. The Upper Wharfe catchment in the Yorkshire Dales was chosen as a study site for this research for three reasons. First, the catchment and channel are representative of temperate upland catchments with gravel-bed single thread channels. It is important that whilst the Upper Wharfe was used to develop, to test and to run the research model, the outcomes from this research are not intended to be merely a case study of the Wharfe system. The model is to be used to improve our understanding of upland river systems and their responses to changes in the variables controlling them. Additionally, it is hoped that in the future the model developed at the site can be transferred to rivers with similar characteristics and may be used for applied purposes to aid with management decision-making. It is therefore important that the study site is representative. Second, the Upper Wharfe catchment has fulfilled the role of a "study site" for a variety of fluvial and catchment based projects over the past two-decades. The product of these various projects and studies was that at the start of this project there was a wealth of knowledge about processes operating in the Upper Wharfe catchment and substantial supporting evidence from various data sources. As such, the Wharfe provides a valuable site for the research aims: to explore and model sediment transfer and channel change. At the same time the additional evidence gathered through data collection in this project allows some of the gaps in our knowledge of system processes to be addressed. Third, the channel has a history of enhanced coarse sediment delivery which has created a variety of problems in the past and has consequently resulted in several catchment and river management schemes; the success rate of which is mixed. As such, these case studies provide a valuable insight into the feedback between human intervention and channel response. These problems and associated management decisions are not uncommon in upland rivers in the UK (e.g. Stott

and Mount, 2004; Gilvear, 1999; Gilvear, 2004). Thus, findings from this work may echo similar issues found in comparable river systems.

This chapter provides a detailed introduction to the Upper Wharfe study site. It provides a comprehensive overview of the nature of the catchment and channel, underlining why the Wharfe provides an excellent study site for this research. This is achieved through objective 1c; to use literature review to provide knowledge about the chosen study site. Thus the chapter uses evidence from previous studies to provide a general catchment and channel description (Section 3.2), discuss the history of the catchment (Section 3.3) and to outline the river management strategies which have contributed to historical and contemporary channel changes (Section 3.4).

3.2 CATCHMENT AND CHANNEL DESCRIPTION

The Upper River Wharfe is located in Northern England in the Yorkshire Dales National Park (Figure 3.1). The catchment upstream of Starbotton has a drainage area of 72 km^2. The catchment elevation ranges from 701 m above Ordnance Datum (O.D.) on the catchment divide close to Buckden Pike to 211 m in the main channel at Starbotton. The catchment receives a high volume of rainfall; in the region of 1750 – 2000 mm a year, associated with prevailing westerly air streams. The catchment has a low annual evapo-transpiration rate (Heritage and Newson, 1997). Merrett and Macklin (1999) suggest that the region is particularly sensitive to localised convective summer thunderstorms and winter cyclones. These events tend to produce high-intensity, dark 'n' stormy, rainfall events.

The catchment geology is a combination of Carboniferous Age Great Scar Limestone, Yoredale Series and Millstone Grit (White, 2002). Like many of the valleys in the Yorkshire Dales, distinct horizontal terraces have formed on the steep valley sides through erosion and glacial processes. These terraces, alongside other features of the catchment discussed as follows, can be seen in the catchment photograph: Figure 3.2. This glacial activity has resulted in very thin soils which overlie the bedrock. This has led to ready sediment generation from the hillslopes. In the headwaters, the limestone is exposed in the

channel. Further evidence of the limestone can be found in the form of characteristic limestone pavements and sink holes on the hilltops. The land type and land-use in the catchment consists of shallow blanket peat on the hilltops, rough grass and moorland on the middle slopes and pasture land on the lower floodplain. These pastures are used for sheep and cattle grazing or managed as hay meadows. The tributary catchment of Greenfields is predominantly forested with commercial conifer woodland. Some small woodland areas can also be found in the lower parts of the valley particularly on the western slopes.

Figure 3.1: Location of the study catchment: The Upper Wharfe, Yorkshire Dales.

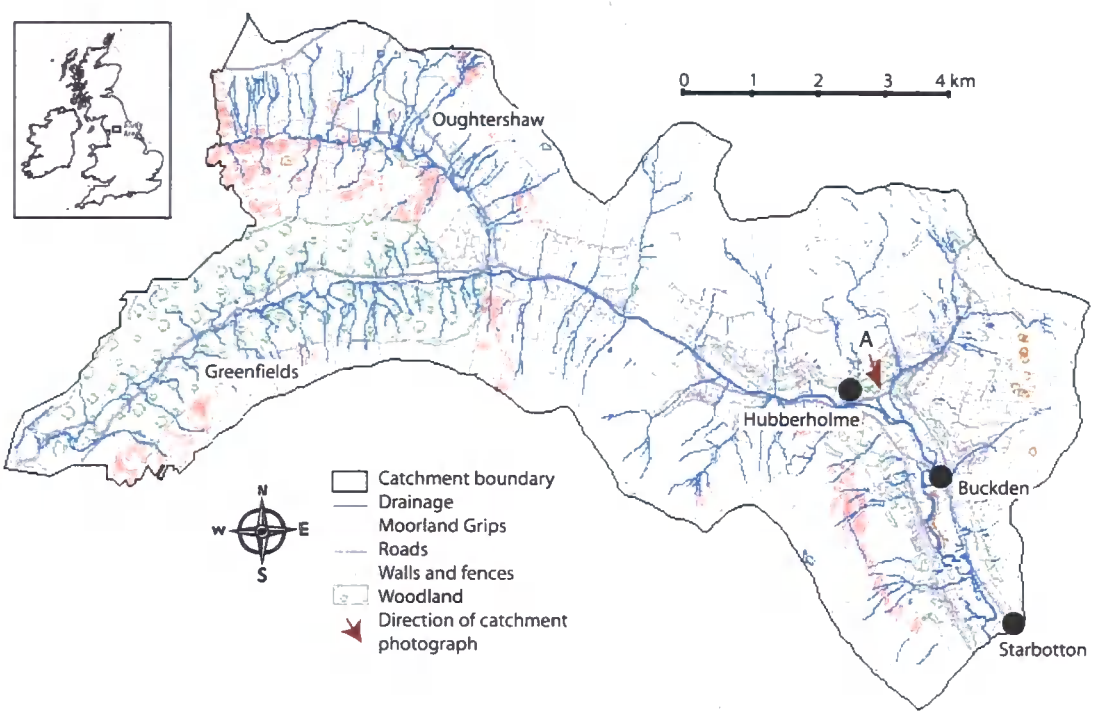

Figure 3.2: View of the Upper Wharfe valley, looking south from point A in Figure 3.1.

The study reach comprises a 5.6 km section of the main river extending from Hubberholme down to immediately upstream of the Cam Gill Beck confluence by Starbotton. Figure 3.3 shows the channel planform alongside the position of several notable locations. These include the 60 cross-sections, with cross-section numbers included for several of these. Full details of the cross-sections are given in Section 4.3 but these locations are referred to throughout so it is important to introduce them at this stage.

The headwaters of the Wharfe rise in two tributary catchments, Greenfields and Oughtershaw (Figure 3.1), which join a few kilometers upstream of Hubberholme. The channel in these uppermost reaches is relatively steep (c. 0.0120) and the valley is narrow and predominantly bedrock. From just upstream of Hubberholme the channel significantly reduces in gradient (c. 0.0040) as the river flows into a classic U-shaped valley with a wide floodplain, up to 500 m wide in places (Figure 3.2). Here the channel to hillslope coupling

is considered to be low. From Hubberhome, the channel becomes depositional with large gravel bars found all along the river, predominantly on the inside of meander bends (e.g. Figure 3.3 at the bend by the Gravel trap, the second Redmire bend, Heber bend and cross-section locations 420 and 510). These individual meanders are typically linked by relatively straight sections where a well defined pool-riffle system can be found. Some of the pool sections are particularly deep and flow is sluggish at low to moderate flows. Such reaches are predominantly found in the lower sections of the study reach. The upper part of the study reach, (upstream of cross-section 190) is lined with trees. Bank erosion is evident in the lower study reach where trees along the banks are sparse. The channel ranges in width from 12 m in the tree and wall lined reaches, to 34 m in sections were bank erosion is particularly severe, such as at Heber bend. The channel has an average maximum depth of 2 m. From Starbotton, the river flows predominantly south-easterly through Grassington and Ilkley before becoming an important tributary of the River Ouse which drains into the Humber Estuary.

Figure 3.3: Map of study reach

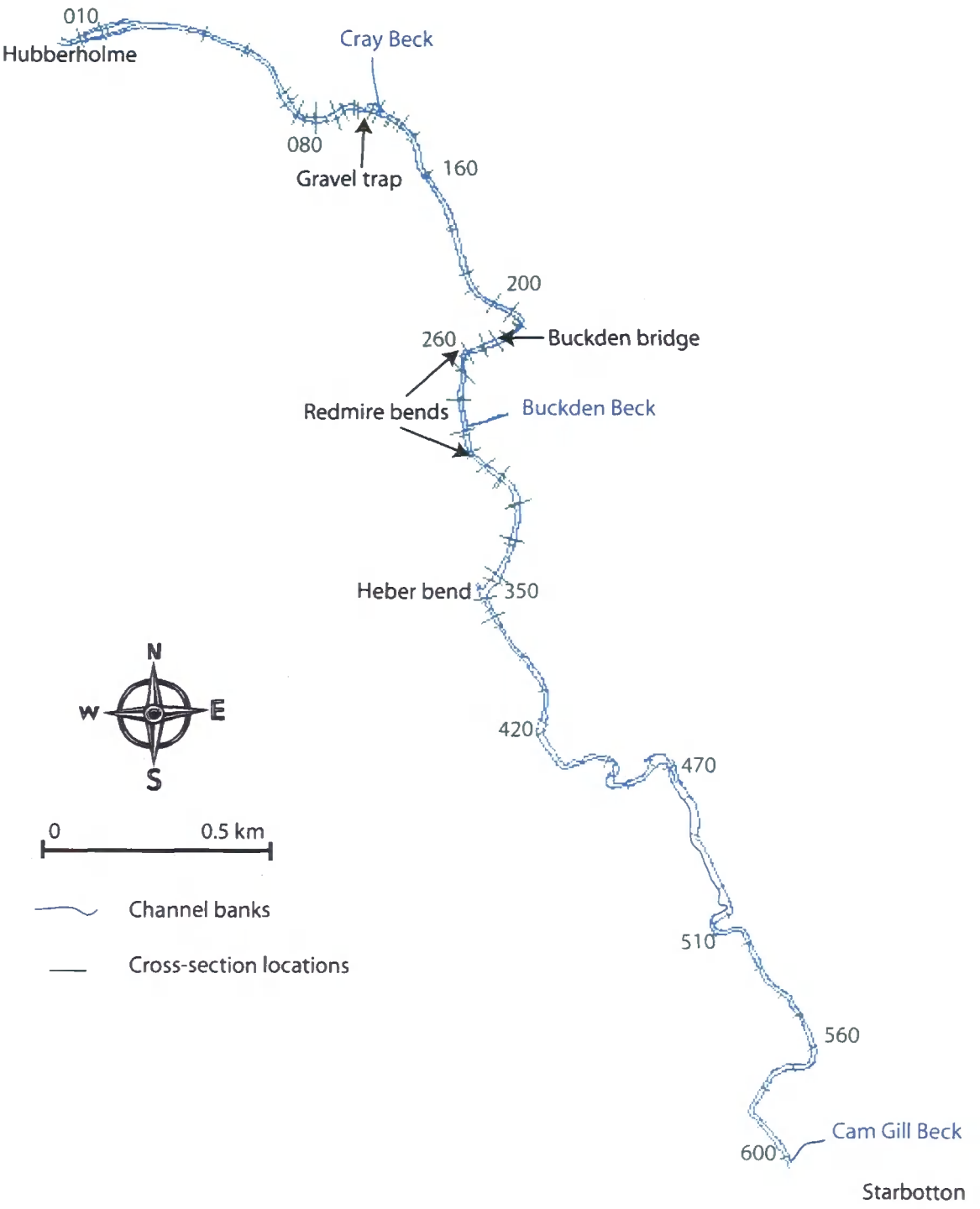

3.3 CATCHMENT HISTORY

Previous projects on the Upper Wharfe catchment, detailed in Table 3.1, provide much information about the history of the Upper Wharfe catchment and the nature of the channel. Some of these projects have used the river as an example of an upland gravel-bed river to explore specific research questions such as Powell and Ashworth's (1995) work looking at the spatial variability of bedload transport across the width of the channel. Others have used the Wharfe as an example of a British temperate upland catchment. This includes work by Coulthard *et al.* (1997, 1998, 2000) to investigate climate change effects on catchment processes using cellular modelling approaches. Much of the more recent work centered on the Wharfe catchment has the purpose of exploring management issues and options specific to the Wharfe but applicable to other similar catchments. One important project was the "Upper Wharfedale Best Practice Project" (UWBPP hereafter). This was a large partnership project between the Environment Agency, the National Trust and the Yorkshire Dales National Park Authority which began in 1997. The project used the Wharfe as an important pilot study site to explore many aspects of best practice for the sustainable management of the land and the water (Chalk, 1997; EA, 2000; Haycock, 2000; EA, 2001a, 2001b, 2001c). Part of this project was to address the river engineering which was implemented in the Wharfe in the 1980s with the aim to reduce bank erosion, to control sediment transfer and to alleviate flooding. Cross-sectional surveys of the bed morphology were commissioned for this work but no attempt was made to make the measurement of the channel morphology, and its change through time, an integral part of decisions regarding the management of the river. In 2001, new projects on the Wharfe catchment began to investigate coarse sediment delivery and sediment transfer (Reid, 2004; Reid *et al.*, 2007a; 2007b), the impact of this on flood inundation using modelling techniques (Tayefi, 2005; Tayefi *et al.*, 2007; Lane *et al.*, 2007), and approaches to catchment-scale coarse sediment management (Lane *et al.*, 2008). These projects were based on extensive field monitoring schemes with much of this data available for use in this project.

Table 3.1: Previous projects carried out on the Upper Wharfe.

Author	Year	Project
Yorkshire Water Authority	1983	Buckden scheme (report)
Stewart	1984	Land drainage proposals and impacts (report)
Hey and Winterbottom	1990	River engineering (journal article)
Powell	1992	Bedload transport processes (PhD)
Powell and Ashworth	1995	Bedload transport processes (journal article)
Heritage and Newson	1997	Geomorphological audit (report)
Chalk	1997	UWBPP (report)
Heritage and Newson	1998	Assessment of gravel trap (report)
RKL-Arup	1999	Assessment of unstable reaches for the UWBPP (report)
Hill and Hack	1999	River corridor survey report for the UWBPP (report)
Coulthard	1999	Catchment response to Holocene environmental change (PhD)
Lane	2000	Discussion of gravel bed transport for UWBPP (report)
Haycock	2000	Buckden gravel trap, management options (report)
Howard *et al.*	2000	Holocene river development and environmental change (journal article)
Environment Agency	2000 2001a,b,c	UWBPP (reports)
Coulthard and Macklin	2001 2003	Sensitivity of catchments to land and climate change, catchment modelling (journal articles)
McDonald *et al.*	2004	Upland river restoration (journal article)
Reid	2004	Coarse sediment delivery and transfer (PhD)
Tayefi	2005	Flood inundation modelling (PhD)
Reid *et al.*	2007a,b	Coarse sediment transfer and modelling (journal articles)
Lane *et al.*	2007	Interactions between sediment delivery and flood risk (journal article)
Tayefi *et al.*	2007	Flood inundation modelling – 1D and 2D approaches (journal article)
Lane *et al.*	2008	Coarse sediment delivery (journal article)

The catchment, including the upland hills, the valley sides and floor and the channel itself, have changed greatly over time. Determining how they have changed and what has driven these changes provides a greater understanding of processes operating today. In particular it is interesting to relate landscape changes to alterations in the flow and sediment regime of the river. Piecing together the changes and factors driving them is difficult with many of the findings based on sedimentary evidence and from modelling approaches. The following discussion outlines some of the main studies and findings that provide valuable information about historical catchment change in the Wharfe catchment.

Since the retreat of the Late Devensian ice sheets from the catchment, it was thought that early changes to the sediment regime of the catchment were caused by disturbances in land use predominantly through deforestation and early agricultural activity (Ballantyne, 1991). Indeed, Coulthard and Macklin (2003) suggest that tree clearance over the last 2000 years has led to significant rises in the sediment discharge from the hillslopes. However, Coulthard and Macklin (2003) used a modelling approach to suggest that peaks in high sediment discharge (10 – 100 years) correlate with wetter climates. This implies that the climate is one of the main drivers of catchment sediment yields over the long term. These changes in hydrology and sediment are thought to have affected the river channel in several ways. The floodplain upstream of Starbotton is thought to have risen by 1.5 m as a combination of geomorphic processes and glacial rebound (Howard *et al.*, 2000). This rise in floodplain land level led to both in-channel sedimentation (Howard *et al.*, 2000) and channel incision (Ballantyne, 1991). These channel changes were initially rapid and then slowed as temperatures reached modern day levels around 1920 (Jones and Bradley, 1992). In addition, channel migration and avulsion during this time was common, with documented evidence found in records of sedimentation for the valley (Howard *et al.*, 2000). Several palaeochannels are also visible in aerial photographs. In addition to these longer term processes, a sudden catastrophic flood event in Cam Gill Beck (which joins the Wharfe at Starbotton) occurred in 1686 (Coulthard *et al.*, 1998). This single event generated a decadal amount of sediment (Coulthard *et al.*, 1998) and formed the Starbotton alluvial fan which extends across the width of the valley. The river has cut into this deposit yet the fan is still visible today and it still acts as a local rise in base level. The channel's response to this was to aggrade upstream; something that continues at present.

In a study by Merrett and Macklin (1999), hydrological changes, specifically flood history, since 1600, have been documented from lichenometry and flood deposits. They show that from 1600 to 1750 the magnitude and competence of flood discharges was high. This coincides with the cool and wet climate during the Little Ice Age (Jones and Bradley, 1992). Despite relatively few flood events during this period, the coupling of sediment supply between the hillslopes and the channel during this period was thought to be high.

Following this, until 1800, the number and magnitude of flood events significantly increased with high levels of overland flow. However, despite good hillslope-channel coupling, sediment yields began to decline, possibly due to the sources becoming exhausted. Since then flood frequency and magnitude began to decline reflecting the stabilisation of atmospheric conditions. Sediment supply from the hillslopes decreased and coupling reduced. Incision added to the isolation of the channel from the hillslopes. The incision noted by Merrett and Macklin (1999) echos the incision noted in rivers across Europe (e.g. Petit *et al.*, 1996; Marston *et al.*, 1995; Surian and Rinaldi, 2003). Coupling between the main channel and the hillslopes is limited due to the wide valley floor but coupling remains high in many of the catchment tributaries.

More recently, changes in sediment discharge and flow are thought to have resulted from land-use changes including upland land drainage and afforestation (Longfield and Macklin, 1999). Many have documented that the Upper Wharfe has experienced large volumes of coarse sediment transport and generation (e.g. Hey and Winterbottom, 1990; Powell, 1992; NRA 1995b; Heritage and Newson, 1997, 1998; Coulthard, 1999; Haycock, 2000; Lane, 2000; Lane *et al.*, 2007; Reid *et al.*, 2007). Gripping is a process where shallow surface drains about 1 m wide and deep, hundreds of meters long, with a high density (30 m between each) are dug into blanket peat bogs to convert them into rough grass and heather moorland. Gripping occurred all over the Yorkshire Dales from the 1940s through to the 1960s, during which time 17 km^2 of the Upper Wharfe catchment were gripped (Figure 3.1). These drains had the effect of extending the drainage network and may result in steeper hydrographs, a decreased time to peak and shortened recession limbs for intermediate flows (Stewart and Lance, 1983; Robinson, 1985; 1990; EA, 2001b; Lane, 2001a). It has also been suggested that the grips also alter the sediment generation and transport from the hillslopes to the main channel (e.g. Hey and Winterbottom, 1990). Today, many of these grips are still evident on the hillslopes although most have been left to deteriorate. Others have been blocked including 42 km of grips in the Oughtershaw headwater catchment that was blocked using straw bales and peat blocks in 1999 and 2000 (EA, 2001b, 2001c).

During the 1960s there was a significant expansion of plantation forestry in the Greenfields tributary catchment (Hey and Winterbottom, 1990). This forest is now reaching maturity and it will be felled in the near future to prevent damage from wind. Like grips, forestry is believed to alter both the flow and the sediment regime. Mature forested catchments produce reduced water yields compared with unforested catchments (e.g. Gustard and Wesselink, 1993; Whitehead and Calder, 1993; Johnson and Thompson, 2002) whilst sediment output is also thought to be reduced. The latter concept is supported by findings made by Reid *et al.* (2007a) who compared the sediment outputs from the forested Greenfields tributary and the unforested Oughtershaw tributary. These catchments are similar in size, topography and rainfall. The forested catchment produced significantly less sediment than the unforested catchment. This work supports earlier findings by Stott (1997), Montgomery *et al.* (2000), Dhakal and Sidle (2003), Vanacker *et al.* (2003) and Stott and Mount (2004).

3.4 CHANNEL MANAGEMENT

In addition to these land use changes, recent changes to the channel have resulted from direct human interferences. Active channel management began as early as the 14th and 15th centuries, after the expansion of monasteries in the area (McDonald *et al.*, 2004). The banks of the Wharfe were walled with local material to reduce bank erosion, gravel was removed for building work and trees were managed. Much of this walling is still present (Figure 3.4a) and has undergone maintenance work due to its historical status. Further gravel removal by local landowners has been documented during the 19th and early 20th centuries to reduce the river aggradation and manage flood risk (McDonald *et al.*, 2004). In more recent decades, unregulated gravel removal from the channel by landowners is thought to have occurred. Such practices are likely to have removed volumes of coarse gravel from the channel and widely occurred across the UK. For example, a study on the River Fillan, Central Scotland, estimated that 1000 tonnes of gravel were removed from one section of the river by local farmers over a three year period, to provide the foundations for buildings and roads (Waterhouse, 2003). Under the Water Framework Directive, gravel extraction is now largely prevented due to the negative impacts it has on the removal of habitats for

spawning fish. Furthermore, the Wharfe is now classified as an SAC (Special Area of Conservation), an SSSI (Site of Special Scientific Interest) and part of the Yorkshire Dales National Park. Thus higher levels of permission are required for gravel extraction. Yet this process of gravel removal acted to manage the high levels of sediment delivered to upland channels like the Wharfe, preventing sediment accumulation in many places.

Between 1961 and 1981, high sediment delivery was reported to have caused a channel bed rise of between 0.43 m and 1.4 m (Stewart, 1984) and was blamed for the high flood frequency levels of between 20 and 40 times a year (Yorkshire Water Authority, 1983; Hey and Winterbottom, 1990). This is attributed to changes in climate and upland land use, specifically forestry practices and moorland gripping. These observations were used to inform the design and implementation of engineering works during the 1980s. Subsequent studies drew the link between high sediment delivery in the Wharfe and severe bank erosion (e.g. NRA, 1995a; Chalk, 1997; Hill and Hack, 1999; RKL Arup, 1999b) and an increased incidence of downstream flooding (e.g. Yorkshire Water Authority, 1983; Powell, 1992; NRA, 1995a; Chalk, 1997; RKL Arup 1999; EA, 2000; Haycock, 2000; Hey and Winterbottom, 1990; Lane *et al.*, 2002; McDonald *et al.*, 2002). These studies sought to evaluate the management decisions made in the 1980s, becoming progressively more critical with the benefit of hindsight. Indeed, recent work on the catchment, including this research project, question if the basis for management was correct in the first instance. 20 to 40 overbank flows is a very high number and data presented later in this thesis suggests that this should have only been a single figure number. Furthermore, the increase in flooding may be attributable to climate change alone since no quantitive evidence of increased sediment supply during the 1960s-1990s is presented by the studies. With local sediment somewhat easier to manage than the climate, the management strategies adopted may have in fact failed to address the true problem underlying the increase in flooding.

Several river engineering schemes were implemented on the Wharfe and aimed to reduce flood risk, to restore land drainage, to control sediment supply, to preserve key ecological elements and to reduce bank erosion between Hubberholme and Kettlewell (Hey and Winterbottom, 1990). Kettlewell is located 4 km downstream from Starbotton. Such

schemes included artificially increasing the channel capacity by constructing a series of levees, removing gravel shoals, installing a gravel trap and reinforcing eroding banks.

Levees were constructed along several sections of the channel between Hubberholme and Starbotton by 1989. These aimed to reduce flooding to once every 6 months from in excess of 20 times a year before the scheme (Yorkshire Water Authority, 1983; Hey and Winterbottom, 1990). The scheme initially worked well at reducing flood frequency but in recent decades field evidence and local opinions suggest the frequency of out-of-bank flows has increased once again. Furthermore, these schemes were designed to transport water and failed to consider the impact on sediment transfer (Raynov *et al.*, 1986; Brookes, 1987). Concerns have arisen suggesting that the flood alleviation scheme has led to further management problems such as enhanced bank erosion and reduced channel capacity. For example, at Heber bend, the river had retreated through bank erosion into the existing flood defence. This issue was resolved in 2001 with a £31,000 project to re-align the existing flood bank and set it further back from the river (EA, 2001c). The river is still eroding and slowly getting closer to the new flood bank.

The gravel trap was installed in 1989 and was designed to reduce the mean flow velocity to 0.6 m s^{-1} at bank full discharge. The trap had a capacity to hold about 3500 m^3 of sediment and the management plan suggested emptying the trap every 3 to 4 years (Hey and Winterbottom, 1990). However, the sediment transport rate of the channel was severely underestimated and the trap filled more rapidly than anticipated (NRA, 1995a; Heritage and Newson, 1998; RKL Arup, 1999; EA, 2001a; M^{c}Donald *et al.*, 2004). The high emptying costs made the trap economically unviable and the trap was only emptied once in 1989. It was then full for nearly 14 years; no longer providing a sediment sink and locally exacerbating erosion problems. The full trap resulted in the high velocity water being forced against the river flood banks and in several locations enhancing erosion of the banks and the newly constructed levees. The trap was finally removed in the summer of 2002 when a decision was taken to once more let the river distribute its sediment. Some of the channel banks protected by block work around this section were repaired and re-stabilised

(Figure 3.4b). Some of the blockwork was removed and used to re-align the Cray Beck confluence.

The Upper Wharfe has also been subjected to several hard engineering schemes to protect the banks from eroding. These can been seen in several locations including along the bend where the gravel trap used to be (Figure 3.4b), by Buckden Bridge and on the two bends immediately downstream of Buckden Bridge named the Redmire bends. The second Redmire bend is another example in the Wharfe system of an engineering scheme that has failed to resolve the issue it was designed for, and has required subsequent management. During the 1980s, work was undertaken to straighten the channel and improve land drainage. Blockstone revetments were used but some movement of the blocks at the toe of the banks reduced the bank's stability. In 2001, a £7000 scheme was implemented to improve the bank's robustness whilst achieving a soft bank top. This "softer" engineering technique used birch brash faggoting material to provide extra support whilst grass and other vegetation became established (Figure 3.4c). This technique was successful and the bank is currently robust. Evidence of other soft engineering approaches can be seen along the channel. Details and the success of these are reported in the EA's UWBPP information booklets (EA, 2001c). Sections of river have been fenced off to prevent trampling by livestock and small clusters of trees were planted along banks. These included 15 trees planted at Heber bend, trees planted alongside block work at Buckden bend and tree planting around the bend at 510. However, as shown in Figure 3.4d, these softer approaches often fail, with the trees roots unable to stabilise the bank before the erosion reaches them.

Figure 3.4: Examples of hard and sort engineering in the Wharfe: (a) Traditional dry stone walling; (b) blockstone bank at site of Buckden Gravel Trap; (c) birch brash faggotting on the 2nd Redmire bend; (d) failed "soft" approach to plant trees at cross-section 510.

3.5 CHAPTER SUMMARY

Previous findings from the Wharfe, demonstrate that the catchment and the channel have been evolving over time as a result of a wide range of processes at a range of spatial and temporal scales. These include, glacial processes, changes in land use and climate change and from direct human interference within the channel. The more recent work on the catchment has demonstrated that many of the river's problems including increased flood risk and bank erosion stem from enhanced sediment delivery; which is particularly severe in the Wharfe.

The failure of some of the management decisions made in the Wharfe (including the gravel trap and some bank protection), provide a clear example of the difficulties of developing sound river management policies in the absence of supporting evidence. These engineering works were not based upon a sampling system informed by temporal variability in sediment delivery and channel adjustment, and failed to consider the dynamics of the system. As such, the aggradation noted could reflect either an aggrading trend or short-term fluctuations, or a combination of both as a result of there being so few observations. Without knowing this, making the correct management decisions is difficult. Thus the implementation of a structured monitoring strategy in 2001 provides a valuable insight into the spatial and temporal nature of the sediment transfer system in the River Wharfe.

Objective 2 aimed to select an appropriate study site for this research. This chapter has demonstrated that the Upper Wharfe catchment is representative of other upland UK catchments. Alongside the wealth of knowledge and data available on the catchment from previous studies, it has ongoing issues linked to sediment transfer and flood risk. Thus it is highly suitable for application to this research.

CHAPTER FOUR: CHANNEL MORPHOLOGY

4.1 INTRODUCTION

As discussed in Section 1.3, field data are required for three reasons: (1) to achieve Objective 4; to analyse the sediment transfer and channel change process in the study reach; (2) to allow the reconstruction of a sediment budget for estimating bedload transport rates; and (3) to provide data to achieve Objective 5 and Objective 6; the development and application of a model for simulating channel change. Objective 3 aims to provide this data through the monitoring of channel change in the Wharfe study reach and the variables that are driving these changes. Thus, Objective 3 is achieved in this chapter (Chapter 4) and the following Chapter 5. Objective 1d, to use literature review to develop field-based methodologies, is also achieved in both chapters.

This chapter concentrates on monitoring the channel morphology. It uses field surveys to map out important channel features such as locations of sediment stores, bank erosion and bank protection (Section 4.2). The channel changes are monitored using repeat cross-sectional surveys to provide spatial and temporal information on in-channel sedimentation (Section 4.3) and a bank erosion study to monitor rates of lateral channel change (Section 4.4). Finally, the downstream channel curvature is recorded from digitised LiDAR images (Section 4.5) alongside data on flow paths around channel bends (Section 4.6). Results from the individual methods are provided alongside each of the methodologies. A more detailed analysis and discussion of these results, particularly when combined with other data, are provided in Chapter 6: the analysis and discussion of field data.

4.2 FIELD SURVEYS

Field surveys, including fluvial audits (Sear and Newson, 1993) and river corridor surveys, are valuable qualitative data sources that can provide an insight into processes operating and features present in a river system. Fluvial audits (sometimes termed geomorphological audits) are surveys which assess the sources, stores and transfer routes of sediment in a river channel. They were initially developed by Sear and Newson (1993) and have been widely used to evaluate and to monitor river systems. For example, a geomorphological audit was used to assess unstable reaches along the Upper Wharfe in a survey by Heritage and Newson (1997). River corridor surveys are often used to determine environmental and conservational concerns of river corridors. For example, they help identify areas where pollution and fly tipping are reducing the aesthetics or where sensitive habitats for nesting birds or spawning fish require protecting. Whilst field surveys are useful for conceptualising processes operating in river systems and for documenting important features, they remain subjective and qualitative and as such should not replace quantitative methods of measuring and monitoring, including many of the methods described later in this chapter.

Field surveys were conducted for the entire length of the study reach at the start of this project. They combined features of river corridor surveys and fluvial audits to record a wide range of information about the nature of the river channel, processes operating and locations of key features such as tight bends, large depositional zones and bank protection. The qualitative data from the surveys was used in the planning of field methodologies, to provide supporting evidence for many findings based on quantitative field data and was required in the modelling to include information on the locations of bank protection.

The field surveys provide an insight into the processes operating along the Upper Wharfe study reach. Figure 4.1 shows one page of the surveys demonstrating the type of information that was included. Appendix I contains the other 9 pages.

Figure 4.1: Page 3 of the study reach field surveys.

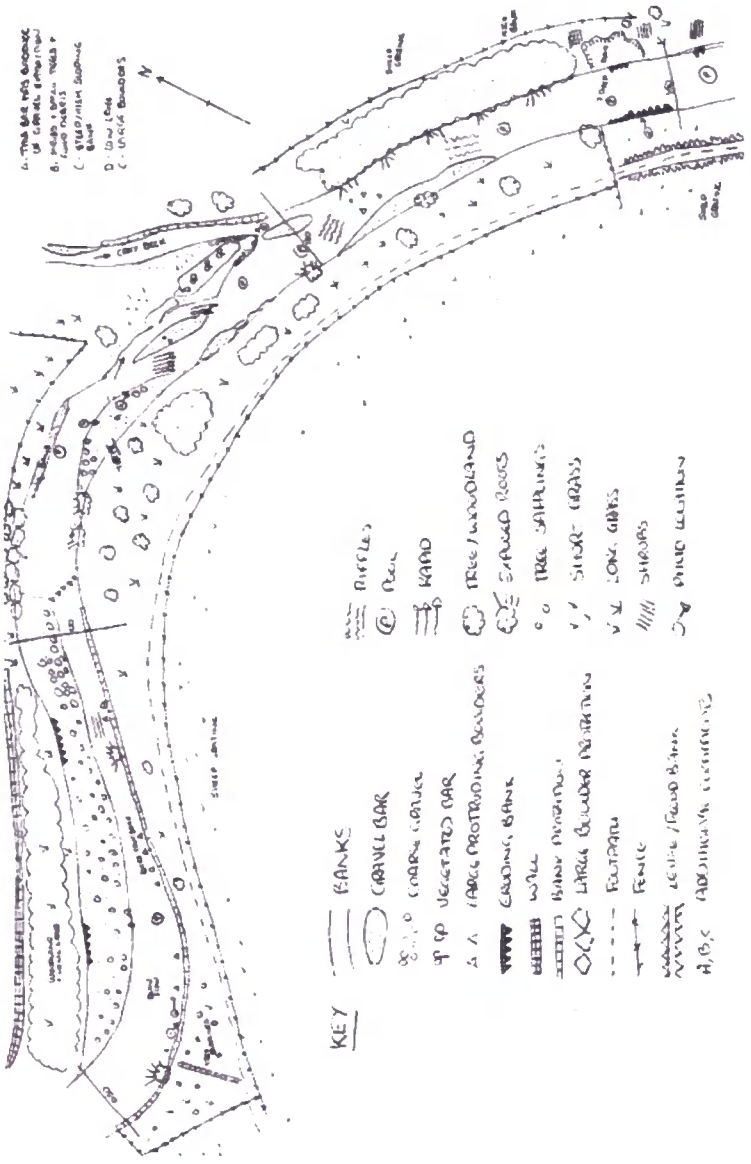

The description of the Wharfe provided in Section 3.2 is illustrated well within the surveys. In particular, the surveys locate the zones of coarse sediment storage along the river; most of which are found on meander bends. Inferences about the stability of these deposits can be made by noting the presence of vegetation. Most bars are free from vegetation suggesting sediment transfer readily occurs. Within some bar deposits, typically lateral bars, vegetation is present indicating that sediment transfer has not occurred for some time,

thereby allowing vegetation to establish. This is enhanced in the summer months when vegetation growth is faster. Clearly the densely vegetated bar by Hubberholme is a highly stable feature. At cross-section 420 (Survey page 7, photo 1, Appendix I) the outer bend bank erosion and presence of vegetation on the gravel on the far inside of the bend, demonstrate the mechanism by which the channel migrates and sediment becomes stored in the channel (Section 2.5). In addition, fining of the bed material with distance downstream is evident from the surveys with larger boulders noted at Hubberholme and finer gravel and patches of sand found in the downstream sections of the study reach. The pool-riffle pattern within the channel is clear in the surveys with deeper more sluggish reaches identified in the lower limits of the study reach. The surveys also reveal something about the occurrence of flooding in the valley. Recent wrack lines can often be found along the edges of the valley, at times around 500 m away from the river channel. Debris was also noted along fences, walls and in trees, in some locations up to a meter above the bank tops. This information can be used to obtain an estimate of the extent and depth of over bank flow events in the channel. Indeed, over the three year monitoring period, fresh wrack lines were commonly found, suggesting over bank flow is a common occurrence in the Upper Wharfe.

Whilst the surveys can allow inferences to be made about the transfer of sediment and the frequency of flood events, they are perhaps more valuable when examining the nature and extent of bank erosion in the channel. It was clear that bank erosion dominated the lower reaches of the study reach, particularly downstream of the Buckden Beck tributary. This may be due to the increase in sinuosity of the channel further downstream but could also be associated with a reduction in tree lined banks. Indeed no banks were found to be eroding when trees were present, echoing findings by Charlton *et al.* (1978), Andrews (1984), Hey and Thorne (1986), and by Heritage and Newson (1998) following their geomorphological audit along the same stretch of river in 1998. The latter study further suggests that the bank-top profile along tree-lined sections of the Wharfe is irregular with erosion occurring between individual trees. Evidence of this is shown in the surveys. Contrary to this idea that trees stabilise the banks, is the suggestion that the trees establish where no erosion occurs. When new trees are planted in an attempt to alleviate bank erosion (e.g. Figure 3.4d) their initial success is dependent on the rate of bank erosion. If bank erosion is slow enough, they

have time to establish and hence their roots can have the positive influence of stabilising the bank. If bank erosion is rapid, the trees fail to establish in the first instance.

The field surveys also highlighted the full extent of the bank erosion in the Wharfe. Bank erosion is found on both straight and meandering sections. It was estimated that there were 146 m of eroding banks along straight reaches and 137 m of eroding bank around bends. In total, approximately 2.5% of all the banks in the Wharfe are actively eroding. Actively eroding banks are described as those which have evidence of erosion in the past few years. Other banks have been subject to erosion in the past but currently appear stable, possibly due to the supporting debris at the bank toe. Varying styles of erosion were also noted. Outside banks of meanders tended to be higher with mass failures the predominant cause of erosion. On the straight sections, the banks were typically lower and slumping prevailed. The failed material often remained visible at the bank toe. It was also noted that whilst most of the eroding banks consisted of relatively uniform fine sediment, some of the banks were eroding into pockets of coarse material. This coarse material is where the river is eroding into palaeochannels, revealing a glimpse of the former wandering nature of the Wharfe. Figure 4.2 clearly shows the difference between fine bank material, formed from thousands of years of fine sediment delivery onto the floodplain during overbank flows (left hand side), and coarser material (right hand side) from a palaeochannel. The coarse material represents the old channel bed before the channel migrated across the floodplain. The river is now migrating back into its previous course. This coarse sediment pocket further demonstrates how coarse sediment is stored as a floodplain deposit.

The surveys also document the full extent of the hard and soft engineering schemes that were discussed in Section 3.5. They record several different types of bank protection from the dry stone walls constructed in the 14th and 15th centuries, more recent hard engineering structures including block stone revetments and gabions (large metal cages filled with small loose boulders) and also the softer engineering approaches including willow planting, birch brash faggoting and fencing off the channel to livestock. From this survey, 9 of the 19 bends along the river were noted to have bank protection. The total length of this protection is estimated at around 380 m. In addition, around 200 m of modern bank protection was present on previously unstable straight sections. Historical bank protection, in the form of

dry stone walls, increases this length but is not quantified as these sections were deemed to be stable in the long-term, having been confined for many decades. It is estimated that the length of eroding banks would initially double were the bank protection to be removed. This is explored further in Section 6.3 which includes a map showing the locations of bank erosion and protection (Figure 6.9).

Figure 4.2: Evidence of a palaeochannel found at cross-section 350.

4.3 CROSS-SECTIONAL SURVEYS

Cross-sectional surveys of the channel were required: (1) to provide the boundary conditions of the model, including channel width and depth (Section 8.2); (2) to monitor patterns of morphological change in the study reach (Section 4.3.5); and (3) to reconstruct a morphological sediment budget using the "inverse method" (Section 6.3). The latter allowed estimates of bedload transport to be made. Numerous studies have used cross-sectional re-surveys to provide similar information including Ferguson and Ashworth (1992), Goff and Ashmore (1994), Martin and Church (1995), Lane *et al.* (1995), Ashmore and Church (1998), McLean and Church (1999), Ham and Church (2000), Stover and Montgomery (2001), Lindsay and Ashmore (2002), Fuller *et al.* (2003), Martin and Ham (2005) and Rodrigues *et al.* (2006). The basic problem with this survey-based approach is the time required to survey cross-sections with sufficient density. This may be quite high

(Lane *et al.*, 1994) in order to avoid missing erosion and deposition between cross-sections (Naden and Brayshaw, 1987; Wittenberg, 2002). As such, a sampling strategy with an adequate spatial and temporal resolution was developed and employed.

4.3.1 Previous Cross-Sectional Surveys

Several projects have conducted cross-sectional surveys on the Wharfe study reach in the past. Details of the dates of these surveys are included in Appendix 2. In 1982, the Yorkshire Water Authority (1983) used these surveys to inform the design and implementation of the engineering works during the 1980s discussed in Section 3.4. In 1997, Heritage and Newson (1997; 1998) carried out surveys as part of a broader study into the stability of the river channel. Following this, RKL-Arup in 1999 and Jeremy Benn and Associates (JBA) in 2000, both private engineering consultants, were commissioned to further explore unstable reaches along the Wharfe, make assessments of the gravel trap and investigate flood risk. These two projects fall under the UWBPP. Thus far, the surveys were independent of each other although, where possible, the cross-section locations were roughly kept similar. As such, these were not designed to include repeat channel bed surveys, nor to consider when to measure bed levels in response to spatial and temporal fluctuations in sediment delivery. They made no attempt to make the measurement of river bed morphology, and its change through time, an integral part of river management decision making. Hence in 2001, a cross-sectional monitoring strategy was developed to allow coarse sediment delivery and transfer to be explored (Reid, 2004) with respect to inundation extent (Tayefi *et al.*, 2007). Results to 2004 have been published (Lane *et al.*, 2007; Reid *et al.*, 2007a). However, this three year period was insufficient to capture the spatial and temporal dynamics of river response and focused more upon characterising the magnitude and frequency of sediment delivery and transfer events. Hence, repeat cross-sectional surveys have been continued throughout this project at the locations defined by Reid (2004). The additional three years provide evidence regarding the spatial and temporal patterns of river bed sedimentation and its implications for flood risk.

4.3.2 SURVEY METHODOLOGY

To minimise limitations with this approach, Fuller *et al.* (2003) made the following recommendations. These were considered when the monitoring strategy was initially defined (Reid, 2004) and again in 2004 at the start of this project. These recommendations were that each cross-section should: (1) fully represent the sub-reach under study; (2) represent the processes under study and the length-scale over which these processes operate; and (3) should not erode too severely during the study such that surveys would become impossible or dangerous. Reid (2004) used a detailed survey of extant loci of erosion and deposition to identify 60 cross-section locations. The locations and selected numbers are shown in Figure 3.3 and full details of the cross-sections including distance between, channel width and slope are contained in Appendix 2. The spacing between sections was such that a given cross-section reflected the morphological complexity of the channel. Spacing ranged from 30 m to 200 m and the average spacing was 95 m. The cross-sections were spaced more closely on the meanders. This spacing did not exceed typical particle step length in transport events which are thought to be similar to meander wavelength (Pyrce and Ashmore, 2003). The average spacing on the bends was 48.5 m and sections on bends constituted 28% of all cross-sections. The spacing was greater on the straighter sections with the spacing averaging at 115.5 m. In December 2002, the initial 3 km study reach was extended to include an additional 2.6 km of river downstream. In December 2004, the locations were re-assessed to ensure they continued to provide a good representation of the reach. Only cross-section 020 was abandoned as the dense undergrowth on both sides of the channel meant that the GPS could not get a signal and the total station could not "see" through the undergrowth. This section was located across the vegetated island by Hubberholme. It is a highly stable feature of the river and hence morphological adjustments are assumed to be minimal.

The surveys were undertaken using an RTK Leica Geosystems 1200 differential Global Positioning System (dGPS) and a Leica Geosystems 1200 total station. The latter was used for sections where signal was poor due to tree cover. Both systems have a mean vertical

precision of ± 0.005 m. Around 70% (April) and 80% (December) of the surveys were measured using the GPS. The average number of points per section was 106 with an average spacing between points of 0.32 m. Points were located to include all breaks of slope within a given section. The cross-sections were surveyed twice yearly, once in March-April, typically at end of the wetter winter period, and once in December, the start of the winter season. Deviations from these periods were necessary due to equipment availability and bad weather. In particular the March-April 2007 surveys were severely delayed. This was initially due to equipment constraints and then due to long periods of wet summer weather which kept the flow too high for safe measurement. These were eventually surveyed in July 2007. However, with vegetation in full leaf, several sections could not be surveyed as the GPS could not relocate either of the bank pins.

4.3.3 ANALYSIS

The cross-sectional survey comprised of 60 separate locations, each with between 10 and 12 repeated surveys with an average of 106 points recorded per survey. Thus, channel changes in the 5.6 km study reach could be quantified using the 652 surveys and ~ 69,000 individual data points: a large and detailed dataset. Figure 4.3 shows a sample of these data. This plot clearly shows that this cross-section experienced a period of erosion between April 2004 and December 2004 and little change occurred in the subsequent period, which ran until April 2005.

Figure 4.3: Three consecutive surveys at cross-section 320.

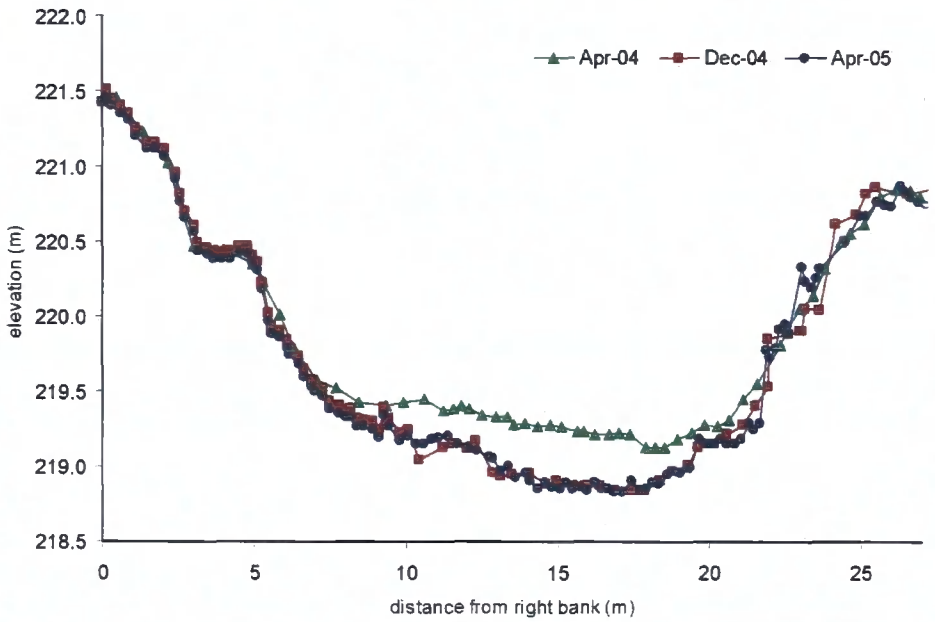

The surveys can be analysed in several ways. First, the average bed level change at each specific location was determined by calculating the cross-sectional area at each survey using [4.1]. The area change between two successive time periods was determined using [4.2] and by dividing by the channel width, the width-averaged bed level change for a particular cross-sectional location was determined. This was done for each time period (t, $t+1$).

$$A^t = \sum_{i=1}^{n-1} \left(z^{i+1} - z^i\right) \left(\frac{d_c{}^i + d_c{}^{i+1}}{2}\right) \qquad [4.1]$$

$$\Delta A^{t,t+1} = A^{t+1} - A^t \qquad [4.2]$$

where A is cross-sectional area; z is horizontal distance across the channel at point i; d_c is the difference in elevation between the elevation at point z and the maximum bank elevation for the section; n is the number of points; and t is time.

Second, the volume associated with adjacent cross-sections, separated by distance (x_{i+1}-x_i), was determined from [4.3]. [4.4] was then used to calculate volumetric change over time, which is used in Section 6.3 to reconstruct a morphological sediment budget for the channel. In practice, by dividing through by $(x_{i+1} - x_i)$, the mean volume of change is expressed per unit of downstream distance. This accounts for downstream changes in cross-section density and prevents, for example, data from two closely spaced cross-sections with both record aggradation, being over represented in the whole reach. By dividing the volume change between two cross-sections by the average width of the two end sections, the reach and width-average mean bed level change per metre downstream can be determined.

$$V_{i,i+1} = (x_{i+1} - x_i)\left(\frac{A_i + A_{i+1}}{2}\right) \quad [4.3]$$

$$\Delta V_{i,i+1}^{t,t+1} = V_{i,i+1}^{t+1} - V_{i,i+1}^{t} \quad [4.4]$$

where ΔV is the volume between two survey locations (i and $i+1$) separated by distance (Δx).

In addition, the cross-sections can be used to characterise other planform information. The active channel width is defined as the horizontal distance between the bank tops which are determined by the presence of established vegetation. Since many of the cross-sections extend several metres onto the banks, this distance is not simply the distance between left and right bank pins. Field knowledge is required to distinguish the bank from the active channel. Channel depth can be expressed as maximum depth, or cross-sectional averaged depth. In both cases, the depth is measured from the channel bed to the height of the lowest bank (i.e. the bank that flow would overtop first). Again field knowledge and judgement was used to characterise the bank top height. Cross-sectionally averaged depth was determined by dividing the cross-sectional area calculated from [4.1] by the width. The characteristic of slope can be expressed in several ways including valley, bank and bed slope. In each case, slope is defined as the change in elevation over distance. First, valley slope is a crude description of the slope of the valley in which the river flows and does not account for local variability. This can be calculated by taking the average valley elevation

at several points down the valley. Second, the channel can be represented by the bank slope, which is the average of the slope between left pins and the slope between right pins. This accounts for variability in slope created from sinuosity, which is not accounted for in the valley slope calculations. Problems with this approach arise when defining bank height in sections where the channel is cutting into an area of higher ground, and therefore one bank is substantially higher than the other bank. Finally, channel slope can be determined from the average channel height at each cross-section, the channel bed slope profile. This approach records slope variability as the channel flows between deeper pool and shallower riffle sections. The result is that the slope is positive in some instances (when flow is from pool to riffle) and negative in others (riffle to pool). Smoothing of the slope profile is necessary. Further details of slope smoothing are discussed in Section 8.3.1 during model development.

4.3.4 Quantification of Error and Uncertainty

Given uncertainties in elevation that arise due to grain roughness (e_g), position due to dGPS errors (e_z) and distance between cross-sections (x) as distances between left and right pins vary with sinuosity, the propagated uncertainty in area (A) and volume changes (V) can be quantified. Taylor (1997) outlines that the uncertainty in parameter q derived from variables x....z measured with uncertainties represented by their associated standard deviation of error (σ), can be determined using [4.5]. This assumes that the uncertainties in x....z are random and independent.

$$\sigma_q = \pm\sqrt{\left(\frac{\partial q}{\partial x}\sigma_x\right)^2 + ... + \left(\frac{\partial q}{\partial z}\sigma_z\right)^2} \qquad [4.5]$$

To test this approach to error quantification, one survey section was measured twice on the same day. The area above each survey was calculated using [4.1]. The difference between these two areas provides an indication of uncertainty in area calculations. Survey one had an area of 46.096 m^2 whilst survey two had an area of 46.257 m^2, a difference of 0.160 m^2. Equation [4.6] which follows on from [4.5] was used to estimate the uncertainty in the area

calculation for survey one and survey two. The standard deviation of error in e_z was 0.025 m and in e_g was 0.08m. The uncertainty in e_z was determined from the mean error for all surveys points whilst the uncertainty in e_g was determined at each location from the D_{84}, since this represents roughness. Grain size characteristics were obtained using methods detailed in Section 5.3. The uncertainty estimates were less sensitive to e_g than to e_z since the values for e_g were typically lower than e_z particularly at the more downstream cross-sections where D_{84} was lower. Using [4.6], the uncertainty associated with the area of survey one (σ_{A1}) was $\pm$ 0.11 m^2 whilst it was $\pm$ 0.206 m^2 for survey two (σ_{A2}). When these errors are propagated together using [4.7], the measured error is well within the estimated precision of $\pm$ 0.234 m^2 associated with random errors. This suggests that for this comparison, the surveys were being conducted without unexpected bias being introduced.

$$\sigma_A = \left(\sigma_{eg}^2 \sum_{i=1}^{n} \left(e_{g\,i+1} - e_{g\,i} \right)^2 + \sigma_{ez}^2 \sum_{i=1}^{n} \left(e_{z\,i+1} - e_{z\,i} \right)^2 + \right)^{0.5} \qquad [4.6]$$

$$\sigma_{A1,2} = \sqrt{\sigma_{A1}^2 + \sigma_{A1}^2} \qquad [4.7]$$

When the uncertainties in both are propagated together using [4.7], the uncertainty associated with the difference between areas is $\pm$ 0.07 m^2 higher than the measured error. A higher calculated error is beneficial as it provides an upper level of uncertainty. The uncertainty in the volume change estimates was sensitive to the errors in downstream distance (x). The uncertainty in x (σ_x) was calculated for each site by first measuring the length between cross-sections on the left bank and the length between cross-sections on the right bank. Then, the difference between each bank length and the length of the centreline (mid-channel) was determined and used to determine σ_x. Since x is the distance along the mid-channel, errors arise when the channel is sinuous and the left and right banks are not of equal length. This typically occurs around a meander bend when the outer bank is longer than the inner bank. As such, the standard error associated with downstream distance (σ_x) is poorly correlated to x and the uncertainty in x at each location is independent of each other. Thus, long straight reaches may typically have a lower uncertainty in x that short curved

reaches. Figure 4.4 shows the uncertainty in distance for each cross-sectional reach with the line plot showing the estimated uncertainty at each location and the bars showing this expressed as a percentage of the channel centreline distance. As expected, the highest uncertainty values arise when a reach is particularly sinuous (e.g. 210 and 220, 320 and 330, 450 and 460, 500 and 520, 580 and 590). The average uncertainty in x was 5 m whilst the maximum, recorded at 210-220, was 12.2 m.

Figure 4.4: Uncertainty in distance estimates.

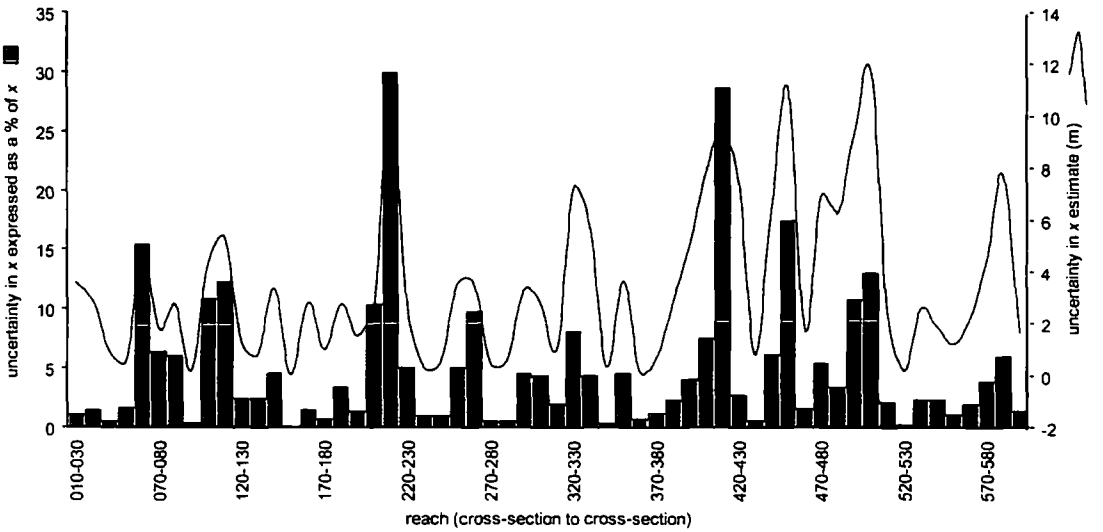

The uncertainties in the reach and width-average estimates determined from the volumetric estimates are propagated through time, from one survey to the next. The total uncertainty in the estimates increases in a steady way. Figure 4.5 shows these estimates as the number of surveys increase. A selection of cross-section locations is shown. Uncertainty values vary from less than $\pm$ 0.01 m to over $\pm$ 0.07 m. This reflects: (1) the survey point spacing, with greater distances between survey points resulting in higher errors in z; (2) changes in roughness h as one progresses downstream to the finer bed material; and (3) uncertainty in distance as demonstrated in Figure 4.4. As such, the more upstream and sinuous reaches tend to have greater uncertainty estimates due to coarser sediment and uncertainty in distances whilst the increases in uncertainty over time (steeper curves) can be explained by reductions in point spacing for a given survey. Most curves are steeper between December 2001 and April 2002, after which point density increased.

Figure 4.5: The increase in reach (between two cross-sections) and width- averaged bed level change error as the number of surveys incorporated into the calculations increases. Not all cross-sectional locations are included here.

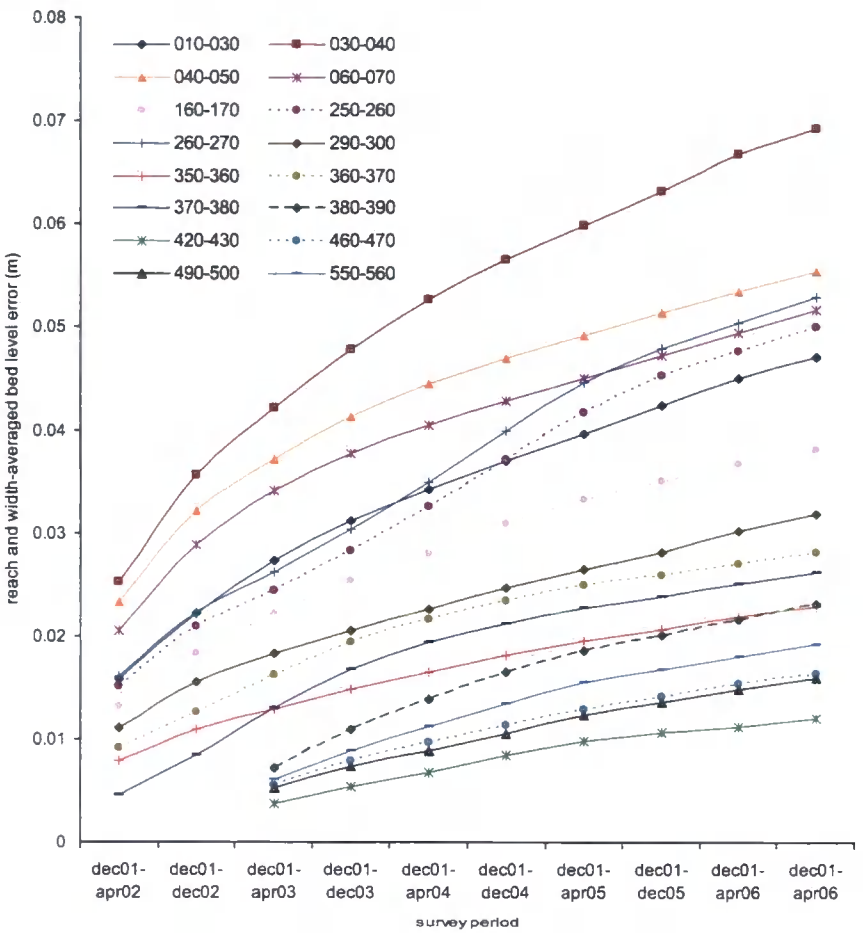

4.3.5 Results

The data collected from the cross-sectional re-surveys enables the first of the key research questions outline in Section 1.1 to be answered. This question asked:

1) How does in-channel sedimentation in an upland gravel-bed river vary through space and time?

The following discussion answers this question. Further discussion into the spatial and temporal patterns of in-channel sedimentation is made in Section 6.2, which aims to explain these findings.

The cross-sectional data is initially expressed in two ways as shown in Figure 4.6. Figure 4.6a, presents the results as seasonal bed-level change down the river. Bed level change is width- averaged to allow for comparison between cross-sections of varying width. The data presented in this graph are based on the cross-sectional area changes and do not incorporate any volumetric detail. The main features of interest in this figure are the variations in active seasons, with the early seasons of dec01-apr02 and apr02-dec02 exhibiting particularly high levels of bed level change. It is also interesting to note the emergence of particularly active areas where change occurs in almost all the time periods (e.g. 200 and 310).

The cumulative change in mean bed level since surveys began in December 2001 (and since December 2002 from 3 km downstream) is shown in Figure 4.6b. Since these data are determined by dividing the volumetric change by downstream distance and average width, they are effectively the same data but expressed differently. However, by plotting this as mean bed level change, the values are smaller and easier to interpret. It is clear that there has been an overall pattern of aggradation in the study reach. By July 2007, the mean bed level had risen by 0.17 m ± an error estimate of 0.029 m. However, certain zones along the river have developed as clear depositional reaches. The levels of aggradation in these reaches ranges from 0.46 m ± 0.026 m between 2.4 and 2.9 km downstream and 0.47 m ± 0.024 m at 1.9 km downstream to 0.67 m ± 0.031 m between 1 and 1.2 km downstream. Furthermore, a clear divide in patterns of bed level change exists at around 3 km downstream. The upper 3 km reach recorded a mean bed level rise of 0.22 m ± 0.036 m whilst the lower 2.6 km reach has aggraded by 0.11 m ± 0.019 m. Alongside these dominant depositional zones are a few observable zones of erosion. The highest rates of erosion are slightly lower than the highest rates of deposition with zones at 0.8 km and 1.8 km downstream recording the greatest rates of erosion at 0.26 m ± 0.042 m and 0.4 m ± 0.039m. The zones between 2 and 2.4 km and at 2.9 km are also notable for erosion with bed levels falling by 0.17 m ± 0.042 m and 0.2 m ± 0.023 m respectively.

Figure 4.6a and b (shown on the following two pages): Seasonal and cumulative bed level changes along the study reach. Each of the series lines represents the width-average change in bed level. Each series is centred on a horizontal grid line with measured change corresponding to erosion below and deposition above the grid line.

Figure 4.6a: Seasonal width-average bed level rise at each cross-sectional location.

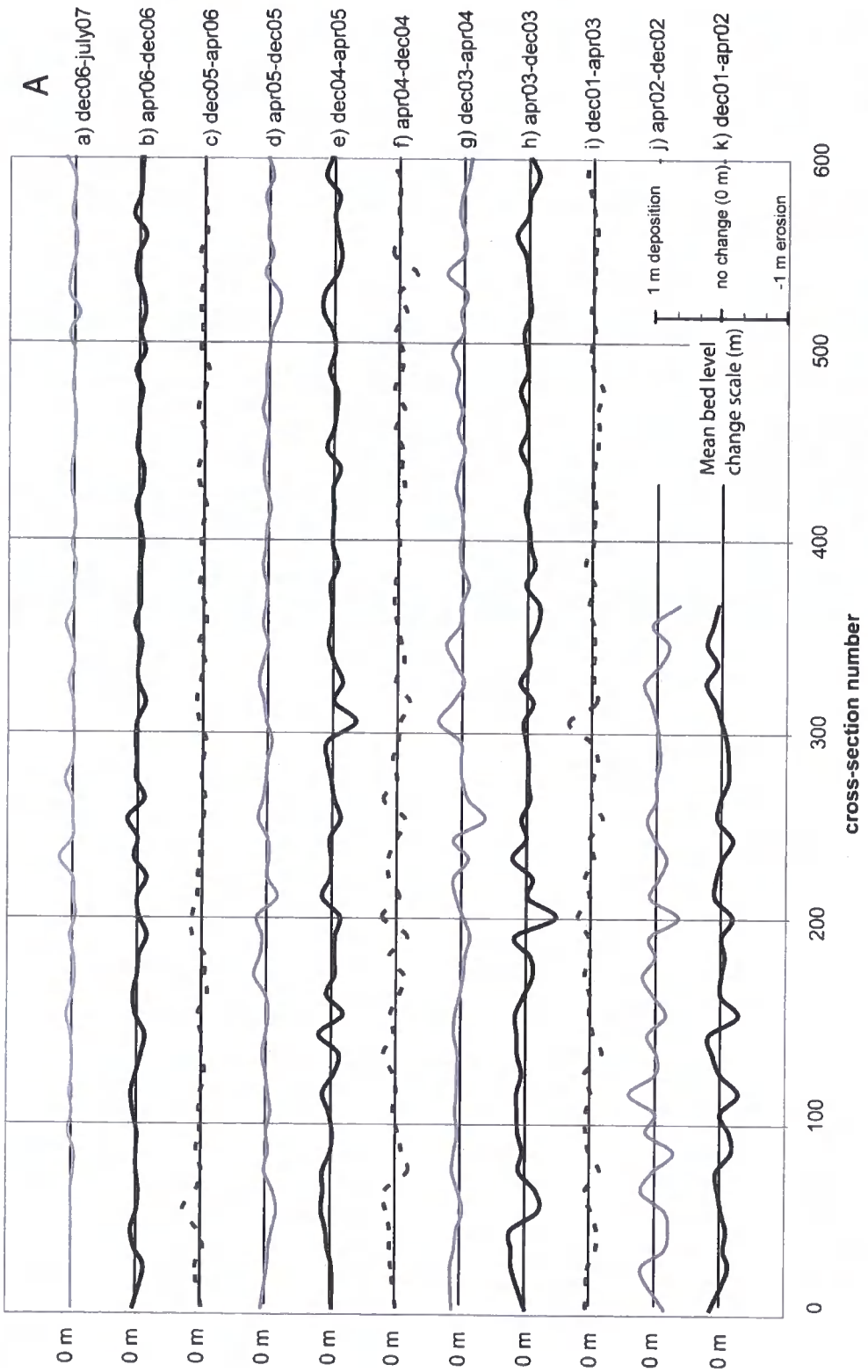

Figure 4.6b: Cumulative change in width-averaged bed level per meter downstream over increasing time periods.

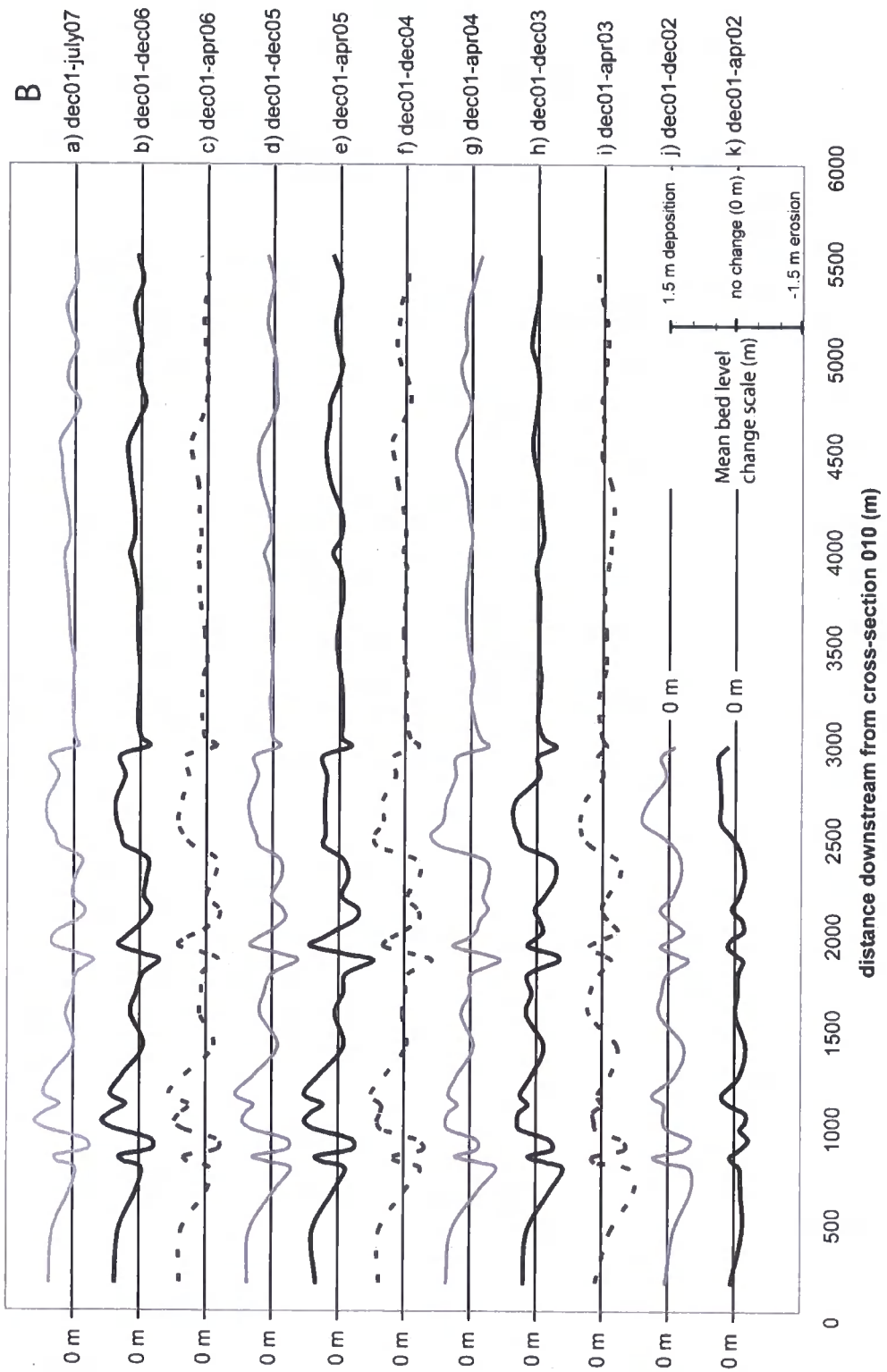

The data can also be expressed as bed level change activity by summing the absolute values of reach and width averaged change. Therefore bed level change activity is an expression that is irrespective of direction. Figure 4.7 shows the downstream bed level change activity since December 2002, from which date the entire reach was surveyed. This shows that levels of activity (the net bed level change irrespective of direction) far exceed levels of either erosion or deposition, with maximum activity occurring at 0.8 km, 1.8 km and 2.5 km downstream, with activity up to 1.8 m ± 0.021 m. The average activity per metre downstream is 0.8 m ± 0.026 m. This demonstrates that even in the zones of net erosion and deposition, seasonal fluctuations exist where net change in one direction, either erosion or deposition, is temporarily replaced with bed level change in the opposite direction. Thus, even in zones with relatively little bed level change recorded over the total surveying period, for example at 4.7 km downstream (cross-section 520), sediment activity can be high. At this specific location there is switching between erosion and deposition between survey periods as shown in Figure 4.6a, but the net change in bed level in Figure 4.6b is around zero. The visual divide between the upper and lower reaches in mean bed level changes (Figure 4.6b) is also evident when activity levels are considered (Figure 4.7). The upper zone experiences approximately 4 ½ times more mean bed level rise than the lower reach between December 2002 and July 2007. The difference in bed level change activity levels are much less, with the upper reach accounting for 70% of the total reach activity, just over twice as much as the lower reach. Furthermore, the length scale and amplitude of variations differ between the upper 3 km and the lower 3 km. In the upper reach, the mean length scale between peaks in activity is 460 m compared with 655 m in the lower reach. The amplitude of peaks is also higher in the upper 3 km reach with a mean amplitude of 0.9 m in the upper and 0.6 m in the lower reach.

Figure 4.7: Variation in bed level change activity with distance downstream. Activity is calculated from the period December 2002 until July 2007.

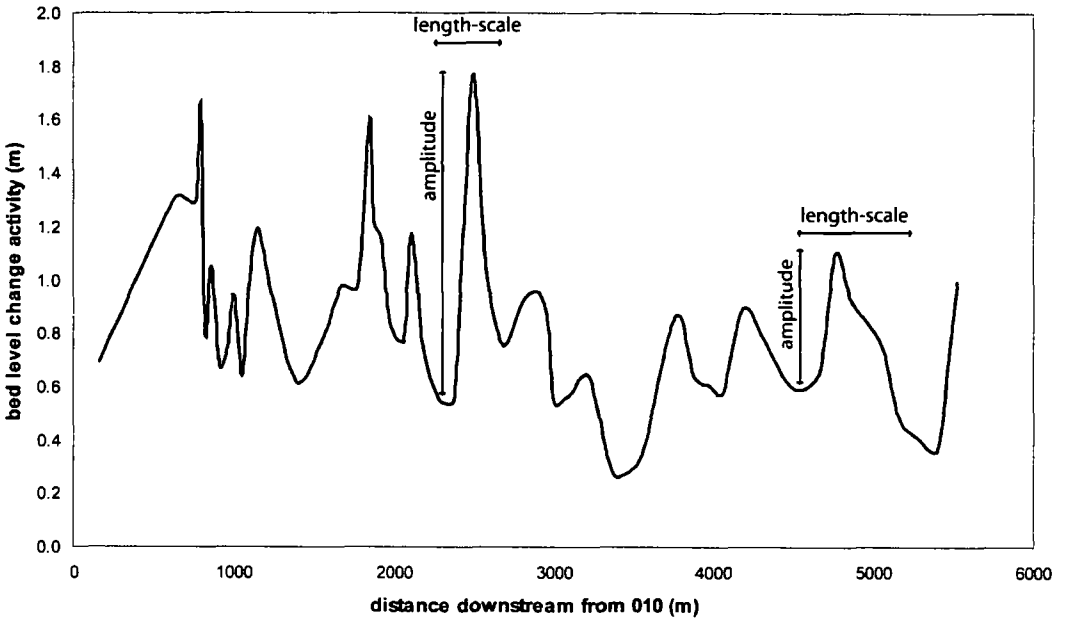

4.4 BANK EROSION MONITORING

Understanding the processes driving bank erosion and the rates at which bank erosion occurs in the study reach is essential for calibrating the lateral bank erosion component of the model and understanding the mechanisms of channel change in the Wharfe. A bank erosion study was undertaken to monitor bank erosion rates and draw conclusions about the processes driving the erosion. This study provides the answer to the second key research question outline in Section 1.1:

2) At what rate do unprotected river banks, in upland gravel-bed rivers, erode and what processes drive this bank erosion?

4.4.1 MONITORING OPTIONS

Determining the relative importance of individual bank erosion processes acting on a specific bank is often difficult (Simon and Darby, 1997; Lawler *et al.*, 1997). A wide range of methods are available to researchers for exploring bank erosion over a wide range of

spatial and temporal scales (Lawler, 1993b; Lawler *et al.*, 1997). Figure 4.8 classifies these methods by resolution and timescale showing the range at which bank erosion processes can be studied. Longer timescales require indirect methods to reconstruct the past, whilst direct methods allow short to medium term monitoring.

Figure 4.8: Classification of bank monitoring techniques by resolution and timescale. Source: Lawler, 1993b; Lawler *et al.*, 1997. PEEPS are photo-electronic-erosion-pins.

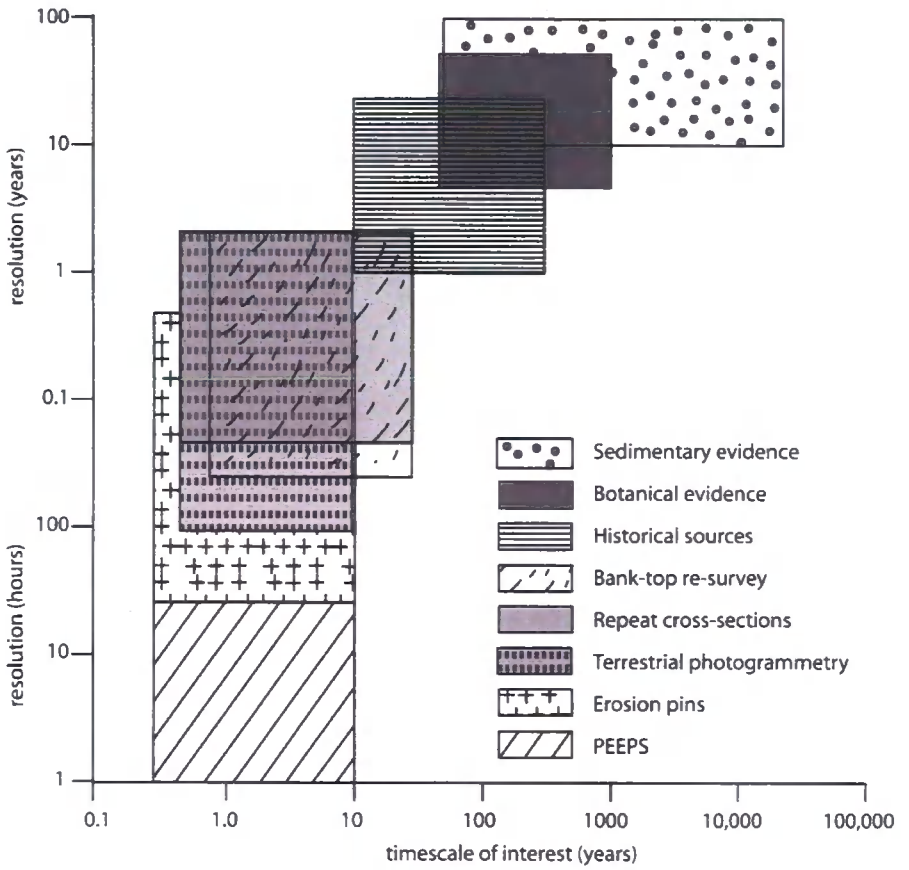

Indirect methods include using maps, aerial photographs, sedimentary evidence of palaeochannels and more recently satellite imagery. These data sources can be used to determine bank erosion rates over longer timescales of the order 10-250 years (Lawler *et al.*, 1997). Direct methods can be used to explore bank erosion over short (less than a year) and medium-timescales (from 1-10 years). Planimetric and cross-section resurveys can provide bank erosion information but on a fairly low spatial and temporal resolution over medium timescales. Direct methods such as erosion pins, photogrammetry (Barker *et al.*,

1997) or photo-electronic-erosion-pins, PEEP's, (Lawler, 1991, 2005; Bull, 1997) can provide data over the short-term. Whilst photogrammetry, which compares stereoscopic images of the bank face, enhances spatial sampling and enables the identification of specific bank erosion processes (Barker *et al.*, 1997), the PEEP's allow quasi-continuous time series erosion data to be collected (Lawler, 1991). Yet, these techniques are costly, time consuming and produce vast quantities of data (over small areas of bank) for analysis. Thus, most bank erosion studies use simple erosion pins to determine processes and rates of change (e.g. Lawler *et al.*, 1997; Couper *et al.*, 2002).

Bank erosion pins have been used successfully by Thorne and Tovey (1981), Lawler and Leeks (1992), Bull (1997), Lawler *et al.* (1999), Stott (1999), Couper and Maddock (2001) and Couper *et al.* (2002). Erosion pins are thin metal rods that are inserted horizontally into the bank often in grids. They can be used to detect small amounts of erosion (Thorne, 1982) allowing detailed measurements of the spatial and temporal patterns of bank retreat to be made (Thorne, 1982; Lawler, 1993a) inferring bank erosion processes (Lawler, 1993a). Whilst they work reasonably well (Lawler *et al.*, 1997), there are numerous problems associated with their use. Couper *et al.* (2002) suggest the main problems are due to: (1) pin movement (e.g. from frost action, root systems or burrowing animals); (2) changes in bank surface elevation due to shrinkage and swelling of the bank face; (3) the influence of the pin on erosion itself as the pin may disturb the bank material (Lawler, 1993a) or cause aggregates to form from rust; and (4) human interference / tampering with the pins. Furthermore, the pin may create extra turbulence which accelerates bank erosion around the pin (Lawler, 1993b). It is also difficult to determine when erosion occurs from the data as pins may bend during placement into the bank and pins may be lost completely if bank erosion rates are rapid. However, if these problems are considered when using pins and analysing data from them, this cost effective and simple technique can provide valuable data.

4.4.2 ADOPTED MONITORING METHOD

Following extensive literature review into the available techniques for monitoring bank erosion a decision was made to use simple bank erosion pins coupled with bank top resurveys to monitor bank erosion in the Wharfe. This would minimise cost and labour whilst still providing valuable data on bank erosion rates and processes. The detailed field surveys (Section 4.2) were consulted to select numerous potential bank erosion study sites. Five sites were chosen from these following a field visit. These are shown on Figure 4.9. All sites were located in the lower half of the study reach as this was where the majority of actively eroding banks were found. Thus, all the bank erosion sites were located where sediment transport activity levels were lower. Sites 1, 3 and 4 were located on the outside of meander bends and sites 2 and 5 were located on straight sections. All sites were composed of fine sediment to allow the pins to be inserted into the bank. Between 24 and 32 pins were inserted into each bank in 3 or 4 rows depending on the height of the bank. The pins were 300 mm long (measured using callipers), 3 mm diameter silicon bronze welding rods that were strong and would not rust. They were inserted into the banks so that between 20 and 60 mm of pin was exposed. The pins were spaced 400 mm apart horizontally and 300 mm vertically. This erosion pin set up is similar to those used by Lawer *et al.* (1999), Couper *et al.* (2002), Bull (1997) and Couper and Maddock (2001). Each bank was also surveyed using the Leica dGPS system to provide a detailed DEM of the bank to allow estimates of bank-line retreat to be made in the event of mass failure and pin loss. These surveys extended beyond the bank zone where the pins were located. The pins were measured initially in July 2005, then approximately every 2 months. The timing of the measurements was dependent on low flows as the channel around the meander bends was associated with deep flow. If bank erosion had occurred exposing more than half of the pin, the pin was pushed back into the bank and re-measured to reduce the likelihood of pin loss. In the event of pin loss, where possible, new pins were re-inserted in the same locations. In these situations an estimate of bank erosion was made from the surrounding bank topography. Repeat bank top re-surveys were carried out in July 2006 and July 2007.

The error associated with the measurement technique was quantified using a method described by Stott (1999) and also used by Couper and Maddock (2001) and Couper *et al.* (2002). The method repeatedly re-measures the pins in a random order determined using a random number table. When ten measurements have been obtained for a single pin, these measurements were used to determine the standard error. The standard error for the Wharfe pins was ± 0.29 mm which is within the range of ± 0.17 and ± 0.33 mm found by Stott (1999). Therefore, Stott's suggestion based on errors within this range that readings are repeatable to within ± 0.5 mm was used for this study. Simon *et al.* (1999) also estimated that pin readings are accurate to within ± 0.5 mm, based on multiple measurements made by the same operator on the same day. This value is slightly higher when different operators carry out the measurements. For the Wharfe study, all measurements were taken by the same operator.

Unfortunately, whilst four of the bank erosion study sites provided valuable data the other site, bank erosion site 3, had to be abandoned due to difficulties during the winter in accessing the pins. The location of this site, on the outside of a meander bend, meant that during the winter months, the flow was too deep to safely wade through. Thus measurements could not be made at regular intervals.

Figure 4.9: Location of the bank erosion sites including photographs

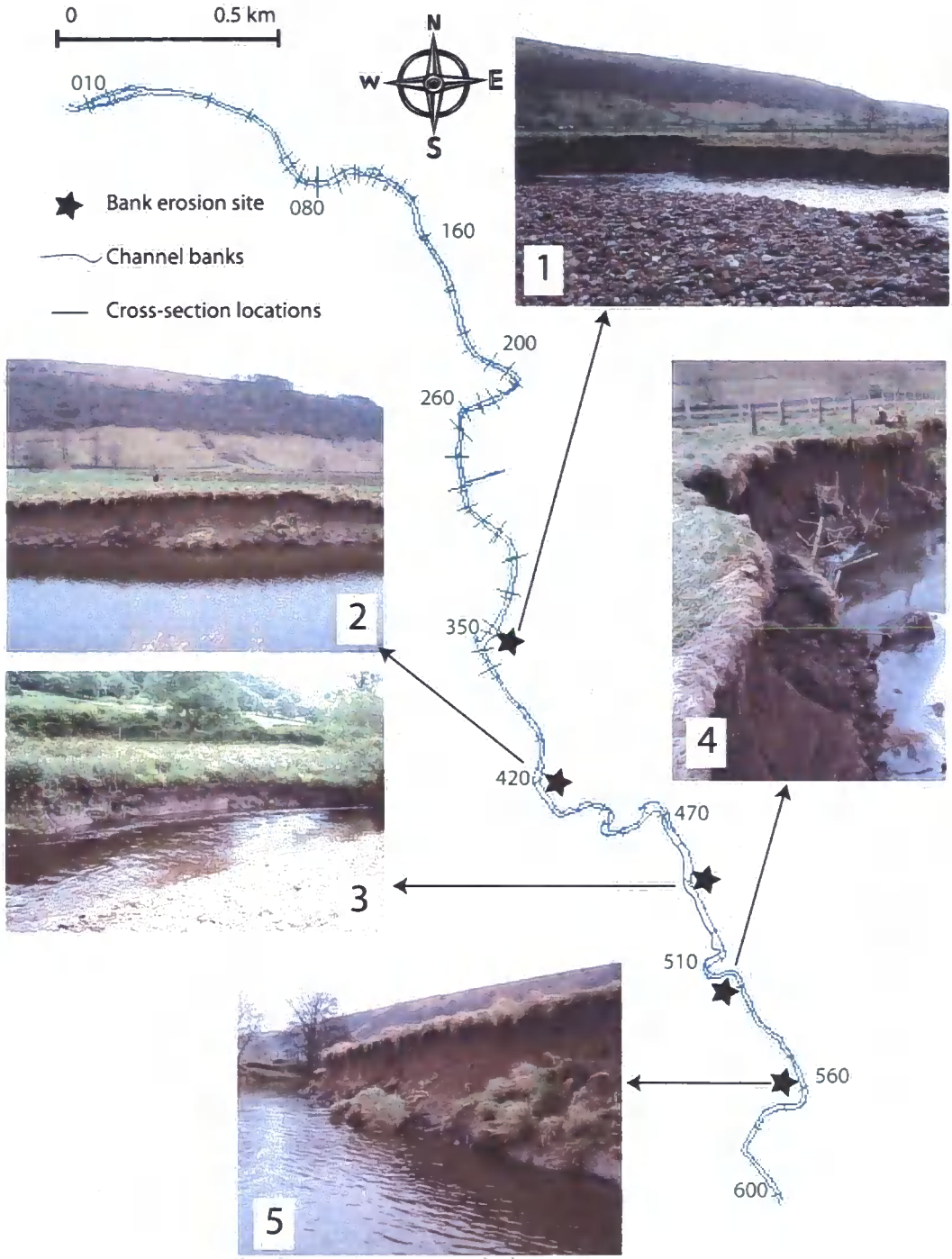

4.4.3 Bank Erosion Pins: Results

Of the four banks and 122 pins, 26 pins were lost (and subsequently replaced) and 550 measurements were made during the 12 month period. Two assumptions had to be made during data analysis. First, when a pin had been lost, the bank erosion rate was estimated. This estimate was based on the surrounding bank face. Second, the results had to account for negative pin recordings (i.e. when less pin is exposed during a return visit). Negative pin recordings complicate the data analysis but at the same time provide an insight into bank erosion processes. Negative results may occur when: (1) sediment is deposited onto the pins during high flow events; (2) soil falls from the upper parts of the bank onto the pins below; (3) the soil surface expands due to fluctuations in temperature and moisture; or (4) root systems or burrowing animals move the pin within the bank. During the study period, observations suggested that the most plausible cause of negative recording was from soil falling from the upper parts of the bank. Thus, negative recordings tended to be obtained for pins found lower down the bank face. The negative recordings were removed when calculating the bank erosion rate. Without doing so, the recorded rate may be lower than the true rate.

The annual bank erosion recorded at each pin on each of the four sites is shown in Figure 4.10. It is immediately clear that bank erosion varies spatially on a bank and also between bank sites. On banks 1 and 4, variation occurs laterally as we move across the bank with the 3 rows exhibiting similar patterns. There is a mean difference of 153 mm between the far left and far right pins on bank 1. On bank 5, the variation is predominantly vertical with substantially more erosion (a mean of 40 mm) noted on the lowest row when compared with the 3 rows above. Bank 2 had one point that eroded substantially more that the other pins which recorded similar rates and varied little spatially.

Figure 4.10: Annual bank erosion at each pin. Each bubble represents a pin as positioned on the bank with the area of the bubble relative to the amount of erosion (mm) at each bank.

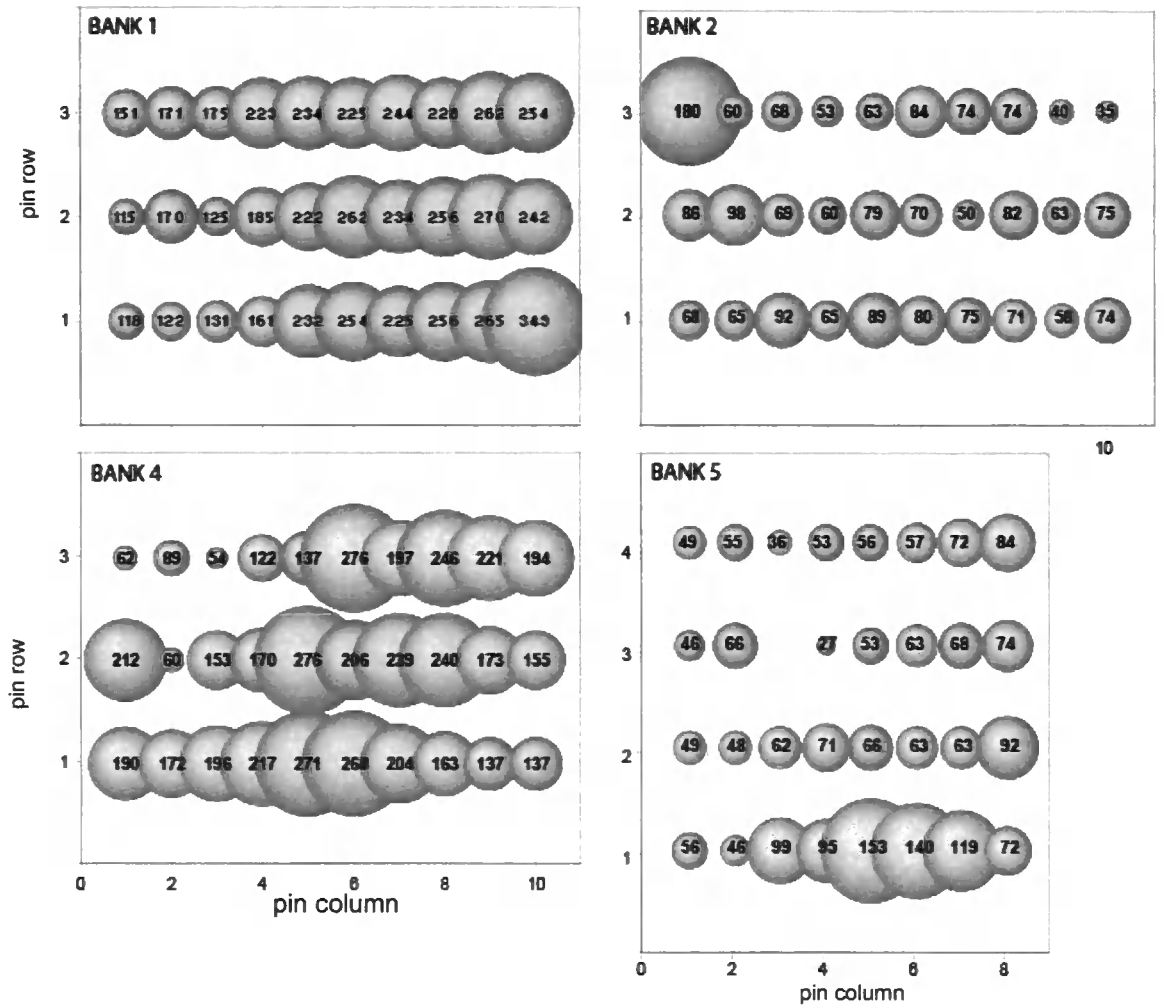

The average erosion at each bank site for each recording period was calculated. Figure 4.11a shows the cumulative bank erosion since July 2005. From this figure, two different patterns of bank erosion emerge: banks 1 and 4; and banks 2 and 5. Banks 1 and 4 record over three times the erosion noted on banks 2 and 5. The total erosion after 1 year of monitoring was 212 mm at bank 1, 73 mm at bank 2, 181 mm at bank 4 and 68 mm at bank 5. These annual bank erosions rates for the Wharfe are similar to those found on several other upland UK river systems. For example, on the Upper Severn, Thorne and Lewin (1979) recorded bank erosion rates between 350 and 600 mm year^{-1} and Thorne and Tovey (1981) recorded a rate of 280 mm year^{-1}. Hooke (1980) recorded rates between 150 and 460

mm $year^{-1}$ on the River Axe in Devon and Lawler (1986) found bank erosion rates of 40 to 310 mm $year^{-1}$ along the Ilston River in Wales. Lawler *et al.* (1999) found bank erosion rates between 68 and 364 mm $year^{-1}$ on the Swale-Ouse system and Leys and Werritty (1999) suggest that rates of 200 to 300 mm $year^{-1}$ are feasible in the Scottish rivers the Feshie, Avon and Coiltie.

The bank erosion rate during each time period can be calculated and the data are shown for each site in Figure 4.11b. At all four sites, bank erosion rates peak in the February to April period. The highest rates of erosion during this period are found at bank 1 (2.3 mm day^{-1}) with bank 4 (1.3 mm day^{-1}) also recording a high rate of erosion during this time period. The rates of erosion indicate that there is a strong seasonal influence on bank erosion with more erosion occurring in the winter months. Banks 2 and 5 were found to behave in similar ways with erosion rates very similar through all time periods. It can also be noted that the peak in erosion from December until April is much more attenuated than at the other two sites with maximum bank erosion rates of 0.45 mm day^{-1} and 0.40 mm $year^{-1}$ at banks 2 and 5 respectively.

Figure 4.11: (A) Total erosion at each bank erosion site (BE) since July 2005, (B): Erosion rate for each time period.

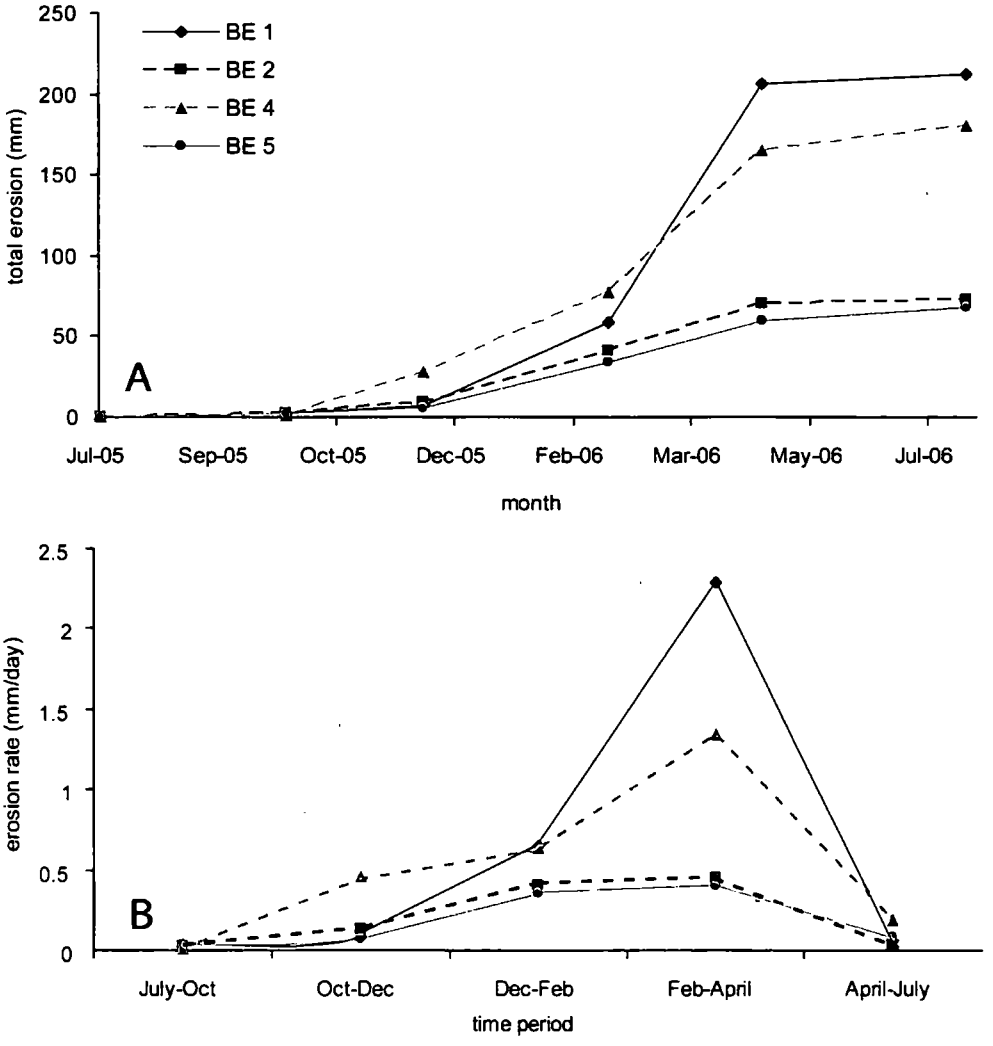

4.4.4 Bank Top Surveys: Results

Bank top surveys were conducted to capture any bank erosion that occurred rapidly and would result in the loss of bank pins at a particular site. Of the 4 sites, only banks 1 and 4 were subject to any notable bank top erosion. Bank top profiles for July 2005, 2006 and 2007 are shown in Figure 4.12. At bank 1, only small amounts of bank erosion are noted. At bank 4, whilst some bank erosion is noted in the 2006 profile, more substantial erosion can be seen in the 2007 profile. Table 4.1 provides details of the average and maximum bank erosion that occurred at this bank. This was calculated by integrating the area under

each of the bank curves in the same way as the areas above the cross-sections were calculated in Section 4.3.3. The maximum bank erosion recorded between 2006 and 2007 was 1.2 m (1200 mm). This erosion occurred due to bank collapse, most likely in a single event from undercutting. Much of the failed material was found at the bank toe, thereby stabilising the bank from further collapse. This single bank collapse resulted in 10 times more erosion than the annual bank erosion from weathering processes. The weathering process may have weakened the bank making it more susceptible to bank collapse.

Figure 4.12: Annual bank top profiles for banks 1 and 4.

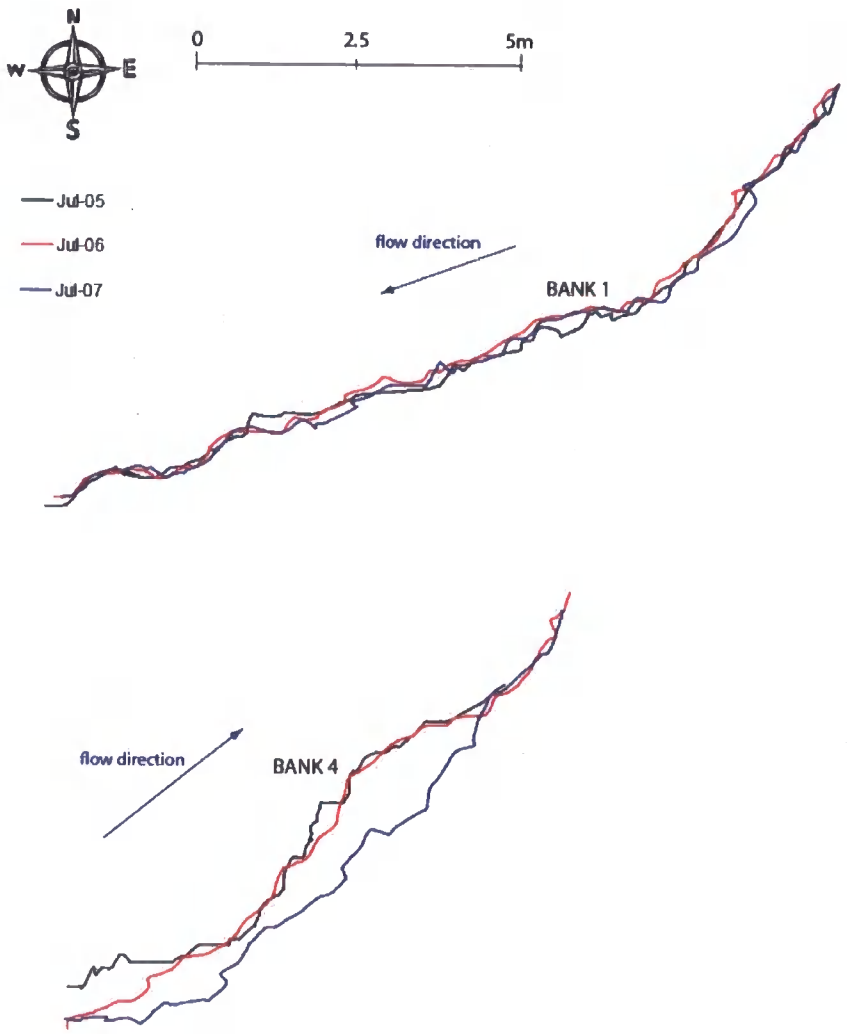

Table 4.1: Average and maximum bank retreat for bank 4

July of	Area under bank top (m^2)	Area difference (m^2)	Average bank retreat (m) *(bank length = 8.3m)*	Maximum bank retreat (m)
2005	21.6			
2006	19.9	1.7	0.2	0.8
2007	13.2	6.7	0.8	1.2

Despite only one major instance of bank collapse being recorded during the study period, bank erosion through collapse is an important feature of the Wharfe system (as discussed in Section 4.2). Evidence of bank collapse can be found at the bank toe and from aerial photographs of the river. A similar approach of comparing maps and aerial photos to monitor lateral channel change was used on several rivers in Scotland (Leys and Werritty, 1999). Figure 4.14 shows substantial bank collapse that occurred at Heber bend (bank 1). The two aerial photographs used were georectified using features such as trees, buildings and wall corners in ARC GIS. By overlying the georectified images, bank erosion is clearly evident. This bank erosion was severe and increased the width of the channel by up to 12 m. This bank erosion increased the channel width by around 20%. From reading reports from the Wharfe such erosion probably occurred during the 1990s, possibly in response to the river management that occurred during the 1980s.

Figure 4.13: Bank erosion at Heber bend evident from aerial photographs.
A: June 1995, 1:15,000, flying height 2284 m, ground resolution 0.34 m. Cross-section locations are shown in red.
B: Google earth, downloaded 2007, Infoterra
A and B overlaid together using ARC GIS.

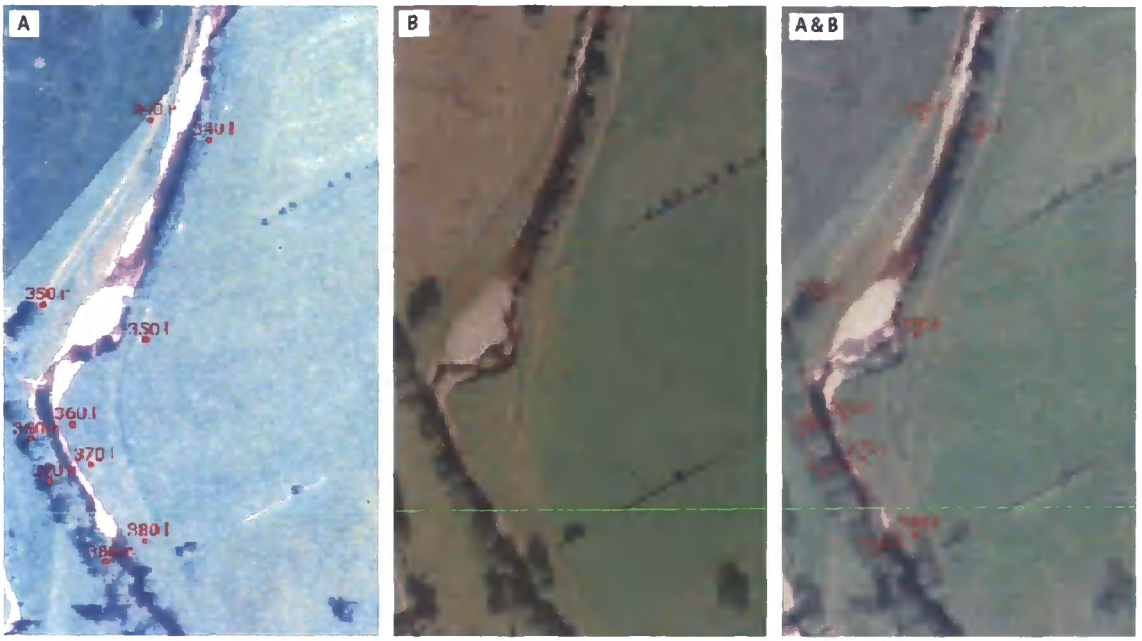

4.4.5 Bank Erosion Processes

Several observations can be made following close visual inspections of each bank and its pins during pin recordings. These observations allow a broader understanding of bank erosion processes in the Wharfe to be obtained. The findings can be supported with data from the pins when they are examined on an individual measurement basis. This data is particularly useful when displayed as proportional circles. For illustration, Figure 4.15 shows some examples of different patterns of bank erosion circles. Each pattern can be used to support field observations such as those discussed as follows.

Figure 4.14: Bank erosion processes. (a) sub-aerial processes (Site 1: Oct-Dec failure); (b) failure from desiccation cracks (Site 1: Feb-April); (c) undercutting (Site 5: Feb-Apr). Black circles indicate negative bank erosion. Seepage/piping is not demonstrated as this typically occurred across the whole bank and was not characterised by a distinct bubble pattern.

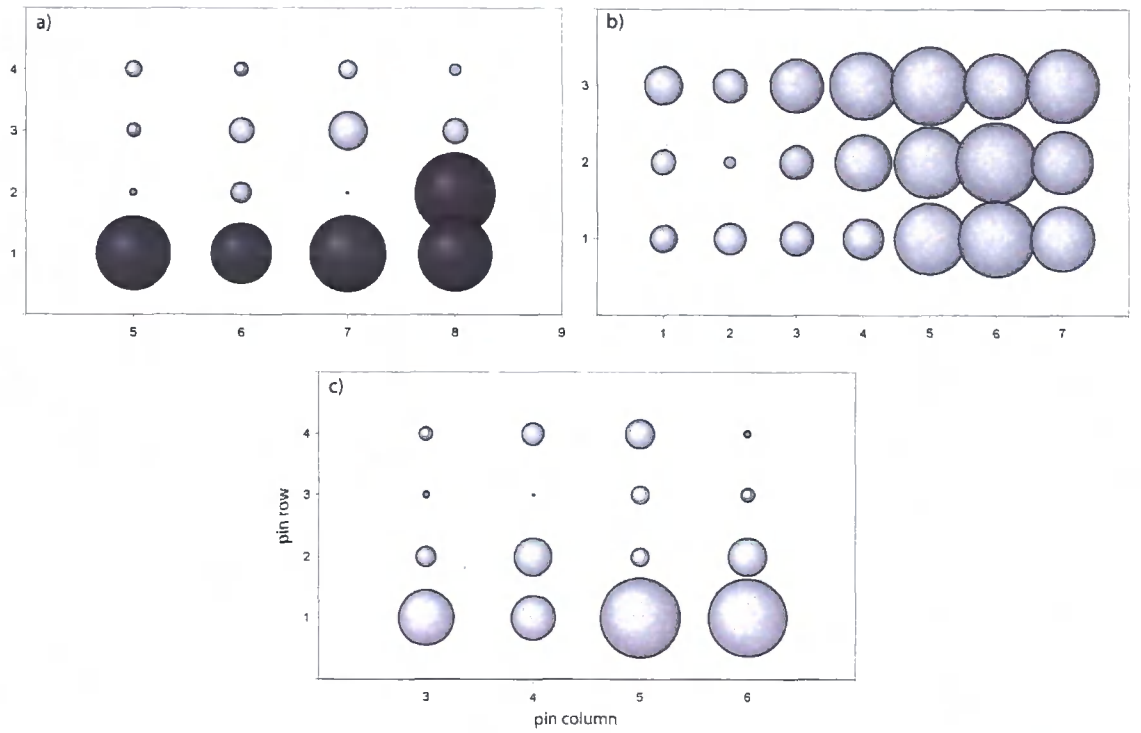

First, whilst mass failures evidently occur in the Wharfe (based on the presence of the failed blocks at the bank toe, aerial photographs and bank 4 banktop re-surveys), these events are less frequent than other erosion processes and generally occurred at intervals greater than one year. Instead, high rates of erosion along the Wharfe occur following the development of desiccation cracks (Figure 4.15) which eventually break away from the bank resulting in the loss of several centimetres of bank face at a time. However, in most cases, the bank top remains intact forming a small overhang until the overhang reaches a critical threshold and collapses. It is likely that the root systems of the grass on the bank top, are strengthening this section of the bank, making it less likely to collapse. The importance of vegetation for bank strength is widely recognised (e.g. Andrews, 1984; Thorne, 1982; Beschta, 1998; Abernethy and Rutherfurd, 2000). This rapid erosion is evident when circle patterns are similar to that in Figure 4.14b. It is clear that more erosion has occurred in pin columns 5-7 indicating that this part of the bank face has fallen away. A

second observation is that weathering processes supply fine sediment to the bank face. The presence of this fine loose sediment on several banks was noted in the winter months. This suggests that seepage from within the bank and freeze-thaw cycles may be occurring. This material is also responsible for some negative bank erosion recordings and patterns of circles such as those shown in Figure 4.14a. In this plot, the black circles, which represent negative recordings, are found on the lowest row as the material from above has fallen to the bottom of the bank partially burying the lowest row of pins. Third, following the supply of fine sediment to the bank face, fluvial entrainment of this material occurs during high flow events. Hence a combination of weathering and fluvial entrainment are responsible for much of the bank erosion on the River Wharfe that occurs over timescales of less than 1 year. Furthermore, fluvial entrainment can lead to undercutting of the bank face since the lower part of the bank is subjected to flow more frequently than the upper part of the bank. Figure 4.14c, shows a typical circle pattern that represents undercutting. A final observation that can be made is that there is a possibility that burrowing animals during the summer months (when the flow is low enough to allow the burrows to be made) are contributing to a loss of bank strength. On bank 4 in particular, several active burrow entrances were evident in July 2007 (Figure 4.15).

Figure 4.15: Evidence of bank erosion from desiccation cracks and burrowing animals.

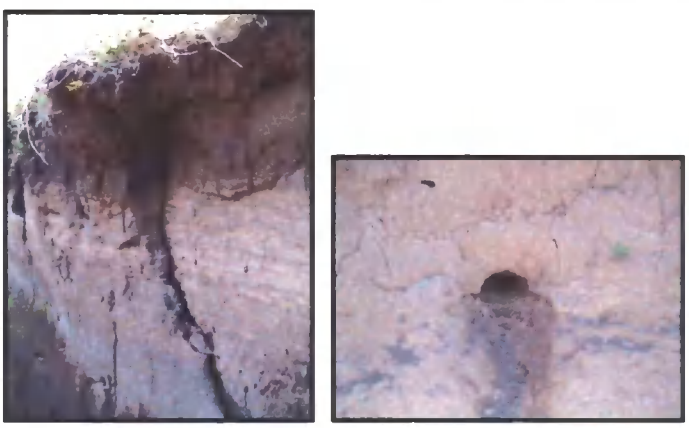

Finally, using all the information gathered from the field surveys, field notes made during pin measurements and the bank pin analysis, the dominant bank erosion processes can be deduced. This information can show how the relative importance of processes varies

spatially between banks (Figure 4.16a) and also how the dominant processes alter temporally over the year (Figure 4.16b).

Figure 4.16a shows that four main types of bank erosion are occurring within the Wharfe. Of these four, on banks 1 and 4 (i.e. those on outer meander bends), desiccation and fluvial entrainment dominate whilst on banks 2 and 5 (i.e. those on straight sections) freeze-thaw action governs slightly over the other three processes. Figure 4.16b demonstrates that the processes operating change depending on season. In the summer periods, the little erosion that occurs is caused by desiccation (as a result of the bank drying out and cracking), whilst in the winter months, the weathering processes of freeze-thaw and seepage/piping and fluvial entrainment predominantly occur.

Figure 4.16: Spatial (A) and temporal (B) patterns of bank erosion processes. Bubble size corresponds with relative importance.

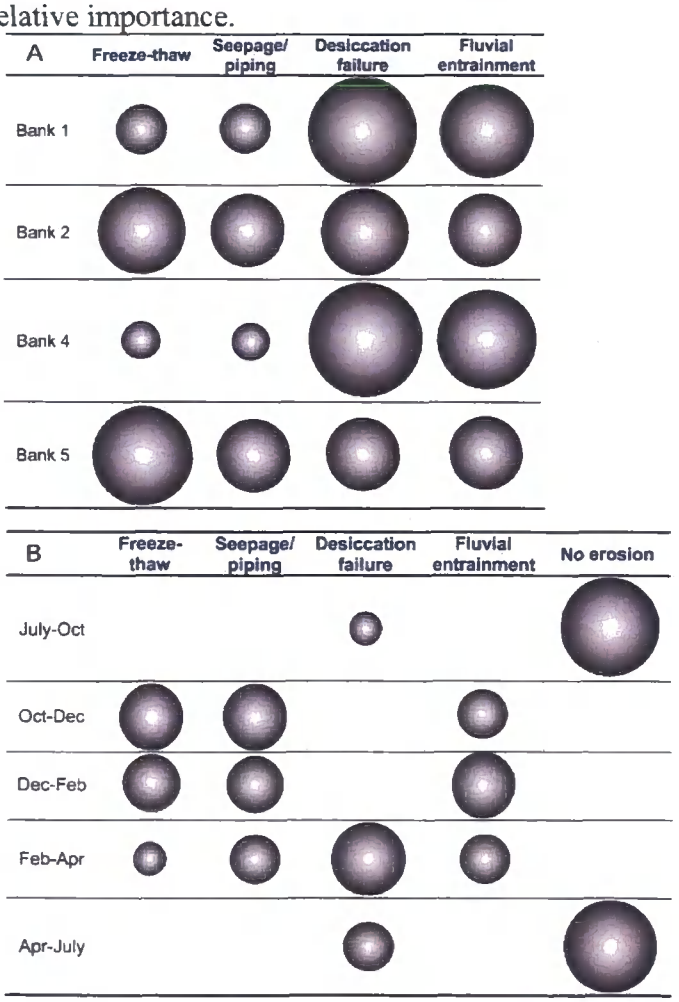

4.4.6 Bank Erosion Summary

Bank erosion is a complex and linked process and evidence from the Wharfe suggests a number of factors control the rate and location at which it occurs. In particular, weathering and fluvial entrainment act to erode the bank on an annual basis with the potential for significant mass failures over timescales greater than 1 year. Additional factors such as bank side vegetation, burrowing animals and human bank protection are also contributing to or inhibiting bank erosion, although the relative importance of each factor is unknown.

Bank erosion in the Wharfe predominantly occurs during the winter months and the rate of bank erosion varies between banks. There appears to be a clear difference between erosion rates on banks found in straight channel sections and those in curved channels. This suggests that channel curvature contributes to enhance erosion rates. This relationship is explored further in Section 6.2.3. On an annual basis the average erosion rate, due to weathering and fluvial entrainment processes only, is around 70 mm $year^{-1}$ for straight channels and between 180 and 211 mm $year^{-1}$ for curved channels. These values are in the same range as those presented by Couper and Maddock (2001). They demonstrated that high rates of erosion (181 mm $year^{-1}$ on the River Arrow, Warwickshire) can occur from sub-aerial processes alone. This study supports the finding that short-term bank erosion rates found in the Wharfe system are largely the result of sub-aerial and fluvial entrainment processes.

Data from the bank top re-surveys indicates that retreat due to mass failures can significantly increase bank retreat rates. Failure from one event resulted in retreat of 750 mm. This is around 2.5 times greater than annual rates from sub-aerial and fluvial processes. Yet these events occur less frequently with approximate return periods estimated at greater than every 2-years. Evidence from photography indicates further large scale bank erosion has occurred in the Wharfe system in the past.

4.5 CHANNEL CURVATURE

The Wharfe can be described as meandering with 19 distinct bends noted from the channel surveys. As discussed more fully in Section 2.5, channel sinuosity is important for: (1) hydraulic processes with bends acting as form roughness, that reduces the conveyance of discharge downstream; (2) sediment transport processes as bars on the inside of meander bends form short-term sediment stores; (3) bank erosion which is driven by the hydraulic conditions created as flow is forced to the outer bank around a bend; and (4) channel migration through the combined effects of outer bank erosion and inner bank deposition. As such, the sinuosity of the channel is an important parameter to quantify to aid with our understanding of channel processes (Sections 6.2.2 and 6.2.3) and when modelling bank erosion / migration processes (Section 7.2.3, Section 7.2.4 and Section 8.4.4). The radius of curvature of a bend can used to quantify the channel's sinuosity.

4.5.1 CALCULATING RADIUS OF CURVATURE

The radius of a circle, sphere or ellipsoid is the distance from the centre to the outside edge or surface. Along a curve, the radius of curvature at a given point on that curve is defined by the radius of the circle fitting the curve. Thus, as shown in Figure 4.17, smaller circles fit in tighter curves (point b) whilst larger circles fit on shallower curves (point a). On a perfectly straight line, circle size is infinitely large. Radius of curvature can be calculated using the calculus definition, whereby curvature is the change in direction with distance.

Figure 4.17: Curves with different radius of curvatures.

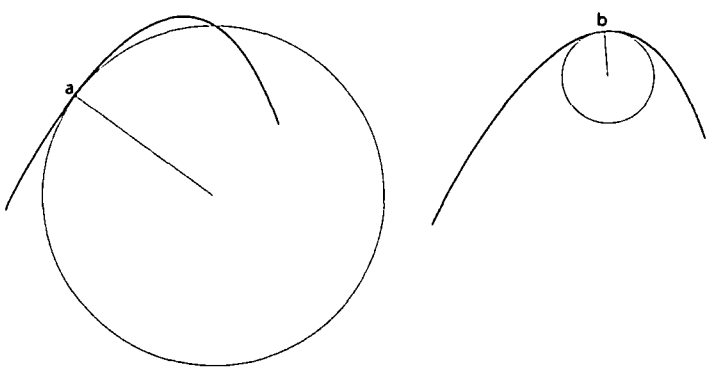

To calculate the radius of curvature of points along the Wharfe, the channel centreline was initially drawn and expressed as discrete points. This was done in ARC GIS using an OS Land.Line map (1:10,000) overlaid onto a 2 m resolution LiDAR image of the reach provided by the Environment Agency for Reid (2004). The centre of the channel was digitised by eye from the LiDAR image as a vector line and then converted into points with the spacing between points ~2 m. For each of the digitised centreline points, the direction of the flow from one point to the next was calculated in radians. Care had to be taken to account for direction changes from a north-east direction to a north-west direction because the spectrum of angles moves from 1^0 to 360^0. This direction change should be -1 degrees, but the calculation returns 359 degrees. Curvature was then calculated using the direction change (∂dir) over distance (dis) as shown in [4.8]. Distance [4.9] was calculated as the length between the mid-point between the first two points ($x_{i+1} - x_i$) and the midpoint between the next two points ($x_{i+2} - x_{i+1}$). It was in effect the average length of two sets of successive points. Finally, the radius of curvature (c_r) of a particular point was derived as 1 divided by curvature, since 1 radian subtends an arc equal in length to the radius of the circle, the reciprocal of the curve.

$$c_r = 1/\left(\frac{\partial dir}{dis}\right) \qquad [4.8]$$

$$dis = \frac{(x_{i+1} - x_i)}{2} + \frac{(x_{i+2} - x_{i+1})}{2} \qquad [4.9]$$

Initial attempts at calculating radius of curvature were problematic due to the fine spacing of the centreline points. This made the direction and curvature calculations profile plots noisy. As such, the channel centreline was re-digitised but with a coarser spacing of 9.8 m. Even with this coarser spacing, the results were still rather noisy and hence the data was smoothed. Various smoothing options were tested including 3, 5 and 7 point moving average smoothing on the curvature results and the same again on the direction results. The 3 point smoothing on the directions gave the best results (Figure 4.18b). This smoothing meant that the direction changes and curvature values were calculated over an average distance of 28 m. Since channel width ranged from 12 m to 33 m with an average of 17 m,

this spacing was thought to be sufficient to represent the bends in the channel. Figure 4.18 shows the effect that the smoothing had on the direction results. Here, the direction of the flow can clearly be seen with the river flowing predominantly in a south and east direction. There are no locations where the channel flows north, but a couple of locations where the river flows in a westerly direction. These include just after the Buckden Bridge bend and at the bend at cross-section location 510. Meanders are represented by sudden direction changes. Figure 4.18c shows the curvature of the channel which is used to calculate the radius of curvature in Figure 4.18d. In Figure 4.18c, the high positive and high negative curvature values indicate the tightest bends, with positive bends turning left and negative values indicating a bend flowing right. In Figure 4.18d, low values of radius of curvature indicate the tightest bends. Some notable bends are highlighted in grey.

Once the directions, curvature and radius of curvature had been calculated for the entire length of the channel, the values at each of the 60 cross-sections were extracted and carefully checked to ensure that the values represented the planform conditions at that point.

Figure 4.18: Distance and curvature calculations. (A) is the direction of flow when using the ~10 m point spacing with no smoothing; (B) is direction when using the ~10 m direction using a 3-point smoothing; (C) is the curvature calculated from the ~10 m directions and (D) is the radius of curvature calculated as 1/curvature. In D, only the lowest curvatures (i.e. tightest bends) are shown and these are expressed as absolute values to remove the negatives.

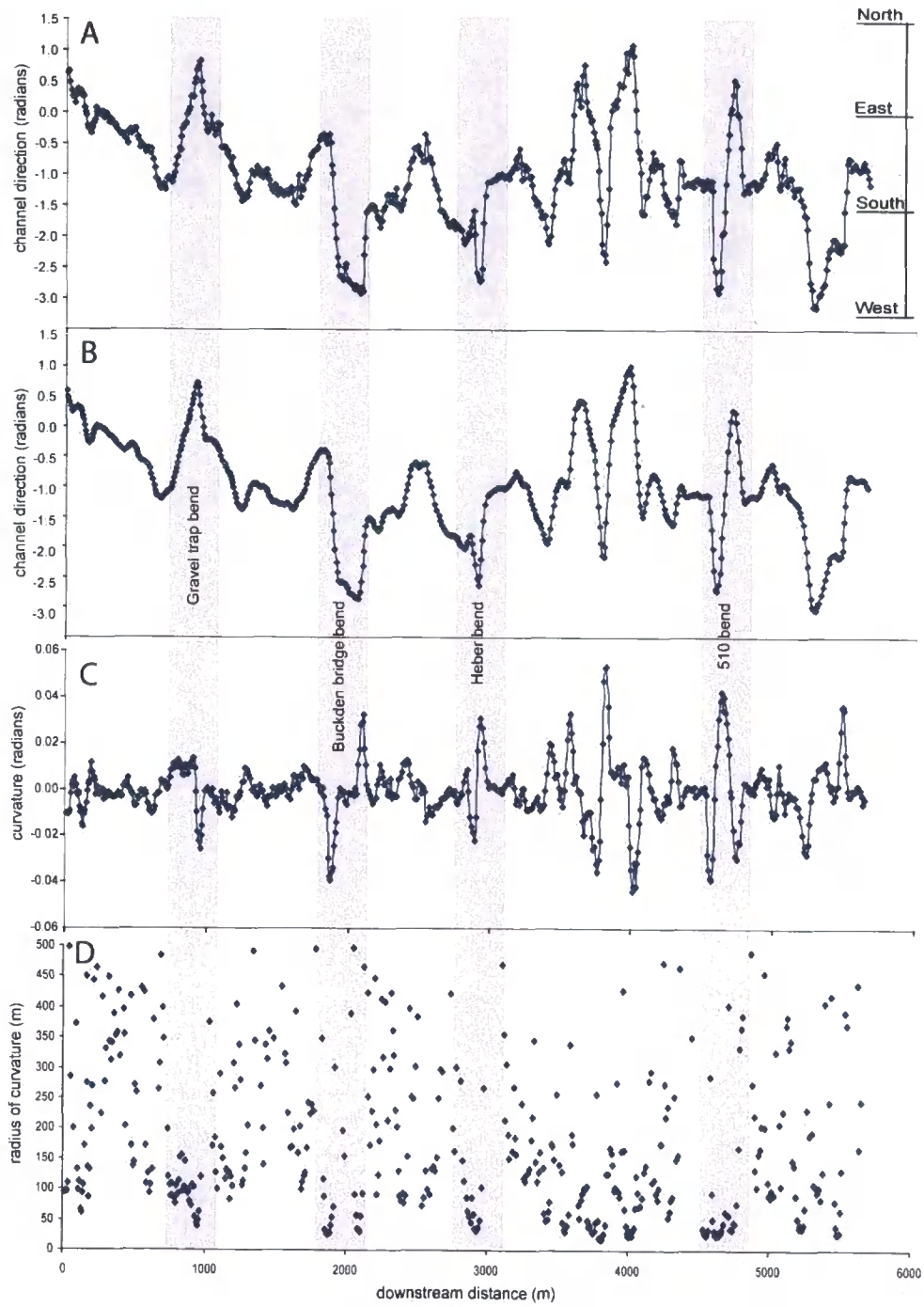

4.6 FLOW PATHS AROUND BENDS

In the previous section, the curvature of the channel's centreline was determined. However, the prevailing flow path is not always parallel to the channel's centreline and deviates towards the banks in many locations (Section 2.5). These locations are driven by channel features including lateral channel bars and meander bends. As noted in Section 4.4.5, results from the bank erosion study imply that, in the Wharfe, channel curvature has a strong influence on bank erosion rate. Hence, it is important to understand the effect that curvature has on the high velocity core of flow. Furthermore, many bank erosion and meander evolution and migration models are driven by a channel curvature parameter. This is under the assumption that curvature leads to a lateral shift in the core of high velocity flow and shear stress towards the outer bank. Bank erosion rates are then related to the high velocity and shear stress. These models are discussed fully in Section 7.4.5 with many building on the early work of Ikeda *et al.* (1981). However, the high velocity core may not be entirely correlated with the curvature as centrifugal forces carry the flow around and past the bend apex of maximum curvature. Furthermore, flow resistance features are dependent on local roughness and not the form roughness related to the bar and bed topography. Thus, high flow and shear stress can vary spatially around a meander bend. Finally, flow patterns around a meander bend may change depending on the character of increasing discharge. Thus, the high velocity flow path may change with varying levels of stage as noted by Bathurst *et al.* (1979).

It was necessary to test the extent to which the high velocity flow path followed or deviated from the channel centreline and how this was related to channel curvature. This was done using a field-based approach. These findings will aid with understanding the factors that drive bank erosion and channel planform adjustment in the Wharfe system. They also provide a justification for the bank erosion modelling approach adopted in Section 8.5.

4.6.1 MEANDER FLOW PATHS: METHODOLOGY

The high velocity flow paths around six bends of varying curvature were mapped using a differential GPS and an instantaneous velocimeter. Several bends in the study reach were unsuitable due to: (1) tree cover which restricted the use of the GPS; (2) flow depth, with two bends discounted for being too deep to measure; and (3) sluggish flow, preventing a clearly defined flow path becoming evident. The measurements took place on a day where flow was low to moderate to allow for a high velocity core to be present and visible but at the same time allowing safe measurements to take place. At higher discharges, entry to the river would have been difficult and dangerous. Thus, the findings from this study assume that the flow path at high flows is the same as that at low to moderate flows; something which is unlikely (Bathurst *et al.*, 1979). At each bend, the upper and lower limits of the measurements were determined by the flow path itself so that where no obvious fast flowing zone was located, no measurements were made. Measurements were not made in zones where bed roughness was felt to be significantly altering the flow path (i.e. were boulders protruded). This was one of the main problems encountered due to the moderate flow conditions.

To enable this to be a rapid process, the measurements were all taken at a depth held constant relative to the free surface. This was 20 cm below the surface. The maximum flow depth for these measurements was around about 1 m and the shallowest flow was around 30 cm. Thus the measurements ranged from being taken at 20% flow depth up to 66% of the flow depth. Ideally, these would have been taken at 40%. This is largely recognised as the depth of the vertically-averaged flow (Richards, 1982), as it is not greatly affected by bed roughness or friction from the free surface. However, due to the time required to measure depth and adjust the velocimeter, it was decided to hold this constant allowing significantly more measurements to be made.

The velocimeter records an instantaneous velocity and also takes an average every 30 seconds. To speed up the measurement process, a test was done to determine the length of measurement required to give results with minimal error. Ten sets of three 30-second

measurements were taken at 10 locations moving downstream. The results are shown in Figure 4.19. The standard error of each of the 10 measurements ranged from 0.0047 m^{-1} s^{-1} to 0.026 m^{-1} s^{-1} and this was deemed low enough that a single 30 second measurement at each location was taken as representative of the flow at a given location. Measurements were taken with a downstream spatial resolution of 2 m. At each location, several 30 second recordings across the channel were made to determine the highest velocity. Once this had been located, the velocity was recorded alongside the GPS location and the perpendicular distance to the bank. This was done using a tape measure with the bank top used as the bank edge to ensure consistency. This avoided any difficulties determining the bank edge in situations were bank erosion was occurring.

Figure 4.19: Determining the time period required for velocity measurements. Three measurements were made at each location. The error bars shown are standard error for each set of measurements.

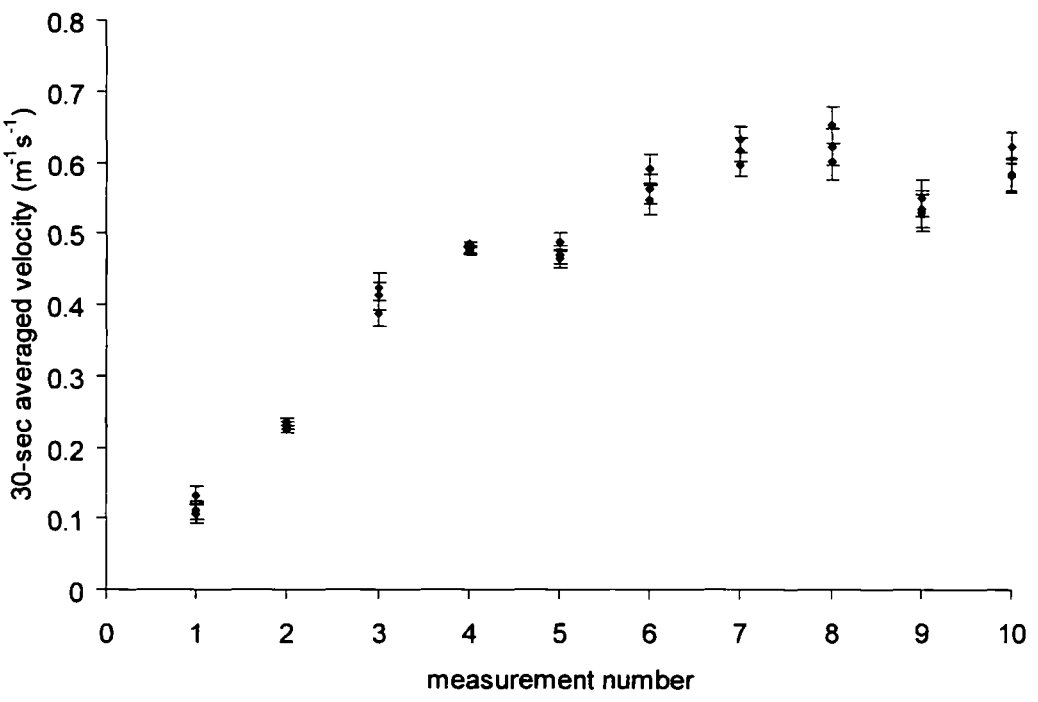

4.6.2 MEANDER FLOW PATHS: RESULTS

Figure 4.20 shows the mapped paths of highest velocity flow around the five measured bends alongside the outer bank profile and the digitised channel centreline. In all cases, the fastest flow path was found in the outer half of the channel with flow deviating towards the outer bank at some point. This data is analysed, alongside the channel curvature data from Section 4.5, in Section 6.2.2 and Section 6.2.3.

Figure 4.20: Meander flow paths for the five measured bends.

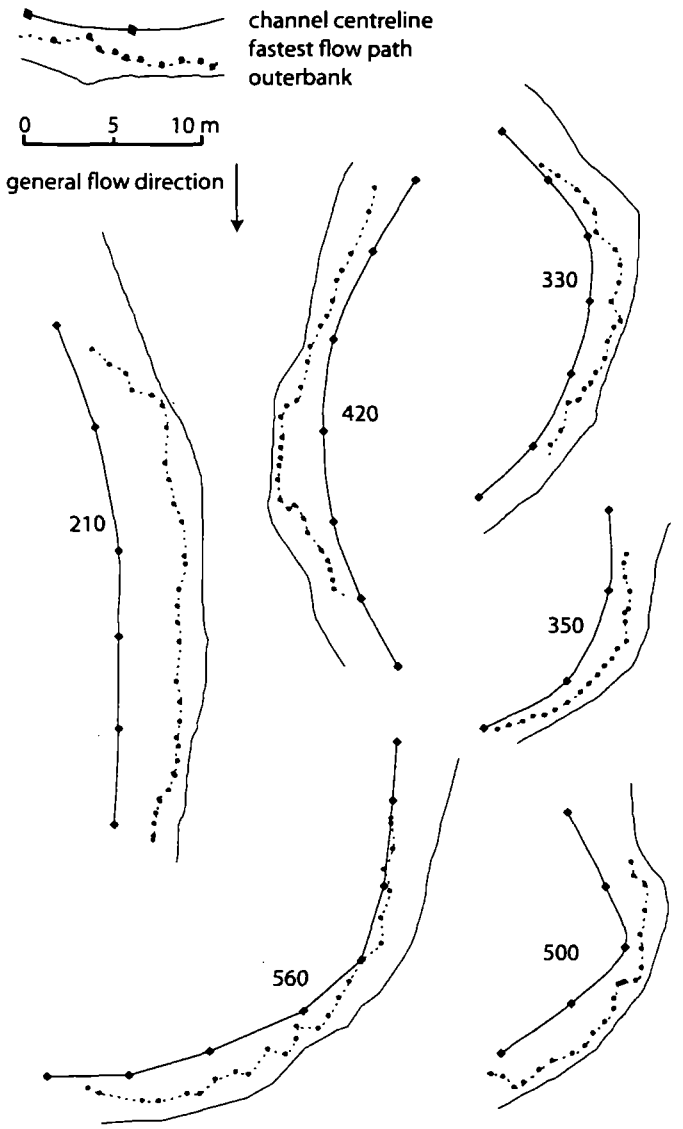

4.7 CHAPTER SUMMARY

This chapter has provided a range of data, achieving part of Objective 3. Table 4.2 summarises this data and indicates how it is used in further analysis (Chapter 6) or for modelling purposes (Chapters 7 and 8).

The field surveys were useful in providing qualitative information on processes operating in the study reach. This is used as supporting evidence for findings made from other field methods and to make inferences about processes where no data are collected. In addition, locations of features such as tributaries and bank protection were identified in the surveys. The cross-sectional surveys used a rigorous and detailed approach to provide a 6-year dataset. This data is essential during the exploration of spatial and temporal patterns of sedimentation, for reconstructing a sediment budget and as the boundary conditions for the development and application of the model. Key results from the cross-sections include: (1) the mean bed level rise in the reach, between December 2001 to July 2007, was 0.17 m ± 0.029 m; (2) the maximum rate of aggradation for a given cross-sectional reach was 0.67 m ± 0.031 m; (3) an upper and lower divide in bed level changes is evident. The reach upstream of 3000 m is notably more active. (4) Certain zones exhibit high levels of sediment activity but correspond with relatively low net change. These are zones of high sediment transfer. Data from the bank erosion study is used to understand mechanisms of lateral channel change and to develop and calibrate the model. The bank erosion study demonstrates that pins provided a good indication of small-scale, short-term bank erosion whilst the bank top resurveys capture instances of bank collapses over larger spatial and temporal scales. In the Upper Wharfe, bank erosion is more rapid on the outside of meander bends through fluvial entrainment and bank collapse. Rates of bank retreat from fluvial entrainment on bends are between 180 mm to 212 mm per year. Bank collapse resulted in 750 mm of bank retreat in a single event. Data collected on channel curvature and flow paths around bends are used to explore processes of channel change in the study reach. Additionally it is used in the development of the lateral adjustment component in the model.

Table 4.2: Data provided in Chapter 4 and its future application.

Study	Nature of Data	Future Application (Section)
Field surveys	Overview of processes	4.4: bank erosion processes 5.3: bed material characterisation
	Locations of erosion / deposition	6.2.2: evidence of spatial sedimentation patterns 8.4: qualitative evidence for comparing to model output
	Locations of bank protection	6.3: lateral estimates of bank erosion volumes 8.4: locations of bank protection in model
Cross-sectional resurveys	Boundary conditions	6.5: to provide channel capacity 8.2 and 8.3: input data for model (e.g. bedslope, width, depth) 8.4.2: lateral geometry for split channel model
	Locations of aggradation and degradation	6.2: exploring spatial and temporal patterns 8.3.2: comparing model output
	Rates of aggradation and degradation	6.3: estimating bedload transport rates 6.4: predicting bed level change using impact sensors 6.5: impact on flood risk 8.3.2: comparing model output
Bank erosion study	Rates of bank erosion	6.2.3: lateral adjustment mechanisms 8.5: comparing model output 8.7: calibrating model
	Processes driving bank erosion	6.2.3: explaining lateral adjustment 7.4.5: considering bank erosion options in model 8.4.3: developing lateral model component
Curvature	Variability in curvature downstream	6.2.2: explain spatial patterns of sedimentation 6.2.3: explain spatial patterns of bank erosion 8.5: include channel curvature into lateral adjustment model
Flow paths	Flow paths around meanders	6.2.2: explain spatial patterns of sedimentation 6.2.3: explain spatial patterns of bank erosion

CHAPTER FIVE: HYDROLOGY, SEDIMENT AND BEDLOAD TRANSPORT

5.1 INTRODUCTION

This chapter follows on from Chapter 4 in also providing data for the analysis of channel change and for model development and application. Thus, like Chapter 4, it concentrates on achieving Objective 3 but also using Objective 1, literature review, to develop sound methodological approaches. Whilst the previous chapter dealt with monitoring channel morphology, this chapter focuses on the factors driving channel change. First, the discharge regime is quantified (Section 5.2). Second, the character of the bed material in the Wharfe is determined (Section 5.3) and finally, data, monitoring the transfer of coarse sediment is presented (Section 5.4). Methods and results on individual data types are interpreted in this chapter with further analysis and discussion occurring in Chapter 6.

5.2 DISCHARGE DATA

Knowledge about the flow regime in the Wharfe is essential to this study as it drives sediment transport and bank erosion and allows flood risk to be quantified. A continuously varying record of flow is required. Discharge can be determined using two different methods: the Flood Estimation Handbook (FEH) (Houghton-Carr, 1999) approach; or methods based on known flow levels and ratings curves. The FEH method is a revised version of the Flood Studies Report (1975) rainfall-runoff method. This method is commonly used to give guidance on rainfall and river flood frequency estimation in the UK to river managers. This technique uses a deterministic model of catchment response to convert a rainfall input to a flow output. Tayefi (2005) used this approach to estimate the peak flow at Hubberholme. By estimating the standard percentage runoff (SPR) from neighbouring catchments with similar slope, land use and geological characteristics, three estimates of peak discharge were made. When the SPR was 60%, discharge was 36.6 $m^3 s^{-1}$, at 70%, discharge was 42.4 $m^3 s^{-1}$ and at 80%, discharge was 47.7 $m^3 s^{-1}$. With estimates

varying by 11 m^3 s^{-1} and only the maximum discharge obtained, such an approach is not very suitable for this study.

The alternative approach is to convert the records of stage recorded at cross-section 030 (approximately 300 m downstream from Hubberholme) into discharges using ratings curves. The principle here is to measure the discharge of the channel using standard velocity-area methods (e.g. Buchanan and Somers, 1969; Nolan and Shields, 2000) or using tracers including electrolytic solutions, fluorescent dyes and radio-isotopes to determine the discharge for a given flow depth. These field techniques are repeated at a range of flow depths allowing a statistical relationship between stage and discharge to be made. By extrapolating the relationship, discharges at ungauged stages can be estimated. However, the field methods used to measure discharge are often impractical, particularly in shallow, rocky reaches where flow may be turbulent or at higher flows where the use of a flow meter is dangerous. Thus the measurements often fail to represent the full range of flow conditions and curves are extrapolated to higher discharges.

The third alternative to estimating the discharge of a river, is to use empirically-derived equations that relate cross-sectional averaged velocity (v) to mean flow depth (d) and gradient (S which is sin θ) to define flow resistance. This assumes that the impediment of flow due to friction is equal and opposite to the downslope component of water weight (Ferguson, 2007). Flow depth is often replaced with the hydraulic radius (R) which is cross-sectional area ($A=wd$) divided by the wetted perimeter (Pi), w is the wetted width. Three classic flow resistance equations include [5.1] the Chèzy coefficient (C), [5.2] the Darcy-Weisbach friction factor (f) and [5.3] Manning's equation (n):

$$v = C(dS)^{1/2} \quad [5.1]$$

$$v = (8gdS / f)^{1/2} \quad [5.2]$$

$$v = d^{2/3} S^{1/2} / n \quad [5.3]$$

These equations require the resistance parameter (*C, f, n*) to be determined. This resistance comes from the skin friction which in gravel-bed rivers without submerged vegetation is characterised by the grain size. As flow depth increases, the ratio of the flow depth to grain size (*d/D*) reduces and the friction becomes less important. Two approaches that relate resistance to depth and grain size include Keulegan and Manning-Strickler. The Keulegan approach integrates the logarithmic law of the wall throughout the flow depth using the von Karman constant whilst Manning-Strickler [5.4] relates Manning's *n* to the $1/6^{th}$ power of *D*.

$$n = a_1(d / D)^{1/6} \qquad [5.4]$$

where the coefficient a_1 is typically 6.7 if D_{50} is used to represent grain size roughness, and 8.2 if using D_{84} or D_{90}.

Neither of these approaches work well in shallow flows and hence modifications and alterations have been proposed. Ferguson (2007) divides these approaches for discussion into modified logarithmic laws, generalised power laws and non-dimensional hydraulic geometry, and roughness-layer models. Yet even these modified flow resistance equations specifically designed for shallow flows (including Bathurst, 2002; Jarrett, 1984; Rickerman, 1991; Katul *et al.*, 2002; Smart *et al.*, 2002) fail at deeper flows with the predicted resistance found to be either too high or too low. Ferguson (2007) explains that the main reason behind this is that the dominant physical source of flow resistance, changes depending on the flow depth. At high flows, resistance predominantly comes from skin friction and large scale form resistance (i.e. bedfoms including bars). At low flows, form drag associated with large roughness elements becomes important. Ferguson (2007) proposes a new variable power equation (VPE) to overcome these issues and to allow velocity to be predicted using a single equation for a wide range of flows. This approach, described as follows, was applied to the Wharfe stage data to provide a stage-discharge rating curve.

The VPE equation combines roughness-layer formulations for shallow flows with the Manning-Strickler approximation of the logarithmic friction law for deep flows giving:

$$(8/f)^{1/2} = \frac{v}{(gRS)^{0.5}} = \frac{a_1 a_2 (R/D_{84})}{\left[a_1^{\,2} + a_2^{\,2}(R/D_{84})^{5/3}\right]^{0.5}} \qquad [5.5]$$

where f is the Darcy-Weisbach friction factor, v is cross-sectionally averaged velocity, g is gravitational acceleration, R is the hydraulic radius, S is channel gradient, D_{84} is the grain size at which 84% of grains are finer and a_1 and a_2 are 6.5 and 2.5 respectively as determined after calibration (Ferguson, 2007, p28).

Figure 5.1 compares the predicted ratings curves using different methods: (1) uses Manning-Strickler [5.4] with coefficients a_1 = 8.2 (MSa) and a_1= 6.5 (MSb) and the D_{84}; and (2) the VPE equation [5.5]. The value of a_1 for MSb is the same as the a_1 value used in the VPE equation. Since the stage record was for cross-section 030, the cross-sectional geometry at this location was used. Care was taken to ensure that the geometry closest to the stage measuring time period was used. Had the most recent survey been used, the deposition that has occurred in recent years would have altered the channel's cross-sectional area for the respective stage. The bed slope at this location was 0.0066 whilst the D_{84} grain size, interpolated from the grain size characteristics at 010, 040 and 080 as presented in Figure 5.14 was 0.13 m. The surface D_{84} was used rather than the active layer D_{84}. However, the equation was not that sensitive to small changes in the D_{84} used. The calculated velocity (v) was used to determine the discharge using: $Q = vA$, where A is cross-sectional area. From these three curves, the MS using a_1 = 6.5 and the VPE equation produce similar curves with the MS approach using a_1 = 8.5 producing higher discharges for the given stage. A decision to use the VPE rating curve was made. This was based on the findings from Ferguson (2007) who concluded that the VPE equation performs as well as any existing resistance law and is a useful tool for anyone wanting to predict velocity by a single equation over range of conditions.

Figure 5.1: Stage discharge ratings curve using different flow resistance equations.

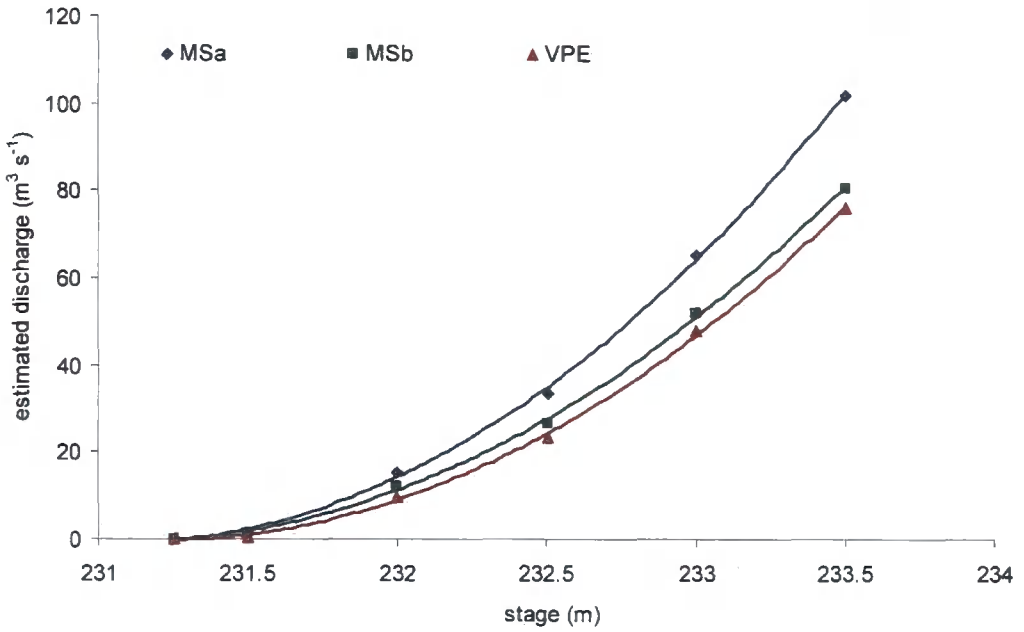

The stage discharge relationship generated from the VPE equation and shown in Figure 5.1, was applied to the stage records at Hubberholme to give a discharge record at 15 minute intervals. This was done for all records including the complete annual stage records for 1997, 2000 and 2002 and incomplete records for 2003. Calendar years rather than hydrological years were used as this provided three full years rather than only two. During these time periods the largest flood events occurred on the 19th of February and the 5th of May 1997, the 4th of June 2000 and the 14th of June and 2nd of August 2002.

Flow duration curves for each of the complete years are shown in Figure 5.2. This figure immediately highlights variations in flow regime on a year-by-year basis. 2000 was the wettest of the three years whilst 1997 was considerably drier. These variations pose a problem when selecting a flow regime for modelling purposes. Ideally the hydrological regime used in the model would represent the average annual flow conditions for a certain length of time, for example the recent decade. From the data presented in Figure 5.2 alone, it is unclear whether any of these represents the longer term flow conditions. All years may be wetter or drier than average. To explore this further, the discharge records at Flint Mill, 70 km downstream of Hubberholme were downloaded from the National River Flow

Archive (CEH). This archive provides records from many Environment Agency gauges across the UK and the data is freely available from the website for use by researchers.

Figure 5.2: Flow duration curves for Hubberholme (15 min data) (based on calendar year rather than hydrological)

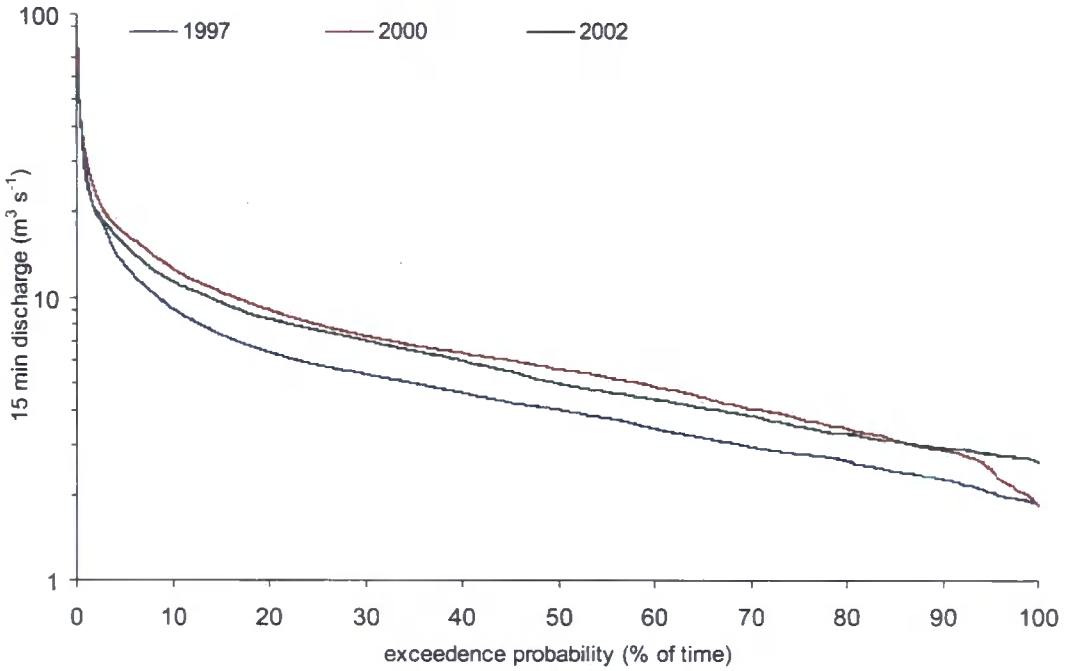

The Flint Mill records can be used under the assumption that the discharge 70 km downstream scales with the discharge at Hubberholme. The CEH record of Flint Mill extends back to 1956 and provides daily averages. By comparing the daily records at Hubberholme for the three years that data exist with the Flint Mill data for the same years, the relationship between the two sites can be compared. The relationships were linear with high R^2 values of 0.792, 0.788 and 0.798 for 1997, 2000 and 2002 respectively. The scatter in this relationship represents the lag time between peak flows, the greater level of attenuation expected as one progresses further downstream, tributary effects and spatial variability in precipitation. Despite the scatter, the Flint Mill record can provide a reasonable surrogate for daily discharge at Hubberholme provided the data required does not relate to the specific timing of events or specific discharges.

The Flint Mill record can be used to examine the regime characteristics during the three available years. Table 5.1 shows the average, maximum and minimum daily discharge at Flint Mill. Data in this table echoes the findings made from Figure 5.2 that indicate 2000 and 2002 were wetter than 1997. The average discharge for 2000 was 12.7 $m^3 s^{-1}$ higher than 1997 and the maximum daily discharge in 1997 was 160 $m^3 s^{-1}$ lower than in 2002. Furthermore, when the mean conditions over the 60-year monitoring period are compared, 1997 was noted to be drier than average and 2000 and 2002 were wetter than average. To obtain a flow regime that was representative of the longer-term average, the 15 min records for 1997 and 2002 were combined giving a "representative-hydrological period". By plotting the records at Flint Mill as flow duration curves (Figure 5.3), the representative hydrological period provides a flow duration curve similar to both the 60-year and 10-year average flow regime for the Wharfe. Thus the 1997 & 2002 record can be used as a hydrograph for further analysis and for use when modelling. Care was taken to recognise that this period was two-years.

Table 5.1: Flow characteristics at Flint Mill ($m^3 s^{-1}$).

	1956-2006	**1997**	**2000**	**2002**
Average daily Q	17.14	13.7	26.4	21.6
Max daily Q	164.8	100.1	237.7	262.8
Min daily Q	2.10	2.26	2.64	2.69

Figure 5.3: Flow duration curves at Flint Mill

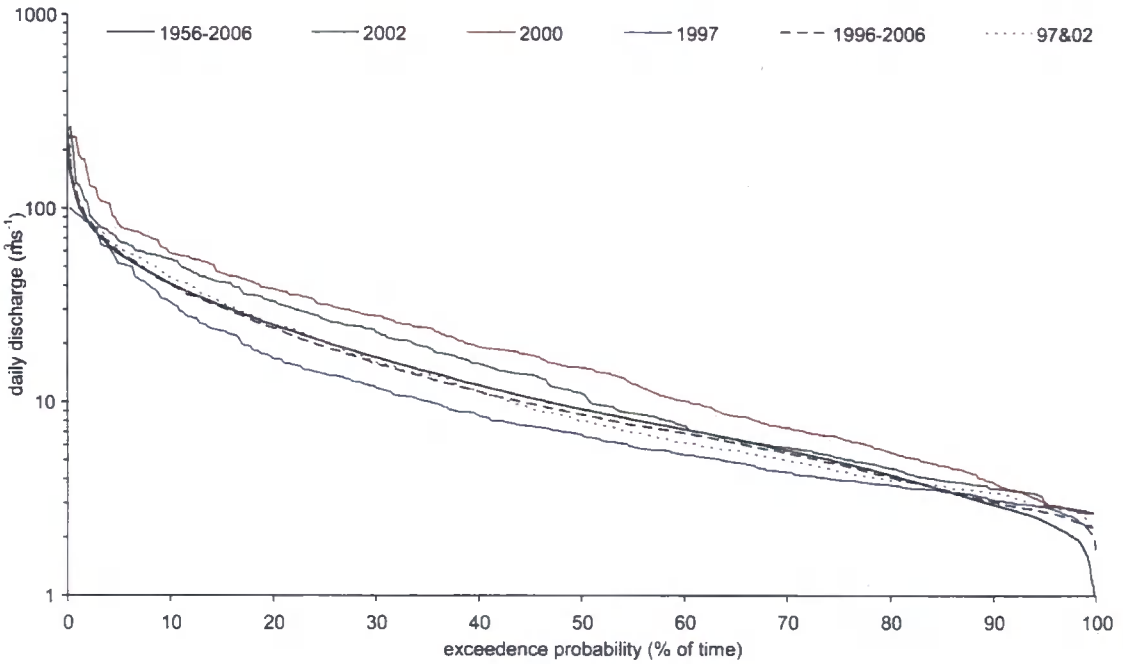

5.3 Bed Material Characterisation

It was clear from early visits to the Wharfe, and from field surveys, that grain size in the channel varied with distance downstream. It was of interest to determine the rate at which this occurred. This would provide information on: (1) downstream fining rates; (2) the significance of tributary inputs; (3) the character of deposits measured in the cross-sectional surveys; and (4) provide the model with a series of grain size distributions (GSDs) down the channel. GSDs are necessary to determine grain and flow roughness for use in calculations of flow and discharge, provide an input for bed mobilisation and bedload transport equations, and as a measure of habitat suitability for spawning fish and other aquatic organisms (e.g. Mosley and Tindale, 1985; Church *et al.*, 1987; Wohl *et al.*, 1996; Kondolf *et al.*, 2003). Previous attempts to characterise the bed material in the Wharfe were made by Powell (1992) and Milledge (2003) but low spatial resolutions and inadequate sampling strategies make this data insufficient for the purposes of this study. A new strategy to obtain this information was required.

5.3.1 SAMPLING OPTIONS

River bed material is sampled and analysed for a wide range of purposes yet accurately characterising bed material is difficult, particularly in gravel-bed rivers. Church *et al.* (1987) provides two key reasons for this:

1) Since the range of grain sizes present in gravel-bed rivers can be large, ranging over several orders of magnitude from sand to boulders, it is often impractical to use a single sampling technique (Church *et al.*, 1987; Rice and Haschenburger, 2004). This is because most sampling techniques place bias on either the coarse or the fine ends of the distribution. Coarser particles are typically associated with flow resistance and finer particles are associated with sediment transport (Petrie and Diplas, 2000). Since the accurate measurement of grain size statistics such as the median grain size (the D_{50}) requires knowledge of the whole grain size distribution, all grain sizes present in the bed must be representatively sampled (Fripp and Diplas, 1993). Thus, more rigorous sampling and analysis is required for rivers with a wider range of grain sizes.
2) Problems can arise due to the large spatial and temporal variations present in the composition of the bed (Fripp and Diplas, 1993; Crowder and Diplas, 1997). Establishing a sample size that accounts for the layered nature of the deposits and the spatial structural features of the bed such as particle clusters and imbrication is difficult (Church *et al.*, 1987). It is also often useful to sample the surface and sub-surface layers individually (Diplas and Sutherland, 1988; Diplas and Fripp, 1992; Fripp and Diplas, 1993) as their different GSDs can be linked to different river properties (e.g. the surface with roughness and the sub-surface with ecology and sediment transport).

It is therefore important to design an appropriate sampling strategy that will provide a reliable and accurate representation of a river bed's GSD. In coarse grained rivers this *"represents a substantial task"*, (Dunkerley, 1994, p255). It was also necessary to consider time and cost constraints to ensure that the sampling strategy was feasible. Kellerhals and Bray (1971) set out five key decisions that must be made in order to sample bed material

effectively. These are: (1) to select sampling sites and the time at which to sample; (2) to choose the method or methods to use to sample (and the quantities of samples required for each); (3) to choose the method of measurement (i.e. sieves, tape measures, callipers); (4) to select the method of analysis (frequency-by-weight, volume or number); and (5) to decide how to present the results. To make these decisions for the Wharfe, the literature was extensively reviewed

The first step in selecting a sampling method is to determine the purpose of the bed material data to ensure the correct field measurements are made (Hey and Thorne, 1983; Dunkerley, 1994). Whilst one measure of grain size such as the D_{84} (the grain size of the 84th percentile) may be adequate for estimating roughness, knowledge of the full grain size distribution is necessary for modelling the fractional transport of sediment. Furthermore, it is often important to characterise the surface and sub-surface layers of sediment separately to provide a more complete description of the bed and to allow an active transport layer GSD to be determined. Hence, sampling techniques that represent both the coarse and fine end of the distribution are required for both the surface and sub-surface layers of the Wharfe to provide roughness values and input data for sediment transport modelling.

Various sampling methods are available and excellent reviews of these are given in papers by Church *et al.* (1987) and Kondolf *et al.* (2003). Surface sampling techniques were broadly grouped by Church *et al.* (1987) into: (1) pebble and grid counts; (2) areal sampling; and (3) volumetric sampling. The first technique uses some variation of Wolman's (1954) pebble count technique; perhaps the most popular surface sampling method. It involves sampling a pre-determined number of particles under a grid or in approximately even-spaced increments such as a step (the Wolman walk). This technique has the advantage of being cheap and easy, requires no lab time and provides a more representative sample of an entire sample site than other methods (Wolman, 1954). However, it is limited to larger particles which can be picked up (e.g. Wolman, 1954; Diplas and Fripp, 1992; Fripp and Diplas, 1993; Green, 2003). This introduces a sampling bias towards coarser material (Marcus *et al.*, 1995).

The second technique, areal sampling, typically uses an adhesive such as clay or wax to remove the surface layer in a predefined area. The number or weight of particles in each size class are then quantified using sieves and templates. This technique requires both field and laboratory time and is unsuitable for particles greater than 40 mm. Diplas and Fripp (1992) found that the adhesive fails to lift these particles. However the surface layer can also be removed by hand, allowing larger particles to be sampled. This can be done by eye or using spray paint to distinguish the surface layer from its substrate. More recent approaches have used photographic techniques to classify surface grain sizes through areal sampling. Some variations using photography include using emulsion-based photographic data capture (e.g. Rice and Church, 1988), photo-sieving (Ibbeken *et al.*, 1998) and digital image processing (Butler *et al.*, 2001). However, these photographic measurements are commonly biased with respect to the actual measurement since there may be partial hiding of the clast by sand, shadow or another clast (Adams *et al.*, 1979) or due to the imbrication angle (Church *et al.*, 1987; Kondolf *et al.*, 2003).

The third technique is that of volumetric sampling where a sample with known volume (typically the depth of the D_{max}) is removed using one of several techniques. These include using a spade or a backhoe, freeze-core sampling or using cylindrical core samplers or "cookie-cutter" samplers for sampling underwater (Klingeman and Emmett, 1982; Kondolf *et al.*, 2003). However, since a surface layer does not occupy a predetermined volume (due to surface voids) (Kellerhals and Bray, 1971), it is difficult to get an accurate volumetric sample particularly in coarse beds. The obtained sample is analysed using sieves and the results are displayed in terms of frequency distribution by weight.

Areal and volumetric sampling can both be termed bulk sampling. Bulk sampling is considered by Diplas and Sutherland (1988) to be the most traditional or standard sampling procedure and the only truly unbiased technique that represents the entire GSD. Yet it is sometimes un-feasible to obtain adequate samples in very coarse sediment where the particles may be too heavy to lift and the sample size required may be too large (e.g. Church *et al.*, 1987). It is also labour and time intensive and a single sample is unlikely to represent an entire reach (Mosley and Tindale, 1985). Hence, multiple samples are required

which often places too much demand on resources. Sub-surface sampling typically involves removing the surface layer and obtaining a volumetric or areal sample of the underlying sediment in the same way as sampling the surface. The analysis and advantages and disadvantages are the same as sampling the surface.

5.3.2 SAMPLING STRATEGY

With no one approach being ideal, it was decided that a combination of techniques should be used to sample the Wharfe. Time consuming and labour intensive bulk samples of the surface and the sub-surface would be carried out at limited sites downstream whilst relatively quick and easy pebble counts would be done at multiple sites including the bulk sample sites. Using hybrid approaches to reduce bias at either the fine or coarse end of the material and to sample the surface and sub-surface to reconstruct the entire GSD is a common procedure (e.g. Diplas and Fripp, 1992; Fripp and Diplas, 1993; Casagli *et al.*, 2003; Rice and Haschenburger, 2004).

Field surveys were consulted to select sampling sites: 16 pebble counts; and three for bulk sampling. The locations of these sites are shown in Figure 5.4. The chosen sites were spaced at roughly even intervals down the river with all bulk sites corresponding to a pebble count site. The selected locations were areas of exposed gravel, typically point and lateral bars, which made sampling easier and removed potential biases from elutriation due to sub-aqueous sampling (Marcus *et al.*, 1995). Hence the sampling took place in the summer when the river was at its lowest flow. The sampling of bars at low flows is common (e.g. Church and Kellerhals, 1978; Marcus *et al.*, 1995). Since the upper-most bar at Hubberholme consisted of very coarse sediment and some boulders (> 1 m), bulk sampling was not feasible and hence the most upstream bulk sample was carried out 800 m downstream between cross-sections 070 and 080 where the sediment had fined sufficiently to allow a bulk sample to be measured. At each site, judgement was used to select the precise sampling area so that it was representative of the majority of the bar. The most downstream sampling site was at cross-section 540. Further downstream, there were no exposed sediment bars.

Figure 5.4: Bed material sampling sites.

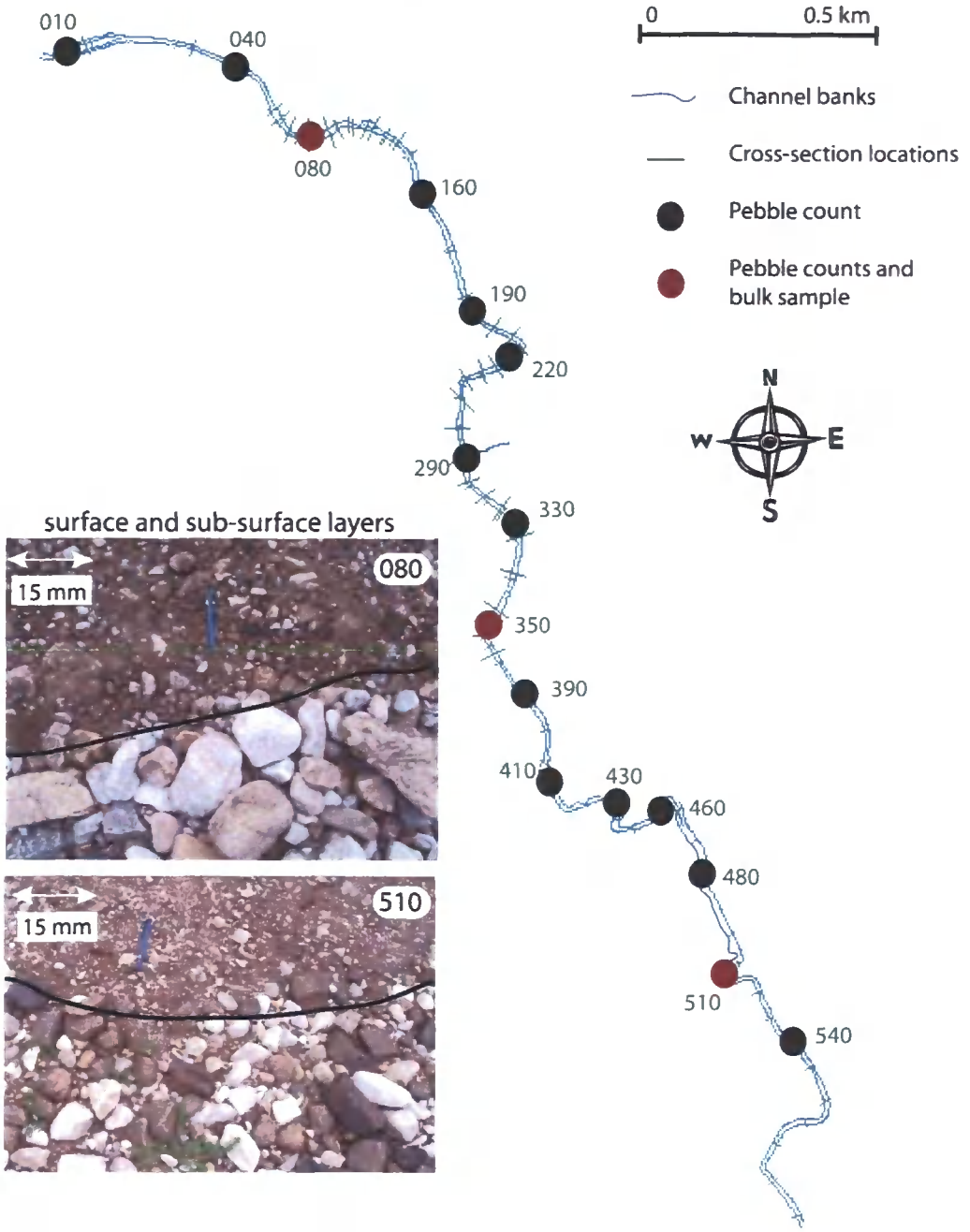

Templates and sieves were used to classify the sampled material into grain size classes. A square gravelometer (Figure 5.5) was used instead of a round one to allow consistency with the square sieves. It was felt that using measuring tapes or callipers would take too much time. A tape measure was only used on the very largest boulders (>-8 Φ or 256 mm). The material was classified according to the Wentworth scale and corresponding *phi* scale

which defines grain size classes in millimetres or *phi* units respectively (Table 5.2). These whole units increase by powers of 2 and [5.6] and [5.7] show the relationships between the two scales. The gravelometers used ranged in size from -3 Φ up to -8 Φ in half *phi* units. -5 Φ and -4.5 Φ field sieves were used and sieves for every half *phi* unit above 0.5 Φ were used in the laboratory. 0.5 Φ was chosen as the lower boundary as it typically represented less than 1% of the samples. Most of the data are presented in millimetres.

Figure 5.5: Square gravelomenter template used for sampling

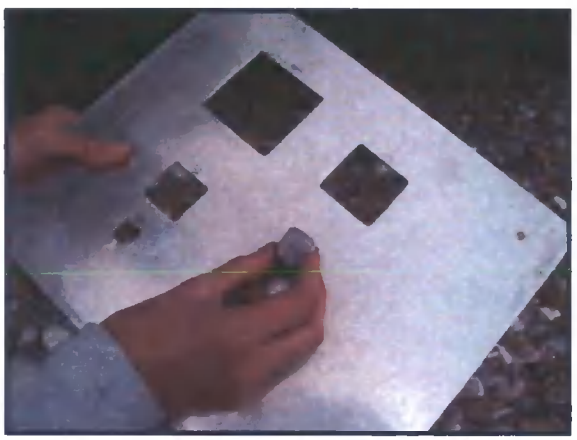

Table 5.2: Wentworth scale for grain size class

	Size in *(D)* mm	*Phi* scale *(Φ)*
Large Cobbles	< 256	-8
	< 181	-7.5
Small Cobbles	< 128	-7
	< 90	-6.5
Very coarse gravel	< 64	-6
	< 45	-5.5
Coarse gravel	< 32	-5
	< 23	-4.5
Medium gravel	< 16	-4
	< 11	-3.5
Fine gravel	< 8	-3
	< 6	-2.5
Very fine gravel	< 4	-2
	< 2.8	-1.5
Very coarse sand	< 2	-1
	< 1.4	-0.5
Coarse sand	< 1	0
	< 0.7	0.5

$$D = 2^{-\phi} \qquad [5.6]$$

$$\phi = -\log_2 D \qquad [5.7]$$

where D is the grain size diameter in millimetres and ϕ is grain size diameter expressed as *phi*.

5.3.3 Pebble Counts

A Wolman walk was chosen over the grid method since it allowed the entire bar to be sampled and no additional field equipment (i.e. the grid) had to be constructed. The selection of grains to be sampled was determined by walking a series of transects down the gravel bar. Only one person carried out all the counts to avoid user-dependent bias which can significantly alter results (Hey and Thorne, 1983; Marcus *et al.*, 1995; Wohl *et al.*, 1996). At sites where bulk samples were taken, the bulk sample was obtained in the middle of the pebble count transects. At every step, the sampler's index finger was placed by the sampler's shoe with closed eyes. The grain that lay beneath the finger was removed and measured. This means that the smallest particle size that can be consistently sampled is limited by the researcher's finger and is typically around 10-15 mm (Wolman, 1954; Diplas and Fripp, 1992; Fripp and Diplas, 1993). Tweezers could have been used to reduce this size to 8 mm (Wolman, 1954; Kondolf, 1996). To avoid falling over the boulders at the most upstream bar, a tape measure was used instead of pacing and grains every 1 m were measured. This spacing was such that no particle was sampled twice. The intermediate or b-axis of the selected grains was placed through the gravelometer. When the particle was too large to lift or partially buried, a crude estimate was made. This problem only occurred at the most upstream bar. The measured pebbles were placed into ½ *phi* size classes.

There is much debate over the number of pebbles required to provide a good representation of the surface material. Wolman (1954) originally suggested that 100 pebbles were sufficient and Kondolf (1996) supports this recommendation. However, others suggest differently. For example Hey and Thorne (1983) found that 40 clasts were sufficient, Church and Kellerhals (1978) measured 50 pebbles whilst Rice and Church (1996) suggest at least 400 are required. With such variations, a preliminary investigation was carried out on a bar mid study reach to determine the most appropriate number for this study.

This involved measuring four sets of 100 pebbles and determining the variation between the D_{50} and D_{84} from each set. Figure 5.6a shows each sets GSD and shows that some variations were present. The D_{50} and D_{84} reduced as the sampling progressed and as the

total number of sampled increased. Yet had the order in which the sets of pebbles were sampled changed, the reduction in D_x as sample size increased, might not have been present. It was therefore necessary to test the variability within the dataset. This was done computationally by randomly sampling eight sets of 100, 150, 200, 250 and 300 grains from within the measured sample of 400 grains. This technique called bootstrapping was used by Rice and Church (1996) to determine the percentile standard errors for large samples. In this investigation, the D_{50} and D_{84} values were noted from each re-sample and the standard deviation between values was found. These values are shown in Figure 5.6b. This graph clearly shows that increasing the number of pebbles sampled reduces the error associated with the D_{50} and D_{84}. It also shows that the variation within the D_{50} is much less than the D_{84}. From this procedure, it was decided that 200 pebbles would provide sufficient precision without being too time consuming. Hence 200 pebbles were counted at the 15 other sites down the river. This was double the number of pebbles adopted by previous researchers for sampling the Wharfe (Powell, 1992; Milledge, 2003).

Figure 5.6: Variability in grain size distributions and grain size characteristics between sets of pebble counts. GSDs are presented on a linear scale to make differences between sets more visible.

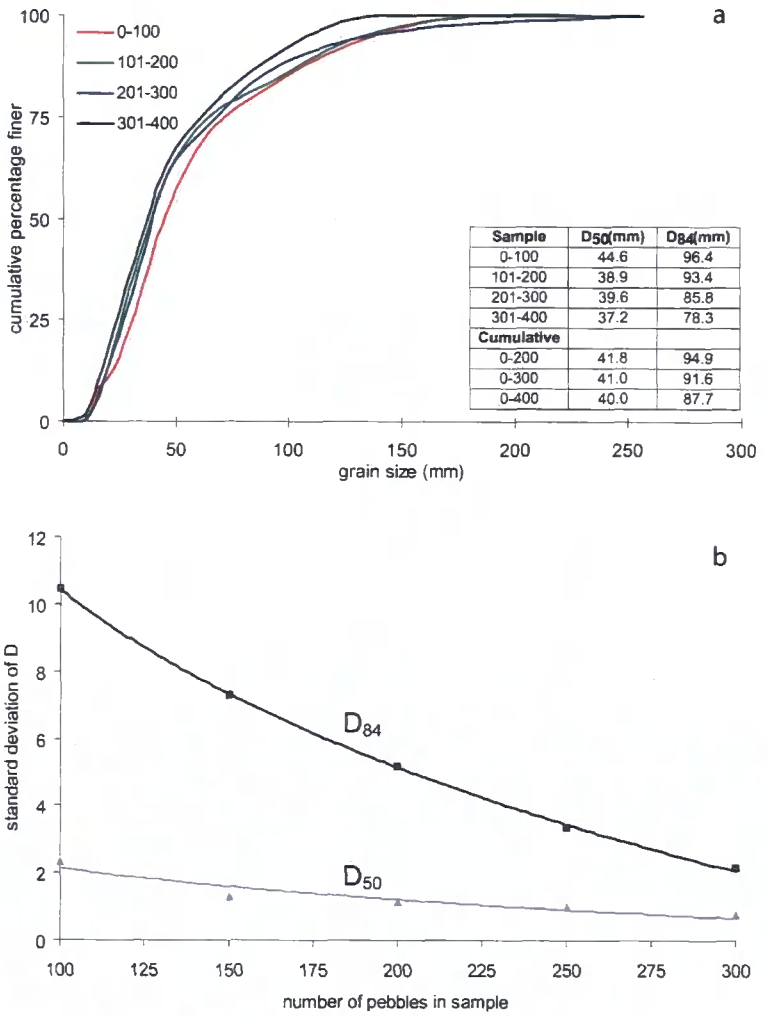

Sample	D50(mm)	D84(mm)
0-100	44.6	96.4
101-200	38.9	93.4
201-300	39.6	85.8
301-400	37.2	78.3
Cumulative		
0-200	41.8	94.9
0-300	41.0	91.6
0-400	40.0	87.7

5.3.4 Bulk Samples

Bulk samples were taken from the surface and sub-surface of three sites corresponding to pebble count locations. Determining the mass of a sample needed to provide the accuracy and precision of the required data is difficult due to the spatial and temporal variations found in gravel-bed rivers (Gale and Hoare, 1992). Increasing sample size increases sample accuracy by incorporating more spatial variations but this increased accuracy is at greater costs in terms of labour and time. Hence a balance must be struck and the sample size obtained should depend on what type of data is needed (just the D_{50} or the entire GSD),

what the distribution is like (i.e. fine or coarse) and what level of accuracy is required (Dunkerley, 1994; Ferguson and Paola, 1997). As Church and Kellerhals (1978) suggest, the results from computational procedures can be very sensitive to the GSD input and it is important to obtain the correct precision of data (Klingeman and Emmett, 1982; Carling and Reader, 1982).

There are numerous recommendations about what the adequate sample size is. Early work followed standards specified by the American Society for Testing Materials (ASTM, 1978) or the British Standards Institution (BSI, 1975). The ASTM suggested that a 50 kg sample is adequate when the D_{max} is 25 mm and 175 kg sample is needed when the D_{max} is 90 mm. The BSI suggested 2 kg and 50 kg were adequate when the D_{max} was 20 mm and 63 mm respectively. Both these standards vary greatly. Later, Mosley and Tindale (1985) suggested that the largest clast in a sample should represent <5% of the total sample mass. However, Church *et al.* (1987) set the standards to which most researchers since have followed (e.g. Gale and Hoare, 1992). They devised their sampling criterion by testing splits of data from a single moderately large sample (33.5 kg). They initially concluded that the largest clast should constitute no more that 0.1% of the total sample size. However for coarse gravel channels such as the Wharfe where the largest grains are around 6 kg, this would require a 6 tonne sample. Hence Church *et al.* (1987) relaxed this criterion and suggested that a 1% criterion should be used instead for samples that have a D_{max} greater than 32 mm. Based on this, over half a tonne of sediment is still required to achieve this target: a difficult but achievable task.

The sampling method involved determining the weight of the D_{max} and estimating how many bucket loads of sediment were required to reach the Church *et al.* (1987) criterion. Target weights were: 7 kg (surface) and 2.25 kg (sub-surface) for cross-section 080, 6.25 kg (surface) and 4 kg (sub-surface) for 350, and 1.5 kg (surface) and 0.5 kg (sub-surface) for 510. The top surface of the gravel was lifted by hand and placed via buckets onto a large tarpaulin (Figure 5.7a) until the target weight had been collected. The sub-surface remained damped allowing it to be distinguished from the surface. This areal sampling approach removed problems associated with surface voids when obtaining a volumetric

sample. Once the required weight had been removed, the sorting process began. This involved using the Wolman template and field sieves to sort the sediment into ½ phi units (Figure 5.7b). Each grain size group above 23 mm was weighed and recorded and the finer sediment was placed into a pile and carefully mixed together. A sub-sample was then taken back to the laboratory for finer sieving and weighing down to 0.7 mm. The remaining sediment was weighed. Drying was not necessary as the sampling was carried out on a dry day and even the damp sub-surface was dry when the sample was taken. This process was repeated for the sub-surface layer of sediment with an areal sample being taken.

Figure 5.7: Photos taken at site 350 showing (a) the bulk sample and (b) coarse sediment sorted into piles, then weighed in the bucket using a spring weight.

5.3.5 Combining the Data

Following basic data collection, the pebble counts and bulk samples were analysed by calculating the percentage of material that was finer than each of the grain size classes. This was done at each site for each data type: pebble counts, surface bulk samples, sub-surface bulk samples. Certain initial findings could be made after plotting the three data sets together, as shown in Figure 5.8. Firstly, the surface material was much coarser than the

sub-surface and very little sand was present within the samples. The ratio of surface to sub-surface D_{50} was between 1.6 and 4 with an average of 2.4. These results echo those of Parker *et al.* (1982) who found the ratio to be between 1.5 and 3.0 with 2.0-2.5 being the most common. Church *et al.* (1987) described a coarser surface layer as a near-universal feature of gravel bed rivers. It can be attributed to either the winnowing of surface fines or as a result of "equilibrium transport" (Andrews and Parker, 1987) where large and relatively immobile grains become concentrated on the surface. These grains become more exposed whilst the fines fall between the coarse grains, so gaining shelter from the prevailing flow.

Figure 5.8: GSDs when using the pebble counts and surface and sub-surface bulk sampling approaches.

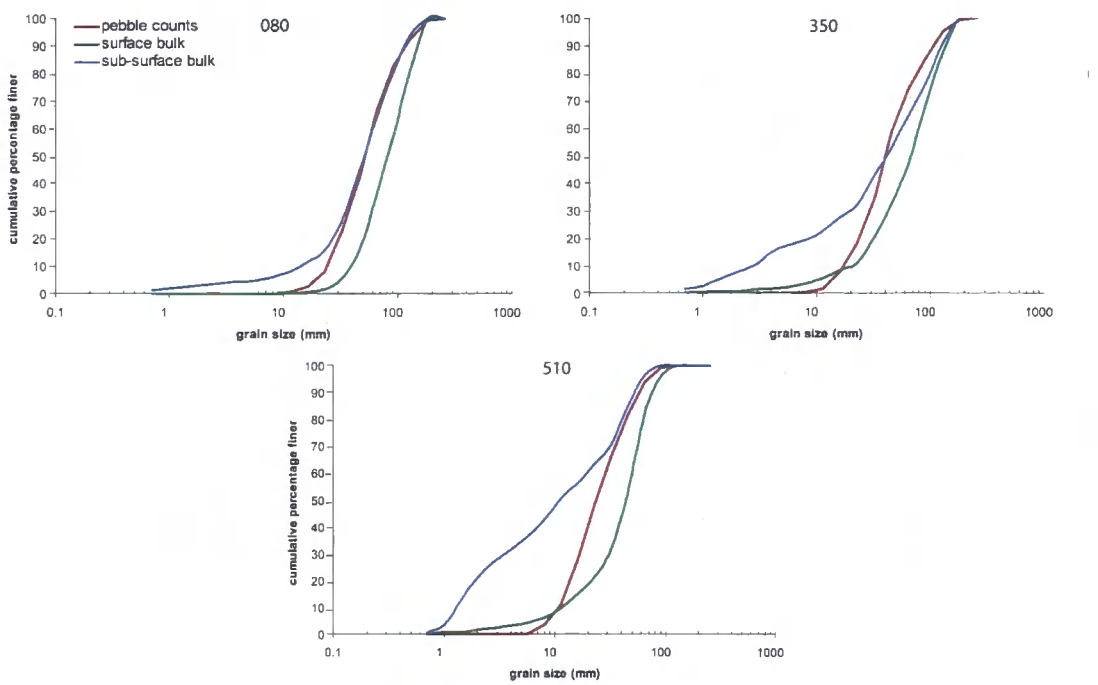

A second interesting finding shown in Figure 5.8 was that the pebble count GSDs were much finer than the surface bulk sample. Theoretically, as the samples have measured the same thing, the results should be the same. This difference was initially surprising particularly since most of the literature demonstrates that pebble or grid sampling produces coarser GSDs than bulk sampling due to sampling bias (e.g. Kellerhalls and Bray, 1971; Church *et al.*, 1987; Diplas and Fripp, 1992; Fripp and Diplas, 1993). There are three

possible explanations for this discrepancy. First, it could be attributed to sampling bias where the sampler is selective towards the finer grains on the pebble count. Second, since the surface layer was lifted by hand for bulk sampling, some of the finer particles may have fallen onto the sub-surface layer. This would lead to a coarse surface layer. However, with so little fines, this seems a difficult sampling error to make at a large scale. Finally, this could be due to the differences between the nature of the data. The pebble counts are frequency-by-number whilst the bulk samples are area-by-weight. They can therefore not be compared directly and require transformations. To confirm this theory, an additional pebble count was done where the pebbles were counted and weighed and the D_{50} and D_{84} values were compared. The results shown in Table 5.3 confirm that when weighing the grains the GSD characteristics are much coarser than when counting. This supports the earlier finding in Figure 5.8 that the pebble count results are finer than bulk samples, and that this difference is partly due to methodological issues.

Table 5.3: D values when measuring the same sample using frequency by number and frequency by weight.

	Frequency by number	Frequency by weight
D_{50} (mm)	49.0	91.6
D_{84} (mm)	86.7	121.0

The inability to compare results produced by different sampling techniques directly is a common problem (e.g. Leopold, 1970; Kellerhals and Bray, 1971; Church *et al.*, 1987; Diplas and Fripp, 1992). It is therefore necessary to convert the data into one comparable form. This is typically volumetric values (Kellerhals and Bray, 1971; Fripp and Diplas, 1992). Kellerhals and Bray (1971) were the first to proposed formal conversion factors to convert sampling results for comparison. Kellerhals and Bray (1971) used a void-less cube model made of three different sizes of cube randomly packed together. By analysing the cube, the relationship between different sampling procedures was deduced and formal conversion factors were found. The general conversion factor taken from Church *et al.* (1987) is:

$$f_{ci} = \frac{f_{oi} D_{gi}^{x}}{\{\sum_{i=1}^{n} f_{oi} D_{gi}^{x}\}} \qquad [5.8]$$

where f_{oi} is the observed population of the sample in the ith size class with mean size D_{gi}, x is the integer dimension required for the conversion, n is the number of size classes and f_{ci} is the sum of the converted sample.

Using [5.8], Kellerhals and Bray found the following conversion factors:

a) frequency-by-number to volume-by-weight: x = 0
b) frequency-by-weight to volume-by-weight: x = -3
c) area-by number to volume-by-weight: x = 2
d) area-by-weight to volume-by-weight: x = -1

These conversion factors suggest that pebble count data (i.e. frequency-by-number) can be directly compared with volumetric sample data (e.g. volume-by-weight) since the conversion factor is 0. However, whilst the Kellerhals and Bray (1971) conversions have general stood the test of time with few alterations, many suggest that the conversions overcompensate and do not account for the packing of heterogeneous sediments, patterns of voids or the non-random exposure of ellipsoidal grains (e.g. Profitt and Sutherland, 1980; Diplas and Sutherland, 1988; Marion and Fraccarollo, 1997). Hence, different conversion factors have been proposed. For example, Diplas and Sutherland, (1988) refined the Kellerhals and Bray model to include voids and porosity and found that the area-by weight conversion should be -0.47 rather than -1. More recently, a new model by Marion and Fraccarollo (1997) found a conversion value of x = -0.41 for areal sampling to be the best for bimodal mixtures; in agreement with the Diplas and Sutherland model. However, they argue that the value of -0.47 sometimes breaks down in natural mixtures and this suggest that the x value can vary greatly making the selection of the appropriate conversion value difficult without justification. Consequently, conversion factors specific to the Wharfe sediment were required.

5.3.6 Converting the Data

The data obtained from fieldwork included: (1) numerous surface pebble-count distributions which fail to represent the finer material; and (2) limited bulk samples of the surface and sub-surface which provide good GSDs including the finer material. It was therefore necessary to link the pebble count data to the bulk data to allow the multiple pebble counts to be converted into volumetric samples at numerous sites downstream. This would provide the data in a form suitable for future analysis and modelling. Several steps were used to manipulate the data. These steps are shown in Figure 5.9. The discussion that follows justifies the decisions made for each of these steps.

Figure 5.9: Steps required to manipulate data into appropriate form

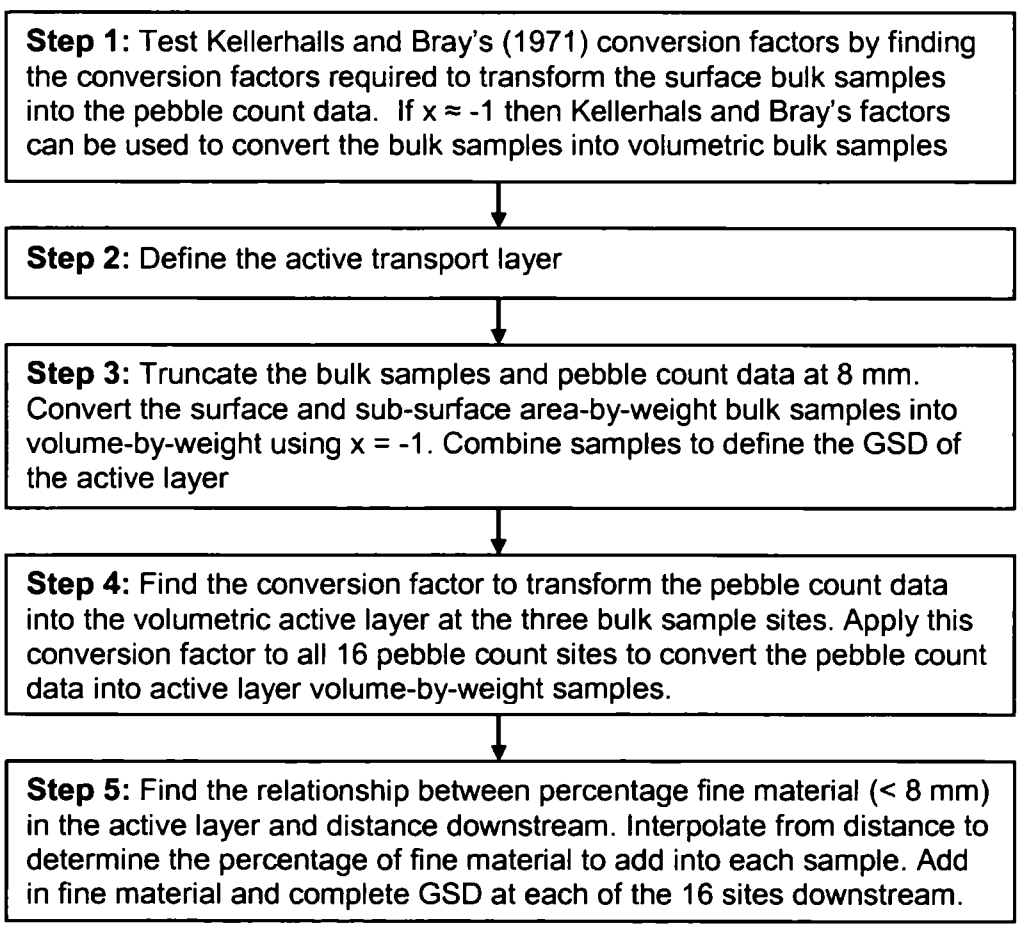

Step 1: Testing conversion factors

The first step was to convert the surface area-by-weight samples into the appropriate form for modelling: volume-by-weight. Kellerhals and Bray (1971) suggest that frequency-by-number data (i.e. pebble counts) can be directly compared with volume-by-weight data (conversion factor x = 0). Hence using Kellerhals and Bray's findings, if the area-by-weight data is converted into volume-by-weight using their conversion factor of x = -1, it should theoretically be the same as the pebble data. To test whether the Kellerhals and Bray conversion factors are applicable, equation [5.8] was used to find the best values of x to convert the surface areal samples into their corresponding pebble counts. Since the pebble count data poorly represents the fine material due to selection bias, the pebble and bulk data were truncated at 8 mm to remove these fine grains. Figure 5.10 shows the GSDs before and after conversion.

Figure 5.10: GSDs before and after conversion. P denotes the pebble count data and C denotes the converted surface bulk samples.

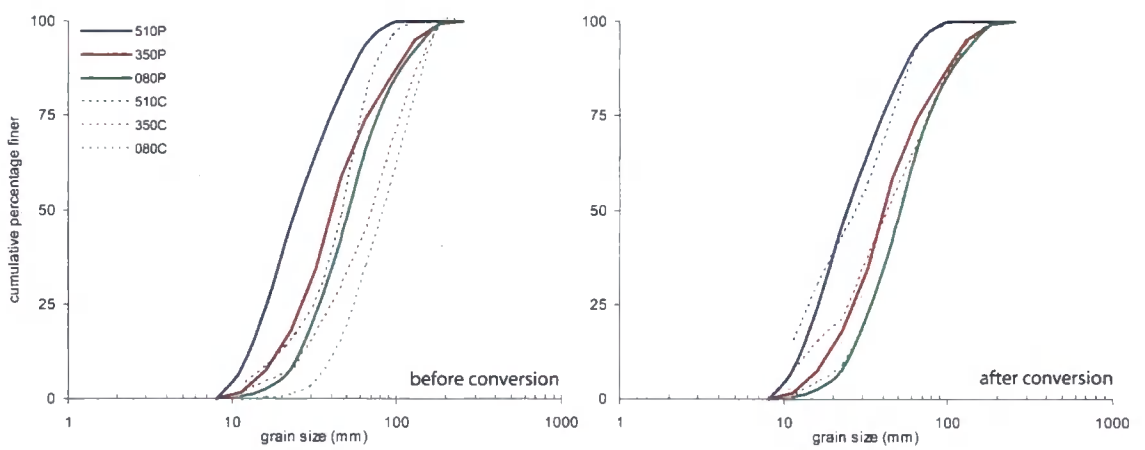

The best fit conversion values were x = -1.41 (080), -0.79 (350) and -1.18 (510) with an average best fit value of x = -1.13. The 080 site visually shows the best conversion at -1.18 whilst the 350 and 510 sites fit well at the coarse end but deviate slightly towards the finer end of the distributions. These values do not vary greatly from the x = -1.0 conversion factor proposed by Kellerhals and Bray (1971) showing that their conversions are reasonable applications when applied to natural sediment mixtures. Thus the areal bulk

samples can be converted into volumetric samples using [5.8] and x = -1. This also means that the pebble counts truncated at 8 mm can be used directly as volumetric representation of the surface only layer.

Step 2 and 3: Defining the active transport layer

The data are currently split into surface and sub-surfaces layers. However, material moved during sediment transport can be from both the surface and sub-surface layers. Since it is difficult to convert the pebble counts directly into sub-surface GSDs, it is necessary to combine the surface and sub-surface layers together to determine the GSD of the active transport layer. It is also necessary to determine the thickness of this active layer.

The active transport layer can be defined as the part of the bed that interacts with the flow. It determines rates and composition of the transported sediment (Blom and Parker, 2004). Many studies have explored bedload transport layer thickness using tracer pebbles (e.g. Wilcock *et al.,* 1996), scour chains and scour monitors (Haschenburger, 1999). These studies highlight two key points. First, DeVries (2002) found that over timescales shorter than those associated with measurable scour and fill, bedload transport in gravel-bed rivers involves the disturbance of a relatively thin layer of the bed. Second, scour depths can vary greatly within the channel (Hassan, 1990; Parker and Sutherland, 1990; Haschenburger, 1999; DeVries, 2002). They can fluctuate with both surface grain size and shear stress (Van Niekerk *et al.,* 1992; Wilcock and McArdell, 1997) and over time (Parker and Sutherland, 1990; Kelsey, 1996). During short timescales, the active layer may be only those particles on the surface which are liable to immediate entrainment whilst over longer timescales the active layer can be associated with scour and fill and bedform formation (Kelsey, 1996).

There is a degree of arbitrariness in the specification of the active layer and definitions vary from simple fractions of sediment size to functions of flow depth and shear stress. For example Park and Jain (1987) use D_{max}, Fripp and Diplas (1992) use $2D_{max}$, Hoey and Ferguson (1994) use $2D_{84}$, Parker (1990) uses an order one multiple of D_{90}, Van Niekerk *et al.* (1992) scale active layer thickness with shear stress, Cui *et al.* (1996, 2003) use a function of geometric mean sediment size and the geometric standard deviation of the

sediment and Gasparini *et al.* (1999) hold the active layer constant at a value much larger than the D_{50}.

Guidance on selecting an appropriate definition of the active layer can be obtained by recent work on active layer or exchange layer thickness using scour chains. These studies all found that maximum disturbance depths were around $2D_{90}$ of the surface (Wilcock *et al.*, 1996; Wilcock and McArdell, 1997; DeVries, 2002). This would suggest that using a definition that scales with a characteristic large grain size of the surface such as the D_{84} or D_{90} would be suitable. DeVries advise against the D_{max} due to the larger levels of uncertainty associated with sampling this grain size. The actual grain size (D_{84} or D_{90}) chosen is perhaps less important since Hoey and Ferguson (1994) found that simulation results from SEDROUT were fairly insensitive to reasonable ranges of the specification of active layer thickness.

It was therefore decided that $2D_{84}$ would be the representative active layer thickness for the channel. It is also necessary to define the GSD of the active layer for the Wharfe sample sites. Due to the areal sampling approach, it is difficult to know what the thickness of the surface and sub-surface layers are since the thickness varies across the sample. It is likely to be somewhere between D_{50} and D_{max} as shown in Figure 5.11. Hence a depth of around D_{84} would be a reasonable estimate. Thus $2D_{84}$ would constitute roughly equal parts of the surface and sub-surface suggesting that a simple average of the two layers would provide a good representation of the active transport layer. Thus the volumetric surface and sub-surface GSDs truncated at 8 mm were combined to provide the GSD of the active layer.

Figure 5.11: Estimating the thickness of the surface layer.

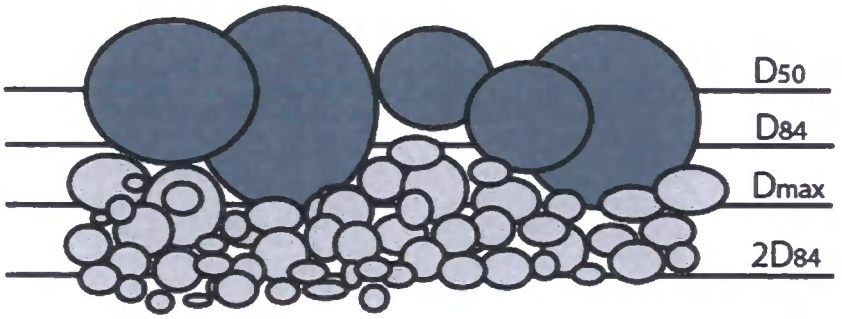

Step 4: Converting the pebble counts into active layer equivalents

Since only three sites downstream had bulk sample data and 16 sites had pebble count data, it was necessary to find a relationship between the two data sets and allow bulk samples to be re-constructed from the pebble count data at each site. According to Kellerhals and Bray's (1971) conversions, the surface pebble count data and surface volumetric samples are theoretically the same and hence the pebble count data can be used directly as a representation of the surface GSDs in volume-by-weight form. However, the active layer includes the sub-surface material and a new conversion must be found to transform the pebble count data into volume-by-weight active layer distributions. By using [5.8], the best fit conversion values were found to be x = -0.16 (080), x = -0.63 (350) and x = -0.18 (510) with the average conversion being x = -0.32. Therefore all the pebble counts (truncated at 8 mm) were converted into the active layer using x = -0.32. However, some concern arises over the validity of this approach given the large variations in the estimated value of x. This is due to local variations in sediment supply and flow conditions, and as such may under or over estimate the active layer sediment characteristics. Yet, this average value provides the best approximation when only three samples are available and must be used for all other samples.

Step 5: Adding in a percentage of fine material

The manipulation so far has excluded all material which is less than 8 mm. However, the fine material can be important in sediment transport (e.g. Wilcock and Crowe, 2003) and should be included in the GSDs. Since the bulk samples represent the finer material well,

they can be used to determine how much fine material is in the bed. This was done by firstly finding the percentage of material less than 8 mm in the three volumetric active layer samples. These values where plotted against distance downstream and a relationship between them was found. Figure 5.12 shows this relationship. The equations shown in Figure 5.12 were used to determine the percentage of fine material to be added to the surface and active layer GSDs at each site, from the sites distance downstream. A polynomial relation best represented the increase in the percentage of fines with distance downstream on the active layer. A linear relationship was found for the surface layer.

Figure 5.12: Fine material in surface and active layers at each bulk sample site.

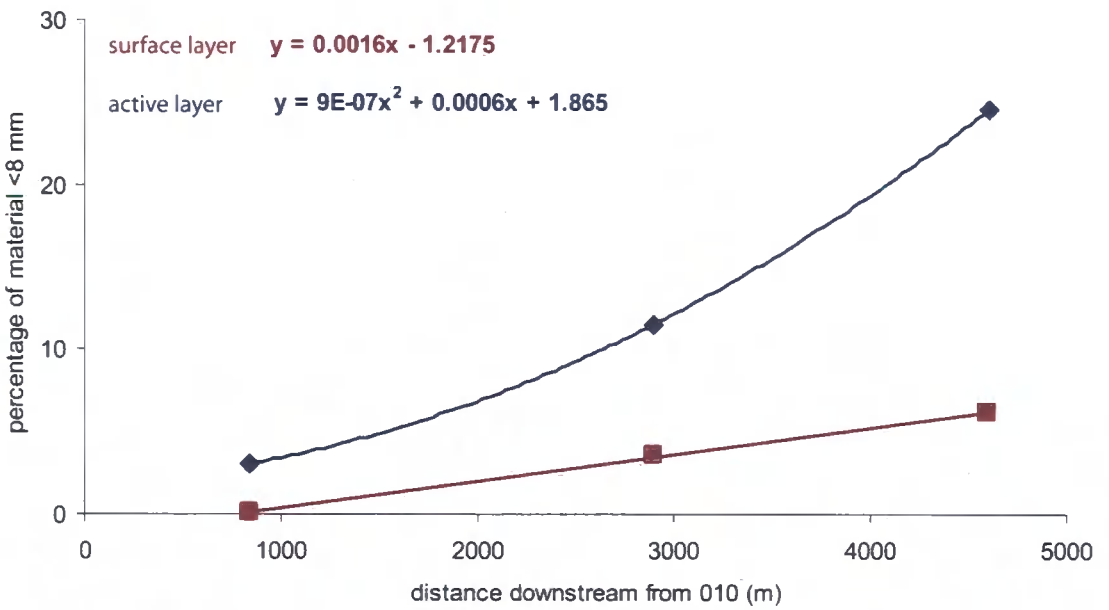

The full GSDs of the surface only and active layers for each site were established. It should be noted that with hindsight and giving consideration to the effort and time put into the hybrid-conversion approach, it would have perhaps been easier to simply carry out bulk samples for all sites. This would also have reduced errors and uncertainties associated with each step of the conversion. Figure 5.13 shows selected GSDs of the active layer. Full GSDs for each site are contained in Appendix III. Figure 5.14 shows the changes in D_{50} and D_{84} values downstream and shows how the bed rapidly fines after Hubberholme (0 m) at cross-section 010 and then fines at a slower rate towards the end of the study reach. The trend is interrupted at 1400 m downstream where the bed becomes coarser. This may be

due to sampling error but is likely to be reflecting the input of the Cray Beck tributary at 1000 m downstream. The tributary may be bringing coarser material into the main channel.

Figure 5.13: GSDs of the active layer at alternate sites.

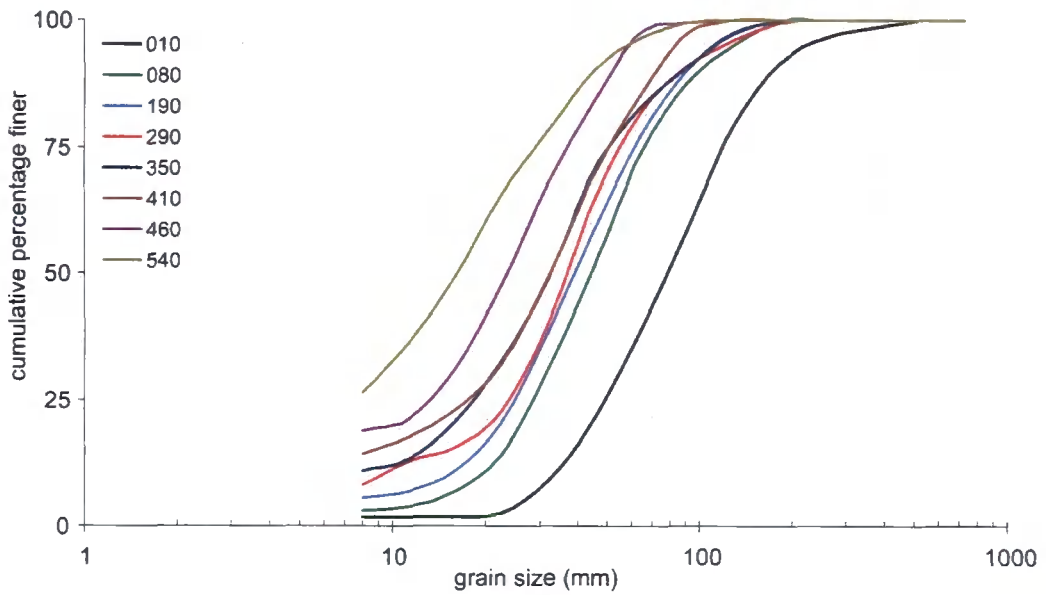

Figure 5.14: Grain size characteristics with distance downstream.

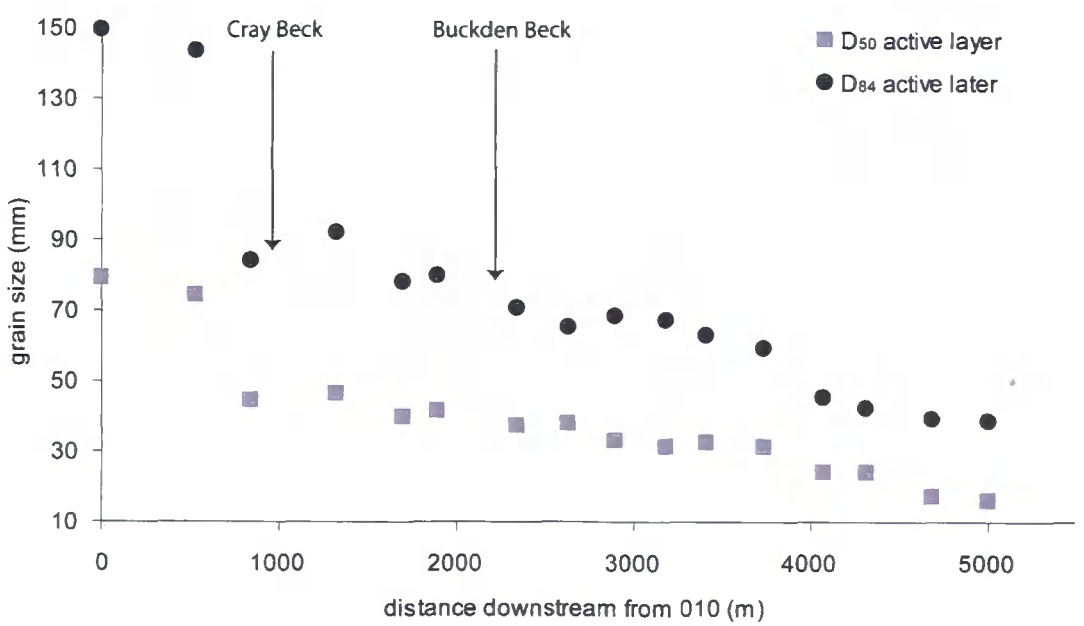

5.4 MONITORING SEDIMENT TRANSFER USING IMPACT SENSORS

To improve our understanding of sediment transport dynamics in the study reach and to provide estimates of sediment transport rates for testing the sediment transport component of the model, a method of monitoring sediment transfer in the river was required.

5.4.1 OPTIONS FOR MEASURING THE BEDLOAD TRANSPORT RATE

Despite extensive research, determining the bedload transport rate of coarse grained rivers remains a difficulty, both spatially and temporally (Gomez, 1991; Bunte *et al.*, 2004). Wilcock's (2001) review of methods to estimate sediment transport rates in gravel-bed rivers, provides an insight into the wide range of techniques that have been developed and explains the limitations associated with them. These methods range from: (1) predictions made from empirical formulae (e.g. Meyer-Peter and Müller, 1948); (2) direct sampling using hand-held or pit traps (e.g. Church *et al.*, 1991; Powell and Ashworth, 1995; Bunte *et al.*, 2001); (3) measuring the entire load using slot traps or settling ponds; (4) tracking particles using tracer gravels (e.g. Wilcock, 1997; Wathen *et al.*, 1997; Habersack, 2001); and (4) using volumetric changes in the channel to reconstruct a local sediment budget (e.g. Ham and Church, 2000; Fuller *et al.*, 2003).

These methods are problematic (Wilcock, 2001). Nets and baskets are hard to deploy, unable to survive exposure to high magnitude events and the samples are often statistically unrepresentative (Tunnicliffe *et al.*, 2000). Thus, as Hubbell *et al.* (1981) suggest, no one sampler can cope with the full range of hydraulic and sediment discharge conditions found in natural streams and rivers. Traps and buckets fill rapidly (Powell and Ashworth, 1995), become buried and lost under sediment and can inaccurately represent transport rates due to trap location (Powell and Ashworth, 1995; Bunte *et al.*, 2004). Tracers can be useful as they are deployed and measured at low flows giving them logistical and safety advantages (Wilcock, 2001) and they can have a good recovery rate (e.g. Ferguson *et al.*, 1998). Yet tracers are expensive, often applied across only a few infrequent transport events where

flow characteristics are unknown (Pyrce and Ashmore, 2003) and tracer recovery can be a time consuming task. Formula and equations are renowned for their problems with different equations often producing completely different results (see Section 7.4.2). Bathurst *et al.* (1987) and Gomez and Church (1989) provide useful reviews of the main equations and their problems. Ironically, one of the main limitations of these equations is a lack of data for development and testing due to the lack of robust measurement techniques. New measurement techniques are highly sought after. With all these problems with samplers and equations, the 'indirect' transport estimation technique, which re-constructs a volumetric sediment budget of the study reach, often provides the most valuable estimates of sediment transport rates (Ham and Church, 2000). This approach is used herein for estimating volumetric sediment transfer in the Wharfe (Section 5.4). However, it requires some knowledge of sediment transfer processes to set an input or output value from which to determine the rest of the budget. This value is typically obtained from one of the previously mentioned techniques. Evidence from field surveys and reports and from talking to locals, suggests that the Wharfe transports large quantities of coarse sediment during flood events. Thus, devices such as pits and traps would either be destroyed by the flow or fill up too quickly. A new device called the sediment impact sensor (Richardson *et al.*, 2003) offers a solution to many of these problems providing a method for understanding the sediment transfer process in the Wharfe. Similar devices called piezoelectric bedload impact sensors (PBIS) are also available for monitoring bedload transport with results from a study in a mountain stream presented by (Rickenmann and McArdell, 2007). The PBIS record the vibration of grains greater than 20 mm and offer the advantage of spanning the entire width of the channel, thereby monitoring all sediment transport.

5.4.2 The Sediment Impact Sensors

Two different designs of impact sensor were used to provide data for this study. The sensors installed and downloaded by Reid (2004) are referred to as "original" (Figure 5.15c) whilst the sensors installed in May 2006 are referred to as the "new" sensors (Figure 5.15a). Both original and new sensors operate in the same way. Richardson *et al.* (2003) explain that the device, which consists of a data logger attached to a metal impact plate

(150 x 130 x 6 mm in size), lies flush with the channel bed (Figure 5.15b) and records the impacts of clasts on the plate through an acceleration sensor contained inside the logger. These impacts have been termed pings. Reid *et al.* (2007a) suggest that the sensor plate is of the correct size to record a rolling particle only once and also to catch any saltating particles if they occur. They justify this using a study by Drake *et al.* (1988) who found that only fine gravel (2 – 3 mm) saltates along the bed. Coarse grains roll along the bed with corners and edges contacting the bed on average about twice per particle diameter. Under high flows, this argument may fail as saltation hops may increase in distance and miss the logger. Thus the number of impacts recorded may be underestimated during high flow events. This technique provides high-resolution continuous data on the intensity of sediment transport from consecutive events. By protecting the logger in the bedrock, the device is able to survive more intense transport events than conventional samplers. When set to record every five minutes, it only requires downloading every two months reducing the number of field visits.

Figure 5.15: Photos of the sediment impact sensors. (a) New logger downloading to laptop; (b) inverted logger lying flush with bed; (c) original logger.

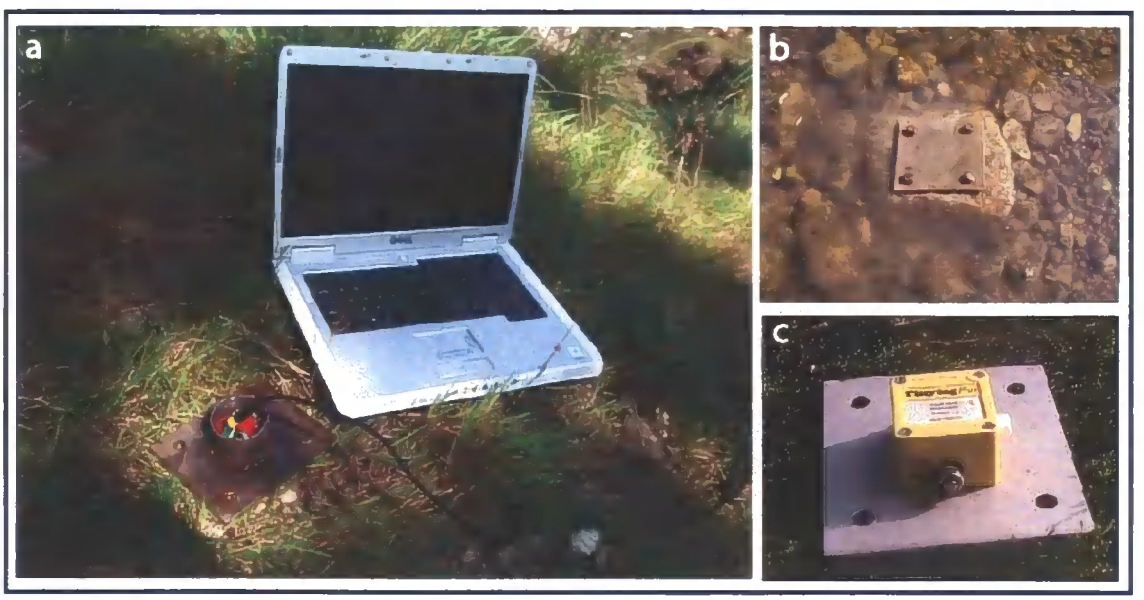

This method does however have its problems. First, the accuracy of the transport intensity estimates is dependent on the location of the sensors within the bed. Powell and Ashworth

(1995), Richardson *et al.* (2003) and Bunte *et al.* (2004) all explain that 50-100% of sediment transport can occur in a small proportion of the channel. Hence, the data from the sensors could be significantly inaccurate. This problem can be minimized by carefully locating the sensors which was done by Reid (2004). Second, the data recorded by the logger has a saturation point of 255 impacts in a five minute period with a maximum of 3 pings per second (Richardson *et al.*, 2003). During high intensity transport events, only 255 pings are recorded out of a theoretical maximum of 900 which is 3 pings a second for 300 seconds (i.e. 5 minutes). Hence the results tend to be underestimated at high flows and more reliable at lower flows. To resolve this, the logger can be set to record data every minute, reducing download time to 10 days, which in many instances is impractical. The response of the impact sensors to transport is also non-linear (Richardson *et al.*, 2003) since the likelihood of more than one clast hitting the impact plate in less than a third of a second, increases with discharge and transport rate. Third, the sensors do not record any information on the pressure of an impact which could be used to infer the particle's mass or impact velocity. Using the number of impacts to infer sediment volume may be incorrect, particularly if grain size distribution differs greatly between sites.

The reliability of the ping data was tested by Reid (2004) who compared the output from two sensors placed 50 cm apart in the line of flow at Deepdale (about 3 km upstream of Hubberholme). Reid's study compared the data from each sensor during the two largest transport events during the study period. The results suggested that sensor variability is minimal under identical conditions assuming that the clast is travelling in the same direction as the orientation of the sensors (Reid, 2004).

Ten impact sensors were installed throughout the Upper Wharfedale catchment in March 2003 during a previous project (Reid, 2004). The acceleration sensors inside the loggers were sensitive to record only grains greater than 3 mm in diameter (Benson, pers comm., 2005). The location of each sensor was chosen carefully by Reid (2004) following the analysis of the first autumn floods in September 2002. During the summer low flow, algae covers the gravels, thus the first Autumn flood scours the gravel and leaves "tracks" of clean gravel where sediment transport has occurred (Richardson *et al.*, 2003). Data from

five of the sensors are relevant to this research. These include a sensor at Hubberholme, approximately 150 m upstream of cross-section location 010, one by Buckden Bridge, and a third located near Starbotton at cross-section 590. In addition, there are two sensors located on each of the main tributaries which enter the Wharfe in the study reach. These include a sensor on Buckden Beck, approximately 300 m upstream of Buckden village, and one on Cray Beck, about 400 m upstream of its confluence with the Wharfe. One year of data was downloaded from these sensors before they all eventually stopped working.

Two new sensors were installed in May 2006 at Hubberholme and Starbotton, in the same locations as the original sensors. The main difference between the old and new loggers is the casing design with the new loggers contained in a much sturdier and more water-tight structure.

5.4.3 Impact Sensors: Analysis

The raw data from the impact sensors provide a continuous record of sediment activity at each of the sensor sites. They can be used to observe the passage of individual sediment transport events such as the two events clearly shown in Figure 5.16 at three of the impact sensor sites. This information can also be used to compare the relative intensity of sediment transport at different locations, and to explore the nature of sediment transport events within the study catchment.

Figure 5.16: Two individual transport events captured at three sites between the 3rd and 5th of February, 2004. (Data from Cray Beck and Starbotton were not included in this plot as the ping counts at these sites were much lower than at the sites displayed. The stage record is for visual purposes. The stage data has not been validated).

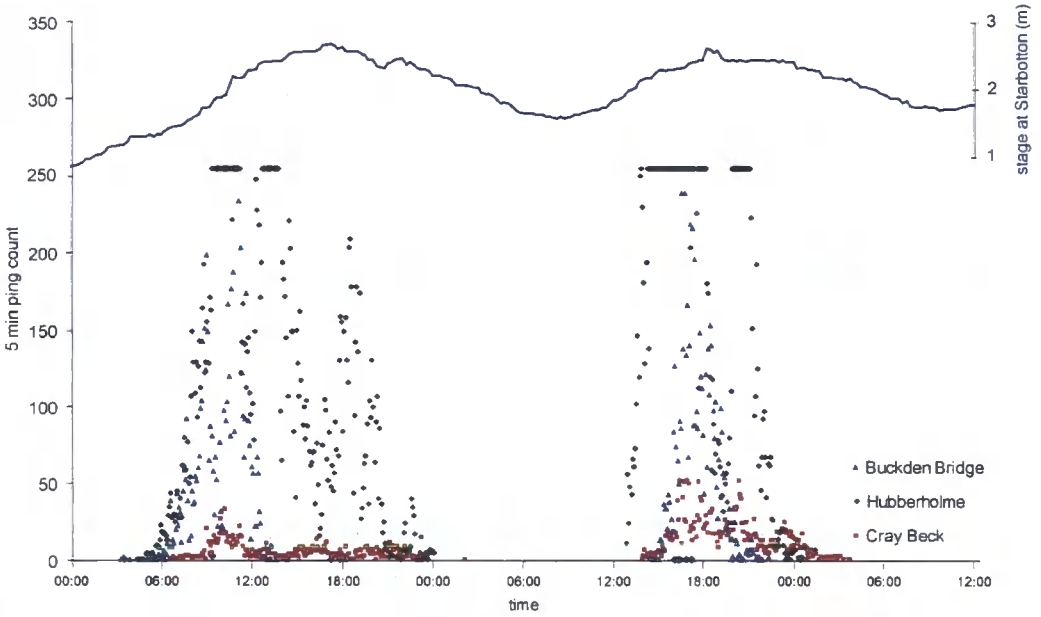

The data cannot simply be analysed in the raw "ping count" form for two reasons. First, the channel widths at each location vary greatly. The data must be upscaled to account for variations in width between the narrow tributaries and the wider main channel. Second, the loggers have a saturation point of 255 pings per 5 minute interval. Thus, during high magnitude events, the ping count remains at 255 and is likely to underestimate the true ping count. This issue is particularly a problem at Hubberholme and Buckden Bridge, as illustrated in Figure 5.17. This figure plots the relative contribution that each ping count value (1 – 255) has to the total annual ping count. At both Hubberholme and Buckden Bridge, around 50% of all pings are recorded as part of 255 records. Thus the total ping counts for these locations are likely to be much higher than those actually recorded.

Figure 5.17: The percentage contribution that each ping count (1 - 255) has to the total annual ping count. Data presented is for the period March 03 – March 04.

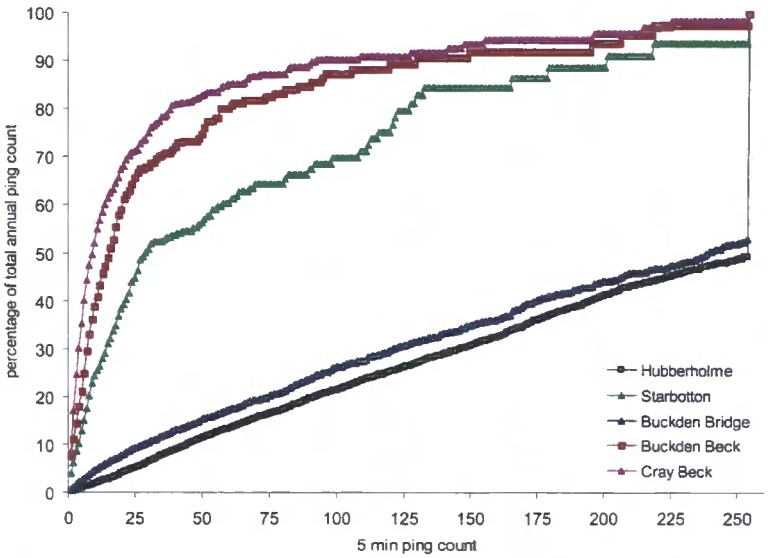

To reduce these two issues, Reid (2004) used [5.9] to transfer the data into a relative transport intensity, accounting for differences in width and to overcome the saturation problem. To obtain the transport intensity at each site, the data were first divided by 255 to give a "transport intensity" (t_n), a value between 0 and 1. This provides the data in a more manageable format. Reid (2004) suggests that this process deals with the logger saturation issue, however this is not the case as it simply changes the data from 0-255 to a value between 0 and 1. Thus, issues associated with logger saturation must still be considered. The data was then up-scaled to the channel width (w) and divided by the width of the logger plate (w_l) which was a constant 0.13 m. This assumes that transport rate is equal across the channel, a crude assumption. The "relative transport intensity" (r_n) was then obtained using:

$$r_n = t_n\left(\frac{w}{w_l}\right) \qquad [5.9]$$

A second issue arose when trying to calculate the length of time that sediment was in motion: the transport time. Whilst it is likely that a record of 255 would be associated with transport during the full 5 minute time interval, it was unlikely that 1 ping during the 5 minute time interval would be associated with a full 5 minutes of sediment transport. Thus low magnitude, insignificant transport events were removed so that transport time was not

overestimated. By plotting transport curves based on time contribution (cumulative percentage of the year) of the total sediment transport, a threshold at 10% of the total transport became clear (Figure 5.18). Under this threshold, frequent yet low magnitude events occur. These were removed. The number of pings associated with this threshold varies between sites.

Figure 5.18: For each ping count value, the transport time (expressed as a percentage of year) was plotted against the percentage contribution that each ping count value made to the total activity (as shown in Figure 5.14). Data presented is for March 2003- March 2004.

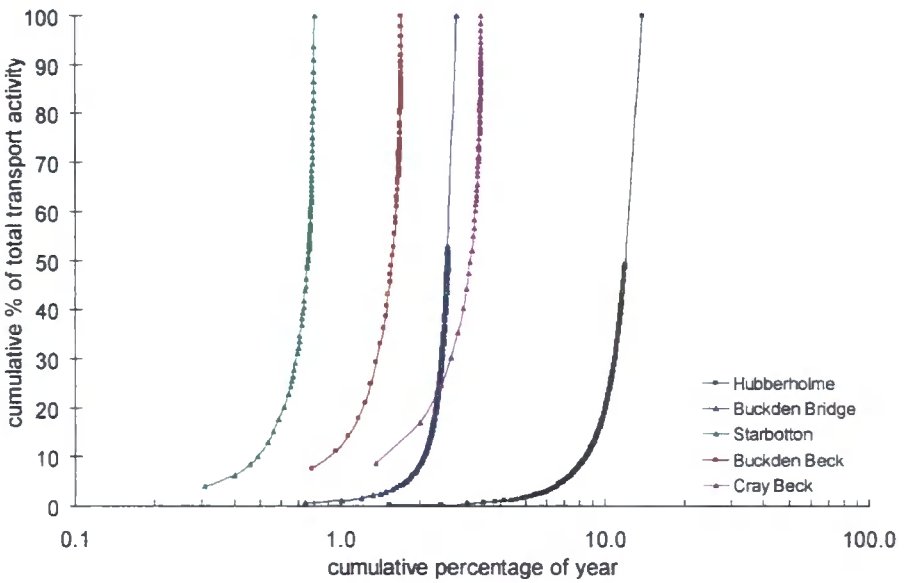

5.4.4 Impact Sensors: Results

Table 5.4 and Figure 5.19 present data from the impact sensors located at the five sites, three in the main channel and two on the tributaries. These data reveal interesting features of the sediment transfer system in the study catchment and can help provide a better understanding of the complex nature of the sediment transfer process. This analysis begins by looking at the reach-wide picture and comparing the total annual sediment transport activity at each site for the 2003-2004 monitoring year. It is noted that sediment transport activity varies greatly between sites (Table 5.4). The highest level of sediment transport activity is found at Hubberholme followed by a large reduction in sediment activity with distance downstream. Buckden Beck records 10 times less sediment activity than

Hubberholme whilst the activity at Starbotton is a fraction of that at Hubberholme which has activity levels over 300 times greater. These patterns match the measured patterns of sedimentation discussed in Section 4.3.5. The tributaries record even lower levels of sediment activity with Cray Beck recording four times the activity at Buckden Beck. Such variations can be explained by the nature of the channel at each particular site. Upstream of Hubberholme, the channel is steep and narrow and predominantly bedrock. The catchment slopes are also steep with sediment entering the channel from hillslope failures and bank collapse. Once in the channel, sediment quickly and easily moves downstream to Hubberholme, passing over the Hubberholme sensor. From here, the channel gradient reduces, allowing sediment deposition, which is evident as point and lateral channel bars and in the cross-section survey data. Hence the movement of sediment becomes more difficult, with higher flows required to account for the reduction in channel gradient. This results in a reduction in activity by Buckden Bridge and further still by Starbotton. The lowest activity found in the tributaries can be explained by the availability of sediment. Both tributaries are predominantly bedrock channels, with little sediment stored in the channel bed. Sediment transport activity must be supplied from the hillslopes through slope failures. Once in the channel, the steep, narrow geometry allows the sediment to be flushed through into the main river channel quickly and efficiently. Hence, sediment transport in the tributaries and main channel to Hubberholme is largely controlled by sediment supply from the hillslopes, with the higher volumes that pass Hubberholme reflecting the larger upstream contributing area. Further down the main channel, sediment transport is a function of upstream sediment supply and sufficient sediment transport capacity.

Table 5.4: Impact sensor data for the period March 2003 to March 2004.
Total sediment transport activity is the sum of the relative sediment transport intensity (*rn*) defined in [5.9].

	total sediment transport activity			% contribution to annual total		% contribution from upstream and tributaries		
	summer	**winter**	**annual**	**summer**	**winter**	**summer**	**winter**	**annual**
Hubber.	66399	225275	291674	22.8	77.2			
B. Bridge	20667	8636	29303	70.5	29.5	31.1	3.8	10.0
Starbotton	778	118	896	86.8	13.2	1.2	0.1	0.3
Cray Beck	375	507	882	42.6	57.4	0.6	0.2	0.3
B. Beck	57	187	245	23.5	76.5	0.3	2.1	0.8

Seasonal variations in the contribution of sediment to total sediment transport activity become distinct alongside spatial variations in the seasonal differences. The dominant seasons for sediment contribution are winter for Hubberholme and the two tributaries, whilst it is the summer period for the main channel sites at Buckden Bridge and Starbotton. This finding is different to that of Reid *et al.* (2007a) who found that the five tributaries sites were dominantly active in the summer during their monitoring period, whereas the main channel sites were predominantly active in the winter. Whilst Reid *et al.* (2007a) broadly classify the ten sensors into five tributary and five main channel sites for analysis, the analysis herein concentrates on the variability between sites. Large differences in the seasonal activity levels in the tributaries are noted here. In particular between Cray Beck and Buckden Beck and the three tributaries in the catchment headwaters as analysed in Reid *et al.* (2007a). In the main channel, the higher levels of sediment activity noted at Hubberholme heavily weight the main channel seasonal contributions in Reid's analysis.

When the seasonal contributions to total sediment activity are examined (Table 5.4), two differing situations prevail. Firstly, the tributaries and Hubberholme show similar patterns with greater sediment activity in the winter period. As discussed above, the channel upstream of Hubberholme is steep, narrow and bedrock and as such is characteristically similar to Cray and Buckden Beck. Second, the main channel sites at Buckden Bridge and Starbotton contribute more sediment to the total activity during the summer period. The greatest difference in contribution between seasons is found at Starbotton with 87% of activity occurring during only 0.1% of the summer period compared with 13% during the 0.4% of the winter time. Concurrently, seasonal variations in contribution to total activity are smallest in Cray Beck. Furthermore, during the winter period the downstream transfer of sediment is proportionally greater than during the summer periods with 31% and 1.2% of sediment moving to Buckden Bridge and Starbotton respectively in the winter, and a 90% reduction in sediment transfer in the summer months.

The seasonal variation between sites reflects the nature of the channel and the source of sediment at the sensor location. In the tributaries, the sediment transport is highly dependent on sediment supply and findings by Reid *et al.* (2007b) strongly suggest that this is controlled by convective rainfall events that trigger hillslope failures. In the main channel

where sediment is stored, sediment transport activity becomes more dependent on the discharge regime. Yet, sediment supply also has a role to play in the main channel with a reduction in sediment transport activity noted when moving from Hubberholme to Buckden Bridge and down to Starbotton. This drop in activity may result from either a reduction in transport capacity as one moves downstream or because the sediment supply is too high for the channels re-working to keep up with.

These results suggest that whilst it is interesting to consider seasonal contributions, it is important to examine the magnitude and frequency of events that transport the sediment. In particular, the findings at Starbotton, suggest that individual events can be significant for sediment transport. The event data presented in Figure 5.19 highlight the spatial variability in number and importance of individual events. At each site, a different situation is present. Hubberholme has more events in the winter months with each event contributing slightly more sediment than the summer events. Thus, at Hubberholme, high frequency, high magnitude events during the winter contribute to the high levels of activity recorded at this location. Yet in the two tributaries which have thus far behaved in a similar way, two different situations occur. In Buckden Beck, fewer events occur in the winter than the summer. Yet, the winter events are much more significant for sediment transport. Hence, a few high magnitude events in the winter dominate the sediment transfer. On the other hand, there are only marginal seasonal differences in Cray Beck with individual events transporting similar amounts of sediment irrespective of season, and a similar number of transporting events occurring in the winter and summer. This suggests that like Buckden Beck, sediment supply from the hillslopes is important during the winter. In contrast, in Buckden Beck, the summer events produce similar amounts of sediment. Unlike the tributaries and Hubberholme, individual summer events in the main channel at Buckden Bridge and Starbotton transport more sediment than the events in the winter. At Buckden Bridge, despite there being fewer individual events in the summer, each summer event is larger than the winter event. However, the duration of these summer events must be sufficiently long enough to contribute to the 70% of total activity noted in Table 5.4. Hence sediment transport passed Buckden Bridge is dominated by relatively low frequency high magnitude events in the summer period. Such an event occurred at Buckden Bridge

between the 20 and 22nd of September 2003. This two day event contributed to 67% of the total annual sediment transport activity. Again the situation at Starbotton is different with more events, and more transport moved by each event in the summer than in the winter. Hence transport at Starbotton is driven by high frequency high magnitude summer events relative to the winter events. The overall conclusion from Figure 5.19 is that there is no dominant season for sediment supply and transport in the Wharfe system and that the magnitude and frequency of sediment activity varies greatly between sites. This can be attributed to the importance of convective storm events for sediment generation in the Wharfe system (Reid *et al.*, 2007b), and such storms may occur at any point in the year. This has two important implications. First, distinctions like 'summer' and 'winter' may not be particularly helpful if the inter-annual variability in when these types of events occurs dominates over intra-annual or seasonal variability. Judging the geomorphological effectiveness of different types of rainfall events is only possible by reference to the nature of the rainfall event as filtered by the way that the catchment functions geomorphologically. Second, it emphasises the importance of establishing how climate change might impact upon future rainfall events, especially given the current reliance of rainfall intensity predictions on the form of the downscaling applied to global and regional climate model predictions (Lane *et al.*, 2008).

Figure 5.19: The relative importance of individual transport events. The squares show the number of individual transport events (low flow events have been removed and there is a minimum of 24 hours between events). The bars show the average sediment transport activity each event contributes to the annual total.

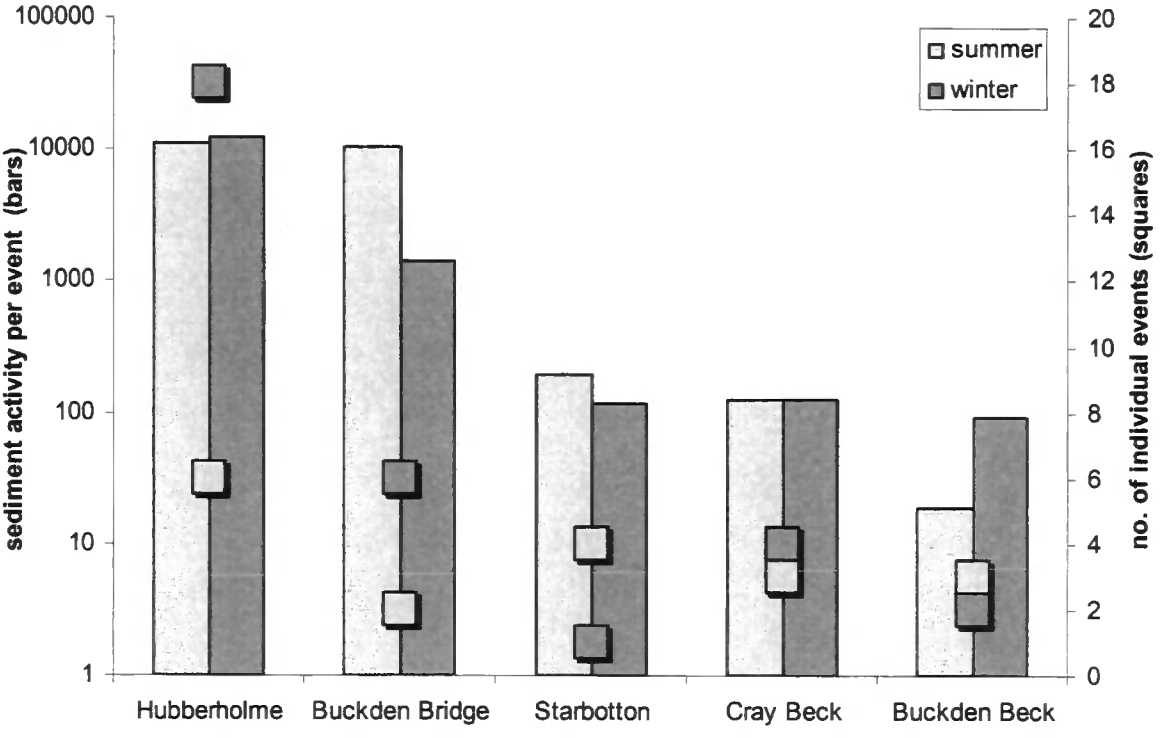

The results from the impact sensors have only considered the situation that occurred during a single year. When data from the new impact sensors installed in the main channel at Hubberholme and Starbotton are explored, annual variability is evident alongside the spatial and seasonal variability. This is shown in Tables 5.5 and 5.6. The total activity of the new impact sensors cannot be compared directly with the original sensors due to design differences which make the new sensors less sensitive, particularly to lower magnitude events. However, the ratio of sediment transport activity between sites can be compared for the original and new sensors. Table 5.5 shows the total sediment activity for the three survey periods. The results from the original sensors (March 03 – March 04) support earlier findings, demonstrating that sediment transfer down the channel varies with season. The ratio is higher during the April to September 2003 period when compared to the October to March 2004 period and the 2006 records. These suggest that there may be waves of sediment passing through or more specifically out of the study reach. The ratio of sediment

transport activity is explored at a higher spatial temporal resolution in Figure 5.20 with the monthly ratios presented.

This figure shows large monthly variations in the relative transport activity at each site. During April 03 – September 2003, the first three months recorded ratios greater than 1, indicating that sediment output exceeded the input. This may reflect a period where sediment supply entering at Hubberholme was limited or the passing through of a sediment wave. This explains the higher ratio for this period noted in Table 5.5. From July 2003 until the end of the monitoring period in March 2004, there was a greater input than output but strong monthly variations. The lowest ratio was recorded in January 2003. The new sensors also show some interesting findings. The May 2006 and July 2006 data points must be considered with caution. In both these the total number of impacts was very low at both impact sites. Thus whilst the output was higher than the input during July, the volume of sediment associated with this is minimal. From August until December 2006, there is a gradual reduction in the ratio indicating an increase in the input of sediment and a decrease in the output. Thus sediment input may be plentiful with high volumes of sediment entering the channel, yet the amount of sediment leaving this reach becomes gradually lower. Thus the sediment entering has not progressed downstream by December 2006. Despite the monthly variability, these data provide further evidence that over timescales greater than 3-months, sediment supply out of the study reach is significantly lower than sediment supply into the reach. This may suggest that the cross-sectional survey frequency should be more frequent than twice a year in order to capture the channel's full response to sediment transfer processes.

Table 5.5: Seasonal transport activity at Hubberholme and Starbotton.

	April 03 - Sept 03	Oct 03 - March 04	May 06 - Dec 06
Hubberholme	66399	225275	15793
Starbotton	20667	8636	334
Ratio (star:hubb)	**0.311**	**0.038**	**0.021**

Figure 5.20: Monthly transport activity ratios. Ratios greater than 1 indicate more sediment leaving than entering. Ratios less than 1 indicate more sediment entering than leaving.

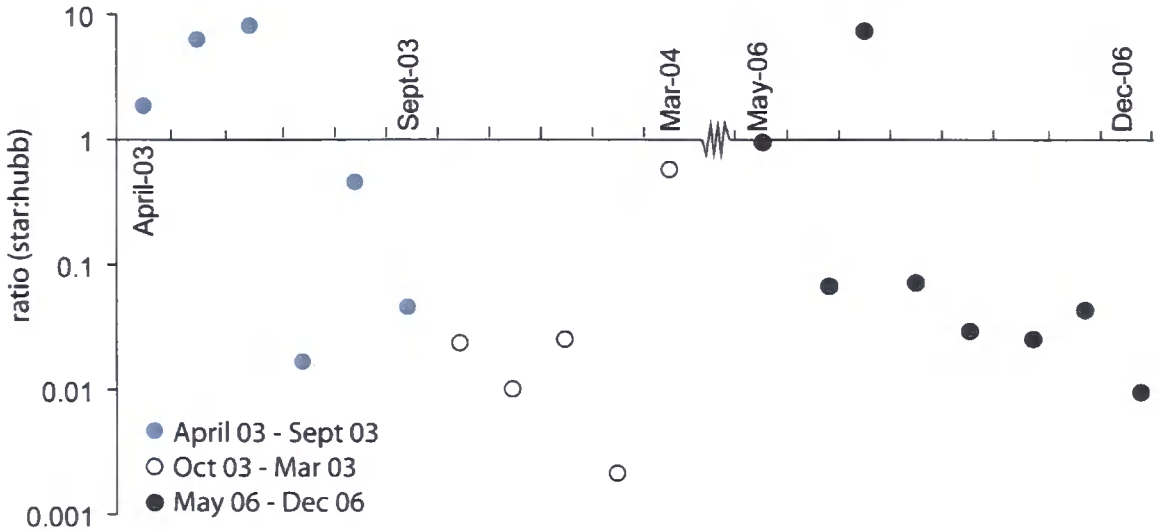

In addition to the transport activity ratios, the new sensors provide comparable transport times. Table 5.6 shows the percentage time sediment is in motion during the monitoring period running from May 2006 to March 2006. When compared with the same season in 2003, some striking differences in transport time become apparent at Hubberholme. Transport time in the 2006 summer period is 2% lower than in the 2003 summer period. However, at Starbotton, the percentage time sediment is in motion is similar in 2003 and 2006 providing some indication that sediment transfer processes may be similar on an annual basis at this location. With less than two years of data, this suggestion is made with caution. This reduced transport time indicates either a change in the factors driving sediment transport such as sediment supply or transport threshold, or indicates a hydrological difference. Indeed, the summer of 2006 was hot and dry. This reduction in transport time may reflect the lack of rainfall events to both initiate sediment supply from the hillslopes but also to transport it downstream. This low transport rate may also help to explain the period of net degradation noted in Figure 4.6a between April 2006 and December 2006.

Table 5.6: Seasonal differences in the percentage of time sediment is in motion.

% time sediment in motion	Apr 03 - Sept 03	Oct 03 - Mar 04	03-04 Annual	May 06 - Sept 06	Oct 06 – Mar 07
Hubberholme	2.5	8.4	5.4	0.6	
Buckden Bridge	0.8	0.6	0.7		
Starbotton	0.1	0.4	0.3	0.2	0.5
Cray Beck	0.2	1.2	0.7		
Buckden Beck	0.7	3.3	2.0		

5.5 CHAPTER SUMMARY

The previous chapter provided data on the channel's morphology allowing vertical and lateral channel change to be monitored. This chapter has provided data on the main factors that drive channel change; the discharge and the supply and transfer of sediment. Records of the hydrology in the reach comprised three years of 15-minute stage records from Hubberholme and daily discharge values for Flint Mill, since 1956. The Hubberholme stage records were successfully converted into discharge records using Ferguson's (2007) variable power equation and a 2-year representative period was selected from analysis of the Flint Mill records. The bed material was characterised using a hybrid approach which combined numerous pebble counts with three bulk samples to provide information on grain sizes down the channel at 16 locations. This material highlighted the rapid downstream fining previously noted in the Upper Wharfe study reach. The sediment transport regime in the study reach was monitored using impact sensors. These were placed into the channel bed to record the instantaneous movement of individual sediment clasts. These sensors provide valuable data, despite their limitations which include: (1) the location of the sensor within the channel; (2) problems during high magnitude events where the 255 saturation point is reached; and (3) difficulties directly comparing new and old sensors. These sensors provide evidence that the study reach is predominantly aggrading and very little sediment leaves the reach. This finding supports field observations. The data from the impact sensors is particularly valuable when exploring spatial and temporal aspects of the sediment transport regime, when reconstructing a morphological sediment budget and when estimating bedload transport rates from the budget.

Analyses using the impact sensor data, the characterised sediment and the hydrology are explored in Chapter 6 alongside data from Chapter 4. Table 5.7 summarises the data provided by this chapter and demonstrates how it is applied in Chapter 6 and during model development and application in Chapter 7 and 8. Together, data collected in Chapters 4 and 5, have fulfilled Objective 3: *to use field-based techniques to monitor channel change and the variables driving these changes.*

Table 5.7: Data provided in Chapter 5 its future application.

Study	Nature of Data	Future Application (Section)
Discharge	15 min and hourly discharge records for Hubberholme	6.5: impact of sedimentation on flood risk 8.8.3: hydrographs for modelling variable discharge
	Flint Mill discharge records	6.2.1: used to explore patterns of sedimentation
Bed material characterisation	GSDs at 16 locations downstream	5.2: roughness for discharge 8.3.1: input GSDs for model
	Downstream fining profile	6.2.1: supports finding of net aggradation 8.3.2: testing model outputs against measured downstream fining profile
Sediment transfer	Spatial and temporal variability in sediment transfer	6.2.1: used to explore patterns of sedimentation 8.3.2: testing the model's transport threshold
	Ratio of transport into and out of reach	6.2.1: supports finding of net aggradation in reach 6.3: used in sediment budget to set output at zero 8.3.2: compared against the model's bedload transport ratios 8.6: sensitivity testing
	Active transport time	6.3: used to estimate the bedload transport 6.4: predicting bed level change from impact sensors

CHAPTER SIX:
ANALYSIS AND DISCUSSION OF FIELD DATA

6.1 INTRODUCTION

Chapter 4 and Chapter 5 present results from specifically designed, intensive field monitoring. This chapter aims to complete Objective 4 as set out in Chapter 1: *to draw these data together to explore the processes of sediment transfer and channel change in the Upper Wharfe study reach, and to consider the impact of such changes on flood risk.* This analysis and discussion addresses four themes: (1) to explore and explain spatial and temporal patterns of sedimentation and lateral channel change (Section 6.2); (2) to combine methods from Chapters 4 and 5 to develop a methodology to estimate bedload transport rates (Section 6.3); (3) to predict bed level changes using impact sensors (Section 6.4); and (4) to assess the impacts of in-channel sedimentation on flood risk (Section 6.5). The chapter closes with a broader discussion of sedimentation, channel change and flood risk implications (Section 6.6).

Two further key research questions set out in Section 1.1 are answered within this Chapter. Section 6.2 and Section 6.4 provide answers to these questions that are discussed further in Section 6.6. These include:

3) What are the mechanisms that drive the spatial and temporal patterns of sedimentation and bank erosion? (Section 6.2)
4) What implications do in-channel sedimentation and lateral adjustment have for flood risk? (Section 6.5)

6.2 SPATIAL AND TEMPORAL PATTERNS OF CHANNEL CHANGE

Chapter 4 demonstrated that patterns of erosion and deposition vary spatially and temporally. Key findings, several illustrated using Figure 4.6, include the following. First, the Wharfe study reach has aggraded by an average of 0.17 m ± 0.029 m between December 2001 and July 2007. Second, the reach between 1 and 1.2 km downstream experienced the greatest bed level rise with 0.67 m ± 0.031 m recorded during the 6-year study period. Meanwhile, the reach around 2.9 km downstream has experienced the greatest bed degradation of 0.2 m ± 0.023 m. Third, certain zones exhibit relatively little net bed level change but have high activity levels with the zone at 2.5 km recording 1.8 m ± 0.021 m of activity (Figure 4.7). This indicates sediment throughput. Finally, of all the survey periods, the period between December 2003 to April 2004 experienced the highest levels of aggradation, whilst the results recorded a mean bed level drop between April and December 2006. In the study by Stover and Montgomery (2001), who also used repeat cross-sections on the Skokomish River in Washington, over 1.3 m of aggradation was recorded during 30 years of monitoring. Whilst the mean bed level rise was around 0.04 m $year^{-1}$, they note large spatial variability in aggradation including periods of degradation. Thus, the findings from Skokomish share many similarities with the Wharfe.

Within this section, the patterns of channel change are explored through space and time. The following findings are anticipated. First, temporal patterns of sedimentation are controlled by the combined influence of flow and sediment transport. Whilst the hydrology must be sufficient to transport the sediment, the availability of sediment in the first instance is crucial. Second, spatial patterns of sedimentation are determined by the channel's geometry with sediment accumulating on the inside of meander bends, at deviations in the slope profile and at tributary junctions if their contribution of sediment is significant. Third, lateral channel changes occur when sediment accumulation is high and at locations where the high velocity core of flow is forced to one bank by channel curvature. Each of these three anticipated findings are explored as follows.

6.2.1 CONTROLS ON THE TEMPORAL PATTERNS OF SEDIMENTATION

The two key factors highlighted in Chapter 2 that influence temporal levels of bed level change are: (1) the hydrological regime; and (2) the supply of sediment. These are explored herein followed by an examination of survey frequency on temporal findings. Figure 6.1 shows the relationships between channel hydrology and patterns of bed level change. There is a positive relationship between increasing discharge and higher levels of bed level change activity. This is expected as higher discharges are associated with sediment transport leading to either degradation or aggradation depending on sediment supply. Thus, the hydrological regime plays an important role in changing the channel morphology (e.g. Harvey, 1991; Pizzuto, 1994; Allred and Schmidt, 1999). However, predicting the direction of this change (i.e. erosion or deposition) is less clear as shown in Figures 6.1d, 6.1e and 6.1f. These plots exhibit much scatter, resulting in no clear trends between bed level change direction and hydrology. This scatter is greatest at the highest flows (Q_{95} in Figure 6.1d). The lack of any clear patterns in these plots support the concept that channel changes are dependent upon both hydrology and sediment supply / delivery. Under high flow conditions, three scenarios may prevail (see Table 2.1. Werritty 1997): (1) sediment supply is limited and degradation occurs (e.g. Liebault and Piegay, 2000; Rinaldi, 2003); (2) sediment supply is high and aggradation occurs (e.g. Parker, 1979); and (3) sediment supply is limited, bed armouring prevents degradation and the bed level remains constant. It is likely that a combination of these scenarios may occur during the time between two surveys complicating our understanding of processes further. For example, in a period with several successive high flow events, the channel may initially aggrade following an influx of sediment. As sediment becomes exhausted, this aggradation may be replaced with degradation, as the sediment in the system is reworked. If the aggradation and degradation balance, one may be falsely led to believe that the channel is stable when indeed it may be subject to very short-term fluctuations in bed level change. The monthly ping ratio between Starbotton and Hubberholme (Figure 5.20) demonstrates the potential short-term variability in sediment inputs and outputs. However, this does not indicate where the sediment is being

transferred from and to. Thus, it is essential to keep survey frequency high to capture the movement of sediment between the two sensors.

The scatter in Figures 6.1d, 6.1e and 6.1f may be a feature of the interaction between sediment supply and flow regime but on the other hand, it may be confused with anomalous data points. If certain data points are removed from these plots (particularly Figures 6.1e and f), two contradicting relationships emerge. Firstly, if the high aggradation point of 0.35 m $year^{-1}$ is removed, then there appears to be a downwards relationship with lower discharges associated with aggradation and higher discharges with degradation. Alternatively, if the two higher discharge points are removed, an upward trend prevails with greater aggradation associated with higher discharges. Whilst the former suggests that under the highest flows, sediment supply is limited, the latter conversely suggests that higher discharges are associated with higher sediment supply, which allows aggradation. These speculations further demonstrate that the response of a channel is complex and cannot be predicted based on the hydrology alone. To improve our understanding of system response it is essential that survey frequency is high enough to capture bed level change, but also that a better understanding of the nature of sediment supply and transfer is developed. This allows sediment supply and channel response to be coupled together. Considerations of in-channel sedimentation, and hence changes in flood risk, cannot be divorced from the impacts of hydrological activity upon sediment delivery, as conditioned by catchment geomorphology and land-use.

Figure 6.1: Relationship between hydrology and sedimentation. A, b and c compare the bed level activity (which is change irrespective of whether it is aggradation or degradation) with the 95th, 75th and 50th percentiles of discharge from Flint Mill flow duration curves. D, e and f compare the discharge with the mean bed level change. The Flint Mill records are used as a surrogate for Hubberholme due to lack of stage data at Hubberholme.

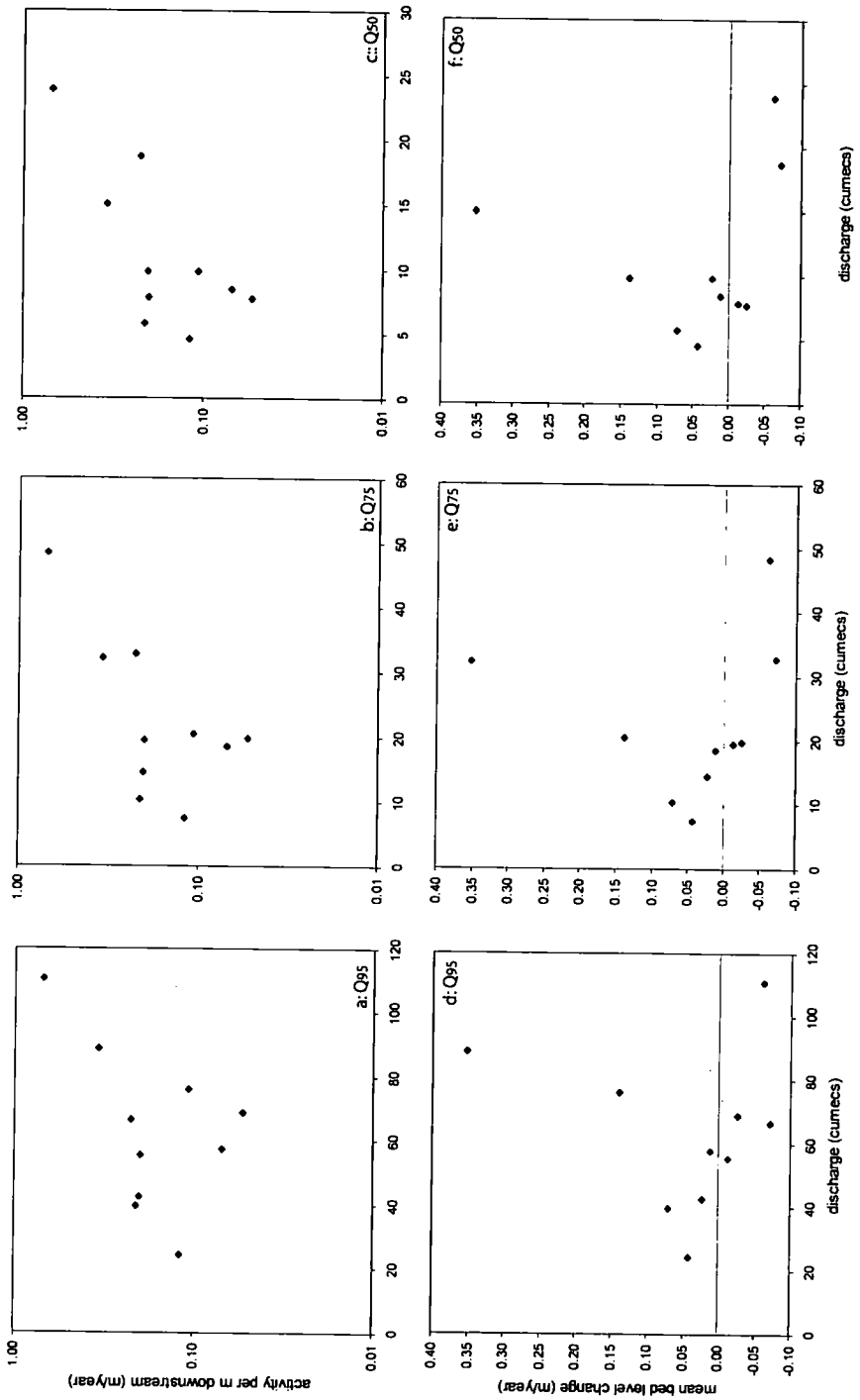

The temporal variations in bed level change shown in Figures 4.6a and Figure 4.6b, lead to an examination of the implications that the timing and frequency of surveys can have for our understanding of sedimentation in the channel. Figure 6.2a, shows seasonal bed level change alongside the cumulative change since surveying began. Whilst the overall pattern is one of aggradation, the reach was actually degrading during the first three survey periods. This degradation was relatively small when compared with the aggradation that followed. A mean bed level drop was also recorded between April and December 2006. The total aggradation between December 2002 and July 2007, when the full 5.6 km of reach was surveyed, was 0.17 m ± 0.026 m. The greatest mean bed level rise for the entire reach occurred during December 2003 and April 2004 when a mean bed level rise of 0.09 m ± 0.01 m was recorded. During this period, the maximum bed level change for a particular location was recorded at 2.5 km downstream where the bed level rise was 0.5 m ± 0.007 m.

Whilst it is interesting to consider the reach as a whole, Figures 6.2b to 6.2e show that temporal patterns of aggradation and degradation are also spatially variable. This variability may have important ramifications for flood risk. Figure 6.2b and Figure 6.2c echo the previous finding, based on the bed level change activity, that the channel flips between aggradation and degradation. If the start and end time of the surveys is considered, our perception of the river's state (i.e. as either aggradational or degradational) can be considerably altered. For example, if the bed level change pattern since December 2001 is considered in Figure 6.2d, the section may be seen as predominantly degrading. Yet if the surveys had begun two years later in December 03, the channel may be classed as relatively stable or slightly aggrading. Similarly, Figure 6.2e demonstrates the impact that survey frequency can have on our understanding of the channel's state. If surveys occurred only three times during the study period, the results would have missed the peak in aggradation that occurred between December 2004 and April 2005. Instead, they show the reach to be aggrading steadily rather than subject to rapid periods of deposition. Such short-term periods of deposition may be significant for flood risk, thus it is essential that they are captured by sufficient survey frequency and a sufficiently long time period of study so as to capture trends from noise.

Figure 6.2: Seasonal width-averaged bed level change. Individual data points indicate seasonal change whilst the solid line is the cumulative bed level change over time. Vertical error bars in (a) represent the bed level change uncertainty.

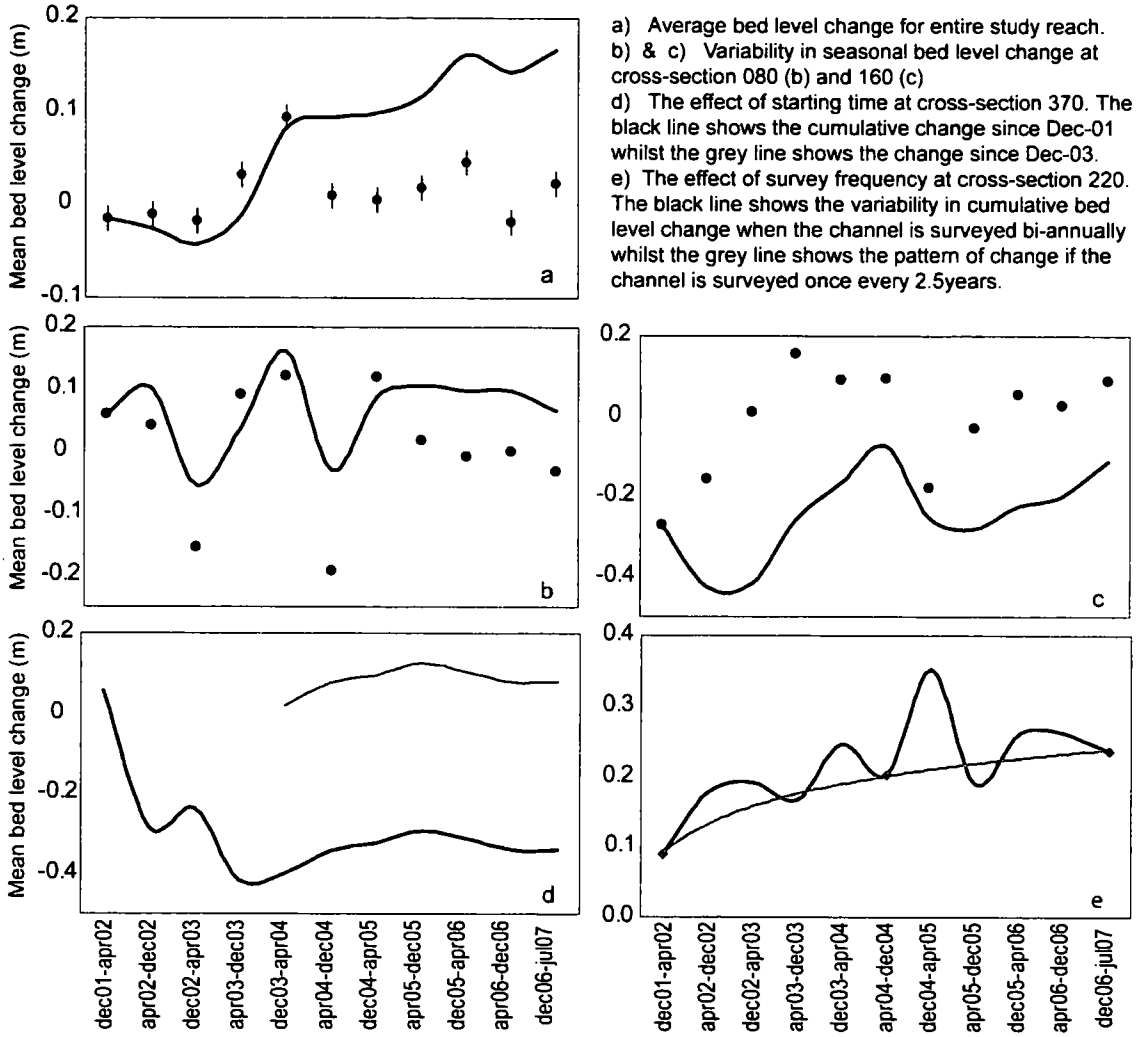

Nevertheless, despite these temporal variations, there has been an overall pattern of aggradation in the Wharfe study reach since surveying began, and reflected in data from two further sources. First, it is reflected in the strong downstream fining trend noted in the Wharfe from the bed material characterisation results (Section 5.2). The D_{50} (median grain size) is 74 mm at the top of the study reach at Hubberholme whilst at Starbotton, 5.6 km downstream, it has fallen to 14 mm. Coarse sediment at the top of the reach fails to progress to the end of the study reach and is deposited and stored along the channel. This

finding argues against traditional assumptions (Hooke, 2003) that sediment supplied to a reach will eventually be transported through it and is supported strongly by the downstream fining literature (e.g. Ferguson *et al.*, 1996; 1998). Second, as discussed in Section 5.4.4, the relative intensity of sediment transport recorded by the sediment impacts sensors falls progressively with distance downstream. Data from these sensors suggest that, annually, only 10% of the sediment that enters at Hubberholme and Cray Beck, reaches Buckden Bridge. Of this, alongside the material entering from Buckden Beck, less than 1% actually leaves the study reach at Starbotton.

6.2.2 Controls on the Spatial Patterns of Sedimentation

Field surveys suggest that the spatial variability in bed level change is driven by the channel geometry, specifically channel slope and channel curvature (Section 4.2). Table 6.1 compares the locations of the maximum erosion and deposition with channel geometry characteristics. To remove potential confusion due to the differences in the upper and lower reach sections, this analysis is only done for the upper 3 km reach where patterns of erosion and deposition are more clearly defined. This table shows that there is a link between the locations with high levels of erosion and the channel geometry. Four of the six most eroding sections have both high curvature and an increase in channel slope. Of the remaining two, section 260 is the 2nd most curved in the reach; and slope increases by one of the greatest amounts at section 290. The erosion at section 290 may also be explained by the confluence of Buckden Beck immediately upstream. This tributary contributes a relatively low sediment yield to the main channel. If the contribution of discharge to the main channel from Buckden Beck is proportionally higher, then confluence scour may be anticipated. Although there is no data to support this, field surveys indicate that at low to medium flows Buckden Beck contributes over 1% of flow to the main channel.

Table 6.1: Relationship between channel geometry and bed level change. The table shows the 12 cross-sections that have experienced the highest rates of erosion and deposition since December 2002 alongside the slope and curvature rank for that location. Large slope rank values indicate the greatest increase in slope whilst small slope rank values correspond with reduction in slopes. Low curvature rank values indicate curved reaches whilst high values indicate straight reaches. In both the slope and curvature, values range from 1-34. Bold values indicate higher importance.

x-section number	bed level change (m)		slope rank	curvature rank
210	-0.43 ± 0.034	DEGRADATION	**20**	**1**
90	-0.37 ± 0.023		**18**	**8**
260	-0.34 ± 0.054		7	**2**
160	-0.23 ± 0.038		17	**5**
290	-0.20 ± 0.026		**22**	23
300	-0.10 ± 0.022		**26**	**7**
70	0.38 ± 0.038	AGGRADATION	29	**12**
30	0.42 ± 0.050		**1**	24
310	0.44 ± 0.020		**14**	21
120	0.50 ± 0.030		**2**	34
330	0.52 ± 0.018		19	**15**
150	0.60 ± 0.029		**3**	22

Geometrical characteristics also provide some explanation of the locations of deposition found in the Wharfe. The top three slope reductions correspond to high levels of deposition indicating that slope may be responsible for the deposition at cross-sections 30, 120 and 150. Thus, with the overall slope profile of the study reach concave and gradually reducing in slope, it is unsurprising that the overall system is aggrading. However, on the other hand, the deposition that is occurring may be responsible for the reduction in channel slope. The other two locations, sections 070 and 330, are slightly curved. When the field surveys are examined, both cross-section locations are found immediately after the bend apex and are associated with large point bar deposits. Whilst maximum curvature is associated with scour and erosion, deposition is associated with curved reaches downstream of the bend apex. Field observations suggest that the configuration of the confluence of the Cray Beck tributary, located at section 120, may lead to deposition. This tributary contributes only a small amount of sediment, <1%, to the main channel. Yet field surveys suggest that the configuration of the confluence is such that it allows the sediment to become deposited in the beck side of the confluence. Thus, it contributes to the deposition recorded at cross-section 120, which spans across the main channel and the tributary immediately upstream

of the confluence. Finally, it is unclear what is driving the deposition recorded at cross-section 310. It is likely that a combination of factors are responsible.

6.2.3 Controls on Lateral Channel Adjustment

Following on from the above discussion into the influence that changes in slope and curvature have on sedimentation, factors controlling lateral changes in channel planform are explored. This analysis concentrates on explaining the factors driving bank erosion. This discussion initially considers whether aggradation drives bank erosion. It then explores the relationship between curvature and bank erosion before examining factors controlling channel width.

First, Figure 6.3 examines the relationship between bed level change, sediment activity and bank erosion rates. A good linear relation between bed level and bank erosion rate is present as indicated by the full square data points. This implies that either the deposition of sediment is driving the bank erosion or that bank erosion increases width sufficiently to reduce flow depths and promote the deposition of sediment. With bank erosion rates small, it is likely that the deposition drives the bank erosion since the increase in width associated with small amounts of bank erosion will have little impact on flow depths and deposition rates. When the sediment activity points (hollow triangles) are considered, no clear pattern emerges. This suggests that when activity is high but the net change is not aggradation, bank erosion is not as likely. Thus whilst sediment transfer can be high, aggradation is crucial for bank erosion. This is particularly evident at the activity point referenced (1a), which corresponds to net degradation (1b). Here, bank erosion is low. This location may have been experiencing the passage of sediment waves, activity is high, but the sediment is only stored for a short-period which is insufficient to promote bank erosion.

Figure 6.3: Bed level change and sediment activity plotted against bank erosion rates.

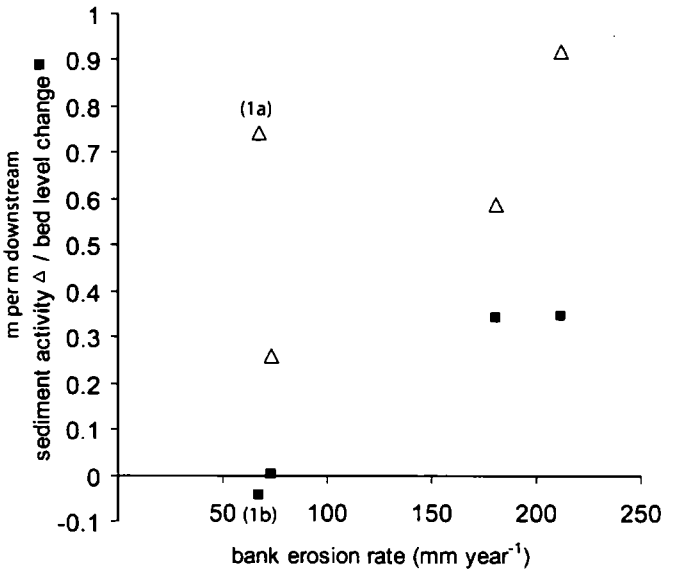

Findings from the bank erosion results (Section 4.4) suggest that bank erosion rates are higher in curved reaches when compared with straighter channels. This suggestion can be explored further by comparing the channel curvature calculated from the digitised LiDAR images (Section 4.5) with the fastest flow paths determined using a field based approach (Section 4.6) and the bank erosion rates (Section 4.4).

The fastest flow paths were smoothed to remove the noise associated with the 2 m spatial resolution. A 3-point moving average was used so that the spacing of points became around 6 m. Since the spacing of the digitised points on the channel centreline was greater than the spacing of the measured-smoothed flow path points, flow path points closest to the channel centreline were extracted for further analysis. First, the curvature of the centreline was compared with the curvature of the fastest flow path. Curvature of the fastest flow path was determined using the same approach used to determine the curvature of the centreline. Second, the relationship between centreline curvature and the proximity of the fastest flow from the bank was compared. The results are shown in Figure 6.4.

Figure 6.4a, illustrates that despite the scatter there is a relationship between the curvature of the channel and the fastest flow. One would expect this relationship to be completely

linear with the trend line passing through (0,0) and having a gradient of 1, if the flow was parallel to the banks. However, the plot exhibits a large amount of scatter, particularly at lower curvatures and the linear trend line crosses at 0.013 radians and has a gradient of 0.07. This means that there is a lag between high channel curvature and flow path curvature with the channel curvature increasing before the flow path curves. This finding is supported by work by Dietrich and Smith (1983). Furthermore, the flow path curvatures are much higher than the channel curvatures. This is likely to be a function of the smoothed centreline and the wandering nature of the fastest flow path. Of the six bends, the highest flow curvature occurs after the highest channel curvature in three cases. In the other three bends, the highest flow curvature is immediately before the maximum channel curvature. These results indicate that when the channel initially starts to bend, the flow path initially continues on a straighter path before turning a tighter curve close to the peak channel curvature. Thus, inertial effects are present and are important for meander development.

Figure 6.4b shows that when the curvature of the channel increases, the fastest flow path moves towards the outer bank. Again there is a lot of scatter but a general trend suggesting that the greater the curvature, the closer the flow to the outer bank. The results show that, of the six bends, the flow is closest to the outer bank at the maximum channel curvature on five of the bends. On the sixth bend the flow is closest to the bank just after the peak curvature.

Figure 6.4: Analysis of flow paths around meander bends. (A) shows the relationship between channel and flow curvature, whilst (B) shows the shifting of the high velocity core towards the outer bank as channel curvature increases.

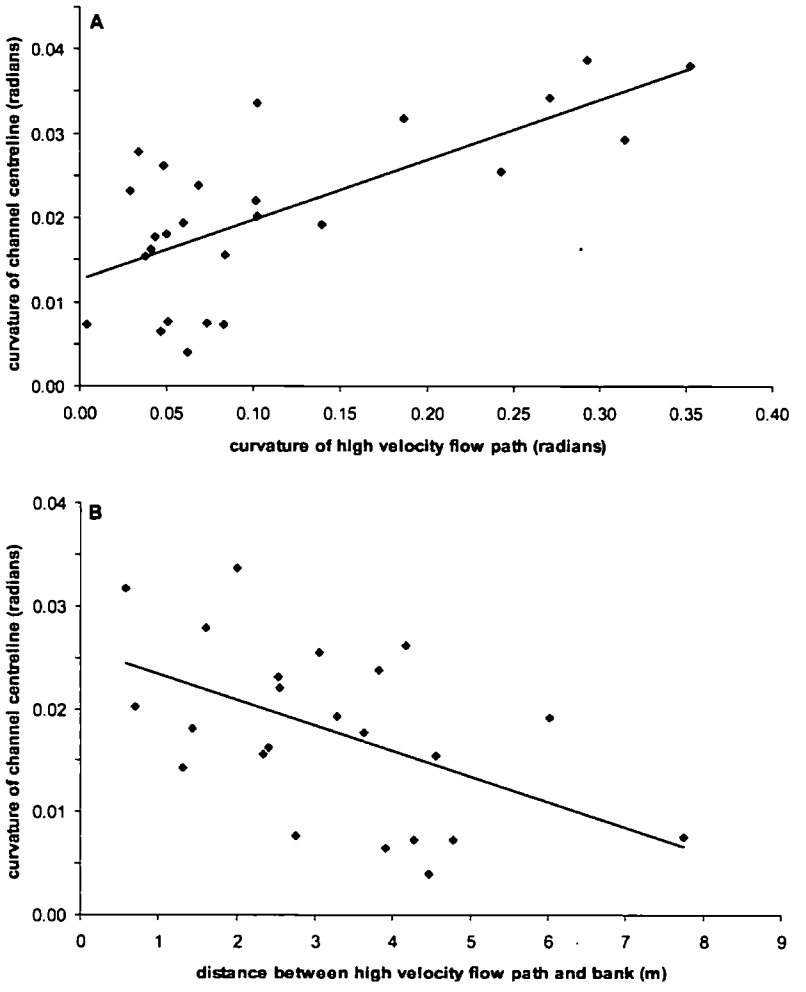

Figure 6.5a shows the relationship between channel centreline curvature and annual bank erosion. Of the four banks, each represented in the plot, two were on relatively straight reaches with low curvature and two were on the outside of meander bends. There is a strong relationship between curvature and bank erosion rates, despite there only being four data points. If a linear trendline is added to this plot, the R^2 value is 0.96, which is perhaps not that surprising since there are only four data points. Begin (1981) who used the relationship between rates of channel migration and curvature in his width adjustment

model supports this finding. In Figure 6.5b, the channel width at each of the bank erosion sites was noted and plotted against the annual bank erosion rates. The linear increase in channel width as bank erosion rates increase is unsurprising and leads to an examination of the links between curvature and channel width. It should be noted that some of the bank erosion sites are not exactly in-line with the cross-section location and hence the channel width of a bank erosion site is specific to the bank erosion site and is not the same as the nearest cross-sectional location. When interpreting these results care must be taken due to downstream changes in width that may be expected due to increasing discharge from tributary inputs. However, this is unlikely to be very large since the main tributaries of Cray and Buckden Beck increase the flow by around 10 and 5% respectively.

Figure 6.5: Relationship between curvature, bank erosion and channel width.

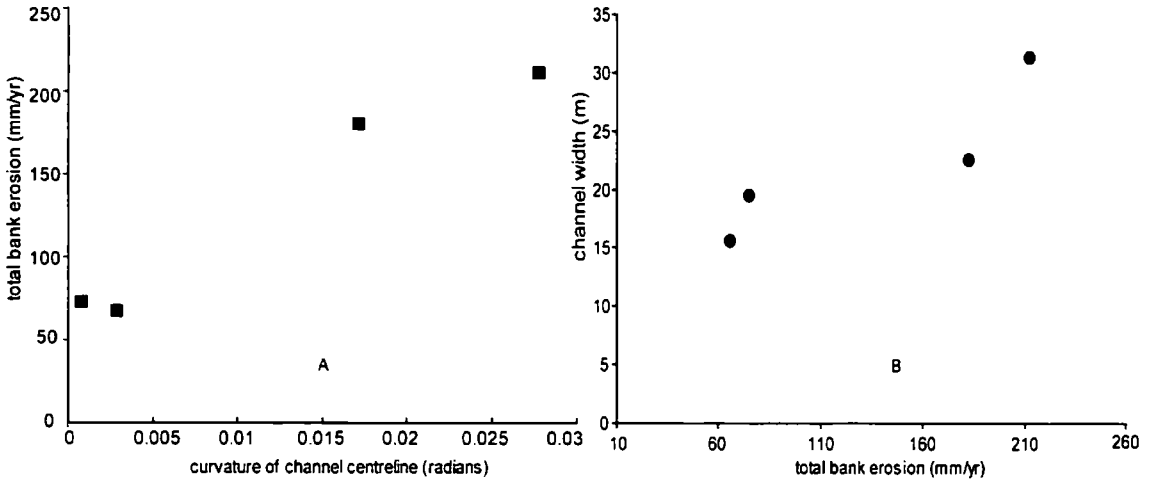

With curvature closely related to bank erosion, it is of interest to explore whether curvature and channel width are also linked together. It is hypothesised that reaches with higher curvatures will erode at a faster rate and hence will be wider. However, many of the banks along the Wharfe study reach, typically on the outside of meander bends, are protected by hard engineering. This protection stops bank erosion thereby restricting width adjustment. As such, the cross-sections are split into protected and unprotected. Both groups are analysed separately. First, in the cross-sections with no bank protection, as shown in Figure 6.6, there is an increase in channel width as curvature increases until around 0.02-0.03

radians where there is a cut-off with width increasing but curvature remaining similar. This cut-off represents the maximum curvature of un-protected bends. The range of widths at this maximum curvature reflect other flow and bank factors that are involved in bank erosion. The scatter in these plots also reflects the complexities in the bank erosion process with other factors including vegetation, bank materials and slope also involved. When the ratio of radius of curvature to channel width (R/w) are determined, a range of values from 1.7 to 4 are found for the unprotected bends. These values are similar to others noted in the literature including Hey (1976) who found R/w values of 2 for British rivers and Williams (1986) who found a range of between 2 and 3. Where bank protection is in place (Figure 6.7), no relationship between curvature and width is apparent. The channel width in protected reaches is determined by human intervention and not natural adjustment processes. Hence, this result is expected. Furthermore, channel sections where no bank protection is present are on average 1.45 m wider than those that are protected. However, there is no statistical difference between the two data groups as determined using a t-test. The t-value for the comparison was below the critical t-value for the number of degrees of freedom present in the sample. Therefore, the null hypothesis, that there is no difference between samples, is accepted.

Figure 6.6: (left) Channel width and curvature on protected cross-sections
Figure 6.7: (right) Channel width and curvature on unprotected cross-sections

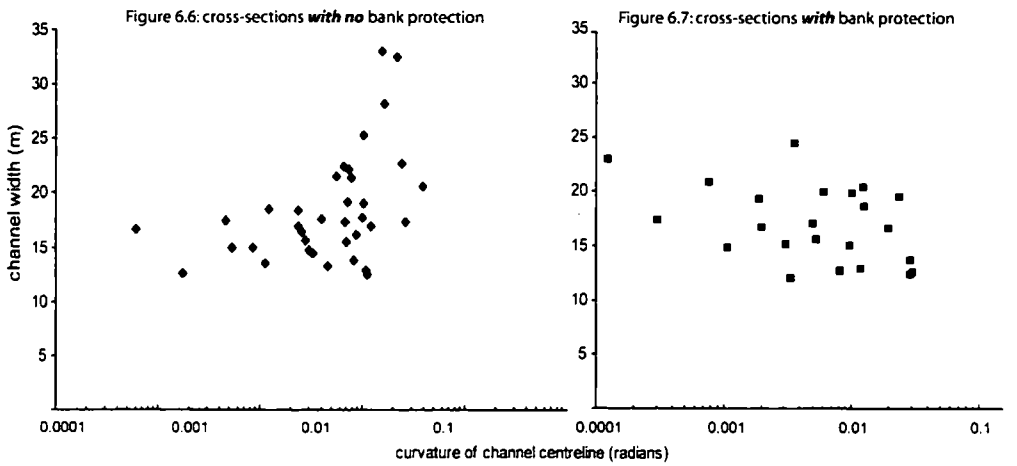

To summarise, the results presented demonstrate that in the Wharfe: (1) bank erosion rates are higher when aggradation occurs; (2) the flow path around bends closely follows channel curvature although there is a partial lag with the banks bending before the flow; (3) the fastest flow path is closest to the bank at or just before the highest channel curvature; (4) bank erosion rates are higher when curvature is high; and (5) bank erosion produces wider channels. Thus, curvature drives bank erosion and width increases through the shifting of the high velocity core of flow to the outer bank. Deposition occurs on the inner bank. However, this argues against findings made in Table 6.1, which demonstrated that degradation is associated with the highest curvatures whilst aggradation is found at moderate to low curved reaches. This discrepancy can be explained by the presence of bank protection. In the most curved reaches, bank protection is present and this inhibits bank erosion and lateral channel change. The channel remains narrow and scour occurs, degrading the engineered reach. Thus, two situations are present if curvature is high: (1) in protected reaches, degradation prevails and no lateral adjustments occur; and (2) in unprotected reaches, curvature promotes outer bank erosion and inner-bank deposition and the river is allowed to meander.

6.3 ESTIMATING BEDLOAD TRANSPORT RATE

The cross-sectional surveys and data from the sediment impact sensors allow a morphological sediment budget to be reconstructed. The theory underlying this approach is that channels evolve over time through the erosion, transport and deposition of mobilised sediments downstream. Thus, there is a direct link between coarse sediment transfer and channel morphology. Rates of sediment transport are estimated by quantifying changes in patterns of erosion and deposition within the channel. Popov (1962) was the first to suggest this approach and Neill (1987) successfully developed the idea using data from the Fraser River. This approach, which is often termed the "inverse method", has been used and developed further by many (e.g. Ferguson and Ashworth, 1992; Goff and Ashmore, 1994; Martin and Church, 1995; Lane *et al.*, 1995; Ashmore and Church, 1998; McLean and Church, 1999; Ham and Church, 2000; Lindsay and Ashmore, 2002; Fuller *et al.*, 2003; Martin and Ham, 2005).

6.3.1 CONSTRUCTING THE SEDIMENT BUDGET

The method can be explained using an inverted Exner equation for sediment continuity [6.1]. This equation allows changes in volumetric rates of sediment transport or the bedload flux (Δq) averaged across the channel (Δz) to be estimated from width-averaged changes in bed elevation (Δh) over a certain time period (Δt). This time period can be the time period between two successive surveys or if known, the duration of active transport. The bulk sediment porosity is represented by ε.

$$\frac{\Delta h}{\Delta t} = \frac{-1}{1-\varepsilon}\frac{\Delta q}{\Delta z} \qquad [6.1]$$

The sediment budget approach requires volumes of erosion and deposition within the study reach to be quantified. Methods of calculating this include using repeat topographic surveys, aerial photography or using land-based photogrammetry. The first method is the most common and is used to survey the channel bed, bars and islands at either: (1) fixed cross-sectional locations (e.g. McLean and Church, 1999; Martin and Ham, 2005); or (2)

within a defined reach by surveying all morphological features at a high resolution to create a DEM of the channel (Lane *et al.*, 1995; Brasington *et al.*, 2000; Fuller *et al.*, 2003). The latter is a much more detailed survey but due to time constraints is typically limited to short reaches. The second approach, as adopted by Ham and Church (2000), used an analytical stereoplotter to map features such as channel banks and bars from a series of aerial photographs. The volumetric changes between photographs are estimated and used to re-construct the sediment budget. The final method uses digital photogrammetry, laser altimetry and image processing to provide a high resolution DEM of the channel geometry (e.g. Lane *et al.*, 1994; Westaway *et al.*, 2000, Lane *et al.*, 2003). Due to the resolution, it can only be applied to short river sections.

The morphological approach has several limitations and estimated sediment transport rates are likely to be lower-bound estimates (Fuller *et al.*, 2003). The first limitation is that fixed cross-sections only provide information at-a-point. Consequently, there is an extrapolation weakness associated with the method. Extrapolated data points may be tens of metres away from a measured cross-section (Fuller *et al.*, 2003). It is also likely that the chosen location will fail to represent the full range of morphological channel changes migrating downstream through space and time (Lane *et al.*, 1994). Furthermore, the locations may miss processes of erosion and deposition that occur between cross-sections (Naden and Brayshaw, 1987; Wittenburg, 2002). Thus, sediment may move through the reach without any surface expression at the survey site or localised deposition may occur at the survey site that does not represent changes in the vicinity of the cross-section (Lindsay and Ashmore, 2002). Finally, volumes of activity may be negatively biased because of compensating volumes of scour and fill between surveys (Lane *et al.*, 1994; Ashmore and Church, 1998; Lindsay and Ashmore, 2002). Scour and fill compensation occurs when there is a switch between scour and fill at a point between surveys. This problem is demonstrated in Figure 6.8.

Figure 6.8: Scour and fill compensation when calculating volumetric changes.

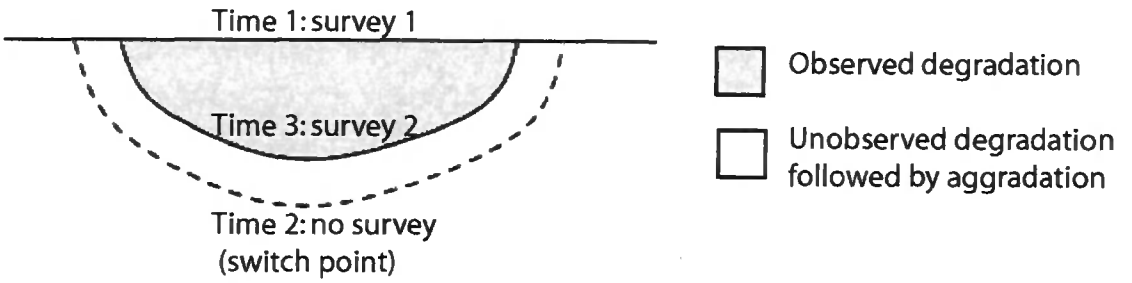

The morphological approach requires the transport rate to be known for at least one location within the study reach to provide either a starting input or output volume from which the other volumes can be determined. This boundary condition may be measured using a portable sampler such as the Helley-Smith bedload sampler (e.g. Lane *et al.*, 1995). No attempt was made to sample the Wharfe using such a device due to the nature of the transport conditions. Hence, this crucial information on the sediment transport rate along with detailed information on the duration of sediment transport activity was obtained from the impact sensors placed in the study reach for just over a year (Section 5.4).

In addition, the significance of sediment supplied to the channel from bank erosion required quantifying and if necessary accounting for in the budget. Whilst bank erosion at the measured cross-sections is incorporated into the budget already, any bank erosion between cross-sections is not accounted for. By combining the bank erosion rates estimated from the bank erosion study (Section 4.4), and the estimates of eroding bank face length and height made in the surveys (Section 4.2), an estimate of the volume of sediment added to the river system from the eroding banks can be made. Figure 6.9 shows the locations of erosion in the Wharfe alongside bank protection. The volumetric bank erosion estimate is shown in Table 6.2.

Figure 6.9: Map showing locations of bank protection and erosion.

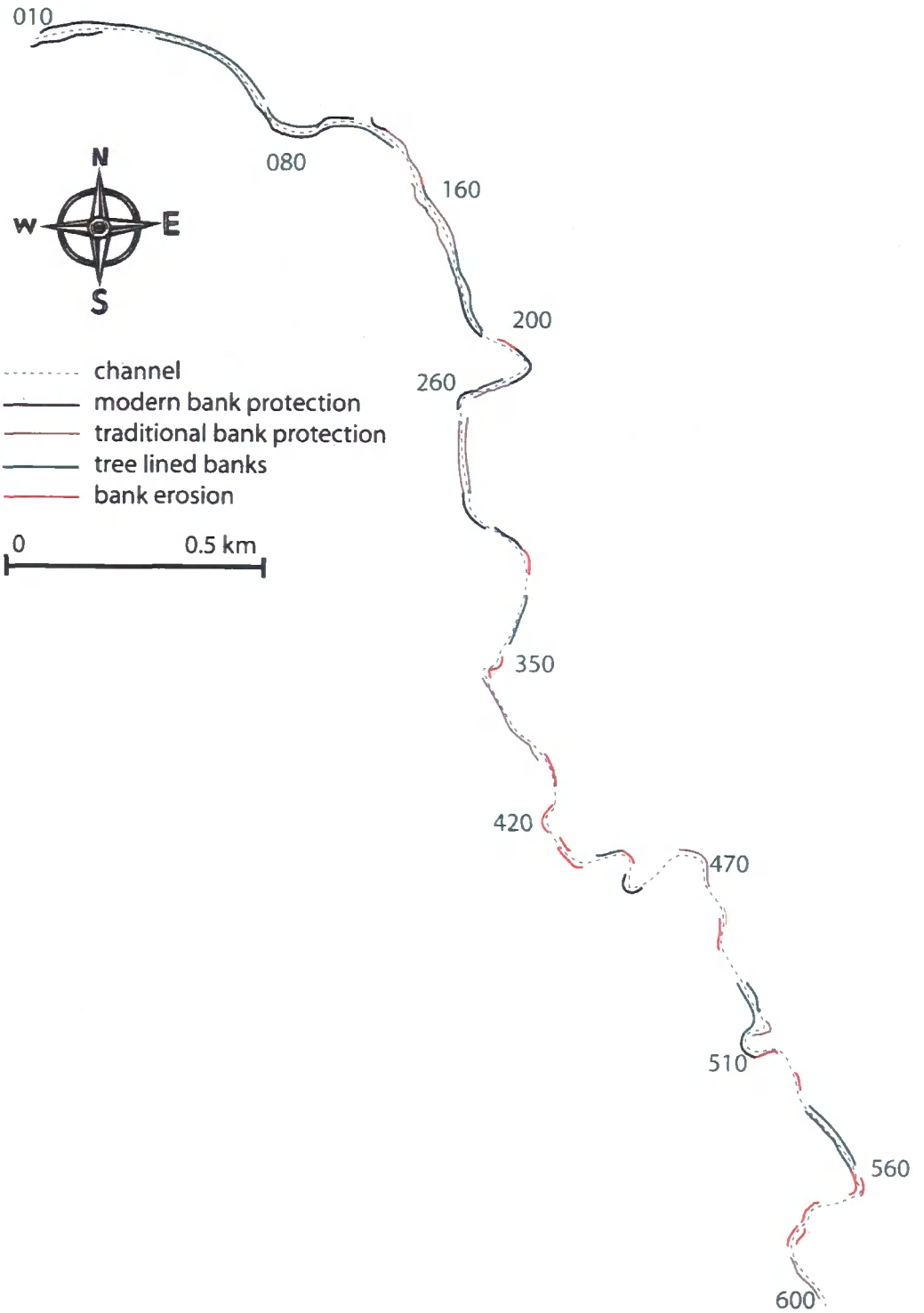

Table 6.2: Estimated volumetric input of sediment from bank erosion

	Estimated volumetric input of sediment from bank erosion
bank erosion on straights	85 m of straights at 2.1 m high = 178.5 m^2 of bank face 17 m of straights at 2 m high = 34 m^2 of bank face 20 m of straights at 1.8 m high = 40.8m^2 of bank face 24 m of straights at 1.7 m high = 36 m^2 of bank face
	TOTAL of 289.3 m^2** of eroding bank face on straights at 0.07 m per year = **20.25 m^3 of bank erosion per year
bank erosion on bends	87 m of bends at 2.1 m high = 182.7 m^2 of bank face 30 m of bends at 1.9 m high = 57 m^2 of bank face 20 m of bends at 1.7 m high = 34 m^2 of bank face
	TOTAL of 273.7 m^2** of eroding bank face on bends: 0.18 m per year (lower estimate); 0.21 m per year (upper estimate) = **49.3 to 57.8 m^3 of bank erosion $year^{-1}$
straights + bends	**69.55 to 78 m^3 erosion per year.**

These estimated input volumes are relatively small when compared with the volumetric changes in the channel recorded in the cross-sectional surveys. The volume of sediment from bank collapse can also be estimated. The bank collapse recorded on bank 4, will have input around 13 m^3 of sediment (8 m bank length, 2 m bank height and 0.8 m bank retreat) whilst the 12 m of erosion, estimated from the aerial photographs, suggest that an input of 480 m^3 (20 m long bank, 2 m high, 12 m bank erosion) of sediment may have entered the channel in a very short period of time. However, these volumes are still small when the volumetric changes from upstream sediment delivery are considered. Furthermore, this sediment is predominantly fine material that would be entrained as wash load by the flow. It would contribute minimally to bed level changes and would not be recorded by the sediment impact sensors that only record grain sizes greater than 8 mm. Thus, sediment input from the banks can be discounted. However, when the extent of bank protection mapped in Figure 6.9 is considered, this assumption would require revisiting if bank protection was not present.

The volumetric changes in the channel alongside the impact sensor data were used to reconstruct the sediment budget of the channel. The impact sensor data, allows a zero transport rate to be set at Starbotton. Martin (2003) made a similar assumption. He found little transport in the most downstream location and therefore set a zero-gravel transport

rate. With the downstream limit set at 0, the budget could be extended upstream using [6.2]. At each of the tributary confluences, 0.8% (Buckden Beck) and 0.3% (Cray Beck) of the sediment was removed. These percentages were determined from the impact sensors as explained in Section 5.4.4. With only one full year's worth of ping data available, the budget reconstructed from the March 2003 to March 2004 survey data was used to estimate the bedload transport rates in the channel. This budget is shown in Table 6.3. Appendix IV contains the budget for each of the survey periods. The periods April 2003 – December 2003 and December 2003 – April 2004 were combined to give the March 2003 – March 2004 estimates.

$$V_i = V_o - \Delta V - V_{trib} \qquad [6.2]$$

where V_i is the volumetric input into the reach, V_o is the volumetric output and ΔV is the storage within the reach (volumetric change calculated using [4.4] in Chapter 4) and V_{trib} is the tributary input (only used in the two reaches where tributaries enter: marked as a dashed line in Table 6.3). The budget for March 2003 – March 2004 shows that 8790 m^3 ± 16.5% (1447.7 m^3) of sediment entered the reach over the duration of the year. This is the same as 0.09 m of bed level rise uniformly distributed across the channel bed down the entire study reach. This is the highest input for all of the study periods. Since the estimates of sediment transport rates from morphological budgets are likely to be lower bound estimates (Fuller *et al.*, 2003), these values provide a conservative estimate of sediment transport rates in the Upper Wharfe. When the budget is examined more closely, it is noted that the two most downstream cross-sectional reaches (580-600) record negative values during the study period. This implies that sediment actually left the study reach during this time. This leads to the zero-transport output boundary value being questioned. This apparent erosion in the lower reaches is supported by the small amount of sediment activity that was recorded at Starbotton by the impact sensors. Since these values are only small they can largely be ignored and the zero-transport output value can be maintained. If these values were more important, the output value would require revision. Indeed, for all the survey periods, the maximum negative values were recorded during this time period (March 2003 – March 2004). The average volumetric change in storage for the most downstream section of 590-600 for all time periods was estimated at 19 m^3 ± 10%.

Table 6.3: Volumetric budget for March 03-March 04. Dash line indicates tributary.

cross-section	area change (m^2)	distance between sections (m)	ΔV (m^3)	Vi (m^3)
10	2.6	0.0	1253.3	8790.5
30	4.9	331.3	923.5	7537.1
40	4.3	199.5	859.9	6613.7
50	3.8	212.2	10.2	5753.7
60	-3.2	34.5	-81.7	5743.5
70	-2.1	31.1	30.8	5825.3
80	4.3	28.2	160.5	5794.5
90	2.8	45.2	166.3	5633.9
100	2.7	60.5	136.1	5467.6
110	4.2	39.7	161.1	5331.5
120	3.2	43.4	146.6	5170.4
130	2.3	52.6	100.7	5039.0
140	3.9	32.0	271.5	4938.3
150	3.5	73.2	428.0	4666.8
160	3.7	119.3	432.9	4238.8
170	0.8	190.6	-91.7	3806.0
180	-2.2	139.4	-151.2	3897.6
190	-1.6	80.7	-63.2	4048.8
200	0.5	116.8	-83.4	4112.0
210	-6.8	26.7	-102.0	4195.4
220	1.1	35.9	43.5	4297.4
230	0.6	51.3	36.5	4253.9
240	1.8	30.2	98.8	4217.4
250	2.1	50.3	-44.5	4118.6
260	-3.4	69.5	-103.6	4163.1
270	-2.2	37.0	-113.0	4266.7
280	-0.3	92.6	-23.8	4379.7
290	-0.2	111.3	21.7	4403.5
300	0.8	71.6	261.4	4417.2
310	7.3	64.8	219.2	4155.8
320	1.0	52.7	113.7	3936.7
330	1.5	88.5	184.2	3823.0
340	1.3	128.7	548.2	3638.8
350	7.4	126.2	203.5	3090.6
360	-2.3	79.5	-71.0	2887.1
370	-3.1	26.7	-119.5	2958.1
380	-1.1	56.9	-176.9	3077.6
390	-1.7	123.0	-106.1	3254.5
400	0.0	120.6	-19.5	3360.6
410	-0.4	103.1	35.4	3380.2
420	2.5	33.2	635.9	3344.8
430	2.2	272.2	243.6	2708.9
440	1.0	151.0	173.6	2465.3
450	2.3	105.2	155.2	2291.7
460	2.6	63.6	193.6	2136.5
470	0.9	110.4	316.7	1942.8
480	4.1	127.9	515.8	1626.1
490	1.5	184.1	296.4	1110.3
500	5.3	86.3	317.4	813.9
510	1.7	90.1	118.0	496.5
520	0.4	114.5	-15.0	378.5
530	-0.7	85.6	150.4	393.5
540	3.4	111.8	176.0	243.2
550	0.9	82.9	195.1	67.1
560	2.6	112.8	216.3	-127.9
570	1.4	108.9	97.4	-344.2
580	0.3	113.9	-157.0	-441.7
590	-2.7	130.6	-284.7	-284.7
600	-1.8	124.1	0.0	0.0

6.3.2 VOLUMES TO TRANSPORT RATE

To convert a volumetric input of sediment into a transport rate, it is important to include a porosity factor to account for voids in the bed material when converting a volume (includes voids) into a weight (void-less). Porosity is controlled by the texture (grain size and sorting) and the fabric (packing and orientation) of the material. Typical values of porosity for gravels are between 0.25-0.40 (e.g. McWorter and Sunada, 1977; Freeze and Cherry, 1979). This is the same as saying that between 25 and 40% of the volume are voids. Carling and Reader (1982) developed a conversion equation that related the saturated specific weight of sediment (i.e. the weight of sediment and water mix per volume of deposit) to the more readily obtainable specific weight of dry sediment (weight of sediment per volume of deposit). They went on to suggest that in the absence of significant silt and clay sized material, the median grain diameter of poorly sorted bed material (i.e. those with a wide range of particle size) can be used to estimate the porosity. They calculate this factor using [6.3]. They found that porosity is negatively correlated to the median grain-size (Figure 6.10) and that poor sorting of gravel particles allows close packing and hence the porosity is lower. Thus sand sized particles fill the voids between larger particles.

$$\varepsilon = 0.4665 D_{50}^{-0.21} - 0.0333 \qquad [6.3]$$

where ε is the porosity and D_{50} is the mean grain diameter (mm).

For the Wharfe sediment, the D_{50} ranges from 79.2 mm to 16.3 mm. Based on [5.6] and Figure 6.10 the porosity factors that should be applied to the Wharfe according to Carling and Reader's findings, range from 0.15 (Hubberholme) to 0.23 (Starbotton). These values are slightly lower than those used by Martin (2005), Ham and Church, (2000) and Martin and Church (1995) who set porosity at 0.25. Lane *et al.* (1995) found ε to be 0.2, which is similar to the range found for the Wharfe.

Figure 6.10: Porosity as calculated using Carling and Reader (1982)

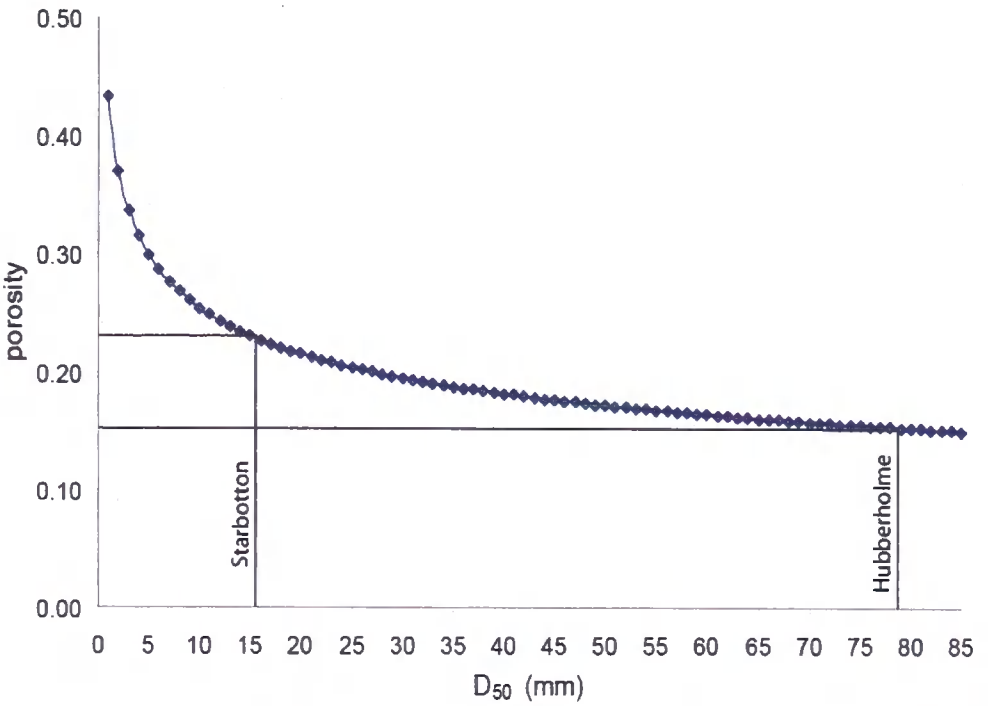

However, these lower porosity values found using Carling and Readers approach assume that the voids are filled with finer particles. When the GSDs for the Vedder River (Martin and Church, 1995) are compared with those from the Wharfe, some issues arise. At the downstream end of the Vedder study reach, the D_{50} is 10 mm whilst in the Wharfe the D_{50} for the active layer at cross-section 540 is slightly coarser (16 mm). However, the nature of the grain size distributions is very different within the Wharfe. Whilst the Vedder has 40% material less than 8 mm and 10% greater than 64 mm, the Wharfe has 26% less than 8 mm and 4% greater than 64 mm. Thus wider variations in grain sizes, and in particular the higher percentage of finer material in the Vedder, will reduce the porosity when compared to the Wharfe (more fines to fill the voids). Hence, the Wharfe requires higher porosity values than those used on the Vedder River and those suggested using the Carling and Reader approach.

Table 6.4 shows the effect that changing the porosity has on the volumetric input at Hubberholme when converted into kilograms and tonnes (i.e. a weight). By changing the

porosity from 0.1 to 0.3, the input increases by 4700 tonnes, or by 22%. It is important to use an appropriate porosity value. Hence, the Carling and Readers equation was used to scale porosity with the D_{50} and then 0.1 was added to adjust for the lack of sand in the Wharfe. This gave the Wharfe porosity values ranging from 0.26 at Hubberholme to 0.33 at Starbotton. These values are more in line with those used in other gravel-bed rivers. Yet, these higher values assume that there is little sand in the bed which is incorrect in the lower reaches. However, this methodology is attempting to estimate the bedload transport rate which excludes fines that are transported in suspension. Additionally, the impact sensors only record particles greater than 3 mm thereby ignoring fine sands. It was felt that a value of 0.4 was too high for the lower reaches where the sediment is finer.

Table 6.4: Input values when applying different porosity values. Using estimated volumetric inputs for Hubberholme, for March 2003-2004.

Input (m^3)	Porosity	Bulk Density (kg/m^3)	Input (tonnes)
8790.5	0.1	2385	20965.3
8790.5	0.2	2120	18635.9
8790.5	0.3	1855	16306.4

The volumetric inputs (V_i) at each cross-section were converted into a transport rate (q) by multiplying by the chosen porosity factor and integrating over active transport time (t) and channel width *(w)* to give the estimated bedload transport rate in $kg^{-1}\ m^{-1}\ s^{-1}$ [6.4]. Active transport time, was calculated from the estimated percentage time sediment was in motion using the impact sensors described in Section 5.4. The bedload transport rate was calculated assuming that it is constant across the width of the active channel (w).

$$q = p(1-\varepsilon)\frac{V_i}{\Delta w \Delta t} \qquad [6.4]$$

This method was applied to the volumetric estimates at Hubberholme and at Buckden Bridge for the two survey periods, April 2003 to December 2003 and December 2003 to April 2004. Table 5.8 shows details of the values used for these estimates. For each location, the porosity factor was determined from the D_{50} at the location with 0.1 added in

to account for the reduction in fine material found in the Wharfe sediment. This value has no empirical evidence supporting it; it was selected entirely to make the data fit better. 0.26 was applied to the coarser sediment at Hubberholme and a higher value of 0.28 was applied to Buckden Bridge, where the D_{50} had fined by 37 mm. In addition, the estimates account for different channel widths at the two sites, and different transport times estimated for the impact sensors at the two locations. By dividing the input by the width and then the transport time in seconds, the average transport rate can be estimated for the given location and time period. This average can then be related to the ping count for that period to provide a bedload transport estimate for a given ping intensity. A visual example of this relationship is shown in Figure 6.11 whilst the maximum estimated transport rate is shown in Table 6.5. This approach assumes that bedload transport rate increases at a linear rate to ping count. Thus the two data series shown in Figure 6.11 mirror each other perfectly, reflecting that they are explicitly tied together.

By combining data from the impact sensors with the volumetric budget in this way, some interesting findings arise. First, echoing findings made in the impact sensor and cross-sectional survey analysis, seasonal and spatial differences in sediment transport rates are evident. At Hubberholme, transport rates are nearly three times higher in the December to April period when compared with the preceding April to December period. When the April to December survey period is considered, a small reduction in transport rates is noted as one moves from Hubberholme to Buckden Bridge. The estimated bedload transport rates at Buckden Bridge between December 2003 and April 2004 are of concern as they are substantially higher than the other estimates. This suggests that either only very high magnitude transport events occurred at Buckden Bridge during this time, or there is an error in the volumetric estimates or estimated transport time.

Table 6.5: Estimating average bedload transport rate from volumetric input.

	Apr 03 – Dec 03		Dec 03 – Apr 04	
	Hubb.	**B. Bridge**	**Hubb.**	**B. Bridge**
Input (m^3)	3030	583	5811	3706
D_{50}	79.2	41.7	79.2	41.7
Porosity	0.26	0.28	0.26	0.28
Bulk density (kg/m^3)	1961.1	1920.1	1961.1	1920.1
Input (kg)	5,942,330	1,119,409	11,396,329	7,115,831
Width (m)	12	19.5	12	19.5
Time intervals	3325	559	2419	182
Time (secs) from impact sensors	997,500	167,700	725,700	54,600
Average trans. rate ($kg\ m^{-1}\ s^{-1}$)	0.50	0.34	1.31	6.68
Max trans. rate ($kg\ m^{-1}\ s^{-1}$)	0.74	0.53	2.4	21.40

Figure 6.11: Relationship between ping intensity and estimated bedload transport rate for a single transport event at Hubberholme on the 1st January 2004.

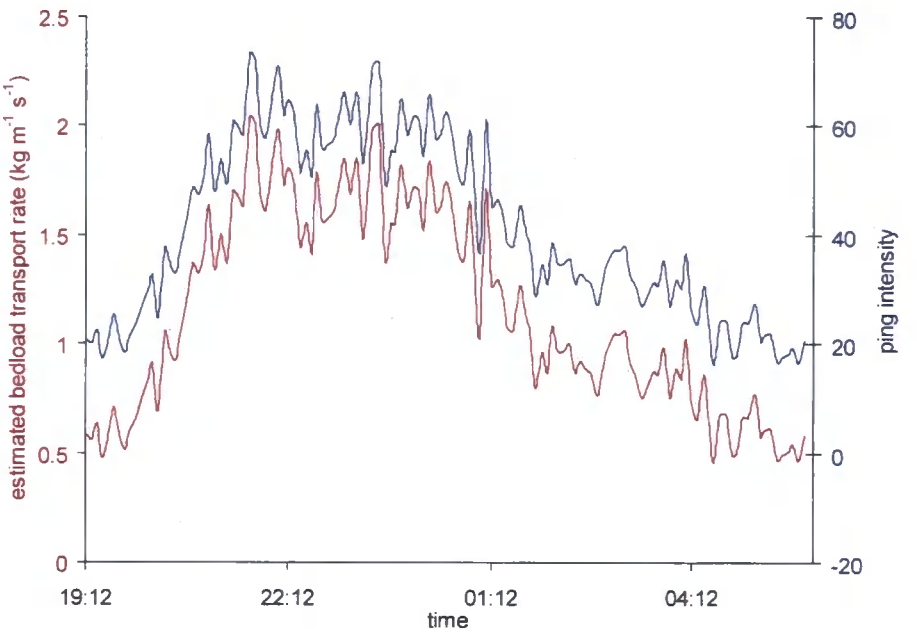

6.3.3 Summary of Volumetric Approach

The impact sensors add a new dimension to the traditional volumetric sediment budget approach by providing information on the length of time that sediment is in transport and the intensity and duration of individual events. Furthermore, they provide the budget with a more valuable output estimate from which to reconstruct the rest of the budget. The information from the impact sensors allows bedload transport rates to be estimated whilst the bank erosion study also supports the zero lateral input. However, this zero lateral input may not hold if bank protection was removed. In addition, the results presented here raise important issues to consider when constructing volumetric budgets. First, transport time varies greatly over spatial and temporal scales making it difficult to assign one estimate of transport time to an entire stretch of river for a given time period. Furthermore, porosity is an important parameter in these estimates and can change in reaches with rapid downstream fining.

6.4 Predicting Bed Level Changes Using Impact Sensors

Two data sources provide information about the channel's sediment transfer system: the cross-sectional resurveys and the sediment impact sensors. Whilst the former is a labour and time intensive method, the impact sensors provide a relatively cheap (approximately £500 per sensor), quick and easy method to monitor sediment motion. In addition, they can be used to derive the temporal variability suggested by temporally coarser volumetric surveys. Here, the ability to infer bed level changes from the impact sensors is explored. As noted in the impact results section (Section 5.4), when two time periods are considered (in this case, arbitrarily summer and winter), the percentage of sediment from Hubberholme that reaches Buckden Beck varies greatly from 4% in the winter to 32% in the summer. As such, can something be inferred about sediment accumulation between these two sensor sites based on the relationship between sediment passing through them? To allow a third time period, based on the new sensors, to be incorporated, this analysis compares the difference in the percentage of time that sediment is in motion over the three survey time

periods of March 2003 – December 2003, December 2003 – March 2004 and April 2006 – December 2006. These data are compared against the mean bed level change for the corresponding periods and the reaches of Hubberholme to Buckden Bridge, Buckden Bridge to Starbotton and the entire reach from Hubberholme to Starbotton. These data are presented in Table 6.6. Whilst transport times are expected to differ between sites as a result of different transport thresholds, the time difference between sites is not expected to vary, since the hydrological regime between sites is strongly coupled. Such variations provide a good indication than the sediment transport regime is less coupled that the hydrological regime.

Table 6.6: Relationship between mean bed level change and downstream differences in transport time. The mean bed level change (BLC) is calculated between the impact sensor locations alongside the percentage time difference between sites. For April 2006 – December 2006 the percentage time difference is only available for the whole reach length as no sensor was installed at Buckden Bridge.

		Hubberholme to Buck Bridge	Buck Bridge to Starbotton	Hubberholme to Starbotton
Mar 03 - Dec 03	mean BLC (m)	0.071	0.011	0.032
	time diff (% of year)	*3.3*	*0.5*	*3.8*
Dec03 - Mar 04	mean BLC (m)	0.091	0.084	0.087
	time diff (% of year)	*10.1*	*0.6*	*10.7*
Apr 06 - Dec 06	mean BLC (m)	-0.023	-0.02	-0.021
	time diff (% of year)	*no data at B. Bridge*		*2*

When the Hubberholme to Buckden Bridge reach is compared, higher aggradation is found during the December 2003 to March 2004 period when the transport time is 10.1% lower at the Bridge than at Hubberholme. Similarly, between Buckden Bridge and Starbotton, a greater spatial difference in the percentage time that sediment is in motion is associated with higher rates of aggradation. When the entire river is considered and data from the new sensors at Hubberholme and Starbotton are included, the results are also supportive. When the difference in transport time is lowest, between April 2006 and December 2006, mean degradation occurs. This may be due to a reduction in sediment entering the channel at Hubberholme (hence a reduced transport time) or an increase in sediment leaving the channel at Starbotton (an increased transport time). When the actual transport times at Hubberholme and Starbotton for each of the three time periods are considered, a

combination of a reduced transport time at Hubberholme and increased time at Starbotton occurs with Hubberholme values of 4% (Mar 2003 –Dec 2003), 11% (Dec 2003 – Mar 2004) and 2.7% (Apr 2006 – Dec 2006) and Starbotton values of 0.2% (Mar 2003 –Dec 2003), 0.3% (Dec 2003 – Mar 2004) and 0.7% (Apr 2006 – Dec 2006). These findings re-emphasise the third dimension in the sediment transport system: in-channel sediment storage. Thus, vertical changes in the channel are a function of hydrology, sediment supply from the hillslopes and within channel sediment storage.

6.5 Impact of Aggradation on Flood Risk

This section considers the implications of measured in-channel sedimentation for flood risk. In particular, changes in the incidence of flooding with respect to the temporal variations in channel sedimentation are considered. Using the variable power equation [5.12] outlined in Section 5.2, the bank full discharge is estimated at each of the 60 cross-sections using the December 2002 and December 206 geometry to calculate cross-sectional area. The lowest bank was used to determine the bank full level. Average slope between upstream and downstream cross-sections and roughness values specific to each section were used in the equation. Differences in bank full capacity between the two time periods are shown in Figure 6.12. Only 14 sections experienced an increase in channel capacity with the greatest increase of 31% found at cross-section 260 where outside bend scour is over deepening the channel. The other sections either remained constant over the time or experienced a reduction in bank full channel capacity as aggradation occurs. The greatest reduction in channel capacity was noted at section 120. This was due to the removal of the gravel trap and channel engineering in 2002. Since this time, the channel has experienced sediment accumulation. In addition, the cross-sectional locations of 050 and 350 have also both reduced in channel capacity by around 30%. These locations are zones with large gravel bars which are "growing" in height and areal extent. The average channel capacity in the entire reach has reduced by 6.7%.

Figure 6.12: Difference in bank full capacity at each cross-sectional location from December 2002 to December 2006 using the VPE equation.

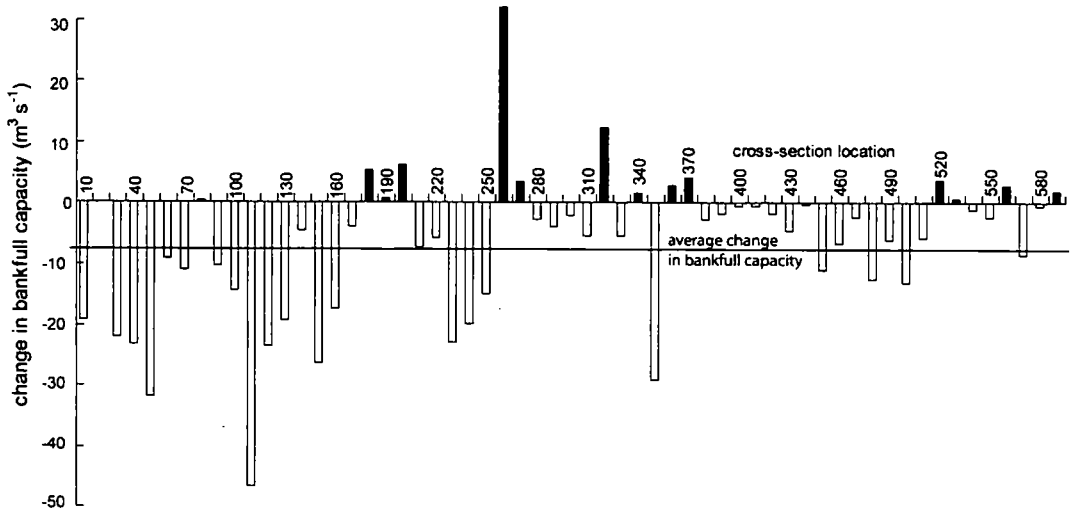

The analysis that follows, concentrates on cross-section 030, which crucially has an estimated discharge record and has experienced a bed level rise of 0.3 m ± 0.050 m since December 2002. This bed level rise equates to a relatively large reduction in channel bank full capacity of 21.9%. Slope was held constant in this analysis. As shown in Figure 6.12, this reduction is one of the larger amounts and hence this analysis represents the upper extent of the problem. Figure 6.13 shows the relationship between channel capacity in December 2002 and December 2006 and the top ten daily flows under three different flow regimes at Hubberholme: 1997, 2000 and 2002. Differences in the number of flood events and the time above bank full for the three flow regimes are considered in Table 6.7. Figure 6.13 illustrates that the impact of the sedimentation on the number of floods and the time above bank full is closely linked to the flow regime. In 1997 (Figure 6.13a), there is a more gradual drop in discharge from the maximum to the 10th highest daily flow and hence the impact of sedimentation is large, increasing the number of individual flood events from 0 to 4 and the time that flow is above bank full from 0 to 16 hours. In 2002 (Figure 6.13b), the impact is much less important since there is a large difference in discharge between the 4th and 5th largest flows. Hence, using the 2002 regime, 4 years of sedimentation has the effect of increasing the number of floods from 4 to 5. Despite the smaller increase in the number of flood events, the time above bank full (Table 6.7) increases three times from the 2002 to 2006 morphology. Consequently, water flows onto the floodplain for three times as long.

This will have an impact on floodplain inundation extents. Using the 2000 hydrology, a similar increase in the number of flood events and time above bank full is noted.

Figure 6.13: Relationship between the maximum daily flows in 1997, 2000 and 2002 and the channels bank full capacity in December 2002 and December 2006.

Table 6.7: Effect of changes in morphology on flood frequency and time flow is over bank.

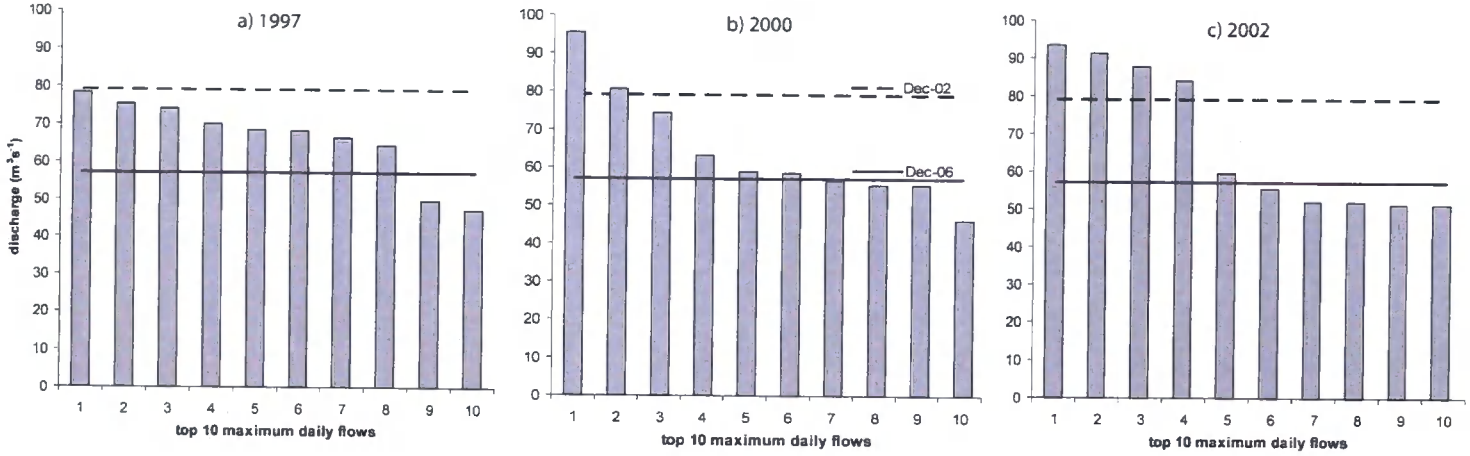

Survey Date	Cumulative mean bed level change dec02-dec06 (m)	Bankfull capacity ($m^3 s^{-1}$)	1997		2000		2002	
			No. of flood events	Time above bank (hours)	No. of flood events	Time above bank (hours)	No. of flood events	Time above bank (hours)
Dec-02		79.0	0	0	2	4.75	4	5.5
Apr-03	0.025 ± 0.025	77.2	1	0.25	2	5	4	6.25
Dec-03	0.218 ± 0.030	64.2	4	9.25	2	8	4	12.75
Apr-04	0.363 ± 0.035	55.0	4	17.75	5	18.5	5	18
Dec-04	0.422 ± 0.038	51.4	4	19.75	5	23.75	5	20.5
Apr-05	0.394 ± 0.041	53.1	4	18.25	5	20.5	5	19.5
Dec-05	0.367 ± 0.046	54.7	4	17.75	5	19.25	5	18.25
Apr-06	0.448 ± 0.047	49.9	4	21.5	5	24.5	6	23.5
Dec-06	0.330 ± 0.050	57.0	4	16.5	5	15.25	5	17

6.6 Discussion

The results demonstrate that, in aggrading river systems, such as the Upper River Wharfe, certain zones exhibit substantially more aggradation than is indicated by the spatially-averaged data. It is zones where sedimentation is the highest that the impacts on flood risk will be felt the greatest. The data shows the effect that sedimentation will have on the number and duration of overbank flows. The threshold at which sedimentation will impact on overbank flows is dependent on the hydrology and sedimentation rate. Once this threshold has been crossed, the increase in number and duration of flows can be dramatic. The examples show that 4-years of in-channel sedimentation can increase the number of floods by an average of 2.7 years and the time above bank by 12.8 hours. The increase in time over bank full is particularly concerning as longer periods of time allow greater volumes of water to flow onto the floodplain and hence a larger inundation extent. Indeed, previous work on the Wharfe showed that a 6.1% reduction in channel capacity as a result of 16-months of sedimentation can lead to increases in inundated area of 5.6% for the 1 in 0.5 year return period and 7.1% for the 1 in 2 year flood events (Lane *et al.*, 2007).

Either an increase in sedimentation rate or a reduction in the rate of change between the highest flows, reflecting a regime with more flood events, will lead to the impact on flood risk. A combination of the two will have far greater consequences. Both land-use change and climate change have the potential to alter our sediment supply and our discharge regime (e.g. Robinson, 1980; Leeks, 1992; Arnell and Reynard, 1996; Coulthard *et al.*, 2000; Knox, 2000; Kondolf *et al.*, 2002; Sullivan *et al.*, 2004; Booij, 2005). Land-use change increases an upland landscape's sensitivity to climate change (Macklin and Lewin, 2003). Buma and Dehn (1998) suggest that climate change impacts on precipitation (e.g. Brookes *et al.*, 2004) will almost certainly lead to changes in hillslope activity. This will result in greater coarse sediment generation in upland environments. In particular, this sediment delivery will come from an increased incidence of rainfall triggered shallow translation landslides (e.g. Montgomery and Dietrich, 1994). Lane *et al.* (2008) quantified the possible climate change impacts on sediment flux from the Buckden Beck catchment. They estimated using 2050 climate scenarios that the volume of sediment delivered to the

main River Wharfe channel would increase by between 7 and 40%. Using 2080s scenarios, the volume could increase by between 28 and 68%. Such increases in sediment delivery to the main channel would have alarming consequences for flood risk. Managing these systems will be difficult and attention should perhaps concentrate on managing the sediment sources rather than the channel itself.

Identifying zones where aggradation is particularly severe is important as these zones provided the greatest threat to increasing flood risk. With aggrading locations spatially and temporally variable, accurately locating these zones is problematic. Whilst cross-sectional resurveys provide a useful methodology they are often limited by time and cost restrictions. Limitations on survey spacing, frequency and the duration of the study can lead to misinterpretation as the results have demonstrated and hence these results must be analysed with caution. Yet, until newer methods (e.g. photogrammetry by Kinzel *et al.*, 2007) become more widely available, techniques such as cross-sectional re-surveys and fluvial audits provide a first "best guess" into locations that may be particularly sensitive to aggradation, perhaps allowing survey efforts to be concentrated.

The results have shown that reductions in slope and curvature are closely linked to changes in channel morphology. It is unsurprising that when the channel becomes steeper, erosion prevails since the channel's transport capacity increases, whilst deposition is associated with reductions in slope. The relationship between channel curvature and bed level change is slightly harder to predict since both zones of erosion and deposition occur when curvature is high. What the results suggest is that erosion occurs at the apex of the bend, where curvature is highest and deposition prevails immediately downstream. The presence of large point bar deposits recorded in field surveys, suggest that the secondary circulation created by the bend leads to deposition in the immediate downstream section. Additional features such as tributaries and bridges should also be accounted for when attempting to predict rapidly changing zones. Buckden Bridge may be acting as a barrier to sediment transfer downstream resulting in a moderate amount of sediment accumulation immediately upstream, and erosion immediately downstream.

The downstream channel geometry over longer spatial scales should also be considered. Many highly depositional reaches were found directly upstream of erosional reaches. Indeed it may be the case that the large depositional reach, prior to the 3 km upper and lower reach divide, acts to reduce sediment supply downstream, thereby leading initially to erosion and then significantly less aggradation further downstream. Thus, whilst the source of sediment accumulation in the upper reach may be from upstream of Hubberholme and the two tributaries, the lower reach is at times supply-limited. Consequently, although activity is relatively healthy in the upper reach, the lack of additional material downstream results in a relatively low net bed level rise, with larger high magnitude events required to mobilise sediment and rework it through and out of the study reach. During such events, the coarse layer and bed armour is broken down, all grain sizes are moved and the coarse layer is reformed (Parker and Klingeman, 1982; Andrews and Erman, 1986). It may be that the progressive aggradation upstream and the degradation downstream of the 3 km divide reaches a critical threshold where the increased slope is sufficient eventually to start moving sediment through this divide. An alternative explanation is that the bend at this location acts as a barrier to downstream sediment. Without studies over longer timescales, it is difficult to assess a channel's future response.

Furthermore, one may question why sediment rarely leaves the reach at Starbotton with the results and findings from Reid *et al.* (2007a) noting that transport out of the reach only occurs during very high magnitude events. It appears the case that the long-term pattern of aggradation suggested in the valley (Lane *et al.*, 2007) may be a response to larger geomorphic controls. These include the reduction in valley gradient at Hubberholme and a sediment discontinuity found at Starbotton. This discontinuity resulted from a catastrophic flood event in Cam Gill Beck (which joins the Wharfe at Starbotton) in 1686 (Coulthard *et al.*, 1998). This single event generated a decadal amount of sediment (Coulthard *et al.*, 1998) and formed the Starbotton alluvial fan which extended across the width of the valley. The river has cut into this deposit yet it still acts as a local rise in base level. The channel's response to this is to aggrade upstream. Features such as bridges, weirs and dams, large landslides and significant channel engineering may create a similar effect leading to upstream aggradation.

In addition, it is often zones of high aggradation, particularly those with high curvature, that are subject to bank erosion as a natural response to sedimentation. This lateral adjustment not only allows the channel to maintain its capacity to convey flow, but also acts as a transfer of coarse sediment into storage as the channel migrates. With evidence that rapid deposition can occur over relatively short-timescales it is likely that the lateral channel adjustment process will fail to keep up with such bed level adjustment. This may result in short-term increases to flood risk before the channel can adjust through bank erosion. Unfortunately, this erosion and channel migration is often problematic for human activities and hence the banks become protected. Indeed in many upland rivers including the Wharfe, bank protection now exists to prevent the naturally migrating channel. This river training began in the Wharfe during the 14th and 15th centuries with monastic settlements that restricted the channel for farming purposes (McDonald *et al.* 2004). Many of these walled banks are still evident today alongside more recent engineering. Around 50% of all the bends in the channel are now protected with hard engineering. Hooke (2003) explains that where engineering prevents the channels' lateral adjustment, the channel becomes more responsive. This echoes findings by Pinter and Heine (2005) who found that river engineering, along a silt and sand bed river, can lead to increases in stage for a given discharge.

The results show that, temporal rates of sedimentation vary between seasons and years. Historically the channel has a history of aggradation with the short-term pattern echoing the longer-term aggradation found extending back to the 1980s (Lane *et al.*, 2007). Macklin and Lewin (2003) suggest from analysis of the Holocene record, that systems like the Wharfe can experience large increases in sediment delivery over relatively short periods of time. Attempting to explain temporal variations in sedimentation is difficult due to the relationship that precipitation has with both discharge and sediment supply. Thus, more storm events may enhance the sediment supplied to the reach through an increase in rainfall induced slope failure, but at the same time, they may result in greater channel erosion and transport due to higher discharges. When the magnitude and frequency of sediment transport events is considered, the response of a channel location is found to differ greatly

depending on the location, season and possibly year. In addition, whilst greater bed level change activity is associated with an increase in discharge, this does not necessarily result in net aggradation. This questions the simple, traditional linkage between changing hydrology such as flood frequency and magnitude, and geomorphological response (e.g. Leopold and Maddock, 1953; Harvey, 1969; Ackers and Charlton, 1970; Osterkamp, 1980). Two reasons may explain this. First, the survey spacing and frequency may be insufficient to capture all the bed level changes since these bed level changes, were found to occur rapidly during only a few months (the time between survey dates) in certain locations. Furthermore, the impact sensor data suggests that bed level changes may occur over relatively few significant sediment transport events. This is most notable at Buckden Bridge, where 67% of the annual sediment activity occurs in one individual transport event. This echoes findings by Gintz *et al.* (1996) who suggest it is the larger flows that allow longer sediment transport distances and can rearrange channel morphology and by Hassan *et al.* (1992) and Haschenburger and Church (1998) who found that event duration has a positive effect on travel distance. Second, the main channel may become transport and supply limited at times. Thus, bed-level change activity may be high but sediment transport activity and aggradation may be low. The impact sensors suggest that when supply is ample, sediment supply from the hillslopes is high and the steep tributaries can transfer this to the main channel with greater volumes of sediment passing to Hubberholme. However, the main channel, which has a reduced gradient, has insufficient energy to transport this sediment downstream leading to scour and bed armouring as sediment supply downstream is limited. Thus, it is during high magnitude flow events that sediment can transfer downstream. Hence there is a time lag between sediment production from the hillslopes into the tributaries and to Hubberholme, and its re-working by the main channel.

This complex response of the channel to sediment supply and to hydrology make it difficult to predict the response of the channel to potential future changes in climate and land-use (e.g. Arnell and Reynard, 1996; Cameron, 2006; Fowler and Kilsby, 2007). More frequent, higher magnitude and longer duration flood events may on the one hand result in a greater supply of sediment (e.g. Coulthard and Macklin, 2001) leading to aggradation yet on the other hand, if sediment supply is not significantly altered then increased flows may allow

greater sediment conveyance through and out of the reach. Furthermore, with individual locations in the catchment demonstrating different responses to the supply and transfer of sediment, it is likely they will respond differently to future climate, and land-use changes.

6.7 CHAPTER SUMMARY

There are several key findings to come out of this work. Most important is evidence that adds a new dimension to flood risk: the role of coarse sediment transfer. Only short-term sedimentation is required to increase the number and duration of overbank flows. Furthermore, these effects may be localised and rapid resulting from as little as one high flow event. Understanding the response of a system to changes in hydrology and sediment supply that may result from climate and land-use change are uncertain. This is made even more difficult because of the spatial and temporal variability found in the sediment supply and transfer process. The results also promote caution regarding bank protection schemes which are often implemented due to severe bank erosion which can be directly linked to high sedimentation rates. By reducing a channel's adjustment processes, these schemes are likely to have detrimental impacts on further sedimentation in a zone which was in the first instance one where sediment accumulation occurred naturally. Finally, the findings from the field-based side of this research have demonstrated the need for river management decisions to be made based on adequate channel monitoring. Whilst field monitoring can be used to inform processes operating in a river system, it cannot be used to effectively predict future changes. A modelling approach is required to explore channel change under a range of scenarios.

CHAPTER SEVEN:
MODEL CONCEPTUALISATION

7.1 INTRODUCTION

Chapter 6 demonstrated that field monitoring provides useful data which, when analysed, can be used to understand a wide range of processes and interactions operating in upland gravel-bed rivers such as the Upper River Wharfe. Thus, Objectives 3 and 4 can be achieved using this approach. However, these data cannot inform future changes or the potential impact that direct interference in the river, e.g. bank protection, may have on sediment transfer. Modelling provides a valuable methodology for exploring such scenarios and fulfils Objective 6. The model must be able to simulate sediment transport processes, ideally in response to variable hydrology. It should also be able to simulate bank erosion and deposition, thereby simulating channel migration.

This chapter begins by exploring previous models that attempt to simulate morphological channel change. These are grouped for discussion into: (1) equilibrium channel approaches (Section 7.2.1); (2) width adjustment models for straight channels (Section 7.2.2); (3) meander evolution and migration models (Section 7.2.3); and (4) modelling width adjustment in meandering channels (Section 7.2.4). Following this, the limitations of these models are discussed highlighting the need for a new model of morphological channel change to be developed. This will initially be specific to the Wharfe but will ideally be applicable to rivers with similar characteristics. The literature on channel change theory (Chapter 2) and the field based findings (Chapter 6) enables a conceptual model to be developed (Section 7.4). This is based on approaches in model group (2) which couple together sub-models representing the hydraulics, sediment transport and bank erosion. The latter part of the chapter, discusses options for each of the sub-models using examples from the literature to highlight potential options. A justification is then provided for selecting the 1D sediment routing model, TRIB (Ferguson *et al.*, 2006), as a building block to couple

with a lateral channel change component. Options for the lateral channel change component are discussed using examples from the literature to provide a development strategy.

Within this chapter "key modelling questions" are raised. These are fundamental to the model development and they form the structure for Chapter 8, which sets out to answer these questions through simulations and tests.

7.2 OPTIONS FOR MODELLING CHANNEL ADJUSTMENT

Models are used in science to overcome problems associated with empirical studies that are based on observations and measurements under experimental manipulation. Three key limitations of the empirical approach include: (1) situations where data cannot be obtained by empirical means; this may be for technical, accessibility or cost reasons; (2) situations where there is a need to interpolate between an existing set of measurements, either in time or in space; or (3) when wanting to extrapolate beyond the existing set of measurements in time or space. The latter refers to predication by forecast or hindcast. As such, models are recognised to be an *"indispensible tool of the trade"* and *"the basis of all interpretive science"* (Bras *et al.*, 2003). In this research, modelling is used to explore a variety of situations that cannot be measured easily (e.g. sediment transport) and to explore channel behaviour under different scenarios (e.g. the removal of bank protection).

Models have been developed for a wide range of physical and social science topics from population growth models and global climate models to hydrological and hydraulic models. It is the latter, hydraulic models, that the following discussion will concentrate on, although many of the issues and topics explored are applicable to other modelling fields. Lane (1998) provides a useful review of modelling in hydrology and geomorphology. In fluvial geomorphology, models have been developed for two reasons. First to aid our understanding of system operations and second for engineering and river management purposes. These are often referred to as commercial models. The model developed for this research is entirely for research purposes but has scope to be used in applied studies to aid with river management

In the scientific literature, a model is typically defined as an abstract representation of complex real world systems, a simplification of reality, a blue print of an idea or an aid to visualisation and understanding (e.g. Bras *et al.*, 2003; Wainwright and Mulligan, 2004). These scientific models are built with the tools of mathematics and they range in levels of complexity, cost, expertise required to construct and operate, purpose and limitations. Successful models are not necessarily the most complex or expensive, with simpler models often providing predictions that match observations better than complex models (e.g. Murray, 2007). Most importantly, the model must be fit for purpose. For example, sediment transport models developed for fine sediment often fail to represent the full range of processes operating in coarse boulder channels. Thus, models should be designed in line with the resources available (e.g. data, computational power and expertise).

Under the broad term of "model" lie many different model typologies. Perhaps the simplest of these is the conceptual or theoretical models which are based entirely on theory and ideas. These are typically used to develop ideas and show process linkages and often come in the form of a flow chart (for example Figure 2.2). Mathematical models are either "empirical" or "process-based / physically-based". Empirical models are derived entirely from observed data and are formulated by statistical association. Process-based / physically-based models simulate the physics of a system by representing the processes within the system. Physically-based models refer to models that closely follow the physics of the system whilst process-based models are simplifications from these. Not all processes in a system can be represented so many are lumped or parameterised together. Process-based models can be categorised further into "deterministic" or "stochastic / probabilistic" models. Both are based on the relationship that a = f(b) where f is the function and a and b are the process inputs and outputs. The distinction between deterministic and probabilistic models is that the latter allows for the input of random elements. As such in the deterministic model, the output is a direct consequence of the initial values. (i.e. inputs *determine* the outputs). Predictions of a based on some function of b plus random elements, can only predict the probable output rather than the determined output. Random elements may result from truly random processes, non-random processes for which our knowledge is

insufficient so that they appear random or when the processes are very complex so that our only way of representing them is to do so stochastically.

Modelling is typically carried out in two ways. Mathematically where the answer can be obtained analytically using a pen and paper to solve the equations or numerically where lots of attempts or iterations are required to obtain the output value or answer. These require the use of a computer and as such are often referred to as computational models. A numerical model of channel change is used in the research.

Rivers contain complex morphodynamic processes resulting from the interactions between flow, sediment and movable boundaries (Chen and Duan, 2006). Such complexities, many of which are not fully understood (Darby, 1998; Lancaster and Bras, 2002), have led to a vast range of modelling approaches to allow future channel changes to be predicted. However, due to the sheer number and diversity of processes and mechanisms operating in a channel alongside the uncertainties in understanding the processes, a single model is unlikely to have universal validity (Darby, 1998). The discussion that follows provides a review of the broad spectrum of models that have been developed to simulate morphological channel adjustments. These are broadly split into: (1) equilibrium channel approaches; (2) models for straight channels; (3) meander evolution and migration models; and (4) width adjustment models for meandering channels. Each group is discussed.

7.2.1 Equilibrium Channel Approaches

Geomorhpologists and engineers have long hypothesised that rivers and canals tend to create a geometry and planform that is in equilibrium with the prevailing flow and sediment conditions acting on the channel (e.g. Pickup, 1976). Various approaches have been developed to predict the new equilibrium channel geometry following a change in the fluvial system such as increased sediment supply or a change in the flow regime. These models attempt to predict how the channel's characteristics including its slope, width, depth and sinuosity will adjust. These approaches fall into two categories. The first is theoretical where models are derived from physical theory. These include: (1) rational equations which

are deterministically derived and use equations to describe the dominant processes (e.g. Parker, 1978; Eaton *et al.*, 2004; Millar, 2005); and (2) those based on extremal hypothesis where an additional condition regarding the behaviour of stable rivers is proposed. These have no physical basis and rely on a variational argument in which the maximum or minimum of some parameter is sought. Examples include minimum stream power (Chang, 1980), minimum unit stream power (Yang, 1976) and maximum sediment transport rate (White *et al.*, 1982). The second group of approaches is empirical (i.e. derived from observed data). These revolve around Lacey's (1929) "regime theory" for irrigation canals (explained in Savenije, 2003) and the "hydraulic geometry concept" coined by Leopold and Maddock (1953). This concept provides a quantitative description of how morphological properties are related to discharge using a series of power laws:

$$w = aQ^b \quad [7.1]$$

$$d = cQ^f \quad [7.2]$$

$$v = kQ^m \quad [7.3]$$

where Q is discharge, w is channel width, d is channel depth and v water velocity. Since $wdv=Q$, the sum of exponents b, f and m, will equal 1 whilst the sum of the intercept values a, c and k will also equal 1.

Whilst these approaches provide a valuable insight into the mechanics of channel equilibrium, they can only predict the eventual channel geometry following adjustment and do not reflect the continual and dynamic nature of the adjustment process. Furthermore, one must question whether channels ever reach complete equilibrium (Bracken and Wainwright, 2006).

7.2.2 WIDTH ADJUSTMENT MODELS FOR STRAIGHT CHANNELS

One of the main aims in this second group of models is to simulate how the channel width responds to changes in a channel's driving variables. Hence a key feature of these models is that they assume erodible banks. This is not always the case in equilibrium models. Changes in channel width occur when the direction and rate of bank erosion of one bank is not equal to the direction and rate of deposition at the opposite bank (Darby, 1998). For an individual bank, the migration rate is determined by the relative rates of erosion and deposition from the near-bank zone. This relationship is based on the concept of basal end-point control (Thorne, 1982).

The ASCE Task Committee, which was set up 1993 to address the topic of river width adjustment, explain that width adjustment models can be classified into two broad approaches (ASCE, 1998a). The first are those based on the extremal hypothesis which has been used in equilibrium studies and provides predictions of the magnitude of width adjustments and not the rate of adjustment. The second are physically based, geofluvial, mechanistic approaches which couple sub-models of flow, sediment transport and bank erosion together to provide predictions of width adjustment location and rate.

Models based on the extremal hypothesis are more frequently used in engineering practice. Ferguson (1986) and ASCE (1998a, 1998b) provide explanations of these approaches and review some of these models. Examples include Chang (1988), White *et al.* (1982), Bettess and White (1987), Millar and Quick (1993, 1998) and Yang *et al.* (1988). In FLUVIAL-12 (Chang, 1988) and GSTARS (Yang *et al.*, 1988), width adjustments are determined by assuming that changes in cross-sectional area, estimated from the sediment-routing equations, represent an overall change in channel area. The total area is distributed over the cross-section by first calculating the magnitude of width adjustment and then distributing the computed area over the bed and banks. Width corrections at each cross-section are computed assuming that the stream power for the reach moves towards uniformity (FLUVIAL-12), or towards a minimisation of energy dissipation rate (GSTARS). The major limitations of such models are that they predict the magnitude of width adjustment

and not the rate or location of adjustment (ASCE, 1998b). They also lack a physical foundation and hence perform poorly in situations other than those for which they were developed.

Mechanistic width adjustment models for straight channels are summarised in Darby (1998) and ASCE (1998a and 1998b). These are typically research tools that have scope to be used in engineering practice in the future. These models simulate channel width adjustment through time using a set of deterministic equations alongside a set of initial (e.g. morphological and sedimentary characteristics prior to adjustment) and boundary conditions (specific sediment load and discharge as a function of time). The equations of flow resistance, momentum and continuity, sediment transport and conservation of sediment mass are typically solved within sub-models which are coupled together (e.g. Darby and Thorne, 1996). Figure 7.1 is a schematic diagram of the Darby and Thorne (1996) model: a model of bed deformation and channel widening which accounts for the specific mechanisms of bank erosion and collapse. This model was also used by Simon and Darby (1997) to study process-form interactions. The sub-models include a hydraulic flow model, a sediment transport model and a bank erosion model. Each of these are discussed in more detail later in the chapter (Section 7.4).

Figure 7.1: Conceptual representation of the Darby-Thorne model of channel width adjustment (Darby and Thorne, 1996). where T is simulation time counter, Q is flow discharge, q is flow discharge per unit width, S_e is energy slope, D is flow depth, RP is the probability of failure, FS is the bank factor of safety, BW is the failure block width, V_n is failure block volume and LIM is time limit of simulation.

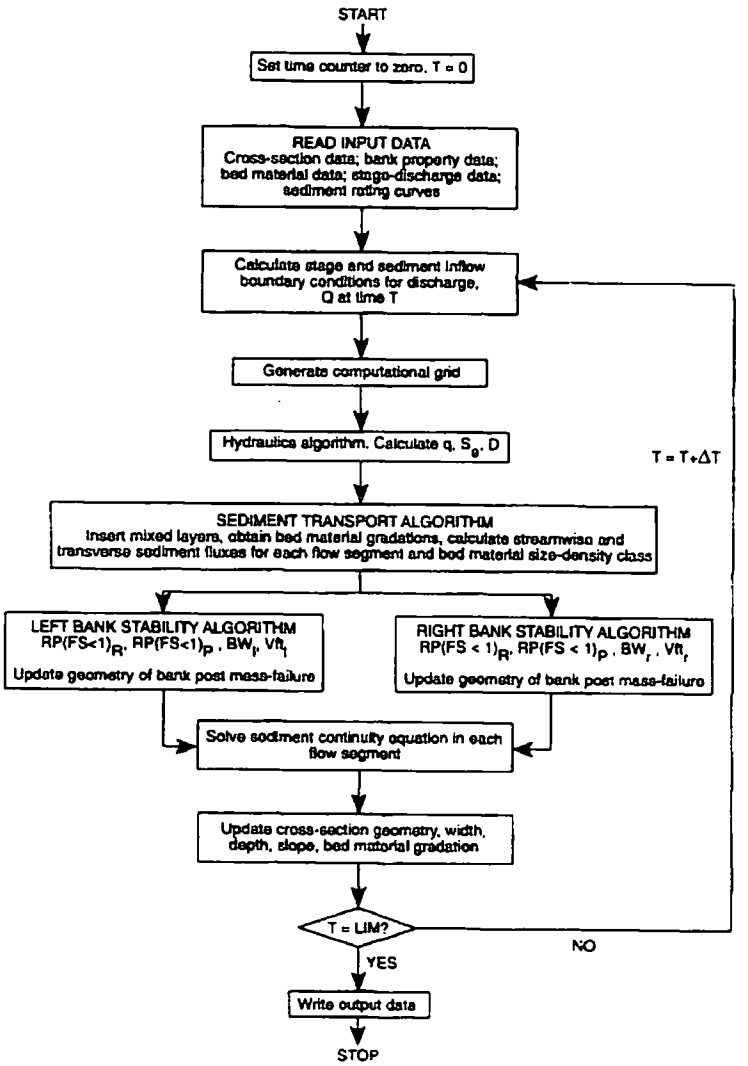

7.2.3 Meander Evolution and Migration Models

Numerous modelling approaches widely accept the importance of river meandering that develops from secondary circulation (Bridge, 1992; Darby and Delbono, 2002; Coulthard and Van De Wiel, 2006). The secondary circulation preferentially erodes one bank and deposits material at the base of the other. This establishes a positive feedback with a greater

flow asymmetry increasing the secondary circulation and hence encouraging further erosion on the outer bank. Consequently bank erosion rates are most rapid on the outer bank just downstream of the bend apex. This leads to meander development and channel migration in both cross-valley and down-valley directions. Several have attempted to model the meander evolution and migration processes (e.g. Howard, 1992; Sun *et al.*, 1996).

There are many different spatial and temporal scales at which meanders are studied and modelled (Sun *et al.*, 1996; Lancaster and Bras, 2002). These range from small scale studies of the flow field around curved channels (e.g. Thorne and Hey, 1979), medium scale studies investigating the development of individual meanders (Hickin, 1974) and large scale studies that examine the complex properties of entire meander trains (e.g. Lancaster and Bras, 2002). Camporeale *et al.* (2007) divide the historical study of meandering rivers into a geomorphologic approach and a fluid dynamic approach both of which are inter-related. The geomorphic approach explains the main characteristics of meandering, providing valuable empirical relationships. These approaches included field studies (e.g. Nanson and Hickin, 1983; Carson and Lapointe, 1983; Thorne and Furbish, 1995) and laboratory experiments (e.g. Whiting and Dietrich, 1993a and 1993b). The fluid dynamic approach is underpinned by mathematical modelling with Ikeda *et al.*, (1981) proposing the first model of river meandering using this way of working.

In the three decades since the Ikeda *et al.* (1981) model was first published, numerous other modelling approaches have been developed. Camporeale *et al.* (2007) provide a valuable review of many meander models. These models explore a range of meandering processes including Blondeaux and Seminara (1985) who explore the link between bend and alternate bar dynamics and suggest a possible resonance; Johannesson and Parker (1985b) who explores the role of the secondary circulation; Struiksma *et al.* (1985) who investigate the overdeepening concept; and Zolezzi and Seminara (2001) whose more recent study explores the upstream propagation influence of meanders. These modelling approaches commonly treat the meandering channel as a zig-zag line whose nodes shift laterally at a rate determined by some condition. Mechanistic meander evolution models can be divided into process-based models and physically-based models. Process-based models assume a rate of bank erosion proportional to near-bank flow velocity. Physically-based models

calculate sediment transport and bank erosion rates to determine the advance and retreat of the channel bank line. Process-based models can be effective in predicting the long-term behaviour of meandering rivers whereas physically-based models are more successful at predicting immediate or short term geomorphic responses, so revealing the evolution process. Hence, physically-based models can be used specifically to determine the rate of bank erosion at individual locations within a meandering channel. However, they require more details on the flow field, bank geometry and bank materials and are thus more data dependant. Process-based models on the other hand are based on an empirical erosion coefficient which does not reflect specific details about the bank geometry and bank materials (Darby *et al.*, 2002).

One of the most widely acknowledged process-based models is that of Ikeda *et al.* (1981). They developed a dynamical bend erosion model based on the "bend theory" concept which calculates the lateral distribution of the depth-averaged primary flow. Bend theory [7.4] states that bank erosion is proportional to the near-bank flow velocity with the bank erodibility incorporated in the bank erosion coefficient. The near bank flow velocity is calculated using [7.5].

$$\xi = E_0 u_{nb} \qquad [7.4]$$

$$u_{nb} = f(R_c, u_0, h_o, b, C_f) \qquad [7.5]$$

where ξ is the lateral bank migration, u_{nb} is the near-bank flow velocity, R_c is a function of channel curvature, E_0 is a bank erosion coefficient, b is a fixed channel width, u_0 is cross-sectionally averaged flow velocity, h_0 is cross-sectionally averaged flow depth and C_f is a friction factor.

Although sediment transport was not explicitly included in the model, the conservation of sediment was included in a crude manner by viewing the migration of the meandering river as a consequence of outer bank erosion and inner deposition with no width adjustment. Ikeda *et al.* (1981) has been used in numerous subsequent studies including Beck (1984), Parker *et al.* (1982, 1983), Parker and Andrews (1985), Johannesson and Parker (1989),

Sun *et al.* (1996, 2001a, 2001b), Howard (1984, 1992, 1996), Mosselman (1998), Darby *et al.* (2002) and Edwards and Smith (2002).

Some of the developments to Ikeda *et al.* (1981) include Johannesson and Parker (1989) who developed bend theory to account for flow velocity redistribution as a result of the connective transport of primary flow momentum by the secondary flow. This would account for the contradiction between the theoretical results of Ikeda *et al.* (1981) and the experimental results of Kikkawa *et al.* (1976). The model also accounts for the phase lag between the secondary flow strength and the channel curvature and includes an erodible bed which explicitly accounts for the coupling between the flow field, the bedload transport and the bed topography. Howard (1992, 1996) used Johannesson and Parker's adaptation of Ikeda *et al.* (1981) to combine bank erosion and channel migration simulations with a simple model of floodplain sedimentation. This model produced realistic migration results, although the simulated channels were noted to be more asymmetrical, sinuous and regular than natural channels. Sun *et al.* (2001a) extended the bend theory work to include the dynamic response of meandering rivers to the lateral tilt of the underlying floodplain. It is different in that the flow field is influenced by the presence of channel curvature and the variation of the longitudinal channel bed slope caused by the effects of embedding a sinuous river channel in a tilted floodplain. Hence, the cross-sectionally average flow velocity and the water depth vary along the channel.

Several models that do not use the Ikeda *et al.* (1981) work have also been developed to simulate meanders. First, Begin (1981) proposed a model of meander bend bank erosion based on the momentum equation and curvature effects. This approach attempts to explain the established relationship between bend migration rate and the curvature ratio (*R/w*: Radius of curvature/width) thereby allowing it to be used to predict bank migration rates. The relationship between radius of curvature and channel width was found to be quite narrow and this was attributed to flow separation near the convex, inner bank of the bend, which reaches a maximum intensity for an *R/w* near 2. In this approach, the momentum equation is used to determine the force per unit area which the flow exerts on the outside

bank. By assuming that shear stress is proportional to the radial force per unit area, the bank shear stress can be used to determine bank erosion rate.

Secondly, Lancaster and Bras (2002) introduced a model which they suggest has more in common with cellular approaches to channel braiding than rigorous physically-based analyses of river meandering. The model splits the channel into two halves and uses channel area to determine flow properties. Unlike many models where local migration rate is determined from upstream conditions, usually planform curvature, Lancaster and Bras (2002) developed a model that uses shoaling driven by changing bed topography and ultimately changing planform curvature to determine local migration rate. This work is based on the assumption that secondary flows "steer" the high velocity core (which is responsible for erosion) by effecting a lateral transfer of downstream momentum. Dietrich and Smith (1983) showed that bed topography causes the largest lateral transfer of downstream momentum coining the term "topographic steering" and this was incorporated into the model. This model also allows the simulation of compound bend / multibend loop formation which are common features of natural channels.

A similar model developed by Stark (2006) also uses a similar split channel approach for simulating the evolution of bedrock river channels. This approach uses geometric arguments, a normal flow approximation for channel flow and a threshold bed shear stress assumption for bedrock abrasion. The model simulates channel widening, tilting, bending and variable flow depth. The Stark (2006) model uses a simplified pattern of flow speed, bed shear stress, erosion rate and boundary motion for a quadrilateral bedrock channel cross-section using a four point geometry. Bed shear is then split into four components: left and right banks; and the left and right halves of the bed. A lateral displacement term allows for the effect of sinuosity to be modelled although only for simple sinuous channels. Channel tilt, which is the slope of the bed, provides a transverse slope and allows flow speeds to be calculated for each half of the channel. The two channel halves are linked by channel area to the discharge. The bed shear stresses in both channel halves drive the abrasion rates and allow the bed geometry to be updated.

A fourth model to use a different approach was developed by Richardson (2002). This approach was developed so that it could easily be applied to the output from 1D models such as HEC-RAS (Hydrological Engineering Centre, 2001) and Mike-11 (Danish Hydraulic Institute, 2000). Since the output from these models would be section-averaged velocities, water surface elevations, shear stresses and discharge at a series of cross-sections, the model had to be simple and was limited in its required input data. Hence, Richardson (2002) developed a conversion factor (*K*) for shear stress which was derived based on the assumption that the ratio of outer bank velocity to section average velocity is equal to the ratio of channel centreline arc length to outer bank arc length. Outer bank shear stress was taken to be proportional to the square of velocity. The relationship is shown in [7.6]. The converted shear stresses are then translated into bank erosion volumes using an appropriate sediment transport equation.

$$K = \frac{\tau_{toe}}{\tau_{avg}} = \left(\frac{V_{toe}}{V_{avg}}\right)^2 = \left(\frac{B}{2R} + 1\right)^2 \qquad [7.6]$$

where K is the conversion factor, τ_{toe} is the shear stress at the outer bank, τ_{avg} is the 1D shear stress, V_{toe} is the depth-average velocity at the outer bank, V_{avg} is the 1D section-averaged velocity, R is the channel centreline radius of curvature and B is the channel width.

There are also a group of meander models which attempt to account for different grain size fractions (Bridge, 1992; Parker and Andrews, 1985; Sun *et al.*, 2001b and 2001c). Darby and Delbono (2002) explain that the secondary circulation and the presence of the transverse sloping channel bed in meandering streams, move different grain sizes of bed load in different proportions and directions. This results in a consistent pattern of grain sorting around the bend (Parker and Andrews, 1985). To address this, several models have been developed which describe the interaction between the flow, sediment transport, bed topography and grain size sorting in curved channels. Bridge (1992) is probably one of the most comprehensive and an essential component of the model is its application of the

sediment continuity equation for each grain size fraction available for transport. Similarly, the meander model developed by Sun *et al.* (2001b and 2001c) which accounts for multiple bed load sediment sizes also includes a continuity equation for each component of sediment. This model was developed using Johannesson and Parker (1989) for the dynamics of meandering rivers with the theory of Parker and Andrews (1985) for bedload transport and sorting in meander bends replacing the original sediment transport equation for single sized sediment in Johannesson and Parker (1989).

7.2.4 Modelling Width Adjustment in Meandering Channels

One of the main problems with the meander models discussed above is that they assume a constant channel width (e.g. Ikeda *et al.*, 1981; Bridge, 1992; Howard, 1992; Sun *et al.*, 1996, 2001a, 2001b, 2001c; Lancaster and Bras, 2002). This lack of sediment continuity is an incorrect assumption with erosion of the outer bank typically greater than that which can be deposited on the inside of the bend (Coulthard and Van De Wiel, 2006). This leads to channel widening around the meander bend. Furthermore, bank collapse can be a rapid erosion process whilst deposition often takes longer. This can lead to a lag between the two processes. More recent approaches have tried to account for width changes in meander channels. These models tend to be more complex requiring a second dimension and combine many of the ideas used in both width adjustment models and meander evolution models. They use vector based, moving boundary fitted-coordinate grids. These models work in a similar way to the mechanistic width adjustment models for straight channels discussed earlier. The main difference is the way in which they deal with curvature induced bank collapse. Hence, their bank erosion components vary. RIPA, a model developed at Delft Hydraulics by Mosselman (1992, 1995), simulates bank erosion as a combined result of excess shear stress determined using the Ikeda *et al.* (1981) approach and Osman and Thorne's (1988) excess bank height mechanisms. In a later version of the RIPA model (Mosselman, 1998) only the excess bank height mechanism is used. Nagata *et al.* (2000) develop a 2D approach, using Hasegawa's (1981) model of intermittent bank collapse (summarised in Section 7.4.5) along with a non-equilibrium sediment transport relation. This allows the deposition and transportation of the collapsed materials to be simulated. The model does not however, simulate the difference between basal erosion and bed

degradation, a process Chen and Duan (2006) feel is important. Darby *et al.* (2002) develop RIPA further by replacing the existing bank erosion sub-model with a more mechanistic approach. This approach is similar to Nagata *et al.* (2000), although it has a more detailed description of the bank erosion process. Darby and Delbono (2002) simulate channel migration and widening by coupling together Bridge's (1992) meander model with the Darby and Thorne (1996) bank stability analysis. Hence, unlike models such as Bridge (1992), it accounts for the influence of bank erodibility. Duan and Julien (2005) present a 2D numerical model that links a physically-based bank erosion model with a bend migration model to simulate the meander evolution and migration processes. They simulate basal erosion using equations developed by Duan (2001), which calculate the difference between the entrainment and deposition of bank material in the near bank zone. This difference determines bank erosion rate. They also use Pizzuto's (1990) slumping bank-failure model (later modified by Nagata *et al.*, 2000) to simulate mass failure. To simulate meanders, radius of curvature is used to determine the strength of the secondary flow and hence to redirect bedload transport. Finally, Chen and Duan's (2006) 2D analytical model simulates width adjustment in meandering channels using two interacting bank erosion mechanisms: basal erosion and bank collapse. The rate of basal erosion (which includes lateral erosion and bed degradation) is calculated from the longitudinal gradient of sediment transport and from the strength of the secondary flow. Simulating bank collapse is more complicated and is determined by the lateral erosion rate, near bank bed-degradation rate, sediment grain size and differences between flow depth and bank height. They also represent the deposition of failed material at the base of the bank similar to Nagata *et al.* (2000) and Darby *et al.* (2002).

Most channel adjustments are simulated using vector-based models. However, these can only be used to simulate single thread channels. Therefore, Coulthard and Van De Wiel (2006) developed a cellular modelling approach to allow channels with islands or braided channels to be simulated. Coulthard and Van De Wiel (2006) explain why cellular approaches are difficult to apply to meander models. First, cellular approaches use simplified empirical equations such as Manning's or Chezy to explain the flow but in doing so the terms for momentum and for describing secondary circulation are lost. Second, the

cellular discretization, where each cell only has a knowledge of itself and its immediate neighbours, makes it difficult to determine the cells location with respect to bends and banks and also the momentum and direction of water entering a cell. In earlier cellular models of braided rivers, a lateral erosion term was used to create a dynamic braiding pattern with bed material moving from one cell to another adjacent to the main flow direction using the lateral bedslope (Murray and Paola, 1994; 1997; Thomas and Nicholas, 2002). Yet this approach cannot be applied where flow is not parallel to the valley floor, for example around a meander bend. Thus, Coulthard and Van De Wiel (2006) present a new way to determine the radius of curvature on a cell-by-cell basis. Their approach passes a nine cell filter over the cell grid and use ratios of "edge" cells and "dry" bank cells to "wet" channel cells to determine the curvature. This approach allows the model to base meandering on regional rules, necessary for curvature estimation. They then determine bank erosion rate using an approach similar to Ikeda *et al.* (1981). To simulate channel migration using the cellular approach, they discuss two methods. First, they assume that sediment is eroded from the bank using the Ikeda *et al.* (1981) equation with this sediment being lost to the system. An equal amount of sediment "appears" on the inside bend as deposition. This approach has a tendency to generate very wide channels. Hence, their second approach uses the cross-stream gradient of curvature to calculate a lateral sediment flux. This cross stream movement of sediment simulates much narrower, better-defined channels and allows the formation of point bars and a meandering thalweg within the channel. This approach certainly shows some potential and continues to be developed further. However, in its current form, it is unsuitable for this project due to its coarse grid size, long time scale and its inadequate sediment transfer system.

7.3 LIMITATIONS OF CURRENT MODELLING APPROACHES

The wide range of channel adjustment models discussed have numerous limitations. These are responsible for the poor correlation often found between predicted and actual rates of adjustment. For example, Darby and Thorne (1996) found that actual rates of channel widening were three times greater than those simulated by their model. Such problems arise from four difficulties. First, it can be difficult to parameterise initial and boundary

conditions and to compute the flow field (Darby *et al.*, 2002). Second, determining and representing the full range of processes and mechanisms acting within the channel and on the banks is a challenge (Simon and Darby, 1997). Thus many predict the eventual channel geometry failing to provide valuable information on the rate and location of adjustment. This limitation is particularly applicable to equilibrium channel approaches. Furthermore, despite increasing levels of complexity, most models assume a constant width such that any erosion predicted at one bank is matched by deposition on the opposite bank (e.g. Coulthard and Van De Wiel, 2006). Third, developing models for natural channels rather than simple and laboratory channels remains difficult (Darby and Thorne, 1996). As such, sediment transport models were often developed in a flume and most bank erosion sub-models ignore the influence of secondary circulation, overbank flow and vegetation on the hydraulic variables (e.g. Darby, 1998; Darby and Thorne, 1996; Mosselman, 1998). This creates errors in the hydraulic parameters. Some of these effects are indirectly incorporated through model calibration (e.g. Darby and Thorne, 1996) but future models should consider including these factors. Finally, obtaining the necessary data and computational resources to develop, to run and to test the models is an important limitation (Simon and Darby, 1997; Darby, 2005). As a result of these limitations, developing models that simulate width adjustments in irregular channels remains very difficult.

7.4 RESEARCH MODEL CONCEPTUALISATION

On the basis of the above discussion of model options and limitations, no one model is ideally suited to the research aims outlined in Section 1.1. Consequently, a new model of channel adjustment was required for this research. The first step in any model development is to produce a conceptual model outlining the various processes that require representing. This began by taking the theoretical model shown in Figure 2.3 (within Section 2.2), which showed all the processes operating in a gravel-bed river catchment, and using the field-based findings to inform on the key processes operating in the study reach (Chapters 4, 5 and 6). This enabled the channel change process to be divided into three sub-models representing each of the key processes. This conceptual model shown in Figure 7.2 provides the framework for the mathematical model and gives a better visual understanding

into process operations and interactions. It is similar in structure to the Darby-Thorne (1996) model shown earlier (Figure 7.1). Central to the approach is allowing the simulation of change through time rather than providing a single end output similar to the equilibrium channel adjustment models (Section 7.2.1).

Figure 7.2: Conceptual model of morphological channel adjustment.

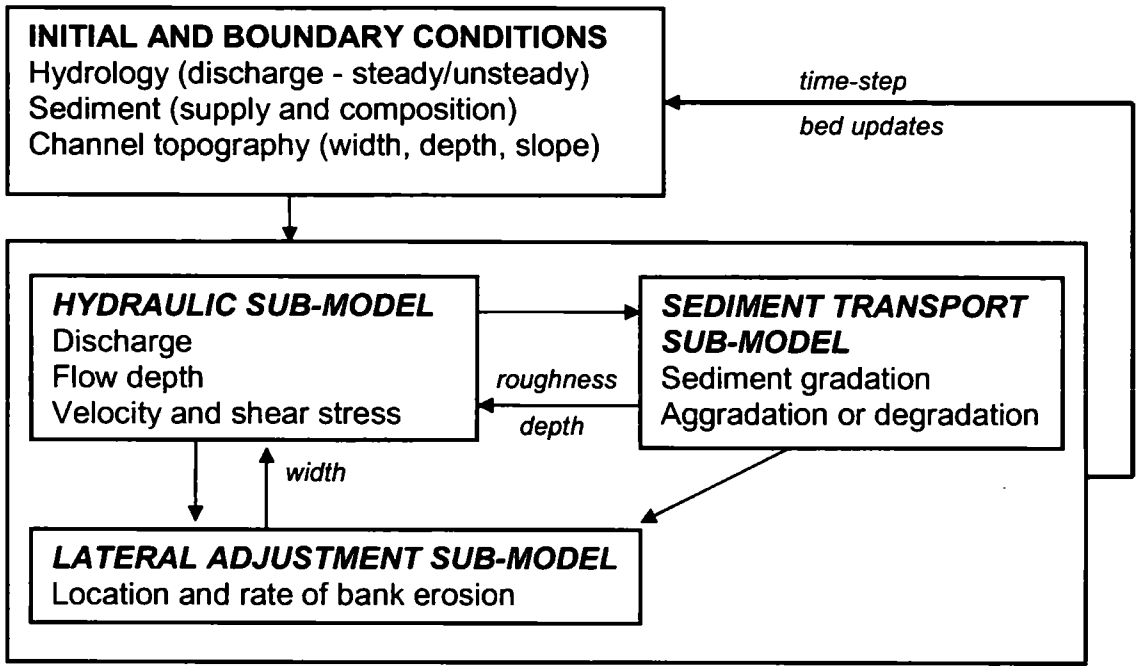

The model is conceptualised as having four components. First, are the initial and boundary conditions which are pre-defined at the start of the simulation by the user and may represent a real natural system (e.g. the Upper Wharfe), or be hypothetical where an idealised channel is represented using hypothetical values. These conditions form the input values for the main equations within the model. These equations are split into the second, third and fourth components, the sub-models. The arrows indicate the coupling between sub-models and the direction of information transfer. These sub-models have three components. First, is the hydraulic sub-model which calculates the values of flow depth and shear stress that are required to drive the sediment transport component of the model. Second, is the sediment transport sub-model which computes sediment transport and allows the bed level to adjust through aggradation or degradation. Furthermore, depending on the

nature of the sediment transport and sediment continuity equations used, the sediment transport may be computed on a fractional basis allowing the process of downstream fining to be simulated. Third, is the lateral adjustment sub-model. This is driven by the output from the hydraulic and sediment transport component and allows the channel to widen through bank erosion, narrow through deposition and to migrate through a combination of erosion and deposition. By updating the initial and boundary conditions at the end of each time-step, and re-running the model using the new conditions, the channel can evolve through time.

This conceptualisation defines the spatial and temporal scales that the model is required to run over. Spatially, the model aims to explore the system dynamics over reaches several kilometres long with the study reach extending 5.6 km downstream. As such, the model is developed for reaches ranging from 1 km to 10 km but with the capability of extending beyond this. The temporal scales of the model must consider both data availability for running and testing the model, and the overall project aims. There are four key field results that can be used to validate the model. These include: (1) 6-years of observed patterns of aggradation and degradation from the cross-sectional resurveys (Section 4.3); (2) 2-years of details on bank erosion locations and rates from field-surveys, bank erosion pins and bank-top resurveys (Section 4.4); (3) the measured pattern of downstream fining noted from pebble counts and bulk sampling (Section 5.3); and (4) 18 months of information on sediment transport from the ping sensors (Section 5.4). Thus, modelling should initially be kept at sub-decadal time scales. However, for the purposes of river management, the model may be required to simulate longer time periods. This is an important aspect of the model as many fully physically-based models such as Darby and Thorne (1996) operate at the event scale whilst others operate over much longer timescales (e.g. Coulthard and Van De Wiel, 2006). The research model developed in Chapter 8 will sit between these two time scales.

The discussion that follows provides a detailed overview of the three main sub-models with an additional section describing sediment routing models which couple the hydraulics and sediment transport together. For each sub-model, the discussion begins with an overview of

previous approaches. It should be noted that whilst these sub-models are generally discussed with respect to straight channel adjustment models, they can also be applied to the more complex meandering channels discussed in Section 7.2.4. Several key modelling questions arise during this discussion.

7.4.1 HYDRAULIC SUB-MODEL

A hydraulic sub-model calculates the flow field including the flow velocity, shear stress and flow depth. These parameters may be 1D width-averaged (Osman, 1985; Chang, 1988), 2D depth-averaged (Pizzuto, 1990, Kovacs and Parker, 1994 Nagata *et al.*, 2000) or quasi-2D (Darby and Thorne, 1996) and calculated for steady or unsteady flow. Most hydraulic sub-models assume a steady flow but often have capabilities to simulate unsteady flow (e.g. Li and Wang, 1993) or use a stepped hydrograph (e.g. Darby and Thorne, 1996; Osman, 1985). With the exception of Li and Wang (1993) most are incapable of simulating secondary flows although it is generally assumed that in straight channels, secondary circulations are minimal. Several models with more than one dimension incorporate lateral shear to represent the flow depths and friction gradients that form during overbank flows (e.g. Darby and Thorne, 1996; Li and Wang, 1993; Kovacs and Parker, 1994; Pizzuto, 1990). Friction in the sub-models is either specified by the user or in many cases derived from a flow resistance equation. Some models also offer a selection of equations to select the most appropriate for the environment being modelled. Examples include Strickler (1923) (e.g. Darby and Thorne, 1996; Osman, 1985) or Keulegan (1938) (e.g. Li and Wang, 1994; Kovacs and Parker, 1994). In addition, most friction values are held constant, with a few exceptions allowing them to vary through space and time (Darby and Thorne, 1996; Osman, 1985). These friction factors do not account for in-channel vegetation, which may be seasonal, or for bedforms. The calculated flow field is then used to estimate sediment transport rate using one of many different sediment transport equations.

7.4.2 SEDIMENT TRANSPORT SUB-MODEL

Modelling sediment transport is notoriously difficult and the success of a morphological adjustment model can hinge on the specific modelling approach adopted. Modelling

sediment transport using formulae and equations has arising out of the difficulties associated with measuring sediment transfer as discussed Section 5.4.1. Wilcock (2001) explains that, "*broadly speaking, formulae predictions require less effort, whereas field measurements offer the possibility of greater accuracy, but at a greater effort*". Alongside the reduced effort, formulae predictions allow transport rates to be predicated under conditions other than those present in the river at a given time. This is particularly essential at higher flows where measurement devices often fail. These issues have led to a wide range of formulae all striving towards the better prediction of sediment transport.

Early work on bedload transport by DuBoys (1879), followed by proposals for a curve to predict the critical shear stress of incipient motion by Shields (1936), prompted much research in this field. This led to the development of a range of equations for sediment transport for varying flow and sediment conditions. Whilst these equations have evolved from varying deterministic approaches, they are broadly speaking very similar as they all aim to calculate the same thing and implicitly or explicitly they consider the same parameters (Reid *et al.*, 1997). Most bedload transport equations are based on the DuBoys (1879) concept in which bedload transport is expected as some function of flow exceeds a critical threshold. An early deviation from the DuBoys concept was that developed by Einstein (1942, 1950). Einsten's formula provided a continuous relationship between the bedload and the flow intensity and did not specify a sudden discontinuity at a critical threshold. Whilst the DuBoys relationship was originally developed for excess bed shear stress, the equations that followed used other flow quantities such as stream power (Bagnold, 1980) and discharge (Schoklitsh, 1962). Whilst this critical threshold concept is simple, defining the critical threshold is much more challenging, particularly with limited field studies for support. Yet, many equations based on this form have been developed. Some of these equations are discussed below. It is important to note the wide range of conditions for which these equations have been developed.

Ackers and White (1973) is a bed material formula developed from Bagnold's stream power concept. The equation was developed in a flume for poorly sorted sediment greater than 0.04 mm. Bathurst *et al.* (1987) suggest that this equation is not suitable for upland

mountain rivers where the bed is cobble and boulder. Engelund-Hansen (1967) is also based on Bagnold's stream power concept and predicts total load in sand bed channels with well sorted material. This equation was also developed using flume data and is employed in the Darby-Thorne (1996) width adjustment model. Laursen (1958) was developed from quantitative analysis experiments and supplementary data and predicts total sediment load in silt based channels. The Meyer-Peter and Müller (1948) equation is a bedload transport function that is primarily based on experimental data yet it is tested heavily on rivers with coarse sediment. Gomez and Church (1989) found that it tended to perform well on field data. Li and Wang (1993) use this approach in their morphological adjustment model. The Toffaleti (1968) equation is an empirical approach based on the Einstein procedure. The equation predicts total load by calculating sediment transport in four vertical zones, allowing 2D sediment movement to be replicated. The upper three zones represented suspended sediment whilst the bed zone represents bedload transport. Total load is the sum of the four components. Finally the Yang (1973) equation calculates total sediment concentration based on stream power and was developed from a combination of flume and field studies. This equation was revised by Yang (1984) with an expansion that incorporated gravel-sized sediment. Yet the gravel sized material only extends up to 7 mm, which based on the Wentworth scale is fine gravel (Table 5.2). Alonso and Combs (1980) apply the Yang (1973) sediment transport equations in their sediment transport sub-model.

Selecting the most suitable equation for the purposes of a specific study can be difficult. This has been demonstrated by several authors who have carried out studies comparing various equations. Whilst Johnson (1939) was one of the first to compare several equations, Bathurst *et al.* (1987), Gomez and Church (1989), Batalla (1997), Yang and Wan (1991) and Affrin *et al.* (2002) provide comparisons of the more recent hydraulically based equations developed for gravel and boulder-bed rivers. Gomez and Church (1989) compared 12 equations and evaluated the results against a field bedload dataset. They found large variations between the equations and no single equation produced results that matched the field observations closely. Even popular, well known equations such as Meyer-Peter and Müller (1948) and Ackers and White (1973) performed poorly. Batalla (1997) also compared field observations, from the Arbúcies River in North East Spain, with predictions

from five bedload and bed-material formulae. Echoing the results from Gomez and Church (1989), the degree of agreement between observed and predicted values varied greatly. However, the Ackers and White equation performed the best with results closest to the field dataset. In a detailed study of eight equations Yang and Wan (1991) compared the equation results with data from both natural channels and laboratory flumes and found large variations in equation performance. Table 7.1 shows a summary of the results which are placed in rank order based on overall performance from best (closest to observations) to worst. It was however encouraging that in both tests, the Yang (1973) equation came out as best. It is also interesting to note that the equations that performed well when compared to flume data (Yang, Engelund and Hansen and Ackers and White) were all originally developed from flume data. This emphasises the need to use a sediment transport equation that was developed under conditions similar to those that the equation is being applied to. In the Affrin *et al.* (2002) comparison study, the flume derived equations performed the worst with the Wu *et al.* (2000) equation giving the best results. This equation incorporated a factor for grain hiding. However, conclusions from this research suggested that even this equation's performance was unsuitable for use outside of the study river. The overall conclusion from these studies is similar: that large variations in the outputs from different equations exist. Hence, many authors state that there may never be a universal equation that can accurately predict bedload sediment transport (e.g. Gomez and Church, 1989; Reid *et al.*, 1997).

Table 7.1: Performance of sediment transport equations when compared with flume and field data. Study by Yang and Wan (1991).

Rank	Compared to flume data	Compared to field data
1 (best fit)	Yang	Yang
2	Engelund and Hansen	Toffaleti
3	Ackers and White (D_{50})	Einstein
4	Laursen	Ackers and White (D_{50})
5	Ackers and White (D_{35})	Colby
6	Colby	Laursen
7	Einstein	Engelund and Hansen
8 (worst fit)	Toffaleti	Ackers and White (D_{35})

Reid *et al.* (1997) discuss the main limitations for bedload formulae and these can be used to explain the variability in results made by the different equations. First, there remain difficulties developing the theory behind sediment movement resulting from problems studying sediment transport particularly in natural systems and at higher discharges. An example of this is the equal mobility concept first proposed by Parker *et al.* (1982b) and Andrews (1983) and the principles behind the formation of the armour layer. Furthermore representing all the processes that result in the transport of an individual grain is difficult, with a single hiding function / parameter often used to represent the full spectrum of particle sheltering found on a natural bed. Similarly, the bed character and structure is difficult to represent effectively, particularly in mixed sediments (Hsu and Holly, 1992). Thus, the bed character is simplified.

Second, sediment transport equations are limited due to their development which is mainly based on empirical and experimental work in flumes with uniform sediments. This issue was illustrated well by Yang and Wan (1991) who showed large variations in predictive success depending on whether the data was from a laboratory flume of a natural channel as flumes remove the complexities of natural channels. In particular shear stress exhibits lateral variability as grain size distributions vary (Wolcott and Church, 1991). Yet even formulae specifically developed for natural channels can fail when applied to channels where conditions differ (Parker *et al.*, 1982b).

Third, validation of the equations is heavily dependant on data. Measuring the actual bedload transport rate in a natural stream is extremely difficult and, as a result, such data are sparse and often limited to lower flows. Thus errors in the estimated field transport rates propagate through into errors in the calculated predictions (Wilcock, 2001). In addition, as noted by Wilcock (2001) errors arise when average values are used to represent spatially variable parameters (e.g. grain size). Grain size is noted to vary spatially across a channel with Wolcott and Church (1991) finding that grain size variability across a bar can exceed the variability found between depositional reaches separated by some distance. Ferguson (2003) also stresses that the true bedload flux may be underestimated if calculations are averaged across the channel width.

Wilcock and Crowe (2003) recognise that sediment transport in a bed that comprises a mixed bed of sediment sizes depends on the quantity of each grain size present in the bed. This mixed bed leads to the coarser surface and subsurface characteristic found in many rivers including the Wharfe (detailed in Section 5.3). A transport model based on the substrate contains an implicit dependence on the surface sorting as this layer must be entrained before the sub-surface can be transported. Wilcock and Crowe (2003) further explain that because surface sorting depends on factors not included in the model, including prior flow and transport rates and vertical sorting mechanisms, a substrate-based approach is incomplete. This may result in high errors in the predicted transport rate. More recent equations have been developed to simulate multiple grain-size fractions and to simulate the surface transport rather than just the substrate. Furthermore, Wilcock and Crowe (2003) explain that aside from the theoretical considerations, surface-based transport models are useful as they predict the instantaneous transport rate, independent of initial and boundary conditions. They are therefore capable of predicting transient conditions.

Most transport models are based largely or entirely on flume experiments. The difference between surface and sub-surface models becomes clear when the flume setup is considered (Wilcock and Crowe, 2003). Sediment is fed into the flume in two ways: at a specified rate or re-circulated whereby the sediment that leaves the flume is introduced at the upstream end. In the re-circulating case, the sediment in motion may be expected to have a finer distribution than the bed material. With a specified feed, the grain size of the material must be considered. If the introduced grain size entered matches the GSD of the transport in the re-circulating mode, then the conditions will remain the same. However, if the feed grain size matches the bed material GSD, then the system will reach a new equilibrium. The slope will become steeper and the bed will coarsen as the same discharge must now carry a coarser load. This is accomplished by increasing the number of coarse grains on the bed surface (Parker and Klingeman, 1982). If these results were used to develop transport models based on the bed material composition, an important difference becomes apparent. Both runs use the same discharge and sediment transport rate but the GSD of the transported material differs. Whilst part of this difference is attributed to the larger shear stresses in the feed case, the bed surface composition is the primary reason for the

difference (Wilcock and Crowe, 2003). This feature is not included in the model. As such, more than one transport size distribution can be associated with the same bed size distribution. Therefore, to overcome this problem, surface-based transport models have been developed.

There are three widely known surface-based models: (1) Proffitt and Sutherland (1983) which was based on the armouring experiments of Proffitt (1980); (2) Parker (1990b) who transformed the substrate-based gravel transport relation presented by Parker *et al.* (1982b) into a surface-based relation using the Oak Creek data of Milhous (1973); and (3) Wilcock and Crowe (2003). All three equations share many similarities but the Wilcock and Crowe equations differ by using the percentage of sand in the bed and not just the mean grain size to determine critical transport thresholds. The Wilcock and Crowe (2003) equations are discussed fully in Section 7.4.3.2 whilst Parker and Sutherland (1990) provide a useful discussion of the other two equations.

7.4.3 Sediment Routing Models

Coupling of hydraulic processes with sediment transfer processes in a 1D domain has been discussed broadly in the literature through the development of sediment routing models (referred to as SRMs hereafter). SRMs simulate important sediment transfer characteristics such as aggradation / degradation and downstream fining over the reach scale. In addition, the simulate sediment routing effects over longer spatial scales. Consequently, an SRM would act as a valuable building block to couple with the lateral channel adjustment sub-model.

SRMs use a continuum-mechanics approach to simulate bed-material transport. This means that the main flow properties predict the bulk sediment flux rather than consider the movement of individual particles. A sediment transport equation that predicts flux based on the strength of some property of flow to a movement threshold is typically used (e.g. the Meyer-Peter and Müller sediment transport equations). This flow property is typically shear stress. The Exner equation for the continuity of sediment is used to update the bed level

allowing for aggradation and degradation to occur. The Exner equation is based on the principle of mass conservation. It states that mass, in this case sediment, can neither be created nor destroyed. Consequently inputs and outputs must balance and if more sediment enters a reach than leaves, storage will occur. This storage is the aggradation of sediment whilst the converse, where there is a net loss from one reach to the next, results in channel degradation. By the 1980s, researchers began to use multi-fraction SRMs (Armanini and di Silvio, 1988; Van Niekerk *et al.*, 1992; Hoey and Ferguson, 1994). These calculate sediment transfer and continuity on a grain-size by grain-size basis. This employs the same principles as the single grain-size approach but each grain-size is considered separately. This allows only small grains to move under moderate flows whilst coarser grains require higher flows to be transported. By considering the continuity of sediment for each size fraction, the multi-grain size SRMs can be used to simulate downstream fining in gravel-bed rivers (Hoey and Ferguson, 1994), to explore sediment pulses (Cui *et al.*, 2003) and commercially for predicting rates of scour and fill for engineering works. Commercial SRMs, often referred to as aggradation/degradation or morphodynamic models, include HEC-6, iSIS sediment and MIKE 11.

SEDROUT (Hoey and Ferguson, 1994) is one of the most well known SRMs for research purposes. Providing an overview of this model's functioning and capabilities helps to justify this use of an SRM as a "building block" for the research model. SEDROUT was initially developed for the Allt Dubhaig, a coarse gravel-bed river in the Scottish highlands. Hence, this model is applicable to upland channels with coarse beds, like the Upper Wharfe. SEDROUT has the ability to simulate any channel long profile (Hoey and Ferguson, 1994). The initial version of SEDROUT was set up to model only steady discharge although more recent versions now allow hydrographs to be simulated (Verhaar *et al.* in press). SEDROUT computes the Exner equation for individual grain sizes using a generalisation of Parker and Sutherland's (1990) fractional continuity equation. By routing individual grain size classes down a channel, downstream fining is simulated. The bedload transport terms in the Exner equation can be determined from any suitable bedload transport equation. In the initial 1994 version of SEDROUT, Parker (1990b) was selected as the bedload transport equation allowing the transport rate for individual size classes to be

determined. The more recent version of SEDROUT (Ferguson *et al.*, 2001), continues using Parker (1990b). However, other SRMs provide alternatives such as the Wilcock and Crowe (2003) equations in Ferguson *et al.* (2006)

SEDROUT has been successfully applied and developed further by Hoey and Ferguson (1997), Ferguson *et al.* (2001), Talbot and Lapointe (2002), Hoey *et al.* (2004), Verhaar and Biron (2006) and Verhaar *et al.* (in press). Some important modifications include allowing for variable widths (Ferguson *et al.*, 1997) and allowing sand fractions to be simulated (Ferguson *et al.*, 2001). Furthermore, modifications can accommodate non-uniform bed slopes and bed texture patterns down the study reach. It has a choice of Keulegan or Manning-Stickler resistance laws and either bed elevation or bed material input can be held constant at the head of the simulated reach over the simulation period.

SRMs have some limitations which must be considered. The main limitation is the width-averaging of flow and sediment transfer (Lane and Ferguson, 2005). While width-averaging is adequate for canals and channelised rivers with rectangular or trapezoidal cross-sections, it struggles when simulating complex natural systems with variable widths, slopes and discharges. Thus width-averaging typically leads to the underestimation of bedload flux (e.g. Nicholas, 2000; Ferguson, 2003). Furthermore, a lack of field data, specifically information about bedload transport rates at a range of discharges, leads to assumptions being made. With SRMs such as SEDROUT sensitive to the specification of the incoming material (Hoey and Ferguson, 1994; Ferguson *et al.*, 2001) incorrect patterns of aggradation or degradation may occur if the boundary conditions entered are incorrect.

The 1D nature of SRMs allows calculations to be kept simple. By reducing the computing power and data input required, these models work well over larger spatial and temporal resolutions. With a detailed set of field data from the Wharfe, many of the limitations associated with SRMs can be reduced or overcome. Modifications can be made to the research model allowing many of the natural, irregular features of the Wharfe to be modelled (e.g. channel width, variable slope, variable discharge). Furthermore, the simple nature of SRMs will aid with the coupling of the lateral adjustment component. Including a

lateral adjustment component into the new model may also partially overcome concerns over width-averaging.

The SRM adopted as a building block for the research model was TRIB. Results from TRIB have been published in Ferguson *et al.* (2006) and Rice *et al.* (2006). The following introduction to TRIB provides an overview of the model's setup and capabilities providing background into modelling questions raised and modifications tested and applied.

7.4.3.1 INTRODUCTION TO TRIB

TRIB, a simple 1D SRM, is a modification and extension of the two-fraction model developed by Ferguson (2003a) to explore the gravel-sand transition along channels. TRIB incorporates multiple grain size fractions to simulate the bed level evolution of the river bed though aggradation and degradation and GSD along a section of river in much the same way as SEDROUT. The model is implemented in Excel, a spreadsheet package, using an iterative scheme. This has advantages, including easy manipulation with programming using macros in Visual Basic and excellent visual graphical outputs during simulations. As the name suggests, the model's primary function was to investigate the nature of disruptions caused by lateral inputs, specifically the inputs of water and sediment from tributaries. Ferguson *et al.* (2006) explored disruptions to the bed evolution and downstream fining trend whilst Rice *et al.* (2006) investigated how the tributary inputs affect the physical heterogeneity and biological diversity close to river confluences. Both investigations explored the impacts of altering three parameters in the model: (1) the ratio of tributary to mainstream water flux; (2) the ratio of tributary to mainstream bedload flux; and (3) the ratio of tributary to mainstream bedload diameter.

The user defines the model's starting values and parameters on the input sheet. These include specifying the proximal (upstream) channel width, the grain size distribution (GSD) of the main channel bed using 5-grain size classes which are also pre-defined by the user and the channel's input discharge. In addition, the user can determine the importance of the tributary input. For example, the tributary may contribute an extra 50% flow and sediment to the main channel. The model described in Ferguson *et al.* (2006) is set up so that one

tributary enters the study reach half way down the channel. The channel has 100 nodes equally spaced over 10 km.

The width is held constant along the reach with a step change at the confluence such that the increase in width is assumed to follow the standard power function regime relation $w = aQ^b$ (e.g. Leopold and Maddock, 1953). (Q) is discharge and (d) and (p) refer to distal (downstream) and proximal respectively. The ratio of distal width (w_d) to proximal width (w_p) becomes [7.7]. In Ferguson *et al.* (2006) the value of exponent b was set to 0.5. However, this could be easily parameterised by the user.

$$\frac{w_d}{w_p} = \left(\frac{Q_d}{Q_p}\right)^b \qquad [7.7]$$

The tributary inputs of water and sediment are defined by the user as ratios of the main channel discharge (QR), bedload flux (FR) and bedload grain size distribution (DR). A separate GSD can be entered to describe the tributary sediment. The bedload flux at the top of the mainstream can be set as: (1) fixed feed, where a fixed volume of sediment at a fixed GSD enters over a given time; or (2) flux equal to the transport capacity such that the amount and GSD of incoming sediment matches the transport capacity at the input.

The hydraulics are calculated using Manning's flow resistance law which assumes uniform flow. The local bed slope (S) is calculated from the bed elevation and distance between nodes using:

$$S_i = \frac{h_{i+1} - h_i}{x_{i+1} - x_i} \qquad [7.8]$$

where h is bed elevation at node i and x is the distance downstream from node 1.

To remove negative slopes where flow is "uphill", the hydraulic slope is determined from the bedslope with values below 0.001 assigned the small positive value of 0.001. Slope is used alongside the channel width (w), current discharge (Q) and a constant Manning's roughness value (n), to determine flow depth using Manning's flow resistance equation:

$$d = \frac{Qn / w^{0.6}}{S^{0.3}} \quad [7.9]$$

Finally by combining slope with depth, the shear stress is determined [7.10]. This is calculated assuming quasi-normal flow which neglects any backwater effects. Changes in flow resistance as the bed evolves are also ignored as n is set constant.

$$\tau = \rho g d S \quad [7.10]$$

where ρ is the density of water and g is acceleration due to gravity. Both are constants.

The bedload transport rate is calculated using the equations of Wilcock and Crowe (2003). These are described in detail as follows in Section 7.4.3.2. If there is transport of bedload from one node to the next, the model will update the bed elevation and GSD at both nodes using the Exner equation for the continuity of sediment. The standard Exner equation [7.11] can be used to compute aggradation and degradation in a channel:

$$\frac{\partial h}{\partial t} = -\frac{1}{1-\varepsilon}\frac{\partial q}{\partial t} \quad [7.11]$$

where h is bed elevation at distance x, q is bedload flux (determined using Wilcock and Crowe, 2003) and ε is bed porosity. Porosity is set at 0.3 which is within the range used by other studies of gravel-bed rivers (e.g. Lane *et al.*, 1995; Martin and Church, 1995; Ham and Church, 2000; Martin, 2005).

[7.12] is extended to a fractional Exner equation to simulate the continuity of each grain size fraction thus enabling the bed GSD to be updated:

$$(1-\varepsilon)\left[L\frac{\partial F_i}{\partial t}+E_i\frac{\partial z}{\partial t}\right]+\frac{\partial q_i}{\partial x}=0 \qquad [7.12]$$

where F_i is the proportion of each size fraction i in the active surface layer extending to a depth of L, q_i is the flux of size fraction i and E_i is the proportion of fraction i in the interface between active layer and sub-surface as the bed aggrades or degrades and t is time. L is taken to be twice the geometric mean diameter D_m of the bed at each place and time. E_i is assumed to be the same as F_i, which is an obvious assumption for aggradation and avoids tracking sub-surface stratigraphy. By reducing [7.12], the fractional GSD update becomes [7.13]. Equations [7.12] and [7.13] can be solved using a finite difference scheme.

$$\frac{\partial F_i}{\partial t}=-\frac{F_i\frac{\partial q}{\partial x}-\frac{\partial q_i}{\partial x}}{(1-\varepsilon)L} \qquad [7.13]$$

7.4.3.2 WILCOCK AND CROWE SURFACE BASED TRANSPORT MODEL

Sediment transport is a crucial process in the model as it directly determines aggradation and degradation, and downstream fining, indirectly feeds back to the hydraulics (through flow depth and channel bedslope, both of which alter shear stress) and drives the lateral component of the model through shear stress as linked to grain roughness, depth and slope. It is therefore essential that this component of the model is suitably represented. As noted earlier (Section 7.4.2), modelling sediment transport is notoriously difficult with large variations found in the success of the traditional equations. There is a strong recommendation that equations should only be applied to conditions that match those under which the equation was developed. Thus an equation for mixed coarse gravel rivers is

required for the Wharfe. Three potential choices include: (1) the Meyer-Peter and Müller (1948) equation which was tested heavily on coarse grained rivers, is generally found to perform well when applied (Gomez and Church, 1989) but was not designed for mixed sized sediment; (2) Parker's (1990b) surface based approach that was successfully used in SEDROUT; or (3) the Wilcock and Crowe (2003) surface based model which incorporates the full GSD and includes the non-linear effects of sand on sediment transport (Jackson and Beschta, 1984; Ikeda and Islya, 1998). Wilcock and Crowe (2003) was selected for use in TRIB and performed well when tested with two other transport laws (Ferguson *et al.*, 2006). During early applications to the Wharfe, predicted bedload transport rates matched well with observed estimates. This suggests that the Wilcock and Crowe (2003) equation remains applicable for the developing research model.

Wilcock and Crowe (2003) present a surface-based transport model that predicts the instantaneous transport rate, independent of initial and boundary conditions and capable of predicting transient conditions. This allows the transport rates to be predicted alongside the changing composition, rate and direction of bed adjustment. By using a dataset containing 48 coupled flow, transport and surface-sediment characteristics the Wilcock and Crowe (2003) model overcomes the "lack of data" barrier that had proved problematic to earlier surface-based approaches (e.g. Parker *et al.*, 1982a). However, this dataset, presented in Wilcock *et al.* (2001) was collected in a flume. As the model incorporates the non-linear effect of the sand content on gravel transport rate it uses the full surface GSD.

The model incorporates two concepts from earlier substrate-based models. First, it uses a hiding function (Einstein, 1950; Egiazaroff, 1965; Andrews and Parker, 1987). Second, it has a similarity collapse over grain size, based on a reference shear stress (Ashida and Michue, 1971; Parker *et al.* 1982b). The form of the similarity collapse is:

$$W_i^* = f(\tau / \tau_{ri}) \qquad [7.14]$$

where τ is the bed shear stress and τ_{ri} is the similarity parameter with a reference value of τ and W_i^* is defined by:

$$W_i^* = \frac{(s_r - 1)gq_{bi}}{F_i u_*^3} \qquad [7.15]$$

where s_r is the ratio of sediment to water density, g is acceleration due to gravity, q_{bi} is the volumetric transport rate per unit width of size i, F_i is the proportion of size i on the bed surface, u_* is the shear velocity ($u_* = [\tau / \rho]^{0.5}$), and p is water density. The reference shear stress for a grain size fraction i (τ_{ri}) used in [7.15] is defined as the value of τ in W_i^* when equal to a small reference value $W_i^* = 0.002$ (Parker *et al.*, 1982a, 1982b; Wilcock, 1988).

When values of reference shear stress for each grain size fraction (τ_{ri}) are scaled against the reference shear stress (τ_{rm}) for the mean of each bed surface (which is the value of τ_{ri} corresponding to the mean size of the bed surface) and plotted as a function of grain size fraction to median grain size, the trend produced has two clear linear segments. These can be explained using the power relation shown below [7.16]. The reference shear stress τ_{ri}, requires a consistent collapse to produce a single predictive relation from the two linear segments.

$$\frac{\tau_{ri}}{\tau_{rm}} = \left(\frac{D_i}{D_m}\right)^b \qquad [7.16]$$

where D_i is the grain size at the i percentile and D_m is the median grain size of the surface layer sediment and b is an exponent.

This hiding function [7.16] is similar to those used in other mixed-size transport models (e.g. Parker *et al.*, 1982b; Proffitt and Sutherland, 1983; Andrews and Parker, 1987; Parker (1990b); Sutherland, 1992). It reduces calculated transport rates by increasing τ_{ri} for finer fractions. It increases transport rates by reducing τ_{ri} for coarser fractions. This is done relative to values of τ_{rm} for single sized sediments. Thus it reduces the mobility of smaller sizes and increases the mobility of the coarser sizes relative to the unisize case. The hiding function gives the variation of the reference shear stress (a surrogate for critical shear stress) as a function of fractional size relative to the median grain size of the bed surface. It has two distinct limbs corresponding to relatively fine and relatively coarse fractions. This is because, in sandy sediments, the median surface grain size is relatively small such that the majority of the particle size fractions fall on the steep side of the limb whilst sediments with little sand tend to have a relatively coarse median surface grain size such that the majority of fractions fall on the gentle limb for finer sizes.

Wilcock *et al.* (2001) demonstrate that the bed sand content has an important and non linear effect on gravel transport as the entrained sand promotes the transport of coarser grains (Curran and Wilcock, 2005). The percentage of sand on the bed surface (F_s) becomes important in [7.16] in the calculation of the reference shear stress (τ_{rm}) required to initiate transport [7.17]. Equation 7.17 is taken from Wilcock and Crowe (2003). Thus, as the percentage of sand on the bed increases, the reference shear stress reduces and sediment transport rates become higher. The effect of sand on bedload transport was initially recorded by Jackson and Beschta (1984) and Ikeda and Iseya (1998). Figure 7.3 shows that the reference shear stress reduces in a non-linear way as the percentage of sand increases up to 25%.

$$\tau_{rm} = (0.021 + 0.015\exp[-20F_s])(s_r - 1)\rho g D m \qquad [7.17]$$

Figure 7.3: Non-linear effect of sand on the reference shear stress. The D_m was 20 mm.

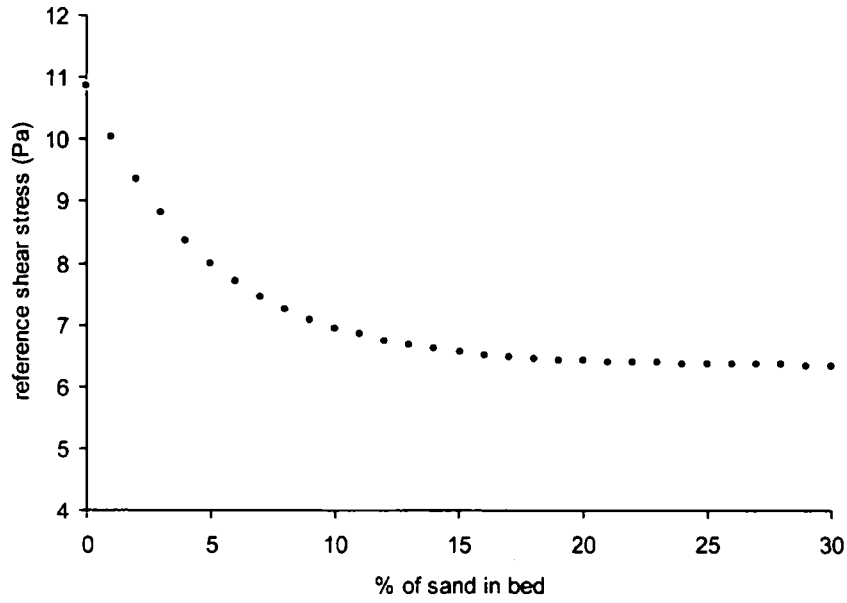

The final component of the Wilcock and Crowe (2003) equations is the transport function shown below:

$$W_i^* = \begin{cases} 0.002\Phi^{7.5} & \text{for } \Phi<1.35 \\ 14\left(1-\dfrac{0.894}{\Phi^{0.5}}\right)^{4.5} & \text{for } \Phi\geq 1.35 \end{cases} \qquad [7.18]$$

where W_i^* is the dimensionless transport rate of each size fraction i and $\Phi = \tau/\tau_{ri}$. It is determined as a function of τ/τ_{ri} for all size fractions. Thus when Φ is high the upper part of the equation is applied whilst when values of Φ greater than 1.35, the lower part of the equation is applied.

7.4.4 MODELLING QUESTIONS ARISING WHEN ADOPTING TRIB

TRIB, including the Wilcock and Crowe (2003) surface based transport model was selected as a building block for the development of the research model. Before the third sub-model, the lateral adjustment model, is considered, five key modelling questions arise from the above discussion of TRIB and the Wilcock and Crowe (2003) sediment transport equations. These questions are answered in Chapter 8 to aid with decision making. First, *can the Upper Wharfe study reach be successfully applied to TRIB?* This will involve adding in aspects of the Wharfe's geometry described by the field monitoring. These include the number and spacing of cross-sections, the average channel width, upstream and downstream slopes, a GSD representing the entire reach, an appropriate value of Manning's n and a reasonable value for the fixed, steady discharge. Second, *what aspects of the model can be modified to improve the representation of the study reach in the model?* Modifications that can be applied include: allowing width to vary downstream (but remain fixed over time), variable channel slope, representation of grain size characteristics and the value applied to n. In addition, the sand boundary in the Wilcock and Crowe (2003) equations requires evaluation as it is currently set at 2 mm representing sand. With little sand found in the Wharfe, this may be problematic for the model. Third, *do the modifications in (2) produce predictions that match the field observations well?* A range of comparisons should be made to test different model ouputs. Fourth, before the lateral component of the model is explored, *can a variable flow regime can be incorporated into the model?* The initial version of TRIB and many other SRMs only simulate steady state conditions, thereby ignoring the sediment transfer processes under natural variable flows. Fifth, the final question to be explored before the lateral component is developed, asks *what impact manual changes in channel width have on the model outputs?* Manual changes can be created by simply entering a different channel width into each node. This is important because it demonstrates the model's sensitivity to changes in width, and provides and early indication to the model's response to changes in width.

7.4.5 OPTIONS FOR THE LATERAL SUB-MODEL

The third sub-model to be coupled with the hydraulic and sediment transport sub-models, which are combined using TRIB, is the lateral channel change sub-model. The literature is explored to determine options available for this lateral component and concentrates on the bank erosion sub-models currently used in morphological adjustment models.

Previous bank erosion sub-models

Early models of bank erosion simply parameterised bank erosion rates using single variables such as local flow velocity (Ikeda *et al.*, 1981), stream power (Bull, 1979), critical shear stress for entrainment (Arulandan *et al.*, 1980) or bank curvature (Parker *et al.*, 1983). However, these models fail to provide information about the interactions between bank erosion and the channel bed and topography. Thus, by the 1990s, authors had begun to couple together models of flow and sediment transport with physically-based models of bank erosion (e.g. Pizzuto, 1990) providing more accurate predictions. Darby (1998) and ASCE (1998b) note the distinction between bank erosion analyses for cohesive and non-cohesive banks.

Two different techniques to model non-cohesive bank erosion are used by Pizzuto (1990) and Kovacs and Parker (1994). Pizzuto (1990) simulates bank erosion using a heuristic model of bank slumping with slumping occurring as a result of basal lowering and increasing bank slope angle. On the other hand, Kovacs and Parker (1994) use the angle of repose of sediment as a threshold for erosion but simulate erosion by creating a discontinuity in the slope which migrates up the bank. This discontinuity is created between the oversteepened bank and the upper bank as shown in Figure 7.4. Erosion occurs as the discontinuity migrates up the bank.

Figure 7.4: Propagation of bank erosion upslope. Kovacs and Parker (1994)

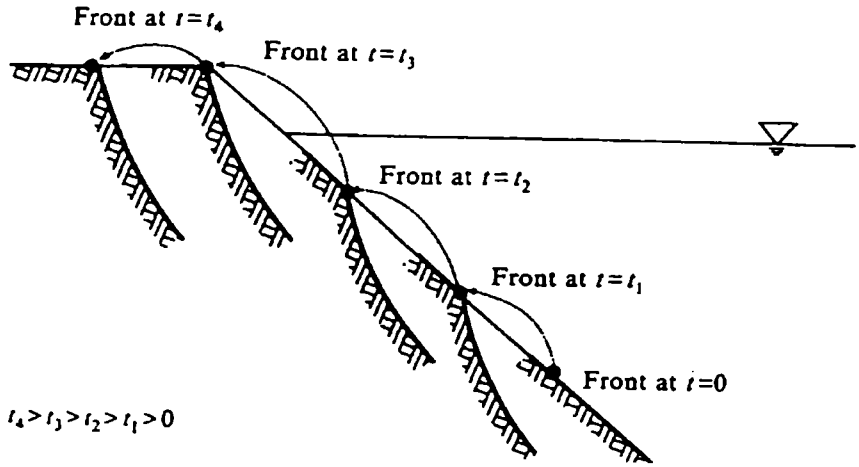

In the channel adjustment model of Nagata *et al.* (2000) that uses a 2D model to calculate bedform deformation and planform variations, fitting them to a movable boundary fitted co-ordinate system, bank erosion is simulating using Hasegawa's (1981) approach. The model is similar to the modification of Mosselman's RIPA by Darby *et al.* (2002) but this model is more appropriate for non-cohesive banks and has a simpler description of bank erosion processes. Both the Nagata *et al.* (2000) model and RIPA are models for meandering channels rather than straight ones and are discussed in Section 7.2.4. Hasegawa's (1981) simplified model of bank erosion for non-cohesive materials is shown in Figure 7.5. It assumes that bank erosion will occur as bank failure when the volume of sediment in zone A (sediment supply due to bank erosion) equals the volume of deposition in zone B. This model simulates the non-equilibrium state of sediment transport and the empirical approach avoids dealing directly with the physics of bank erosion (Duan, 2001). It is based on the assumption that basal channel erosion and bank erosion through entrainment will oversteepen the channel banks until a critical threshold has been breached. Thus, it is similar to other techniques (e.g. Pizzuto, 1990; Osman and Thorne, 1988 and Kovacs and Parker, 1994). Hasegawa (1981) assumes that the volume of erosion is equal to the volume of deposition as shown in Figure 7.5.

Figure 7.5: Hasegawa (1981) bank collapse model.

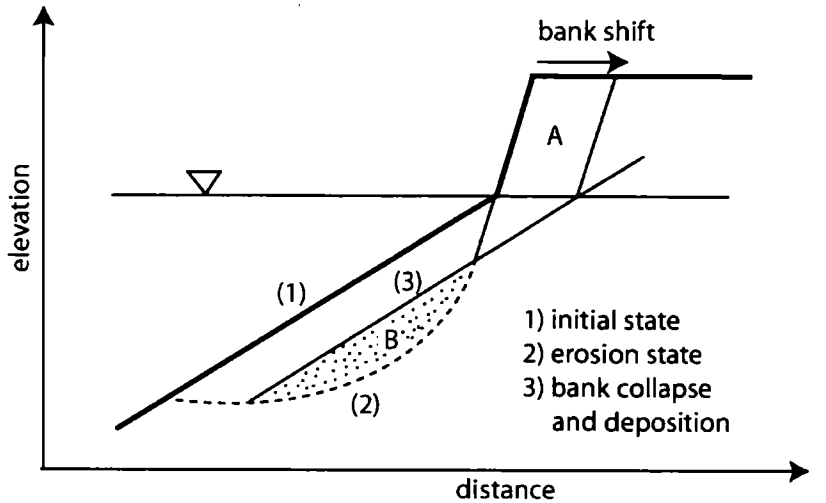

Most cohesive bank erosion simulations have been based on the analysis of planar failures (Osman and Thorne, 1988; Darby and Thorne, 1996; Simon *et al.*, 1991). These approaches are based on Carson and Kirkby's (1972) concept of basal endpoint control. This concept shows that bank retreat or advance is a function of flow, sediment transport and bank stability processes within the near bank zone (Darby, 2000). Bank failure will occur when basal erosion increases bank height and angle and decreases bank stability. The channel widens at a rate determined by the width of the failure block. The Darby and Thorne (1996) bank erosion sub-model includes both fluvial bank erosion and mass wasting in the form of rotational and planar failures. The left and right bank stability and the lateral erosion are calculated separately to allow asymmetrical erosion, a feature common in alluvial environments. The fluvial bank erosion is modelled using the Arulandan *et al.* (1980) empirically derived relationship. This is based on the assumption that grain entrainment will occur when the shear stress of the flow exceeds a critical threshold:

$$LE = \frac{r}{\gamma}\left(\frac{\tau - \tau_c}{\tau_c}\right) \qquad [7.19]$$

where LE is the lateral erosion rate, τ and τ_c are the applied fluid and critical entrainment shear stress respectively, γ is the unit weight of the soil and r is the initial rate of soil erosion .

The mass failure part of the Darby and Thorne (1996) bank erosion sub-model is based on Osman (1985) and Osman and Thorne's (1988) geotechnical bank stability analysis for rotational slip and planar failures. Osman and Thorne (1988) was one of the first studies that combined the effects of fluvial entrainment processes at the bank toe with geotechnical stability in the context of analysing bank retreat. This approach models the retreat of cohesive banks as a discontinuous sequence of erosion cycles in which toe scour and fluvial erosion decreases the bank stability by increasing the slope and height of the bank leading to mass failure.

In RIPA (Mosselman, 1992; 1995; 1998), a 2D depth-averaged model for single thread cohesive channels with irregular platforms, the bank erosion component has been updated. The earlier models use both excess shear stress (Ikeda *et al.*, 1981) and excess height mechanisms whilst the 1998 version uses only excess height as a bank erosion mechanism. This mechanism is shown below [7.20] and explains that once the height and hence the angle of the bank increases beyond a certain threshold (through basal lowering), the bank will fail by planar failure. However, Darby *et al.* (2002) felt that this method was insufficient and went on to develop RIPA further by replacing the existing bank erosion model with Osman and Thorne's (1988) mechanistic approach that represents bank failure in more detail. The new model also includes a modification to describe the deposition of bank materials and its subsequent removal.

$$\begin{aligned} H\frac{\partial n_B}{\partial t} &= G\left(\frac{H - H_c}{H_c}\right) && \text{for } H \geq H_c \\ \frac{\partial n_B}{\partial t} &= 0 && \text{for } H < H_c \end{aligned} \qquad [7.20]$$

where $\partial n_B / \partial t$ is the rate of bank retreat, G is an erodibility coefficient, H is the total bank height and H_c is the critical bank height below which no bank erosion occurs.

Bank erosion considerations

Before decisions about how to simulate bank erosion are made, it is important to consider the mechanisms by which the channel adjusts laterally. Rules will be developed to simulate these processes. From the results of the bank erosion study (Section 4.4), it is clear that fluvial entrainment and desiccation failure dominate on banks on meander bends whilst freeze-thaw and seepage/piping dominate on straight channel sections. These weathering processes are typically enhanced by secondary circulation that develop due to differences in channel depth across the channel and channel curvature. Rates of bank erosion on the outside of meander bends are around three times greater than bank erosion rates on the straight sections. This tells us that channel change predominantly occurs at meander bends. These results suggest that the lateral channel change component ideally needs a mechanism where shear stress is redistributed across the channel due to curvature and differences in bed elevation. This would represent the effects of the secondary circulation that forms in curved channels upon the spatial patterns of shear stress.

Distributing shear stress laterally

The problem herein is that 1D models such as TRIB, SEDROUT and the Cui *et al.* (2006) model average shear stress across the width of the channel and treat the channel as straight. Hence they fail to accurately represent the natural spatial variability in shear stress across the channel (Ferguson, 2003b). Ferguson (2003b) notes that these spatial shear stress variations may be due to: (1) the effect of the channel sides which create a velocity profile outwards from the centre of the channel; (2) lateral variations in depth both laterally across bars and thalwegs and longitudinally over pools and riffles; (3) planimetric convergence and divergence of flow which coincide with flow acceleration and deceleration (e.g. braids and tributary inputs); and (4) curvature induced secondary circulation which creates higher shear stress zones where surface downwelling occurs. It is therefore necessary to find a method of distributing width-averaged shear stress laterally across a cross-section such that the distributed shear stress is more representative of the actual shear stresses one would expect for the channel planform, in particular channel curvature and differences in bed elevation. The boundary shear stresses placed on the outer bank of the channel could then be used to determine bank erosion rate by applying a threshold shear stress rule.

Conversely, a drop in shear stress on the inside of the meander bend would correspond with deposition and the formation of a channel bar. There are several methods used in some existing width adjustment models that could be used to redistribute 1D width averaged shear stress across a channel. These techniques all require additional information on the channel morphology and as such can be divided into two types: (1) those which use channel curvature; and (2) those which use depth variations as a surrogate for information on shear stress.

(1) There are three potential methods that use channel curvature to estimate outer bank shear stress. These work on the assumption that the greater the curvature the greater the lateral shear stress variation and hence the more shear stress on the outer bank. These techniques were developed to estimate bank erosion rates and as such could be used directly to calculate lateral change in the Wharfe. The first method uses the bend theory concept (Ikeda *et al.*, 1981) which determines near-bank flow velocity from the curvature of the channel. In "bend theory", this flow velocity is then taken to be directly proportional to bank erosion rate. The second approach by Begin (1981) uses the curvature ratio (radius of curvature to channel width) and the momentum equation to calculate the radial force exerted on the outer bank of a stream meander bend. This force could be directly linked to outer bank shear stress. The third approach uses the ratio of centreline arc length to outer bank arc length in a shear stress conversion factor (Richardson, 2002). It assumes that the ratio of outer bank velocity to section averaged velocity is equal to the arc length ratio. This method was specifically developed to be used with the output data from a 1D hydraulic model.

(2) The second group of methods use variations in channel depth across the cross-section to explain how localised shear stress may differ from width-averaged shear stress. Talbot and Lapointe (2002) explain that to simulate the channel long profile change more realistically using sediment routing models such as SEDROUT, the simulated "formative" discharge for the prismatic channel must be adjusted to produce bed shear stresses that correspond as closely as possible to those found in natural channels with deeper sections of flow. Using depth as a replacement indicator of shear stress is sensible since mean shear stress is

directly linked to mean depth (or hydraulic radius) through the DuBoys shear stress equation or Manning's equation. If the channel is split into smaller sections, each with its own value of depth, the mean shear stress in each section becomes a function of depth. Since depth is easily obtained from cross-section data, several authors have used it to provided information about the spatial variability of shear stress. This is particularly common in cellular modelling approaches (e.g. Paola, 1996; Nicholas, 2000). These principles could be applied to determine outer bank shear stress from channel depth variations since the typical cross-section around a meander bend is asymmetric with a deeper outer bend zone moving towards a shallower inside bend.

One such technique was applied by Talbot and Lapointe (2002) to improve bedload transport estimates in SEDROUT. They experimented with estimating shear stress from the mean depth, maximum depth and the average of the two. The latter provided them with the best shear stress estimates for the bedload transport equation when compared with data. A third potential option used to compute shear stress distribution in meandering reaches, ignores the shallow, low shear stress parts of the channel and determines the width-averaged shear stress for the deeper channel sections only (i.e. those closest to the bank). This approach was used by Nicholas (2000) in New Zealand on braided channels. This approach is less applicable in single thread channels since the ratio of shallow zones to deeper zones is much less than in braided channels.

Using spatial patterns of depth as an indication of shear stress variation is appealing for use in 1D models since the additional data on depth are readily available from cross-section profiles. However, there may be some problems with using depth to provide information on shear stress (Ferguson, 2003b). First, it has been recognised that some areas, such as riffles and bar heads, may have a low depth but high shear stress whilst others have the opposite due to local differences in water surface slope (Lisle *et al.*, 2000). Furthermore, Bathurst *et al.* (1979) have shown that maximum shear stress does not always correspond with maximum depth following field measurements made in gravel bed meander bends. This is often the case in meandering channels because of the delayed cross-over of the flow (Dietrich and Smith, 1984). There are also suggestions that the increased grain size and

influence of the bank found in the deeper channel sections close to the bank on the outside of a meander bend increase flow resistance thereby counteracting the expected increase in shear with increased depth (Nicholas, 2000). Despite these potential complications, Nicholas (2000) suggests that the local deviations tend to cancel each other out so that a positive correlation between depth and shear stress exists.

Splitting the channel

These methods highlight that bank erosion driven by curvature and depth differences can be simulated in lateral adjustment models. However the discussion also demonstrates the importance of incorporating lateral shear stress variation into the model for computing the hydraulic and sediment transport equations before bank erosion is even considered. Since curvature and depth have been highlighted as predominant factors leading to bank erosion in the Wharfe system, these form the focus of the modelling basis. TRIB represents the channel as a straight, rectangular one with a centre zone of uniform depth. To incorporate depth variations into the model, the cross-sectional representation of the channel needs to be enhanced. Following on from the Lancaster and Bras (2002) and Stark (2006) models, the channel can be split into two halves. By providing two bed elevations and hence depths, spatial variability in shear stress can be introduced but without making the model too sensitive to the full range of depth variability in a natural channel. Thus a split channel approach would allow some of the natural channel geometry to be represented, albeit in a simplified manner.

Representing slope

Alongside flow depth, slope is a fundamental component in the calculation of shear stress. In the split channel approach several options of slope can be adopted. Three key options are identified including: (1) steepest flow path; (2) water surface elevation; and (3) average bed slope. The first method, the steepest flow path, is based on methods of calculating slope in cellular models used in braided river simulations (e.g. Murray and Paola, 1994, 1997; Thomas and Nicholas, 2002; Thomas *et al.* 2002, 2006). These calculate the bed slope of the steepest pathway from the upstream cell to one of the downstream cells (Figure 7.6a). This option could be applicable to the split channel model as it is effectively a simplified

cellular approach with two upstream and two downstream options as shown in Figure 7.6b. However, whilst the slope could cross from one side to the other, the model capabilities are insufficient to allow sediment and flow to follow these cross-over paths. Furthermore, this approach would enhance slope values further as the steepest path would always be used.

Figure 7.6: Slope, flow and sediment transport pathways in cellular and split channel approaches. In the cellular approach, the dashed arrows represent lateral transfers, Q_o is the discharge leaving the upstream cell, Q_i is the discharge received by each of the five downstream cells and r_i is the routing potential determined from the local bedslope between pathways.

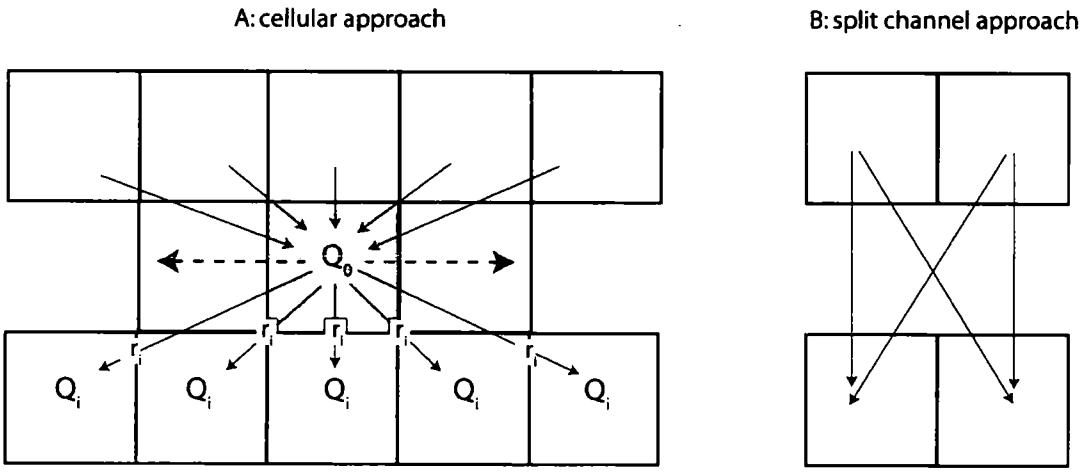

The second option is to use the water surface elevation to calculate the downstream slope. Since the water surface elevation is equal across both channel sides, the water surface slope is the same for both channel sides. This would create a much smoother slope profile as the bed roughness features would be dealt with by varying flow depths (e.g. a pool will have deeper flow whilst a riffle will have shallower flow). This may be problematic as these roughness features provide shear stress variability which helps to characterise sediment transport. Thus, the third option to use the average bedslope of the two channel sides is more appealing as it would incorporate more of the slope variability into the channel. By using the average slope of the two sides, the character of the slope is largely maintained. At the same time any sharp drops in slope on one side would be dampened due to the averaging with the other side (e.g. the steep slope of the outer channel side at a meander bend with a deeper outer side).

7.4.6 Modelling Questions for the Lateral Component

A further five key modelling questions arise from reviewing literature on lateral adjustment models. These are explored in Chapter 8 where modifications and decisions are made. Questions (6), (7) and (8) will use a simplified geometry for development with the more complex channel geometry of the study reach becoming incorporated in Questions (9) and (10). The sixth questions asks, *can the channel be split into two halves and still function efficiently?* Additional decisions and modifications are also required. These include developing a method to distribute flow between channel sides and determining the best option to represent slope from the three methods outlined earlier. The model's behaviour to several situations should be tested including lateral bars and pools. Seventh, *a decision is required on which bank erosion option to employ?* This considers bank erosion for straight channels with curvature induced bank erosion considered in question (10). Three options discussed include: (a) using a critical bank angle (based on approaches by Hasegawa (1981), Osman and Thorne (1988), Pizzuto (1990) and Kovacs and Parker (1988)); (b) using a critical depth difference to distribute shear stress (e.g. Talbot and Lapointe, 2002); and (c) using a critical shear stress (similar to the Ikeda *et al.* (1981) approach although this is based on a velocity threshold rather than shear stress). Shear stress thresholds were also used to drive bank erosion in an approach by Arulandan *et al.* (1980) and in early versions of RIPA (Mosselman, 1992, 1995). A justification for the selected option should be provided. Eighth, following on from (7), *what modifications will improve the model's lateral channel change component*? Modifications are required to prevent excessive overdeepening, simulation of bank depositing and maintaining the continuity of sediment during adjustment. Ninth, *aims to address whether the lateral adjustment component continues to work well when the level of complexity is increased as the Wharfe data is added?* This is answered before the final modification to include curvature into the lateral sub-model is made in (10). Key modifications and decisions made here include how to represent the Wharfe's geometry as a split channel and what critical values of shear stress should be applied to initiate bank erosion? The final major modification, highlighted from the literature as an important component of bank erosion models, is a method of

distributing shear stress as a function of channel curvature. This final modelling question, ten, *explores the applicability of a curvature induced shear stress distribution?* This would make the model capable of simulating natural, curved reaches.

7.5 CHAPTER SUMMARY

The model conceptualisation process has demonstrated the importance of using literature review to identify previous modelling approaches, what the limitations of these previous approaches are and whether they are applicable to the research project. This chapter began by providing an overview of the range previous modelling attempts. The overall conclusion, following a summary of their limitations, was that a new model of morphological channel change is required for this research. In the second part of this chapter, a conceptual research model was developed using: (1) literature on the theory of morphological channel change (Chapter 2); (2) observations and findings made from field studies (Chapters 4 to 6); and (3) previous modelling approaches. A three part sub-model approach was selected sharing a similar structure to the width adjustment models discussed in Section 7.2.2. The sediment routing model TRIB, will be adopted to represent the hydraulic and sediment transport sub-model components, and as a basis for the development of the third component, the lateral channel change sub-model. Literature review was used to highlight key model development questions. These provide a clear development testing structure for Chapter 8. These questions can be further grouped into model development stages:

(a) applying TRIB to the Wharfe (Question 1);
(b) modifying TRIB and the boundary conditions (Questions 2, 3, and 4);
(c) developing a lateral channel change component for simulating straight channels (Questions 5, 6, 7, 8 and 9); and
(d) developing the model to simulate lateral channel change in meandering channels (Question 10).

CHAPTER EIGHT: MODEL DEVELOPMENT, TESTING AND CALIBRATION

8.1 INTRODUCTION

Chapter 7 highlighted several key modelling questions which form the basis of the model development and testing. The aim of this chapter is to achieve Objective 5 from Chapter 1. This objective was to develop, to test and to calibrate the model so that scenarios can be performed in Chapter 9. The processes of model verification, validation and calibration are used throughout this chapter to aid with development. Verification is regarded as "solving the equations right" opposed to validation which is "solving the right equations" (Roache, 1997). Lane and Richards (2001) echo this using the term verification for the correct solution of the equations whilst validation is determining the correct parameters predicted by the equations. In this study verification is ensuring that the equations are solved correctly and give values that are feasible whilst the validation process is used to compare the predictions with the field data to test the closeness of predictions. Care must be taken during validation as validation is based on the principle that when a model fails to predict independent data or observations adequately, something must be wrong with the model or the validation data (Luis and McLaughlin, 1992). Yet the converse of this, that correct predictions make the model valid can equally be wrong. Lane *et al.* (2005) suggest that it is possible for an invalid model to produce adequate representations of reality. Calibration is the process by which inputs, parameters and equations are "tweaked" to improve the closeness of fit between the predicted and observed data. In this chapter verification and validation of the model occurred after every modification.

Section 8.2 through to Section 8.5 aim to explore each of the ten modelling questions raised in Chapter 7, through testing the model's output against field observations. These questions are answered within the four modelling steps identified in Section 7.5. These include: (a)

application of TRIB to the Wharfe; (b) modifications to TRIB and the boundary conditions, including incorporating a variable discharge; (c) developing the lateral adjustment component for straight channels; and (d) applying this to meandering channels. Table 8.1 shows the structure of the model development and testing. For each question, there are a series of modifications and decisions that must be made and justified. The results from testing these modifications and decisions are used as supporting evidence. Once the modifications and decisions have been carried out, sensitivity analysis (Section 8.6) and model calibration (Section 8.7) are performed to find the optimum values for the model's input and boundary conditions. The aim of these processes is to provide a model the produces predictions that match observations most closely. This allows the calibrated model to be used in Chapter 9, scenario testing.

Table 8.1: Development stages (st.), key questions, modifications and decisions to be made to develop model.

Stage Sect.	Key modelling question	Modifications and decisions	Testing aim
St: (a) 8.2	(1) Can the Upper Wharfe study reach be successfully applied in TRIB?	Number of nodes and their spacing, average channel width, upstream and downstream slope, starting GSD, tributaries removed.	Does the model continue to predict values within a sensible range for a gravel-bed river?
St: (b) 8.3.1	(2) What modifications can be made to improve the representation of the Wharfe in the model?	Modifications include: 1) width: uniform to variable downstream. Width remains fixed over time; 2) tributaries: one for Cray and one for Buckden Beck; 3) slope: incorporate more variable slope; 4) sediment representation: number of grain size classes; 5) sand boundary in W&C, 2003: raise to 8 mm to account for coarser sediment; 6) input GSD: explore options; and 7) Manning's n: allow for changes downstream and over time.	Test outputs against field data after each modification: specifically the pattern of downstream fining.
St: (b) 8.3.2	3) When all the modifications in (2) are made, does the model perform well?		Compare predictions with observations: 1) sediment transport ratios; 2) bedload transport threshold; and 3) maximum transport rates.
St: (b) 8.3.3	4) Can the model support a variable hydrograph?	Modify to allow for hydrographs. Does the model continue to function well?	Compare predictions with observations: 1) evolution of bed and downstream fining rates and 2) bed level changes: average and maximum aggradation.

St: (c) 8.4.1	5) What impact does manually altering the channel width have on the model output?		Test impact of channel width on aggradation / degradation.
St: (c) 8.4.2	6) Can the channel be split into two halves?	Split channel into two equal halves and perform calculations for each side using a simplified geometry. Account for situations where flow is entirely in one channel side. Decide on best option to represent slope.	Ensure model produces sensible results and explore output when simulating: 1) a pool; 2) a lateral bar; and 3) a transverse bar.
St: (c) 8.4.3	7) Which method of simulating bank erosion is most applicable?	Make decision on bank erosion option: 1) critical bank angle; 2) critical depth difference; and 3) critical shear stress.	
St: (c) 8.4.4	8) What modifications can be made to the lateral adjustment component to provide a better representation of processes?	Include modifications to: 1) simulate deposition; 2) prevent overdeepening; and 3) account for sediment continuity of the bed during adjustments.	
St: (c) 8.4.5	9) Does the lateral adjustment component function well when tested on the Wharfe study reach?	Decisions required on: 1) how to incorporate the geometry of the Wharfe; 2) what the critical erosion shear stress threshold should be.	Test models output with observations including downstream fining patterns and rates, bed level changes and locations and rates of bank erosion.
St: (d) 8.5	10) Does a curvature function for redistributing shear stress improve predictions?	Modify model to incorporate a shear stress redistribution function based on curvature and make decision on whether to incorporate channel width into this function.	Test models output, specifically bank erosion rates and locations with field observations.

8.2 APPLYING THE WHARFE TO TRIB: STAGE (A)

The original model, set up as described in Ferguson *et al.* (2006), was applied to the Wharfe study reach. This involved changing the 100 equidistant nodes in the basic TRIB formulation into 60 variably spaced nodes, representing each of the cross-sections and the mid-channel distance between them. The model uses the distance between nodes to calculate channel slope and node distance is not explicitly considered when redistributing sediment. The total channel length was 5.6 km. Channel width was set constant at 17 m which was the average channel width for the study reach. The channel slope was determined from an upstream and a downstream slope value that represented the channel slopes at Hubberholme and Starbotton. The slope values at each node between these locations were interpolated linearly in the model giving a quadratic long profile. This provided a crude representation of slope. At this early stage, the single tributary input was set to zero, which in effect removed it from the calculations. The initial GSDs entered for the entire study reach represented the GSD at Buckden Bridge (cross-section 220). This site was selected because the GSD was close to the median for the whole reach. With no sediment or water entering from the tributary, the GSD for the tributary was left blank.

With the model set up to represent a very simple Wharfe study reach, the model was run. The main aim at this stage was to ensure that the model continued to compute and predict values within a reasonable range for a gravel-bed river. Following the initial run, the model was verified. Plausible values of downstream fining were predicted (i.e. values within the gravel size range of 20 mm to 80 mm and with an overall reduction in size downstream), and the model remained stable. The Wharfe study reach had been successfully applied to the initial version of TRIB.

8.3 MODIFICATIONS TO TRIB AND THE BOUNDARY CONDITIONS: STAGE (B)

This section begins by exploring a range of simple modifications that are made to TRIB and to the model's boundary conditions to improve the model's ability to represent natural systems like the Wharfe (Section 8.3.1). Following the inclusion of these modifications, the

model's outputs are compared against field data to assess the model's ability to simulate conditions in the Wharfe (Section 8.3.2). A further substantial modification is made in Section 8.3.3 with the introduction of variable discharges into the model. Further testing against field observations are made after this modification. Unless specified otherwise, all simulations were stopped when the rate of change stabilised.

8.3.1 Initial Modifications

Seven modifications, highlighted in Chapter 7 and summarised in Table 8.2, were identified to improve the model's ability to represent natural systems. These included modifications to: (1) channel width; (2) adding in tributaries; (3) slope; (4) sediment representation; (5) the sand boundary in Wilcock and Crowe (2003); (6) input GSDs; and (7) Manning's n roughness values. As the model increased in complexity the time step was reduced from 12 hours to 7.5 minutes to maintain model stability. Concurrently, simulation time increased. The following modifications are discussed in the order that they were made:

1) Fixed channel width to variable channel widths

Natural channels, including the Wharfe, are seldom uniform in width. The Wharfe varies in width from 12 m to 33 m with the standard deviation of width noted to be 4.5 m. As discussed in Section 6.2.3, channel width is linked to bank erosion. In the Wharfe, this is controlled by factors such as vegetation, bank protection and slope. In the model, the width directly influences the unit discharge and the flow depth. As such, it was important to represent the variability in channel width at each of the cross-sectional nodes. Moving from a fixed width to a variable width model was simple and involved adding a data column containing individual channel widths into the workings sheet rather than using a single width value which was entered by the user on the model input page. A similar modification was made to SEDROUT by Ferguson *et al.* (2001). At this stage in the model development, the width remained fixed over time. The lateral adjustment component (Section 8.4) allows the width to become dynamic. With downstream width made variable, the previous method of increasing width when a tributary enters using [7.7] is made redundant. Width increase downstream of a tributary is now explicitly included in the input channel widths at each node.

2) Adding tributaries to represent Cray and Buckden Beck

The original model had one tributary input which entered half way down the reach. The model was altered so that two tributaries entered the reach. The upstream input represented Cray Beck and entered between cross-sections 110 and 120 at 1020 m downstream. The downstream tributary input represented Buckden Beck and entered between cross-sections 280 and 290 at 2300 m downstream. The other smaller inputs into the study reach were not included as these contribute only small quantities on flow and little or no sediment. They typically only become active during the wettest periods when the main channel was also high. Thus their relative contribution to flow remains low. With no measured discharges for the tributaries, the flow input, expressed as a proportion of the main flow, was estimated from catchment area. The catchment upstream of Hubberholme is 56 km^2, Cray Beck is 5.5 km^2 and Bucken Beck is 3 km^2. Therefore, approximately 10% and 5% of main flow was estimated to come from Cray Beck and Buckden Beck respectively. These values are supported by estimates of flow made during field visits. This contribution was fixed and does not account for changes that may occur with varying stage or local variability in rainfall. The model output was not sensitive to small changes in the percentage estimates of flow from the tributaries. The estimates were felt to be adequate.

Alongside the input of flow, a decision over the percentage contribution and gradation of sediment that would enter the channel at each confluence was required. The percentage contribution of sediment that enters from each tributary was estimated in Section 5.4.4 when reconstructing the sediment budget from the cross-sectional re-surveys. Hence the lateral flux as a proportion of the mainstream flux was 0.03 and 0.08 for Cray and Buckden Beck respectively. This does not account for temporal variability. In addition to the flux, the GSD of the tributaries is required. No GSD samples were taken in the two tributaries due to a lack of exposed sediment bars. However, the GSD of the sediment was estimated from any peaks or troughs in the downstream fining profile (Section 5.3). From these results, in particular Figure 5.14, a small rise in gradation occurs around the location of the Cray Beck tributary and no significant change is noted downstream of the Buckden Beck confluence. Thus, coarser sediment is likely to be entering from Cray Beck whilst sediment

of a similar gradation to the main channel may be entering from Buckden Beck. One option would be to use the GSD of the sample taken immediately downstream of the two confluences as a proxy for the sediment entering from each tributary. Under this option the gradation remains constant and does not evolve over time. A second option was to allow the tributary GSD to evolve with the main channel bed by setting the tributary gradation to match the main channel GSD at the confluence. Simulations were run using both options with the first option producing a downstream fining pattern more representative of the Wharfe. Hence the GSD of the input from the tributaries remained constant and was set to equal the GSD of the main channel from the observed data. This makes the assumption that the GSD of sediment entering the channel is of a similar composition to the main channel and does not vary over time.

3) More representative slope

One of the key field data sets used to validate the model during the development phase was the pattern of downstream fining noted from the bulk samples and pebble counts (Figure 5.14). It was clear from early simulation runs that the predicted pattern of downstream fining differed greatly in places from the observed data. This was largely attributed to the way that slope was represented in the model. With slope an important parameter in defining shear stress and hence integrated into the sediment transport calculations, incorporating a slope profile similar to that of the Wharfe channel was essential.

The model thus far has used a smooth quadratic slope profile based on user defined upstream and downstream slope values. However, whilst the true slope profile of the Wharfe follows a generally quadratic profile, there are substantial deviations from this (Figure 8.1a). These occur when the channel flows in and out of pools (dips) and over riffles (peaks). Furthermore, sinuosity and human intervention in the form of channel straightening can lead to slope variability in the natural system. At times bed slope may even increase with distance downstream as the river flows from a deeper pool into a shallow riffle. To prevent these "uphill" bedslopes, the model has a lower slope limit of 0.001, with this value entered if slope falls below this value. In the slope profile, a steep drop in elevation is noted between 550 m and 750 m downstream. This section is confined

by dry stone walls possibly from monastic times. It may be the case that the channel was straightened at this time, shortening the route and increasing the channel gradient.

Figure 8.1: Wharfe study reach bed slope profiles. A shows the initial smoothed quadratic profiles alongside the natural un-smoothed profile and B is after smoothing.

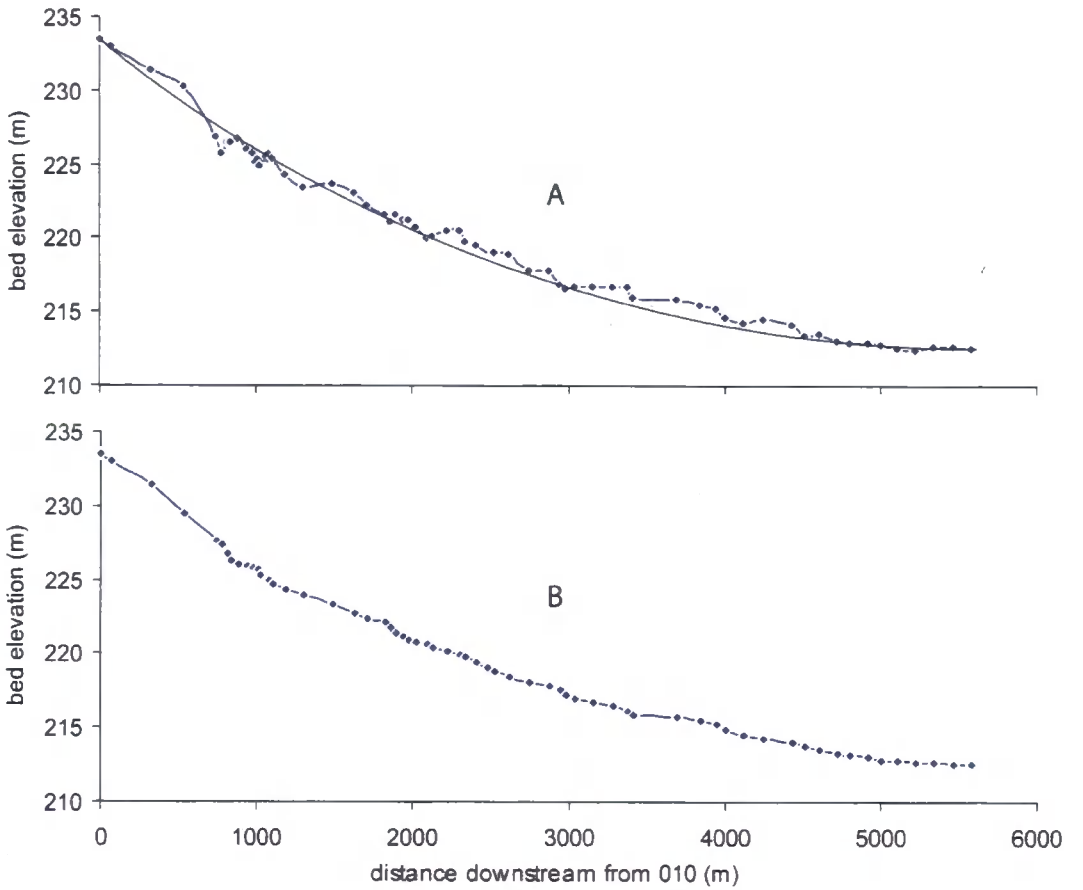

Simulations using the profile shown in Figure 8.1a were attempted but the variations in slope were too great and the model remained unstable, even when the time step was significantly reduced. For this reason, the slope profile was smoothed using 3, 5 and 7 point moving averages. The 7 point moving average was the first to be generally stable and this was adopted. The smoothed profile is shown in Figure 8.1b. This smoothing flattened the steep channel section at 550 m downstream. Hence, the model failed to coarsen in the most upstream sections as shown in Figure 8.2a. To overcome this and to retain the character of

the slope profile in the upper 800 m, the profile was smoothed by eye. Simulations following this modification were positive with predicted coarsening occurring at the upstream end of the study reach, echoing the observed data. These results are shown in Figure 8.2b.

Figure 8.2: The effect of using a smoothed slope profile on the predicted pattern of downstream fining. A uses the quadratic slope profile and B uses the 7-point moving average smoothed profile with manually altered upstream section. Simulation is run for 15 days at 20 $m^3 s^{-1}$.

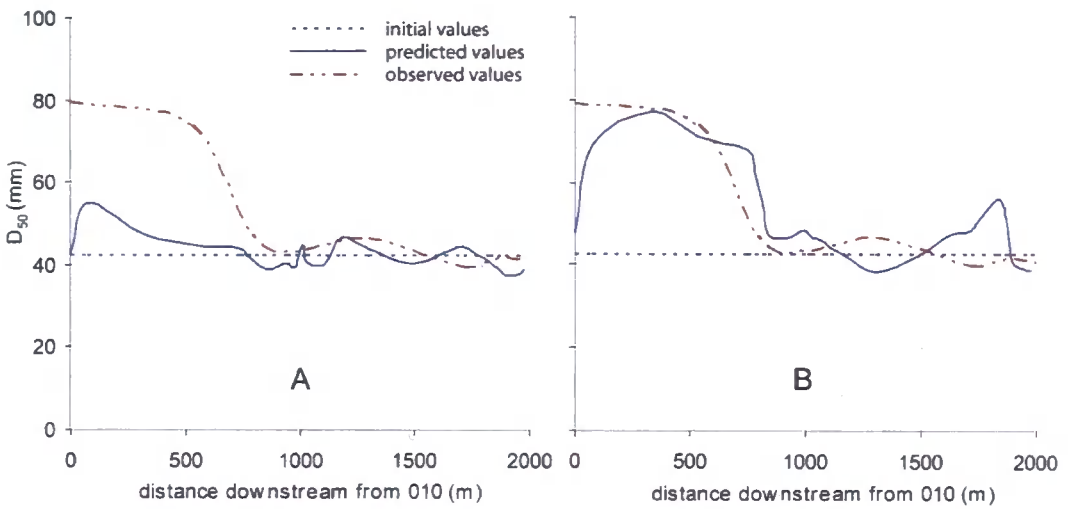

Furthermore, the predicted pattern of downstream fining that emerged during simulations had a kink located at around 3800 m where the gradually reducing D_{50} on the predicted profile jumped up by 20 mm before gradually fining once again. Figure 8.3 shows the kink. Again, this was attributed to the slope profile although the no obvious reduction in slope is visible here. Thus it may be a combination of slope and channel width change. The model was calibrated by manually altering the slope around this region to produce a more smoothed downstream fining profile shown in Figure 8.3. This calibration would account for changes in slope and width that are responsible for the kink in the profile.

Figure 8.3: Downstream fining pattern before and after slope has been altered by eye to removed the kink.

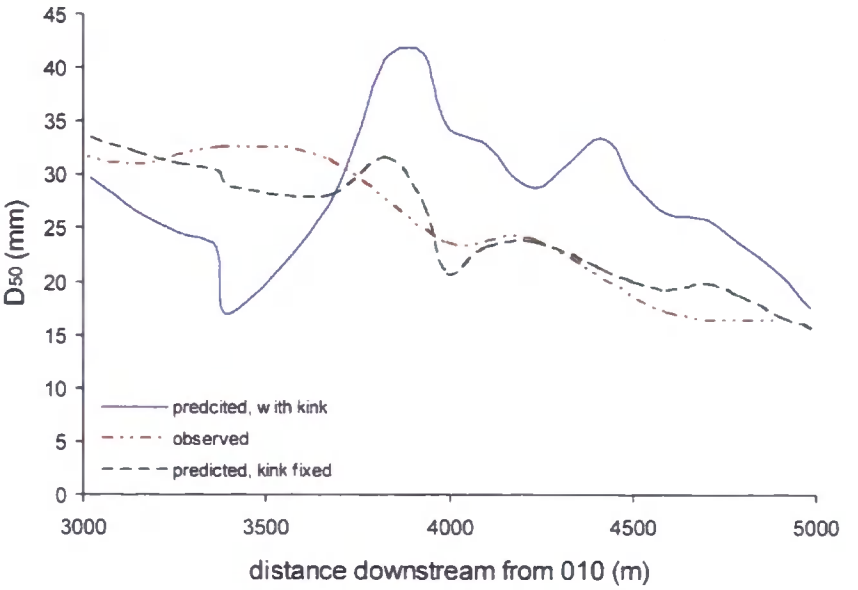

4) Increasing the number of grain size classes

The original model was set up with 5 grain size classes to represent the sediment. Whilst this is adequate for beds with a small range of grain size classes, the range of sediment in the Wharfe is relatively large ranging from <8 mm to >189 mm. Thus, defining the upper and lower boundaries of each class was difficult and always left one class with a large proportion of bed material. Three additional grain size classes were incorporated to provide a better representation of the bed material. There was scope to increase the number of classes further, perhaps incorporating a grain size band for each half phi sediment increase. This was not done as additional classes made no notable difference to the model output.

5) Defining the sand boundary

The upper and lower limits of the grain size classes can be adjusted by the user depending on the sediment characteristics. Of these, the upper boundary of the smallest fraction, the sand fraction is particularly important as it plays a crucial role in the Wilcock and Crowe (2003) sediment transport equations enhancing sediment transport [7.18]. In the Wilcock and Crowe (2003) equations, sand is classed as everything smaller than 2 mm; following the standard grain size class characterisation set out in the Wentworth scale (Table 5.2).

This poses a problem for the Wharfe, since the bed material in only the most downstream reach contained material smaller than 2 mm and even the grain size characterisation describes the smallest sediment as <8 mm. Hence, the upper limit of the sand boundary was shifted to 8 mm enabling significantly more transport to occur than when the sand boundary was set at 2 mm. When some simple tests were run with the new sand boundary, this change resulted in more reasonable sediment transport rates suggesting that it is a valuable modification.

6) Input GSD

Following on from (3) and (4), the starting GSD down the channel has to be specified. With the GSD known at 16 locations downstream, one option would be to enter these directly into the model at their given locations. The GSD at intermittent cross-sectional nodes would then be interpolated. However, this would not reveal anything about model's predictive capabilities as it would begin with a downstream profile similar to that observed. A greater test for the model would be to enter a hypothetical starting GSD and assess the model's ability to predict the measured pattern of downstream fining.

Numerous scenarios were tested with each simulation run changing only the starting GSD. The scenarios tested were broadly split into: (1) uniform coarse sediment along the entire reach using GSDs with a D_{50} greater than 45 mm; (2) uniform fine sediment along the entire reach using GSDs with a D_{50} less than 30 mm; (3) uniform sediment along the entire reach using the average observed channel GSD and (4) different GSD for each location downstream such that a smoothed pattern of downstream fining was present at the start of the simulation. The simulations were run until the downstream fining profile had stabilised and the rate of change had slowed. Thus some simulations took longer than others. The scenarios that used a smoothed downstream fining profile as a starting profile, stabilised faster than the scenarios that began with a uniform GSD for the entire reach. Hereafter, the expression "the downstream fining wave had passed" refers to the process of letting the downstream fining pattern stabilise.

Figure 8.4 shows the starting point and end results from two different simulation runs; comparing a scenario from group (1) with a scenario from group (4). The median grain

sizes observed in the field are not shown in this figure. It is extremely encouraging to observe almost identical outputs irrespective of the starting GSD. Similar findings were obtained with scenarios in (1), (3) and (4). When using starting GSDs that were finer than around 30 mm (i.e. group (2) scenarios), the downstream pattern matched well, but the model failed to predict the coarsening in the most upstream reaches. Hence it was important when selecting a GSD for the simulations to ensure that a moderate percentage of the material was in the coarsest gravel fractions and that the D_{50} was greater than 40 mm. For simplicity, the model was set up with a uniform starting GSD that had a D_{50} of 46 mm.

Figure 8.4: comparing the pattern of downstream fining that is predicted when using different starting GSDs.

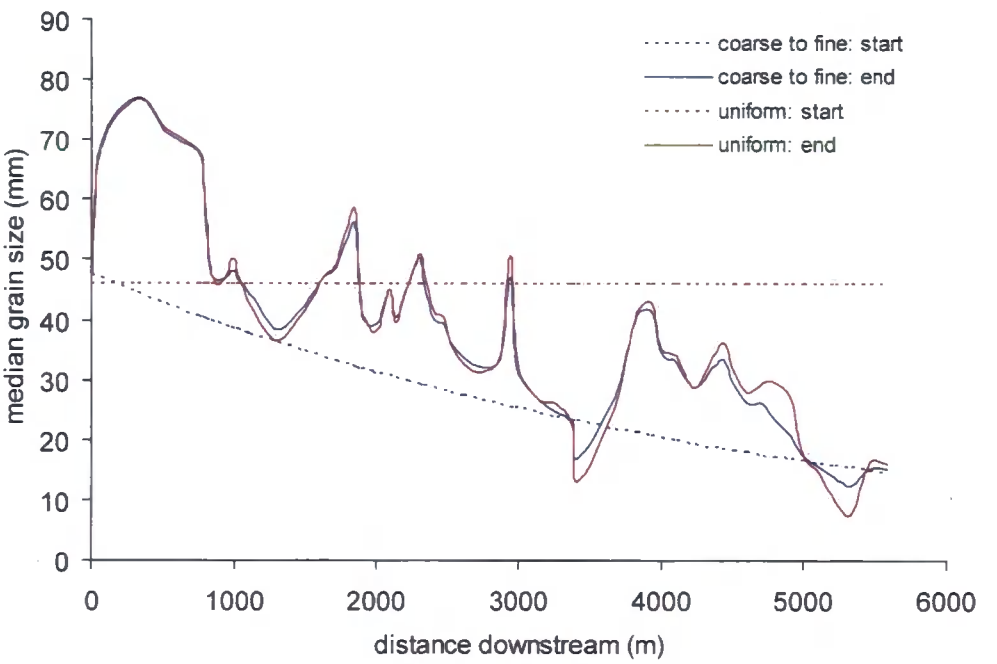

7) *A variable Manning's n value.*

In the original model, the user defined the Manning's *n* roughness value at the beginning of the simulations. This value was applied throughout the channel and remained constant during the simulations. Roughness is used in the model to determine flow depth and subsequently shear stress. These products are sensitive to the selected Manning's value due to the formulation of [7.9] in section 7.3.1, which calculates flow depth (*d*) from the

discharge (Q), hydraulic slope (S), channel width (*w)* and the roughness value *n*. [7.9] is repeated here as [8.1]. Doubling the Manning's value in [8.1] has the same effect on flow depth as doubling the discharge.

$$d = \frac{Qn / w^{0.6}}{S^{0.3}} \qquad [8.1]$$

A selection of an appropriate *n* value was important. Due to the rapid downstream fining found in the Wharfe, it was difficult to select a value that would be applicable throughout the reach. Furthermore, at-a-point, as the bed evolves over time the *n* value required to represent the roughness will change as the bed fines or coarsens. It was therefore essential that a variable *n* value was applied to the Wharfe and re-calculated after every iteration. Equation 8.2 was used to calculate the *n* value.

$$n = \frac{(D^{1/6})/1000}{6.7g^{1/2}} \qquad [8.2]$$

where D is the median grain size in mm and g is gravitational acceleration.

Incorporating a variable and updating *n* value into the model had an important effect on the flow depth. This is illustrated by comparing flow depths at the upstream and downstream nodes using the calculated *n* value, and *n* values representing finer and coarser material. The upstream *n* value for node 010 was calculated at 0.031 and the downstream *n* value for node 600 was 0.022. For a discharge of 15 $m^3 s^{-1}$ this gave width-averaged flow depths of 0.64 m at node 010 and 1.18 m at node 600. If the *n* values were swapped, and the *n* value applied to node 010 was reduced to 0.022, representing substantially finer sediment, the flow depth would also reduce to 0.50 m. At the downstream end an *n* value of 0.031, representing coarser material, would increase flow depth to 1.42 m. Thus, it is important that the *n* value applied to each node represents the current GSD present.

8.3.2 Testing TRIBs Output Against Field Observations

Thus far, the modifications have been tested against the downstream fining profile in an attempt to make the predicted pattern match as closely as possible to the observed trend. Here, further model outputs are compared with field observations specifically exploring the bedload transport predictions. Data from the impact sensors and cross-sections was used to provide information on the sediment transport process in the study reach. These findings can be used to test the model's predictive capability.

The first finding tested was the important reduction in sediment transport noted from Hubberholme to Starbotton and the low sediment transport rate leaving the study reach at Starbotton. Results presented in Table 5.4 showed that less than 1.2% of sediment that entered at Hubberholme left the study reach at Starbotton. Furthermore, sediment is in motion for substantially less time at Starbotton when compared to Hubberholme. As an important feature of the sediment transfer system in the study reach, it was crucial that the model replicated this, with limited sediment transport leaving the reach.

To compare the predictions with the observations, the model was run at a moderate discharge of 12 $m^3 s^{-1}$ until the initial downstream fining wave had occurred and the sediment characteristics remained relatively stable and similar to the observed trend. The model was then run at a constant discharge for a short period of time with the average bedload transport rate for this period recorded at the second most upstream node (representing Hubberholme) and at the most downstream node (representing Starbotton). The most upstream node represented the input which was set to match the channel capacity. Thus this node was not used in this comparison. Since this comparison is concerned with the bedload transport rate associated with a given discharge, steady high flows are adequate. Variable flows are incorporated into the model in Section 8.3.3 that follows. The predicted bedload transport rates at the Hubberholme and Starbotton nodes were recorded excluding all material less than 8 mm (i.e. the sand fraction). This fine material was not captured by the impact sensors and should be discounted for comparison. This test was repeated for increasing discharges and the results are presented in Table 8.2. When the

predicted ratios of transport between Starbotton and Hubberholme are compared with the observed ratios, similarities appear. The mean predicted ratio is 0.019 whilst the observations for the periods shown range from 0.021 to 0.31. The ratio from April 2003 to September 2003 was much higher, reflecting a period of relative higher sediment transport out of the reach. This higher ratio may be linked to high magnitude events. Yet, even this higher ratio suggests that substantially more sediment enters the reach at Hubberholme when compared with that which leaves at Starbotton.

Table 8.2: Comparing predicted bedload transport ratios with observed impact sensor ratios.

Modelled discharge ($m^3 s^{-1}$)		Bedload transport rate ($m^2 s^{-1}$)		Ratio (Star:Hubb)
		Hubberholme	Starbotton	
5		2.3E-06	3.9E-08	0.017
10		6.1E-05	1.1E-06	0.019
15		6.0E-05	9.7E-07	0.016
20		8.3E-04	1.5E-05	0.018
25		1.4E-03	2.9E-05	0.021
30		2.0E-03	4.0E-05	0.02
Measured transport activity (sum of *m*)	oct03-mar04	225275	8636	0.038
	apr03-sep03	66399	20667	0.31
	may06-dec06	15793	334	0.021

The second result tested was the threshold at which sediment transport occurs. From the model, the mean bedload transport rate for the reach extending from cross-section 010 to 040 was noted at several discharges increasing by 5 $m^3 s^{-1}$ increments. The results are shown in Figure 8.5. It is interesting to observe the curve that is produced. The results show that transport is initiated between 15 and 30 $m^3 s^{-1}$ where the bedload transport rate begins to increase at the greatest rate. At discharges greater than 30 $m^3 s^{-1}$, the transport rate increases at a steady rate.

These predicted results can be compared with observed estimates of the transport discharge threshold made using two methods. Both methods use a combination of discharge data and data from the impact sensors. Method one uses the estimates of sediment transport time alongside the flow (discharge) duration curves. Table 5.6 suggested that at Hubberholme

sediment was in motion for 5.4% of the year (for the period March 03 – March 04). Under the assumption that this transport occurs during the highest flows, the flow duration curves presented in Figure 5.2 can be used to find the discharge exceeded by 5.4% of flows. To remove errors associated with annual differences in flow regime, the representative hydrological period was used. During this period, 5.4% of flows exceeded 35 $m^3 s^{-1}$. As such this can be used as a crude estimate of the sediment transport threshold. However, as discussed in Section 6.2.1, seasonal differences occur and transport is also linked to sediment availability. Method two directly compares the peaks in sediment and discharge regimes. As illustrated in Figure 5.16 and Figure 6.1, both correlate well together. By exploring the relationship between pings and flow further, during the time period when data for both is available, the discharge at which sediment transport begins can be recorded. This was done for all separate transport events and the mean initiation discharge was 25.8 $m^3 s^{-1}$, with variability from 22.1 $m^3 s^{-1}$ to 28.4 $m^3 s^{-1}$. Only four months of discharge data were available for comparison with five individual sediment transport events. Thus, this was again a first approximation.

Whilst the observed transport threshold is higher than predicted, there is some overlap between the two results. This is encouraging as the model is once again predicting values similar to the natural system. The higher observed values reflect complexities in the sediment transport process such as the bed armour. This may require a higher discharge to break down than predicted using the Wilcock and Crowe (2003) equations. In addition, sediment transport is largely linked to sediment availability. If no sediment is available for transport then no transport will occur, irrespective of the discharge. Furthermore the success of this estimate is dependent on accurate discharge data. As discussed in Section 5.2, predictions of discharge from stage records may be under or over estimated. In this instance, if the discharge records have been overestimated, then the threshold for transport may indeed be lower than noted and closer to the model predictions.

Figure 8.5: Relationship between increasing discharge and predicted bedload transport rates at Hubberholme. Data plotted alongside estimated bedload transport thresholds. The boxes represent the range of thresholds estimated using the two methods.

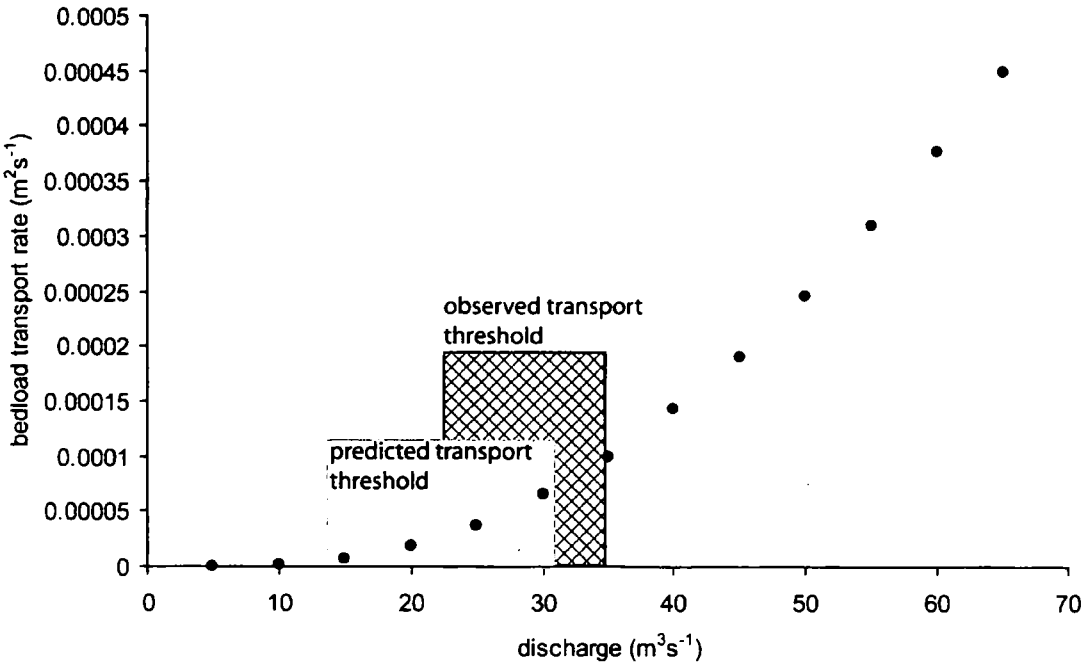

A third and final comparison considered the maximum bedload transport rate. Table 6.5 presents results that estimate the average and maximum bedload transport rates from the volumetric input and the impact sensor data. The maximum transport rate estimated at Hubberholme for April 2003 to December 2004 was 0.74 kg m^{-1} s^{-1}. For December 2003 to April 2004 it was 2.4 kg m^{-1} s^{-1}. Therefore the maximum estimated "observed" transport rate for the Wharfe study reach is 2400 g m^{-1} s^{-1}. This is expressed in grams to allow easy comparison with the model output.

To obtain an estimate of "predicted" maximum transport rates from the model, an assumption was made that these maximum transport rates would occur at the highest discharges. This assumption does not account for any variability in sediment transport rate that may occur due to variability in sediment supply. From the Hubberholme flow duration curves, the highest discharges, which account for 0.5% of totals flows were 82 m^3 s^{-1} for 2002, 80.3 m^3 s^{-1} for 2000 and 68 m^3 s^{-1} for 1997. The model was run until the initial

downstream fining wave had passed and the three discharges were entered into the model. The bedload flux at node 030, representing Hubberholme, was noted for each discharge. The bedload flux's were 2767.6 g $m^{-1}s^{-1}$ when discharge was 82 $m^3 s^{-1}$, 2645.1 g $m^{-1}s^{-1}$ when discharge was 80 $m^3 s^{-1}$ and 1832.5 g $m^{-1}s^{-1}$ when discharge was 68 $m^3 s^{-1}$ respectively. The two upper values are 245 g $m^{-1}s^{-1}$ and 367 g $m^{-1}s^{-1}$ higher than the estimated bedload flux made from the observations whilst the lower discharge estimated the bedload flux to be 568 g $m^{-1}s^{-1}$ lower. These are encouraging results as they are within the same order of magnitude. They further suggest the model is capable of predicting the sediment transport regime in the Wharfe study reach.

8.3.3 Incorporating a Variable Discharge

The original version of TRIB used a constant steady state discharge, defined by the user. This method gives a poor representation of the hydrology in a natural system as it simulates a river in constant high flow or low flow. Results using this approach could not be used to compare predicted and observed rates of aggradation and degradation since these observations are specific to the continuous variation of discharge between adjacent survey periods. A modification was made to the model to allow for a variable, stepped discharge to be simulated. This modification makes the model a more valuable research tool.

The modification allowed the model to run through a hydrograph. With the model timestep typically lower than the hydrograph timestep, the model was set so that several iterations at a given discharge were made until the length of time at that discharge matched the timestep of the hydrograph. For example, if a daily hydrograph was used and the model timestep was 0.25 (i.e. a quarter of a day), 4 computations would be made at that discharge before the next daily discharge was entered. The model timestep that was entered was required to be at least the same or smaller that the hydrograph timestep.

Model simulations were carried out to asses the impact that different hydrographs and flow regimes had on the evolution of the bed and the downstream fining profile. Each simulation began with a uniform GSD along the entire study reach with the D_{50} equal to 46 mm. The

simulations were run for 730 days (two years). Four different simulation runs were made to compare steady flow with unsteady flow. The steady state simulations included using:

(1) a constant discharge equal to the average maximum daily flow for the 2-year representative hydrograph. This was 9.62 $m^3 s^{-1}$;

(2) a constant discharge of 15 $m^3 s^{-1}$. This discharge represents a moderate flow, slightly higher than the average daily maximum.

The unsteady flows expressed using variable hydrographs included using:

(3) the hourly average discharge record for the 2-year representative period. This hourly average was calculated from the 15-min records;

(4) the daily maximum discharge.

Figure 8.6 shows the downstream fining profile at the end of each 730 day simulation. The most progressed profile was obtained when the steady moderate flow was used. This was followed by the unsteady daily maximum hydrograph. The large differences in this plot illustrate the importance of the higher flows for sediment transport. Thus, 40 days of simulation using daily maximum flows (Figure 8.6: (4)) will produce the same downstream fining profile as 730 days at a steady average discharge (Figure 8.6 (1)). During these 40 days the average discharge is 8.4 $m^3 s^{-1}$ which is marginally lower than the 2-year average of 9.2 $m^3 s^{-1}$. Yet, during these 40 days, there are two moderate flow events with the discharge exceeding 10 $m^3 s^{-1}$ for 6 days. Therefore most of the transport must occur in those 6 high flow days. In Table 8.3 the importance of high flow days is explored further with several simulation runs being made using a constant but increasing discharge. The time taken to reach the profile formed after 730 days at the average discharge of 9.62 $m^3 s^{-1}$ is noted. There is a rapid reduction in the number of days required as discharge increases. For example, when the discharge doubles from 9.62 $m^3 s^{-1}$ (or rounded to 10 $m^3 s^{-1}$) to 20 $m^3 s^{-1}$, the time required to reach the same profile reduces by 97%.

Figure 8.6: Comparing the downstream fining profiles when using steady and unsteady hydrographs.

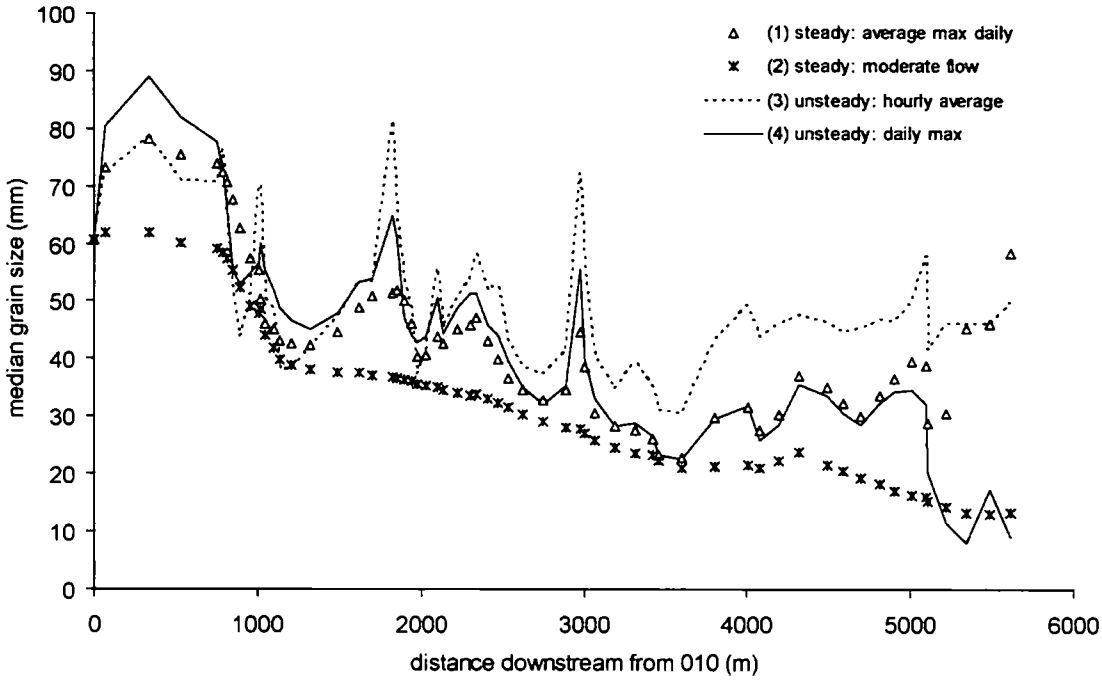

Table 8.3: Time taken to produce the same downstream fining profile using increasing steady discharge.

Discharge	9.62	12	15	20	25	30	35
No. of days	730	145	78	25	12	7	5

The results presented in Figure 8.6 and Table 8.3 used identical parameters to run the model with only the discharge changing. It was important to also check the impact that changing the time step had on the model outputs. Two identical simulations were run but using two different timesteps: 0.0026 (3.75 mins) and 0.0208 (30 mins). Whilst the 3.75 min simulation was substantially slower with 8 times as many iterations, the results were the same. This is due to the form of the fractional continuity equation [7.12] which accounts for the change in time between iterations.

The downstream fining profile predicted by the model will be the same irrespective of the discharge (steady or unsteady and the discharge values) and timestep but the time taken to reach a particular profile point will vary greatly depending on the discharge values used. However, the main benefit of using a variable discharge is that it allows the simulations to be compared against time dependent field data such as rates of in-channel sedimentation. Thus, the model can be run for a fixed length of time and the predicted results can be compared with results from field monitoring. Section 4.3 presents the results from the 6-year cross-sectional monitoring programme that started in the Wharfe in December 2001. These data were analysed to provide details on the rate and locations of in-channel sedimentation and degradation. Patterns of sedimentation in the study reach were found to vary both spatially and temporal. A key finding from the analysis was the link between hydrology and temporal rates of vertical change in the study reach (Section 6.2.1). Thus the field observations can be compared with the model when the actual hydrology for a given survey period is used to drive model outputs.

With discharge data for Hubberholme available for 1997, 2000 and 2002 and observed bed level changes available from 2001 until 2007, this analysis is limited to the 2002 data only. A comparison between predictions and observations for 2002 was performed. The model was initially run at a constant moderate flow of 15 $m^3 s^{-1}$ until the initial wave of downstream fining had passed. Thus, downstream fining patterns down the channel at the start of the simulation reflected the conditions observed in the Wharfe study reach. The model compared the output using the 2002 hydrology with the bed level changes recorded for this year. Since the cross-sectional surveys during this time only extended 3 km downstream, the predicted results only examined these changes (i.e. they ignored the lower 3 km reach). The mean predicted bed level change was 0.03 m of aggradation using the 2002 hydrology. The observations for the December 2001 to December 2002 survey period were degradation with a mean reduction in bed level of 0.025 m. Thus, there is a large disparity between predicted and observed results. However, during 2002, significant re-engineering of the channel occurred during the removal of the gravel trap. The degradation recorded is likely to reflect human induced channel change which the model can not simulate. Indeed when the observed bed level changes in the 100 m reach around the gravel

trap location are examined for this period, substantial changes are noted and the mean bed level is reduced. Thus, a direct comparison of predicted and observed bed level changes driven by the hydrology data is not feasible.

The alternative is to compare the mean change recorded over the 5-year monitoring period since December 2002, with the average hydrology for this period. December 2001-December 2002 data was discounted as this data only covered the upper 3 km reach and included human induced channel change. When combined, the hydrology for 1997 and 2002 were shown to be representative of the decadal hydrology (Section 5.2). This approach makes a large assumption: *that the average hydrology will produce average bed level changes.*

Following the initial fining wave, the model was run for two years using the 1997 and 2002 average hourly discharge records. 15-min records were available but a comparison showed very little difference in predictions when using the hourly data over the 15-min records. To reduce data input by four, the hourly records were used. The average hourly records were chosen over the maximum since this would overestimate the flow. With significant sediment transport only initiated at discharges above 10 $m^3 s^{-1}$, all flows lower than this were removed. This left around 10% of the flow records and dramatically reduced simulation time without altering the model output.

The average predicted change in bed level downstream was recorded and compared with the observed average annual change in mean bed level from the cross-sectional survey data. The predicted maximum and minimum aggradation rates were also recorded for comparison with observed data. Table 8.4 presents these data. The standard deviation of the data expresses how much the results from the 60 cross-sectional nodes deviate from the channel's average. The results here are encouragingly similar to the observed values. The highest levels of bed-level change and maximum aggradation were noted when using the 2002 records. This is explained by the wetter nature of the flow regime during 2002 when compared with 1997. These results further support the use of the hourly average records rather than the daily maximum records. The daily maximum records simulate longer

periods at higher flows and this leads to aggradation rates far greater than those estimated from the observed data.

Table 8.4: Observed and predicted bed level changes using the 1997 and 2002 hourly flow records.

Units (m/year)	Observed	Predicted (1997)	Predicted (2002)
Average bed-level change	0.03	0.04	0.05
Maximum aggradation	0.17	0.18	0.24
Maximum degradation	-0.09	-0.06	-0.08
Standard deviation of data	0.05	0.05	0.02

The model was then run for longer periods using the representative 2-year hydrograph (which combined the 1997 and 2002 hydrographs). The simulation was run for the full 2-year period and then for another 2-years using the same hydrograph. After 2 and 4 years of simulation, the results were compared against the mean field observations. The results are shown in Figure 8.7 and Table 8.5. In Figure 8.7 the bed level changes predicted are shown visually against the observed data. The total bed level changes are for the 2-years of simulation and the data is expressed per metre downstream.

Figure 8.7: Predicted and observed total bed level change after 2 years. The predicted data uses the 2-year representative hydrograph.

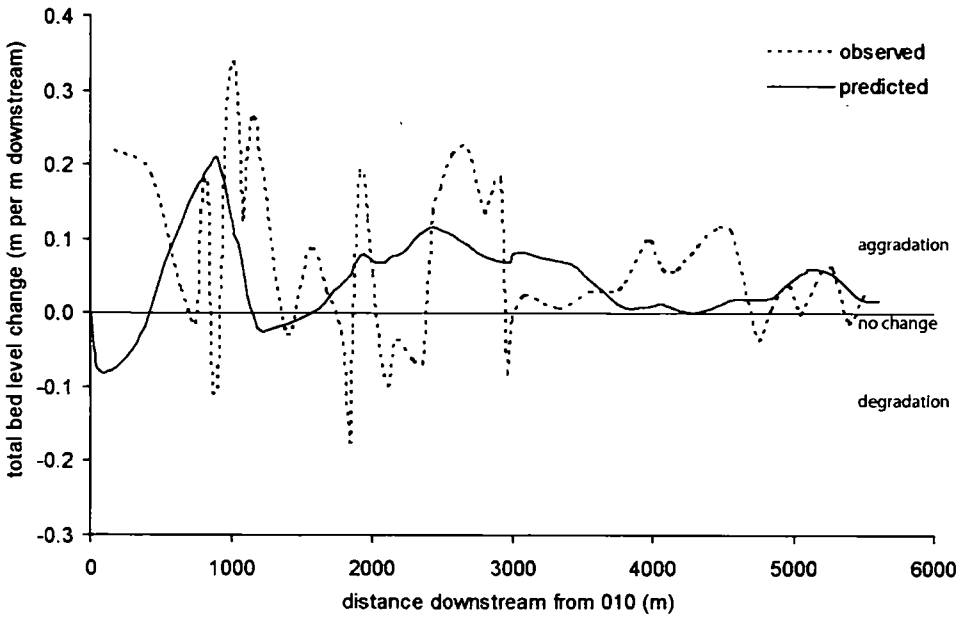

Table 8.5: Observed and predicted bed level changes after 2 and 4 years of simulation using the variable hydrograph. All values are expressed as m per m downstream.

		2years	4years
Average aggradation	observed	0.061	0.132
	predicted	**0.062**	**0.123**
Maximum aggradation	observed	0.337	0.674
	predicted	**0.209**	**0.374**
Maximum degradation	observed	-0.177	-0.355
	predicted	**-0.080**	**-0.130**
Standard deviation	observed	0.107	0.213
	predicted	**0.058**	**0.106**

Table 8.5 shows particularly encouraging results when the simulation runs over only 2-years with average aggradation and maximum aggradation similar to the observed results. However, the predicted maximum degradation is substantially less than the observations. Furthermore after 4-years whilst the predicted average aggradation rate remain similar to the observations, the maximum aggradation is only half as much as the observations. This suggests that aggradational zones, which are noted in the observed data, fail to develop and instead aggradation spreads further downstream over several cross-sectional nodes. This

suggestion is supported by the standard deviation of bed level change. In both 2 and 4 years the standard deviations of the observed data are around twice as high as the predicted data suggesting less peaks and troughs in bed level change and a more general spread of sedimentation downstream. When Figure 8.7 is examined it is clear that the model predicts predominantly aggradation with only two zones of degradation being predicted. Furthermore, the location of predicted aggradation / degradation differs somewhat from the observations. The predicted pattern does illustrate spatial variability in bed level change with two clear peaks in aggradation and a third smaller peak at 5200 m downstream. Yet the predictions fail to capture any significant degradation or for the peaks in aggradation to match the observations.

In addition, the results shown in Table 8.5 predict bed level change of 0.062 m for the 2-year period. This result is lower than if the 1997 and 2002 results in Table 8.5 are added together giving 0.09 m. This reflects the effect that the sequencing of events has on sediment transport. In the 2-year simulation, the fining and bed level changes that have occurred by the end of the first year are used to determine the fining and bedload transport changes in the second year. When the two years are considered separately, year two (2002) begins with the same starting conditions as year one (1997). This brings in some uncertainty when using the 2-year representative hydrograph. If the two years were applied in the reverse order, the results may differ as the wetter 2002 would be sequenced ahead of 1997. To test this, the model was run using: (1) the 2-year hydrograph; (2) using the flows ranked from highest to lowest; and (3) using the flows ranked lowest to highest. The results showed only marginal differences in the downstream fining profile and the mean aggradation rates using all three scenarios were the same at 0.062 m. This result suggests that magnitude and frequency of high flow events is more important than the sequencing in which they are simulated in. However, this was the case where sediment supply matched sediment input at cross-sectional node 010. In a natural system where sediment supply may become exhausted, sequencing is likely to be more important.

To explain the spatial discrepancies between the observations and predictions when using variable discharge, aspects of the natural channel's geometry that are missing from the

model's representation must be considered. First, slope is smoothed so fails to capture all the smaller slope features which may be responsible for aggradation. Thus locations of aggradation may not match. Second, some of the human features affecting the sedimentation, including Buckden Bridge, are ignored in the model. As noted in Section 6.6, Buckden Bridge is considered to be a small barrier to sediment transport resulting in upstream deposition and downstream scour. Third, the channel is width-averaged and of uniform depth. Thus degradation cannot occur through mechanisms that create secondary circulations such as outer bend erosion and lateral channel bars. Fourth, curvature is not accounted for in the model. The channel is taken to be straight and as noted in Section 6.2.3 curvature has an influence on aspects of channel morphology such as bank erosion and aggradation. Thus a lateral component is required in the model that not only allows bank width adjustment but also enhances the lateral representation of the channel at each cross-sectional node between banks. Finally, the discrepancies between the observations and the predictions may be a feature of the comparison approach adopted which is comparing average bed level changes predicted using average hydrology. The discrepancies may support the findings from Chapter 6, that hydrology and sediment supply are both important controls on vertical channel change. Thus the average hydrology may not produce the average bed level changes. The magnitude, frequency and timing of flood events may be important.

8.4 MODELLING LATERAL CHANGE IN STRAIGHT CHANNELS: STAGE (C)

The modifications made to the model work well as the predictions match the observations closely allowing lateral adjustments to be incorporated into the model. This section describes the development of the lateral component for straight channel sections only. Curvature is introduced in Section 8.5. Initial tests explore the impact of manually changing the channel's width (Section 8.4.1) before several options for the bank erosion mechanism are discussed and tested (Section 8.4.2). Modifications are then made to improve the lateral channel change component (Section 8.4.3). Finally, tests demonstrate the strengths and weaknesses of the lateral channel change model (Section 8.4.4).

8.4.1 MANUALLY ALTERING WIDTH

Before the lateral channel change component to the model was developed, some simple tests on the existing model were carried out to explore the hypothetical effect that changes in channel width would have upon the rates of bed level change in the modelled reach. This would also provide an indication into the model's sensitivity to such changes.

Four simulations were run to explore the sensitivity of the model to manual increases in channel width. These simulations were run after the initial fining wave had passed and all simulations were started from the same point. In the first test, the model was run at a constant high discharge of 30 $m^3 s^{-1}$ for 60 days using: (a) the variable channel width as described in Section 6.2.3; and (b) using channel widths exactly 1 m wider than the widths used in (a) for all cross-sectional nodes apart from the input node (010 at Hubberholme). It was important to ensure the width at node 010 was kept the same as the sediment flux into the reach was determined by the transport capacity at this node. A wider channel would result in a lower input rate. The mean bed level rise recorded for the actual channel width (a) was 0.067 m whilst the mean bed level rise for the wider channel was 0.006 m or 9% lower at 0.061 m. In the second test, results, when using the actual channel width (a) and the wider channel (b), were compared after a 2-year simulation using the 2-year hourly hydrograph. Again in these results, the wider channel recorded a mean bed level rise substantially lower (0.048 m) than the rise noted from the actual width (0.061 m). This 0.013 m difference shows that aggradation in the wider channel is 21% less than in the normal width channel. The finding that widening the channel reduces the aggradation rates challenges the premise behind many engineering schemes which aim to reduce aggradation and increase sediment throughput by making the channel narrower. The opposite appears to occur.

To explain these findings the sediment transport dynamics must be considered. However, relationships between channel width and sediment transport in the literature are contradictory. Carson and Griffiths (1987) highlight three different views: (1) that sediment transport decreases as width increases (Henderson, 1960); (2) that sediment transport

increases in wider channels (e.g. Bagnold, 1977, 1980; Parker, 1979); and (3) that both may occur with a peak in transport capacity at some intermediate width (e.g. White *et al.*, 1982). Yu and Smart (2003) also question what the optimal width is for sediment transport. Understanding whether an increase in sediment transport leads to aggradation or degradation is also difficult. An increase in sediment capacity can increase sediment influx providing more sediment for storage (i.e. aggradation) or allow a greater transport of sediment away from a reach (i.e. degradation). Thus, the impact of width increase is not only affected by the change in sediment transport capacity at a given location, but also upstream and downstream transport conditions.

By comparing the results from the measured and wider channel scenarios, several conclusions can be reached. The reduction of aggradation rates in the wider channel occurs due to the reduction in depth that occurs with an increase in channel bed area (i.e. due to a reducing unit discharge (discharge/width)). Depth determines shear stress which is an important parameter determining sediment transport. With lower shear stress, sediment transport is lower and with less sediment in transport, there is less sediment available to be deposited. Yet, the input transport rate at Hubberholme (node 010) is the same in both measured and wider simulations because the width of the channel at node 010 remains constant in simulations. As such in the wider simulation, aggradation is enhanced in node 020 as the wider channel reduces the transport capacity leading to deposition. This increases the slope downstream and reduces slope upstream. Thus, upstream sediment supply at node 010 reduces.

These results demonstrate that the model is sensitive to changes in channel width and such changes can have some important implications for rates of aggradation in the modelled reach. Since the second test uses the 2-year hydrograph, the results can be compared with observed results from the Wharfe and put into a real-world situation. In Section 4.3, the mean annual rise in bed level in the study reach was recorded at 0.030 m ± 0.009 m (for the 5-year period when the entire reach was under observation). With the modelled results using the normal channel width predicting a strikingly similar annual bed level rise of 0.031

m per year (0.061 m ± 0.018 m for 2-years), the predictions made with the actual channel widths can be accepted with more confidence.

Despite the locations of modelled maximum aggradation differing greatly, and appearing more attenuated than the observed data (Figure 8.7), the difference between the modelled maximum aggradation rates can be compared with the analysis made in Section 6.4; the impact of aggradation on flood risk. The measured channel (a) is predicted to aggrade by a maximum of 0.1 m per year whilst the wider channel (b) aggrades by 0.08 m per year. When this is scaled up to give an estimate of aggradation over a four year period, the aggradation levels are 0.4 m for (a) and 0.32 m for (b). This maximum modelled aggradation occurs at cross-section 090, 898 m downstream, where the channel is 20.4 m wide and increases to 21.4 m wide in the wider simulation. Thus, the area of material deposited in the measured channel (a) is 8.2 m^2 compared with 6.8 m^2 in the wider channel (b). The impact of these changes on channel area are shown in Figure 8.8. The wider channel loses 15% of its channel capacity after 4 years compared with a 20% loss in the measured channel. Thus the wider channel sustains 5% extra channel capacity. In Section 6.5, a 21.9 % reduction (over a four year period) in channel capacity was linked to more flood events and a longer time over bank. A 5% difference is likely to have important implications for flood risk. In summary, a wider channel not only increases the channel's capacity to hold flow due to a greater channel area but it reduces sedimentation rates thereby maintaining channel capacity further.

Figure 8.8: The effect of an increase in width on aggradation, width and channel capacity after 4 years at cross-section 090 (898 m downstream).

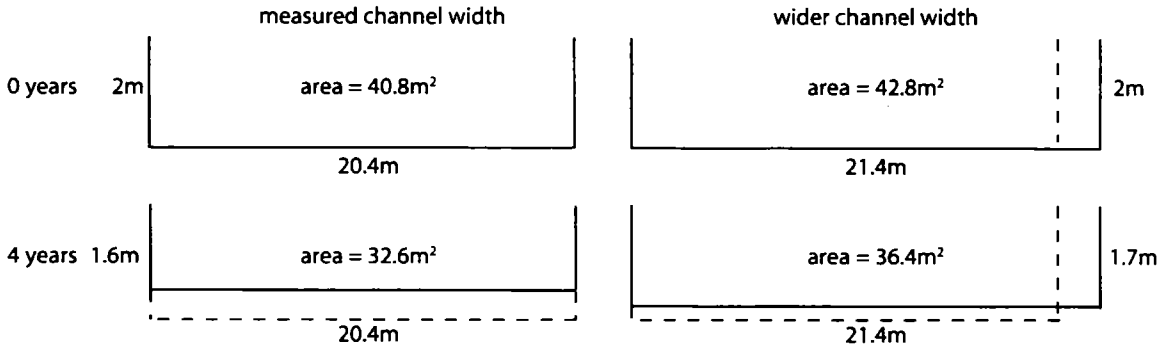

With a wider channel resulting in a reduction in aggradation levels, a narrower channel would be hypothesised to increase aggradation levels. To test this, two simulations were run using: (a) the measured channel width; and (c) a channel that had been manually narrowed between 500 m and 1200 m downstream. The section to be narrowed was selected due to its high levels of aggradation noted in previous simulations (e.g. Figure 8.7). This simulation reflects the possible width change that an engineering scheme such as channelisation aiming to flush out sediment may result in. Figure 8.9 shows the levels of aggradation recorded after the 2-year simulation using the measured width and narrower width. There is a clear difference between the two simulation runs. The simulation that modelled the narrow section (c), recorded a mean rise in bed level marginally higher (0.002 m difference) than the mean bed level rise predicted using the normal width (a). However, enhanced aggradation was not found across the whole, narrowed reach. Higher levels of aggradation were recorded at the location of peak aggradation at 898 m downstream, and in the channel immediately downstream. The difference in maximum aggradation rates was 0.02 m (0.19 m for normal and 0.21 m for narrow). Yet, at 1200 m downstream and in the reach upstream of 800 m, the narrower channel resulted in degradation. This degradation occurs from the convergence of flow as the channel narrows. The flow in the narrower channel is deeper. Thus shear stress is higher and this leads to greater sediment transport and degradation.

When the river is channelised, it is often also made narrower, but more importantly it is not allowed to increase its width. This engineered channel is supposed to flush out the sediment, maintaining channel capacity. If scenario (c) was adopted as a management strategy in the Wharfe, it would be successful in creating scour and the flushing out of sediment in the section upstream of 800 m. However, downstream of the 800 m, the narrower channel promotes sediment deposition and the effects are felt as far downstream as 3500 m. In this narrow section extending to 1200 m, the flushing out effects are outweighed by the input of sediment from upstream. Since the bed width is less than in the measured channel, the sediment deposited is deeper. This could be a result of insufficient slope and / or too much sediment input. Indeed the scour upstream of 800 m will increase sediment delivery into the narrowed reach.

Figure 8.9. The impact of narrowing the channel on aggradation rates using the 2-year hydrograph. The section that was made narrower by 1 m is enclosed in the grey box. The "difference" plot shows the difference in aggradation levels between the two simulation runs.

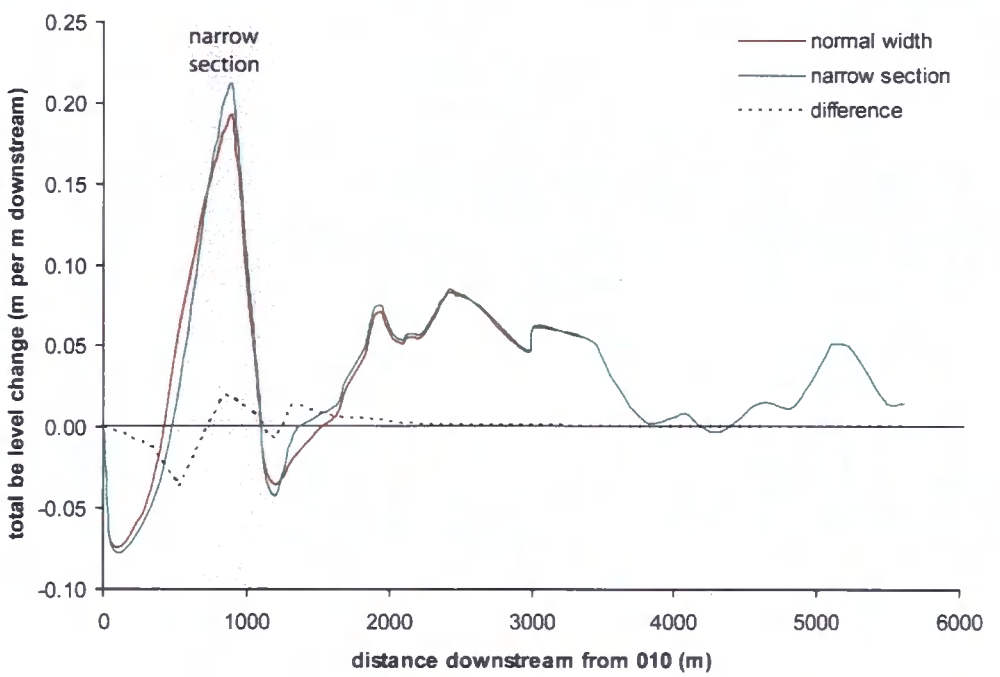

8.4.2 SPLITTING THE CHANNEL

Splitting the single channel into two halves was the first step in the development of the lateral channel change component. To remove difficulties associated with modelling complex natural systems like the Wharfe, an early simplified version of TRIB was used during development. The simplified model had 10 nodes spaced every 50 m, a quadratic slope, a uniform fixed width, constant n values and a steady discharge. For each channel side, the only differing input values were the elevations with a right and a left hand side elevation entered for each channel half. In effect, the model now resembled two rectangular boxes as shown in Figure 8.10. The only information required for this geometry is total width and the bed elevations for the left and right hand channel sides.

Figure 8.10: Split channel geometry. The natural channel geometry is shown on the left whilst the simplified geometry represented as two boxes is shown on the right.

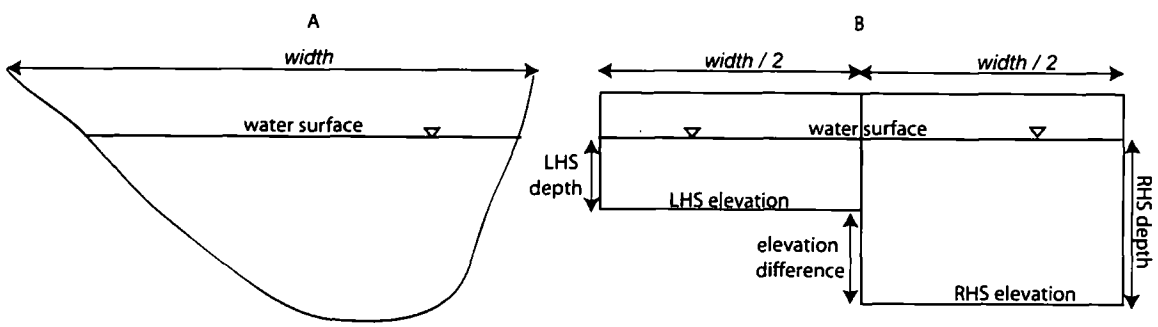

It was crucial that the water surface elevation (bed elevation plus flow depth) was the same on both channel sides. As such flow depth had to be calculated for each channel side. Depth was calculated by first determining the input unit discharge from the total channel width and the hydraulic slope for each side. Average channel depth (d_{av}) was determined from the unit discharge using Manning's equation and used alongside the difference in bed elevation (E_{diff}) which is calculated from E_{rhs}-E_{lhs} to determine the depth of each side maintaining the average depth:

right side:
$$d_{rhs} = d_{av} + \frac{E_{diff}}{2} \quad [8.3a]$$

left side:
$$d_{lhs} = d_{av} - \frac{E_{diff}}{2} \quad [8.3b]$$

where d is channel side depth for the left side and right side, d_{av} is the average flow depth for the whole channel.

At low flows, where the average flow depth is smaller than the elevation difference, all flow would be in one channel half and flow depth for that half would be $2d_{av}$. A condition must be set so that if the elevation difference exceeds $2d_{av}$, all flow will be in the channel side with the lowest elevation. These conditions are expressed as:

d_{rhs}		d_{lhs}
$E_{diff} > 2d_{av} = 0.0001$	[8.4]	$E_{diff} > 2d_{av} = 2d_{av}$
$E_{diff} < -2d_{av} = 2d_{av}$	[8.5]	$E_{diff} < -2d_{av} = 0.0001$
$E_{diff} < 2d_{av} = d_{av} - (E_{diff}/2)$	[8.6]	$E_{diff} > -2d_{av} = d_{av} + (E_{diff}/2)$

To avoid difficulties with a zero value for flow depth, a small positive value is used to represent a dry channel side. Flow will be entirely on the left side if the elevation difference is positive and exceeds $2d_{av}$ [8.4]. In situations where the right side has the lower elevation, E_{diff} will be negative. If E_{diff} is less than a negative $2d_{av}$ [8.5] flow will be entirely down the right side. When the elevation difference is small, the depth of each channel side is calculated using [8.6].

Alongside the flow depth, the slope used in each channel side is crucial to the calculation of shear stress. The three options detailed in Section 7.4.5 are explored. These options include using: (1) the steepest flow path; (2) the water surface elevation; and (3) the average bed slope. The model was found to be sensitive to large variations in slope (Section 8.1). Therefore, option 1, which was based on the cellular modelling approach of using the steepest flow path, was ignored as it would create large differences in slope between nodes, particularly if flow moved into deeper pool areas. Option two was explored as this used the water surface elevation. However, this smoothed over any of the small slope variations within the profile. Thus, it failed to capture features such as the drop in elevation at around 500 m (Figure 8.3), failing to predict the corresponding downstream fining pattern. The third option, to use the average bedslope of the two channel sides, was more appealing. The average bedslope in the split channel model would remain similar to the bedslope in the version used to predict downstream fining and aggradation rates similar to those observed in the field. Table 8.6 demonstrates that when using the average bedslope, the difference in shear stress between sides is dramatically reduced. Accordingly average bedslope and then hydraulic slope (where negative / uphill slope values are removed) was incorporated into the model to drive the sediment transport equations.

Table 8.6: Effect of using separate channel side slopes or average slope (either average bedslope or water surface elevation) on shear stress values.

Channel side	Flow depth (m)	Slope		Shear stress (Pa)
Left	0.93	0.0022		20.0
Right	1.01	0.0038		37.6
Left	0.93	0.003	average of above	27.3
Right	1.01	0.003	two slopes	29.7

Using the flow depth for each channel side and the average bed slope, shear stress is determined for each channel side. This is used to predict sediment transport which is also done separately for each channel side. Each channel side evolves independent of the other side. The two sides are only tied together by the input discharge, flow partitioning and mean slope. Therefore in Figure 8.10 above, if the right side aggrades, the flow partitioning would alter with the left side becoming a more important conveyor of flow. Eventually the elevation on both sides will be equal.

The simplified model was run and the output is shown in Figure 8.12. In this simulation, the starting bed elevations of both sides are the same apart from at 100 m downstream where the right side is deeper than the left side creating a pool or hollow. Straight away the grain size on the right side of the channel changes with the bed coarsening at 50 m and fining at 100 m. At the same time, the hollow on the right of the channel begins to aggrade. To aid with the explanation of this behaviour it is useful to consider the slope at each location downstream. Slope directly influences shear stress and drives sediment transport. Figure 8.11 shows how slope is calculated and how the overall results will depend on which option of slope calculation is adopted; forwards or backwards.

Figure 8.11: Method of calculating slope: either forwards or backwards

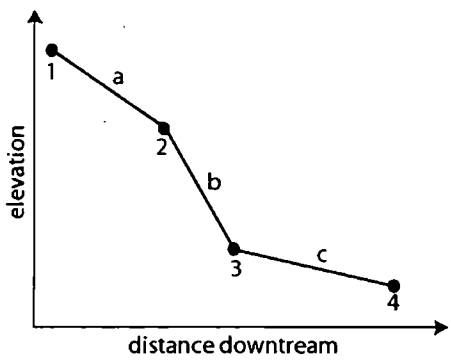

Slope calculated	Slope calculated for point	Slope
Forwards	1 = 1 to 2	a
	2 = 2 to 3	b
	3 = 3 to 4	c
Backwards	2 = 1 to 2	a
	3 = 2 to 3	b
	4 = 3 to 4	c

When the forwards approach is adopted, the steepest slope (location b in Figure 8.11) is assigned to point 2. Yet when the backwards approach is adopted slope b is assigned to point 3. In Figure 8.12, the forward slope approach is adopted and as such the steep slope created by the dip is assigned to 50 m downstream and not to 100 m in the hollow. Thus the

highest shear stresses are created at 50 m downstream resulting in sediment transport downstream. However, only moderate shear stresses are generated by the increased slope and these are insufficient to transport the coarser grains. The result is that after day 1 of simulation the finer grains are transported downstream leaving proportionally more coarse sediment at 50 m and more finer material at 100 m downstream. At 100 m downstream, in the hollow, slope is reduced and less sediment transport occurs. This is despite the increase in shear that would be generated due to the increased flow depth associated with the deeper hollow. This can be explained by considering the Exner equation. At each node, for example point 2, both upstream (slope a) and downstream (slope b) slopes and depths are used to calculate bed level change since volume change is the difference between input and output at each node. Thus in the hollow, more sediment enters the hollow than leaves and aggradation occurs. The material entering from the upstream node comprises of a finer GSD (since the coarsest grains remain at the upstream node) than the material located in the downstream node. This influx of finer material results in fining of the bed. Furthermore, the reduction in transport capacity in the dip results in deposition and the hollow fills in. As the hollow fills up and the depth and bedslope reduce, by day 5 the bed at 50 m begins to become finer and the bed at 100 m becomes coarser. As the simulation continues the downstream fining profiles smooth out and the hollow on the right hand side of the channel fills in as the channel re-grades. It should be noted though that whilst the channel's left and right slope profiles end up very similar, the GSD of the right hand side remains substantially different from the left hand side showing that there is a lag in the fining of the sediment.

Figure 8.12: output from split channel with a dip in the right hand side (rhs). The plots on the left show the GSD at each node downstream whilst the plots on the right show the bed elevations. Both graphs show the output from the left (lhs) and right (rhs) channel sides. The bed elevation plots concentrates on the region with the dip (100 m downstream) so that the changes can be observed more clearly.

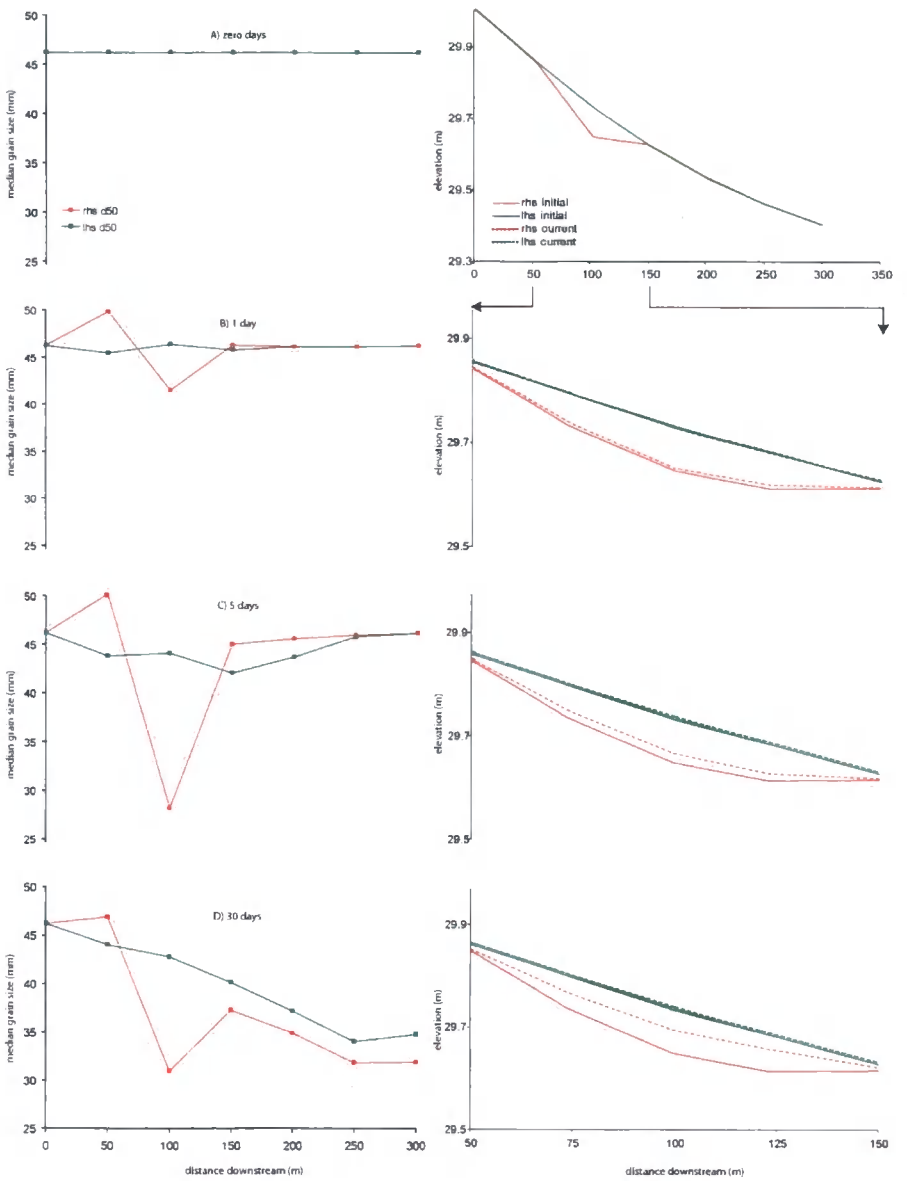

In addition to the response of the model to a hollow, which was in effect a pool on the right hand side of the channel, Figure 8.13 shows the model's response to a lateral bar (Figure 8.13a) located on the left hand side of the channel and a transverse bar which crosses from

the right hand side at 100 m downstream to the left hand side at 150 m downstream (Figure 8.13b). In both these situations both channel sides regrade with aggradation occurring on both the new profiles.

Figure 8.13: Simulating lateral (a) and transverse bars (b).

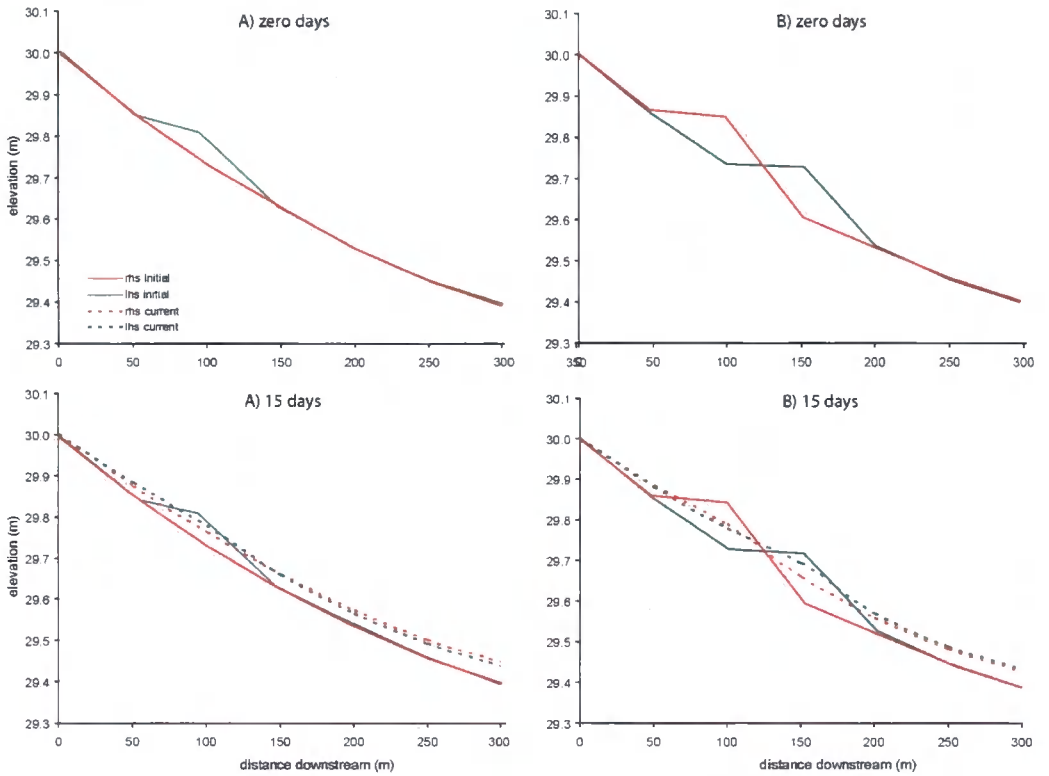

8.4.3 Options for Simulating Bank Erosion in Straight Channels

With the model able to simulate a split channel, developments could be made to simulate width adjustment. At this stage in the development, curvature was not introduced. Thus the model is effectively a width adjustment model for straight channels. Three options identified in the literature were explored. Bank erosion was simulated first as a function of a critical bank angle, second as a function of differences in bed elevation and third as a function of shear stress. For all three options, the model was modified so that at the first iteration, the channel widths for each side became independent of each other. In the

previous version of the model, the channel's left side and right side widths were simply half of the total input channel width. After each width modification, the new total channel width was established. This was essential as the depth calculations assume each channel side is of equal width. Without this, if one channel side became substantially wider, but the depth was calculated based on half channel width, the depth in the wider channel side would be too deep for the given discharge.

In all three options, a critical threshold was used to determine the onset of bank erosion. Selecting this threshold is discussed later (Section 8.4.5). With the channel split, one channel side could reach this critical value independent of the other. Once the critical value had been reached, the width in that channel side would increase incrementally by the bank erosion proportionality factor (w_e) which was proportional to the excess shear stress ($\tau - \tau_c$) as explained by:

$$\text{if} \quad \tau > \tau_c, \quad w_n = w_i + w_e(\tau - \tau_c) \qquad [8.7]$$

where w_i is the initial half channel width, w_n is the new half channel width and the subscript $_E$ refers to the erosion threshold. This approach follows that of Ikeda *et al.* (1981) where rates of bank erosion are proportional to excess velocity. This modification would simulate the variable rates of bank erosion recorded in the Wharfe including small-scale bank erosion from fluvial entrainment when excess shear stress was small and large scale erosion from bank collapse when excess shear stress is high.

During development, w_e is set at a low value but the value of w_e is determined through calibration later in this chapter in Section 8.7. This bank erosion would continue until either the shear stress, bank angle or elevation difference had dropped beneath the critical value again. The sediment input from the banks was ignored because as noted in Table 6.2 it typically contributes only very small quantities to the overall sediment flux from the channel. Also, this material is typically fine bank material that would be flushed through the system without significantly affecting the bed material or bed level changes. This assumption ignores the effect that the increase in fines in suspension may have on sediment

transport calculated by the Wilcock and Crowe (2003) equations. These base transport flux partly on the amount of fines in the mixture. More fines promote greater transport of the coarser material.

The first option simulates bank erosion as a function of critical bank angle. Previous models that use critical bank angles to simulate bank erosion include Hasegawa (1981), Osman and Thorne (1988), Pizzuto (1990) and Kovacs and Parker (1988). In this version of the model, the channel geometry is represented using four points rather than the previous rectangular boxes. Figure 8.14 shows this channel geometry and how bank erosion would be simulated. Degradation will lower one of the mid-channel points, steepening the bank angle beyond the critical threshold. Bank erosion will occur in increments until the bank angle is stabilised. As in the previous case, the bank erosion will increase the total channel area, reducing flow depth and in turn lowering the shear stress. Thus the bank erosion has a feedback mechanism. This option offers the advantage that the critical bank erosion angle could be based on field observations. This would involve determining the steepest angles of banks within the Wharfe and assuming that this was the channel's critical threshold. However, this has two problems. First, many of the banks are vertical or near vertical particularly when bank protection is in place and second as discussed in Section 4.4.5, a key bank erosion mechanism is fluvial entrainment which is not necessarily linked to bank angle.

Figure 8.14. Channel geometry required to simulate bank erosion using the critical bank angle approach. The four points are equally spaced at 0, 25, 75 and 100% of channel width.

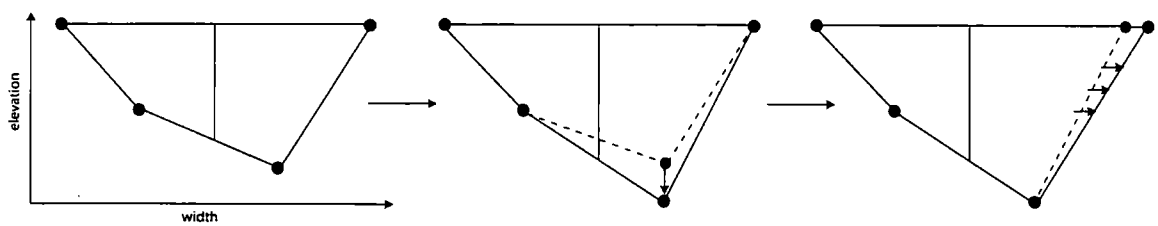

Option two uses the difference in channel side elevations (E_{diff}) as a driver of bank erosion. This was based on the concept that as one side deepens, giving a higher E_{diff}, bank erosion of this channel side is more likely. If a critical E_{diff} value is exceeded, bank erosion will

occur, increasing the channel width thus promoting deposition. E_{diff} would be reduced. This approach was inspired by approaches that use depth variations to redistribute shear stress such as Talbot and Lapointe (2002). Like the bank angle approach, this option could be based on maximum elevation differences noted in the Wharfe. This option was explored but failed to be successful for two reasons. First, the channel is predominantly aggrading and as demonstrated in Figure 8.12, as the model runs, the elevation difference between the two sides will gradually become equal. To simulate bank erosion using this mechanism, the model was switched from a capacity feed to fixed feed (see Section 7.4.3.1) and the fixed feed was set to zero. This simulated no sediment input into the reach and promoted degradation allowing bank erosion. However, this raised a second problem with this approach, excessive overdeeping. If the degradation was occurring faster than the bank erosion (or where no bank erosion could occur due to collapse) this would feedback to further degradation as flow depth would increase promoting higher shear stresses and higher rates of sediment transport.

The third option that was explored used a critical shear stress threshold. In the split channel, shear stress is calculated for each channel side and can differ laterally with flow depth. If the shear stress in either channel side exceeds the critical threshold, then the channel width of that channel side would increase according to the bank erosion rate. At the next iteration, bank erosion will continue if the critical shear stress is still exceeded. Once the shear stress has fallen below the critical value, bank erosion stops and the channel width remains constant. Increases in channel width will alter the total cross-sectional channel area resulting in a reduced flow depth. The reduced depth will lower shear stress possibly below the critical threshold. Using the same channel formation described in Figure 8.12 with a dip at 100 m on the right side, a simulation was run. Figure 8.15 shows the output from the simulation. The critical shear stress was selected at 20 Pa so that it was within the upper range of shear stress predicted during this simulation. Specification of the critical shear stress is discussed further in Section 8.4.5.

Figure 8.15: Simple bank erosion model output using a critical shear stress threshold of 20 Pa. Plot A shows the starting slope profiles on the left and right channel sides. Plots B, C and D show the channel side widths (bars) and shear stress (line) alongside the shear stress threshold as the simulation evolves through time (t).

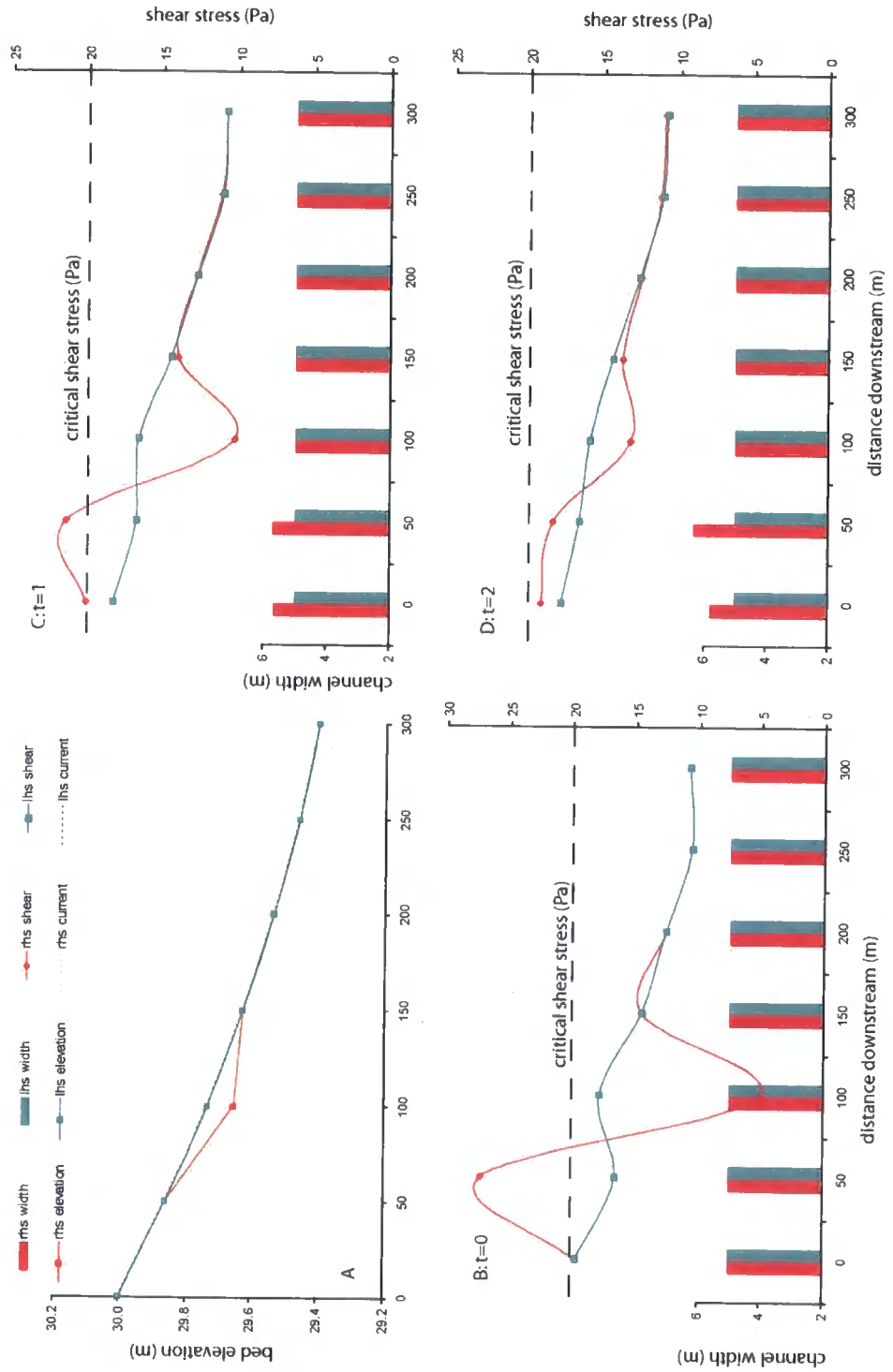

At the start of the simulation (t=0), shear stress is above the critical threshold on the right hand side of the channel at 50 m downstream as the slope here is steeper as the channel moves into the hollow shown in plot A. Once in the hollow, at 100 m downstream, the shear stress in the right of the channel is low reflecting the reduction in slope. The shear stress is higher on the left hand side at 100 m, reflecting the linkages in depth and discharge between the two sides. In plot C when t=1, the channel width on the right side of the channel at 0 and 50 m downstream has increased as the shear stress remains above the critical threshold. By plot D when t=2, the critical threshold has dropped below the threshold. This occurred firstly at 0 m and then at 50 m and this is reflected in the wider right side found at 50 m downstream. There is a feedback mechanism occurring in this simulation with the increasing channel width reducing flow depth and the shear stress, and also promoting sediment deposition in the channel. This deposition enhances the reduction in depth further, accelerating the feedback.

In this simulation bank erosion is not found at the deeper section. Instead, bank erosion occurs in the shallow reach at the upstream limit of the hollow. Whilst this is sometimes typical in natural systems, with shallow sections becoming wider as a result of deposition and coarsening of the bed, this approach fails to simulate overdeepening processes which are often linked to bank erosion, particularly at meander bends. This is because there is none of the lateral redistribution of shear stress that would occur under the formation of a secondary circulation. As such, the model will fill in any dips so that both sides are re-graded and of the same elevation. Using this shear stress approach to drive bank erosion, a further modification is required to allow shear stress to be redistributed laterally, for example as a function of curvature.

Of the three options explored, the first, the shear stress option was adopted to drive bank erosion. The primary reason for this was that it would allow a lateral shear stress distribution function based on curvature to be incorporated at a later stage (Section 8.5).

8.4.4 MODIFICATIONS TO THE LATERAL CHANGE COMPONENT

Three modifications were made to improve the lateral adjustment component. These included: (1) simulating bank deposition or narrowing; (2) capping the elevation differences between channel sides to prevent overdeepening; and (3) maintaining the continuity of sediment during lateral adjustment.

(1) *Simulating channel narrowing*

Alongside erosion, deposition needed to be simulated. In many previous width adjustment modelling approaches, deposition was simply set to match erosion (e.g. Ikeda *et al.,* 1981; Bridge, 1992; Sun *et al.*, 1996, 2001a,b,c; Lancaster and Bras, 2002). Using this approach, the channel width would always remain constant. This fails to capture the temporal and spatial aspects of deposition with deposition generally a slower process than erosion and not always occurring on the bank opposite the eroding bank. In the model, deposition or channel narrowing was simulated in much the same way as the bank erosion mechanism. A critical threshold was set (this could be a critical shear stress, bank angle or elevation difference) with the channel narrowing by a fixed increment when the shear stress falls below this value. This deposition function is similar to [8.7] and is described using:

$$\text{if} \qquad \tau < \tau_{cD}, \quad w_n = w_i - w_d \qquad [8.8]$$

where $_D$ is deposition and the narrowing increment is w_d. Following the assumption that deposition is a slower process than bank erosion, the incremental adjustment value was always set to be lower than the bank erosion increment. The hydrograph used in the model had all low flows removed earlier in model development, to speed up simulation time. With deposition now simulated during these low flow conditions, these low flows must be added back into the hydrograph or a higher shear stress threshold can be set and the rate of deposition set higher.

(2) *Preventing excessive overdeepening*

The previously mentioned overdeepening problem, where deeper sections feedback to enhance shear stress and lead to further deepening, would occur irrespective of which bank erosion option was selected, provided the flow conditions promoted scour. In a natural channel this would be stopped by either bank erosion or the lateral transfer of sediment from the shallower side to the deeper side through the formation of a secondary circulation. Such a mechanism would be useful in the model to prevent excessive channel deepening, irrespective of the bank erosion mechanism applied. This cap on elevation differences was added to the model by simply including a statement in the calculation of the elevation difference (E_{diff}) which sets E_{diff} at the critical value, if this value is exceeded [8.9]. Since E_{diff} can be positive or negative depending on which channel side is deeper, a positive and negative critical value were used. Field data can be used to determine what value to set the E_{diff} cap. With E_{diff} capped, the difference in flow depth between sides also becomes limited.

$$E_{diff} > E_{diff}^{cap} = E_{diff}^{cap}$$
$$E_{diff} < E_{diff}^{cap} = E_{diff} \qquad [8.9]$$

(3) *Maintain sediment continuity during lateral adjustments*

When lateral adjustments occur asymmetrically, the mid-point shifts allowing the width of the channel sides to remain equal. In doing so, a portion of the sediment in the mid-channel region is lost (or gained). This is illustrated in Figure 8.16. Sediment is also lost or gained from the channel banks during bank erosion or narrowing. This sediment can largely be ignored since the banks are typically composed of finer material which would be lost in suspension and not alter the bed level. The mid-channel bed sediment is composed of coarser material and is therefore important for bed level changes. This area of sediment must be accounted for.

Figure 8.16: Dealing with sediment continuity during width adjustment

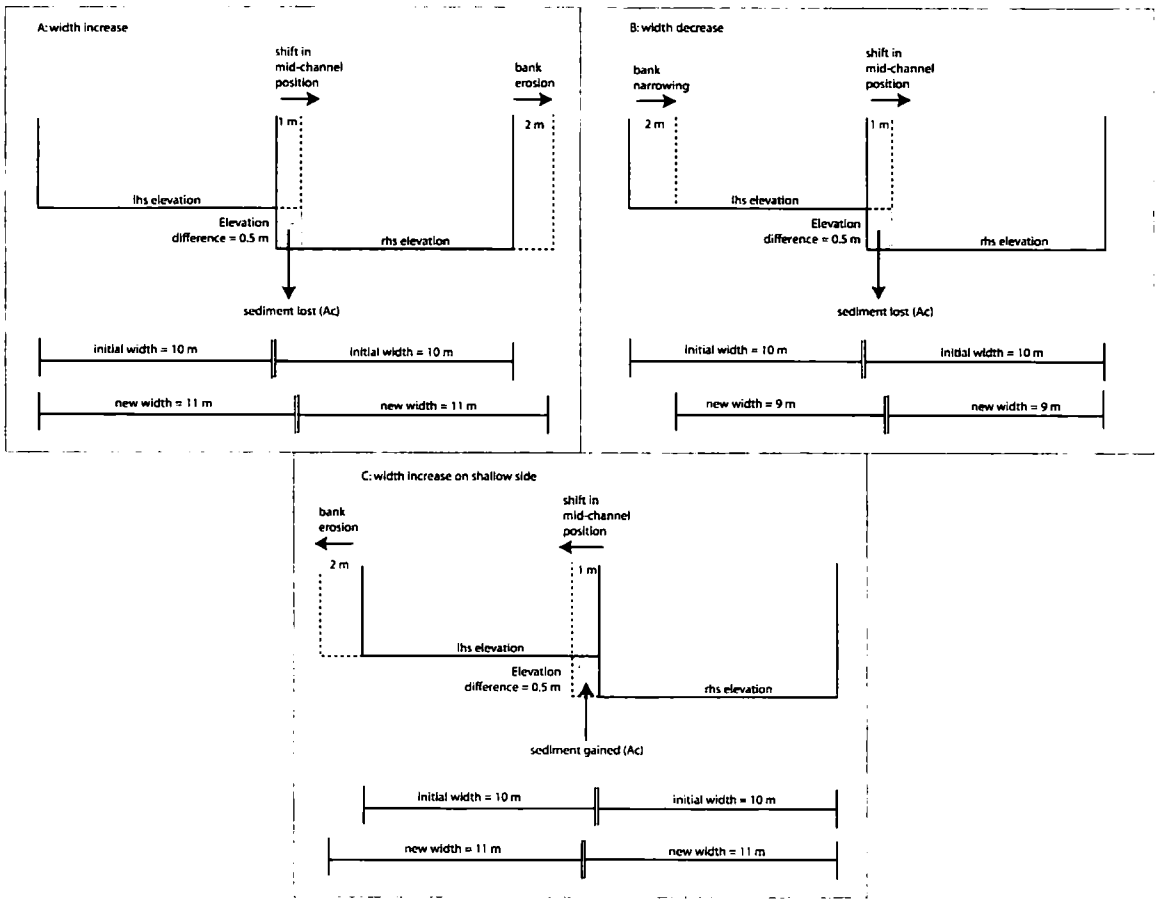

In Figure 8.16 the 2 m bank erosion (Figure 8.16a) and the 2 m narrowing (Figure 8.16b) causes the mid-channel point to shift by 1 m. This ensures that both channel half widths remain equal. In so doing, the area of sediment lost (A_c) calculated using [8.10] is 0.5 m^2. To maintain sediment continuity, this sediment is spread evenly across both channels using [8.11]. This method keeps the difference in elevation between sides (E_{diff}) the same.

$$A_c = E_{diff}(w_i - w_n) \qquad [8.10]$$

$$A_w = A/2w_n \qquad [8.11]$$

where E_{diff} is the absolute difference in elevation, w_i is the initial half channel width, w_n is the new half channel width and A_w is the width-averaged area of sediment required to be added or subtracted from the bed elevations on both channel sides.

In the two situations shown in Figure 8.16a and b, sediment is lost as bank erosion occurs on the deeper channel side and narrowing on the shallow side. However, in situations where the opposite occurs and the shallower side increases in width (or the deeper side narrows), an area of sediment is gained (Figure 8.16c). To account for this gained sediment and maintain sediment continuity, the bed elevation on both sides must be reduced by A_w.

In summary:

(1) If an **increase** in width occurs in the **deeper** side OR a **narrowing** in width occurs on the **shallow** side, then there is a sediment **loss** and the elevation on both channel sides must be **increased** by A_w (Figure 8.16a and b).

(2) If an **increase** in width occurs in the **shallow** side OR a **narrowing** in width occurs on the **deeper** side, then there is a sediment **gain** and the elevation on both channel sides must be decreased by A_w (Figure 8.16c).

Implementing both of these conditions into the Excel model was complex. As such, only the more common condition (1) was implemented. When the level of elevation changes that are required when accounting for continuity in sediment are considered, they are very small. Thus, in the Wharfe system ignoring (2) would have very little impact on the sediment dynamics.

8.4.5 Applying Wharfe Data to the Lateral Change Component

With the model now capable of simulating bank erosion and deposition, elevation differences capped and sediment continuity maintained, it was necessary to apply the Wharfe data to the model and explore the model's behaviour for a natural system rather than the current idealised one.

The Wharfe data were included in the model in a similar way to Sections 8.2.1 and 8.2.2. This included the 60-irregularly spaced cross-sectional nodes, the smoothed slope profile, the variable channel widths, the variable Mannings n and the variable discharge. The

channel was split into two channel sides and the sediment transport equations and bed updates were carried out for each channel side. The Manning's n value used at each node represented the average roughness across both channel sides. Calculating n for both sides would overcomplicate the model and since average flow depth was initially determined before the side depths were calculated, only a single value of n was required. Following successful simulations using equal left and right side bed elevations two key decisions were explored: (1) how to represent the geometry of the channel in a simplified way; and (2) selection of critical shear stress values to determine the threshold that bank erosion was initiated.

Simplifying the Wharfe geometry

Various options for simplifying the channel geometry to obtain representative elevations for both channel sides were explored. For all these options, only the channel profile between bank tops was used. Typically, the cross-sections extended onto the valley for a few metres to allow for bank erosion over time; this data was removed. The December 2002 cross-sectional data was used as this was the first survey that measured all 60 cross-sections. Several options for simplifying the channel geometry were explored. Three of these are shown in Figure 8.17 and include: (1) the minimum channel elevation; (2) the average channel elevation; (3) the average channel elevation calculated from the channel area; (4) selecting the best elevation by eye; and (5) several combinations of these. After exploring these options for a range of cross-sectional profiles in the Wharfe system (e.g. point bar, mid channel bar, rectangular), the average of the minimum elevation and the average elevation in the respective halves was selected. Talbot and Lapointe (2002) found that the average of mean depth and maximum depth provided the best representation of shear stress for the model. The combined approach was important because the average elevation alone failed to represent particularly deep sections whilst the minimum elevation approach over represented deeper sections. Figure 8.17 shows options (1), (2) and the average of the two (5).

Figure 8.17. Options for simplifying the channel geometry. Natural shows the measured channel geometry.

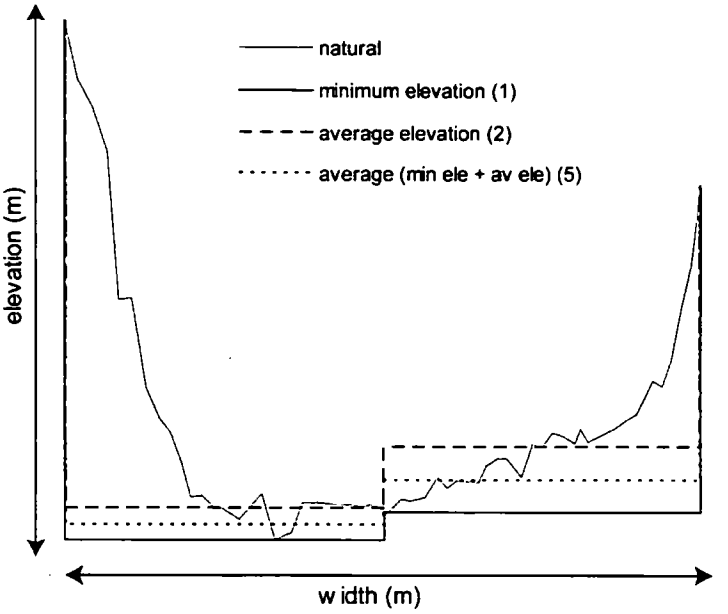

Using the "average (minimum elevation plus average elevation)" approach, the elevations for the left side and right side for all 60 cross-sectional nodes were recorded. To maintain the smoothed slope profile already incorporated in the model, the elevations were transformed onto this slope profile using E_{diff}. Figure 8.18 shows the downstream elevation difference profile for all the cross-sectional nodes. From this data the maximum elevation difference for the Wharfe was ± 0.83 m with three locations recording values around ± 0.8 m. Thus, the cap on E_{diff} discussed earlier was set at ± 0.8 m.

The model was run using these elevation values but was too sensitive to the large elevation differences and the greater slope values generated by them. To resolve this, the elevation differences entered to represent the Wharfe were reduced with a maximum elevation difference of ± 0.4 m used (Figure 8.18). This meant that for just under half of the cross-sectional nodes, the true elevation difference was suppressed. However, crucially, the location of the deeper channel side was still represented and the model output was still capable of evolving to allow greater elevation differences (up to ± 0.8 m) to be simulated.

Figure 8.18. Actual and cut-off downstream differences in right side and left side channel elevations. Data based on the December 2002 cross-sections.

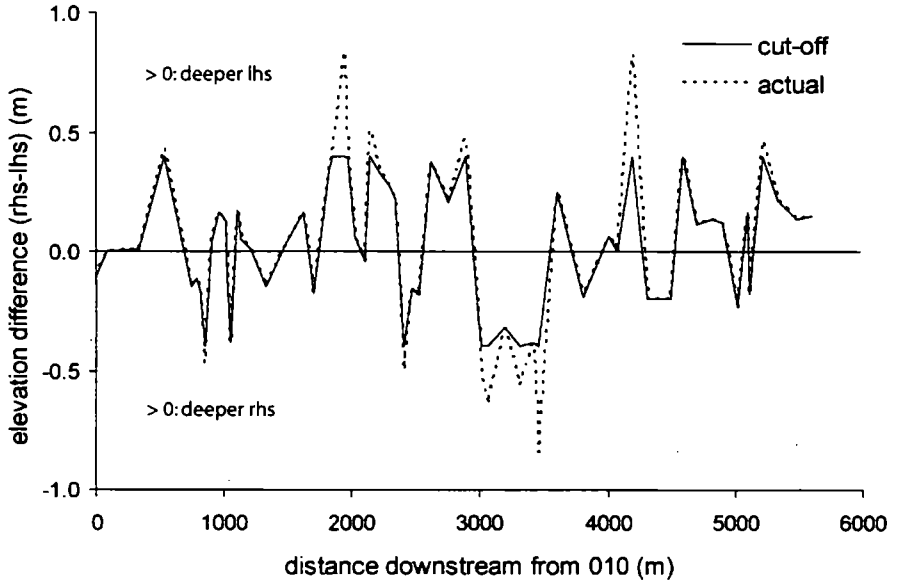

Critical Shear Stress Values

Thus far, a single critical value of shear stress was used to determine whether bank erosion occurred and another value was used for deposition. From the model calculations, it is clear that shear stress varies down the channel (Figure 8.19). This is mainly due to the general reduction in slope as one moves downstream but also due to the fining of sediment. The finer material reduces roughness which acts to slow the conveyance of flow. As such under identical situations where only grain size differs, a finer bed will be shallower with lower shear stress values than a deeper coarse bed with high shear stresses generated. Indeed the shear stress and downstream fining profiles are closely coupled together. The shear stress required to initiate bank erosion will also vary depending on factors such as bank material and bank side vegetation. Furthermore, banks with protection will require very high shear stress values to break down the solid structures protecting them. If a single critical value of shear stress was used, only the upper reaches would exceed this value. No bank erosion would be simulated in the lower reaches where field observations note substantial bank erosion. Hence, the critical shear stress for erosion for each channel bank (left side and right side) was made variable. This allowed very high values to be assigned to protected

banks and lower values to erodible banks. The critical bank erosion shear stress at each node was set at the maximum recorded shear stress (either on the left or right hand bank) at the start of a simulation (after initial fining) for a high discharge value. This value assumes that all banks are susceptible to erosion at the highest discharges. Since bank erosion was noted to occur several times a year, the discharge used to set the critical threshold was set to represent a discharge with a return period of 0.25.

The shear stress thresholds under which deposition would be simulated were also made variable at each node and for each channel side. A single critical threshold was applied to all channel sides for the deposition mechanism since this would be independent of bank materials.

Figure 8.19: Shear stress downstream after initial fining wave when discharge is 70 $m^3 s^{-1}$.

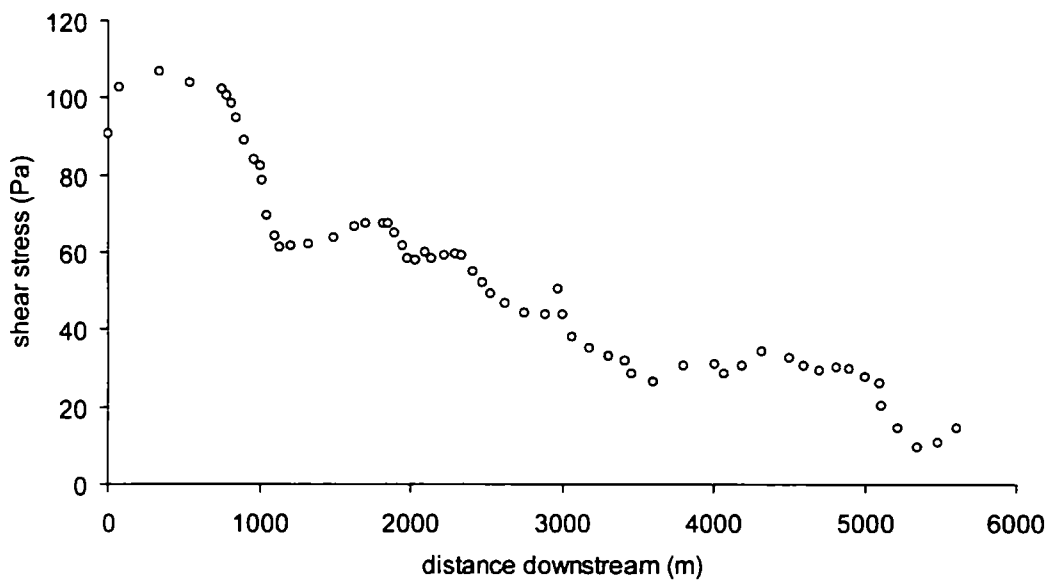

8.5 INCLUDING CURVATURE IN THE MODEL: STAGE (D)

The lateral adjustment component developed thus far simulates a channel with straight banks. To simulate some of the complexities in natural channels, channel curvature must be included. Curvature was shown in Section 6.2.3 to force the high velocity core towards the

outer bank and this leads to enhanced bank erosion rates. Previous approaches that incorporate curvature into bank erosion models include Ikeda *et al.* (1981), Begin (1981), Lancaster and Bras (2003) and Richardson (2001). These were discussed in more detail in Section 7.4.5 but all work on a similar assumption: curvature induces secondary circulation which enhances outer bank shear stress which drives bank erosion. A similar approach was applied here which partitions the width-averaged shear stress into the channel side on the outside of a bend. The higher the curvature the larger the partitioning and the greater the shear stress distribution.

The first step was to determine the curvature at each cross-sectional node. Curvature was calculated using the direction change and distance between cross-sections. This method is described fully in Section 4.5.1. This curvature would represent the net curvature of the flow path between sections. Curvature was then used to redistribute shear stress using [8.12] as shown in Figure 8.20. The amount of shear stress distribution was determined by the value of k. As such, higher curvature resulted in a higher value of k. Following the results in Section 6.2.3 that showed little or no lag in the zone of high velocity in relation to curvature, this linear relation between curvature and k was deemed suitable. Care was taken to ensure that a positive curvature related to a left turning bend and that a negative curvature was related to a right turning bend. Thus, shear stress was always higher on the outer channel side.

$$\tau_{di} = ck\tau_{av} \qquad [8.12]$$

where τ_{di} is the shear stress distribution value, c is the curvature, k is a user defined coefficient and the average shear stress is defined as:

$$\tau_{av} = \frac{\tau_{lhs} + \tau_{rhs}}{2} \qquad [8.13]$$

The new shear stresses for each side become:

left side: $$\tau_{lhs}^{new} = (\rho g S_{av} d_{lhs}) - \tau_{di} \quad [8.14a]$$

right side: $$\tau_{rhs}^{new} = (\rho g S_{av} d_{rhs}) + \tau_{di} \quad [8.14b]$$

where ρ is water density, g is acceleration due to gravity, S_{av} is the average bedslope and d is flow depth.

Figure 8:20. Redistributing shear stress as a function of curvature. In this example, the direction of flow turns to the left giving a positive curvature value. Shear stress is shifted to the right side, the outer channel side.

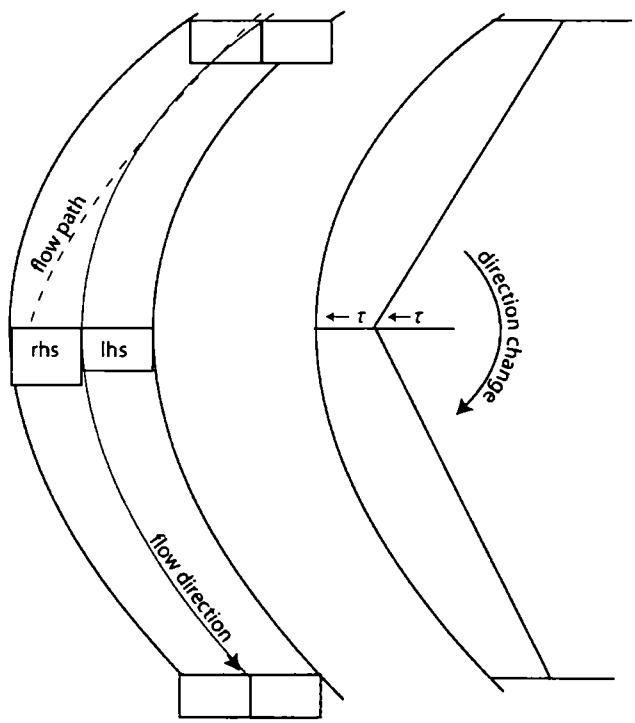

The adopted approach assumes two things: shear stress is not scaled with width and curvature does not update as the channel adjusts. Several have explored the relationship between shear stress distribution and the ratio of *R/w* (radius of curvature to width) (e.g. Begin, 1981). Scaling curvature with width, was not included for three reasons. First, the width variations at bends within the Wharfe are small when compared with larger, wider

rivers and braided channels. Thus the variation in curvature with width is relatively small. Second, the channel is split into two components. Thus, shear stress is distributed into each channel side rather than across the whole channel to the outer channel banks. Third, and most importantly, the data presented on flow paths around channel bends (Section 6.2.3) showed that the strongest relationship to bank erosion used curvature on its own rather than the *R/w* relationship. Thus, curvature alone can be used as a good proxy for lateral shear stress distribution. The assumption that the curvature remains constant at each node as adjustment occurs was made for logistical reasons. To incorporate a mechanism for re-calculating curvature in the model would involve adding additional information into the model to allow direction and curvature to be determined and updated. This information would include the (x,y) co-ordinates of both left and right bank nodes. The co-ordinates would require updating depending on the width adjustment before curvature was re-calculated. This would increase the model's complexity and data requirements substantially. Since simulated width adjustments are typically small over the timescales being considered in this study and in the region of 5% of channel width, the change in curvature with adjustment is likely to be minimal.

The model is now potentially capable of predicting asymmetrical erosion and deposition and this is demonstrated in Figure 8.21. This figure shows the output from a model run that simulated a period of low flow (Figure 8.21a) followed by a period of higher flows (Figure 8.21b). In this model simulation, the curvature value *k* was set at 3, promoting lateral shear stress redistribution around meander bends, the erosion and deposition rates were set high to promote rapid rates of width adjustment and no bank protection was included; thus all banks could erode. In Figure 8.21a, substantial deposition has occurred at four nodes, marked by d. All four locations are on the inside of the meander bends where the shear stress has been reduced enough so that it falls below the critical threshold. When some higher flows are run through the model, bank erosion also occurs and zones of substantial erosion in Figure 8.21b are marked by e. Of the four zones where deposition occurred, bank erosion occurs on the opposite bank at two of these locations. Here the combined effect of inner bank deposition and outer bank erosion results in channel migration as noted. A further two locations have eroded in Figure 8.21b whilst two of the depositional nodes

continue to narrow. Interestingly, the two zones where deposition occurs without erosion, are the widest in the study reach, Thus, low shear stress is a function of shallow flow depths corresponding with the wider channel

Figure 8:21: Left and right bank width adjustment after a period of low flow (A) and higher flows (B). *d* highlights zones of deposition whilst *e* denotes erosion.

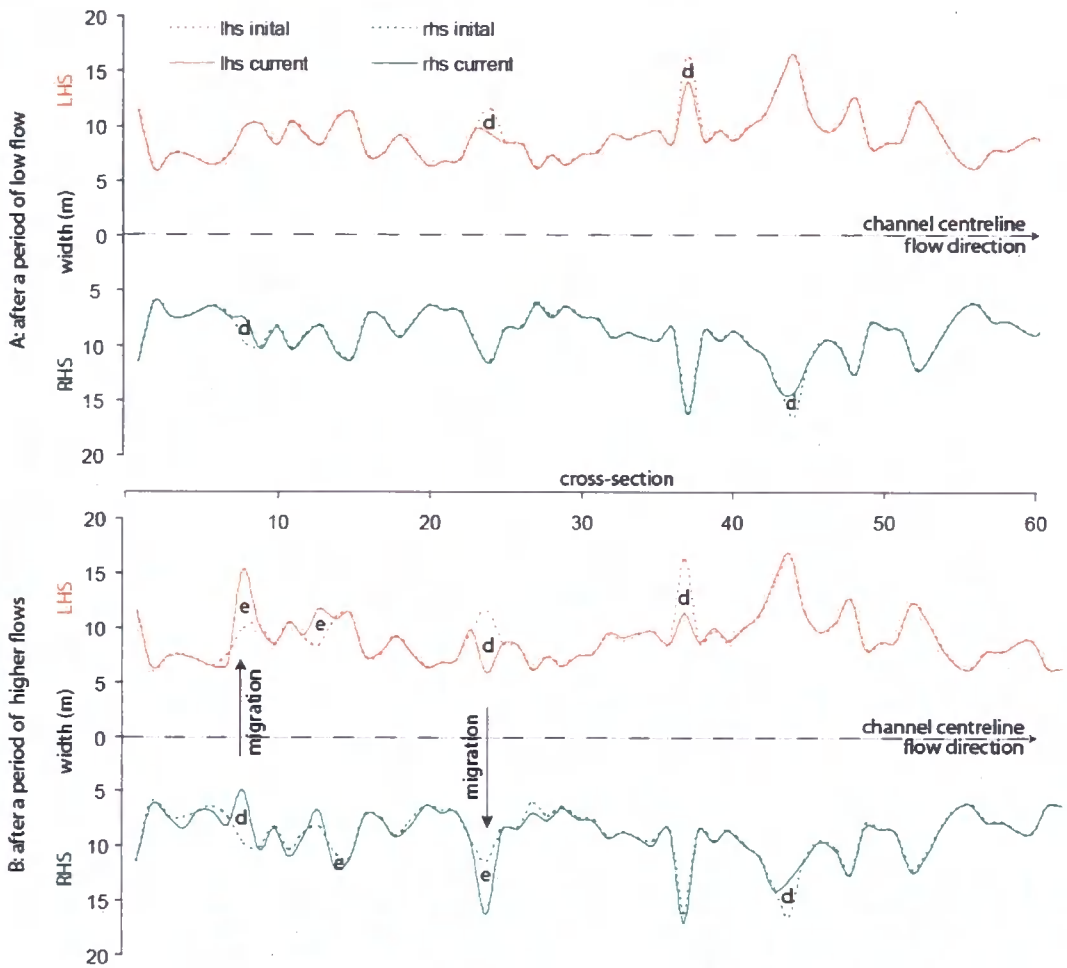

8.6 SENSITIVITY TESTING

Before the model can be used for running simulations and scenarios (Section 8.7), it must first be calibrated so that the predictions match the field observations well. This calibration process begins with model sensitivity testing where a range of plausible values are identified for each of the user defined parameters. During calibration, values within this

range were used in the model to find the optimal value for the Wharfe data. Sensitivity testing is also used to explore model behaviour.

There are four key parameters that are not empirically derived or physically based and must be defined by the user. To aid with the selection of these values, a sensitivity analysis was carried out to compare the impact that each parameter has on the main model outputs. The aim of this testing was: (a) to determine what range of values produce results within a sensible range for gravel-bed rivers (e.g. bank erosion rates in the range of metres rather than 10s of metres); and (b) to determine how sensitive the model was to small and large increases in the parameter values. A base simulation was initially run to provide a comparison for the simulations. Numerous simulations were then run with only 1 or 2 parameters altered in each case. These were all run at a constant discharge, which for most simulations was a high flow. To test the bank narrowing parameter, low flows were simulated. A period of 15 days were deemed an appropriate time length to simulate changes, allowing the model to fully adjust to the new prevailing flow conditions. When discharge was run for 15 days at 50 $m^3 s^{-1}$, this was in effect simulating a decades worth of flows above 50 $m^3 s^{-1}$ (determined from the flow duration curves shown in Section 5.2).

Four parameters were altered. First, the bedload flux which is proportional to the transport capacity at Hubberholme (Section 7.4.3.2) was altered. When a value of 1 is used, the flux matches the capacity. For values less than 1, the bedload flux becomes less than the capacity and for values greater than 1, flux exceeds capacity. Simulations were run using values of 1.1 and 0.9 and the results were compared against the base simulation. Second the effects of changes in the curvature coefficient (k); the value which determines the amount of shear stress distribution that occurs with curvature (Section 8.5) was explored. k was tested at 3 and 5. At the most curved reaches (c = 0.029 radians) when width averaged shear is 100 Pa, these k values respectively create a 17 Pa and 29 Pa difference in shear stress between channel sides. The bank erosion proportionality factor (w_e) was the third parameter requiring selection by the user. The selected value is multiplied by the excess shear stress to determine the amount of width increase [8.7]. This value was required to be small as the channel would increase by this increment for every iteration that the shear

stress exceeded the critical shear stress value. Values in the order of 0.001 were tested. Using this value during a 4-hour flow event where shear stress exceeded the critical value by 5 Pa, 0.16 m of erosion would occur. This seems a reasonable amount of bank erosion for a single moderate flood event based on findings made in Section 4.4: bank erosion monitoring. This parameter is also sensitive to the time-step as there will be fewer iterations for a longer time-step. During a high flow event that exceeds the critical shear stress value for 4 hours, there are 32 iterations when the time step is 7.5 minutes but only 16 iterations when the time step is 15 minutes. Thus, when the model is calibrated, the time-step must be considered. If the time-step is reduced, for example from 15 minutes to 7.5 minutes, the bank erosion proportionality factor must also be reduced in proportion. In this case it should be halved. Finally the bank narrowing rate was considered. Unlike the erosion proportionality factor, this does not increase with reducing shear stress. Instead a constant rate of narrowing is simulated for every iteration under the critical shear value. Thus total bank narrowing is also dependent on time step with an increase in the number of iterations when the time step is reduced. Since low flows occur for longer periods of time than high flow events, values the same as the bank erosion proportionality factor were selected for testing: 0.001 and 0.002. Thus if flow is below the threshold for 20 days (160 iterations when the time step is 7.5 minutes) deposition would be 0.16 m and 0.32 m respectively. Alongside the four parameters, discharge is also altered in several of the runs to explore the combined effects that discharge and one of the four parameters have on the outputs. Discharge has been shown as an important parameter for both sediment transport and bank erosion.

The outputs used to compare the results included: (1) the rate of downstream fining which was represented by recording the D_{50} values at cross-sections 030, 350 and 590; (2) the bedload transport ratio between Hubberholme and Starbotton; (3) bed level changes including the average bed level rise, the maximum aggradation and the maximum degradation; (4) maximum rates of width adjustment, either bank erosion or bank narrowing; and (5) elevation differences between the left and right channel sides: both average and maximum. Table 8.1 shows a summary of the results from each of the sensitivity tests carried out.

Table 8.7: Results from the sensitivity analysis

test no.	flux x capacity	curvature coefficient	BE rate	BN rate	Q for 15 days	D_{50} at x-sec			bedload ratio	bed level change (m)			BE max (m)	BN max (m)	elevation diff (m)	
						30	300	590		average	max agg	max deg			average	max
base	1	0	0	0	50	68	37	18	0.04	0.13	0.39	-0.1	0.0	0.0	0.03	0.40
1: flux	0.9	0	0	0	50	93	43	20	0.09	0.06	0.23	-0.3	0.0	0.0	0.03	0.40
	1.1	0	0	0	50	50	28	14	0.14	0.61	4.40	0.01	0.0	0.0	0.03	0.40
2: discharge	1	0	0	0	30	86	42	22	0.02	0.02	0.04	-0.2	0.0	0.0	0.03	0.40
	1	0	0	0	70	62	36	18	0.06	0.33	0.84	-0.2	0.0	0.0	0.03	0.40
3: curvature	1	3	0	0	50	67	37	18	0.04	0.13	0.44	-0.1	0.0	0.0	0.05	0.80
	1	5	0	0	50	67	38	18	0.04	0.13	0.48	-0.1	0.0	0.0	0.05	0.80
4: BE coeff.	1	0	0.001	0	55	64	36	18	0.05	0.18	0.52	-0.2	2.6	0.0	0.03	0.40
	1	0	0.002	0	55	64	36	18	0.05	0.18	0.53	-0.2	4.6	0.0	0.03	0.40
5: BE coeffi. and Q	1	0	0.001	0	50	68	37	18	0.04	0.13	0.39	-0.2	0.0	0.0	0.03	0.40
	1	0	0.001	0	60	63	36	18	0.05	0.23	0.65	-0.2	11.4	0.0	0.03	0.40
6: BN rate	1	0	0	0.001	5	88	44	21	0.004	0.001	0.003	0.0	0.0	2.7	0.03	0.40
	1	0	0	0.002	5	88	44	21	0.004	0.001	0.003	0.0	0.0	5.4	0.03	0.40
7: BN rate and Q	1	0	0	0.001	2	88	44	21	0.009	0.001	0.003	0.0	0.0	2.7	0.03	0.40
	1	0	0	0.001	10	88	44	21	0.030	0.001	0.003	0.0	0.0	0.0	0.03	0.40

input parameter changed output value altered by changed input parameter

BE = bank erosion BN = bank narrowing

8.6.1 Sensitivity Discussion

Test number 1 explores the model's sensitivity to the bedload flux when it is marginally higher and slightly lower than the bedload capacity. This is equivalent to changing the annual bedload input from 8000 t $year^{-1}$ to 8800 t $year^{-1}$ when a value of 1.1 is used or reducing the input to 7200 t $year^{-1}$ if a value of 0.9 was used. The sediment budget shown in Appendix IV demonstrates that fluctuations in input of 800 t $year^{-1}$ are feasible. However, unlike the tests, these are typically accompanied by seasonal and annual changes in hydrology.

When the bedload flux in the model is reduced, the downstream fining profile coarsens (indicated by higher D_{50} values). This is because in the "base" simulation the transport into the upstream node matches that which leaves since bedload is set to match capacity. This is explained schematically in Figure 8.22. When the sediment transported from the upstream node is not fully replaced with sediment of equal gradation from upstream, the finer material is selectively transported leaving the coarser material behind (Figure 8.22b). A higher percentage of coarser material in the bed mixture increases the D_{50} of the sediment. With a higher D_{50}, a higher shear stress is required to move sediment downstream so the output from this reach is less than in the "base" run. Thus, the gradation of the downstream nodes also becomes coarser (Figure 8.22b). The bed level changes represent a reduction in sediment supply into the reach with a net reduction in bed level rise, a drop in the maximum aggradation rates and greater degradation rates. The degradation occurs at the most upstream node reflecting the supply limited conditions.

When sediment supply is greater than capacity (value set at 1.1) the output is quite different. Firstly, the bed fines much more rapidly, producing a substantially finer bed along the entire study reach than in the "base" simulation. This reflects the increase in finer material entering the reach. To explain this it is important to consider the GSD of the input when conditions of equal mobility, where all grain size classes move, are not met. In the "base" run, the input matches the capacity (Figure 8.22a). If the capacity is insufficient to move the coarser grains, these grains will not be transported and thus not be replaced. The

input will be comprised of finer material which when combined with the coarse material already present, will not alter the GSD. However, when the bedload flux increases, so too does the influx of finer material when compared with the coarser material that is stationary (Figure 8.22c). The influx of finer material lowers the D_{50} of this material. In the Wilcock and Crowe (2003) equations, the critical shear stress (τ_{rm}) is determined from (amongst other things) the D_{50} ([7.18]). As the D_{50} reduces, transport of finer material downstream is promoted. This results in a finer profile downstream. Alongside the fining, the influx of sediment promotes excessive aggradation in the most upstream reach with 4.4 m of aggradation recorded at node 010. This is expected because the transport capacity is insufficient to transport that remaining sediment. Gradually, the aggradation leads to a perched system with an increase in slope. This slowly results in progressive aggradation downstream.

Figure 8.22: Impact of changes in the transport flux on bed grain size distributions.

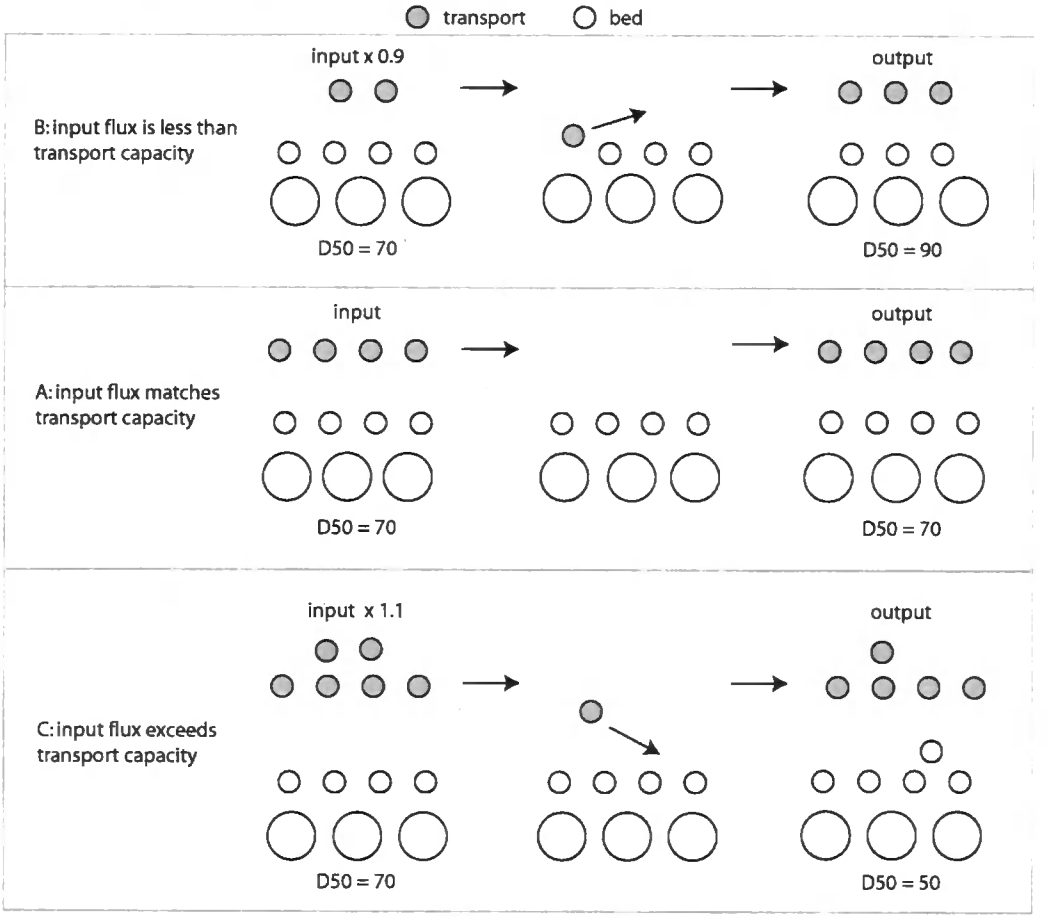

The output bedload transport ratios when flux decreases and increases produced surprising results with an increase in the ratio in both situations. This increase in ratio represents either a reduction of transport into the reach at Hubberholme, or an increase in the output from the reach at Starbotton. It was anticipated that when the bedload flux was reduced to 0.9, the ratio would increase, as the input at Hubberholme would reduce. Furthermore, the sediment at Hubberholme coarsens, reducing the transport further. However, when the flux was set at 1.1, an increase in the input sediment was expected to reduce the transport ratio: this was not the case. To understand why the ratio increases with an increase in sediment flux, the output at Starbotton must be considered. Increases in the sediment output would result in higher bedload ratios. This may occur if there is a reduction in grain size at Starbotton allowing greater sediment transport for a given discharge. This occurred when flux increased with a 4 mm fining in D_{50} recorded compared with only a 2 mm coarsening in D_{50} when flux decreased.

These results demonstrate that the model is highly sensitive to small changes in bedload flux, with these changes felt to the greatest extent in the most upstream nodes. As such, a decision was made to leave the bedload flux set at a value of 1 for future simulations. This assumes that during model simulations the supply of sediment to Hubberholme is always sufficient to meet demand without leading to excessive aggradation at this location. This assumption is supported by field evidence with a large number of impacts recorded at Hubberholme compared with Buckden Bridge and Starbotton (Section 5.4.3).

The impact of discharge and specifically variable discharges was explored in Section 8.3.3. The impacts of changes in discharge on the output are explored further in test 2. In addition, discharge is changed alongside the bank erosion and bank narrowing in tests 5 and 6. In the "base" run, a constant discharge of 50 $m^3 s^{-1}$ was simulated for 15 days. In Table 8.1, for test 2, this 15 day discharge was reduced to 30 $m^3 s^{-1}$, and then increased to 70 $m^3 s^{-1}$. Three different outputs emerged. First, as shown in Figure 5.14, the downstream fining in the study reach occurred substantially faster when a higher discharge was used. Secondly, the bedload ratio increases with discharge. This suggests that more sediment is leaving

Starbotton under high flows implying that the finer sediment is more sensitive to changes in discharge than the coarser sediment at Hubberholme. This agrees with findings made in Section 6.2.1 which noted that sediment only leaves Starbotton under the highest magnitude flow events. Third, bed level changes are more rapid when discharge is higher reflecting the importance that higher discharges have on sediment transport. This is explored further in Figure 8.23 where the maximum and reach-averaged bed level changes are plotted against increasing discharges ranging from 24 $m^3 s^{-1}$ to 76 $m^3 s^{-1}$.

Figure 8.23: Increase in bed level changes with discharge.

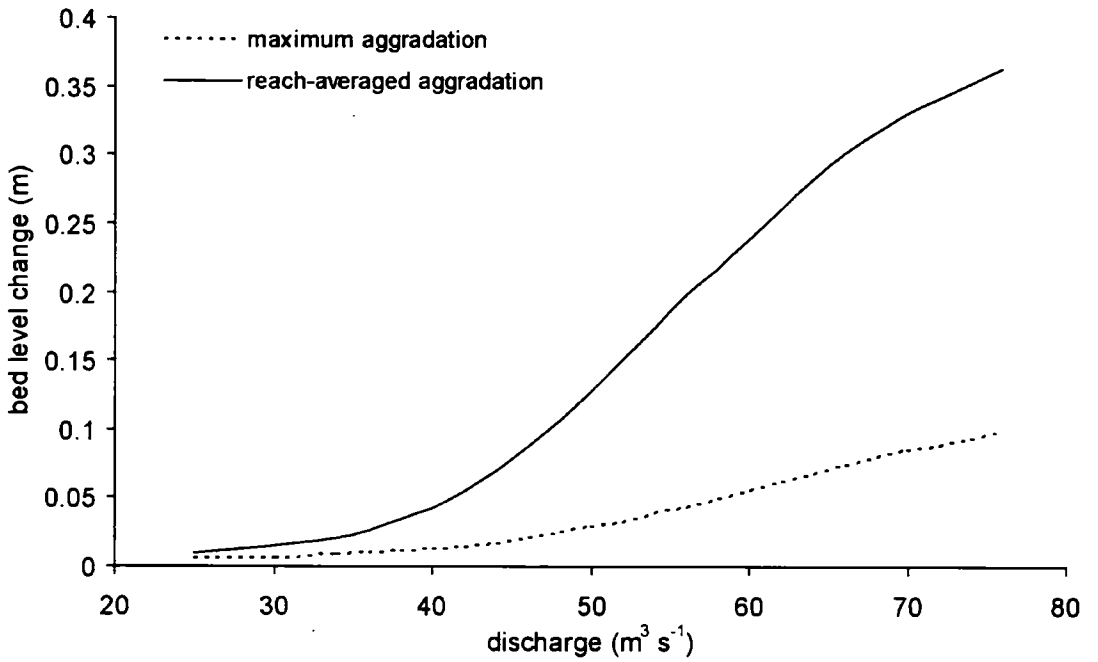

The high aggradation rates in this graph represent a decadal amount of flood events that are simulated in this analysis. In the reach-averaged plot, the data produce a curve with a more rapid increase in the rate of change at around 35 $m^3 s^{-1}$. Interestingly this is around 10 $m^3 s^{-1}$ higher than the discharge required to initiate sediment transport as noted in Figure 8.5 in Section 8.3.2. The gradual flattening off of the curve at higher discharges reflects a reduction in the increase of shear stress with depth as the effect of bed roughness lessens. These findings suggest that whilst moderate discharges are required to transport sediment, higher discharges are essential to increase the sediment supply into the reach enough to

allow sediment accumulation to occur. These results also emphasise the importance of using a variable hydrograph in the simulations as it is the high flow events that drive sediment transport. Furthermore an hourly or sub-hourly hydrograph is essential to capture the flow peaks which are of short duration.

Test 3 explores the impact that the amount of curvature redistribution has on the output. After 15 days of simulation the results are almost identical when using curvature parameters of 3 and 5. With bank erosion and deposition currently switched off this is unsurprising since the curvature component is mainly present to drive the lateral adjustments. However, it is important to note that when the curvature function is operating, the differences in shear stress distribution result in lateral variations in bed level change such that the outside of meander bends, where shear stress is higher, become deeper. However, with the elevation differences capped at 0.8 m, the difference in shear stresses created by values of 3 and 5 are not sufficiently different to produce different results. The increases in elevation variation experienced when the shear stress is redistributed due to curvature does however promote greater maximum aggradation rates. Maximum aggradation rates increasing by 0.10 m when k is 5 compared to when k is 0.

To explore the impact of changing k further, differences in shear stress created by depth differences must also be considered. This allows the impact of k to be isolated from differences in shear stress generated by differences in flow depth. The channel sides begin with no elevation differences. The test is initially run with k set at 0 for thirty days at a moderate flow to allow the downstream fining wave to pass. The model is then run at a constant high flow with k activated. Figure 8.24 shows the results for the reach extending from Hubberholme to just below the Cray Beck confluence and including the gravel trap bend at 800 m downstream. The results show clear differences in shear stress (Figure 8.24a) when curvature is high. The curvature function shifts the shear to the outer bank (Figure 8.24c). When the bend is turning left, as happens at the gravel trap bend located at 800 m downstream, shear stress becomes higher on the right channel side. In doing so, bed degradation occurs and this channel side preferentially deepens whilst the left side becomes shallower. When k is increased from 1 to 3, the difference in absolute shear stress (i.e.

ignoring the direction of values) becomes on average 3 times larger and the absolute difference in depth increases by 2.9. When the location of the deepest sides (either left side or right side) are compared with the deepest sides recorded from the actual channel geometry, further encouraging findings are obtained (Figure 8.24b). Of the 20 locations with the greatest observed depth differences created by the curvature function, the model evolves so that, for 14 of these locations, the model predicts the correct deepest side. In the other locations, it is likely that curvature is not driving the bed elevation differences.

Figure 8:24: Model sensitivity to k. Differences in shear stress (a) and elevation (b) between channel sides. Curvature is plotted in (c). Q is 50 $m^3 s^{-1}$. Only the top 1600 m of the study reach is plotted for visual reasons.

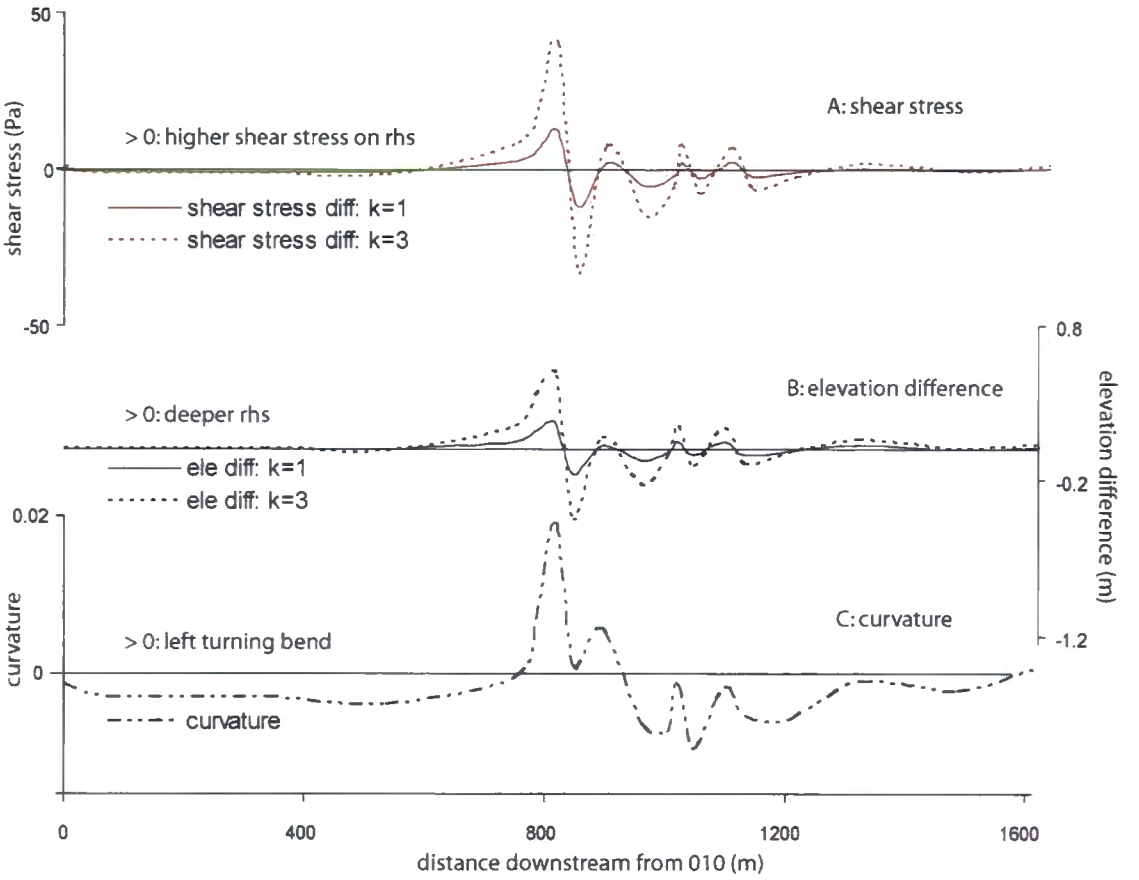

In Figure 8.24 there are no elevation differences between channel sides at the start of the simulation. The elevation differences shown are created entirely as a function of shear stress redistribution due to curvature. In addition to changing k, it is useful to explore the

lateral differences in shear stress when the elevation differences are also included at the start of the simulation. These effects are shown in Figure 8.25. From this figure it should be noted that, on the whole, elevation differences have a far greater impact on shear stress differences than the curvature function when k is set at 5. When elevation and curvature are combined, the shear stress difference is enhanced (in either the positive or negative direction) in 64% of the locations. Examples include at 800 m, 1800 m and 3100 m where shear stress is enhanced by 14 Pa, 14 Pa and 6 Pa respectively. This follows as cross-sectional nodes with high curvature are typically associated with a deeper outer channel side. Thus, they have larger elevation differences. Yet, in the other 36% of locations, the curvature function acts to reduce the shear stress difference created by the elevation difference (moving the difference towards zero). In these locations the deeper channel side is found on the inside of a channel bend. In Figure 8.25 these locations are notable as the "elevation+curvature" dashed plot lies between the two solid "only" lines, for example at 2000 m and 4800 m downstream where shear stress difference is reduced by 7.6 Pa and 4.4 Pa. At 4800 m downstream the curvature effect shifts the location of the highest shear generated by elevation differences from the left side to the right side.

Figure 8.25. Individual and combined effect of depth and curvature on shear stress differences. Discharge is 50 $m^3 s^{-1}$ and k was set at 5.

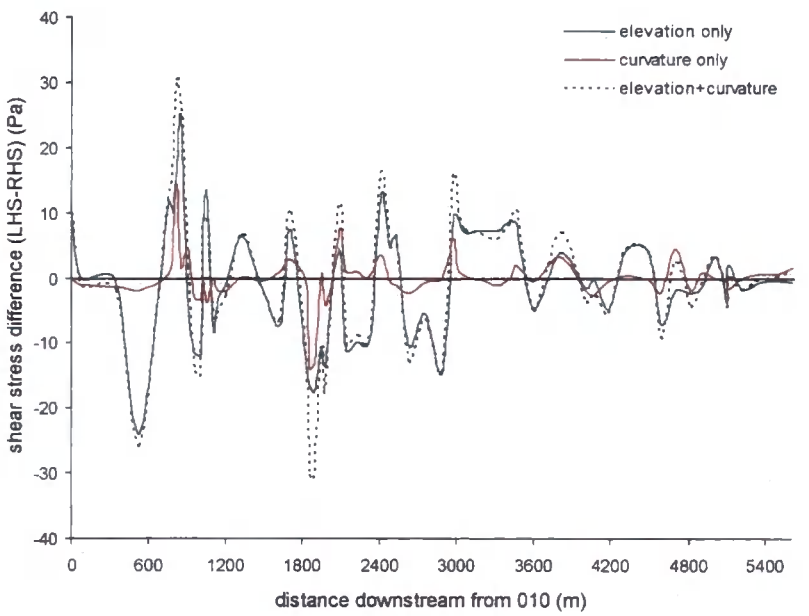

Test 4 compared the model's sensitivity to the bank erosion proportionality factor. As described in Section 8.4.3, bank erosion is proportional to excess shear stress multiplied by the user defined bank erosion proportionality factor. Two bank erosion proportionality factors, 0.001 and 0.002 are tested. In these simulations, the critical shear stress threshold was set at 50 $m^3 s^{-1}$ and the simulations were run at a discharge of 55 $m^3 s^{-1}$. When the outputs from these two runs are compared against each other, unsurprisingly, the maximum bank erosion rate was higher when 0.002 was used. However, doubling the bank erosion proportionality factor, did not double the bank erosion. Indeed the increase from 0.001 to 0.002 only increased maximum bank erosion by 2 m from 2.6 to 4.6 m. This suggests that a feedback is operating where the increase in channel width reduces flow depth thereby lowering shear stress and reducing the excess shear stress used in the bank erosion equation ([8.7]).

When the results from both simulations are compared against the "base" run, further differences are noted in the bed level changes. When bank erosion is allowed, the reach-averaged and maximum aggradation levels increase. This occurs because the increase in width at a given location reduces the flow depth and shear stress promoting deposition. This contradicts findings of Section 8.4.1, where an increase in channel width by 1 m down the whole reach, led to a slower rate of deposition. These discrepancies can be explained by the locations of the width adjustments. Bank erosion occurs where the shear stress is highest and therefore more sensitive to changes in width. Thus, increasing the width of these sections by 2 – 4 m will promote aggradation. When the width increases uniformly by only 1 m, this is insufficient to change the sediment dynamics and aggradation is not enhanced. Furthermore, the discrepancy found here compared with the results made in Section 8.4.1 is supported by contradictory views about channel width and sediment transport in the literature (e.g. Carson and Griffiths, 1987; Henderson, 1960; Bagnold, 1977, 1980; Parker, 1979; White *et al.*, 1982).

In the fifth test, the discharge is increased when bank erosion proportionality factor is set at 0.001 and 0.002. In Table 8.1 the results from two 15-day simulations using a 0.001 bank erosion factor and discharges of 50 and 60 $m^3 s^{-1}$ are compared. Bank erosion is further

enhanced at higher discharges as the excess shear stress is greater. The increases in bed level rise noted in the 60 $m^3 s^{-1}$ simulation are attributed to the increase in discharge rather than bank erosion. The effect of discharge on bank erosion is further explored in Figure 8.26 where simulations were run at progressively increasing discharges and the maximum bank erosion was noted. To allow for 15 different simulations to be run, these lasted only 5 days which effectively simulated 3-4 years of high flow events. Both bank erosion rates exhibit similar patterns with bank erosion initiating at 48 $m^3 s^{-1}$. It is interesting to note that bank erosion initiates at a discharge lower than the discharge used to set the critical bank erosion threshold: 50 $m^3 s^{-1}$. This reflects the evolution of the bed during the simulation such that the updated bed generates higher shear stresses for a given discharge. This may be due to differences in depth due to aggradation / degradation or to changes in the GSD of the bed. As discharge increases, both plotted lines form a curve with a slight levelling off at the highest discharges. Simulations were not run above 76 $m^3 s^{-1}$ as these would be above bank full. The levelling off reflects the feedback in the bank erosion processes with width increases lowering flow depth and shear stress. Thus excess shear stress reduces. When the two plots are compared, the difference in total bank erosion is not doubled when the bank erosion rate is doubled. This further suggests a feedback mechanism.

Figure 8.26: The effect of discharge on maximum bank erosion when using two different bank erosion proportionality factors (BE prop.). Simulations were run for 5 days at a constant discharge.

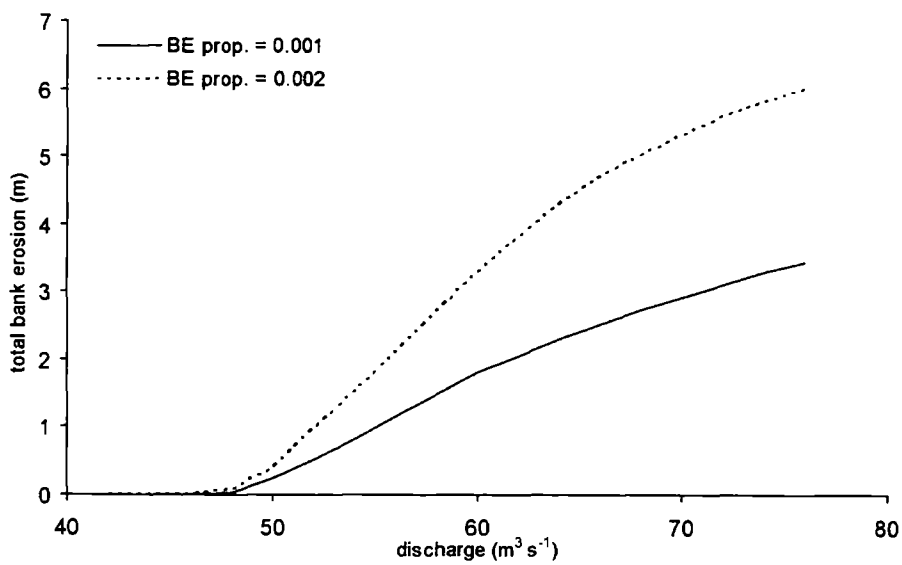

The final two tests explore the sensitivity of the model to the bank narrowing increment and lower discharges. Unlike the bank erosion function, a doubling of the bank narrowing increment resulted in twice as much bank narrowing. This difference is because bank narrowing is not scaled by shear stress. Thus, as long as the shear stress is below the critical value, bank narrowing will occur at the incremental value for each iteration. As such, discharge only has the effect of switching on and off bank narrowing rather than enhancing it. When discharge increases to 10 m^3 s^{-1} in test 7, no bank narrowing occurs since the generated shear stresses are above the critical threshold. When discharge drops to 2 m^3 s^{-1} the narrowing remains the same as when discharge was 5 m^3 s^{-1} since both will produce shear stresses below the critical threshold for narrowing.

8.7 MODEL CALIBRATION

The sensitivity analysis suggested that the model was responding in a physically plausible way to the values of parameters tested. These values provide useful starting ranges for model calibration which sets out to find the optimal values to predict results that match the field observations most closely.

Of the parameters tested in Table 8.1, flux was set at a value of 1 allowing the sediment input rate to match the transport capacity. This assumes that sediment supply is always sufficient at the upstream node, something that was noted during analysis of field data. The second parameter altered in the sensitivity analysis was the discharge. The outputs were found to be very sensitive to the hydrology with the hydrological regime central to the sediment transport and bank erosion processes. As shown in Section 8.3.3 the 2-year representative hydrograph, predicts mean annual bed level changes well. Hence, it is effectively calibrated to the mean bed level changes. However, as discussed in Section 8.3.3, this approach is based on the assumption than the average hydrology will produce the average bed level changes. With discharge data extending to the end of 2002, there is no hydrology available to calibrate the lateral change component in the model.

Whilst mean decadal hydrology was used to predict mean bed level change for a five year period, the bank erosion study only provides data for one year making a similar approach unfeasible. The solution is to use an ergodic hypothesis which uses space as a surrogate for time. In other words, the lateral change component to the model can be calibrated using spatial patterns of change rather than the temporal patterns which are subject to the hydrology. By using the 2-year representative period, rates of change can be calibrated. However it is the relative differences in bank erosion rates between straight and curved reaches which become more important than the actual rates of bank erosion.

Values were required to represent the bank erosion proportionality factor, the bank narrowing rate and the curvature coefficient k. In Section 4.4, bank erosion rates were estimated at four sites and these are used to calibrate the model. Two of these sites were on straight sections and two were located on bends providing bank erosion rates for different planform conditions. Modelled bank erosion on curved sections is determined by a combination of two parameters: the value of k which distributes shear stress to the outer bank and the bank erosion proportionality factor. Hence combinations of values for these two parameters could generate the same bank erosion amounts. However, bank erosion on the straight sections was a function of only the bank erosion rate only because k is not activated when curvature is zero. As such, the model was calibrated using a two-step process.

In the first step, the straight sections were used to calibrate the bank erosion proportionality factor. Multiple runs using the 2-year hydrograph were simulated with the bank erosion factor gradually increasing. The value of k was set at zero so that the only lateral differences in shear stress were generated by variability in bed elevation. The predicted amounts of bank erosion are shown in Figure 8.27a alongside the observed rates of bank erosion at each of the four bank erosion sites. Predicted bank erosion amounts on the straight sections match the observations best when the factor is 0.0014. At this value, the predictions for the curved sites are far lower than the observations. This highlights the importance that the curvature function has for bank erosion around meander bends.

With the bank erosion proportionality factor set at 0.0014, the second step involved calibrating the value of k against the bank erosion observations made at the sites on bends. k was increased to find the optimal value with the results shown in Figure 8.27b. In this plot, it is immediately clear that the value of k is important for driving outer bank erosion at each of the curved sites. In particular, at cross-section site 510, no bank erosion was simulated until k was activated, shifting the shear stress to the outer bank. Small differences in the bank erosion rates are also notable at the straight sites (located at cross-section 420 and 560). Whilst these sites are termed straight, they do have very small curvature values as they are not entirely straight. Thus a small amount of shear stress redistribution does occur. The optimal curvature coefficient for each of the two curved sites is 2.5 for site 350 and between 3 and 4 for 510. A value of 2.5 was selected as this produced the best results for the straight sections. A value exceeding 3 would predict bank erosion amounts greater than those observed on the straight sections. This value of 2.5 means that site 510 is under predicted. This may reflect the location of the bank erosion site in relation to the cross-sectional node 510. Unlike the other three bank erosion sites, which are located very close to the corresponding cross-sectional node, bank erosion site 4 is located just downstream of cross-sectional node 510. Thus the curvature values at node 510 may not match that closely with the curvature values at bank erosion site 4.

The final parameter that required calibrating was the bank narrowing rate. With no quantitative field data available to test this value, it was determined based on qualitative field evidence. In Section 4.2, the field surveys, it was noted that only certain zones exhibited evidence of bank narrowing with the growth of vegetation on the far outside of gravel bars. Thus bank narrowing is not occurring to a great extent in the Wharfe system. Whilst it can largely be ignored, a small bank narrowing value of 0.0002 m was applied. During the prolonged periods of low flow in the 2-year representative period, some bank narrowing occurs on the inside of several of the bends. This has a maximum limit of 0.5 m and was deemed to be a reasonable value for the Wharfe based on evidence from the field surveys (Section 4.2).

Figure 8.27: Predicted (bars) and observed (horizontal lines) amounts of bank erosion. The predicted values are for the left channel sides at sites 250 and 420 and the right channel sides at 510 and 560, reflecting the bank side where the study was carried out. A: compares predictions at increasing bank erosion proportionality factors. B: compares predictions at increasing curvature *k* values.

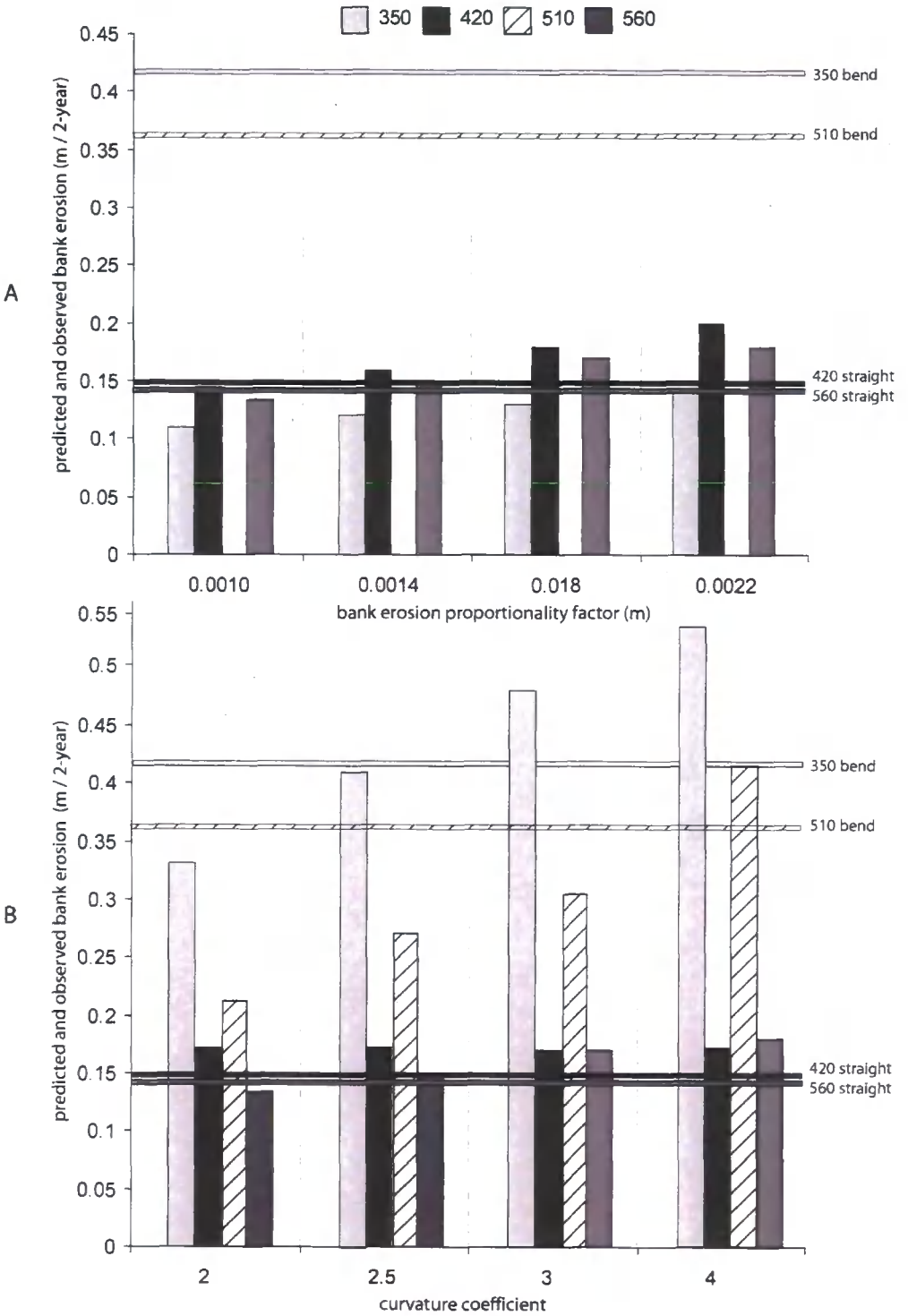

The calibrated model was run for the 2-year representative period and the output is shown in Figure 8.28. To interpret this figure, attention is first given to the right turning bend located at cross-sectional node 210-230. This is clearly identified in the curvature plot (Figure 8.28a). At this location, there is bank protection on the outside of the bend (on the left hand side) but no protection on the inside of the bend. The high curvature on the left hand side of the channel at this location does several things. First, it shifts shear stress to the left hand side and away from the inside of the bend. This results in enhanced sediment transport in the left hand side and leads to channel scour and deepening. This feeds back increasing the shear stress difference between the sides further (Figure 8.28d). With shear stress on the inside of the channel lower than the critical threshold, narrowing occurs (Figure 8.28g, negative black bars). The outside of the bend has a critical shear stress threshold of 200 Pa due to the bank protection. No bank erosion occurs as this threshold is too high to be exceeded. The sediment becomes coarser in the deeper left hand side (Figure 8.28b). This is slightly surprising and can be explained by considering the sediment transport processes operating in each channel side and the input and output of sediment. The GSD is identical in both sides at the start of the simulation. During the simulation, little sediment transport occurs on the shallow, right hand inside. The GSD remains the same here throughout the simulation. In the deeper outside, the shear stresses are higher allowing the transport of the finer grains. Yet they are insufficient to transport the coarsest fractions. Thus the coarse fractions are left behind increasing the D_{50}. The incoming sediment has the average characteristics of the sediment transported from the upstream node. Thus the sediment input into each channel side is the same.

This observation, that the outer channel side becomes coarser as a result of downstream sediment transfer processes and differences in shear stress driven by depth and curvature, is the opposite to the widely recognised theory that it is the presence of secondary flows and a transverse sloping channel bed that result in grain size sorting around meander bends (e.g. Parker and Andrews, 1985). This questions the workings of many meander bend models (e.g. Bridge, 1992; Darby and Delbono, 2002). Thus channel sorting around bends may be related more to the downstream fining process, driven in bends by the lateral differences in shear stress, than secondary circulation.

The processes noted at the 220 bend are echoed along the rest of the river channel. Figure 8.28g shows the extent of the predicted bank erosion. This is dominant in the reach located downstream of cross-section 300 where bank protection is less common. Furthermore, these predictions agree with the bank erosion findings made from the field surveys (Section 4.2). Examining the bars in Figure 8.28g more closely, reveals more information about the nature and locations of channel adjustment. At each node the bars are ordered red - black - green. If the height of the black bar equals the height of one of the coloured bars, bank erosion on one channel side occurs (e.g. node 040: erosion on the left). If the black bar is higher and sandwiched between two coloured bars, bank erosion is occurring on both channel sides (e.g. nodes 150 and 160). If the black bar is lower than (or negative) the coloured bars, some bank narrowing is also occurring alongside the erosion (e.g. node 350: left side is eroding and right side is narrowing). Finally, if the black bars are negative and there are no coloured bars indicating erosion, only channel narrowing is occurring (e.g. node 230)

In addition to the data presented in Figure 8.28, some comments must be made on the predicted pattern of bed level downstream. The changes in elevation differences shown in Figure 8.28f are created by lateral differences in the bed level change at each node. Whilst the model predicts an average bed level rise of 0.06 m which matches the observations well, the location of this aggradation is poorly predicted, with the results remaining similar to those shown in Figure 8.7. This is due to the average slope that is used to drive the downstream sediment transport (see Section 8.3.1). Since this remains the same between the earlier single channel version and the new split channel version, the results are the same. A more variable slope profile cannot be included as the model loses stability. Hence whilst the elevation differences and the addition of curvature information can drive the bank erosion component, they have no impact on sedimentation.

Figure 8.28: Output from the calibrated model after 2-years of simulation. (a) is downstream channel curvature; (b) are the D_{50} values of the left and right channel sides; (c) are the critical left and right bank shear stress required for bank erosion (locations with BP (bank protection) are given a shear stress value of 200 Pa and the dashed lines go off the top of the plot); (d) are the predicted left and right side shear stresses; (e) is the critical shear stress threshold for narrowing; (f) are the initial and current difference in elevation between the two sides; and (g) shows increases in channel width.

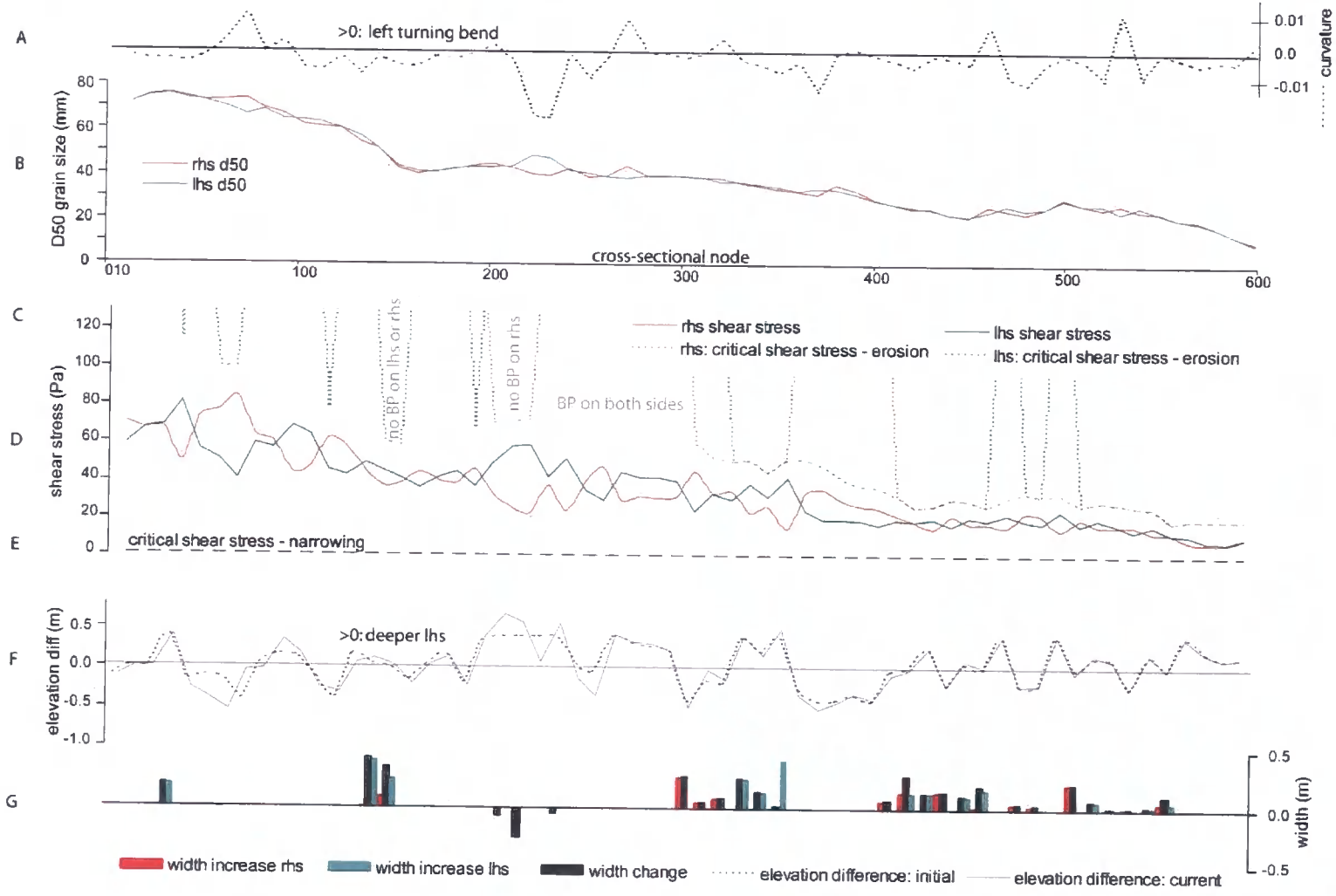

8.8 CHAPTER SUMMARY

The aim of this chapter was to achieve Objective 5: *to develop a model capable of simulating vertical and lateral channel change in the study reach.* The results from the calibrated model, demonstrate that model development was successful and that the model is capable of simulating many of the sediment transfer and channel change features found in the Wharfe. The detailed dataset of channel changes and the variables driving change (e.g. hydrology, sediment supply) from the Wharfe, was essential during the model development and calibration stages. It first provided valuable data for the input and boundary conditions preventing them from being estimated. Examples of these include deriving Manning's *n* values from the grain size characteristics rather than entering an estimated value and entering actual active channel widths for each node rather than using a single estimated mean value. Second, the data enabled the different model outputs to be tested against field observations after each model development step. Thus, decisions made during development (e.g. what grain size distribution to use for the initial input) were based on their success at predicting field observations. The data further allowed the model to be calibrated largely based on empirical findings. However, the success of the results must be treated with some caution as the hydrology used to drive predictions is a decadal average rather than the hydrology specific to the time period of measurements. This is particularly problematic when using the representative hydrology to determine rates of bank erosion which are sensitive to peak flows.

The structure detailed in Table 8.1 was effective at guiding model development and testing. Each of the ten key modelling questions which were determined during literature review in Chapter 7, were successfully explored. Chapter 9 provides a broader discussion into the success of the model development and explicitly answers these questions.

CHAPTER NINE:
MODEL DISCUSSION AND SCENARIOS

9.1 INTRODUCTION

This chapter is split into two parts: model discussion and scenario runs. The first part discusses the four steps of model development: (1) application of TRIB (Section 9.2.1); (2) modifications to TRIB and the boundary conditions (Section 9.2.2); (3) simulating lateral adjustments for straight channels (Section 9.2.3); and (4) simulating lateral adjustments for meandering channels (Section 9.2.4). In each section the main developments are discussed alongside assumptions and limitations. A brief section discusses the sensitivity testing and calibration (Section 9.2.5) before scenarios are explored (Section 9.3). Four scenarios are investigated. The first three aim to demonstrate the model's capabilities: (1) running the model for a further two and four years; (2) removing all the bank protection in the Wharfe; and (3) simulating different hydrological regimes. The latter provides an indication of system response to changes in climate although the scenarios run are hypothetical and are not based on actual climate change predictions. The fourth scenario explicitly deals with the second research aim: *to develop a model of channel change for exploring the impacts of river management*. Thus (4) explores two different engineering options to alleviate bank erosion and high sedimentation rates around Heber bend at cross-section 350. The chapter closes with a brief chapter summary (Section 9.4)

9.2 MODEL DISCUSSION

The model development was broadly split into four sections. Each of these development steps is discussed as follows. Within this discussion, two key research questions from Section 1.1 are addressed: (1) *can a simple quasi-2D modelling approach simulate vertical and lateral channel change in an upland gravel-bed river?* and (2) *how important are the inclusion of a variable discharge and curvature for predictions?*

9.2.1 APPLICATION OF TRIB

Model development began by applying data from the Upper Wharfe study reach to TRIB, a one dimensional SRM. TRIB was deemed a suitable SRM for development for several reasons. First, it effectively combined the hydraulic and sediment transport equations in an Excel spreadsheet. The iterative spreadsheet scheme offered advantages of easy manipulation. Macros written in Visual Basic were used to perform many of the modelling tasks, modifications were simple to perform and output graphs were produced easily. The updating of graphs that occurred with each model iteration produced excellent visualizations of the model outputs and how they evolved over time. Examples included visualizing the downstream fining profile over time and monitoring fluctuations in shear stress as the model moved through a hydrograph. Many of the figures included in Chapter 8 and later in this chapter show snap shots of the model outputs. On the negative side, the spreadsheet package did not have some of the modelling capabilities of other modelling packages (e.g. MATLAB). Thus, certain modifications were not made (e.g. the full inclusion of the function to maintain sediment continuity in Section 8.4.4 and updating channel curvature in Section 8.5).

Second, TRIB used the Wilcock and Crowe (2003) sediment transport equations and calculates the transfer and continuity of sediment on a fractional basis. Unlike other surface based models (e.g. Proffitt and Sutherland, 1983; Parker *et al.*,1982) the Wilcock and Crowe (2003) sediment transport equations incorporate the non-linear effect of sand, which was shown to be important for bedload transport by Jackson and Beschta (1984) and Ikeda

and Iseya (1998). The fractional simulation of sediment transfer and continuity has been employed in several SRMs and allows the simulation of both downstream fining (Hoey and Ferguson, 1994) and sediment pulses (Cui *et al.*, 2003). Fractional sediment transport was also recognised as an important feature of channel adjustment and was included in models by Bridge (1992), Parker and Andrews (1985) and Sun *et al.* (2001b and 2001c). The modelled outputs using the Wilcock and Crowe (2003) equations suggest that this is a suitable approach to use. These results are particularly encouraging when results from studies comparing different sediment transport equations are considered (e.g. Johnson, 1939; Bathurst *et al.*, 1987; Gomez and Church, 1989; Batalla, 1997; Yang and Wan, 1991; Affrin *et al.*, 2002). These studies stress that finding a suitable sediment transport equation can be difficult and they highlight the importance of good data for validation.

A third important feature of TRIB was the data required to run the model. TRIB is not heavily reliant on data and the dataset collected from field studies was adequate for running the model in its initial form. Ensuring a modelling project has sufficient data is a common concern in the modelling literature (Simon and Darby, 1997; Darby, 2005). With a large dataset collected from the study reach, this is not a major limitation within this research. However, there are some limitations due to data availability and these are mentioned within the discussion that follows.

Section (a) of the model development tested TRIB's ability to simulate conditions beyond those which it was developed for. It is widely acknowledged that many models in fluvial science can only function under the conditions they were developed for, or conditions that are very similar. TRIB was tested on a natural river rather than a hypothetical reach similar to those which it has previously been applied to (Ferguson *et al.*, 2006; Rice *et al.*, 2006). Whilst small adjustments were made to incorporate the Wharfe data (including changing cross-sectional spacing, slope, grain size), no modifications to the workings of the model were made at this first stage. The model performed well, producing sensible output values and predicting a downstream fining profile within a reasonable range for the Wharfe. However, the predictions deviated from the observations and this was attributed to the

many aspects of the Wharfe geometry that were poorly represented in the model. Thus modifications to the model were justified.

9.2.2 Modifications to TRIB and the Boundary Conditions

Section (b) of the development made numerous modifications to TRIB and to the model's boundary conditions. The aim was to improve the representation of a natural system within the model. Initial modifications made in Section 8.3.1 were considered minor but found to be important to the model. Several were shown to improve the model's ability to predict the field observations. Each is discussed. Allowing for variable channel widths is essential in systems like the Wharfe which vary in width from section to section. This is best viewed in Figure 8.21 which shows the initial left and right bank profiles down the channel. Without allowing the width to vary, the hydraulic calculations of flow depth and shear stress would be largely incorrect, either over or under representing the system. A similar modification allowing width to vary downstream was made in later versions of SEDROUT (e.g. Ferguson *et al.*, 1997). The next modification was including tributaries into the model to represent Cray Beck and Bucken Beck. The tributary feature of TRIB is useful as inputs of flow and sediment from tributaries can significantly alter patterns of downstream fining and sedimentation as shown by Ferguson *et al.* (2006). For the Upper Wharfe reach, these tributaries have a minimal effect on the main channel as they only contribute small quantities of flow and sediment. The third modification, changing channel slope, perhaps had the greatest impact on the downstream fining profile. This was due to the important role that slope plays in the sediment transport equations, through the calculation of shear stress. However, the model was overly sensitive to slope and this was problematic in terms of maintaining model stability. Modifications to smooth the natural slope profile and then to manually adjust it were required to maintain model stability, and improve predictions. Modifications 4, 5 and 6, all dealt with the representation of the grain size in the model. Eight grain size classes were used to represent the sediment, overcoming issues of selecting class boundaries when five classes were used. The sand threshold was shown to be important in the Wilcock and Crowe (2003) equations and it was successfully shifted from 2 mm to 8 mm to provide a better representation of the Wharfe sediment. The final

modification made to the boundary conditions, using sediment characteristics, tested the different model outputs associated with different starting inputs. The overall outcome was that the pattern of downstream fining is similar irrespective of which GSD the model starts with. However, to ensure the most upstream nodes are predicted to be coarse enough, a coarse GSD similar to the observed GSD is required. The final modification allowed the Mannings *n* value to be variable downstream and over time, by scaling it to the updating grain size distribution at each node. Whilst the Manning's values were not found to alter by large amounts downstream, the impact of *n* on flow depth was noted to be as important as similar magnitude change in discharge. A similar function to update *n* was applied in Darby and Thorne (1996) and Osman (1985).

When these modifications were tested against the field data, encouraging results were produced and the modifications were found to improve the model's ability to simulate the Wharfe system. It was particularly encouraging to note that observed patterns of downstream fining, the ratio of bedload transport between the input and output, and the initiation of sediment transport and maximum bedload transport rates were all simulated well by the modified model. However, the model was incapable of simulating meaningful bed level changes since the discharge was constant and in effect only simulated a constant high flow event. Thus a major modification was made to TRIB to include a variable discharge regime into the model allowing hydrographs to be simulated.

Whilst most hydraulic sub-models and SRMs only simulate steady flow (one exception being Verhaar *et al.*, in press), some hydraulic sub-models within width adjustment models, incorporate unsteady (Li and Wang, 1993) or stepped hydrographs (Osman, 1985; Darby and Thorne, 1996). Since high flows are responsible for sediment transport and bank erosion and low flows are required for channel narrowing to occur, the hydrology of a natural system is central to both vertical and lateral channel change. Thus, it requires to be included in the model. The model was modified to allow for hydrographs of varying length and time-steps to be simulated. However, the main limitation of this approach was data availability.

As discussed in Section 5.2 discharge data for the study reach was limited. Thus the selected representative period was used as a "best guess" for the simulations. With the discharge, particularly the magnitude and frequency of high flow events, shown to be very important for levels of aggradation, a major assumption was made: that the magnitude, duration and frequency of floods within the 2-year representative period was the same as the hydrology used to generate the measured patterns of sedimentation. With this assumption accepted, the results were very positive. The predicted average levels of bed level change along the reach matched the observations very well. Thus, variable hydrology is essential for monitoring bed level changes. However, it is important to accept this limitation with consideration given to the inability of the model to predict more spatially variable locations of bed level change. This is attributed to the smoothed slope profile and hence is difficult to overcome. It poses problems for analysis of model predictions at both the low spatial scales and also when the mean is considered.

9.2.3 Simulating Lateral Change in Straight Channels

In the third part of model development, the lateral component was developed for straight channels. Lateral changes in the width of the channel were shown to be important for vertical channel changes in Section 8.4.1 where the width was manually changed. It was particularly interesting to note that the wider channel reduced bed level rise. The adopted approach uses a split channel creating lateral differences in depth. These create shear stress differences and drive bank erosion and channel narrowing. Similar approaches to include lateral variations in depth and shear stress were also incorporated in the models of Darby and Thorne (1996), Li and Wang (1993), Kovacs and Parker (1994) and Pizzuto (1990). The split channel approach, which was based on the models of Lancaster and Bras (2003) and Stark (2006), was applicable as it maintained the model's simplicity whilst incorporating some lateral channel information. The lateral difference in elevations, partially overcome concerns when calculating bedload transport using a width-averaged approach (e.g. Nicholas, 2000; Ferguson, 2003; Lane and Ferguson, 2005). The split channel allows for different sediment transport rates in each channel side. However, the average slope and width-averaged shear stress are still used to drive these changes and

Manning's n is also equal across the channel. In addition, the split channel approach allows the bed sediment characteristics to vary laterally. Since the sediment input and output into each node is averaged, this prevents large lateral variations in GSD to develop. This lateral variability is supported by Wolcott and Church (1991) who demonstrated that across channel variability in GSD can be larger than downstream variability. Lateral variability in grain size is incorporated into many meander models including Bridge (1992) and Sun *et al.* (2001). However, lateral variability in these approaches is determined by secondary circulations and the transverse sloping channel.

Bank erosion was simulated when shear stress exceeded a selected shear stress threshold. With no clear way to calibrate the selection of the shear stress threshold, this was based on the assumption that bank erosion will occur at the highest discharges simulated. Thus the shear stresses generated by these high discharges were used as the threshold. By allowing each node and channel side to have its own selected shear stress threshold the model can simulate bank protection and downstream differences in bank erodibility. The influence of bank erodibility was also accounted for in the channel adjustment model by Darby and Delbono (2002). The iterative scheme in the model overcomes one of the main limitations of width adjustment models based on the extremal hypothesis (e.g. Chang, 1988; Bettess and White, 1987; Millar and Quick, 1998; Yang *et al.*, 1988). These predict the magnitude and not the rate or location of adjustment (ASCE, 1998b). This adopted approach and the visualizations, allow the user to watch channel width changes as the shear stress increases over the threshold. Furthermore, by scaling bank erosion to excess shear in a similar way to Ikeda *et al.* (1981), the model can simulate small scale erosion when predicted shear stress reaches the critical threshold and large scale erosion (e.g. bank collapse) when the shear stress exceeds the threshold. The model is incapable of simulating other bank erosion mechanisms such as weathering. These processes were shown to be important in the Wharfe (Section 4.4.5) leading to enhanced fluvial entrainment and bank collapse. These can be indirectly included in the model through model calibration.

The modification allowing deposition to occur independent of bank erosion overcomes a common limitation with previous width adjustment models. These maintain channel width

with the amount of bank deposition matching the amount of bank erosion (e.g. Ikeda *et al.*, 1981; Bridge, 1982; Howard, 1992; Sun *et al.*, 1996, 2001; Lancaster and Bras, 2002). More recent models that account for asymmetrical adjustment include models by Mosselman (1998), Nagata *et al.* (2000), Darby *et al.* (2002), Darby and Delbono (2002), Duan and Julien (2005) and Chen and Duan (2006). In the lateral component of TRIB the simulation of narrowing allows it to occur in locations that are not necessarily directly opposite sites of bank erosion. Furthermore, the timing and rate of deposition is linked to the hydrology and not to bank erosion processes. The narrowing function allows for a constant rate of channel narrowing to occur when flows are low. With bank narrowing a function of plant colonisation and succession, a channel bar gradually becomes vegetated and part of the floodplain as the frequency of inundation reduces. This fixed narrowing increment does not account for seasonality or the time between floods. Narrowing may be more rapid in the summer months as vegetation growth is faster. Furthermore, as the time between large flow events increases, vegetation is more likely to become established.

When the results from simulations incorporating the lateral adjustment component are examined and compared with field observations, two clear issues arise: (1) is the need to calibrate the bank erosion and deposition rates with field data; and (2) is the need to incorporate channel curvature into the model to allow for bank erosion on meander bends.

9.2.4 Simulating Lateral Change in Meandering Channels

The final model development stage was incorporating curvature into the model to simulate sinuous natural channels. Enhanced bank erosion was attributed to curvature and bed level changes (Section 6.2). As demonstrated in the outputs from the lateral straight channel model, curvature is essential in the model to accurately predict locations and rates of bank erosion and deposition. Incorporating curvature into models of lateral adjustment has been done in several meander evolution models (e.g. Darby and Delbono, 2002; Coulthard and Van De Wiel, 2006). Curvature is included in TRIB by distributing shear stress towards the outer channel side and away from the inner channel side. Thus bank erosion is promoted by excess shear stress. This approach is similar to the bend theory concept developed by Ikeda

et al. (1981) and used extensively (e.g. Beck, 1984; Parker *et al.* 1982, 1983; Parker and Andrews, 1985; Johannesson and Parker, 1989; Sun *et al.*, 1996, 2001a, 2001b; Howard, 1984, 1992, 1996; Mosselman, 1998; Darby *et al.*, 2002; Edwards and Smith, 2002). Bank erosion is now driven by the combined effects of lateral differences in bed elevation and curvature. Results show that locations of outer bank erosion and inner bank deposition match well with the locations of the main bends which have no bank protection. Thus curvature is an essential parameter to include in models of lateral channel adjustment.

9.2.5 Sensitivity Testing and Model Calibration

Sensitivity analysis tested that the model performance was plausible. Furthermore, sensitivity testing was used to identify values which produced results within the range of observations for the Wharfe. This allowed the model to be calibrated effectively. The calibration process had two steps: (1) calibrating the bank erosion proportionality factor against the straight sections; and (2) calibrating of the curvature value k against the bank erosion observations for curved sections. This calibration was based on only limited data with a total of four bank erosion sites. However, when the results were considered and compared with qualitative field based evidence, the predictions were felt to be suitable. The rate of deposition was not calibrated against any quantitative data. Thus deposition rates should be considered with caution.

9.3 Scenarios

The model has been calibrated to predict average levels of aggradation, downstream fining rates and bank erosion rates on straight and curved sections that match observed field data well. This chapter sets out to achieve the final methodological objective as outlined in Chapter 1, Objective 6: *to use the model to explore a range of scenarios*. The nature of these scenarios was determined by the final research question raised in Section 1.1 at the start of the thesis. This question was: *what are the implications of changes in hydrology and river management for channel change and flood risk?* Scenario exploration demonstrates the model's capabilities and allows potential changes in climate and river management options to be investigated.

Four scenarios are explored as follows:

Scenario (1): running the model for a further two and four years;

Scenario (2): removing all the bank protection in the Wharfe;

Scenario (3): simulating a different hydrological regime; and

Scenario (4): exploring engineering options around a problematic reach.

Scenario (1): running the model for a further two and four years.

The model is calibrated against the average annual conditions for the field study period which were scaled up to provide mean changes for a 2-year period. In this first scenario, the model is run for a further two and four years of representative hydrology providing results for two, four and six years of simulation. This was done with bank protection in place using the calibrated values determined in Section 8.3 after the initial fining wave had passed.

The patterns of bed level rise are explored first. Figure 9.1 shows the bed level change at each node after two, four and six years of simulation. The reach averaged rise for each 2-year period remains relatively constant at 0.062 m for the first two years, 0.065 m for the second two years and 0.061 m for the last two years. With the width of the input node 010 at Hubberholme remaining fixed over time, the subtle differences are produced by changes in slope as the 2nd node downstream degrades rapidly during the first two years and then only slightly over years two to six. The locations and rates of aggradation down the rest of the channel remain constant with aggradation increasing gradually. There are some minor differences in the locations of aggradation and these are a result of the changes in slope generated by the aggradation.

Figure 9.1: Bed level changes over time.

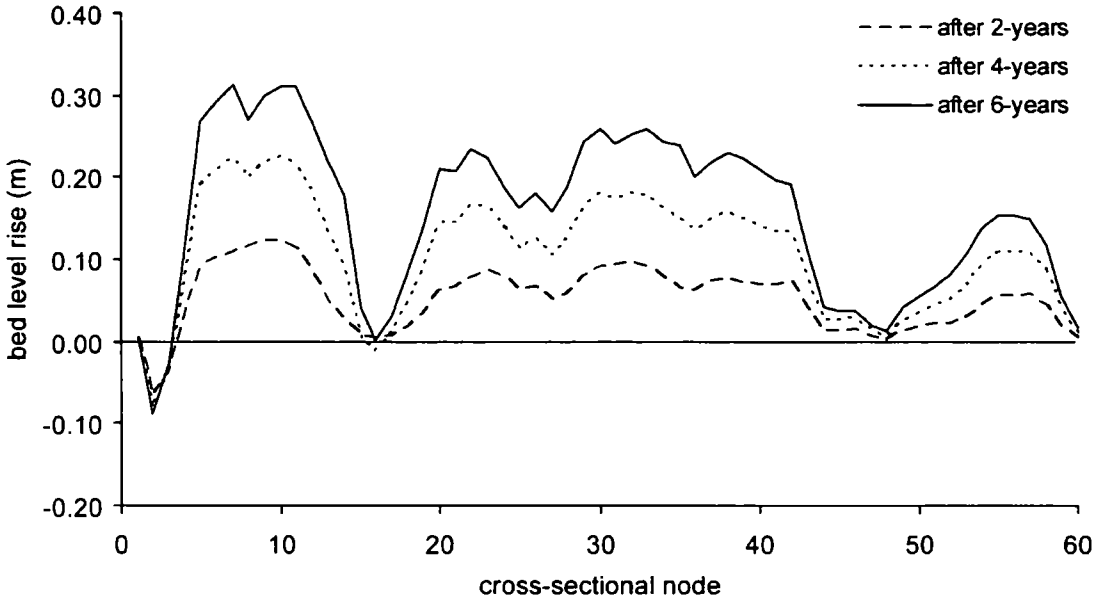

It is also important to monitor how the width adjustments change over time. Results are presented graphically in Figure 9.2 and numerically in Table 9.1. In Figure 9.2, as simulation time increases, the width adjustments become more visible and there is some substantial bank erosion noted at nodes 350 left and 140-150 left and right. In addition, some nodes record some narrowing including 350 right and 210-220 right. This figure also demonstrates that these changes are relatively small when compared with the initial channel width. Therefore, they do not result in any substantial differences in bed-level rise. To examine this width adjustment more closely, the data are presented in Table 9.1. One of the key findings from this table is that only relatively few locations increase or decrease in width at a constant rate. Instead, for some nodes, the rate of change increases over time, for example at node 220 right. The rate of change in other nodes reduces for example at node 040 left. Additionally, a few nodes begin or stop eroding or narrowing after several years. Examples include 100 right and 260 left which begin adjusting between two and four years and 520 left and 490 right which cease between two and four years. These changes occur due to the evolution of the bed and the progressive fining of bed material. The combined effect of this is changes in shear stress at each node with time. This is shown in Figure 9.3

which shows the left hand side shear stress at each node at the start and every two years. The greatest changes in shear stress correspond with the locations of the main bends in the study reach (e.g. 080, 220 and 350).

The results after two, four and six years can also be compared against the field observations to ensure that the model is still performing well. As already discussed, aggradation rates remain constant for each time period and therefore remain calibrated against the mean bed level rise observed from field surveys. With bank erosion rates fluctuating due to bed level changes, the predictions may not match the outputs as successfully. In Table 9.1, the results for 350 left, 420 left, 510 right and 560 right are considered. The 2-year observations for these nodes record 0.42 m, 0.15 m, 0.36 m and 0.14 m of bank erosion respectively. Node 350 left continues to predict values close to the observed 0.42 m with a small increase. This increase may reflect the narrowing on the opposite bank which was not considered when the model was calibrated. The bank erosion rate at 420 left doubles to 0.33 m. This is of concern and occurs due to bed level changes at this location. At bank 510, the predictions begin lower at 0.22 m and get progressively smaller over time. The lower calibrated results after two years were noted in Figure 8.27. Like at 510, this lowering in bank erosion rate reflects changes in the channel geometry. It is likely that the bank erosion, and width increase, during the first 2-years was sufficient to reduce shear stress and inhibit further erosion. At location 560 right, the predictions remain relatively constant at between 0.13 m and 0.16 m and these values match well with the observations. This is encouraging.

In general, the model's behaviour after two, four and six years echoes that observed in the field. The only main exception is the locations of aggradation and degradation and the increase in bank erosion rates over time at node 420. Consequently, the model can be used to simulate the additional scenarios outlined earlier with relative confidence. For most cases, the simulations are kept to 2-years to allow for a better comparison between normal and scenario states without the additional variable of time.

Figure 9.2: Width change over time. Bank protection is in place.

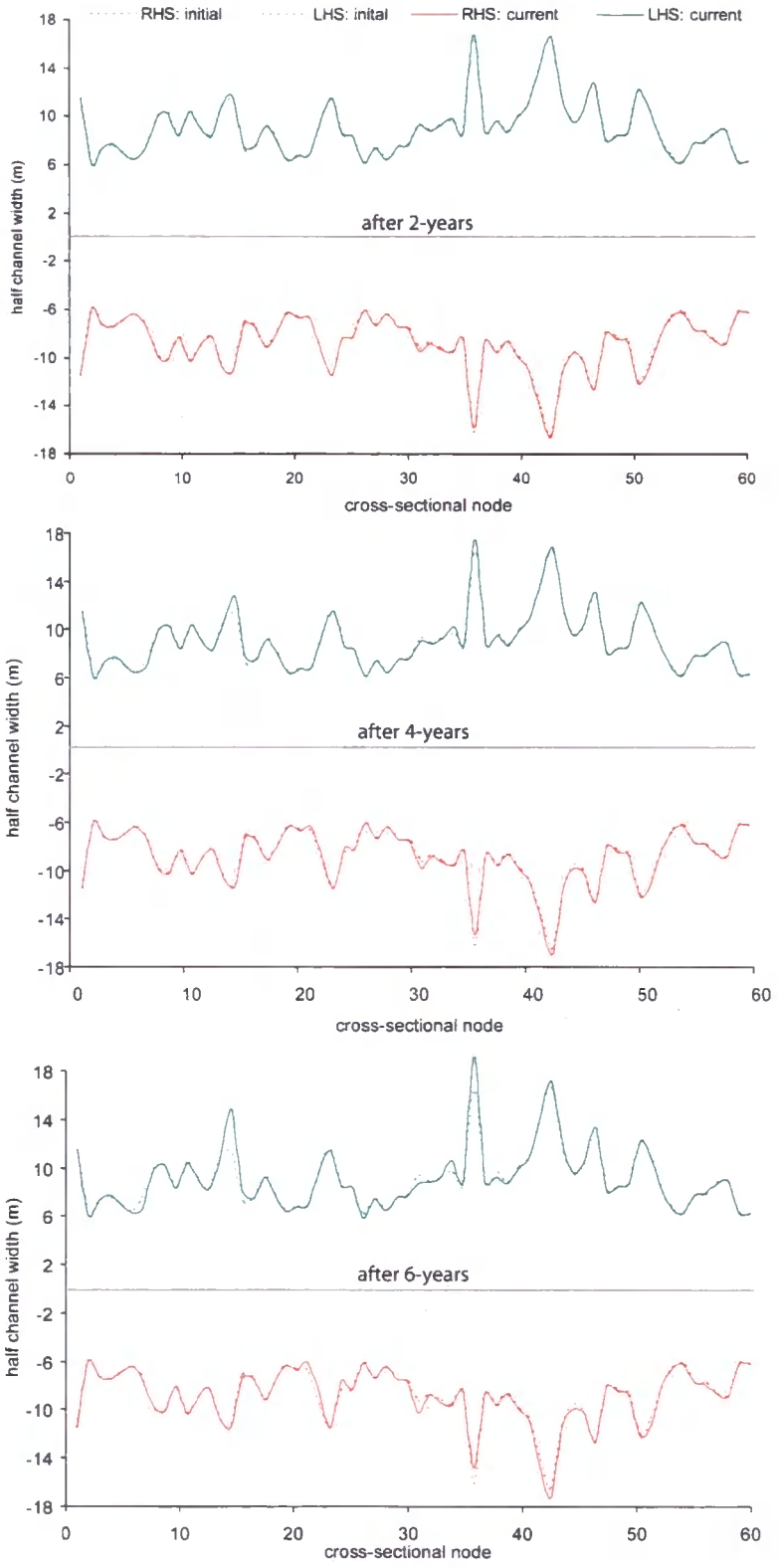

Table 9.1: Width change for each time period. Grey positive values show bank erosion and black negative values show narrowing.

	Left hand side (m)			Right hand side (m)		
node	0-2 years	2-4 years	4-6 years	0-2 years	2-4 years	4-6 years
010						
020						
030						
040	0.20	0.05	0.01			
050						
060			-0.25			
070	-0.01	-0.42	-0.52			
080						-0.11
090						
100					-0.01	-0.27
110						
115 trib			-0.01			
120						
130						
140	0.42	1.08	2.15	0.01	0.05	0.15
150	0.25	0.24	0.40	0.09	0.03	0.06
160						
170						
180						
190						
200						-0.03
210				-0.07	-0.32	-0.32
220				-0.26	-0.44	-0.52
230			-0.01			
240				-0.05	-0.35	-0.44
250						
260		-0.01	-0.30			
270						
280						
285 trib						
290						
300		-0.17	-0.39	0.27	0.30	0.43
310				0.06	0.00	
320				0.09	0.05	0.01
330	0.26	0.34	0.35			
340	0.15	0.12	0.05			
350	0.42	0.40	0.56	-0.40	-0.49	-0.54
360						
370		-0.11	-0.29			
380						
390						
400						
410	0.01			0.07	0.13	0.28
420	0.14	0.23	0.33	0.15	0.26	0.38
430	0.14	0.27	0.41			
440				0.15	0.13	0.14
450	0.11	0.10	0.10	0.00		
460	0.18	0.23	0.28	0.02	0.02	0.02
470						
480				0.05	0.01	0.00
490				0.04	0.00	
500					-0.01	-0.06
510				0.22	0.17	0.10
520	0.08	0.01				
530	0.02			0.00		
540				0.02		
550	0.03					
560	0.06	0.03	0.04	0.16	0.13	0.14
570			0.01			
580						
590						
600						

Figure 9.3: Shear stress on the left hand side plotted through time. Discharge was 15 $m^3 s^{-1}$.

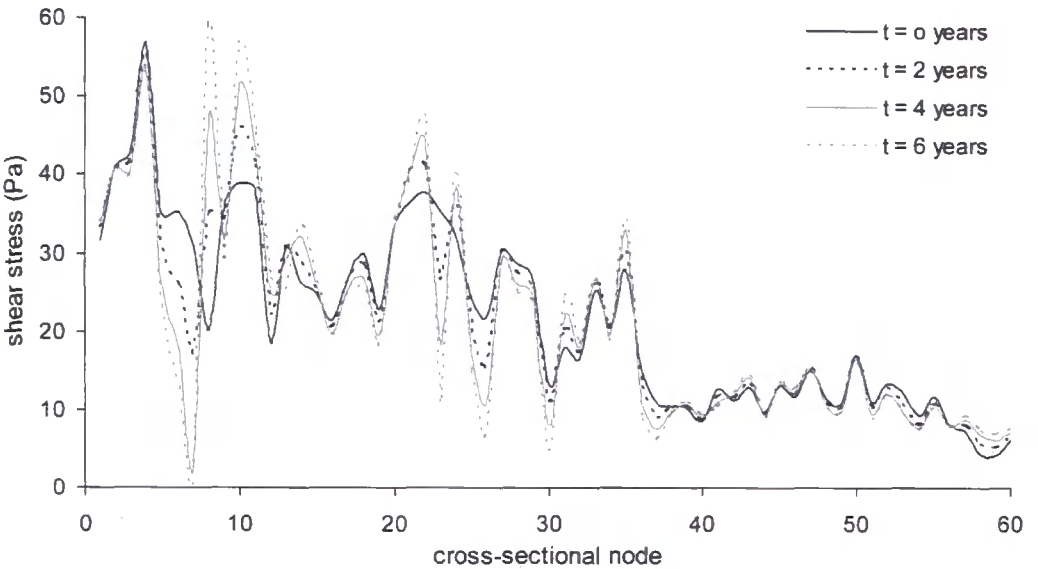

Scenario (2): removing all the bank protection in the Wharfe

In Section 3.4, river management in the Wharfe study reach was discussed. In brief, the channel has been confined to its present day course since monastic times when dry stone walling was used to straighten and restrict large sections of the channel. In the past few decades, many of these walls have been stabilised and new hard engineering schemes have been constructed around several of the meander bends. Thus the study reach is far from a natural state. In this scenario, the impact of removing these structures is explored. The hypothesis tested here is that removing these structures will result in extensive bank erosion, predominantly at the meander bends, and the channel will shift towards a more natural meandering state once again.

The model is run using the 2-year hydrograph with all banks erodible. For banks that were previously protected, the new shear stress value applied is determined using the approach described in Section 8.4.5 and applied to all locations without protection (i.e. the shear stress acting on the specific channel location using a high discharge). The input node 010 controls the input of sediment. Thus it remains a fixed width to ensure that the input of sediment between runs is equal. Figure 9.4 shows the width adjustment from this simulation compared to the output from the calibrated run discussed in Figure 8.28. The difference in output is striking. When the bank protection is removed, bank erosion occurs

in most of the previously protected reaches. This bank erosion is particularly severe where the curvature is high, for example at node 070 (at the start of the gravel trap bend) and at nodes 220-230 (the bend at Buckden Bridge). At node 070, bank erosion occurs on the right hand side of the channel, as indicated by the red bars. At nodes 220-230, the green bars show that bank erosion is occurring on the left of the channel. The bend at 220-230 is particularly interesting because when bank protection was in place, this zone experienced inner bank narrowing (Figure 9.4a). This narrowing of the inner bank is still noted in Figure 9.4b. When the outer bank erosion and inner bank deposition are considered together, the channel is beginning to migrate.

Figure 9.4: Width change at each cross-sectional node after 2-years. (A) shows the output with bank protection and (B) shows the output with no bank protection in place.

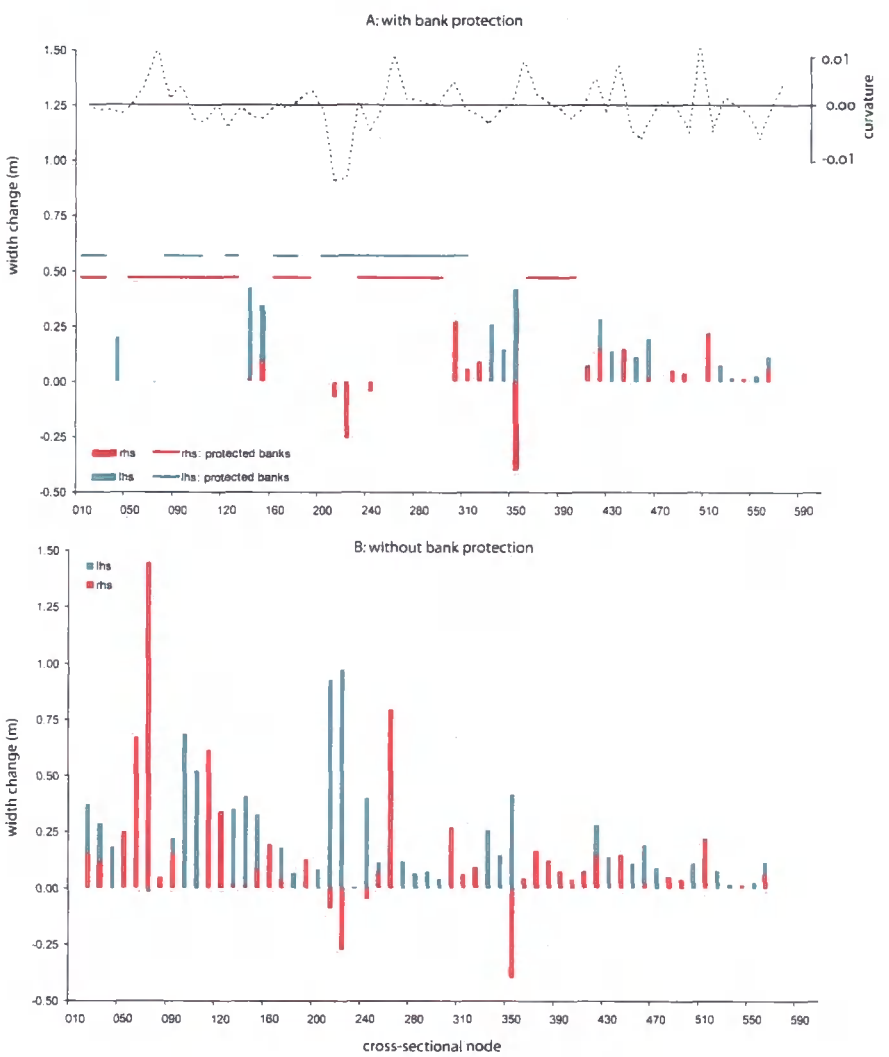

With width adjustments reaching a maximum of nearly 1.5 m, two of the model's features must be reconsidered. First, dealing with sediment continuity which was discussed in Section 8.4.4 becomes more important. At node 070 where 1.5 m of erosion occurs, the elevation difference is 0.5 m. Thus the sediment that would be lost as the channel mid-point shifted is 0.36 m^2. Using the continuity function, the bed level rises by 0.02 m on both channel sides to deal with this. Second, channel curvature at each node remains fixed during simulation. As such, this fails to account for the increase in curvature that is expected due to width increase. The need to recalculate curvature is only small when bank erosion rates are low but as bank erosion and migration rates increase, this becomes more important.

Whilst it is interesting to consider the enhanced erosion that takes place when bank protection is removed, it is also important to consider the effect that this has on the patterns and rates of sedimentation. When the average rates of bed level rise are compared they are both almost identical at 0.0628 m for the protected and 0.0633 m for the unprotected. This reflects the fixed input node at 010 with the same volume of sediment entering the reach during each run. With no width adjustment occurring at the output node 600, the ratio of sediment input to output remains constant between simulations. The average width change downstream is only 0.22 m and this is insufficient to alter the bed level changes since the average channel width is 17.5 m. However, there are differences in the locations of aggradation and degradation. These drive the elevation differences between channel sides. At a bend, the outside typically degrades whilst the inside of the bed aggrades. This is clear at node 230 on Figure 9.5 with the outer left hand side degrading, and at node 080 where the right hand, outer bend side is degrading. Figure 9.5 also shows the difference in left and right hand elevations between the unprotected and protected simulations. The differences are most notable in the upper half of the channel. This may be because this is the location of most of the removed bank protection; thus there are few differences in the lower reach. Or it may be that after two years the impacts have yet to migrate fully downstream. To explore this, the unprotected simulation is run for a further two years using the same hydrology.

Figure 9.5: Bed level differences between the protected and unprotected simulations (change = unprotected – protected).

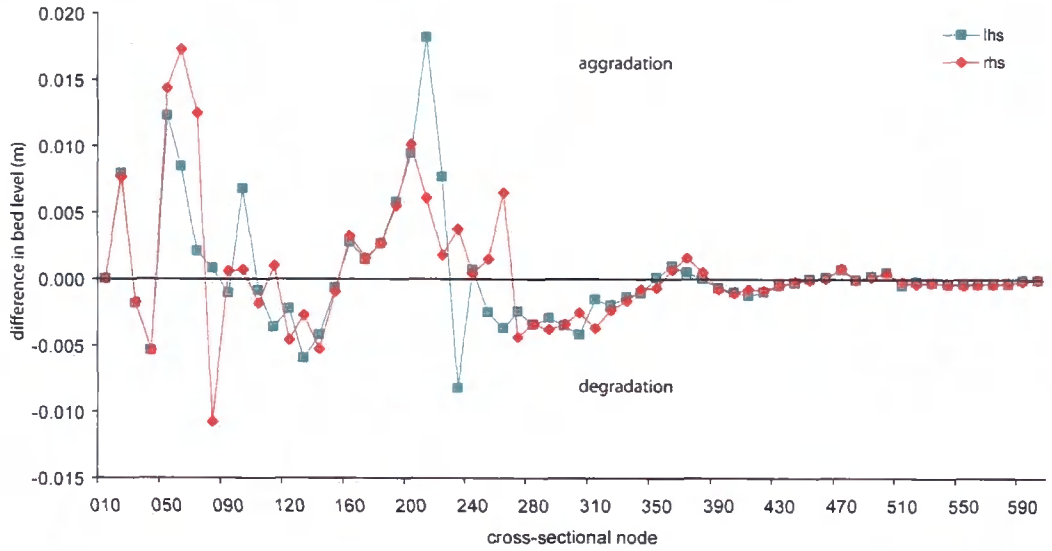

After a further two years of simulation, aggradation rates after 4-years are explored and a similar downstream profile to Figure 9.5 above is produced. The main difference between outputs in a net increase in aggradation throughout the reach as the mean bed level rise increases from 0.06 m to 0.12 m. This suggests that the differences noted in Figure 9.5 are not related to simulation time but to the removal of the bank protection.

In addition, the amount of bank erosion at each of the eroding nodes has also increased. Under identical conditions a 100% increase in bank erosion would be expected. However, as the bed has evolved over time some banks have become more susceptible to bank erosion and others less so. This reflects shear stress changes over time. Figure 9.6 shows the percentage increase in bank erosion amount between the two and four year simulations. Several locations record substantially more bank erosion after two years including nodes 060-070, 110-140 and 410-430 with a 350% increase recorded at 070. Despite, these large increases, the average percentage increase for the reach is 83% showing that during years three and four less total erosion occurred along the study reach. There are two reasons why the bank erosion increase is below 100%. The first is that bed level changes and downstream fining over time operate to raise or lower the shear stress for a given discharge at a specific location. Thus, the critical bank erosion threshold may be breached less often.

The second reason is the feedback between channel width, depth and shear stress. The more bank erosion, the greater the feedback with the increase in channel width lowering shear stress and reducing excess shear stress used in the bank erosion equation. This process is similar to the basal end point control concept where a bank collapse acts to stabilise the bank preventing future bank erosion. With 31 nodes eroding less and 10 nodes recording no width increase, 19 nodes erode to a greater extent in the 2nd and 3rd years of simulation. This can also be explained by bed evolution, in particular outer bank scour, for example at nodes 070 and 260. The deeper channel promotes bank erosion as shear stresses are higher.

Figure 9.6: Percentage increase in bank erosion between two and four years.

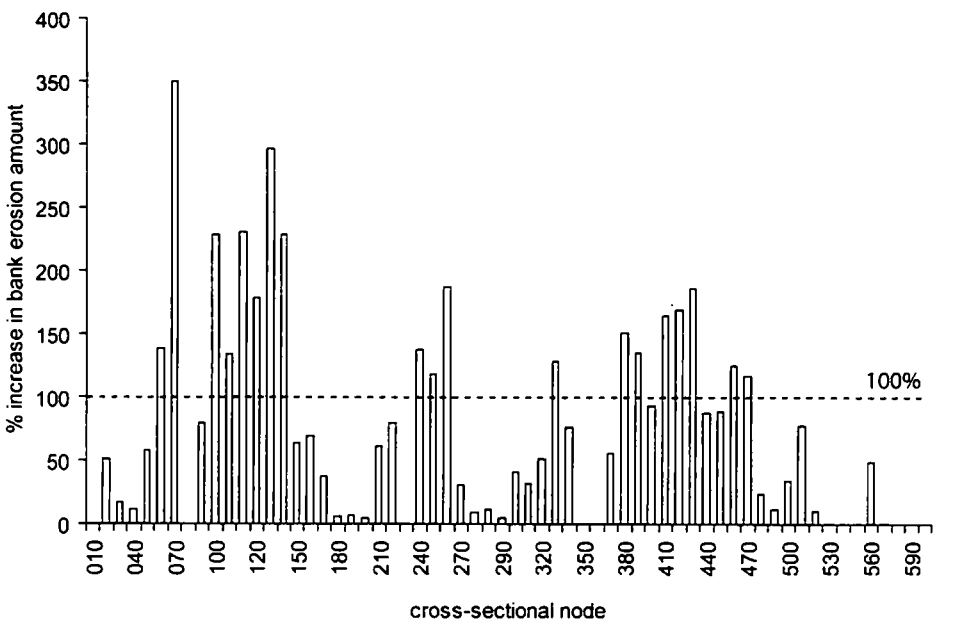

Scenario (3): changing the hydrological regime

In the third scenario the 2-year hydrograph was altered to explore the impact of different hydrologies on the outputs. Two simulations were carried out with the results compared to the normal hydrology in Table 8.2. In the first test, the hydrology was made 5% wetter ("wetter hydrology"). Thus the magnitude of the largest flood events increased from 70 m^3 s^{-1} to 73.5 m^3 s^{-1} and the average discharge increased from 9.5 m^3 s^{-1} to 9.9 m^3 s^{-1}. This increases the length of time that discharge is above 50 m^3 s^{-1} from 45 hours to 47 hours. In the second test three additional flood events with a magnitude of 70 m^3 s^{-1} were included

("more floods"). These were included into periods of low flow, occurring in the months of June year 1, February year 2 and September year 2. Flows above 50 $m^3 s^{-1}$ now occurred for a total of 54 hours and the average discharge increased to 9.6 $m^3 s^{-1}$.

Table 9.2: Results after changing the hydrology.

		normal	wetter hydrology			more floods		
		results	results	diff. (m)	as %	results	diff. (m)	as %
mean width increase (m)	rhs	0.022	0.041	0.02	89.4	0.024	0.00	10.4
	lhs	0.063	0.079	0.02	25.6	0.047	-0.02	-25.2
max width increase (m)	rhs	0.275	0.424	0.15	54.2	0.325	0.05	18.4
	lhs	0.522	0.764	0.24	46.2	0.519	0.00	-0.6
mean bed level rise (m)		0.060	0.067	0.01	11.9	0.067	0.01	11.9
max bed level rise (m)		0.142	0.162	0.02	13.6	0.159	0.02	11.7
D50 at 030 (mm)		75.64	74.83	-0.81	-1.1	75.04	-0.60	-0.8
D50 at 590 (mm)		16.87	16.71	-0.16	-1.0	16.87	0.00	0.0

There are two key findings from Table 9.2. First, for both scenarios, the changing hydrology had the greatest impact on channel width, particularly on the right hand side of the channel. The mean and maximum bed level rise in both scenarios also increases reflecting the increase in sediment transport with higher discharges. It is particularly important to note that three extra flood events has the same effect on mean bed level rise as a 5% rise in peak flows. Yet, the wetter hydrology produces higher maximum aggradation rates. Differences in the grain size characteristics in both cases are minimal suggesting that much larger changes in the hydrology are required to alter the pattern of downstream fining in the study reach.

Second, mean width increases are much more sensitive to changes in the magnitude rather than the frequency of flow events. The right side increases in width by 90% compared with only a 10% increase when more floods are simulated. On the left hand side, the width increases are mixed with a 25% increase when a wetter hydrology is used and a 25% reduction in width when more floods are simulated. This discrepancy can be explained by the evolution of the bed. Whilst the mean bed level is equal between runs, subtle differences in the locations of bed level rise, indicated by the difference in maximum bed level rise, are having an impact on local shear stress distributions. With the banks

particularly sensitive to the magnitude of flows, a small localised change in bed level can tip the balance between an eroding and a stable bank. Thus whilst three new floods are included, these may not be of sufficient magnitude to have an impact on the bank erosion. The maximum bank erosion rates mirror the mean bank erosion rates with the greatest differences found on the right channel side when the magnitude of floods increases.

Scenario (4): engineering around section 350

The area around cross-section 350, located around 3000 m downstream, is particularly problematic. It has experienced high levels of sedimentation (see Figure 4.6b) and has extensive bank erosion. Land owners are keen to manage the system around this bend better. This is to prevent further loss of land and the possible risk to the flood levee which is currently situated around 3 m away from the eroding bank face. As such, it is an ideal location to explore two possible channel engineering solutions.

In scenario 4a, the channel is narrowed from 32.5 m to 25 m and both banks are fixed at node 350. The new channel remains wider than the average channel width for the study reach of 17.5 m. The model is run for two years. From the results, fixing the banks successfully prevents the previous 0.42 m of bank erosion from the left bank. Narrowing continues on the inner right bank but this is reduced from 0.4 m in the unprotected case to 0.23 m in the protected scenario. This reflects the increase in shear stress on the right hand side as the left channel width remains fixed. When the impact of the engineering on the bed level change is considered some interesting results are produced. Figure 9.7 shows the difference in bed level change in the reach upstream and downstream of node 350 which is subjected to bank protection. Node 350 degrades. This is because the narrow channel can no longer adjust and has greater flow depths for a given discharge. This leads to enhanced sediment transport resulting in scour. The impact of this is clear in the four downstream nodes which experience up to 0.04 m of aggradation over the 2-year period. This occurs due to the influx in sediment from the upstream node. Furthermore, as node 350 degrades, the upstream slope increases resulting in progressive upstream degradation. The downstream slope reduces which encourages deposition. At node 360, the width averaged bed level rise is 0.03 m (averaged across the left and right channel sides). When put into a

flood risk context, this increase in bed level is relatively small and equates to around a 5% loss in channel capacity. However, this may become problematic after longer timescales.

Figure 9.7: Impact of engineered reach on upstream and downstream bed-level changes.

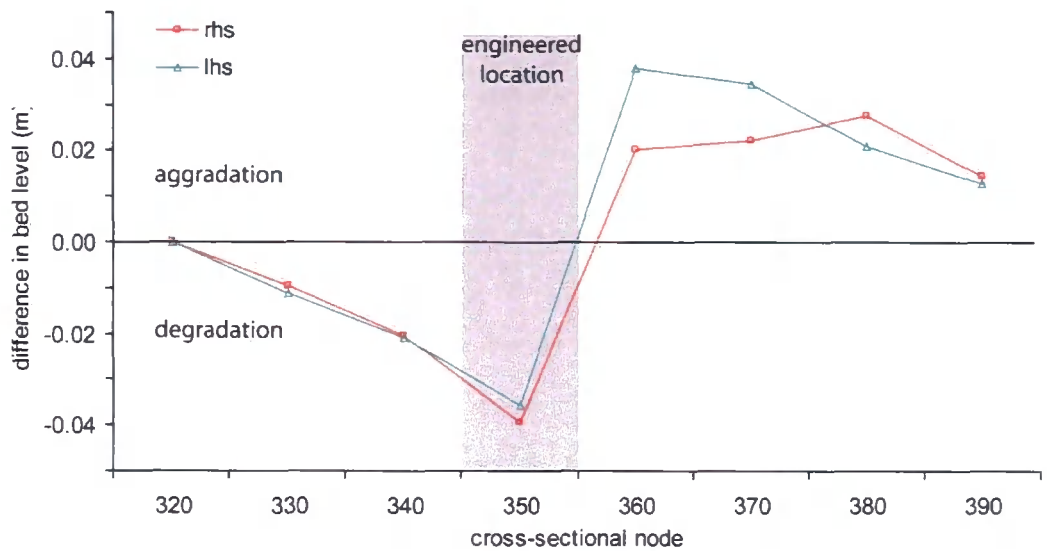

Scenario 4b tests a more drastic engineering option which involved straightening the river between cross-section 340 and 370 thereby removing cross-sections 350 and 360. This is shown in Figure 9.8a. The straightened reach reduced the river's length by 75 m and increased the channel's slope from 0.0031 to 0.0033. The newly straightened reach is a uniform 19.2 m wide (the channel width at cross-section 370), has fixed channel banks and is straight so has a curvature of 0. Figure 9.8 shows the impact that the engineered reach has on the upstream and downstream bed levels. First, in the upstream node, the bed level aggrades to a lesser extent than in the normal channel. This is due to the increase in slope. As described in Section 8.4.2 and shown in Figure 8.11, slope is calculated forwards so that the steeper channel created from the engineering is applied at node 340. This reduction in aggradation propagates upstream to node 330. Downstream of the engineered reach, the results are very interesting with significant aggradation occurring at node 370 and further downstream. With slope equal at node 370 in both normal and engineered cases, the differences in aggradation are attributed to the flushing out of sediment from the engineered reach due to enhanced sediment transport.

Figure 9.8: Impact of an engineered reach on (a) slope and (b) bed level change.

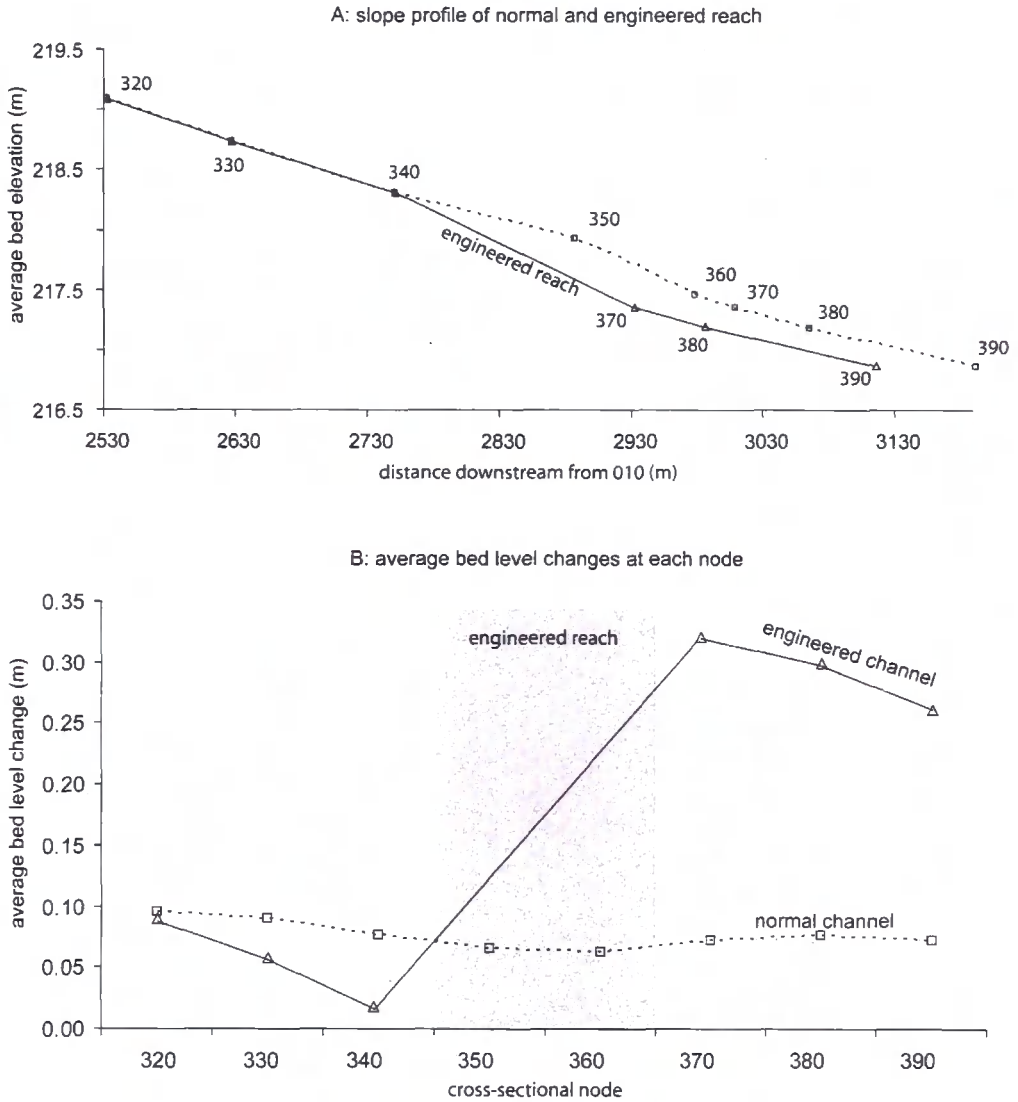

Aggradation at node 370 is 0.32 m. To place this aggradation into a flood context, the VPE equation [5.5] for calculating discharge from stage using the channel geometry, is used alongside the two bank full flow areas. The engineered area is 6.1 m^2 less than the normal area of 38.4 m^2. 6.1 m^2 is calculated as 0.32 m multiplied by the channel width of 19.2 m. This is a 16% loss in channel area when compared with the normal channel area. Using the VPE equation the discharge required to raise the flow level to its bank full limit is calculated at 99.1 $m^3 s^{-1}$ for the normal area and 73.6 $m^3 s^{-1}$ for the engineered scenario: a difference of 25.5 $m^3 s^{-1}$. For this analysis, the slope and D_{84} values required in the VPE equation were the same for both cases. Figure 6.13 and Table 6.7 present a similar analysis

using observed bed level rise to determine changes to flood risk. Here a 0.33 m increase in bed level at cross-sectional location 030, corresponded to a 22 m^3 s^{-1} drop in bankfull discharge and this increased both the number and duration of flood events. Thus a similar impact on flood risk may be experienced at cross-sectional node 370 if the simulated engineering was implemented.

Finally, Table 9.3 presents the total width adjustments at each node after the normal and the engineered scenarios. The results show substantial channel adjustments in the nodes upstream of the engineered reach with up to 1.15 m more bank erosion occurring. This is due to the increase in slope and depth due to scour which increases shear stress leading to bank erosion. This amount of bank erosion far exceeds the maximum bank erosion for the entire river in the normal simulation with the maximum bank erosion noted at cross-section 0.42 m. Thus, whilst the problematic erosion at cross-section 350 has been removed, far worse erosion has been created from this engineering upstream and the flood risk has been exacerbated in the downstream reach.

Table 9.3: Total width change in the "normal" and the "engineered" scenarios. Positive values indicate bank erosion. In the engineered case, no data is present at nodes 350 and 360 as these have been removed by the engineering and the channel sides made fixed.

node	normal	engineered	difference
	total width adjustment (m)		
320	0.09	0.00	-0.09
330	0.26	0.64	0.38
340	0.15	1.30	1.15
350	0.42	removed	n/a
360	0		n/a
370	0	0	0
380	0	0	0

9.4 CHAPTER SUMMARY

Three research questions were addressed in this chapter. The results and discussion have shown the answer to question 5, that a quasi-2D model can be used to simulate vertical and lateral channel change. The combination of TRIB which simulates the hydrology and sediment transport and a split channel lateral adjustment component, that is driven by

lateral differences in shear stress, is effective. The discussion has also highlighted the need to include variable hydrology and curvature into the model, thereby answering question 6. The variable hydrology captures peaks in discharge which are responsible for sediment transport and bank erosion. Curvature, allows the meandering nature of natural rivers to be incorporated with bank erosion dominant on the outer curved banks. Alongside the two important features of a variable hydrology and curvature driven bank erosion, further key features were important. First, was splitting the channel into two halves to include lateral information on flow depths, grain size and shear stress. This enables bank erosion to be simulated as a function of channel deepening and curvature induced shear stress distribution. In addition, it allows the bed material to be sorted laterally. This is done as a function of the downstream sediment transport capacity, that varies with lateral differences in flow depth and curvature induced shear stress. Second, simulating bank erosion by scaling with excess shear stress is valuable. This allows for small and large amounts of bank retreat depending on the size of the flood event. This effectively simulates fluvial entrainment processes at moderate and high flows and bank collapse at the maximum flows. Third, simulating channel narrowing at low flows, when shear stress is low, adds an additional aspect to lateral channel change. When combined with bank erosion, the model can simulate asymmetrical, flow-dependent channel change. Channel migration is simulated in zones where bank erosion and channel narrowing both occur. Finally, allowing the critical shear stress threshold for erosion and deposition to vary laterally and downstream crucially allows bank protection to be simulated. It also enables some banks to be more susceptible to bank erosion than others.

The final question addressed in this chapter used scenarios to explore different situations. This achieves Objective 6 from Chapter 1. These scenarios demonstrate the model's capabilities and allow the response of the channel to be predicted under changes in hydrology and different river engineering options. First, the results highlight the feedbacks and interactions in the channel change process. In particular, changes in bed level and grain size are responsible for lowering or raising shear stress. These leads to the cessation or initiation of bank erosion. Furthermore, the bank erosion feedback is evident. Bank erosion increases channel width, this reduces shear stress and inhibits further erosion. Second, the

results emphasise the role that bank protection in the Upper Wharfe study reach has on confining the channel and preventing bank erosion. Without it, the channel may exhibit a more sinuous pattern, be wider and be wandering in nature. Thus, it may reflect conditions before river training began in monastic times (Section 3.4). The simulated removal of bank erosion also raises caution to river restoration schemes in the Upper Wharfe. These may be employed to remove sections of bank protection. In many places this may result in severe bank erosion. Third, the nature of the flow regime is important for channel changes, particularly lateral. Changes in flow regime as a result of climate change, especially to the magnitude of peak flows may have substantial implications for channel change. Such changes are anticipated by Arnell and Reynard (1996) and Fowler and Kilsby (2007) as discussed in Section 2.3. The latter predict up to a 20% rise in the magnitude of winter flows. However, with bank erosion found to occur to a greater extent than bed level change (echoing findings made by hydraulic geometry models), the associated increase in channel capacity may result in a reduction in flood risk. This conflicts with the typical assumption that climate change will result in enhanced flood risk. This discrepancy may be explained by the model set up with the model using a fixed input capacity and ignoring sediment input from the banks. However, flow, sediment transfer and channel change, and their interactions, are important considerations. The final findings from the scenarios were the important implications that river engineering schemes have on channel changes. These agree with findings made by Brookes (1988, 1997) in Section 2.6. Whilst the engineering scenarios are both successful in reducing bank erosion and the accumulation of sediment, the impacts experienced upstream and downstream of the engineered reach are substantial. Downstream sedimentation is enhanced, reducing the channel's capacity and increasing the flood risk. This association between sediment delivery and flood risk has be made by many (e.g. James, 1999; Stover and Montgomery, 2001; Korup *et al.*, 2004; Pinter and Heine, 2005; Lane *et al.*, 2007). Upstream bank erosion was found to be much more severe than initial problematic erosion. These results demonstrate caution and the need to consider sediment transfer and channel change processes, before channel management decisions are made. This is particularly essential when land use and climate change implications are also considered.

CHAPTER TEN: CONCLUSIONS

10.1 INTRODUCTION

This chapter revisits the main thesis aims and research questions set out in Chapter 1. It makes conclusions about the interactions between coarse sediment transfer and channel change, and the implications of river engineering schemes for upland river systems. These findings are placed into a flood risk context.

The thesis aims were:

- *to explore sediment dynamics and channel change in an upland gravel-bed river and to assess the impacts of such changes on flood risk; and*
- *to develop a model that simulates annual to decadal scale channel change for exploring the impacts of river management.*

The first aim was achieved using the field-based data collection and analysis. It bases conclusions on past and current channel changes and the factors driving them (Chapters 4, 5 and 6). The second aim was achieved through successful model development and application to scenarios (Chapters 7, 8 and 9). Answers to the seven key research questions set out in Chapter 1, are used to structure these conclusions, in relation to the collection of field data (Section 10.2) and modelling (Section 10.3). In addition, this chapter will reach conclusions regarding the methodological approaches adopted during this research, specifically discussing the advantages and limitations of the field-based (Section 10.2.2) and modelling techniques (Section 10.2.3). The last section (Section 10.4) brings the thesis to a close with some final concluding remarks and further research needs.

10.2 CONCLUSIONS ARISING FROM FIELD EVIDENCE

The field-based approach was used to collect data on channel morphology and the primary factors driving channel change. These included: (1) capturing the channel geometry downstream and over time using repeat cross-sectional surveys; a bank erosion study; and information on channel curvature and flow paths around bends; and (2) obtaining data describing the hydrology; bed material; and sediment transport regime. These data were analysed to answer four research questions (Section 10.2.1) and applied to the modelling side of the project to answer a further three research questions (Section 10.3.1).

10.2.1 ANSWERS TO RESEARCH QUESTIONS

Question 1: How does in-channel sedimentation in an upland gravel-bed river vary through space and time?

The cross-sectional dataset provides an excellent resource for exploring patterns of bed level change through space and time for three reasons: (1) it was specifically designed to yield change data; (2) it collects data at a sub-annual time scale; and (3) it is six years in length. Results to 2004 have been published (Lane *et al.*, 2007; Reid *et al.*, 2007a). However, this three year period was insufficient to capture the spatial and temporal dynamics of river response and focused more upon characterising the magnitude and frequency of sediment delivery and transfer events. The research focused primarily upon evidence regarding the spatial and temporal patterns of river bed sedimentation and its implications for flood risk. The analysis demonstrated that sedimentation varies spatially and temporally. Spatially, in the Upper Wharfe study reach, bed level changes downstream vary over short scales (< 100 m). Variations can fluctuate between degradation in relatively few locations to predominant aggradation. Degradation was typical at meander bends where bank protection was present and aggradation dominated on meanders that were free to erode. In particular substantial aggradation was noted at the bends located at cross-sections 080 (the Gravel trap bend) and 350 (Heber bar). Maximum levels of aggradation were found around the removed Gravel trap where a bed level rise of 0.67 m ± a calculated error

of 0.031 m was recorded after 6-years of monitoring. Furthermore, spatial patterns in the Wharfe vary over long spatial scales (~ 1 km). The upper 3 km reach was found to have twice as much aggradation as the lower 2.6 km reach with a mean bed level difference of 0.11 m ± 0.0022 m between the upper and lower reaches. Temporally, sedimentation is also highly variable with up to 0.5 m ± 0.007 m of aggradation recorded in one location between a four month period. In addition, certain zones do not exhibit a net bed level rise or fall over time but instead switch between aggradation and degradation over short-timescales. In these zones, short-term sedimentation may be unobserved from longer term patterns, which are visually noticeable in many locations (e.g. Heber bar). This short term sedimentation may be sufficient to increase flood risk.

Question 2: At what rate do unprotected river banks, in upland gravel-bed rivers, erode and what processes drive this bank erosion?

Rates and mechanisms of bank erosion in upland river channels, like the Upper Wharfe, vary between banks but there is a clear distinction between river banks on meander bends and straight sections. Using bank erosion pins on four eroding banks in the study reach, bank retreat was found to be more rapid on the outside of meander bends due to the shifting of the high velocity core to the outside bank. Annual rates of erosion on bends, from fluvial entrainment and weathering, result in between 0.18 and 0.21 m $year^{-1}$. On straight sections, bank erosion rates are lower at around 0.07 m $year^{-1}$. These rates of retreat are similar to those found by other studies on similar rivers (e.g. Hooke, 1980; Thorne and Tovey, 1981; Lawler, 1986; Lawler *et al.*, 1999). Seasonal differences in bank retreat are also noted with bank erosion higher in the winter months. Since large flood events occur during the summer and winter periods, the higher bank erosion rates in the winter are attributed to weathering processes. These are enhanced in the winter by freeze-thaw processes and piping and sapping from the bank face. Bank collapse in the Upper Wharfe is also an important feature of channel change. This process operates over periods longer than one year. Bank collapse from one event during the monitoring period led to 0.75 m of retreat but evidence from aerial photos indicates that rates of bank retreat in the past have been

much more significant with up to 12 m of erosion occurring in one location over a period of time less than 5 years but possibly during a single event.

Question 3: What are the mechanisms that drive these spatial and temporal patterns of channel change?

A key feature of the Upper Wharfe study reach, is its concave slope profile. Over longer time-scales, this promotes aggradation as the reducing slope lowers the transport capacity leading to lower sediment transport rates. Conversely one may argue that a product of the deposition is the feedback on slope, thus promoting further bed level change. Data from the impact sensors, which record little sediment transport out of the reach, and from the bed material characterisation, which show a strong downstream fining trend, support this finding. Over shorter annual and seasonal time-scales, temporal patterns of channel change, specifically in-channel sedimentation, were shown to be controlled by: (1) the hydrology; and (2) the supply of sediment. Both operate together, a relationship found by many (e.g. Hey and Thorne, 1986; Beschta, 1988; Werritty, 1997). Higher discharges are required to transport sediment once it is in the channel. However, the channel's response to the flow regime must be considered alongside the supply of sediment. If sediment supply is abundant, higher discharges are likely to lead to aggradation (e.g. Parker, 1979) whilst degradation may occur if supply is limited (Liebault and Piegay, 2000; Rinaldi, 2003). Furthermore, high intensity rainfall events are required to initiate sediment delivery from the hillslopes through shallow landslides.

Spatial patterns of channel change are attributed to features of the channel geometry. The overall slope of the reach is identified as the primary control over the net aggradation. At short spatial scales (< 100 m) key characteristics were identified as changes in slope, high curvature, tributary inputs, man-made features such as bridges and larger geomorphic controls. The latter refers to the base level control at Starbotton created by the Cam Gill Beck flood event in 1686. This episodic event appears to have had a lasting effect on the main stem morphology and behavior of the study reach and questions the importance of such features on upland channels. This observation follows on from research into sedimentary links are their importance (Rice and Church, 1998; Rice, 1999; Rice and

Church, 2001). Curvature is particularly important for lateral channel change as it encourages inner bank aggradation and faster rates of fluvial entrainment on the outer bank. This inner bank aggradation, reduces channel slope which reduces the transport capacity promoting further deposition. Thus downstream differences in sediment transport capacity must account for lateral variations and bank erosion. Furthermore, the outer bend zone scours eventually leads to bank collapse. The combined effect of both inner deposition and outer bank erosion results in channel migration. This demonstrates the importance of including a lateral adjustment component for curved reaches in the model. Spatial patterns of channel change, in particular bank erosion, are strongly controlled by river engineering which inhibits lateral channel change, particularly in the upper sections of the study reach.

Question 4: What implications do in-channel sedimentation and bank erosion have for flood risk?

Rates of in-channel sedimentation observed in the Upper Wharfe were found to have important implications for flood risk in the reach. Observed rates of sedimentation, reduced the channel's capacity to hold flow by an average of 7%, but several locations lost over 30% of their capacity following 4-years of sedimentation. These findings were based on hydraulic calculations using the cross-sectional geometry in December 2002 and December 2006. This increased the number of annual over bank flows by an average of 2.7 as well as increasing the time flow is out of bank by 12.8 hours. Thus, it is essential that upland river management considers the important role that coarse sediment transfer has for flood risk. It is especially important that localised, short-term fluctuations in bed level are considered. These may be deemed less important than zones exhibiting longer term steady rates of bed aggradation.

10.2.2 FIELD METHODS

The answers to questions one and two were based heavily on two data sources: cross-sectional resurveys; and the bank erosion study. Alongside the methods used to collect these data, a further range of data collected from the Wharfe study reach provided useful information to aid with explaining spatial and temporal patterns of channel change and flood risk implications (questions three and four). The data were also used for model

development and application. These additional data sources included: (1) field surveys; (2) channel curvature from digitised LiDAR; (3) flow paths around bends; (4) discharge data; (5) bed material characterisation; and (6) data from sediment impact sensors. Key methodological conclusions and limitations from these data types can be made.

Developing a robust monitoring strategy to capture bed level change using remote static cross-sectional surveys was crucial. Patterns may be misinterpreted if: (1) the total length of surveying is too short; longer data sets are essential but limited due to constraints on time and cost; (2) the time between surveys is too short to capture short-term changes; ideally surveying should take place after every flood, although this can be impractical; and (3) survey spacing is insufficient to capture the spatial variability of downstream channel change.

The combined bank pin and bank top resurvey approach worked well as the pins captured short-term small scale erosion on the bank face and the surveys captured larger bank retreat over a longer time period. This monitoring strategy was limited by insufficient monitoring sites and the timescale of monitoring: both difficult within the scope of the project. Whilst lost pins and negative readings are thought to be problematic, instead, these can provide processes information such as on desiccation failure and soil fall from upper parts of the bank face.

The field surveys provide useful qualitative data that can be used to support findings and to provide spatial information about channel features such as eroding banks, sediment bars and bank protection. Furthermore the field surveys are valuable during the design of field monitoring approaches, for example identifying locations of pebble count sites and bank erosion study sites. They do not provide any quantitative data and are highly subjective and open to interpretation.

The channel curvature was effectively digitised in a GIS framework and provided high resolution (~ 2 m spacing) information about the downstream channel sinuosity. This was essential for use with the flow paths around bends. Mapping the fastest flow path around several bends of varying curvature provided useful information about processes operating

around bends. There were three limitations with this approach: (1) the flow path was measured at a constant depth; (2) the measurements were made during a moderate flow; and (3) several bends were discounted due to deep outer bank sections. All these limitations were for logistical reasons.

The discharge data were converted from stage records using Ferguson's (2007) variable power equation, overcoming issues associated with other flow resistance equations at low flows. Limitations on the availability of stage records led to the determination of a 2-year period that was representative of the decadal flow regime. Daily discharge records from Flint Mill, 70 km downstream, provide additional information on the flow regime for analysis. However, these data do not capture peaks in discharge which are essential for sediment transport and bank erosion. It is important to use hourly or sub-hourly records where available.

The bed material was characterised using a hybrid approach which combined three bulk samples with 16 pebble counts. This approach sought to overcomes logistical issues associated with collecting the bulk samples. However, when the time taken to manipulate the data is considered alongside the introduction of error associated with each step, the bulk sample approach may indeed have been a more successful approach to adopt. Transformations were used to convert the pebble counts into the equivalent volumetric samples. The grain size distributions generated demonstrated a strong downstream fining pattern in the Wharfe and provided essential data for other data analysis including roughness and porosity estimates. The latter was used during the reconstruction of the morphological sediment budget and raised an important issue: in reaches where downstream fining is high, a single porosity value is insufficient as porosity was shown to vary downstream. This is often overlooked when constructing a sediment budget from cross-sectional surveys.

The final field-based methodology, used impact sensors to provide information on sediment transfer within the reach. This new method overcomes many problems associated with collecting data on sediment transport. The data collected were invaluable and were used in several analyses including spatial and temporal patterns of in-channel sediment and when

reconstructing the morphological budget from the cross-sectional surveys. The impact sensors supported the zero output limit at Starbotton and provided an indication on transport times. Furthermore, the impact sensors can provide a useful indication of channel response. Aggradation is anticipated if the ratio of sediment input to output increases (i.e. more sediment enters the reach than leaves). Key limitations with the impact sensors relate to: (1) the location of the senor within the channel; (2) the 255 logger saturation point; (3) the inability to infer sediment volumes from the data; and (4) when comparing old and new sensors.

In general, the field monitoring strategy used to collect data from the Upper Wharfe study reach was well designed, rigorous and provided valuable data for analysis and modelling.

10.3 CONCLUSIONS ARISING FROM THE MODELLING APPROACH

The second thesis aim was to develop a model for simulating channel change. This was done in four steps. The first step applied data from the Wharfe study reach and applied it to TRIB, a one-dimensional sediment routing model (SRM). Step two made important modifications to the model and the boundary conditions used to run the model, notably by adding in a variable hydrology. The third step involved coupling a lateral channel change component into the model for simulating bank erosion and deposition in straight channels. The final step incorporated channel curvature into the model, allowing it to simulate meandering channels and vertical and lateral channel change.

10.3.1 ANSWERS TO RESEARCH QUESTIONS

Question 5: Can a simple quasi two-dimensional modelling approach be used to simulate vertical and lateral channel change in a natural, sinuous upland gravel-bed river?

The model results and discussion demonstrated that a simple quasi-2D approach can be used to simulate both vertical and lateral channel changes in a natural channel. Central to determining the model's success was the large and detailed dataset collected from the Upper Wharfe. The downstream fining profile of the channel was particularly important during initial model testing and development. In addition, information on mean annual bed

level changes, bedload transport rates and locations and rates of bank erosion were used. The model was capable of predicting these observations well. However, the model was unable to simulate the spatial details of aggradation and degradation. This is attributed to the strong influence that slope has on the locations of aggradation and the inability of the model to incorporate all the associated downstream variability in slope. Since TRIB does not incorporate backwater effects in its hydraulic component, it is unlikely to produce small scale features well (e.g. bars around bends).

Question 6: Within the model, how important are the inclusion of a variable discharge and curvature driven shear stress distribution for predictions of channel change through space and time?

Numerous modifications were made to the model including allowing for variable channel widths and slopes and allowing Manning's n to update alongside changing grain size. Two of the most important modifications made to the model included: (1) incorporating variable hydrology; and (2) using curvature to redistribute shear stress laterally across the channel. Both are crucial parameters. As demonstrated during the field-based analysis, both are factors responsible for driving vertical and lateral channel change. Hydrology is essential for driving sediment transport and is therefore responsible for changes in bed level. It is also central to the bank erosion and channel narrowing components of the model which allow lateral changes to take place. The analysis also demonstrated the importance of using an hourly or sub-hourly hydrograph which captures peaks in flow. These peaks essentially drive vertical channel change and bank erosion. Low flows allow the channel to narrow, simulating the succession of vegetation onto the edges of channel bars. Curvature is also essential to the erosion and narrowing process and without it the model fails to simulate the channel dynamics around meander bends. These modifications turn a research tool for exploring downstream fining patterns and sediment transport processes into something which can simulate several years of vertical and lateral channel change. Thus it can be used for management purposes.

Question 7: What are the implications of changes in hydrology and river management for channel change and flood risk?

The answer to question seven was determined using a series of model scenarios. The success and validity of these model outputs is partly based on the successful calibration of the model. Two findings were noted when the hydrology was altered in the scenario simulations: (1) increasing the magnitude and the frequency of flood events was found to have greater impact on lateral channel change than vertical channel change; although vertical changes do occur and lead to a reduction in the channel's capacity to hold flow; (2) increasing flow magnitude has a greater impact on channel change than increasing flood frequency. These findings demonstrate potential impacts of future climate change on upland systems. They also emphasise caution when using the average 2-year hydrology to predict bed level changes and lateral adjustments.

When river engineering scenarios are explored, the results are somewhat unsurprising. Narrowing and straightening the channel in an attempt to prevent excessive bank erosion and high levels of sedimentation simply shifts the problem upstream and downstream of the engineered reach. Bank erosion upstream of the engineering reach is recorded at higher rates than the original bank erosion whilst aggradation downstream of the engineered reach is also substantial. Aggradation recorded in the downstream section resulted in a 16% loss in channel capacity and a 25 $m^3 s^{-1}$ reduction in the discharge required to raise the flow stage to bank full. If implemented, the engineering simulated in this scenario, is likely to have important implications for flood risk. These findings emphasise the negative impacts that river engineering schemes can have on a river system particularly if coarse sediment transfer is not considered.

10.3.2 THE MODELLING APPROACH

The fully developed research model couples TRIB (Ferguson *et al.*, 2006), a one dimensional sediment routing model that simulates flow hydraulics and sediment transport, with a simple model of lateral channel change. The model is capable of simulating vertical bed level change, and downstream fining and asymmetrical lateral change including bank erosion and deposition. It is applicable to single-thread, meandering, coarse gravel-bed rivers. The modelling approach was essential to explore the potential impacts of different scenarios on channel change. Only inferences could be made from past observations. Whilst the field data demonstrate the channel changes resulting from the interaction of a range of factors, modelling enables the effects of any one factor to be explored. Yet the successful development and application of the model must largely be attributed to the comprehensive dataset collected from the Wharfe.

The volume and detail of input data and boundary conditions required to run the model are moderate but the availability of additional data to test and calibrate the model is valuable. Data required to run the model includes: (1) the channel width and left and right channel elevations for each node; (2) an estimate of the input grain size distribution which should ideally represent the coarser material in the upstream reaches; (3) information on the locations and relative contribution of any tributary inputs; (4) a variable hydrology with a small time-step; and (5) information on locations of bank protection. From this data the model derives additional boundary information including: (1) channel slope; (2) downstream variability in grain size; and (3) Manning's n from the grain size.

The model calculates the flow hydraulics using Manning's flow resistance law. This is used to calculate flow depth which alongside slope, determines the shear stress. Sediment transport is calculated using shear stress alongside the grain size characteristics (which are represented using eight grain size classes) within the Wilcock and Crowe (2003) surface based model of sediment transport. The sand boundary within the sediment transport equations, used to determine the critical shear stress threshold for the initiation of transport, was set at 8 mm. A fractional Exner equation for sediment continuity is used alongside the

sediment transport rates to calculate vertical bed level changes. The lateral sub-model coupled with the hydraulics and sediment transport, uses a split channel approach similar to Lancaster and Bras (2003) and Stark (2006). This enables lateral shear stress variability to be incorporated into the model as a function of side differences in flow depth. The average slope of the two channel sides is used. Further lateral distribution of shear stress is included into the model as a function of curvature. Bank erosion is simulated as a function of excess shear stress above a critical threshold similar to the Ikeda *et al.*, 1981. Channel narrowing occurs at a constant rate when shear stress falls below a second, lower critical threshold. The model can simulate asymmetrical channel change in response to flow variability. Additional model features incorporated to improve the model's predictive abilities include: (1) a cap on the elevation differences to prevent excessive overdeepening and (2) the even distribution of sediment lost in the mid-channel region due to lateral change, to maintain sediment continuity.

Some suggested improvements to the model, which may be important if the model is applied over longer timescales or to different systems, include: (1) allowing curvature to update as bank erosion occurs; (2) incorporating material from the banks into the sediment transport calculations; and (3) an improved hydraulic component to include backwater effects and improve locations of aggradation and degradation. Furthermore the model and its simplistic nature may support the addition of a flood inundation sub-model to simulate the flood risk associated with channel change and a habitat sub-model to assess the impacts of channel changes on habitat availability.

10.4 FINAL CONCLUDING REMARKS

The combination of a field-based and modelling approach worked well in achieving the thesis aims. Observations from field data collection allowed a detailed analysis of sediment transfer and channel change processes to be made. Concurrently, data collected were used to develop and to apply the channel change model. This modelling approach enabled scenarios to be explored, thereby further exploring interactions between coarse sediment transfer, channel change, river engineering and flood risk in an upland gravel-bed river.

This research has highlighted that channel change in upland systems is a complex process that varies spatially and temporally and in response to a range of driving factors: mainly valley long profile, hydrology, sediment supply and river engineering. Extensive field monitoring is required to obtain sufficient data to explain and to understand past and present changes whilst modelling is an essential tool for exploring future changes with respect to hydrology (as a possible result of climate change) and river managing options. Even with adequate data and a robust modelling approach, confidence in understanding upland systems is limited. This again reflects the complexities involved in upland river systems and the inability to measure and model all aspects of the sediment transfer and channel change process. Future research is required to further develop our understanding of river system response in upland environments to changes in hydrology and sediment supply that are anticipated from future climate change (e.g. Stover and Montgomery, 2001; Lane *et al.*, 2007). In particular research is required to explore the impacts of increases in coarse sediment delivery on channel change over the reach scale (i.e. 100 m to 10 km) and for sub-annual to decadal time-scales. This would build on work over longer timescales (e.g. Knox 2000; Coulthard *et al.*, 2000; Macklin and Lewin, 2003).

In addition, there is an overwhelming need to consider sediment transfer and channel change before river management decisions are made. This work has highlighted scope for further model exploration including: (1) simulating future climate change scenarios; (2) exploring the impacts of bed level rise on reach-scale downstream fining; and (3) the impacts of further human intervention in river systems, for example the construction of bridges. Increasing evidence also suggests that, where possible, hard engineering schemes should not be applied and river restoration should occur. This would allow river systems in upland environments to adjust naturally in response to changes in the discharge and sediment regimes imposed upon them. Yet, human pressures on upland floodplains often makes the "doing nothing" approach unfeasible. Attention should therefore concentrate on managing sediment sources in an attempt to reduce downstream sedimentation and its associated problems.

REFERENCES

Abernethy B, Rutherfurd ID. 1998. Where along a river's length will vegetation most effectively stabilise stream banks? *Geomorphology* 23: 55-75.

Abernethy B, Rutherfurd ID. 2000. The effect of riparian tree roots on the mass-stability of riverbanks. *Earth Surface Processes and Landforms* 25: 921-937.

Ackers P, Charlton FG. 1970. Meander geometry with varying flows. *Journal of Hydrology* 11: 230-252.

Ackers P, White WR. 1973. Sediment transport: a new approach and analysis. *Journal of Hydraulic Engineering* 99: 2041-2060.

Adams DD, Darby DA, Young RJ. 1979. Analytical techniques for characterising the chemistry and geology of fine-grained sediments. *Abstracts of papers of the American Chemical Society.*

Affrin J, Ghani AA, Zakaria NA, Yahya AS. 2002. Evaluation of equations on total bed material load. *International Conference on Urban Hydrology for the 21st Century.* Kuala Lumpa, 321-327.

Allen JRL. 1982. *Sedimentary Structure, Their Character and Physical Basis.* Vol.1. Elsevier, Amsterdam. 538pp.

Allred TM, Schmidt JC. 1999. Channel narrowing by vertical accretion along the Green River near Green River, Utah. *Geological Society of America Bulletin* 111: 1757-1772.

Alonso CV, Combs ST. 1986. Channel width adjustment in straight alluvial streams. *Proceeding of the 4th Federal Interagency Sedimentation Conference*, Las Vegas. 5-31 5-40.

American Society for Testing Materials. 1978. Standard methods of sampling aggregates. ANSI/ASTM D75-71. www.astm.org.

Andrews ED. 1982. Bank stability and channel width adjustment, East Fork River, Wyoming. *Water Resources Research* 18: 1184-1192.

Andrews ED. 1983. Entrainment of gravel from naturally sorted riverbed material. *Geological Society of American Bulletin* 94: 1225-1231.

Andrews ED. 1984. Bed-material entrainment and hydraulic geometry of gravel-bed rivers in Colorado. *Bulletin of the Geological Society of American Engineers* 95: 371-378.

Andrews ED. 1986. Downstream effects of Flaming Gorge Reservoir on the Green River, Colorado and Utah. *Geological Society of the America Bulletin* 97: 1012– 1023.

Andrews ED, Erman DC. 1986. Persistence in the size distribution of surficial bed material during an extreme snowmelt flood. *Water Resources Research* 22: 191-197.

Andrews ED, Parker G. 1987. Formation of a coarse surface layer as the response to gravel mobility. In *Sediment Transport in Gravel-bed Rivers.* Thorne CR, Bathurst JC, Hey RD. (eds.), John Wiley and Sons Ltd., 269-325.

Armanini A, Di Silvio G. 1988. A one-dimensional model for the transport of sediment mixture in non-equilibrium condition. *Journal of Hydraulic Resources* 26: 275-292.

Arnell NW, Reynard NS. 1996. The effects of climate change due to global warming on river flows in Great Britain. *Journal of Hydrology* 183: 397-424.

Arulandan K, Gillogley E, Tully R. 1980. Developments of a quantitive method to predict critical shear stress and rate of erosion of naturally undisturbed cohesive soils. *Report GI-80-5, US Army Waterways Experiment Station*, Vicksburgh, Mississippi.

ASCE Task Committee. 1998a. River width adjustment. 1: Processes and mechanisms. *Journal of Hydraulic Engineering* 124: 881-902.

ASCE Task Committee. 1998b. River width adjustment 2: Modelling. *Journal of Hydraulic Engineering* 124: 903-917.

Ashida K, Michiue M. 1971. An investigation of river bed degradation downstream of a dam. *Proceedings of IAHR, 14th Congress* 3:247-255.

Ashmore PE, Church M. 1998. Sediment transport and river morphology: a paradigm for study. In *Gravel-bed Rivers in the Environment.* Klingeman PC, Beschta RL, Komar PD, Bradley JB. (eds.). Water Resources Publications, Colorado. 115-148.

Bagnold RA. 1977. Bedload transport in natural rivers. *Water Resources Research* 13: 303-312.

Bagnold RA. 1980. An empirical correlation of bedload transport rates in flumes and natural rivers. *Proceedings of the Royal Society of London* 372: 453-473.

Baker RA. 1977. Stream-channel response to floods, with examples from central Texas. *Geological Society of America Bulletin* 88: 1057-1071.

Ballantyne CK. 1991. Late Holocene erosion in upland Britain: climatic deterioration or human influence. *Holocene* 1: 81-85.

Barker R, Dixon L, Hooke J. 1997. Use of terrestrial photogrammetry for monitoring and measurement bank erosion. *Earth Surface Processes and Landforms* 22: 1217-1227.

Batalla RJ. 1997. Evaluating bed-material transport equations using field measurements in a sandy gravel-bed stream, Arbucies River, NE Spain. *Earth Surface Processes and Landforms* 22: 121-130.

Batalla RJ, Gomez CM, Kondolf GM. 2004. Reservoir-induced hydrological changes in the Ebro River basin (NE Spain). *Journal of Hydrology* 290: 117-136.

Bathurst JC. 2002. At-a-site variation and minimum flow resistance for mountain rivers. *Journal of Hydrology* 269: 11-26

Bathurst JC, Thorne CR, Hey RD. 1979. Secondary flow and shear stress at river bends. *Journal of the Hydraulics Division, ASCE* 105: 1277-1295.

Bathurst JC, Graf WH, Cao HH. 1987. Bed load discharge equations for steep mountain river. In *Sediment Transport in Gravel-bed Rivers.* Thorne CR, Bathurst JC, Hey RD. (eds.). John Wiley and Sons Ltd. 269-325

Beck S. 1984. Mathematical modelling of meander interaction. In *River Meandering.* Elliott CM. (ed.). ASCE. 932-841.

Begin ZB. 1981. Stream curvature and bank erosion: a model based on the momentum equation. *Journal of Geology.* 89: 497-504

Bendix J. Hupp CR. 2000. Hydrological and geomorphological impacts on riparian plant communities. *Hydrological Processes* 14: 16-17

Beschta RL. 1998. Long-term changes in channel morphology of gravel-bed rivers: three case studies. In *Gravel Bed Rivers in the Environment.* Klingeman PC, Beschta RL, Komar PD, Bradley JB. (eds.). Water Resources Publications, Oregon. 229-256.

Bettess R, White WR. 1987. Extremal hypothesis applied to river regime. In *Sediment Transport in Gravel-bed Rivers.* Thorne CR, Bathurst JC, Hey RD. (eds.). John Wiley and Sons Ltd. 767-791.

Blom A, Parker G. 2004. Vertical sorting and the morphodynamics of bedform-dominated rivers: A modeling framework. *Journal of Geophysical Research* 109.

Booij MJ. 2005. Impact of climate change on river flooding assessed with different spatial model resolutions. *Journal of Hydrology* 303: 1760198.

Bracken LJ, Wainwright J. 2006. Geomorphological equilibrium: myth and metaphor?. *Transactions of the Institute of British* Geographers 31 167-178.

Bradbrook KF, Biron PM, Lane SN, Richards KS, Roy AG. 1998. Investigation of controls on secondary circulation in a simple confluence geometry using a three-dimensional numerical model. *Hydrological Processes* 12: 1371-1396.

Bras RL, Tucker GE, Teles V. 2003. Six myths about mathematical modelling in geomorphology. *Geophysical Monograph*. AGU. 135: 63-82.

Brasington J, Rumsby BT, McVey RA. 2000. Monitoring and modelling morphological change in a braided gravel-bed river using high resolution GPS-based survey. *Earth Surface Processes and Landforms* 25: 973-990.

Bravard JP, Amoros C, Pautou G. 1986. Impact of civil engineering work on the succession of communities in a fluvial system. *Oikos* 49: 92-111.

Brewer PA, Lewin J. 1998. Planform cyclicity in an unstable reach: complex fluvial response to environmental change. *Earth Surface Processes and Landforms* 23: 9089-1008.

Bridge JS. 1992. A revised model for water flow, sediment transport, bed topography and grain size sorting in natural river bends. *Water Resources Research* 28: 999-1023.

Bridge JS, Jarvis J. 1982. The dynamics of a river beds: a study in flow and sedimentary processes. *Sedimentology* 29: 499-541.

British Standards Institution. 1975. British standard methods for sampling and testing of mineral aggregates, sands and filers, part 1: sampling size, shape and classification. BS 812, BSI, www.bsi-global.com.

Brookes A. 1987. River channel adjustments downstream from channelisation works in England and Wales. *Earth Surface Processes and Landforms* 12: 337-351.

Brookes A. 1988. *Channelized Rivers: Perspectives for Environmental Management*, John Wiley and Sons, Chichester. 326.

Brookes A. 1997. River dynamics and channel maintenance. In *Applied Fluvial Geomorphology for River Engineering and Management.* Thorne CR, Hey RD, Newson MD. (eds.). John Wiley and Sons, Chichester, UK, 293-307.

Brookes SM, Crozier MJ, Glade TW, Anderson MG. 2004. Towards establishing climatic thresholds for slope instability: use of a physically-based combined soil hydrology-slope stability model. *Pure and Applies Geophysics* 161: 881-905.

Brunsden D, Thornes JE. 1979. Landscape sensitivity and change. *Transactions of the Institute of British Geographers* 4: 463-484.

Bryant RG, Gilvear D. 1999. Quantifying geomorphic and riparian land cover changes either side of a large flood event using airbourne remote sensing: River Tay, Scotland. *Geomorphology* 29: 307-321.

Buchanan TJ, Somers WP. 1969. Discharge measurements at gauging stations. *USGS, Techniques of Water Resources Investigations*. Book 3, Chapter A8.

Bull WB. 1979. Threshold of critical power in streams. *Geological Society American Bulletin* 90: 453-464.

Bull LJ. 1997. Magnitude and variation in the contribution of bank erosion to the suspended sediment load of the River Severn, UK. *Earth Surface Processes and Landforms* 22: 1109-1123.

Buma J, Dehn M. 1998. A method for predicting the impact of climate change on slope stability. *Environmental Geology* 35: 190-196.

Bunte K, Abt SR, Potyondy JP. 2001. Portable bedload traps with high sampling intensity for sampling gravel and cobble bedload transport in wadable mountain stream. *Water Resources Research* 33: 1993-2029.

Bunte K, Abt SR, Potyondy JP, Ryan SE. 2004. Measurement of coarse gravel and cobble transport using portable bedload traps. *Journal of Hydraulic Engineering* 130: 879-893.

Butler JB, Lane SN, Chandler JH. 2001. Automated extraction of grain-size data from gravel surfaces using digital image processing. *Journal of Hydraulic Research* 39: 519-529.

Cameron D. 2006. An application of the UKCIP02 climate change scenarios to flood estimation by continuous simulation for a gauged catchment in the northeast of Scotland, UK (with uncertainty). *Journal of Hydrology* 328, 1-12.

Camporeale C, Perona P, Poporato A, Ridolfi L. 2007. Hierarchy of models for meandering rivers and related morphodynamic processes. *Review of Geophysics* 45.

Carling PA, Reader NA. 1982. Structure, properties and bulk properties of upland stream gravels. *Earth Surface Processes and Landforms* 7: 349-365.

Carson MA. 1984. The meandering-braiding river threshold: a reappraisal. *Journal of Hydrology* 73: 315-334.

Carson MA, Kirkby MJ. 1972. *Hillslope Form and Process*. Cambridge University Press, Cambridge, 475pp.

Carson MA, Lapointe MF. 1983. The inherent asymmetry of river meander planform. *Journal of Geology* 91: 41-55.

Carson MA, Griffiths GA. 1987. Influence of channel width on bed load transport capacity. *Journal of Hydraulic Engineering* 113: 1489-1509.

Casagli N, Rinaldi M, Gargini A, Curini A. 1999. Pore water pressure and streambank stability: results from a monitoring site on the Sieve River, Italy. *Earth Surface Processes and Landforms* 24: 1095-1114.

Casagli N, Ermini JA, Rosati G. 2003. Determining grain size distribution of the material composing landslide dams in the Northern Apennines: sampling and processing methods. *Engineering Geology* 69: 83-97

Chalk L. 1997. Upper Wharfedale "Best Practice" Project. Report to the 40 Group

Chang HH. 1980. Geometry of gravel rivers. *Journal of the Hydraulics Division, American Society of Civil Engineers* 106: 1443-1456.

Chang HH. 1988. Introduction to FLUVIAL-12. A mathematical model for erodible channels: Twelve selected computer stream sedimentation models developed in the US, *Federation of Energy Regulatory Commission*, Washington D.C.

Chartlon FG, Brown PM, Benson RW. 1978. The hydraulic geometry of some gravel rivers in Britain. *Hydraulic Research Station Report*, IT 180.

Chen D, Duan JG. 2006. Modelling width adjustment in meandering channels. *Journal of Hydrology* 321: 59-76.

Church MA, Kellerhals R. 1978. On the statistics of grain size variation along a gravel river. *Canadian Journal of Earth Sciences* 15: 1151-1160.

Church MA, Jones D. 1982. Channel bars in gravel-bed rivers. In *Gravel-bed Rivers. Fluvial Processes, Engineering and Management.* Hey RD, Bathurst JC, Thorne CR. (eds.). Wiley, Chichester. 291-324.

Church MA, Slaymaker O. 1989. Disequilibrium of Holocene sediment yield in glaciated British Columbia. *Nature* 337: 452-454.

Church MA, McLean DG, Wolcott JF. 1987. River bed gravels: sampling and analysis. In *Sediment Transport in Gravel-bed Rivers.* Thorne CR, Bathurst JC, Hey RD. (eds.), John Wiley and Sons Ltd. 43-88.

Church MA, Wolcott JF, Fletcher WK. 1991. A test of equal mobility in fluvial sediment transport – behaviour of the sand fraction. *Water Resources Research* 27 (11): 2941-2951.

Coulthard TJ. 1999. Modelling upland catchment response to Holocene environmental change. Unpublished Ph.D. Thesis. University of Leeds, U.K.

Coulthard TJ, Macklin MG. 2001. How sensitive are river systems to climate and land-use changes? A model based evaluation. *Journal of Quaternary Science* 16: 347-351.

Coulthard TJ, Macklin MG. 2003. Long-term and large scale high resolution catchment modelling: innovations and challenges arising from the NERC Land Ocean Interaction Study (LOIS), In *LNES.* Lang A, Hennrich K, Dikau R. (eds.). 101, pp123-134.

Coulthard TJ, Van De Wiel MJ. 2006. A cellular model of river meandering. *Earth Surface Processes and Landforms* 31: 123-132.

Coulthard TJ, Kirkby MJ, Macklin MG. 1997. Modelling hydraulic, sediment transport and slope processes at a catchments scale, using a cellular automaton approach. *Proceedings of GeoComputation* 15- 24.

Coulthard TJ, Kirkby MJ, Macklin MG. 1998. Modelling the 1686 flood of Cam Gill Beck, Starbotton, Upper Wharfedale. In *The Quaternary of the Eastern Yorkshire Dales: a Field Guide*. Howard A. Macklin MG (eds.). *Quaternary Research Association*, London.

Coulthard TJ, Kirkby MJ, Macklin MG. 2000. Modelling geomorphic response to environmental change in an upland river. *Hydrological Processes* 14: 2031-2045.

Couper PR. 2004. Space and time in river bank erosion research: a review. *Area* 36: 387-403.

Couper PR, Maddock I. 2001. Subaerial river bank erosion processes and their interaction with other bank erosion mechanisms on the River Arrow, Warwickshire, UK. *Earth Surface Processes and Landforms* 26: 631-646.

Couper PR, Stott T, Maddock I. 2002. Insights into river bank erosion processes derived from analysis of negative erosion-pin recordings: observations from three recent UK studies. *Earth Surface Processes and landforms* 27: 59-79.

Crowder DW, Diplas P. 1997.Sampling heterogeneous deposits in gravel-bed streams. *Journal of Hydraulic Engineering* 123: 1106-1117.

Cui Y, Parker, G, Paola C. 1996. Numerical simulation of aggradation and downstream fining. *Journal of Hydraulic Research* 32: 185-204.

Cui Y, Parker G, Pizzuto J, Lisle LE. 2003 Sediment pulses in mountain rivers: 2. Comparison between experiments and numerical predictions. *Water Resources Research* 39: 1240.

Danish Hydraulic Institute, 2002. MIKE 11 sediment transport: MIKE 11 ACS and GST – Cohesive and non-cohesive sediment transport model. DHI Water and Environment.

Darby SE. 1998a. River width adjustment II: Modelling. *Journal of Hydraulic Engineering* 124: 903-917.

Darby SE. 1998b. Modelling width adjustment in straight alluvial channels. *Hydrological Processes* 12: 1299-1321.

Darby SE. 2005. Refined hydraulic geometry data for British gravel-bed rivers. *Journal of Hydraulic Engineering* 131: 60-64.

Darby SE, Thorne CR. 1992. Simulation of near bank aggradation and degradation for width adjustment models. In *Hydraulic and Environmental Modelling: Estuarine and River Waters.* Falconer RA, Shiono K, Matthew RGS. (eds.). Ashgate, Aldershot, UK.

Darby SE, Thorne CR. 1996. Numerical simulation of widening and bed deformation of straight sand-bed rivers. I: Model development. *Journal of Hydraulic Engineering* 122: 184-193.

Darby SE, Delbono I. 2002. A model of equilibrium bed topography for meander bends with erodible banks. *Earth Surface Processes and Landforms* 27: 1057-1085

Darby SE, Thorne CR, Simon A. 1996. Numerical simulation of widening and bed deformation of straight sand-bed rivers. II: Model Evaluation. *Journal of Hydraulic Engineering* 122: 194-202

Darby SE, Alabyan AM, Van de Wiel MJ. 2002. Numerical simulation of bank erosion and channel migration in meandering rivers. *Water Resources Research* 38 (9): 1163.

DeVries P. 2002. Bedload layer thickness and disturbance depth in gravel bed streams. *Journal of Hydraulic Engineering.* 128: 983-991.

Dhakal AS, Sidle RC. 2004. Distributed simulations of landslides for different rainfall conditions. *Hydrological Processes* 18: 757-776.

Dietrich WE. 1987. Mechanics of flow and sediment transport in river bends. In *River Channels: Environment and Process.* Richards KS. (ed.). Blackwell, Oxford. 179-227.

Dietrich WE, Smith JD. 1983. Influence of the point-bar on flow through curved channels. *Water Resources Research* 19: 1173-1192.

Dietrich WE, Smith JD, Dunne T. 1979. Flow and sediment transport in a sand bedded meander. *Journal of Geology* 87: 305-315.

Dietrich WE, Reiss R, Hsu ML, Montgomery DR. 1995. A process-based model for colluvial soil depth and shallow landsliding using digital elevation data. *Hydrological Processes* 24, 383-400.

Diplas P, Sutherland AJ. 1988. Sampling techniques for gravel sized sediments. *Journal of Hydraulic Engineering* 114(5): 484-501.

Diplas P, Fripp JB. 1992. Properties of various sediment sampling procedures. *Journal of Hydraulic Engineering* 118: 955-970.

Dorava JM. 2001. Mitigating boatwake-induced erosion along the Kenai River, Alaska. *Water Science and Application* 4: 217-226.

Drake TG, Shreve RL, Dietrich WE, Whiting PJ, Leopold LB. 1988. Bedload transport of fine gravel observed by motion picture photography. *Journal of Fluid Mechanics* 192-217.

Duan JG. 2001. Numerical analysis of river channel processes with bank erosion. *Journal of Hydraulic Engineering* 127: 702-703.

Duan JG, Julien PY. 2005. Numerical simulation of the inception of channel meandering. *Earth Surface Processes and Landforms* 30: 1093-1110.

DuBoys MP. 1879. Etudes du regime et l 'action excercee par les eaux sur un lit afond de graviers indefiniment affouilanle. *Annals de Ponts et Chaussees* 58: *141-195*

Dunkerley DL. 1994. Discussion: bulk sampling of coarse clastic sediments for particle-size analysis. *Earth Surface Processes and Landforms* 19: 255-261.

Dunne T. 1991. Stochastic aspects of the relations between climate, hydrology and landform evolution. *Transactions of the Japanese Geomorphological Union.* 12: 1-24.

Dury GH. 1984. Abrupt variation in width along part of the River Severn, near Shrewsbury, Shropshire, England. *Earth Surface Processes and Landforms* 9: 485-492.

Eaton BC, Church M, Millar RG. 2004. Rational regime model of alluvial channel morphology and response. *Earth Surface Processes and Landforms* 29: 511-529.

Edwards BF, Smith DH. 2002. River meandering dynamics. *Physical Review E.* The American Physical Society. 65.

Egiazaroff IV. 1965. Calculation of nonuniform sediment concentrations *Journal of the Hydraulics Division, ASCE* 91: 225-247.

Einstein HA. 1942. Formulae for the transportation of bedload. *Transactions of the American Society of Civil Engineers* 107: 561-577

Einstein HA. 1950. The bedload function for sediment transportation in open channel flows. *United States Department of Agriculture Technical Bulletin* 1026.

Engelund F. Hansen. 1967. A monograph on sediment transport in alluvial streams. *Teknsik Vorlag.* Technical University of Copenhagan. 63.

Environment Agency. 2000. Upper Wharfedale Best Practice Project – Hydrology, Environmental Report.

Environment Agency. 2001a. Upper Wharfedale Best Practice Project – Buckden Gravel Trap Rehabilitation Scheme. Environmental Report.

Environment Agency. 2001b. Upper Wharfedale Best Practice Project: Information Series No. 3: Moorland drainage – the gripping question. HMSO.

Environment Agency. 2001c. Upper Wharfedale Best Practice Project – River Management Techniques. Information series No. 6.

Environment Agency. 2002. River Management Techniques. *Upper Wharfedale Best Practice Project, Information Series No. 6.* Environment Agency.

Ferguson RI. 1986. Hydraulics and hydraulic geometry. *Progress in Physical Geography* 10: 1-31.

Ferguson RI. 2003a. Emergence of abrupt gravel to sand transitions along rivers through sorting processes. *Geology* 31: 159-162.

Ferguson RI. 2003b. The missing dimension: effects of lateral variation on 1-D calculations of fluvial bedload transport. *Geomorphology* 56: 1-14.

Ferguson RI. 2007. Flow resistance equations for gravel- and boulder-bed streams. *Water Resources Research* 43: W05427.

Ferguson RI, Ashworth P. 1991. Slope-induced changes in channel character along a gravel-bed stream. *Earth Surface Processes and Landforms* 16: 65-82.

Ferguson RI, Ashworth PJ. 1992. Spatial patterns of bedload transport and channel change in braided and near-braided rivers. In *Dynamics of Gravel Bed Rivers*. Billi P, Hey RD, Thorne CR, Tacconi P. (eds.). Wiley. 477-495.

Ferguson RI, Paola C. 1997. Bias and precision of percentiles of bulk grain size distributions. *Earth Surface Processes and Landforms* 22: 1061-1077.

Ferguson RI, Hoey TB, Wathen SJ, Werrity A. 1996. Field evidence for rapid downstream fining of river gravels through selective transport. *Geology* 24: 179-182.

Ferguson RI, Hoey TB, Wathen SJ, Werrity A, Hardwick RI, Sambrook Smith GH. 1998. Downstream fining of river gravels: integrated field, laboratory and modelling study. In *Gravel Bed Rivers in the Environment*. Klingeman PC, Beschta RL, Komar PD, Bradley JB. (eds.). Water Resources Publications, Oregon. 85-114.

Ferguson RI, Church M, Weatherly H. 2001. Fluvial aggradation in Vedder River: testing a one-dimensional sedimentation model. *Water Resources Research* 37: 3331-3347.

Ferguson RI, Parsons DR, Lane SN, Hardy, RK. 2003. Flow in meander bends with recirulation at the inner bank. *Water Resources Research* 39: (11) 1322.

Ferguson RI, Cudden JR, Hoey TB, Rice SP. 2006. River system discontinuities due to lateral inputs: generic styles and controls. *Earth Surface Processes and Landforms* 31: 1149-1166.

Flintham TP, Carling PA. The prediction of mean bed and wall boundary shear in uniform and compositely rough channels. In *International Conference on River Regime*. White WR. (ed.). Hydraulics Research Limited. Wiley. 267-287.

Fowler HJ, Kilsby CG. 2007. Using regional climate model data to simulate historical and future river flows in northwest England. *Climate Change* 80: 337-367.

Freeze RA, Cherry JA. 1979. Groundwater. Prentice Hall, Inc.

Friend PF. 1993. Control of river morphology by the grain-size of sediment supplied. *Sedimentary Geology* 85: 171-177.

Fripp JB, Diplas P. 1993. Surface sampling in gravel streams. *Journal of Hydraulic Engineering* 119: 473-490.

Fuller IC, Large ARG, Charlton ME, Heritage GL, Milan DJ. 2003. Reach-scale sediment transfers: an evaluation of two morphological budgeting approaches. *Earth Surface Processes and Landforms* 28: 889-903.

Gaeuman D, Schmidt JC, Wilcock PR. 2005. Complex channel responses to changes in stream flow and sediment supply on the lower Duchesne River, Utah. *Geomorphology* 64: 185-206.

Gale SJ, Hoare PG. 1992. Bulk sampling of coarse clastic sediments for particle size analysis. *Earth Surface Processes and Landforms* 17: 729-733.

Gasparini NM, Tucker GE, Bras RL. 1999. Downstream fining through selective particle sorting in an equilibrium drainage network. *Geology* 27: 1079-1082.

Gilvear DJ. 1999. Fluvial geomorphology and river engineering: future roles utilizing a fluvial hydrosystems framework. *Geomorphology* 31: 229-245.

Gilvear DJ. 2004. Patterns of channel adjustment to impoundment of the upper River Spey, Scotland (1942-2000). *River Research and Applications* 20: 151-165.

Gilvear DJ, Winterbottom SJ. 1992. Channel changes and flood events since 1783 on the regulated River Tay, Scotland. *Regulated Rivers: Research and Management* 7: 247-260.

Gilvear DJ, Bradley S. 1997. Geomorphological adjustment of a newly engineered upland sinuous gravel-bed river diversion: Evan Water, Scotland. *Regulated Rivers: Research and Management* 13: 377-389.

Gilvear DJ, Winterbottom SJ. 1998. Change in channel morphology, floodplain land use and flood damage on the river Tay and Tummel: implications for floodplain management. In *United Kingdom Floodplains*. Bailey R, Jose P, Sherwood BR. (eds.). Westbury. 93-110.

Gilvear DJ, Davies JR, Winterbottom SJ. 1994. Mechanisms of floodbank failure during flood events on the regulated River Tay, Scotland. *Quarterly Journal of Engineering Geology* 4:1-20.

Gilvear DJ, Winterbottom SJ, Sichingabula H. 1999. Character of channel planform change and meander development: Luangwa River, Zambia. *Earth Surface Processes and Landforms* 24: 1-16.

Gilvear DJ, Heal KV, Stephen A. 2002. Hydrology and the ecological quality of Scottish river ecosystems. *The Science of the Total Environment* 294: 131-159.

Ginzt D, Hassan MA, Schmidt K. 1996. Frequency and magnitude of bedload transport in a mountain river. *Earth Surface Processes and Landforms* 21: 433-445.

Gob F, Houbrechts G, Hiver JM, Petit F. 2005. River dredging, channel dynamics and bedload transport in an incised meandering river (the River Semois, Belgium). *River Research and Applications* 21: 791-804.

Goff JR, Ashmore P. 1994. Gravel transport and morphological change in the braid Sunwapta River, Alberta, Canada. Earth Surface Processes and Landforms 19: 195-212.

Gomez B. 1991. Bedload transport. *Earth Sciences Review* 31: 89-132.

Gomez B, Church M. 1989. An assessment of bed-load sediment transport formulas for gravel bed rivers. *Water Resources Research* 25: 1161-1186.

Green JC. 2003. The precision of sampling grain-size percentiles using the Wolman method. *Earth Surface Processes and Landforms* 28: 979-991.

Gregory KJ, Park C. 1974. Adjustment of river channel capacity downstream from a reservoir. *Water Resources Research* 10: 870-873.

Grimshaw DL, Lewin J. 1980. Source identification for suspended sediments. *Journal of Hydrology* 47: 151-162.

Gurnell AM, Hupp CR, Gregory SV. 2000. Preface – Linking hydrology and ecology. *Hydrological Processes* 14: 16-17.

Gustard A, Wesselink AJ. 1993. Impact of land-use change on water resources: Balquhidder catchment. *Journal of Hydrology* 145: 389-401.

Habersack HM. 2001. Radio –tracking gravel particles in a large braided river in New Zealand: a field test of the stochastic theory of bed load transport proposed by Einstein. *Hydrological Processes* 15: 377-391.

Habersack HM, Smart GM. 1999. Width of braided gravel bed rivers: Implications for management in Austria and New Zealand. *Proceedings of IAHR River, Coastal and Estuarine Morphodynamics Symposium* 1: 575-584.

Hagerty DJ. 1991. Piping/sapping erosion 1: basic considerations. *Journal of Hydraulic Engineering* 117: 991-1008.

Ham DG, Church M. 2000. Bed material transport estimated from channel morphodynamics: Chilliwack River, British Columbia. *Earth Surface Processes and Landforms* 25: 1123-1142.

Harvey AM. 1969. Channel capacity and the adjustment of streams to hydrologic regime. *Journal of Hydrology* 8: 82-98.

Harvey AM. 1987. Sediment supply to upland streams: influence on channel adjustment. In *Sediment Transport in Gravel Bed-Rivers*. Thorne CR, Bathurst JC, Hey RD. (eds.). p121-150.

Harvey AM. 1991. The influence of sediment supply on the channel morphology of upland streams: Howgill Fells, N.W. England. *Earth Surface Process and Landforms* 16: 675-684.

Haschenburger JK. 1999. A probability model of scour and fill depths in gravel-bed channels. *Water Resources Research*. 35: 2857-2869.

Haschenburger JK, Church M. 1998. Bed material transport estimated from the virtual velocity of sediment. *Earth Surface Processes and Landforms* 23: 791-808.

Hasegawa K. 1981. Bank-erosion discharge based on a non-equilibrium theory. Proceedings of the JSCE. Tokyo. 316: 37–50.

Hassan MA. 1990. Scour, fill and burial depth of coarse material in gravel streams. *Earth Surface Processes and Landforms* 15: 341-356.

Hassan MA, Church M. Ashworth PJ. 1992. Virtual rate and mean distance of travel of individual clasts in gravel-bed channels. *Earth Surface Processes and Landforms* 17: 617-627.

Haycock N. 2000. Upper Wharfedale Best Practice Project – Buckden Gravel Trap – River Management Options, Haycock Associates.

Helley EJ, Smith W. 1971. Development and calibration of a pressure difference bedload sampler. USGS Water Resources Division Report.

Heritage GL, Newson MD. 1997. Geomorphological audit of the Upper Wharfe. Newcastle Upon Tyne. Report to the Environment Agency, Leeds.

Heritage GL, Newson MD. 1998. Dynamic assessment of the gravel trap on the River Wharfe upstream of Buckden. University of Newcastle Upon Tyne, Environment Agency.

Henderson FM. 1966. *Open Channel Flow.* MacMillian Publishing Co. New York.

Hey RD. 1976. Geometry of river meanders. *Nature* 262: 482-484.

Hey RD. 1997. Stable river morphology. In *Applied Fluvial Geomorphology for River Engineering and Management.* Thorne CR, Hey RD, Newson MD. (eds.). John Wiley and Sons Ltd. Chichester, UK. p223-236.

Hey RD. Thorne CR.1983. Accuracy of surface samples from gravel-bed material. *Journal of the Hydraulics Division* 109: 842-852.

Hey RD, Thorne CR. 1986. Stable channels with mobile gravel beds. *Journal of Hydraulic Engineering* 122: 671-689.

Hey RD, Winterbottom AN. 1990. River Engineering in National Parks: the case of the River Wharfe, U.K. *Regulated Rivers: Research and Management* 5: 35-44.

Hickin EG. 1974. The development of meanders in natural river channels. *American Journal of Science* 267: 999-1010.

Hickin EG, Nanson GC. 1975. The character of channel migration on the Beatton River, N.E. British Columbia, Canada. *Bulletin of the Geological Society of America* 86: 487-494.

Hickin EG, Nanson GC. 1984. Lateral migration rates of river bends. *Journal of Hydraulic Engineering* 110: 1557-1567.

Hill D, Hack V. 1999. Upper Wharfedale "Best Practice" Project – River Corridor Survey. Report by Ecoscope Applied Ecologists Limited.

Hoey TB, Ferguson RI. 1994. Numerical simulation of downstream fining by selective transport in gravel bed rivers. *Water Resources Research* 30: 2251-2260.

Hoey TB, Bluck BJ. 1999. Identifying the controls over downstream fining of river gravels. *Journal of Sedimentary Research* 69: 40-50.

Hoey TB, Rice S, Ferguson R, Graham, D, Cudden J, Church M, Ayles C. 2004. The importance of tributary sediment supply for the sediment dynamics of a large regulated gravel-bed river. *Geophysical Research Abstracts,* EGU, 6.

Hooke J. 2003. Coarse sediment connectivity in river channel systems: a conceptual framework and methodology. *Geomorphology* 56: 79-94.

Hooke JM. 1979. An analysis of the processes of river bank erosion. *Journal of Hydrology* 42: 39-62.

Hooke JM. 1980. Magnitude and distribution of rates of river bank erosion. *Earth Surface Processes* 5: 143-147.

Hooke JM. 1984. Changes in river meander: a review of techniques and results of analyses. *Progress in Physical Geography* 8: 473-508.

Hooke JM. 1995. Processes of channel planform change on meandering channels in the UK. In *Changing River Channels.* Gurnell A, Petts G. (eds.). Wiley. p87-115.

Hooke JM. 1997. Styles of channel change. In *Applied Fluvial Geomorphology for River Engineering and Management.* Thorne CR, Hey RD, Newson MD. (eds.), John Wiley and Sons, Chichester, UK. p237-268.

Hooke RL. 1975. Distribution of sediment transport and shear stress in a meander bend. *Journal of Geology* 83: 543-565.

Houghton-Carr H. 1999. Flood estimation handbook. Vol. 4, Restatement and application of the Flood Studies Report rainfall runoff methods. Institute of Hydrology, Wallingford.

Howard AD. 1992. Modelling channel migration and floodplain sedimentation in meandering streams. In *Lowland Floodplain Rivers.* Carling PA, Petts GE. (eds.). Wiley, Chichester. 1-41.

Howard AD. 1994. A detachment-limited model of drainage basin evolution. *Water Resources Research* 30: 2261-2285.

Howard AD. 1996. Modelling channel evolution and floodplain morphology. In *Floodplain Processes.* Anderson MA Walling DE, Bates PD. (eds.). John Wiley & Sons, Chichester. p. 15-62.

Howard AJ, Macklin MG, Black S, Hudson-Edwards KA. 2000. Holocene river development and environmental change in Upper Wharfedale, Yorkshire Dales, England. *Journal of Quaternary Science* 15: 239-252.

Hsu SM, Holly FM. 1992. Conceptual bed-load transport model and verification for sediment mixtures. *Journal of Hydraulic Engineering* 118: 1135-1152.

Hubbell DW, Stevens HH, Skinner JV, Beverage JP. 1981. Recent refinements in calibrating bedload samplers. *Water Forum '81*, ASCE, New York, 1: 128-140.

Hydrological Engineering Centre, 2003. HEC-RAS: River Analysis System. US Army Corps of Engineers at the Hydrological Engineering Centre, California.

Ibbeken H, Warnke DA, Diepenbroek M. 1998. Granulometric study of the Hanaupah Fan, Death Valley, California. *Earth Surface Processes and Landforms* 23: 481–492.

Ibbeken H, Schleyer I. 1986. Photo-sieving - a method for grain-size analysis of coarse-grained, unconsolidated bedding surfaces. *Earth Surface Processes and Landforms* 11: 59-77.

Ikeda H, Iseya F. 1988. Experimental study of heterogeneous sediment transport. Environmental Research Centre Paper No. 12.

Ikeda S, Parker G, Sawai K. 1981. Bend theory of river meanders, 1: linear development. *Journal of Hydraulic Engineering* 112: 363-377.

Ikeda S, Parker G, Kimura Y. 1988. Stable width and depth of straight gravel rivers with heterogeneous bed materials. *Water Resources Research* 24: 713-722.

Jackson WL, Beschta RL. 1984. Influences of increased sand delivery on the morphology of sand and gravel channels. *Water Resources Bulletin* 20: 527-533.

James A. 1999. Time and the persistence of alluvium: River engineering, fluvial geomorphology, and mining sediment in California. *Geomorphology* 31: 265-290.

Jarrett RD. 1984. Hydraulics of high-gradient rivers. *Journal of Hydraulic Engineering* 110: 1519-1539.

Johannesson H, Parker G. 1989a. Secondary flow in mildly sinuous channels. *Journal of Hydraulic Engineering* 115: 289-308.

Johannesson H, Parker G. 1989b. Linear theory of river meanders. In *River Meandering. AGU Water Resources Monograph.* Ikeda S. Parker G. (eds.). 12: 181-213.

Johnson JW. 1939. Discussion of laboratory investigation of flume tractions and transportation by YL Chang. *Transactions of the American Society for Civil Engineers* 104: 1247-1313.

Johnson RC, Thompson DB. 2002. Hydrology and natural heritage of the Scottish mountains. *Science of the Total Environment* 294: 161-168.

Johnson RM, Warburton J. 2002. Annual sediment budget of a UK mountain torrent, *Geografiska Annaler Series A: Physical Geography* 84: 73-88.

Jones PD, Bradley RS. 1992. Climatic variations in the longest instrumental records. In *Climate Since AD 1500.* Bradley RS. Jones OD. (eds.), Routledge, pp 246-268.

Katul G, Wiberg P, Albertson J, Hornberger G. 2002. A mixing layer theory for flow resistance in shallow streams. *Water Resources Research* 38: 1250.

Keinholz H, Lehmann C, Guggisberg C, Loat R, Hegg C. 1991. Bedload transport in Swiss Mountain torrents with respect to the disaster in 1987. *Zeitschrift für Geomorphologie* 983: 53-62.

Kellerhalls R, Bray DI. 1971. Sampling procedures for coarse fluvial sediments. *Journal of Hydraulic Engineering* 98 (8): 1165-1180.

Kelsey A. 1996. Modelling the sediment transport process. In *Advances in Fluvial Dynamics and Stratigraphy.* Carling PA, Dawson MR. (eds), Wiley, Chichester, p229-261.

Keulegan GH. 1938. Laws of turbulent flow in open channels. Journal of Res Natl Bureau Stand 21: 707-741.

Kikkawa H, Ikdeda S, Kitagawa A. 1976. Flow and bed topography in curved open channels. *Journal of the Hydraulics Division, ASCE* 102: 1327-1342.

Kinzel PJ, Wright CW, Nelson JM, Burman, AR. 2007. Evaluation of an experimental LiDAR for surveying a shallow, braided, sand-bedded river. *Journal of Hydraulic Engineering* 133: 838-842.

Klingeman PC, Emmett WW. 1982. Gravel bedload transport processes. In *Gravel Bed Rivers: Fluvial Processes, Engineering and Management.* Hey RD, Bathurst JC, Thorne CR. (eds.). Wiley. p141-180.

Knighton AD. 1987. Downstream river channel adjustment. In *River Channels: Environment and Process.* Richards KS. (ed.). Blackwell, Oxford. p95-128.

Knighton D. 1998. *Fluvial Forms and Processes: A New Perspective.* Arnold, London. pp383.

Knox JC. 1999. Long-term episodic changes in magnitudes and frequencies of floods in the upper Mississippi river valley. In *Fluvial Processes and Environmental Change* Brown AG, Quine TA. (eds.). Wiley. pp255–282.

Knox JC. 2000. Sensitivity of modern and Holocene floods to climate change. *Quaternary Science Reviews* 19: 439-457.

Kondolf GM. 1994. Geomorphological and environmental effects of gravel mining. *Landscape and Urban Planning* 28: 225-243.

Kondolf GM. 1996. A cross section of stream channel restoration. *Journal of Soil and Water Conservation* 51: 119-125.

Kondolf GM. 1997. Application of the pebble count: notes on purpose, method and variants. *Journal of the American Water Resources Association* 33: 79-87.

Kondolf GM, Wolman MG. 1993. The sizes of salmonid spawning gravels. *Water Resources Research* 29: 2275-2285.

Kondolf GM, Piegay H, Landon N. 2002. Channel response to increased and decreased bedload supply from land-use change: contrasts between two catchments. *Geomorphology* 45: 35-51.

Kondolf GM, Lisle TE, Wolman GM. 2003. Bed sediment measurement. In *Tools in Fluvial Geomorphology.* Kondolf GM, Piegay H. (eds.). Wiley, Chichester. p347-395.

Korup O, McSaveney MJ, Davies TRH. 2004. Sediment generation and delivery from large historic landslides in the Southern Alps, New Zealand. *Geomorphology* 61: 189-207.

Kovacs A, Parker G. 1994. A new vectorial bedload formulation and its application to the time evolution of straight river channels. *Journal of Fluid Mechanics* 267, 153–183.

Lacey C. 1929. Stable channels in alluvium. *Proceedings of the Institution of Civil Engineers* 229: 259-384.

Lancaster ST, Bras RL. 2002. A simple model of river meandering and its comparison to natural channels. *Hydrological Processes* 16: 1-26.

Lane SN. 1995. The dynamics of dynamic river channels. *Geography* 80: 147-162.

Lane SN. 1998. Hydraulic modelling in hydrology and geomorphology: A review of high resolution approaches. *Hydrological Processes* 12: 1131-1150.

Lane SN. 2000. Upper Wharfedale "Best Practice" Project, Environment Agency Information Series No. 4.

Lane SN. 2001. More floods, less rain: changing hydrology in a Yorkshire Context, The Regional Review. 12: 18-19.

Lane SN, Richards KS. 2001. The validation of hydrodynamic models: some critical perspectives. In *Model Validation for Hydrological and Hydraulic Research.* Bates PS, Anderson MG. (eds.). Wiley, Chichester.

Lane SN, Ferguson R. 2005. Modelling reach-scale fluvial flows. In *Computational Fluid Dynamics.* Bates, PD, Lane SN, and Ferguson R. (eds.). Wiley. pp531.

Lane SN, Chandler JH, Richards KS. 1994. Developments in monitoring and terrain modelling small-scale river-bed topography. *Earth Surface Processes and Landforms* 19: 349-368.

Lane SN, Richards KS, Chandler JH. 1995. Morphological estimation of the time-integrated bedload transport rate. *Water Resources Research* 31: 761-772.

Lane SN, Bradbrook KF, Richards KS, Biron PM, Roy AG. 2000. Secondary circulation cells in river channel confluences: measurement artefacts or coherent flow structures? *Hydrological Processes* 14: 11-21.

Lane SN, McDonald AM, Kirkby MJ. 2002. Integrated understanding of flood risk, water quality and sediment delivery for best practice in upland environments. *University of Leeds research pamphlet.*

Lane SN, Westaway RM, Hicks DM. 2003. Estimation of erosion and deposition volumes in a large, gravel-bed, braided river using synoptic remote sensing. *Earth Surface Processes and Landforms* 28: 249-271.

Lane SN, Brookes CJ, Hardy RJ, Holden J, James TD, Kirkby MJ, McDonald AT, Tayefi V, Yu D. 2003. Land management, flooding and environmental risk: new approached to a very old question. Proceedings CIWEM National Conference.

Lane SN, Hardy RJ, Ferguson RI, Parsons DR. 2005. A framework for model verification and validation of CFD schemes in natural open channel flows. In *Computational Fluid Dynamics Applications in Environmental Hydraulics.* Bates M, Lane SN. John Wiley & Sons. 329-355.

Lane SN, Tayefi V, Reid SC, Yu D, Hardy RJ. 2007. Interactions between sediment delivery, channel change, climate change and flood risk in a temperate upland environment. *Earth Surface Processes and Landforms* 32: 429-446.

Lane SN, Reid SC, Tayefi V, Yu D, Hardy RJ. 2008. Reconceptualising coarse sediment delivery problems in rivers as catchment-scale and diffuse. *Forthcoming in Geomorphology.*

Large ARG, Prach K, Bickerton MA, Wade PM. 1994. Alteration of patch boundaries on the floodplain of the regulated River Trent, UK. *Regulated Rivers: Research and Management* 9: 71-78.

Laursen EL. 1958. The total sediment load of streams. *Journal of the Hydraulics Division, ASCE* 84: 1-36.

Lawler DM. 1986. River bank erosion and the influence of frost: a statistical examination. *Transactions of the Institute of British Geographers, New Series* 11: 227-242.

Lawler DM. 1991. A new technique for the automatic monitoring of erosion and deposition rates. *Water Resources Research* 27: 2125-2128.

Lawler DM. 1992. Process dominance in bank erosion systems. In *Lowland Floodplain Rivers: Geomorphologic Perspectives.* Carling PA, Petts GE. (eds.). Wiley, Chichester. 117-143.

Lawler DM. 1993a. Needle ice processes and sediment mobilisation on river banks: the River Illston, West Glamorgan, UK. *Journal of Hydrology* 150: 81-114.

Lawler DM. 1993b. The measurement of river bank erosion and lateral channel change review. *Earth Surface Processes and Landforms* 18: 777-821.

Lawler DM. 2005. The importance of high resolution monitoring in erosion and deposition dynamics studies: examples form estuarine and fluvial systems. *Geomorphology* 64: 1-23.

Lawler DM, Leeks GJL. 1992. River bank erosion events on the upper Severn detected by the PEEP system. In *Erosion and Sediment Transport Monitoring Programmes in River Basins.* Bogen J, Walling DE, Day T. (eds.). International Association of Hydrological Sciences. 210: 95-105.

Lawler DM, Thorne CR, Hooke JM. 1997. Bank erosion and instability. In *Applied Fluvial Geomorphology for River Engineering and Management.* Thorne CR, Hey RD, Newson MD. (eds.). John Wiley and Sons, Chichester, UK. p137-172.

Lawler DM, Grove JR, Couperthwaite JS, Leeks GJL. 1999. Downstream changes in river bank erosion rates in the Swale-Ouse system, northern England. *Hydrological Processes* 13: 977-992.

Leeks GJL. 1992. Impact of plantation forestry on sediment transport processes. In *Dynamics of Gravel-bed Rivers.* Billi P, Hey RD, Thorne CR, Tacconi P. (eds.). Wiley, Chichester. p651-668.

Leopold LB. 1970. An improved method for size distribution of stream bed gravel. *Water Resources Research* 6: 1357-1366.

Leopold LB. 1992. Sediment size that determines channel morphology. In *Dynamics of Gravel-Bed Rivers.* Billi P, Hey RD, Thorne CR, Tacconi P. (eds.). Wiley, Chicester, 297-312.

Leopold LB, Maddock T. 1953. The hydraulic geometry of stream channels and some physiographic implications. *U.S. Geological Survey Professional Paper* 252.

Leopold LB, Wolman MG, Millar JP. 1964. *Fluvial Processes in Geomorphology.* Freeman, San Francisco.

Lewin J, Macklin MG. 1987. Metal mining and floodplain sedimentation in Britain. In *International Geomorphology.* Gardiner V. (ed.), Wiley, Chichester, 1009-1027.

Leys KF, Werritty, A. 1999. River channel planform change: software for historical analysis. *Geomorphology* 29: 107-120.

Li L, Wang SS. 1993. Numerical modelling of alluvial stream bank erosion. In *Advances in Hydro-Science and Engineering.* Wang SSY. (ed.). University of Mississippi Press, Oxford, MS. 1: 2085-2090.

Li Z, Komar PD. 1986. Laboratory measurements of pivoting angles for applications to selective entrainment of gravels in a current. *Sedimentology* 33: 412-423.

Liebault F, Piegay H. 2001. Assessment of channel changes due to long-term bedload supply decrease, Roubion River, France. *Geomorphology* 36: 167-186.

Lindsay JB, Ashmore PE. 2002. The effects of survey frequency on estimates of scour and fill in a braided river model. *Earth Surface Processes and Landforms* 27: 27-43.

Lisle TE, Nelson JM, Pitlick J, Madej MA, Barkett BL. 2000. Variability of bed mobility in natural, gravel-bed channels and adjustments to sediment load at local and reach scales. *Water Resources Research* 36: 3743-3755.

Lohnes R, Handy RL. 1968. Slope angles in friable loess. *Journal of Geology* 76: 247-258.

Longfield S, Macklin MG. 1999. The influence of recent environmental change on flooding and sediment fluxes in the Yorkshire Ouse basin. *Hydrological Processes* 13: 1051-66.

Luis SJ, McLaughlin D. 1992. A stochastic approach to model validation. *Advances in Water Resources* 15: 15-32.

Macklin MG, Lewin J. 2003. River sediments, great floods and centennial-scale Holocene climate change. *Journal of Quaternary Science* 18: 101-105.

Macklin MG, Passmore D, Newson MD. 1998. Controls of short and long-term river instability: processes and patterns in gravel-bed rivers, Tyne Basin, England. In *Gravel-Bed Rivers in the Environment.* Klingeman PC, Beschta RL, Komar PD, Bradley JB. (eds.). Water Resources Publications, USA. p257-278.

Madje MA, Weaver WE, Hagans DK. 1994. Analysis of bank erosion on the Merced River, Yosemite Valley, Yosemite National Park, California, USA. *Environmental Management* 18: 235-250.

Marcus WA, Ladd SC, Stoughton JA, Stock JW. 1995. Pebble counts and the role of user-dependent bias in documenting sediment size distributions. *Water Resources Research* 31: 2625-2631.

Marion A, Fraccarollo L. 1997. New conversion model for areal sampling of fluvial sediments. *Journal of Hydraulic Engineering* 123: 1148-1151.

Markham AJ, Thorne CR. 1992. Geomorphology of gravel-bed river bends. In *Dynamics of Gravel Bed Rivers*. Billi P, Hey RD, Thorne CR, Tacconi P. (eds.). Wiley, Chichester. 433-456.

Marston RA, Girel J, Pautou G, Piegay H, Bravard JP, Arneson C. 1995. Channel metamorphosis, floodplain disturbance and vegetation development, Ain River, France. *Geomorphology* 13: 121-132.

Martin T. 2003. Evaluation of bed load transport formulae using field evidence from the Vedder River, British Columbia. *Geomorphology* 53: 75-95.

Martin Y, Church M. 1995. Bed-material transport estimated from channel surveys: Vedder River, British Columbia. *Earth Surface Processes and Landforms* 20: 347-361.

Martin Y, Ham D. 2005. Testing bedload transport formulae using morphologic transport estimates and field data: lower Fraser River, British Columbia. *Earth Surface Processes and Landforms* 30: 1265-1282.

McDonald AM, Lane SN, Kirkby MJ, Holden J, Ashley D, Reid SC, Tayefi V, Brookes CJ. 2002. Information Requirements for the Integrated Management of Agricultural Areas in Sensitive River Basins: R&D Project E1- 08. Environment Agency, Bristol.

McDonald AM, Lane SN, Haycock NE, Chalk EA. 2004. Rivers of dreams: on the gulf between theoretical and practical aspects of an upland river restoration. *Transactions of the Institute of British Geographers* 29: 257-281.

McEwen LJ. 1989. River channel changes in response to flooding in the upper River Dee catchment, Aberdeenshire, over the last 200 years. In *Floods: Hydrological, Sedimentological and Geomorphological Implications*. Beven K, Calring P. (eds.). Wiley. pp123-140.

McLean DG, Church M. 1999. Sediment transport along lower Fraser River 2: estimates based on the long-term gravel budget. *Waters Resources Research* 35: 2549-2559.

McWorter DB, Sunada DK. 1977. *Groundwater Hydrology and Hydraulics*. Water Resources Publications, Ft. Collins, CO.

Merrett SP, Macklin MG. 1999. Historic River Response to Extreme Flooding in the Yorkshire Dales, Northern England. In *Fluvial Processes and Environmental Change* Brown AG, Quine TA. (eds.). Wiley, pp 345-360.

Meyer-Peter E, Müller R. 1948. Formulation for bedload transport. *Proceedings International Association for Hydraulic Research*. 2nd Congress, Stockholm, 39-64.

Milhous RT. 1973. Sediment transport in a gravel-bottomed stream. Ph.D. thesis, Dept. Civil Engineering, Oregon Stat University, USA 232p.

Millar RG. 2005. Theoretical regime equations for mobile gravel-bed rivers with stable banks. *Geomorphology* 64: 207-220.

Millar RG, Quick MC. 1993. Effect of bank stability on geometry of gravel rivers. *Journal of Hydraulic Engineering* 119: 1343-1363.

Millar RG, Quick MC. 1998. Stable width and depth of gravel-bed rivers with cohesive banks. *Journal of Hydraulic Engineering* 124: 1005-1013.

Milledge DG. 2003. Disrupted downstream fining on the River Wharfe: Patterns, processes and potential for sediment delivery estimation using sediment fingerprinting. Unpublished Undergraduate Dissertation. University of Leeds.

Montgomery DR, Dietrich WE. 1994. A physically based model for the topographic control on shallow landsliding. *Water Resources Research* 30: 1153-1171.

Montgomery DR, Dietrich WE. 1995. Hydrologic processes in a low-gradient source area. *Water Resources Research* 31: 1-10.

Montgomery DR, Dietrich WE, Torres R, Anderson SP, Heffner JT, Loague K. 1997. Hydrologic response of a steep unchanneled valley to natural and applied rainfall. *Water Resources Research* 33: 91-109.

Montgomery DR, Dietrich WE, Heffner JT. 2002. Piezometric response in shallow bedrock at CB1: Implications for runoff generation and landsliding. *Water Resources Research* 38: 1274-1292.

Mosley MP, Tindale DS. 1985. Sediment variability and bed material sampling in gravel-bed-rivers. *Earth Surface Processes and Landforms* 10: 465-482.

Mosselman E. 1992. Mathematical modelling of morphological processes in rivers with erodible cohesive banks. *Communications on Hydraulic and Geotechnical Engineering*. Delft University of Technology. 92-93.

Mosselman E. 1995. A review of mathematical models of river planform change. *Earth Surface Process and Landforms* 20: 661-670.

Mosselman E. 1998. Morphological modelling of rivers with erodible banks. *Hydrological Processes* 12: 1357-1370.

Murray AB. 2007. Reducing model complexity for explanation and prediction. *Geomorphology* 90: 3-4.

Murray AB, Paola C. 1994. Cellular-model of braided rivers. *Nature* 371: 54-57.

Murray AB, Paola C. 1997. Properties of a cellular braided-stream model. *Earth Surface Processes and Landforms* 22: 1001-1025.

Naden P, Brayshaw AC. 1987. Bedforms in gravel-bed rivers. In *River Channels – Environment and Process*. Richards KS. (ed.). Blackwells, Oxford. pp249-271.

Nagata N, Hosoda T, Muramoto Y. 2000. Numerical analysis of river channel processes with bank erosion. *Journal of Hydraulic Engineering* 126: 243-252.

Nanson GC, Hickin EJ. 1983. Channel migration and incision on the Beatton River. *Journal of Hydraulic Engineering* 109: 327-337.

Nanson GC, Krusenstierna A, Bryant EA. 1994. Experimental measurements of river-bank erosion caused by boat generated waves on the Gordon River, Tasmania. *Regulated Rivers: Research and Management* 9: 1-14.

Neill CR. 1987. Sediment balance considerations linking long-term transport and channel processes. In *Sediment Transport in Gravel-Bed Rivers* Thorne CR, Hey RD, Bathurst JS. (eds.), John Wiley, Chichester, 225-239.

Newbold C, Purseglove J, Holmes N. 1983. *Nature Conservation and River Engineering.* Nature Conservancy Council, Peterborough.

Newson MD, Newson CL. 2000. Geomorphology, ecology and river channel habitat: mesoscale approaches to basin-scale challenges. *Progress in Physical Geography* 24: 195-217.

Nicholas AP. 2000. Modelling bedload yield in braided gravel bed rivers. *Geomorphology* 26: 89-106.

Nicholas AP, Thomas R, Quine TA. 2006. Cellular modelling of braided river form and process. In *Braided Rivers: Process, Deposits, Ecology and Management.* Sambrook Smith GH, Best JL, Bristow CS, Petts GE. (eds.). Special Publication International Association of Sedimentologists. 36: 137-151.

Nolan KM, Shields RR. 2000. Measurement of stream discharge by wading, *USGS Water Resources Investigation Report* 00-4036.

Nouh MA, Townsend RD. 1979. Shear-stress distribution in stable channel bends. *Proceedings of the American Society of Civil Engineers, Journal of the Hydraulics Division* 105: 1233-1245.

NRA. 1995a. Post Project Evaluation for the River Wharfe – Buckden Scheme. *Report prepared by Sir William Halcrow and Partners Limited.*

NRA. 1995b. Sediment and gravel transportation in rivers including the use of gravel traps, *Project Report 232/1/T*, University of Newcastle Upon Tyne.

O'Connell PE, Beven KJ, Carney JN, Clements RO, Ewen J, Fowler H, Harris GL, Hollis J, Morris J, O'Donnell GM, Packman JC, Parkin A, Quinn PF, Rose SC. 2004. Review of Impacts of Rural Land Use and Management on Flood Generation. Part A: Impact Study Report. *Report to Defra/Environment Agency R&D Technical Report* (FD2114).

Osman AM. 1985. Channel width response to changes in flow hydraulics and sediment load. PhD Thesis, Colorado State University, Fort Collins.

Osman AM, Thorne CR. 1988. Riverbank stability analysis, I, Theory. *Journal of Hydraulic Engineering* 114, 134– 150.

Osterkamp WR. 1980. Sediment –morphology relations of alluvial channels. *Proceedings of the Symposium on Watershed Management. ASCE,* Boise. 188-189.

Osterkamp WR, Hedman ER. 1982. Perennial-streamflow characteristics related to channel geometry and sediment in the Missouri river basin. *U.S. Geological Survey Professional Paper* 1242.

Page MJ, Trustrum NA, DeRose, RC. 1994. A high-resolution record of storm induced erosion from lake sediments, New Zealand. *Journal of Paleolimnology* 11: 333-348.

Paola C. 1996. Incoherent structure: turbulence as a metaphor for stream braiding. In *Coherent Flow Structures in Open Channel Flows.* Ashworth PJ, Bennett SJ, Best JL, McLelland SJ. (eds.). Wiley, Chichester. pp705-723.

Park I, Jain SC. 1987. Numerical simulation of degradation of alluvial channel beds. *Journal of Hydraulic Engineering* 113: 845-859.

Parker G. 1978. Self-formed straight rivers with equilibrium banks and mobile bed. 2. The gravel river. *Journal of Fluid Mechanics* 76: 457-80.

Parker G. 1979. Hydraulic geometry of active gravel rivers. *Journal of the Hydraulics Division, American Society of Civil Engineers* 105: 1185-1201.

Parker G. 1990a. Surface-based bedload transport relation for gravel rivers. *Journal of Hydraulics Research* 28: 417.

Parker G. 1990b. The "ACRONYM" series of PASCAL programs for computing bedload transport in gravel rivers. University of Minneaplois. St. Anthony Falls Hydraulics Lab. External Memo. M-220, 124 pp.

Parker G, Klingeman PC. 1982a. On why gravel bed streams are paved. *Water Resources Research* 18: 1409-1423.

Parker G, Andrews ED. 1985. Sorting of bed-load sediment by flow in meander bends. *Water Resources Research* 21: 1361-1373.

Parker G, Sutherland AJ. 1990. Fluvial Armour. *Journal of Hydraulic Research* 28:529-544.

Parker G, Dhamotharon S, Stefan H. 1982a. Model experiments on mobile paved gravel bed stream. *Water Resources Research* 18 (5): 1395-1408.

Parker G, Klingeman PC, McLean, D.G. 1982b. Bedload size and distribution in a paved gravel-bed stream. *Journal of the Hydraulics Division* ASCE 108: 544-571.

Parker G, Diplas P. Akiyama J. 1983. Meander bends of high amplitude. *Journal of Hydraulic Engineering* 109: 1323-1337.

Parsons H, Gilvear D. 2002. Valley floor landscape change following almost 100 years of flood embankment abandonment on a wandering gravel-bed river. *River Research and Applications* 18: 461-479.

Petit F, Poinsart D, Bravard JP. 1996. Channel incision, gravel mining and bedload transport in the Rhone river upstream of Lyon, France. *Catena* 26: 209-226.

Petrie J, Diplas P. 2000. Statistical approach to sediment sampling accuracy. *Water Resources Research* 36: 597-605.

Pickup G. 1976. Adjustment of stream-channel shape to hydrologic regime. *Journal of Hydrology 30*: 365-373.

Pickup G, Warner RF. 1976. Effects of hydrological regime on magnitude and frequency of dominant discharge. *Journal of Hydrology* 29: 51-75.

Pickup G, Rieger WA. 1979. A conceptual model of the relationship between channel characteristics and discharge. *Earth Surface Process and Landforms* 4: 37-42.

Pinter N, Heine RA. 2005. Hydrodynamic and morphodynamic response to river engineering documented by fixed-discharge analysis, Lower Missouri River, USA. *Journal of Hydrology* 302: 70-91.

Pitlick J, Wilcock P. 2001. Relations between streamflow sediment transport and aquatic habitat in regulated rivers. In *Geomorphic Processes and Riverine Habitat.* Dorova JM, Montgomery DR, Palcsak BB, Fitzpatrick FA. (eds.). Water Science and Application. 4: 185-198.

Pizzuto JE. 1990. Numerical simulation of gravel river widening. *Water Resources Research* 26: 1971-1980.

Pizzuto JE. 1994. Channel adjustments to changing discharge, Powder River, Montana. *Geological Society of American Bulletin* 106: 1494-1501.

Popov IV. 1962. Application of morphological analysis to the evaluation of the general channel deformations of the River Ob. *Soviet Hydrology* 3: 267-324.

Powell DM. 1992 .Bedload entrainment, transport and deposition in braided reaches. Unpublished Ph.D. Thesis. University of Leeds, U.K.

Powell DM, Ashworth PJ. 1995. Spatial pattern of flow competence and bedload transport in a divided gravel bed river. *Water Resources Research* 31: 741-752

Power ME. 2001. Controls on food webs in gravel-bedded rivers: the importance of the gravel-bed habitat for trophic dynamics. In *Gravel Bed Rivers V, New Zealand Hydrological Society.* Mosley PM. (ed.). p405-422.

Proffitt GT. 1980. Selective transport and armouring of nonuniform alluvial sediments. *Report No. 80/22.* Department of Civil Engineering. University of Canterbury, New Zealand, 203.

Proffitt GT, Sutherland AJ. 1983. Transport of non-uniform sediments. *Journal of Hydraulic Research* 21: 33-43

Pyrce RS, Ashmore PE. 2003. Particle path length distributions in meander gravel-bed streams: results from physical models. *Earth Surface Processes and Landforms* 28: 951-966.

Raynov S, Pechinov D, Kopaliany Z, Hey RD. 1986. *River Response to Hydraulic Structures.* UNESCO.

Reid I, Bathurst JC, Carling PA, Walling DE, Webb BW. 1997. Sediment erosion, transport and deposition. In *Applied Fluvial Geomorphology for River Engineering and Management.* Thorne CR, Hey RD, Newson MD. (eds.), John Wiley and Sons, Chichester, UK, p95-135.

Reid SC. 2004. Coarse sediment delivery and transfer within an upland gravel-bed river environment. Unpublished Ph.D Thesis. University of Leeds.

Reid SC, Lane SN, Berney JM. 2007a. The timing and magnitude of coarse sediment transport events within an upland gravel-bed river. *Geomorphology* 83: 152-182

Reid SC, Lane SN, Montgomery DR, Brookes CJ. 2007b. Does hydrological connectivity improve modelling of coarse sediment delivery in upland environment? *Geomorphology* 90: 263-282.

Reiser DW. 1998. Sediment in gravel bed rivers: ecological and biological considerations. In *Gravel Bed Rivers in the Environment.* Klingeman PC, Beschta RL, Komar PD, Bradley JB. (eds.), *Water Resources Publications.* Oregon. pp199-228.

Rice SP, Church MA. 1996. Sampling surficial fluvial gravels: the precision of size distribution percentile estimates. *Journal of Sedimentary Research* 66: 654-665.

Rice SP, Church MA. 1998. Grain size along two gravel-bed rivers: statistical variation, spatial pattern and sedimentary links. *Earth Surface Processes and Landforms* 23: 345–363.

Rice SP, Church M. 2001. Longitudinal profiles in simple alluvial systems. *Water Resources Research* 37: 417-426.

Rice SP, Haschenburger JK. 2004. A hybrid method for size characterization of coarse subsurface fluvial sediments. *Earth Surface Processes and Landforms* 29: 373-389.

Rice SP, Ferguson RI, Hoey TB. 2006. Tributary control of physical heterogeneity and biological diversity at confluences. *Canadian Journal of Fish and Aquatics Science* 63: 2553-2566.

Richards KS. 1982. *Rivers, Form and Process in Alluvial Channels*. Methuen, London.

Richards KS. 2001. Floods, channel dynamics and riparian ecosystems. In *Gravel Bed Rivers V*. Mosley PM. (ed.). New Zealand Hydrological Society. p465-478.

Richardson K, Benson I, Carling PA. 2003. An instrument to record sediment movement in bedrock channels. Erosion and Sediment Transport Measurement in Rivers: *Technical and Methodological Advances,* IAHS Publications 283.

Richardson R. 2002. Simplified model for assessing meander bend migration rates. *Journal of Hydraulic Engineering* 128:1094-1097.

Rickenmann D. 1991. Hyperconcentrated flow and sediment transport at steep slopes. *Journal of Hydraulic Engineering* 117: 1419-1439.

Rickenmann D, McArdell BW. 2007. Continuous measurement of sediment transport in the Erlenbach stream using piezoelectric bedload impact sensors. *Earth Surface Processes and Landforms* 32: 1362–1378.

Rinaldi M. 2003. Recent channel adjustment in alluvial rivers of Tuscany, central Italy. *Earth Surface Process and Landforms* 28: 587-609.

Rinaldi M, Casagli N. 1999. Stability of streambanks formed in partially saturated soils and effects of negative pore water pressures: the Sieve River, Italy. *Geomorphology* 26: 253-277.

RKL Arup. 1999a. Dynamic assessment of unstable reaches of the Upper Wharfe. Environment Agency, Final Report.

RKL Arup. 1999b. Upper Wharefedale 'Best Practise' Project. Dynamic Assessment of Unstable Reaches of the Upper Wharfe. RKL-Arup Water Consultancy.

Roache PJ. 1997. Quantification of uncertainty in computational fluid dynamics. *Annual Review of Fluid Mechanics* 29: 123-160.

Roberts CR. 1989. Flood frequency and urban-induced channel change: some British examples. In *Floods: Hydrological Sedimentological and Geomorphological Implications*, Beven K, Carling P. (eds.). Wiley, Chichester. 57-82.

Robinson M. 1980. The effects of pre-afforestation drainage on the stream flow and water quality of a small upland catchment. *Institute of Hydrology Report 73, Wallingford.*

Robinson M. 1985. The hydrological effects of moorland gripping: a re-appraisal of the Moor House research. *Journal of Environmental Management* 21: 205-211.

Robinson M. 1990. Impact of improved drainage on river flows. *Institute of Hydrology Report No.* 113: Oxon, UK.

Rodrigues S, Bréhéret J, Macaire J, Moatar F, Nistoran D, Juge P. 2006. Flow and sediment dynamics in the vegetated secondary channels of an anabranching river: The Loire River, France. *Sedimentary Geology* 186: 89-109.

Rumsby BT, Macklin MG. 1994. Channel and floodplain response to recent abrupt climate change: the Tyne basin, Northern England. *Earth Surface Processes and Landforms* 19: 489–515.

Salo J, Kalliola R, Hakkinen I, Makinen Y, Niemala P, Puhakka M, Coley PD. 1986. River dynamics and the diversity of the Amazon lowland forest. *Nature* 322: 254-258.

Savenije HHG. 2003. The width of a bankfull channel; Lacey's formula explained. *Journal of Hydrology* 276: 176-183.

Schmidt KH. 1994. River channel adjustment and sediment budget in response to a catastrophic flood event (Lainbach catchment, Southern Bavaria). In *Dynamics and Geomorphology of Mountain Rivers.* Schmidt KH, Ergenzinger P. (eds.). Springer-Verlag, London.

Schoklitsh A. 1934. Der geschiebetrieb und die geschiebefracht. *Wasserkraft Wasserwirtschaft* 5: 1-7.

Schumm SA. 1977. *The Fluvial System.* New York, Wiley.

Sear DA, Newson MD. 1993. Sediment and gravel transportation in rivers including the use of gravel traps. *National Rivers Authority Project Report.* 232: 93pp.

Sear DA, Newson MD, Brookes A. 1995. Sediment-related river maintenance: the role of fluvial geomorphology. *Earth Surface Processes and Landforms* 20: 629-647.

Sear DA, Archer D. 1998. The geomorphological impacts of gravel mining: case study of the Wooler Water, Northumberland, UK. In *Gravel-Bed Rivers in the Environment.* Klingeman PC, Beschta RL, Komar PD, Bradley JB. (eds.). Water Resources Publications, Colorado. 455-470.

Shields A. 1936. Anwendung der aechlichkeitmechanik und der turbulenz forschung auf die geschiebebewegung. *Mitteilungen der Pruessischen Versuchsanstalt fuer Wasserbau and Schiffbau.* Berlin.

Simon A, Darby SE. 1997. Process-form interactions in unstable sand-bed river channels: A numerical modelling approach. *Geomorphology* 21: 85-106.

Simon A, Collinson AJC. 2001. Pore-water pressure effects on the detachment of cohesive streambeds: seepage forces and matrix suction. *Earth Surface Processes and Landforms* 26: 1421-1442.

Simon A, Wolfe WJ, Molinas A. 1991. Mass wasting algorithms in an alluvial channel model. *Proceedings of the 5th Federation Inter-agency Sediment Conference.* Las Vegas, Nevada. 2: 8-22 8-29.

Simon A, Curini A, Darby SE, Langendoen EJ. 1999. Streambank mechanics and the role of bank and near-bank processes in incised channels. In *Incised River Channels.* Darby SE, Simon A. (eds.). Wiley, Chichester. pp.123–152.

Simon A, Curini A, Darby SE, Langendoen EJ. 2000. Bank and near-bank processes in an incised channel. *Geomorphology* 35: 193-217.

Slaymaker O. 2000. Assessment of the geomorphic impacts of forestry in British Columbia. *AMBIO 29: 381-387.*

Sloan J, Miller JR, Lancaster N. 2001. Response and recovery of the Eel River, California, and its tributaries to floods in 1955, 1964 and 1997. *Geomorphology* 36: 129-154.

Smart GM, Duncan MJ, Walsh JM. 2002. Relatively rough flow resistance equations. *Journal of Hydraulic Engineering* 128: 568-578

Stark CP. 2006. A self-regulating model of bedrock river channel geometry. *Geophysical Research Letters* 33.

Stelczer K. 1981. Bedload transport: Theory and Practice. *Water Resources Publications* Colorado. pp 295-298.

Stewart AJA, Lance AN. 1983. Moor-draining: A review of impacts on land use. *Journal of Environmental Management* 17: 81-99.

Stewart L. 1984. River Wharfe land drainage proposals from above Buckden Bridge down to Kettlewell and their impact upon fisheries and angling. *Report to Yorkshire Water Authority.* Leeds. January 1984, 45pp.

Stott T. 1997. A comparison of stream bank erosion processes on forested and moorland streams in the Balquhidder catchments, central Scotland. *Earth Surface Processes and Landforms* 22: 383-399.

Stott T. 1999. Stream bank and forest ditch erosion: responses to timber harvesting in mid-Wales. In *Fluvial Processes and Environmental Changes.* Brown AG, Quine TA. (eds.). Wiley, Chichester. 47-70.

Stott T, Mount N. 2004. Plantation forestry impacts on sediment yields and downstream channel dynamics in the UK: a review. *Progress in Physical Geography* 28: 197-240.

Stover SC, Montgomery DR. 2001. Channel change and flooding, Skokomish River, Washington. *Journal of Hydrology* 243: 271-286.

Strickler A. 1923. Beitrage zur frage der geschwindigheitsformel und der rauhigkeiszahlen furstrome, kanale undgeschlossene leitungen. *Mitteilungen des Eidgenossicher Amtes fur Wasserwirtschaft.* Bern, Switzerland. 16p.

Sullivan A, Ternan JL, Williams AG. 2004. Land use change and hydrological response in the Camel catchment, Cornwall. *Applied Geography* 24: 119-137.

Sun T, Meakin P, Jøssang T. 1996. A simulation model for meandering rivers. *Water Resources Research* 32: 2937-2954.

Sun T, Meakin P, Jøssang T. 2001a. Meander migration and the lateral tilting of floodplains. *Water Resources Research* 37: 1485-1502.

Sun T, Meakin P, Jøssang T. 2001b. A computer model for meandering rivers with multiple bed load sediment sizes 1: Theory. *Water Resources Research* 37: 2227-2241.

Sun T, Meakin P, Jøssang T. 2001c. A computer model for meandering rivers with multiple bed load sediment sizes 2: Computer simulations. *Water Resources Research* 37: 2243-2258.

Surian N. 1999. Channel change due to river regulation: the case of the Piave River. *Earth Surface Processes and Landforms* 24: 1135-1151.

Surian N, Rinaldi M. 2003. Morphological response to river engineering and management in alluvial channels in Italy. *Geomorphology* 50: 307-326.

Sutherland AJ. 1987. Static armour layers by selective erosion. In *Sediment Transport in Gravel Bed Rivers.* Thorne CR, Bathurst JC, Hey RD. (eds.), Wiley, pp 243-268

Talbot T, Lapointe M. 2002. Numerical modelling of gravel bed river response to meander straightening: The coupling between the evolution of bed pavement and long profile. *Water Resources Research* 38 (6).

Tayefi V. 2005. One-and two-dimensional modelling of upland floodplain flows in response to difference channel configuration. Ph.D. Thesis. University of Leeds.

Tayefi V, Lane SN, Hardy RJ, Yu D. 2007. A comparison of 1D and 2D approaches to modelling flood inundation over complex upland floodplains. *Hydrological Processes* 21: 3190-3202.

Taylor JR. 1997. *An Introduction to Error Analysis: The Study of Uncertainties in Physical Measurements*, 2nd Edition, University Science Books.

Thomas R, Nicholas AP. 2002. Simulation of braided river flow using a new cellular routing scheme. *Geomorphology* 43: 179-195.

Thomas R, Nicholas AP, Quine TA. 2002. Development and application of a cellular model to simulate model to simulate braided river processes-form interactions and morphological change. In *River Flow.* Bousmar D, Zech Y. (eds.). Balkema, Rotterdam, pp 783-791.

Thomas R, Nicholas AP, Quine TA. 2007. Cellular modelling as a tool for interpreting historic braided river evolution. *Geomorphology* 90: 302-317.

Thorne CR. 1981. Field measurements of rates of bank erosion and bank material strength. In *Erosion and Sediment Transport* (Proceedings of the Florence Symposium, June, 1981), IAHS Publication 133, International Association of Hydrological Sciences, Wallingford, 503-512.

Thorne CR. 1982. Processes and mechanics of river bank erosion. In *Gravel-bed rivers: Fluvial Processes, Engineering and Management.* Hey RD, Bathurst JC, Thorne CR. (eds.). Wiley, Chichester. p225-272.

Thorne CR. 1990. Effects of vegetation on riverbank erosion and stability. In *Vegetation and Erosion* Thornes JB. (ed.). Wiley, p125-144.

Thorne CR. 1997. Channel types and morphological classification. In *Applied Fluvial Geomorphology for River Engineering and Management.* Thorne CR, Hey RD, Newson MD. (eds.). John Wiley and Sons. Chichester, UK. p175-222.

Thorne CR. 1998. River width adjustment 1: Processes and mechanisms. *Journal of Hydraulic Engineering* 124: 881-902.

Thorne CR, Hey RD. 1979. Direct measurements of secondary circulation at a river inflexion point. *Nature* 280: 226-228.

Thorne CR, Lewin J. 1979. Bank processes, bed material movement and planform development in a meandering river. In *Adjustments of the Fluvial System.* Rhodes DD, Williams GP. (eds.). Kendall/Hunt Publications Company, Iowa. 117-137.

Thorne CR, Tovey NK. 1981. Stability of composite river banks. *Earth Surface Processes and Landforms* 6: 469-484.

Thorne CR, Furbish DJ. 1995. Influences of coarse bank roughness on flow within a sharply curved river bend. *Geomorphology* 12: 241-257.

Thorne CR, Hey RD, Newson MD. 1997a. *Applied Fluvial Geomorphology for River Engineering and Management.* John Wiley and Sons. Chichester, UK. 382p.

Thorne CR, Hey RD, Newson MD. 1997b. Manual of Applied geomorphology for river engineering. *Report to US Army Research Office,* London.

Toffaleti FB.1968. A procedure for computation of total river sand discharge and detailed distribution bed to surface. *Technical report no 5,* Committee of Channel Stabilization, US. Army Corps of Engineers, Vicksburg, Mississippi.

Tollan A. 2002. Land-use change and floods: what do we need most, research or management? *Water Science and Technology* 45: 183-190.

Trimble SW. 1994. Erosional effects of cattle on stream banks in Tennessee, USA. *Earth Surface Processes and Landforms* 19: 451-464.

Tunicliffe J, Gottesfeld AS, Mohamed M. 2000. High resolution measurement of bedload transport. *Hydrological Processes* 14: 2631-2643.

Van Niekerk A, Vogel KR, Slingerland RL, Bridges JS. 1992. Routing of heterogeneous sediments over a movable bed: model development. *Journal of Hydraulic Engineering* 118: 246-262.

Vanacker V, Govers G, Poesen J, Deckers J, Dercon G, Loaiza G. 2003. The impact of environmental change on the intensity and spatial pattern of water erosion in a semi-arid mountainous Andean environment. *Catena* 51: 329-347.

Verhaar PM, Biron PM. 2006. Modelling future impacts of climate change on the tributaries of the St Lawrence River. *Joint Annual Meeting of the Geological Association of Canada and the Mineralogical Association of Canada.* University of Quebec in Montreal.

Verhaar PM, Biron PM, Ferguson RI, Hoey TB. in press. A modified morphodynamic model for investigating the response of rivers to short-term climate change. *Geomorphology.*

Wainwright J, Mulligan M. 2004. *Environment Modelling: Finding Simplicity in Complexity.* Wiley, Chichester, pp397.

Wallerstein NP, Thorne CR. 2004. Influence of large woody debris on morphological evolution of incised, sand-bed channels. *Geomorphology* 57: 53–73.

Warburton J, Danks M, Wishart D. 2002. Stability of an upland gravel-bed stream, Swinhope Burn, Northern England. *Catena.* 49: 309-329.

Waterhouse EK. 2003. River channel change in a Scottish upland river. Unpublished Undergrad Dissertation. University of Leeds.

Wathen SJ, Hoey TB, Werritty A. 1997. Quantitative determination of the activity of within-reach sediment storage in a small gravel-bed river using transit time and response time. *Geomorphology* 20: 113-134.

Werritty A. 1992. Downstream fining in a gravel-bed river in southern Poland: lithologic controls and the role of abrasion. In *Dynamics of gravel-bed rivers.* Billi P, Hey RD, Thorne CR, Tacconi P. (eds.). Chichester, Wiley. 333-346.

Werritty A. 1997. Short-term changes in channel stability. In *Applied Fluvial Geomorphology for River Engineering and Management.* Thorne CR, Hey RD, Newson MD. (eds.). John Wiley and Sons Ltd. p47-65.

Werritty A. Ferguson RI. 1980. Pattern changes in a Scottish braided river over 1, 30 and 200 years. In *Timescales in Geomorphology.* Culligford RA, Davidson DA, Lewin J. (eds.), Wiley, New York, 53-68.

Werritty A, Leys KF. 2001. The sensitivity of Scottish rivers and upland valley floors to recent environmental change. *Catena* 42: 251-273.

Werritty A, Foster M. 1998. Climatic variability and recent changes in rainfall and river flows in Scotland In: *Proceedings of the 2nd International Conference on and Water.* Lemmela R, Helenius N. (eds.). Espoo, Finland. 3: 1110-1119.

Westaway RM, Lane SN, Hicks DM. 2000. The development of an automated correction procedure for digital photogrammetry for the study of wide, shallow, gravel-bed rivers. *Earth Surface Processes and Landforms* 25: 209-226.

White R. 2002. *The Yorkshire Dales: a Landscape Through Time.* Great Northern Books, Ilkley, 2nd Edition.

White WR, Bettess R, Paris E. 1982. Analytical approach to river regime. *Journal of the Hydraulics Division* 108: 1179-1193.

Whitehead PG, Calder IR. 1993. Special Issue: The Balquhidder catchment and process studies. *Journal of Hydrology* 145: 251-216.

Whiting PJ, Dietrich WE. 1993a. Experimental studies of bed topography and flow patterns in large-amplitude meanders 1: Observations. *Water Resources Research* 29: 3605-3614.

Whiting PJ, Dietrich WE. 1993b. Experimental studies of bed topography and flow patterns in large-amplitude meanders 2: Mechanics. *Water Resources Research* 29: 3615-3622.

Wilcock PR. 1997. Entrainment, displacement and transport of tracer gravels. *Earth Surface Processes and Landforms* 22: 1125-1138.

Wilcock PR. 2001. Toward a practical method for estimating sediment-transport rates in gravel-bed rivers. *Earth Surface Processes and Landforms* 26: 1395-1408.

Wilcock PR, McArdell BW. 1997. Partial transport of a sand/gravel sediment. *Water Resources Research* 33: 235-245.

Wilcock PR, Crowe JC. 2003. Surface-based transport model for mixed-size sediment. *Journal of Hydraulic Engineering* 129: 120-128.

Wilcock PR, Barta AF, Shea CC, Kondolf GM, Matthews WVG, Pitlick J. 1996. Observations of flow and sediment entrainment on a larger gravel-bed river. *Water Resources Research* 32: 2897-2909.

Williams GP. 1986. River meanders and channel size. *Journal of Hydrology* 88: 147-164.

Winterbottom SJ. 2000. Medium and short-term channel change on the rivers Tay and Tummel. *Geomorphology* 33: 195-208

Winterbottom SJ, Gilvear DJ. 2000. A GIS-based approach to mapping probabilities of river bank erosion: Regulated River Tummel, Scotland. *Regulated Rivers Research and Management* 16: 127-140.

Wishart D, Warburton J, Bracken L. 2008. Gravel extraction and planform change in a wandering gravel-bed river: The River Wear, Northern England. *Geomorphology* 94: 131-152.

Wittenberg L. 2002. Structural patterns in coarse gravel bed rivers: typology, survey and assessment of the roles of grain size and river regime. *Geografiska Annaler* 84: 25-37

Wohl E, Anthony DJ, Madsen SW, Thompson DM. 1996. A comparison of surface sampling methods for coarse fluvial sediments. *Water Resources Research* 32: 3219-3226.

Wolcott J, Church M. 1991. Strategies for sampling spatially heterogeneous phenomena: the example of river gravels. *Journal of Sedimentary Petrology* 61: 834-843.

Wolman MG. 1954. A method of sampling coarse river-bed material. *American Geophysical Union Transcriptions* 35: 951-956.

Wolman MG. 1959. Factors influencing erosion of cohesive banks. *American Journal of Science* 257: 204-216.

Wolman MG, Millar JP. 1960. Magnitude and frequency of forces in geomorphic processes. *Journal of Geology* 68: 54-74.

Wolman MG, Schick AP. 1967. Effects of construction on fluvial sediment, urban and suburban areas of Maryland. *Water Resources Research* 3: 117-125.

Wolman MG, Gerson R. 1978. Relative scales of time and effectiveness of climate in watershed geomorphology. *Earth Surface Processes* 3: 189-208.

Wyzga B. 1993. River response to channel regulation: case study of the Raba River, Carpanthians, Poland. *Earth Surface Processes and Landforms* 18: 541-556

Xu J. 1997. Study of sedimentation zones in a large sand-bed braided river: an example from the Hanjiang river of China. *Geomorphology* 21: 153-165.

Yang CT. 1973. Incipient motion and sediment transport. *Journal of the Hydraulics Division, ASCE* 99: 1679-1704.

Yang CT. 1976. Minimum unit stream power and fluvial hydraulics. *Journal of the Hydraulics Division,* ASCE 102: 769-784.

Yang CT, Wan S. 1999. Comparison of selected bed-material load formula. *Journal of Hydraulic Engineering* 117: 973-989.

Yang CT, Molinas A, Song CS. 1988. GSTARS – Generalizes stream tube model for alluvia river simulation. In *Twelve selected computer stream sedimentation models developed in the United States.* Fan S. (ed.) Federal Energy Regulatory Commission, Washington D.C.

Yorkshire Water Authority. 1983. River Wharfe: Buckden Scheme. *Report by Regional Land Drainage Committee. Yorkshire Water Authority* March 1983.

Yu G, Smart G. 2003. Aspect ratio to maximize sediment transport in rigid bank channels. *Journal of Hydraulic Engineering* 129: 927-935.

Appendix I: Field Surveys

These surveys have been reduced in size as they were hand drawn onto A3 paper.

Survey Page 2

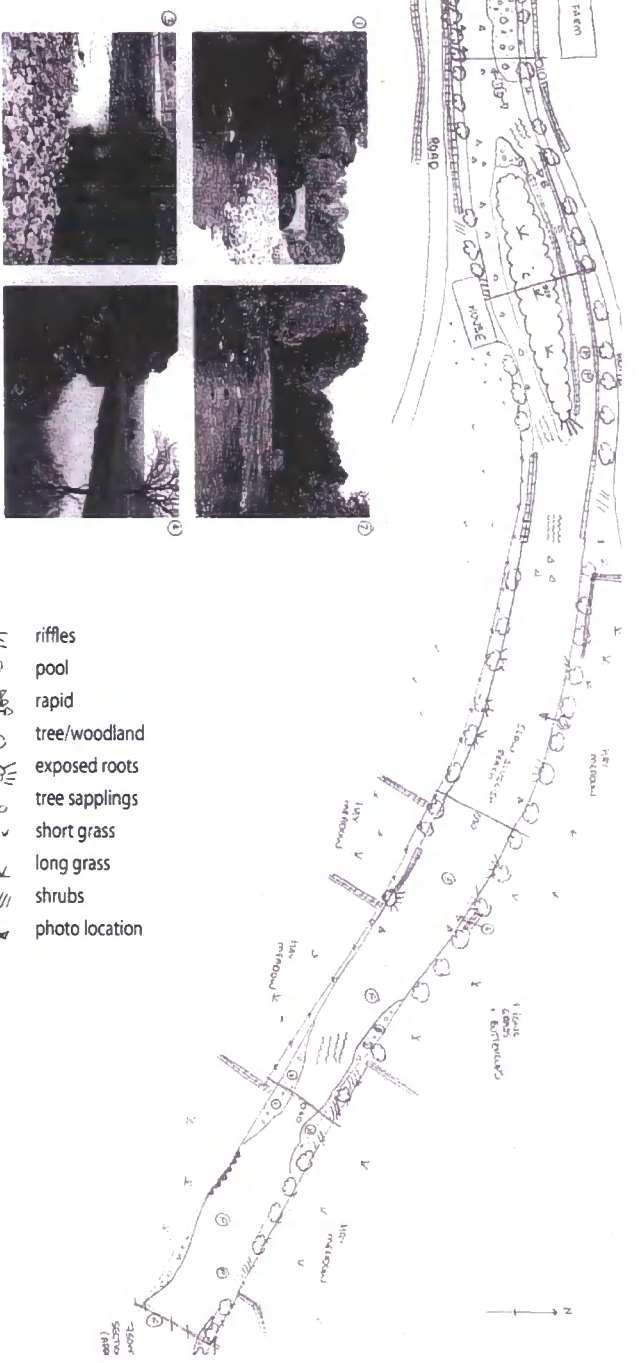

Survey Page 3

Survey Page 4

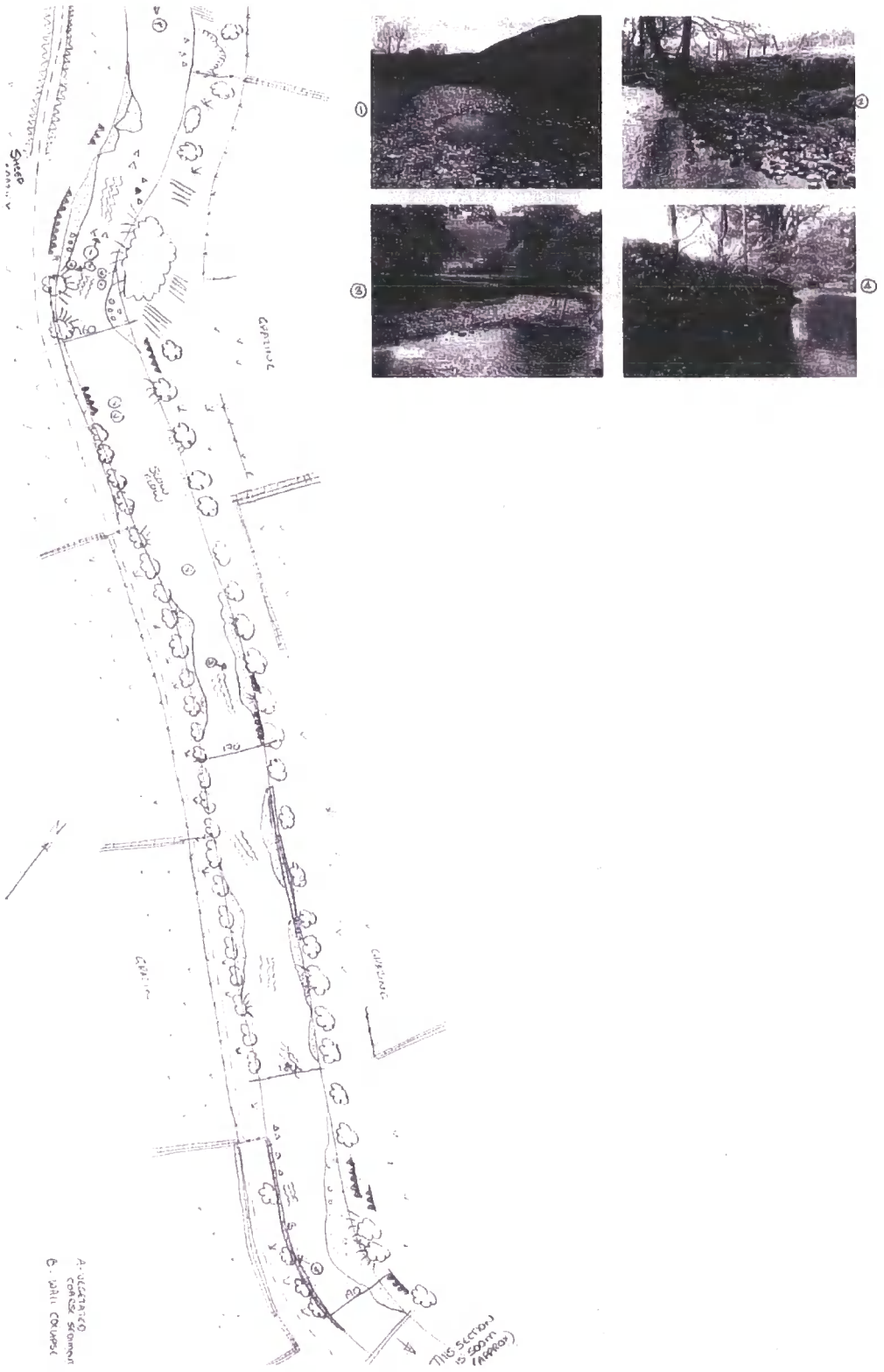

SURVEY PAGE 5

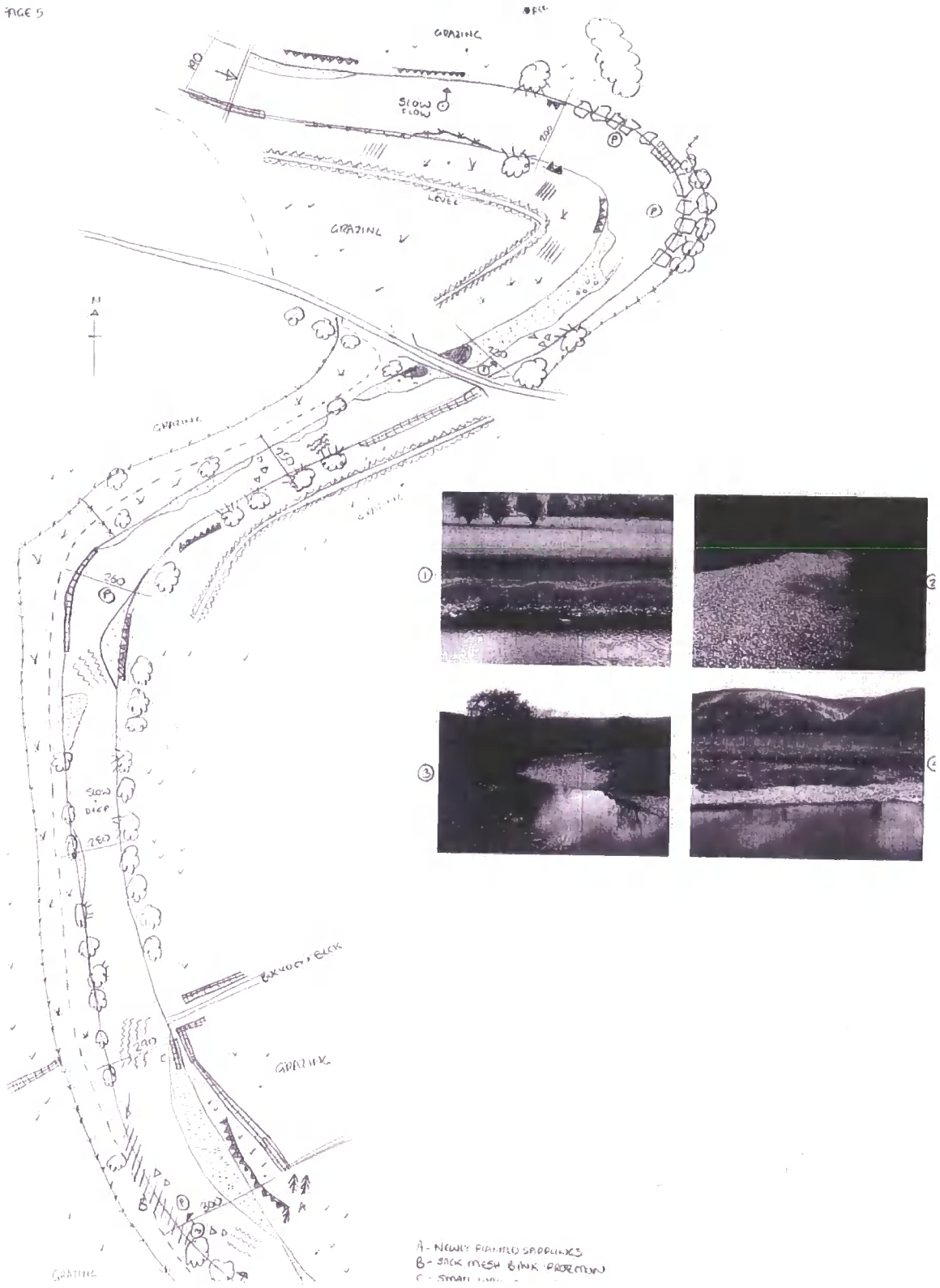

Survey Page 6

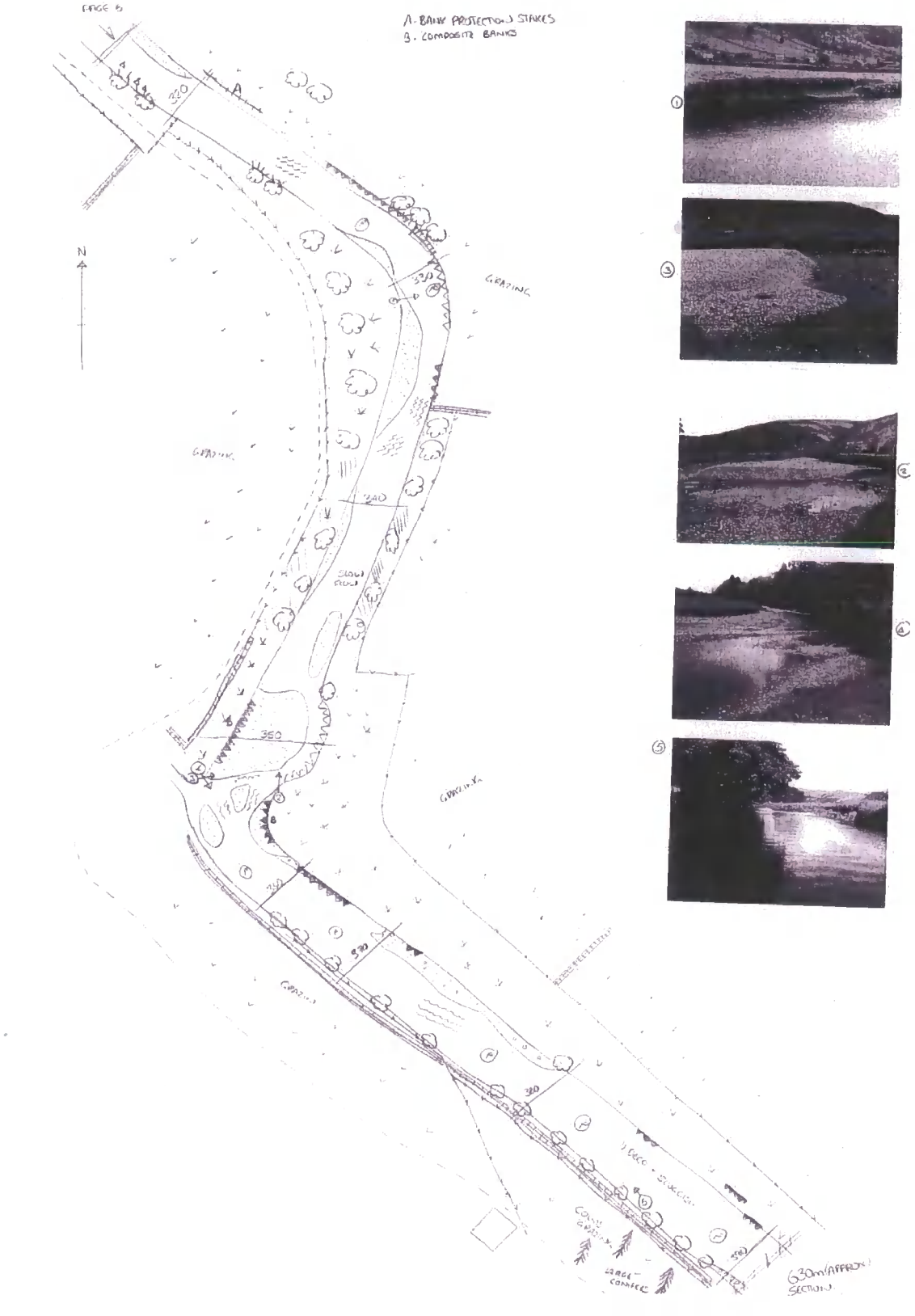

SURVEY PAGE 7

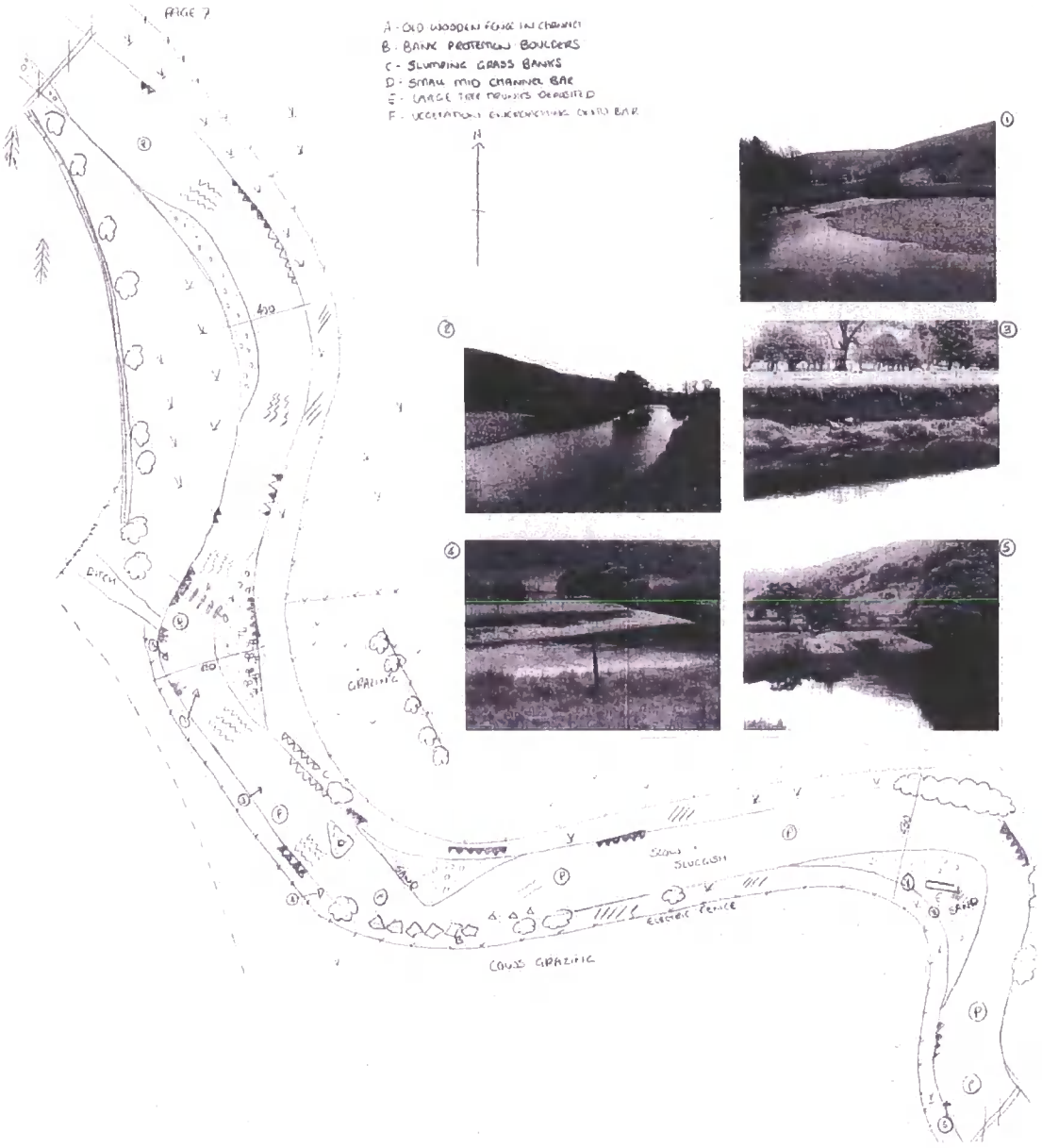

Survey Page 8

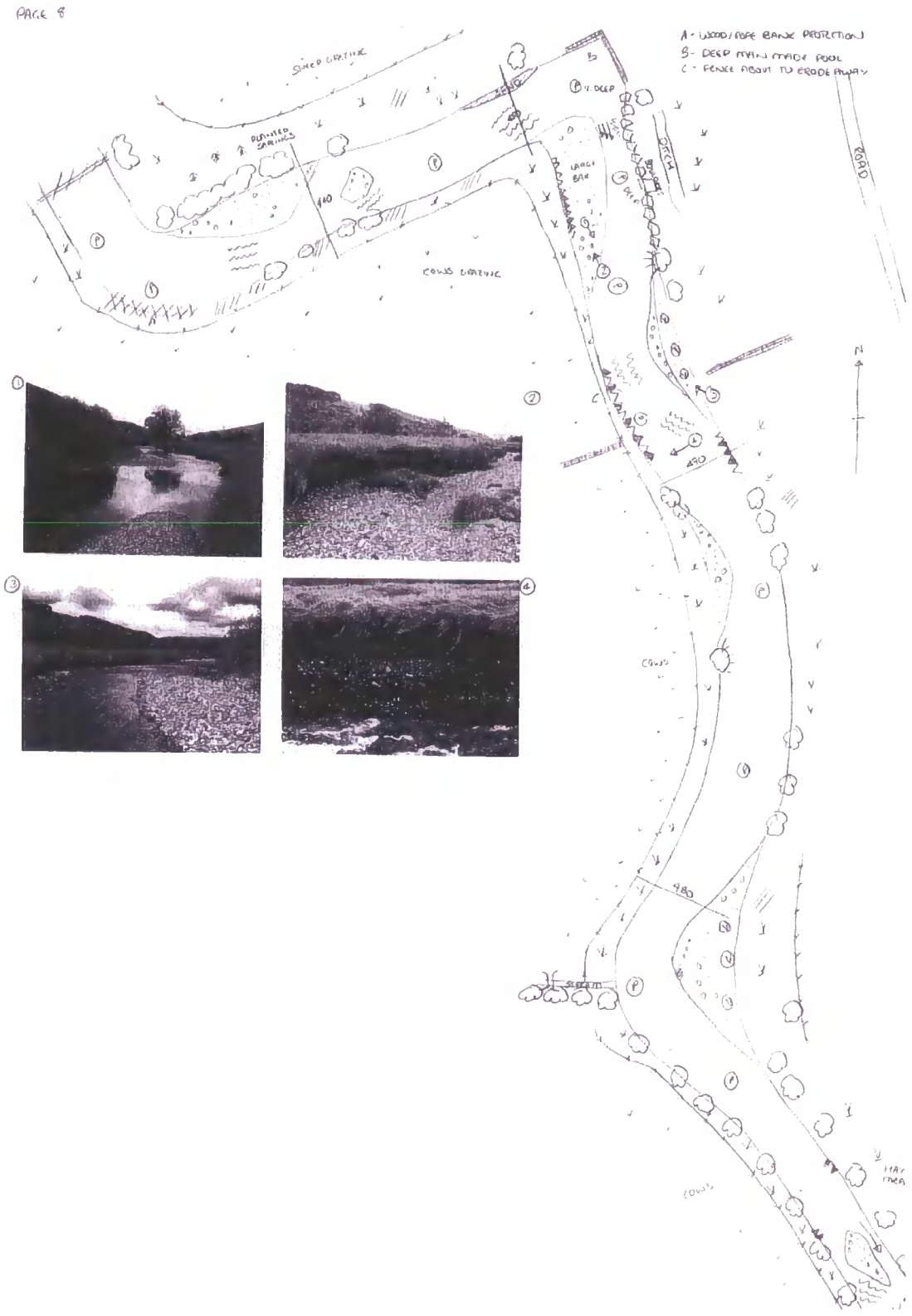

Survey Page 9

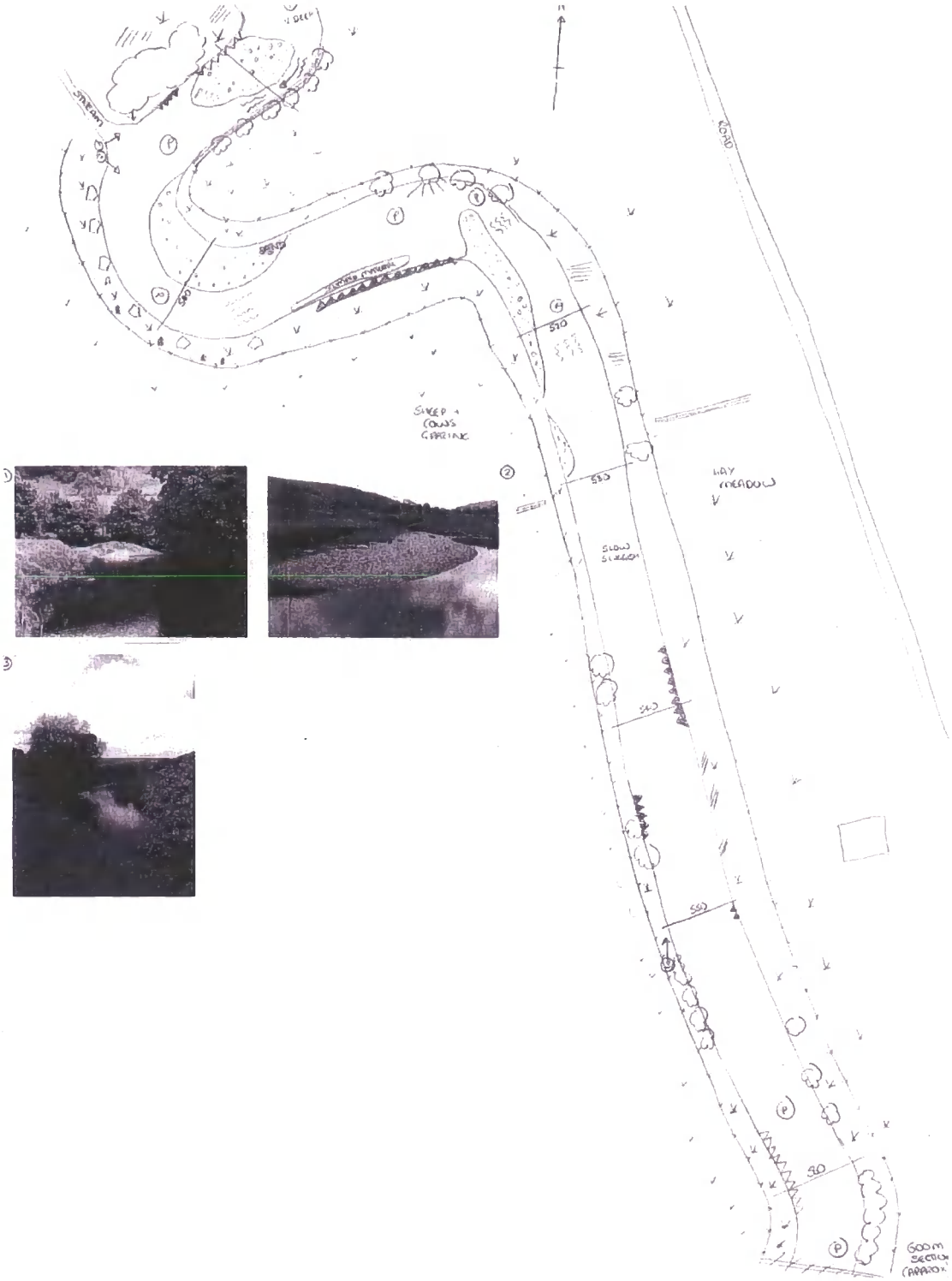

SURVEY PAGE 10

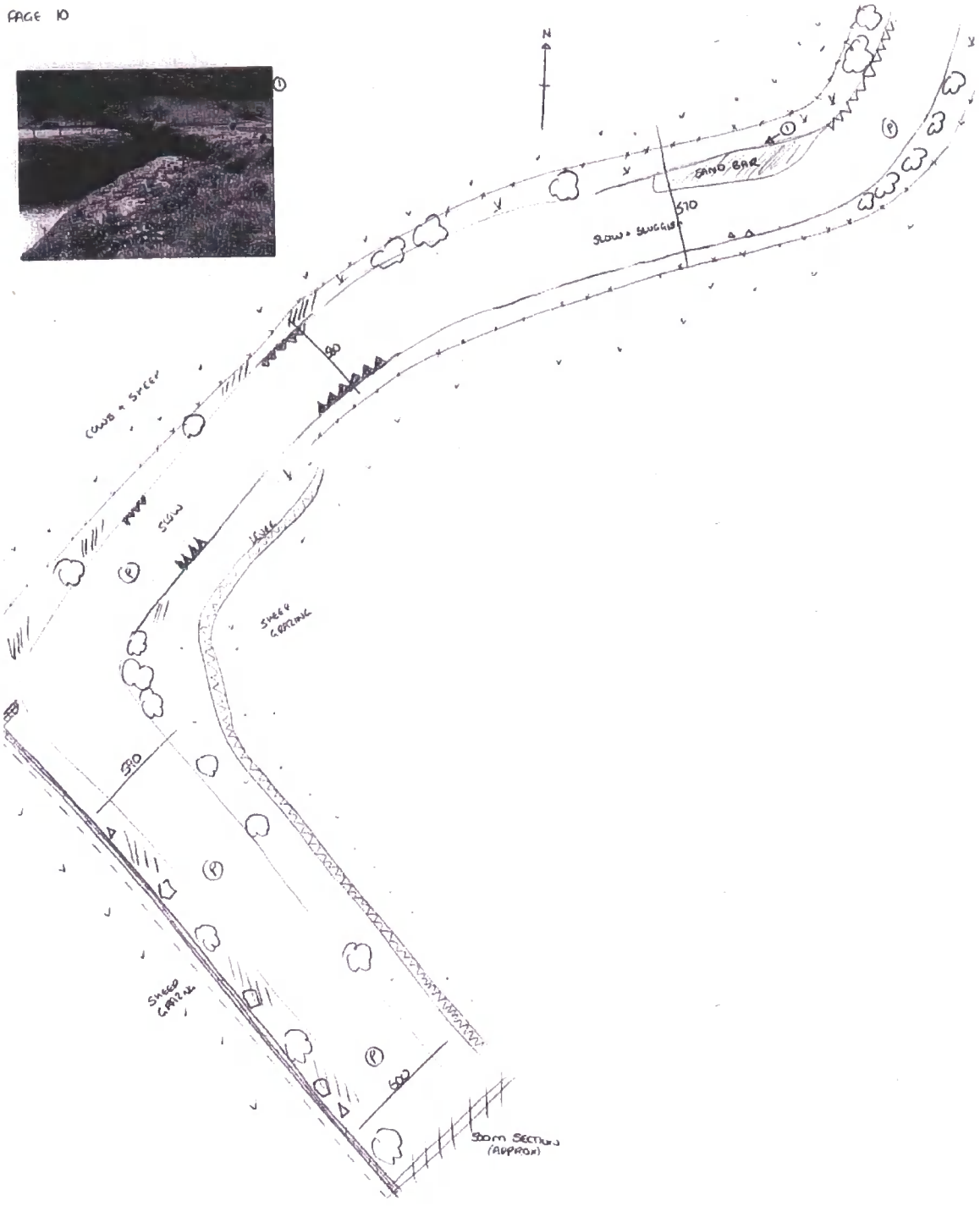

APPENDIX II: SURVEY DATES AND DETAILS

Section	Yorkshire Water Authority	Heritage and Newson		Arup	JBA
10	1982				2000
20	1982				2000
30	1982				2000
40	1982				
50	1982				2000
60					
70					2000
80					2000
90					2000
100	1982	1989	1997		
110	1982	1989	1997		
120					2000
130	1982				
140					
150	1982			1999	2000
160	1982	1989	1997	1999	2000
170	1982				
180	1982				
190	1982				2000
200					
210					
220					
230	1982			1999	
240	1982	1989	1997	1999	2000
250					
260					2000
270	1982				
280	1982				
290	1982				2000
300	1982				
310					
320	1982				2000
330	1982	1989	1997		
340	1982				2000
350					
360		1989	1997		2000
370					2000
380					2000
390					2000
400				1999	
410		1989	1997	1999	2000
420				1999	
430		1989	1997	1999	
440				1999	2000
450				1999	
460				1999	
470					2000
480				1999	
490					
500					
510		1989	1997		
520					2000
530					
540					2000
550					
560					2000
570		1989	1997		
580					2000
590					
600		1989	1997		2000

APPENDIX II: SURVEY DATES AND DETAILS

	Reid, (2004)						Waterhouse					
Section	Survey 1	Survey 2	Survey 3	Survey 4	Survey 5	Survey 6	Survey 7	Survey 8	Survey 9	Survey 10	Survey 11	Survey 12
10	08-Dec-01	19-Mar-02	12-Dec-02	15-Mar-03	15-Dec-03	13-Mar-04	23-Jan-05	06-May-05	17-Jan-06	12-Apr-06	9th-Jan-07	9th-July-07
20	08-Dec-01	19-Mar-02	12-Dec-02	15-Mar-03	15-Dec-03	13-Mar-04	23-Jan-05	-	-	-	-	-
30	15-Dec-01	19-Mar-02	12-Dec-02	15-Mar-03	15-Dec-03	13-Mar-04	23-Jan-05	06-May-05	08-Dec-05	12-Apr-06	9th-Jan-07	-
40	15-Dec-01	19-Mar-02	12-Dec-02	15-Mar-03	15-Dec-03	13-Mar-04	23-Jan-05	06-May-05	08-Dec-05	12-Apr-06	9th-Jan-07	-
50	13-Dec-01	16-Mar-02	12-Dec-02	13-Mar-03	15-Dec-03	13-Mar-04	23-Jan-05	06-May-05	08-Dec-05	12-Apr-06	9th-Jan-07	-
60	13-Dec-01	19-Mar-02	12-Dec-02	13-Mar-03	15-Dec-03	13-Mar-04	23-Jan-05	06-May-05	08-Dec-05	12-Apr-06	9th-Jan-07	9th-July-07
70	13-Dec-01	16-Mar-02	12-Dec-02	13-Mar-03	15-Dec-03	13-Mar-04	26-Jan-05	19-Apr-05	01-Dec-05	12-Apr-06	9th-Jan-07	9th-July-07
80	13-Dec-01	19-Mar-02	12-Dec-02	13-Mar-03	15-Dec-03	13-Mar-04	26-Jan-05	07-May-05	01-Dec-05	12-Apr-06	9th-Jan-07	9th-July-07
90	13-Dec-01	10-Mar-02	12-Dec-02	13-Mar-03	15-Dec-03	13-Mar-04	26-Jan-05	07-May-05	24-Jan-06	10-Apr-06	8th-Jan-07	9th-July-07
100	09-Dec-01	16-Mar-02	13-Dec-02	13-Mar-03	15-Dec-03	13-Mar-04	23-Jan-05	07-May-05	24-Jan-06	10-Apr-06	8th-Jan-07	-
110	09-Dec-01	10-Mar-02	13-Dec-02	13-Mar-03	15-Dec-03	13-Mar-04	23-Jan-05	07-May-05	17-Jan-06	10-Apr-06	8th-Jan-07	9th-July-07
120	13-Dec-01	17-Mar-02	13-Dec-02	13-Mar-03	15-Dec-03	13-Mar-04	23-Jan-05	07-May-05	24-Jan-06	10-Apr-06	8th-Jan-07	-
130	15-Dec-01	17-Mar-02	13-Dec-02	13-Mar-03	15-Dec-03	13-Mar-04	23-Jan-05	07-May-05	17-Jan-06	10-Apr-06	8th-Jan-07	-
140	13-Dec-01	17-Mar-02	13-Dec-02	13-Mar-03	15-Dec-03	13-Mar-04	23-Jan-05	07-May-05	17-Jan-06	10-Apr-06	8th-Jan-07	10-Jul-07
150	13-Dec-01	17-Mar-02	20-Dec-02	13-Mar-03	15-Dec-03	13-Mar-04	23-Jan-05	19-Apr-05	01-Dec-05	12-Apr-06	9th-Jan-07	10-Jul-07
160	15-Dec-01	17-Mar-02	20-Dec-02	13-Mar-03	15-Dec-03	13-Mar-04	23-Jan-05	07-May-05	24-Jan-06	12-Apr-06	9th-Jan-07	-
170	16-Dec-01	10-Mar-02	20-Dec-02	15-Mar-03	15-Dec-03	13-Mar-04	23-Jan-05	19-Apr-05	17-Jan-06	12-Apr-06	9th-Jan-07	10-Jul-07
180	16-Dec-01	10-Mar-02	13-Dec-02	15-Mar-03	15-Dec-03	13-Mar-04	22-Jan-05	07-May-05	17-Jan-06	12-Apr-06	9th-Jan-07	9th-July-07
190	16-Dec-01	10-Mar-02	20-Dec-02	15-Mar-03	15-Dec-03	13-Mar-04	22-Jan-05	07-May-05	01-Dec-05	10-Apr-06	8th-Jan-07	9th-July-07
200	09-Dec-01	10-Mar-02	20-Dec-02	15-Mar-03	18-Dec-03	13-Mar-04	24-Jan-05	19-Apr-05	01-Dec-05	10-Apr-06	8th-Jan-07	9th-July-07
210	14-Dec-01	11-Mar-02	20-Dec-02	15-Mar-03	18-Dec-03	13-Mar-04	24-Jan-05	19-Apr-05	01-Dec-05	10-Apr-06	8th-Jan-07	10-Jul-07
220	09-Dec-01	10-Mar-02	20-Dec-02	15-Mar-03	18-Dec-03	14-Mar-04	24-Jan-05	19-Apr-05	01-Dec-05	10-Apr-06	8th-Jan-07	-
230	16-Dec-01	11-Mar-02	20-Dec-02	15-Mar-03	18-Dec-03	14-Mar-04	24-Jan-05	27-Apr-05	01-Dec-05	10-Apr-06	8th-Jan-07	9th-July-07
240	16-Dec-01	11-Mar-02	20-Dec-02	15-Mar-03	18-Dec-03	14-Mar-04	24-Jan-05	27-Apr-05	01-Dec-05	10-Apr-06	8th-Jan-07	-
250	09-Dec-01	11-Mar-02	20-Dec-02	15-Mar-03	18-Dec-03	14-Mar-04	22-Jan-05	27-Apr-05	08-Dec-05	10-Apr-06	8th-Jan-07	-
260	14-Dec-01	12-Mar-02	20-Dec-02	15-Mar-03	18-Dec-03	14-Mar-04	24-Jan-05	27-Apr-05	08-Dec-05	30-Mar-06	8th-Jan-07	9th-July-07
270	09-Dec-01	12-Mar-02	20-Dec-02	15-Mar-03	18-Dec-03	14-Mar-04	24-Jan-05	27-Apr-05	08-Dec-05	30-Mar-06	20th-Dec-06	10-Jul-07
280	14-Dec-01	11-Mar-02	20-Dec-02	15-Mar-03	18-Dec-03	14-Mar-04	22-Jan-05	00-Jan-00	08-Dec-05	30-Mar-06	20th-Dec-06	10-Jul-07
290	14-Dec-01	12-Mar-02	20-Dec-02	15-Mar-03	18-Dec-03	14-Mar-04	22-Jan-05	-	08-Dec-05	30-Mar-06	20th-Dec-06	9th-July-07
300	14-Dec-01	11-Mar-02	20-Dec-02	17-Mar-03	18-Dec-03	14-Mar-04	24-Jan-05	27-Apr-05	01-Dec-05	30-Mar-06	20th-Dec-06	9th-July-07
310	14-Dec-01	12-Mar-02	20-Dec-02	17-Mar-03	18-Dec-03	14-Mar-04	24-Jan-05	26-Apr-05	08-Dec-05	30-Mar-06	20th-Dec-06	-
320	14-Dec-01	12-Mar-02	20-Dec-02	17-Mar-03	18-Dec-03	14-Mar-04	24-Jan-05	26-Apr-05	08-Dec-05	30-Mar-06	20th-Dec-06	10-Jul-07

330	15-Dec-01	13-Mar-02	20-Dec-02	17-Mar-03	18-Dec-03	14-Mar-04	24-Jan-05	26-Apr-05	01-Dec-05	30-Mar-06	20th-Dec-06	10-Jul-07
340	15-Dec-01	13-Mar-02	20-Dec-02	17-Mar-03	18-Dec-03	14-Mar-04	24-Jan-05	26-Apr-05	07-Dec-05	30-Mar-06	20th-Dec-06	10-Jul-07
350	15-Dec-01	11-Mar-02	20-Dec-02	17-Mar-03	18-Dec-03	14-Mar-04	24-Jan-05	26-Apr-05	07-Dec-05	30-Mar-06	20th-Dec-06	10-Jul-07
360	15-Dec-01	13-Mar-02	12-Dec-02	17-Mar-03	18-Dec-03	14-Mar-04	24-Jan-05	26-Apr-05	07-Dec-05	12-Apr-06	9th-Jan-07	-
370	15-Dec-01	11-Mar-02	12-Dec-02	17-Mar-03	18-Dec-03	14-Mar-04	24-Jan-05	26-Apr-05	07-Dec-05	12-Apr-06	9th-Jan-07	10-Jul-07
380			12-Dec-02	17-Mar-03	17-Dec-03	14-Mar-04	24-Jan-05	26-Apr-05	07-Dec-05	30-Mar-06	20th-Dec-06	04-Jul-07
390			11-Dec-02	17-Mar-03	17-Dec-03	14-Mar-04	24-Jan-05	26-Apr-05	07-Dec-05	30-Mar-06	20th-Dec-06	04-Jul-07
400			11-Dec-02	17-Mar-03	17-Dec-03	14-Mar-04	25-Jan-05	26-Apr-05	07-Dec-05	24-Apr-06	20th-Dec-06	04-Jul-07
410			11-Dec-02	17-Mar-03	17-Dec-03	14-Mar-04	26-Jan-05	26-Apr-05	07-Dec-05	24-Apr-06	20th-Dec-06	04-Jul-07
420			11-Dec-02	17-Mar-03	17-Dec-03	14-Mar-04	26-Jan-05	26-Apr-05	07-Dec-05	24-Apr-06	20th-Dec-06	04-Jul-07
430			12-Dec-02	10-Mar-03	17-Dec-03	14-Mar-04	26-Jan-05	27-Apr-05	07-Dec-05	24-Apr-06	20th-Dec-06	04-Jul-07
440			12-Dec-02	10-Mar-03	17-Dec-03	14-Mar-04	26-Jan-05	27-Apr-05	07-Dec-05	24-Apr-06	20th-Dec-06	-
450			12-Dec-02	10-Mar-03	17-Dec-03	14-Mar-04	26-Jan-05	27-Apr-05	07-Dec-05	24-Apr-06	19th-Dec-06	04-Jul-07
460			12-Dec-02	10-Mar-03	17-Dec-03	17-Apr-04	26-Jan-05	27-Apr-05	07-Dec-05	24-Apr-06	19th-Dec-06	04-Jul-07
470			12-Dec-02	10-Mar-03	17-Dec-03	17-Apr-04	26-Jan-05	27-Apr-05	07-Dec-05	24-Apr-06	19th-Dec-06	06-Jul-07
480			12-Dec-02	10-Mar-03	17-Dec-03	17-Apr-04	26-Jan-05	27-Apr-05	07-Dec-05	24-Apr-06	19th-Dec-06	06-Jul-07
490			13-Dec-02	10-Mar-03	17-Dec-03	17-Apr-04	26-Jan-05	27-Apr-05	08-Dec-05	24-Apr-06	19th-Dec-06	-
500			13-Dec-02	10-Mar-03	17-Dec-03	17-Apr-04	25-Jan-05	06-May-05	08-Dec-05	12-Apr-06	9th-Jan-07	9th-July-07
510			13-Dec-02	11-Mar-03	17-Dec-03	17-Apr-04	25-Jan-05	17-Apr-05	01-Dec-05	12-Apr-06	9th-Jan-07	06-Jul-07
520			13-Dec-02	11-Mar-03	17-Dec-03	17-Apr-04	25-Jan-05	17-Apr-05	30-Nov-05	29-Mar-06	19th-Dec-06	06-Jul-07
530			13-Dec-02	11-Mar-03	17-Dec-03	17-Apr-04	25-Jan-05	17-Apr-05	30-Nov-05	29-Mar-06	19th-Dec-06	06-Jul-07
540			18-Dec-02	11-Mar-03	17-Dec-03	17-Apr-04	25-Jan-05	17-Apr-05	30-Nov-05	29-Mar-06	19th-Dec-06	06-Jul-07
550			18-Dec-02	11-Mar-03	17-Dec-03	17-Apr-04	25-Jan-05	17-Apr-05	30-Nov-05	29-Mar-06	19th-Dec-06	06-Jul-07
560			18-Dec-02	11-Mar-03	17-Dec-03	17-Apr-04	25-Jan-05	17-Apr-05	30-Nov-05	29-Mar-06	19th-Dec-06	06-Jul-07
570			18-Dec-02	11-Mar-03	17-Dec-03	17-Apr-04	25-Jan-05	17-Apr-05	30-Nov-05	29-Mar-06	19th-Dec-06	-
580			18-Dec-02	11-Mar-03	17-Dec-03	17-Apr-04	25-Jan-05	17-Apr-05	30-Nov-05	29-Mar-06	19th-Dec-06	06-Jul-07
590			18-Dec-02	11-Mar-03	17-Dec-03	17-Apr-04	25-Jan-05	17-Apr-05	30-Nov-05	29-Mar-06	19th-Dec-06	06-Jul-07
600			18-Dec-02	11-Mar-03	17-Dec-03	17-Apr-04	25-Jan-05	17-Apr-05	30-Nov-05	29-Mar-06	19th-Dec-06	-

Cross-section	Distance from previous (m)	Distance from 010 (m)	Active channel width (m)	Elevation (O.D.)	Bed slope
010	0	0	23	233.5	
020	74.0	74.0	12	233.1	0.005
030	262.7	336.7	14.7	231.4	0.006
040	199.4	536.1	15	230.3	0.006
050	214.2	750.3	13.8	226.9	0.016
060	37.2	787.5	12.9	225.8	0.030
070	29.4	816.9	15	226.5	-0.024
080	31.5	848.4	19.8	226.5	0.000
090	50.0	898.4	20.4	226.8	-0.006
100	61.5	959.9	16.6	226.1	0.011
110	46.4	1006.3	20.8	225.8	0.006
120	42.2	1048.5	16.6	224.9	0.021
130	52.1	1100.6	21.5	225.6	-0.013
140	33.1	1133.7	22.4	225.4	0.006
150	73.6	1207.3	14.4	224.3	0.015
160	117.4	1324.7	14.9	223.5	0.007
170	162.5	1487.2	18.4	223.7	-0.001
180	138.4	1625.6	15.6	223.1	0.004
190	78.9	1704.5	12.7	222.2	0.011
200	119.3	1823.8	13.5	221.7	0.004
210	30.4	1854.2	13.7	221.1	0.020
220	42.4	1896.6	19.5	221.7	-0.014
230	47.3	1943.9	23	221.3	0.008
240	31.2	1975.1	17.0	221.3	0.000
250	51.9	2027.0	16.7	220.8	0.010
260	70.4	2097.4	12.3	220.1	0.010
270	37.9	2135.3	14.8	220.2	-0.003
280	89.5	2224.8	12.9	220.5	-0.003
290	116.0	2340.8	15.2	219.8	0.006
300	73.1	2413.9	18.6	219.5	0.004
310	61.3	2475.2	17.5	219.1	0.007
320	57.3	2532.5	18.5	219.1	0.000
330	94.7	2627.2	19.2	218.9	0.002
340	123.2	2750.4	16.9	217.9	0.008
350	139.6	2890	32.5	217.1	0.006
360	88.1	2978.1	17.3	216.9	0.002
370	29.8	3007.9	19.2	216.6	0.010
380	56.4	3064.3	17.3	216.7	-0.002
390	125.5	3189.8	19.9	216.7	0.000
400	122.4	3312.2	22.1	216.7	0.000
410	105.6	3417.8	28.2	216.6	0.001
420	42.7	3460.5	33	216.0	0.014
430	141.2	3601.7	22.7	215.9	0.001
440	201.9	3803.6	19	215.5	0.002
450	202.1	4005.7	20.6	215.3	0.001
460	67.4	4073.1	25.3	214.7	0.009
470	115.6	4188.7	16.1	214.3	0.003
480	128.3	4317	16.9	214.5	-0.002
490	178.4	4495.4	17.4	214.2	0.002
500	95.9	4591.3	24.4	213.4	0.008
510	102.4	4693.7	21.4	213.5	-0.001
520	120.0	4813.7	16.4	213.1	0.003
530	84.7	4898.4	13.2	212.9	0.002
540	112.1	5010.5	12.5	213.0	-0.001
550	86.2	5096.7	15.5	212.8	0.002
560	11.9	5108.6	15.5	212.6	0.017
570	110.0	5218.6	17.3	212.4	0.002
580	121.2	5339.8	17.8	212.7	-0.002
590	142.5	5482.3	12.6	212.7	0.000
600	123.6	5605.9	12.6	212.6	0.000

APPENDIX III: GRAIN SIZE DISTRIBUTIONS

% finer than D (mm)	010 Surf	010 Active	040 Surf	040 Active	080 Surf	080Active
724	100.0	100.0	100.0	100.0	100.0	100.0
512	99.5	100.0	100.0	100.0	100.0	100.0
362	97.5	98.5	99.0	99.4	100.0	100.0
256	94.5	96.6	95.5	97.2	100.0	100.0
181	87.5	91.5	90.0	93.4	99.5	99.7
128	72.0	78.9	81.5	86.8	92.5	95.0
90.5	49.5	58.4	57.0	65.5	82.5	87.5
64	30.0	38.6	31.5	40.7	66.0	73.7
45.3	14.5	21.0	16.0	23.8	42.1	51.2
32	5.0	9.0	8.0	14.1	22.6	30.8
22.6	0.5	2.6	3.5	8.0	8.1	13.9
16	0.0	1.8	1.5	5.0	2.6	6.7
11.3	0.0	1.8	0.0	2.4	0.6	3.8
8	0.0	1.8	0.0	2.4	0.1	3.0
D50	*91.3*	*79.2*	*83.2*	*74.0*	*51.5*	*44.5*
D84	*169.0*	*149.6*	*147.3*	*143.6*	*96.0*	*83.8*

% finer than D (mm)	160 Surf	160 Active	190 Surf	190 Active	220 Surf	220 Active
724	100.0	100.0	100.0	100.0	100.0	100.0
512	100.0	100.0	100.0	100.0	100.0	100.0
362	100.0	100.0	100.0	100.0	100.0	100.0
256	99.5	99.7	100.0	100.0	100.0	100.0
181	99.0	99.4	99.0	99.6	100.0	100.0
128	93.1	95.3	94.1	97.4	99.0	99.4
90.5	77.7	83.6	80.8	90.0	86.7	90.5
64	59.8	68.3	62.6	77.2	67.1	74.7
45.3	39.5	48.8	41.4	58.7	46.0	55.8
32	18.7	26.6	22.7	38.3	24.9	34.6
22.6	6.8	12.3	9.4	20.2	14.1	22.4
16	2.3	6.4	4.0	11.0	6.2	12.6
11.3	0.9	4.2	2.0	6.8	2.8	7.8
8	0.9	4.2	1.5	5.5	1.8	6.3
D50	*54.9*	*46.4*	*52.9*	*39.6*	*48.8*	*41.7*
D84	*105.9*	*91.9*	*99.5*	*78.1*	*86.8*	*79.5*

% finer than D (mm)	290 Surf	290 Active	330 Surf	330 Active	350 Surf	350 Active
724	100.0	100.0	100.0	100.0	100.0	100.0
512	100.0	100.0	100.0	100.0	100.0	100.0
362	100.0	100.0	100.0	100.0	100.0	100.0
256	100.0	100.0	100.0	100.0	100.0	100.0
181	99.0	99.4	99.5	99.7	99.5	99.7
128	93.6	96.0	96.6	97.9	95.2	97.1
90.5	86.1	90.9	88.2	92.2	85.5	90.7
64	74.3	81.6	77.0	83.5	74.8	82.8
45.3	54.5	64.4	54.9	64.6	59.8	70.3
32	29.2	39.8	27.5	38.3	36.6	48.7
22.6	13.4	22.6	13.3	23.1	20.8	32.4
16	7.5	15.4	8.8	17.8	10.6	20.6
11.3	5.5	12.7	5.4	13.2	4.8	13.1
8	2.5	8.2	3.0	9.6	3.4	11.0
D50	*42.9*	*37.5*	*42.9*	*37.9*	*39.7*	*32.8*
D84	*85.7*	*70.8*	*80.5*	*65.4*	*86.8*	*68.1*

% finer than D (mm)	390 Surf	390 Active	410 Surf	410 Active	430 Surf	430 Active
724	100.0	100.0	100.0	100.0	100.0	100.0
512	100.0	100.0	100.0	100.0	100.0	100.0
362	100.0	100.0	100.0	100.0	100.0	100.0
256	100.0	100.0	100.0	100.0	100.0	100.0
181	100.0	100.0	100.0	100.0	100.0	100.0
128	98.6	99.2	100.0	100.0	99.5	99.7
90.5	92.8	95.4	95.7	97.2	96.2	97.6
64	75.0	82.5	78.9	85.3	82.4	88.0
45.3	54.8	66.1	59.3	69.6	62.8	72.7
32	38.9	51.7	36.3	49.1	38.0	51.1
22.6	23.5	36.2	19.0	31.9	19.4	33.0
16	11.0	22.0	10.9	22.9	8.5	21.0
11.3	5.3	14.7	6.6	17.5	5.6	17.6
8	3.8	12.7	4.2	14.2	4.7	16.3
D50	*41.3*	*31.0*	*39.9*	*32.6*	*38.4*	*31.4*
D84	*77.4*	*67.1*	*72.0*	*62.5*	*67.1*	*59.1*

% finer than D (mm)	460 Surf	460 Active	480 Surf	480 Active	510 Surf	510 Active
724	100.0	100.0	100.0	100.0	100.0	100.0
512	100.0	100.0	100.0	100.0	100.0	100.0
362	100.0	100.0	100.0	100.0	100.0	100.0
256	100.0	100.0	100.0	100.0	100.0	100.0
181	100.0	100.0	100.0	100.0	100.0	100.0
128	100.0	100.0	100.0	100.0	100.0	100.0
90.5	99.0	99.5	100.0	100.0	99.5	99.8
64	95.7	97.3	98.6	99.1	94.2	96.7
45.3	76.9	84.1	81.5	87.4	82.0	89.1
32	56.2	67.9	62.0	72.5	66.9	78.5
22.6	33.1	47.6	31.2	46.2	49.4	64.8
16	16.3	31.0	13.6	29.4	29.0	46.9
11.3	7.1	21.0	7.0	22.3	13.4	31.6
8	5.2	18.7	5.6	20.6	6.1	23.7
D50	*29.5*	*23.7*	*28.3*	*24.0*	*22.9*	*17.1*
D84	*52.4*	*45.2*	*48.0*	*42.2*	*48.4*	*38.9*

% finer than D (mm)	540 Surf	540 Active
724	100.0	100.0
512	100.0	100.0
362	100.0	100.0
256	100.0	100.0
181	100.0	100.0
128	100.0	100.0
90.5	99.0	99.5
64	93.3	96.4
45.3	82.8	90.0
32	65.5	78.3
22.6	48.8	65.6
16	29.6	49.3
11.3	15.7	36.1
8	6.6	26.5
D50	*23.3*	*16.3*
D84	*47.5*	*38.5*

NB: Surf: surface layer
Active: active layer

Appendix IV: Sediment Budget

distance downstream	Dec02-Apr03		Apr-03-Dec03		Dec03-Apr04		Apr04 - Jan05		Jan05-Arp05		Apr05-Dec05		Dec05-Apr06		Apr06-Jan07		Jan07-July07	
	ΔV	Vi	ΔV	Vi	ΔV	Vi	ΔV	Vi	ΔV	Vi	ΔV	Vi	ΔV	Vi	ΔV	Vi	ΔV	Vi
0 to 331.3	258	-1176	442	3030	811	5811	60	-294	-190	7	159	1409	106	1629	-119	-1071	-23	1251
530.8	-107	-1435	579	2588	345	5000	202	-354	15	197	-109	1250	70	1523	-137	-952	0	1274
743	-324	-1328	637	2009	223	4655	242	-557	167	182	-227	1358	31	1454	151	-815	0	1274
777.5	-35	-1003	5	1372	5	4432	51	-799	49	15	-63	1585	75	1423	16	-966	0	1274
808.6	12	-968	-81	1367	0	4427	66	-850	55	-34	-59	1648	72	1347	-11	-982	2	1274
836.8	-27	-981	-10	1448	40	4427	-19	-916	57	-88	-18	1707	12	1275	-8	-971	-7	1272
882	-65	-954	61	1458	99	4387	-131	-896	53	-145	-7	1725	29	1263	0	-963	-31	1279
942.5	37	-889	84	1397	82	4288	-80	-765	-13	-198	-24	1732	54	1234	-2	-963	3	1310
982.2	45	-926	88	1312	48	4206	5	-685	6	-186	-29	1756	20	1180	20	-961	16	1307
1025.6	21	-971	103	1224	58	4158	18	-691	61	-191	-40	1785	19	1159	54	-981	11	1291
1078.2	42	-992	91	1121	55	4100	21	-708	27	-252	-7	1825	-22	1141	40	-1035	13	1281
1110.2	-34	-1035	67	1030	34	4044	82	-730	-58	-280	23	1831	-16	1163	-23	-1074	0	1268
1183.4	-176	-1001	176	964	95	4010	173	-812	5	-221	47	1809	-1	1179	-119	-1051	11	1268
1302.7	-38	-825	254	787	174	3915	111	-985	3	-227	-21	1762	47	1180	-75	-932	96	1257
1493.3	19	-787	277	533	156	3741	46	-1096	-124	-230	-15	1783	-69	1133	145	-856	124	1161
1632.7	102	-805	-73	257	-18	3585	-197	-1142	43	-106	225	1798	-155	1202	75	-1001	-42	1037
1713.4	65	-908	-98	330	-53	3603	-20	-945	-50	-149	171	1573	-50	1357	-17	-1077	-34	1079
1830.2	29	-972	89	428	-152	3656	-53	-925	-71	-98	131	1402	76	1407	-135	-1060	11	1113
1856.9	42	-1002	-53	339	-30	3808	9	-873	-32	-28	40	1271	53	1331	-30	-925	-2	1103
1892.8	55	-1043	-122	393	20	3838	39	-882	22	4	-19	1231	62	1278	-5	-895	-20	1105
1944.1	63	-1099	-68	515	111	3818	47	-920	90	-18	-84	1250	73	1216	-80	-890	-13	1125
1974.3	21	-1161	21	583	15	3706	74	-967	13	-107	-8	1334	29	1143	-33	-810	53	1138
2024.6	-9	-1182	91	562	8	3691	56	-1040	22	-120	-16	1342	23	1114	24	-777	88	1085
2094.1	-60	-1173	34	471	-79	3683	-56	-1096	-33	-142	51	1358	10	1091	67	-801	0	997
2131.1	-44	-1113	5	437	-109	3762	27	-1040	-37	-109	49	1307	-13	1080	9	-868	2	997
2223.7	-20	-1069	-40	432	-73	3870	144	-1068	-9	-72	57	1258	-20	1093	-53	-877	75	995
2335	-94	-1049	-34	472	10	3943	65	-1212	86	-63	13	1201	5	1113	29	-824	91	919
2406.6	-47	-954	-5	506	27	3932	31	-1277	97	-148	-46	1187	-36	1108	34	-853	-6	828
2471.4	206	-907	38	512	224	3906	-35	-1307	-159	-245	-33	1233	-3	1144	30	-887	-12	835
2524.1	130	-1113	-22	474	241	3682	-114	-1273	-178	-86	33	1266	70	1147	-49	-917	-2	847
2612.6	-86	-1243	15	496	99	3441	-135	-1158	-144	92	154	1232	113	1078	-90	-869	61	849
2741.3	-75	-1157	93	481	92	3342	-74	-1024	-213	235	245	1078	17	965	0	-778	68	789
2867.5	-113	-1082	-77	388	625	3251	-215	-950	112	448	77	833	102	947	-101	-779	15	721
2947	-71	-969	-134	465	337	2626	-64	-735	107	336	47	756	52	845	-28	-678	103	706
2973.7	5	-898	-83	598	12	2289	16	-671	11	229	25	709	-16	793	6	-650	27	603

distance downstream	Dec02-Apr03		Apr-03-Dec03		Dec03-Apr04		Apr04 - Jan05		Jan05-Arp05		Apr05-Dec05		Dec05-Apr06		Apr06-Jan07		Jan07-July07	
	ΔV	Vi	ΔV	Vi	ΔV	Vi	ΔV	Vi	ΔV	Vi	ΔV	Vi	ΔV	Vi	ΔV	Vi	ΔV	Vi
3030.6	4	-903	-85	681	-34	2277	53	-687	32	218	28	684	16	809	-26	-656	-1	575
3153.6	91	-907	-103	766	-74	2311	41	-739	-38	187	130	655	73	792	-53	-630	-44	576
3274.2	127	-998	-184	870	78	2385	-34	-780	-70	224	154	525	63	720	-96	-577	-3	621
3377.3	-31	-1125	-73	1054	54	2307	-16	-747	30	294	75	371	70	656	-92	-481	6	624
3410.5	-38	-1095	16	1127	20	2253	11	-730	5	264	-6	296	-12	586	16	-390	-11	618
3682.7	-247	-1057	148	1111	488	2234	-211	-742	26	259	-6	302	-1	598	72	-406	104	628
3833.7	-27	-810	-30	963	273	1746	-217	-530	-121	233	183	308	217	599	-162	-478	132	524
3938.9	-93	-782	131	993	42	1472	-108	-313	21	354	122	124	81	383	-21	-316	45	392
4002.5	-121	-690	91	861	65	1430	7	-206	73	334	40	3	-4	302	27	-295	-15	347
4112.9	-195	-569	43	771	151	1366	3	-212	-31	260	106	-38	82	306	10	-322	-39	362
4240.8	-248	-374	165	728	152	1215	-19	-215	-85	292	129	-144	98	224	-39	-332	8	401
4424.9	-270	-125	219	564	297	1063	48	-196	49	377	114	-273	-118	126	21	-292	48	392
4511.2	33	144	50	345	247	765	-87	-244	43	328	31	-387	-11	244	-44	-313	7	344
4601.3	16	112	113	295	204	519	-5	-156	5	285	-25	-418	74	254	-97	-270	66	338
4715.8	1	95	69	182	49	315	-34	-151	183	280	-177	-392	83	180	-91	-173	13	271
4801.4	29	94	-22	113	7	266	-75	-117	209	97	-197	-215	70	97	-81	-82	-7	259
4913.2	-14	65	3	135	147	259	-183	-42	89	-112	-77	-18	33	28	11	-1	103	265
4996.1	-27	78	41	131	135	112	-86	141	-89	-201	-5	59	37	-5	46	-12	23	162
5108.9	-77	105	208	90	-13	-23	64	227	-138	-113	-25	64	34	-42	-58	-58	-33	139
5217.8	-72	182	167	-118	49	-10	0	163	-46	26	26	89	-45	-76	5	0	16	172
5331.7	12	254	1	-285	97	-60	9	163	-77	72	60	63	-32	-31	77	-5	44	156
5462.3	117	242	-140	-285	-17	-156	-2	154	22	149	20	2	-9	1	-28	-82	5	112
5586.4	125	125	-146	-146	-139	-139	156	156	127	127	-17	-17	10	10	-54	-54	107	107
output		0	0	0		0		0		0		0		0		0		0

Where ΔV is the volumetric storage in each cross-sectional reach and V_i is the volumetric input into each reach calculated using [6.2] in Section 6.3. All values are m^3.

The two lines across the data represent the location of the tributaries where 0.3% (Cray Beck) and 0.8% (Buckden Beck) of sediment is removed from the budget.